



# UNIVERSIDAD MIGUEL HERNÁNDEZ DE ELCHE

INSTITUTO DE BIOLOGÍA MOLECULAR Y CELULAR

Actividad antitumoral de un extracto de romero (*Rosmarinus officinalis* L.)

en modelos *in vitro* e *in vivo* de cáncer de colon

Tesis Doctoral

Almudena Pérez Sánchez

Elche (Alicante), 2017





**Dr. Antonio Ferrer Montiel**, Director del Instituto de Biología Molecular y Celular de la Universidad Miguel Hernández de Elche,

DA SU CONFORMIDAD a la lectura de la Tesis Doctoral titulada: "Actividad antitumoral de un extracto de romero (*Rosmarinus officinalis* L.) en modelos *in vitro* e *in vivo* de cáncer de colon", presentada por Dña. Almudena Pérez Sánchez para optar al grado de Doctora, la cual ha sido realizada en el Instituto de Biología Molecular y Celular de la Universidad Miguel Hernández de Elche.

Para que consten los efectos oportunos, firma el presente certificado en Elche (Alicante),  
a 22 de Marzo de 2017.

Fdo.: **Dr. Antonio Ferrer Montiel**





*Miguel Hernández*

**Dres. José Antonio Ferragut Rodríguez y Vicente Micol Molina**, Catedráticos de Bioquímica y Biología Molecular de la Universidad Miguel Hernández y **Dr. Enrique Barrajón Catalán**, Profesor Ayudante Doctor de la Universidad Miguel Hernández del Departamento de Ingeniería, Área de Farmacia y Tecnología Farmacéutica,

CERTIFICAN QUE:

El trabajo de investigación que conduce a la obtención del grado de Doctora: “Actividad antitumoral de un extracto de romero (*Rosmarinus officinalis* L.) en modelos *in vitro* e *in vivo* de cáncer de colon”, cuya autora es Dña. Almudena Pérez Sánchez, ha sido realizado bajo nuestra dirección en el Instituto de Biología Molecular y Celular de la Universidad Miguel Hernández de Elche.

Para que consten los efectos oportunos, firman el presente certificado en Elche (Alicante), a 22 de Marzo de 2017.

**Dr. José Antonio Ferragut Rodríguez**

**Dr. Vicente Micol Molina**

**Dr. Enrique Barrajón Catalán**



## Resumen

Los compuestos bioactivos naturales han suscitado un gran interés científico por sus potenciales beneficios en la salud humana, particularmente en la prevención del cáncer, las enfermedades cardiovasculares y neurodegenerativas. Algunos de estos compuestos han mostrado propiedades antitumorales inhibiendo la proliferación de células cancerígenas tanto en modelos *in vitro* como *in vivo*. El objetivo del presente trabajo ha sido determinar la actividad antitumoral de un extracto de romero (ER) enriquecido en terpenoides en modelos *in vitro* e *in vivo* de cáncer colorrectal humano. Además, se ha contribuido a explicar el mecanismo de acción por el cual el ER inhibe la proliferación celular mediante ensayos de viabilidad y de citotoxicidad, así como la implicación de rutas relacionadas con la viabilidad mitocondrial y la respuesta al estrés oxidativo. Posteriormente, se ha estudiado la actividad de dicho extracto en un modelo animal y se ha analizado la permeabilidad intestinal de los compuestos del extracto mediante el empleo de monocapas de células intestinales Caco-2.

Los resultados obtenidos demuestran que el ER presenta una actividad antiproliferativa similar o superior a la observada de manera individual por alguno de sus compuestos más activos, como el ácido carnósico. El mecanismo predominante del efecto antiproliferativo del ER es la muerte celular por necrosis y, en menor medida, un efecto citostático mediante el bloqueo del ciclo celular en la fase G<sub>2</sub>/M. Se propone que esta necrosis sea desencadenada por un aumento exacerbado en los niveles de especies reactivas de oxígeno (ROS) intracelulares, generados a partir de los terpenos presentes en el extracto, y posterior activación de la vía Nrf2 como mecanismo de protección celular. Se propone a los diterpenos ácido carnósico y carnosol y a algún triterpeno como el ácido betulínico como principales responsables del efecto antitumoral observado. La capacidad antiproliferativa del extracto ha sido corroborada en un modelo animal de xenotransplantes humanos de cáncer de colon y se ha verificado en ratas su ausencia de toxicidad a los niveles máximos permitidos por la regulación existente relativa a ensayos animales. Los resultados también muestran que el ácido carnósico presenta la mayor permeabilidad entre los compuestos del extracto seguido del epiisorrosmanol y epirosmanol. La encapsulación del extracto de romero en liposomas no ha mejorado en ningún caso la absorción intestinal de los compuestos identificados. Los resultados obtenidos justifican la utilización de dicho extracto en nuevos ensayos preclínicos para corroborar su eficacia y estudiar en profundidad su mecanismo de acción mediante una aproximación global basada en ciencias ómicas.



## **Abstract**

Bioactive compounds have attracted much scientific interest since they exert various beneficial effects on health, including cancer prevention, cardiovascular and neurodegenerative diseases. Some of these compounds have shown anti-cancer activity by inhibiting the cell proliferation in *in vitro* and *in vivo* models. The aim of this study was to determine the antiproliferative effect of a terpenoid-enriched rosemary extract (RE) in *in vitro* and *in vivo* models of human colorectal cancer. In addition, the mechanism of the antiproliferative/cytotoxic activity was addressed through cell viability and cytotoxicity assays cell cycle analysis, clonogenic survival assay, real time cell growth analysis and migration assay. The role of pathways related to mitochondrial viability and oxidative stress response was also studied. Afterwards, RE activity has been studied in a model animal and the intestinal permeability of the extract compounds has been analyzed through a Caco-2 cell monolayer assay.

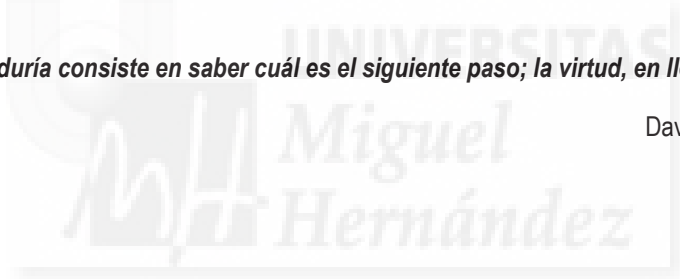
The results indicate that RE shows a similar and/or higher antiproliferative activity than their individually active compounds, such as carnosic acid. The main death mechanism of RE is the necrosis and, to a lesser degree, a cytostatic effect by blocking cell cycle in G<sub>2</sub>/M phase. The exacerbated increase of intracellular reactive oxygen species (ROS) levels, possibly generated by RE terpenoids, could trigger necrosis. Nrf2 pathway was also activated as a part of a cellular protection event against RE action. The anti-tumor effect of the extract was also corroborated in an animal model (human colon cancer xenotransplantation) and no toxicity was found after an acute oral toxicity test in rats.

Carnosic acid, carnosol and some triterpenes such as betulinic acid are postulated as the putative candidates for the observed antiproliferative activity. The results also show that carnosic acid exhibited the highest permeability values followed by epiisorosmanol and epirosmanol in the intestinal cell monolayers. The liposome encapsulation of RE has not improved the intestinal absorption any of the identified compounds. Finally, the results justify further research to verify the efficacy of the RE in preclinical trials and to deeply study its action mechanism through a global approach based on omics techniques



***“La sabiduría consiste en saber cuál es el siguiente paso; la virtud, en llevarlo a cabo”***

David Starr Jordan





## Agradecimientos

En primer lugar, me gustaría dar las gracias a mis directores de tesis, los **Dres. José Antonio Ferragut, Vicente Micol y Enrique Barrajón**, por darme la oportunidad de llevar a cabo este trabajo y por el apoyo incondicional recibido, tanto a nivel personal como profesional.

Quiero agradecer al **Instituto de Biología Molecular y Celular (IBMC)**, a todos los técnicos y a todas aquellas personas que directa o indirectamente me han ayudado a llevar a cabo mi Tesis Doctoral.

Agradezco al personal administrativo, **Javier, May, Carmen y Raquel**, por su amabilidad, paciencia y sobre todo por su excelente trabajo.

Por supuesto, quiero agradecer a todas las personas que han trabajado junto a mí en el grupo de investigación. A **María Herranz**, por su paciencia infinita para enseñarme cultivos y saber responder a todas mis dudas. Una gran compañera, amiga y confidente, con momentos inolvidables a su lado. A **Verónica Ruiz**, mi “Muero de amor”, por su generosidad infinita conmigo y con todos sus compañeros, por estar a mi lado en momentos buenos y no tan buenos, mil gracias por ser mi amiga. A **Luz María Agulló**, mi “Lucecita”, por su ayuda infinita e incondicional en el terreno profesional y personal, por hacerme reír con sus chistes malos del día y sobre todo por ser una gran amiga. A **Mariló Olivares**, por su ayuda, compañía y por momentos muy divertidos a su lado. A **Maite**, mi “María Teresa”, por su gran apoyo en todos los aspectos de mi vida y por estar ahí cuando lo he necesitado. A **Cecilia Jiménez, Teresa Castaño, Adrián Martínez, Noelia Sánchez, María Losada y Víctor Jiménez** por su ayuda y por formar parte de esta experiencia. También agradecer a mis dos italianas favoritas, **Angela Catania** mi “Cucci” y **Silvia Nicolosi** mi “Cachu”, por compartir conmigo momentos maravillosos e inolvidables.



Me gustaría agradecer al grupo de investigación del **Dr. Domingo Saura** y la **Dra. Nuria Martí**, sin olvidarme de **Salud Vegara, Sara Gea** y **María Berenguer**, por su gran apoyo y compañerismo.

Gracias al **Dr. Miguel Saceda** por su ayuda incondicional, amabilidad y por su gran aportación a dicho trabajo.

También agradezco a los **Dres. Alejandro Cifuentes, Elena Ibáñez, Virginia García** y **Carolina Simó** y a su grupo de investigación, por su disposición a acogerme en su laboratorio, enriqueciendo mi formación durante la realización de dicho trabajo. Por supuesto, quiero agradecer al **Dr. Javier A. Menéndez** y a la **Dra. Elisabet Cuyàs** por su gran acogida en su laboratorio y por el enorme apoyo recibido. Y por último, al **Dr. Antonio Segura** y a su grupo de investigación, por su valiosa colaboración en el desarrollo de dicho trabajo.

Además, quiero agradecer a dos grandes amigas, pilares fundamentales en mi vida. A **Sandra Martínez**, mi “Nena”, amigas desde siempre, por compartir momentos buenos y malos a mi lado y por estar siempre ahí cuando más lo he necesitado, como una hermana. A **Cristina López**, mi “Dory”, por su capacidad para sacarme una sonrisa cuando más lo necesito y por su gran amistad.

Por último, y no menos importante quiero agradecer a toda mi familia, en especial a **mis padres** por ser mi mayor apoyo y por creer siempre en todo lo que hago. Me gustaría dedicarles este trabajo para agradecerles todo lo que hacen por mí.

*Mi más sincero agradecimiento a todos*



## Índice

<b>1. INTRODUCCIÓN .....</b>	1
1.1. Cáncer: clasificación e incidencia.....	3
1.2. Cáncer colorrectal (CCR) .....	5
Anatomía.....	5
Clasificación .....	7
Incidencia.....	9
Factores de riesgo .....	12
Sintomatología .....	13
Tratamiento .....	14
1.3. Ciclo celular y cáncer .....	16
Fases del ciclo celular.....	16
Control del ciclo celular .....	18
1.4. Muerte celular: apoptosis, necrosis/necroptosis y autofagia. ....	19
1.5. Compuestos bioactivos naturales.....	21
Polifenoles: estructura y clasificación .....	22
Terpenoides: estructura y clasificación .....	24
1.6. Estrés oxidativo y defensa antioxidante. ....	25
Especies Reactivas de Oxígeno .....	26
Mecanismos de defensa antioxidante .....	28
El elemento de respuesta antioxidante ARE.....	29
Factor de transcripción Nrf2.....	29
1.7. Potencial de Membrana Mitocondrial ( $\Delta\Psi_m$ ). ....	31
1.8. Biodisponibilidad de los compuestos bioactivos.....	33
Absorción y metabolismo .....	33
Transporte en sangre de compuestos fenólicos .....	34
1.9. Extracto de <i>Rosmarinus officinalis</i> L. como fuente de compuestos bioactivos.....	34
1.10. Extracción por Fluidos Supercríticos (FSC), una técnica optimizada para la obtención de extractos enriquecidos en compuestos bioactivos.....	38
<b>2. HIPÓTESIS DE PARTIDA Y OBJETIVOS .....</b>	41
<b>3. METODOLOGÍA.....</b>	45
3.1. Líneas celulares .....	47
Línea celular HGUE-C-1 .....	47
Línea celular HT-29.....	47
Línea celular SW480.....	47
Línea celular Caco-2 .....	48

3.2. Condiciones de cultivo.....	48
3.3. Extracto de romero.....	48
3.4. Aislamiento y purificación de compuestos presentes en el extracto de romero mediante cromatografía semi-preparativa.....	49
3.5. Análisis del extracto de romero y sus fracciones mediante HPLC-ESI-QTOF-MS.....	49
3.6. Determinación de la viabilidad celular.....	51
3.7. Análisis del ciclo celular.....	52
3.8. Detección de apoptosis mediante Anexina-V.....	53
3.9. Determinación de la integridad de la membrana plasmática.....	55
3.10. Determinación de necroptosis y autofagia.....	56
3.11. Cuantificación de Especies Reactivas de Oxígeno (ROS).....	57
3.12. Estudio del Potencial de Membrana Mitocondrial (PMM). <i>Muse Cell Analyzer</i> .....	58
Microscopía de fluorescencia.....	58
3.13. Transfección siRNA.....	59
3.14. Expresión de proteínas mediante <i>Dot-Blot</i> . Extracción de proteínas .....	60
Inmunodetección.....	60
3.15. Ensayos de proliferación y migración. Determinación de la proliferación celular mediante <i>xCelligence Real Time Cell Analysis (RTCA)</i> ....	62
Ensayo de capacidad clonogénica: formación de colonias .....	63
Ensayo de migración celular: <i>wound healing</i> .....	63
3.16. Ensayo de toxicidad oral aguda en ratas.....	64
3.17. Ensayo antitumoral en ratones inmunodeprimidos.....	65
3.18. Preparación de liposomas (LUVs).....	66
3.19. Absorción <i>in vitro</i> de los compuestos del extracto de romero. ....	67
3.20. Análisis de las muestras procedentes del ensayo de permeabilidad en la línea celular Caco-2 mediante HPLC-MS.....	69
3.21. Determinación de la Permeabilidad Aparente ( $P_{app}$ ).....	70
3.22. Análisis estadístico.....	70
<b>4. RESULTADOS .....</b>	<b>71</b>
Fraccionamiento e identificación de los compuestos bioactivos de un extracto de romero que contribuyen al efecto antiproliferativo en células humanas de cáncer de colon .....	73
1. Caracterización cuantitativa del extracto de romero.....	75
2. Fraccionamiento y análisis de los compuestos del extracto de romero. ....	78
3. Efecto antiproliferativo del extracto de romero y de sus fracciones. ....	79

Actividad antiproliferativa y posibles mecanismos de acción del extracto de romero en modelos <i>in vitro</i> e <i>in vivo</i> de CCR.....	83
1. Estudio del mecanismo de acción por el cual el ER inhibe la proliferación celular.....	85
2. Cuantificación de especies reactivas de oxígeno y potencial de membrana mitocondrial en las líneas de cáncer de colon.....	91
3. La implicación del factor de transcripción Nrf2 en el efecto del extracto de romero sobre las células de cáncer colorrectal.....	95
4. Efecto del ER en la proliferación y migración celular en las líneas de cáncer de colon.....	97
5. Toxicidad oral aguda del extracto de romero en ratas.....	102
6. Efecto del extracto de romero en un modelo <i>in vivo</i> de cáncer de colon.....	104
Estudio de la permeabilidad del extracto de romero en monocapas de células intestinales Caco-2.....	107
1. Análisis de las muestras por HPLC ESI-UHD-Qq-TOF-MS.....	109
2. Determinación de los valores $P_{app}$ .....	109
3. Resultados de permeabilidad según familia de compuestos.....	109
Flavonoides y derivados de ácidos fenólicos .....	109
Diterpenos.....	111
Triterpenos.....	112
<b>5. DISCUSIÓN.....</b>	115
1. El extracto de romero produce un efecto antiproliferativo muy similar a sus compuestos aislados en líneas celulares de cáncer de colon.....	117
2. El extracto de romero posee un efecto antiproliferativo en modelos de cáncer de colon debido principalmente a una muerte celular por necrosis y a un bloqueo del ciclo celular.....	120
3. El tratamiento con el extracto de romero induce la generación intracelular de ROS y afecta a la viabilidad mitocondrial.....	122
4. El tratamiento de las células de cáncer de colon con ER activa la vía del factor de transcripción Nrf2 en correlación con el aumento de ROS. El silenciamiento del gen aumenta los niveles de ROS y disminuye la viabilidad celular.....	123
5. El tratamiento de modelos celulares de colon con ER inhibe tanto la proliferación como la migración celular.....	124
6. El extracto de romero no presenta signos de toxicidad oral aguda en ratas Wistar.....	126
7. El extracto de romero disminuye la tumorogénesis en un modelo <i>in vivo</i> de xenotransplantes de cáncer de colon.....	127
8. La absorción de los compuestos del ER en forma libre y liposomada en modelos de monocapas de células intestinales es moderada y se produce principalmente por difusión pasiva.....	128
<b>6. CONCLUSIONES.....</b>	131
<b>7. BIBLIOGRAFÍA.....</b>	137
ANEXO I: Artículos científicos relacionados con la temática de la Tesis Doctoral .....	151
ANEXO II: Otros artículos científicos relacionados con la temática de la Tesis Doctoral .....	179



## Abreviaturas y Acrónimos

<b>7-AAD</b>	7-aminoactinomicina D (del inglés, <i>7-Aminoactinomycin D</i> )
<b>ADN</b>	Ácido desoxirribonucleico
<b>ANOVA</b>	Análisis de la Varianza
<b>AP</b>	Apical
<b>APC</b>	Poliposis adenomatosa familiar (del inglés, <i>Adenomatous Polyposis Coli</i> )
<b>ARN</b>	Ácido ribonucleico
<b>ATCC</b>	Colección Americana de Cultivos Celulares (del inglés, <i>American Type Culture Collection</i> )
<b>ATP</b>	Adenosina trifosfato
<b>BL</b>	Basolateral
<b>CCR</b>	Cáncer colorrectal
<b>DMEM</b>	Medio de cultivo (del inglés, <i>Dulbecco's Modified Eagle's Medium</i> )
<b>DMSO</b>	Dimetilsulfóxido
<b>EDTA</b>	Ácido etilendiamino tetracético
<b>EMA</b>	Agencia Europea de Medicina (del inglés, <i>European Medicine's Agency</i> )
<b>ESI</b>	Ionización por electroespray (del inglés, <i>Electrospray ionization</i> )
<b>EYPC</b>	Lecitina natural de yema de huevo (del inglés, <i>Egg-Yolk Phosphatidylcholine</i> )
<b>FDA</b>	Agencia de Alimentos y Medicamentos (del inglés, <i>Food and Drug Administration</i> )
<b>FSC</b>	Fluidos Supercríticos
<b>HBSS</b>	Solución Salina Equilibrada de Hank (del inglés, <i>Hank's Balanced Salt Solution</i> )
<b>HEPES</b>	Ácido N-2-hidroxietilpiperazina-N-2-etanosulfónico
<b>HGUE</b>	Hospital General Universitario de Elche
<b>HPLC</b>	Cromatografía Líquida de Alta Resolución (del inglés, <i>High Performance Liquid Cromatography</i> )
<b>HRP</b>	Peroxidasa de caballo (del inglés, <i>Horseradish peroxidase enzyme</i> )
<b>IC</b>	Índice Celular

<b>IC<sub>50</sub></b>	Concentración de un fármaco que inhibe el 50% del crecimiento celular
<b>IMIM</b>	Institut Municipal d'Investigació Mèdica
<b>LDH</b>	Lactato Deshidrogenasa
<b>LUVs</b>	Vesículas unilámeras de diámetro grande (del inglés, <i>Large Unilamellar Vesicles</i> )
<b>MS</b>	Espectrometría de Masas (del inglés, <i>Mass Spectrometry</i> )
<b>MTT</b>	Bromuro de 3-(4,5-dimetil-2-tiazolil)-2,5-difeniltetrazolio
<b>Nrf2</b>	Factor relacionado con el factor nuclear eritroide 2p45
<b>PBS</b>	Tampón Fostato Salino (del inglés, <i>Phosphate Buffer Saline</i> )
<b>PMM</b>	Potencial de Membrana Mitocondrial ( $\Delta\psi_m$ )
<b>PEG400</b>	Polietilenglicol 400
<b>QTOF</b>	Cuadrupolo tiempo de vuelo (del inglés, <i>Quadrupole Time-of-Flight</i> )
<b>ROS</b>	Especies Reactivas del Oxígeno (del inglés, <i>Reactive Oxygen Species</i> )
<b>rpm</b>	Revoluciones por minuto
<b>SEOM</b>	Sociedad Española de Oncología Médica
<b>TEER</b>	Resistencia Eléctrica Transepitelial (del inglés, <i>Transepithelial Electrical Resistance</i> )
<b>TR</b>	Tiempo de retención
<b>u.a.</b>	Unidades arbitrarias
<b>UPLC</b>	Cromatografía Líquida de Ultra-Alta Resolución (del inglés, <i>Ultra Performance Liquid Cromatography</i> )
<b>UV-Vis</b>	Ultravioleta-Visible

## Índice de Figuras

<b>Figura 1.</b> Principales partes del intestino grueso (fuente: Asociación Española Contra el Cáncer, AECC).....	6
<b>Figura 2.</b> Capas de tejido en el colon (fuente: AECC).....	6
<b>Figura 3.</b> Diferentes estadios o fases del cáncer de colon (fuente: original de Terese Winslow, 2005). .....	9
<b>Figura 4.</b> Índices de incidencia del CCR (x 100.000) estandarizados por edad para 2012 (fuente: GLOBOCAN, 2012).....	10
<b>Figura 5.</b> Incidencia en porcentaje de tumores en España en el año 2012 (fuente: SEOM).....	11
<b>Figura 6.</b> Fases del ciclo celular.....	17
<b>Figura 7.</b> Distintas vías de muerte celular: apoptosis, necrosis/necroptosis y autofagia (extraída y adaptada de Long and Ryan, 2012).....	21
<b>Figura 8.</b> Elementos básicos del metabolismo primario y su relación con el metabolismo secundario del carbono (extraída y adaptada de Taiz, Lincoln y Zeiger, 2006).....	23
<b>Figura 9.</b> Principales grupos de polifenoles (extraída y adaptada de Câmara, Urrea y Schlege, 2013).....	24
<b>Figura 10.</b> Reducción univalente del oxígeno.....	27
<b>Figura 11.</b> Relación dosis-efecto dependiente entre el nivel de estrés oxidativo y la promoción del proceso de tumoración, mutagénesis y el proceso de apoptosis/necrosis (extraída y adaptada de Valko, 2006).....	28
<b>Figura 12.</b> La vía Nrf2-Keap1. El factor de transcripción Nrf2 juega un papel central en la expresión de genes citoprotectores en respuesta al estrés oxidativo presente en las células.....	31
<b>Figura 13.</b> Estructura y principales compartimentos de una mitocondria.....	32
<b>Figura 14.</b> Planta de romero en floración.....	35
<b>Figura 15.</b> Detalle del tallo, flor y hoja de <i>Rosmarinus officinalis</i> L.....	36
<b>Figura 16.</b> Principales familias de compuestos presentes en el extracto de romero.....	37
<b>Figura 17.</b> Diagrama de fases de una sustancia.....	39
<b>Figura 18.</b> Reducción del reactivo MTT mediante la enzima mitocondrial succinato deshidrogenasa a formazán.....	51
<b>Figura 19.</b> Perfil del ciclo celular obtenido mediante el marcaje de ADN con sondas fluorescentes.....	52
<b>Figura 20.</b> Equipo <i>Muse Cell Analyzer</i> .....	53
<b>Figura 21.</b> Distribución de la población celular según el ensayo Anexina V-7-AAD.....	54
<b>Figura 22.</b> Reducción de NAD <sup>+</sup> a NADH mediante la enzima LDH.....	55
<b>Figura 23.</b> Desesterificación de la sonda H <sub>2</sub> DCF-DA y posterior oxidación dando lugar al compuesto DCF (fluorescente).....	57
<b>Figura 24.</b> <i>Cytation 3 Cell Imaging Multi-mode</i> .....	59
<b>Figura 25.</b> Piezas principales del equipo <i>Dot-Blot</i> de BioRad.....	61
<b>Figura 26.</b> Equipo <i>xCELLigence RTCA DP</i> para determinar proliferación, migración e invasión celular.....	62
<b>Figura 27.</b> Inoculación subcutánea de las células HT-29 en ratones inmunodeprimidos.....	65
<b>Figura 28.</b> Esquema del pocillo formado por el inserto y la monocapa de células Caco-2.....	67
<b>Figura 29.</b> Representación de la medida de la resistencia eléctrica transepitelial (TEER).....	68

<b>Figura 30.</b> Cromatograma de pico base obtenido por HPLC-ESI-QTOF-MS del extracto de romero. Los números de los picos identificados corresponden con su orden de elución.....	76
<b>Figura 31.</b> Gráfico circular con los porcentajes (%) en peso de las familias de compuestos presentes en el extracto de romero.....	76
<b>Figura 32.</b> Curvas de inhibición de la proliferación celular del extracto de romero en las tres líneas celulares de colon, HGUE-C-1, HT-29 y SW480.....	80
<b>Figura 33.</b> Efecto del extracto de romero y sus fracciones en la viabilidad celular de las tres líneas celulares de cáncer de colon, HGUE-C-1, HT-29 y SW480.....	82
<b>Figura 34.</b> Efecto del extracto de romero en el ciclo celular en las tres líneas celulares de cáncer de colon, HGUE-C-1, HT-29 y SW480.....	86
<b>Figura 35.</b> Determinación de apoptosis mediante Anexina-V en las tres líneas celulares de cáncer de colon, HGUE-C-1, HT-29 y SW480.....	88
<b>Figura 36.</b> Efecto del extracto de romero en la liberación de la enzima intracelular LDH en las tres líneas celulares de cáncer de colon, HGUE-C-1, HT-29 y SW480.....	89
<b>Figura 37.</b> Efecto del extracto de romero en la viabilidad celular en las tres líneas celulares de cáncer de colon, HGUE-C-1, HT-29 y SW480.....	90
<b>Figura 38.</b> Efecto del extracto de romero en la generación de ROS en las tres líneas celulares de cáncer de colon, HGUE-C-1, HT-29 y SW480.....	92
<b>Figura 39.</b> Efecto del extracto de romero en el potencial de membrana mitocondrial en las tres líneas celulares de cáncer de colon, HGUE-C-1, HT-29 y SW480.....	93
<b>Figura 40.</b> Efecto del extracto de romero en el potencial de membrana mitocondrial en las tres líneas celulares de cáncer de colon, HGUE-C-1, HT-29 y SW480 mediante el uso de sondas fluorescentes.....	94
<b>Figura 41.</b> Efecto del extracto de romero en la viabilidad celular y la generación de ROS tras el silenciamiento de Nrf2 en las tres líneas celulares de cáncer de colon, HGUE-C-1, HT-29 y SW480.....	96
<b>Figura 42.</b> Nivel de expresión de Nrf2 tras su silenciamiento en las tres líneas celulares de cáncer de colon, HGUE-C-1, HT-29 y SW480 cuantificado por densitometría y normalizado con la proteína β-actina .....	97
<b>Figura 43.</b> Curso temporal de la proliferación celular en las tres líneas celulares de cáncer de colon, HGUE-C-1, HT-29 y SW480.....	98
<b>Figura 44.</b> Efecto del extracto de romero en la formación de colonias en las tres líneas celulares de cáncer de colon, HGUE-C-1, HT-29 y SW480.....	100
<b>Figura 45.</b> Estudio del efecto del extracto de romero en la migración celular mediante el ensayo de <i>wound healing</i> en las tres líneas celulares de cáncer de colon, HGUE-C-1, HT-29 y SW480.....	101
<b>Figura 46.</b> Evolución del peso corporal de los distintos grupos de animales no tratados (control) y tratados con el extracto de romero durante la realización del ensayo.....	103
<b>Figura 47.</b> Estudio de la toxicidad oral aguda del extracto de romero en un modelo <i>in vivo</i> .....	104
<b>Figura 48.</b> Evolución del peso corporal de los distintos grupos de animales no tratados (control) y tratados con el extracto de romero durante la realización del ensayo.....	105
<b>Figura 49.</b> Efecto del extracto de romero en el volumen de xenotransplantes en un modelo <i>in vivo</i> de cáncer de colon.....	106

## Índice de Tablas

<b>Tabla 1.</b> Índices de incidencia y mortalidad de todos los tipos de cáncer (x 100.000) estandarizados por edad para 2012 (fuente: GLOBOCAN, 2012).....	4
<b>Tabla 2.</b> Clasificación de terpenos según Wallach (1887).....	24
<b>Tabla 3.</b> Cuantificación de los compuestos identificados en el extracto de romero. ....	77
<b>Tabla 4.</b> Composición y pureza (%) de las fracciones seleccionadas para los ensayos posteriores de proliferación celular.....	78
<b>Tabla 5.</b> Valores de IC <sub>50</sub> del extracto de romero en las tres líneas celulares de cáncer de colon a las 24 y 48 horas de tratamiento.....	81
<b>Tabla 6.</b> Clasificación de sustancias, según la guía 420 de la Organización para la Cooperación y el Desarrollo Económicos (OCDE).....	102
<b>Tabla 7.</b> Valores de P <sub>app</sub> de los compuestos (cm/s) en el ER libre y ER liposomado y en ambas direcciones estudiadas.....	113





## **1. INTRODUCCIÓN**





## 1.1. Cáncer: clasificación e incidencia.

El cáncer es una enfermedad causada por el crecimiento descontrolado de las células, que modifican su forma, tamaño y otras características. El resultado final es un aumento del número total de células, las cuales se van extendiendo por el órgano y los tejidos adyacentes (**extensión local**), se introducen en los ganglios linfáticos (**infiltración linfática**) o en los vasos sanguíneos y finalmente colonizan otros órganos distantes (**metástasis**).

El cáncer es una de las principales causas de morbilidad y mortalidad a nivel mundial. En 2012 se registraron unos 14 millones de nuevos casos y 8,2 millones de muertes relacionadas con esta enfermedad. Los cánceres diagnosticados con más frecuencia en hombres fueron los de pulmón, próstata, colon y recto, estómago e hígado. En la mujer fueron los de mama, colon y recto, pulmón, cuello uterino y estómago [1]. Más del 60% de los nuevos casos anuales totales del mundo se producen en África, Asia, América Central y Sudamérica (**Tabla 1**). Estas regiones representan el 70% de las muertes por cáncer en el mundo. Se prevé que el número de nuevos casos aumente aproximadamente un 70% en las próximas dos décadas.

Como conclusión, el número de casos de cáncer continúa aumentando principalmente por el envejecimiento, crecimiento de la población mundial y un aumento en hábitos causantes de cáncer, en particular en países en desarrollo. Entre los factores de riesgo encontramos el consumo de alcohol y tabaco, una dieta inadecuada y el sedentarismo; también se incluyen tumores relacionados con infecciones como el virus de Hepatitis B (VHB) y C (VHC) y algunos tipos de Papilomavirus Humanos (PVH).

**Tabla 1.** Índices de incidencia y mortalidad de todos los tipos de cáncer (x 100.000) estandarizados por edad para 2012 (fuente: GLOBOCAN, 2012).

País/Zona		INCIDENCIA			MORTALIDAD		
		Hombres	Mujeres	Todo	Hombres	Mujeres	Todo
ÁFRICA	Este	120,7	154,7	137,8	103,8	110,5	106,5
	Centro	91,8	110,7	100,8	82,3	82,3	81,2
	Norte	133,5	127,7	129,7	99,9	75,7	86,8
	Sur	210,3	161,1	177,5	136,5	98,7	112,5
	Oeste	78,7	112,4	95,3	68,5	75,7	71,6
AMÉRICA	Caribe	207,7	168,0	185,4	119,8	87,7	102,0
	Central	125,8	141,9	133,6	76,6	72,1	73,7
	Norte	344,2	295,4	315,6	123,2	91,7	105,5
	Sur	206,7	180,6	190,6	118,0	88,4	101,2
ASIA	Este	225,4	151,9	186,0	159,3	80,2	117,7
	Sur-centro	98,4	103,3	100,1	74,8	64,7	69,3
	Sur-este	147,6	132,6	138,2	114,4	79,5	94,8
	Oeste	192,8	150,2	168,2	129,3	81,3	103,0
EUROPA	Centro-este	260,0	193,5	216,1	173,4	91,6	123,4
	Norte	298,4	263,9	277,4	126,2	94,4	108,2
	Sur	297,6	220,4	253,6	137,9	78,9	105,2
	Oeste	343,7	263,7	298,7	131,3	83,6	105,2
OCEANÍA	Australia/Nueva Zelanda	365,3	277,9	318,5	115,3	82,6	97,6
	Melanesia	152,1	182,1	164,7	117,9	118,5	116,4
	Micronesia	202,1	146,3	171,4	106,8	55,8	79,7
	Polinesia	226,4	181,6	200,7	125,7	93,3	108,1

Desde una perspectiva estricta pueden definirse tantos tipos de cánceres como enfermos, cada uno con sus alteraciones moleculares y celulares específicas, pero de forma sintética se agrupan por el tejido que les dio origen:

➤ **Carcinomas.** Se trata de cánceres que se originan a partir de células epiteliales, que son células que tapizan la superficie de órganos, glándulas o estructuras corporales. Representan más del 80% de la totalidad de los cánceres, incluyendo las variedades más comunes de cáncer de pulmón, mama, colon, próstata, páncreas y estómago, entre otros.

- **Sarcomas.** Son cánceres que se forman a partir del llamado tejido conectivo o conjuntivo, del que derivan los músculos, los huesos, los cartílagos o el tejido graso. Los más frecuentes son los sarcomas óseos.
- **Leucemias.** Son cánceres que se originan en la médula ósea, que es el tejido encargado de mantener la producción de glóbulos rojos, blancos y plaquetas. Las alteraciones en estas células pueden producir, respectivamente, anemia, infecciones y alteraciones de la coagulación (sangrados o trombosis).
- **Linfomas.** Se desarrollan a partir del tejido linfático, como el existente en ganglios y órganos linfáticos.

## 1.2. Cáncer colorrectal (CCR).

### Anatomía

El colon es la última porción del aparato digestivo. Tiene una longitud aproximada de 1,5 metros y se extiende desde el final del intestino delgado hasta el ano. La primera porción del intestino grueso está situada en la parte inferior derecha del abdomen, es donde desemboca el intestino delgado y se llama ciego. Desde aquí el colon asciende hasta llegar a la zona del hígado (**colon ascendente**) y atraviesa el abdomen (**colon transverso**).

El colon se dirige posteriormente hacia abajo, denominándose **colon descendente**, hasta llegar a una zona denominada sigma que desemboca en el recto y finalmente en el ano que se abre al exterior por el esfínter anal a través del cual se eliminan las heces (**Figura 1**).

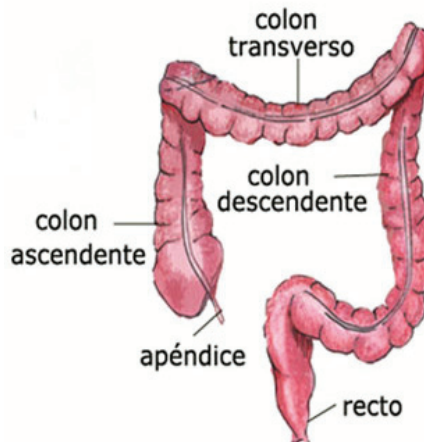


**Figura 1.** Principales partes del intestino grueso (fuente: Asociación Española Contra el Cáncer, AECC).

La función específica del colon ascendente y transverso consiste en absorber agua y electrolitos (sodio, potasio, etc.), mientras que la función del colon descendente y recto consiste en almacenar las materias fecales hasta su expulsión por el ano. Tanto el colon como el recto están constituidos por varias capas de tejido, la más interna es la **mucosa**, que se encuentra rodeada por la **submucosa**. Más externamente se sitúa la **capa muscular** cuya contracción logra el avance del contenido del tubo digestivo, que a su vez está recubierta por la **serosa** (capa más externa) (**Figura 2**). En la mucosa existen glándulas productoras de moco, en ellas es donde se producen con mayor frecuencia los tumores malignos.

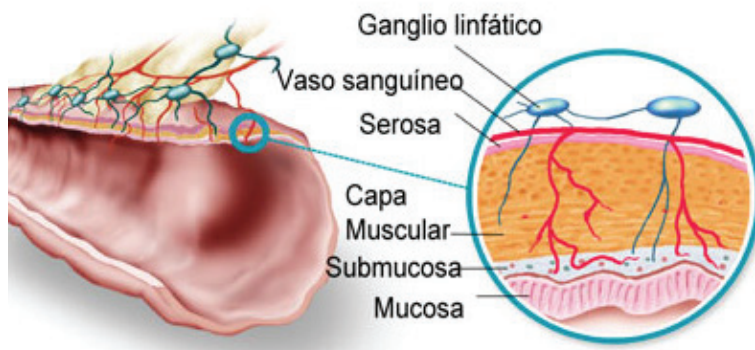


**Figura 2.** Capas de tejido en el colon (fuente: AECC).

La mayoría de los CCRs aparecen sobre un pólipos existente en la mucosa del colon. Dichos pólipos son crecimientos anormales de tejido que surgen de la capa interior o mucosa del intestino grueso y sobresalen a la luz intestinal y que por diversas circunstancias evolucionan a tumor maligno. Este tumor maligno, puede presentar cuatro etapas diferentes:

- **Crecimiento local.** Se produce principalmente al crecer en profundidad invadiendo todas las capas que forman la pared del tubo digestivo, es decir, creciendo desde la mucosa hasta la serosa, pasando por la capas submucosa y muscular. Una vez que el tumor traspasa toda la pared del intestino puede invadir cualquier órgano, bien abdominal o bien a distancia mediante:
  - **Diseminación linfática.** El colon posee una gran red de vasos linfáticos que permiten el drenaje de la linfa a múltiples regiones ganglionares. La diseminación por esta vía se realiza de forma ordenada, afectando primero a los ganglios más próximos y, posteriormente, a los más alejados.
  - **Diseminación hematógena.** Las células tumorales pasan al torrente circulatorio y a través de la sangre pueden dar origen a tumores secundarios en otros órganos y tejidos.
  - **Siembra peritoneal.** Las células cancerígenas pueden “descamarse” del tumor del colon y depositarse en la superficie de otros órganos o estructuras abdominales y pélvicas, como el intestino delgado o los ovarios, produciendo nuevos focos tumorales.

## Clasificación

Para planificar el tratamiento adecuado, el médico necesita saber en qué etapa de la enfermedad se encuentra el paciente. En la actualidad existen dos sistemas que se usan con la misma frecuencia.

## 1. Clasificación TNM

En esta clasificación se miden los tres aspectos que afectan al cáncer. En primer lugar, la **T** se refiere al tamaño del tumor primario en el intestino; la **N** se refiere a la presencia o no en los ganglios linfáticos, mientras que la **M** atañe a la presencia de metástasis a distancia. Como muestra la **Figura 3**, se distinguen los siguientes estadios:

- **Estadio 0 o carcinoma *in situ*.** En esta etapa temprana el cáncer se encuentra en la capa más superficial de la mucosa, no la traspasa y no afecta a los ganglios linfáticos.
- **Estadio I.** El cáncer se ha diseminado a la pared del recto o del colon sin traspasar la capa muscular. En este estadio los ganglios linfáticos tampoco se ven afectados.
- **Estadio II.** El cáncer se ha extendido a la capa más profunda del colon, pero no a los ganglios linfáticos, que, repartidos por todo el cuerpo, producen y almacenan células capaces de combatir las infecciones. En este estadio el tumor puede invadir los órganos de alrededor.
- **Estadio III.** El cáncer se ha extendido ya a los ganglios linfáticos y a los órganos más cercanos.
- **Estadio IV.** El cáncer ha llegado a otros órganos del cuerpo (principalmente tiende a invadir el hígado, los huesos y los pulmones).

## 2. Clasificación de Dukes o Astler y Coller

Esta escala utiliza las letras de la A a la D valorando cuanto profundiza en la pared del colon:

- **Estadio I o A.** En esta etapa se encuentran los pacientes que tienen una lesión sólo en la mucosa y no afecta a los ganglios linfáticos.
- **Estadio II o B.** El cáncer se encuentra en parte de la pared del recto y del colon, pero no lo traspasa, ni afecta a los ganglios.

- **Estadio III o C.** En este nivel el cáncer puede afectar de forma parcial o total a la pared y también a los ganglios linfáticos.
- **Estadio IV o D.** El cáncer afecta a toda la pared y se extiende a órganos más alejados.

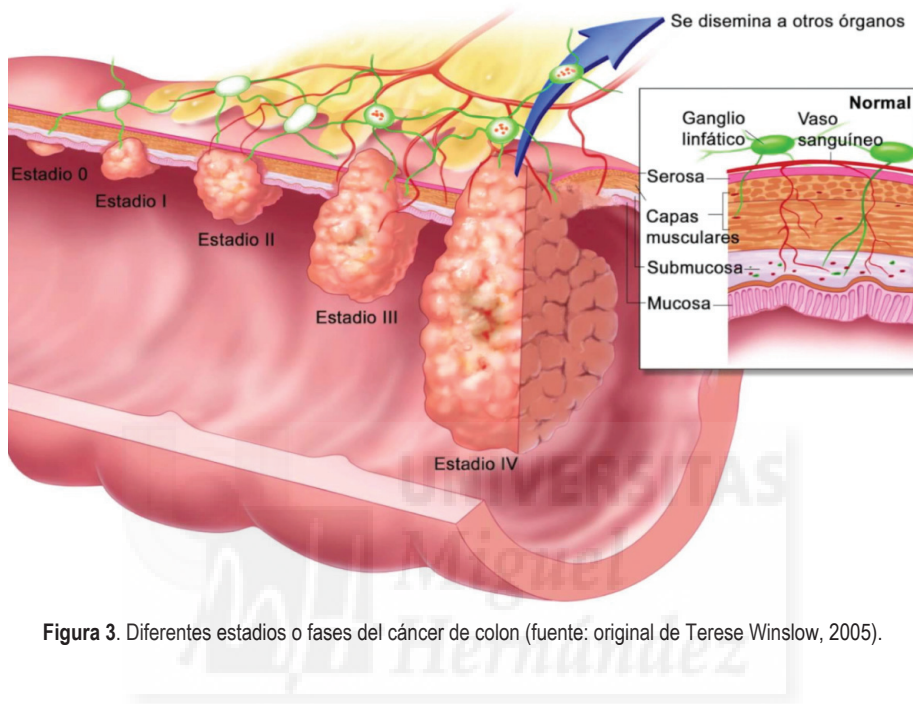


Figura 3. Diferentes estadios o fases del cáncer de colon (fuente: original de Terese Winslow, 2005).

## Incidencia

El CCR representa el tercer tipo de cáncer más común diagnosticado en los hombres y el segundo en mujeres a nivel mundial. Además cabe destacar que la incidencia en hombres es mayor que en mujeres. La mayor incidencia se encuentra en países desarrollados como Australia/Nueva Zelanda y, países pertenecientes a Europa y América del Norte (**Figura 4**).

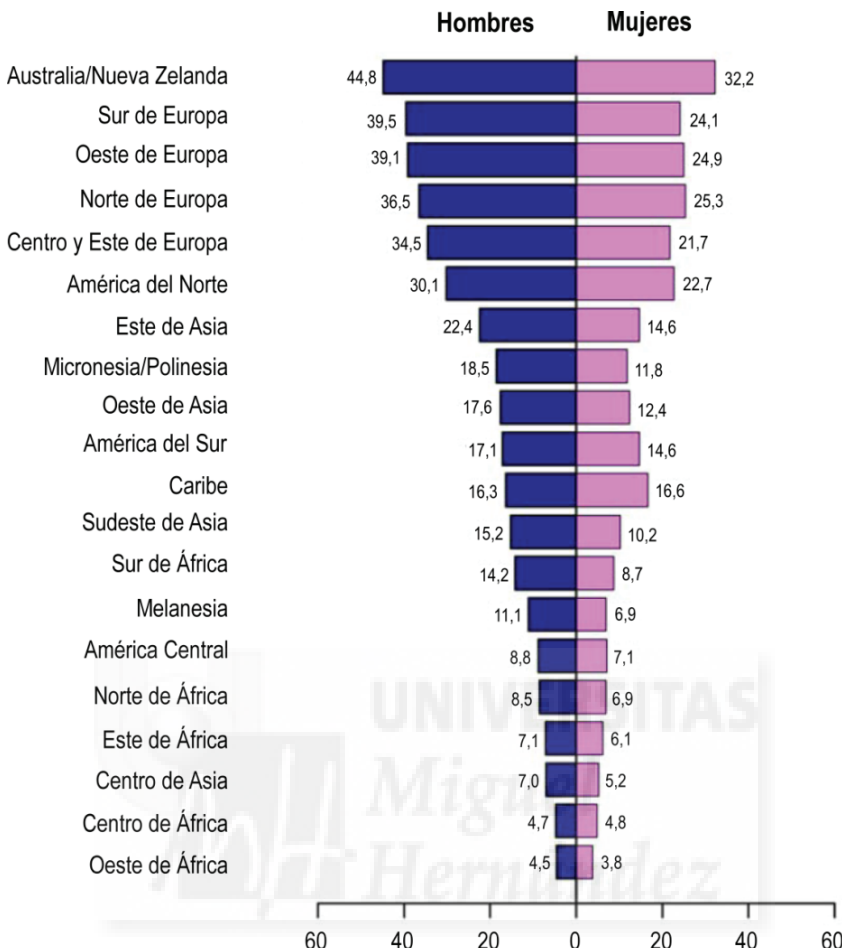


Figura 4. Índices de incidencia del CCR ( $\times 100.000$ ) estandarizados por edad para 2012 (fuente: GLOBOCAN, 2012).

A pesar de la incidencia, las tasas de mortalidad del CCR han disminuido en gran número de países. Este hecho se atribuye a medidas de prevención precoz, la reducción de factores de riesgo y a la mejora de los tratamientos. Sin embargo, su incidencia está aumentando incluso en áreas consideradas históricamente de bajo riesgo de padecer dicha enfermedad, incluyendo España y Este Asiático y Europeo [1].

Tanto la incidencia como la mortalidad del CCR varían considerablemente en todo el mundo e incluso a escala regional, como por ejemplo dentro de los Estados Unidos. Esta

variación geográfica en la incidencia demuestra en gran medida la importancia de los factores ambientales en dicha enfermedad. Se postula que el estilo de vida occidental unido a factores genéticos, así como el aumento de la longevidad en determinados grupos de población, podrían ser variables importantes a la hora de explicar la disparidad en la incidencia entre regiones geográficas.

En España, en los hombres es el tercero en frecuencia, detrás del cáncer de pulmón y próstata. En las mujeres es el segundo en frecuencia, detrás del de mama. Sin embargo, si se tienen en cuenta ambos sexos, el cáncer con mayor incidencia es el colorrectal (15%) (**Figura 5**), el que produce la mortalidad más alta es el cáncer de pulmón (20%) y el que tiene una prevalencia a cinco años más alta es el cáncer de mama (18%). Según datos de la Sociedad Española de Oncología Médica (SEOM) en el año 2012, se calcula una incidencia de 32.240 pacientes al año en España, siendo responsable de 14.700 fallecimientos y una prevalencia a cinco años de 89.705 casos. La mayoría de los casos se diagnostican entre los 65 y los 75 años, con un máximo a los 70, aunque se registran casos desde los 35-40 años. Los casos que aparecen a edades tempranas suelen tener una predisposición genética.

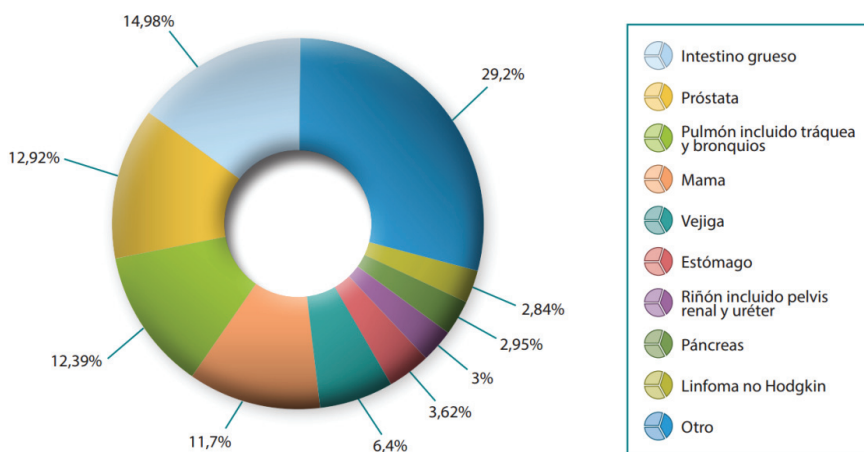


**Figura 5.** Incidencia en porcentaje de tumores en España en el año 2012 (fuente: SEOM).

## Factores de riesgo

En el cáncer de colon y recto los factores que incrementan el riesgo de padecer este tumor son:

- **Alimentación.** Las dietas ricas en grasas animales (carnes rojas) y pobres en fibra, pueden aumentar el riesgo de CCR.
- **Actividad física.** Una vida sedentaria favorece el riesgo de aparición de esta enfermedad.
- **Consumo de tabaco y alcohol.** El tabaco aumenta el riesgo de padecer pólipos, que suelen ser los precursores del CCR. Parece que el alcohol actúa favoreciendo el crecimiento de las células de la mucosa del colon, dando lugar a la aparición de pólipos.
- **Edad.** El riesgo de padecer la enfermedad aumenta con la edad, ya que aumenta la aparición de pólipos en el colon y recto. Es raro que el CCR aparezca en personas de menos de 40 años.
- **Historia personal de pólipos.** La aparición de pólipos adenomatosos aumenta el riesgo de padecer la enfermedad.
- **Historia personal de CCR.** Las personas diagnosticadas de un cáncer a este nivel poseen un riesgo incrementado para padecer un segundo tumor en el colon o recto.
- **Enfermedades inflamatorias intestinales.** Suponen menos del 1% de todos los CCRs. Los dos tipos principales de enfermedades inflamatorias a este nivel son la colitis ulcerosa y la enfermedad de Crohn. La colitis ulcerosa es una enfermedad que se caracteriza por la inflamación prolongada de las paredes del colon, mientras que la enfermedad de Crohn afecta, típicamente, al intestino delgado, aunque en ocasiones el colon también se encuentra inflamado.

➤ **Antecedentes familiares.** En un 5% de los cánceres de colon se han identificado una serie de genes, cuya alteración da lugar a síndromes que predisponen, en mayor o menor grado, a la aparición de CCR. Los dos más importantes son:

1. **Poliposis colónica familiar.** Supone tan solo un 1% de todos los cánceres colorrectales y se caracteriza por la aparición, en la adolescencia, de múltiples pólipos adenomatosos en el colon y recto. Se produce por la alteración de un gen denominado APC (del inglés, *Adenomatous Polyposis Coli*), que se transmite de padres a hijos por una herencia autosómica dominante, es decir, lo pueden heredar tanto varones como mujeres y se padece la enfermedad si uno de los dos genes está alterado.
2. **Cáncer colorrectal hereditario no polipósico.** Supone, aproximadamente, entre un 3% y un 5% de todos los tumores de colon y recto. A diferencia de la poliposis crónica familiar, en la mayoría de los pacientes no se observan pólipos. Es una enfermedad que se transmite de forma autosómica dominante y está causada por la mutación o alteración de uno de los múltiples genes encargados de la reparación de los errores en los mismos.

## Sintomatología

El cáncer de colon produce una serie de síntomas que pueden variar en función de su localización dentro del intestino grueso. Entre los síntomas más relevantes del CCR destacan:

➤ **Sangre en las heces.** Es uno de los síntomas más frecuentes del cáncer de colon. Puede tratarse de sangre roja, más frecuente en tumores de sigma y colon descendente, o de sangre negra, que se mezcla con las heces dando lugar a deposiciones de color negro llamadas melenas. Las melenas aparecen con más frecuencia cuando el tumor está situado en el colon ascendente. Si este síntoma no se diagnostica pronto y el paciente no

recibe el tratamiento adecuado puede agravarse y dar lugar a la aparición de una anemia.

En estos casos el paciente puede sufrir mareos, cansancio o tener la sensación de que le falta el aire, entre otros síntomas. Por otro lado, el enfermo puede detectar que sus deposiciones cambian de tamaño y son más estrechas. Esto se produce porque el intestino se está estrechando.

- **Cambios en el ritmo intestinal.** Los pacientes que tienen cáncer de colon pueden, en algunos casos, tener diarrea y, en otros, estreñimiento. La segunda opción es común en aquellas personas que previamente a la enfermedad tenían un ritmo intestinal normal. Sin embargo, la opción más frecuente es que el paciente sufra períodos de estreñimiento combinados con períodos en los que padece diarrea. Si los tumores están situados en la parte distal del colon, el paciente también puede tener la sensación de que no se completa la deposición y que la evacuación es incompleta.
- **Dolor o molestia abdominal.** Las molestias y los dolores abdominales suelen ser muy comunes. Esto se debe a que el tumor obstruye en parte el tubo intestinal y se produce un dolor y una situación parecida a la de los cólicos. En algunos casos el cierre del tubo puede llegar a completarse y se produce una obstrucción intestinal, en estas situaciones es necesario que el paciente reciba atención médica quirúrgica urgente.
- **Pérdida de peso sin causa aparente, pérdida de apetito y cansancio constante.** Al igual que otras enfermedades relacionadas con el estómago, el cáncer de colon, especialmente cuando se encuentra en un estado avanzado presenta estos síntomas.

## Tratamiento

En el tratamiento del cáncer de colon se sigue un protocolo, es decir, un conjunto de normas y pautas que se establecen, basándose en la experiencia científica, para el tratamiento de dicho tumor. Estos protocolos, que se emplean de forma generalizada en todos los hospitales, recogen las indicaciones o limitaciones de tratamiento en función de una serie de factores:

- Estado general del paciente.
- Localización del tumor.
- Fase en la que se encuentra la enfermedad: infiltración en la pared del colon o recto, afectación ganglionar, afectación de órganos próximos y diseminación de la enfermedad.

Los tratamientos más frecuentemente empleados en el cáncer de colon son la cirugía y la quimioterapia.

- **Estadio 0 o carcinoma *in situ*.** El tumor no ha crecido más allá del revestimiento interno del colon por lo tanto el tratamiento es solamente quirúrgico.
- **Estadio I.** El tumor ha crecido a través de la pared del colon y se puede extender hacia el tejido cercano. El tratamiento es quirúrgico y además podría aplicarse una quimioterapia adyuvante o complementaria a la cirugía.
- **Estadio II.** El tumor ha crecido a través de la pared del colon y posiblemente a los tejidos circundantes, pero aún no se ha extendido a los ganglios linfáticos. El tratamiento es la cirugía para extirpar la sección del colon que presenta el tumor junto con los ganglios linfáticos cercanos (colectomía parcial). Según la valoración médica se podría recomendar quimioterapia adyuvante.
- **Estadio III.** El tumor se ha propagado a los ganglios linfáticos cercanos pero no se ha extendido a otras partes del organismo. El tratamiento es el mismo que se utiliza en el estadio II.

- **Estadio IV.** Si el cáncer se ha propagado ampliamente como para tratar de curarlo con cirugía, la quimioterapia es el tratamiento principal. Luego, si el tamaño de los tumores se reduce, el tratamiento consistiría en extirpar la sección del colon que contiene el tumor junto con los ganglios linfáticos cercanos.

### 1.3. Ciclo celular y cáncer.

#### Fases del ciclo celular

Las células se reproducen mediante un ciclo de división en el que primero se duplica su contenido, y luego se dividen en dos células hijas genéticamente idénticas. Por lo tanto, el tiempo que transcurre desde que una célula se forma por división de una preexistente, hasta que se divide y da lugar a dos células hijas se conoce como ciclo celular. Básicamente el ciclo celular se divide en dos etapas: fase M o mitosis e interfase, que es el periodo que transcurre entre dos mitosis.

En la **interfase** se pueden distinguir diversas etapas:

- **Fase G<sub>1</sub>.** Esta etapa comprende desde el final de la división anterior (fase M) hasta el comienzo de la siguiente etapa. Durante esta fase la célula aumenta de tamaño, expresa su ADN sintetizando proteínas y lleva a cabo el resto de funciones celulares.
- **Fase S.** Es la segunda fase del ciclo, en la que se produce la replicación o síntesis de ADN, como resultado cada cromosoma se duplica y queda formado por dos cromátidas idénticas.
- **Fase G<sub>2</sub>.** Es la tercera fase de crecimiento del ciclo celular en la que continua la síntesis de proteínas y ARN. La célula aumenta de tamaño preparándose para su inminente división en la Fase M.

➤ **Fase G<sub>0</sub>**. Es la fase adicional del ciclo celular en la que la célula se encuentra en un estado de reposo. Si no ha iniciado la replicación del ADN, la célula puede detenerse en G<sub>1</sub> y permanecer en estado de reposo durante días, semanas o incluso años si no recibe estímulos mitogénicos.

La **fase M** (mitosis y citocinesis) es el proceso por el cual una célula progenitora lleva a cabo su división dando como resultado dos células hijas con idéntico material genético. Esta fase incluye la **mitosis**, a su vez dividida en: *profase*, *metafase*, *anafase*, *telofase* y la **citocinesis**, que se inicia ya en la telofase mitótica (**Figura 6**).

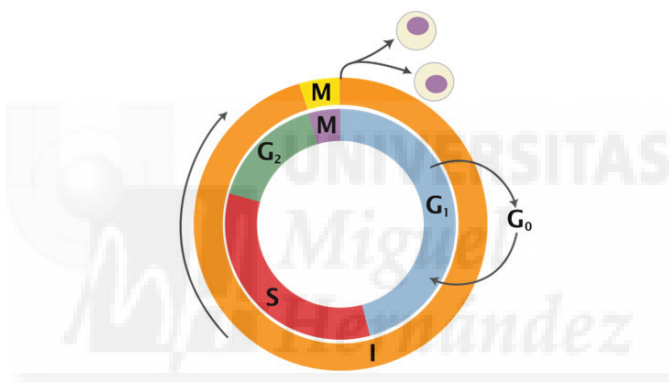


**Figura 6.** Fases del ciclo celular.

La duración de las distintas fases del ciclo varía considerablemente de unos tipos celulares a otros. Una célula que presenta una tasa alta de proliferación en el ser humano completa su ciclo celular en 24 horas; de ellas, 11 corresponderían a la fase G<sub>1</sub>, 8 a S, 4 a G<sub>2</sub> y aproximadamente 1 a la fase M.

En contraste, algunas células del organismo no sufren divisiones a lo largo de su vida, salen de la fase G<sub>1</sub> para entrar en otra etapa del ciclo llamada G<sub>0</sub> en la que se mantienen metabólicamente activas pero no se dividirán a menos que sean apropiadamente estimuladas por señales extracelulares [2].

## Control del ciclo celular

El ciclo de división de una célula consiste en una secuencia de acontecimientos que se repite de forma ordenada y constante. Nunca debe comenzar un proceso sin que el anterior se complete, para ello existe todo un sistema de control que por diversos mecanismos asegura el correcto paso de la célula de una fase a la siguiente.

Uno de estos mecanismos de control consiste en una serie de “frenos moleculares” que detienen el ciclo en determinados puntos con el fin de explorar las condiciones celulares externas e internas. Cuando dichas condiciones son favorables, la célula continúa su avance a través del ciclo, en caso contrario, la progresión se detiene para dar tiempo a que cambie el entorno celular o para que se produzca la reparación de los defectos internos detectados. Estos puntos son los “puntos de control”, también conocidos como *checkpoints*. Actualmente se conocen tres:

- 1) Al final de la fase G<sub>1</sub> se encuentra el llamado punto de control de G<sub>1</sub>. En él se verifica que la célula reciba el estímulo de factores de crecimiento necesarios para la activación del ciclo, que no haya defectos en el ADN que podrían transmitirse a las células hijas y que su tamaño es el adecuado antes de que comience la fase S.
- 2) Otro punto de chequeo ocurre en la fase G<sub>2</sub>. Aquí se comprueba si la replicación del ADN se ha completado y si el tamaño celular es el adecuado para que comience la mitosis.
- 3) En la fase M existe un tercer punto de chequeo capaz de detener el ciclo en caso de que los cromosomas no se encuentren adecuadamente alineados en el huso mitótico.

La habilidad de las células normales para detener el ciclo celular después de sufrir un daño en el ADN, es crucial para el mantenimiento de la integridad genómica. Un fallo en los mecanismos de control del ciclo celular puede llevar a una proliferación celular excesiva y como

consecuencia a la aparición de un tumor. El cáncer resulta de múltiples alteraciones en los genes que controlan la proliferación celular, la diferenciación o la apoptosis. Existen dos grupos de genes relacionados con el desarrollo del cáncer: (a) los oncogenes, que son genes mutados y cuya función normal es estimular la proliferación celular y (b) los genes supresores de tumores, como p53, que restringen el crecimiento celular [3].

#### 1.4. Muerte celular: apoptosis, necrosis/necroptosis y autofagia.

Existen diversos tipos de muerte celular dependiendo del mecanismo. A continuación se exponen los tipos de muerte celular más comunes:

##### **Apoptosis**

La muerte celular programada o **apoptosis**, es el principal mecanismo de supresión tumoral y en células no-malignas se desencadena como un mecanismo protector que elimina células dañadas, ya que de no ser así resultarían perjudiciales para el organismo. Defectos en vías de señalización que median dicho mecanismo de muerte celular pueden resultar en enfermedades hiperproliferativas tales como el cáncer [4, 5]. La apoptosis se caracteriza por la contracción celular, condensación y fragmentación nuclear, formación de vesículas citoplasmáticas y finalmente, la separación de los componentes celulares en cuerpos apoptóticos (**Figura 7**) [6]. Este mecanismo de muerte celular ocurre principalmente por dos vías: la **intrínseca**, en la que las señales de muerte surgen desde el interior de la célula y la **extrínseca**, la cual involucra la activación de receptores de superficie por señales de muerte extracelulares. Ambas vías convergen en la activación de unas proteínas efectoras denominadas caspasas, las cuales conducen finalmente a la célula hasta su muerte [7].

## Necrosis/Necroptosis

La **necrosis** está morfológicamente caracterizada por la permeabilización de la membrana plasmática, que provoca la ruptura y la dilatación de los orgánulos citoplasmáticos, en particular la mitocondria, y por la rápida perdida de los potenciales de membrana [8, 9].

La **necroptosis** es una forma particular de muerte celular programada, ya que está regulada genéticamente y sus principales características son similares a la necrosis (**Figura 7**). Esta forma de muerte celular también se asocia con especies reactivas de oxígeno (ROS) y a diferencia de la apoptosis no implica la fragmentación del ADN [10]. Esta vía se caracteriza por estar estimulada por el factor de necrosis tumoral, TNF- $\alpha$ , por la activación de RIPK1 o RIPK3 (del inglés, *Receptor-Interacting Protein Kinase*) y la inhibición previa de caspasas [11]. La necroptosis puede ser inhibida por medio de la sustancia necrostatina-1.

La característica fundamental que distingue la mayoría de las formas de necrosis de la apoptosis es la rápida pérdida de los potenciales de membrana. Esto puede ser consecuencia de depleción de la energía celular, daño en los lípidos de membrana y/o perdida de la función de bombas iónicas o canales homeostáticos.

## Autofagia

La **autofagia** es un proceso celular que se encarga de la degradación y reciclaje de los componentes celulares. Durante la autofagia, porciones del citosol incluyendo orgánulos completos, son englobados en una doble membrana que se cierra para formar un autofagosoma o vacuola autofágica, que se fusionará con los lisosomas, permitiendo la digestión de los componentes englobados (**Figura 7**). La autofagia tiene un papel fundamental en la obtención de nutrientes, y en la degradación de orgánulos dañados, por lo que supone un mecanismo que permite a las células sobrevivir en condiciones de estrés. La implicación de la autofagia en

cáncer es un tema muy controvertido ya que existen estudios científicos que la señalan como un fenómeno que promueve la muerte celular, mientras que otros defienden que ayuda a la supervivencia de las células tumorales [9].

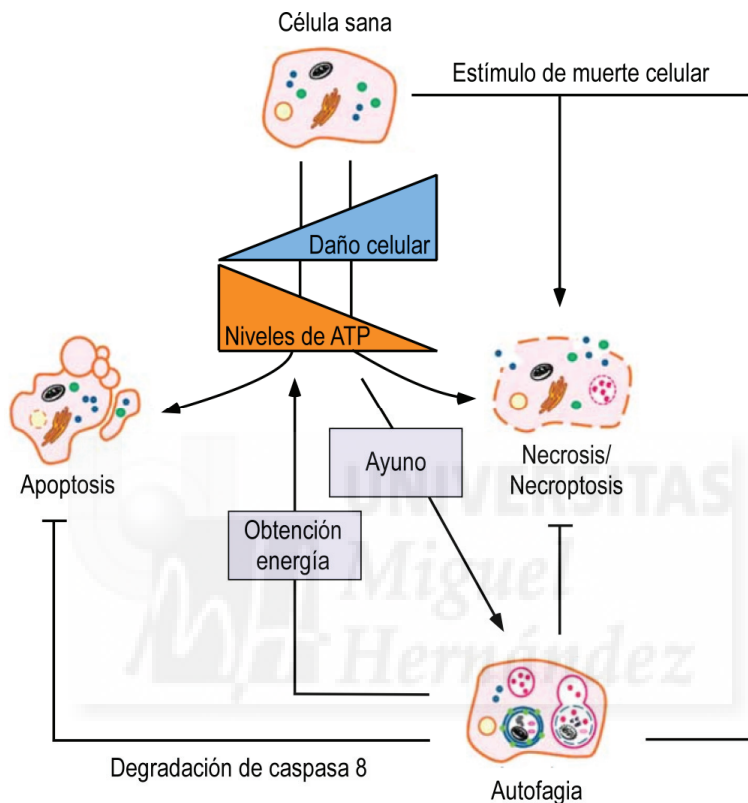


**Figura 7.** Distintas vías de muerte celular: apoptosis, necrosis/necroptosis y autofagia (extraída y adaptada de Long and Ryan, 2012).

### 1.5. Compuestos bioactivos naturales.

Los compuestos bioactivos son sustancias de origen animal o vegetal que influyen en la actividad celular y en los mecanismos fisiológicos, ejerciendo un efecto positivo en la salud de un organismo.

En las últimas décadas, los compuestos bioactivos han suscitado un gran interés desde el punto de vista científico por sus potenciales beneficios sobre la salud, particularmente en la prevención del cáncer [12, 13] y enfermedades cardiovasculares [14, 15]. Muchos estudios han demostrado una actividad antitumoral [16, 17], antiaterogénica [18, 19], antiinflamatoria [20, 21], antimicrobiana [22], antioxidante [23] y analgésica [24] para este tipo de compuestos. Los compuestos bioactivos de plantas se clasifican, según su estructura química en dos grupos [25]:

- **Compuestos resultantes del metabolismo primario.** Procesos químicos que intervienen de forma directa en la supervivencia, crecimiento y reproducción: glúcidos, lípidos y derivados de aminoácidos.
- **Compuestos derivados del metabolismo secundario.** No son esenciales, pero son sintetizados como defensa o adaptación al medio. Los grupos más importantes son los siguientes:
  - Polifenoles
  - Terpenoides
  - Sustancias azufradas
  - Sustancias nitrogenadas (alcaloides)

De estos cuatro grupos, los tres primeros son los que tienen mayor importancia como constituyentes de las plantas, frutas y hortalizas con relevancia en la alimentación humana.

### Polifenoles: estructura y clasificación

Los polifenoles son compuestos ampliamente distribuidos que presentan una estructura molecular caracterizada por la presencia de uno o varios anillos fenólicos. Son productos derivados del metabolismo secundario de las plantas y su biosíntesis tiene lugar a través de dos importantes rutas primarias: la ruta del ácido síquímico y la ruta del ácido malónico [26] (**Figura 8**). Se caracterizan por presentar uno o más núcleos aromáticos sustituidos, como mínimo, con

un grupo hidroxilo que les confiere la propiedad de donar átomos de hidrógeno. Esta cualidad les permite actuar como antioxidantes y desempeñar funciones fisiológicas en los vegetales [27]. Otros participan en funciones de defensa ante situaciones de estrés y estímulos diversos (hídrico, luminoso, etc.).

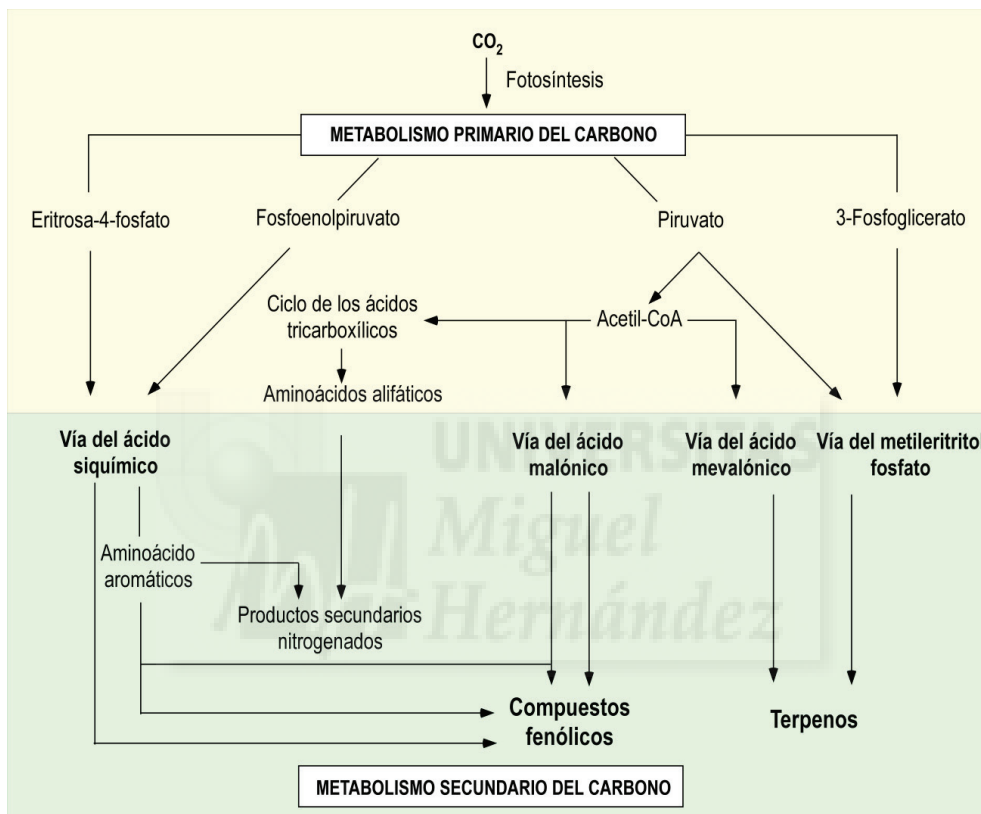


**Figura 8.** Elementos básicos del metabolismo primario y su relación con el metabolismo secundario del carbono (extraída y adaptada de Taiz, Lincoln y Zeiger, 2006).

Existen varias clases y subclases de polifenoles que se definen en función del número de anillos fenólicos que poseen y de los elementos estructurales que presentan estos anillos. Como muestra la **Figura 9**, los principales grupos de polifenoles son: **ácidos fenólicos** (derivados del ácido hidroxibenzoico o del ácido hidroxicinámico), **flavonoides**, **estilbenos**, y **lignanos** [28].

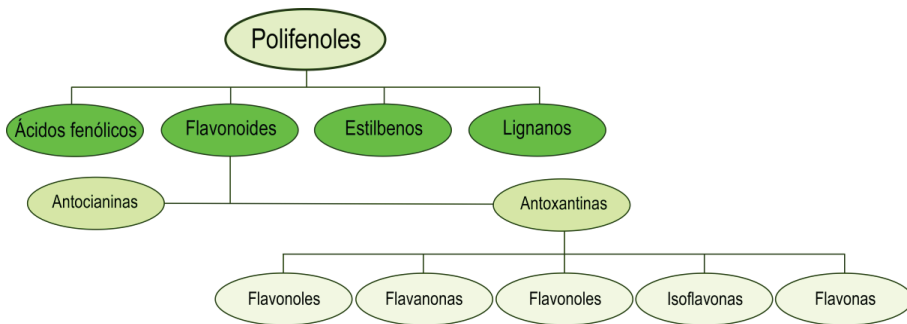


Figura 9. Principales grupos de polifenoles (extraída y adaptada de Câmara, Urrea y Schlege, 2013).

### Terpenoides: estructura y clasificación

Los isoprenoides, más conocidos como terpenoides o terpenos, son un grupo de productos naturales que incluyen todas aquellas sustancias químicas que se sintetizan a partir de dos rutas metabólicas: la ruta del ácido mevalónico y la ruta del metileritritol fosfato (**Figura 8**) [29]. Otto Wallach en 1887 propuso la clasificación de este grupo de compuestos atendiendo al número de átomos de carbono de los mismos (**Tabla 2**). Actualmente esa clasificación es reconocida a nivel mundial y seguida por cuantos trabajan con terpenoides.

Tabla 2. Clasificación de terpenos según Wallach (1887).

Grupo	Nº de átomos de carbono	Nº de unidades de isopreno
Hemiterpenos	5	1
Monterpenos	10	2
Sesquiterpenos	15	3
Diterpenos	20	4
Sesterterpenos	25	5
Triterpenos	30	6
Tetraterpenos	40	8
Politerpenos	5n	n

Los terpenos son los metabolitos secundarios que dan las características organolépticas (aroma y sabor) de las plantas y que constituyen la mayor parte del aceite esencial producido por las plantas aromáticas. En dichos organismos los terpenos ejercen distintas funciones, las dos principales son la protección frente a los insectos y animales herbívoros y la protección contra las temperaturas elevadas. Las plantas reaccionan produciendo terpenos en las zonas depredadas por los insectos y los animales herbívoros y éstos actúan como compuestos amargos inhibiendo la depredación e incluso pueden actuar en algunos casos como insecticida.

### Diterpenos

Los diterpenos son una gran familia de terpenoides que, según las circunstancias, pueden aparecer en los aceites esenciales junto con los monoterpenos y sesquiterpenos. Se trata de compuestos con 20 átomos de carbono (4 unidades de isopreno), por lo que su peso molecular es superior al de monoterpenos y sesquiterpenos, y su volatilidad menor. Pueden actuar, en algunos casos, como sustancias repelentes y también como feromonas atrayentes de insectos [30].

### Triterpenos

Los triterpenos son compuestos con 30 átomos de carbono (6 unidades de isopreno), presentan sólo un tipo de unión y se unen de forma regular “cola-cola” para formar una estructura simétrica, como el escualeno, precursor acíclico de este tipo de compuestos.

### 1.6. Estrés oxidativo y defensa antioxidante.

Los seres vivos se encuentran expuestos a un gran número de agresiones originadas por toda clase de estímulos, como las infecciones microbianas y virales, los agentes xenobióticos, las toxinas provenientes de la dieta y la hipoxia, la mayoría de las cuales inducen la formación de moléculas oxidantes, conocidas como especies reactivas. Dentro de dichas moléculas cabe

destacar las especies reactivas que derivan del oxígeno, **ROS** (del inglés, *Reactive Oxygen Species*), del nitrógeno, **RNS** (del inglés, *Reactive Nitrogen Species*) y del cloro, **RCS** (del inglés, *Reactive Chlorine Species*).

Cuando el aumento del contenido intracelular de ROS sobrepasa las defensas antioxidantes de la célula, se produce el estrés oxidativo, a través del cual se induce daño a moléculas biológicas como lípidos, proteínas y ácidos nucleicos. Por tanto, la capacidad de adaptación al estrés generado por el medio ambiente es un requisito indispensable para la viabilidad celular y la supervivencia de los organismos.

### Especies Reactivas de Oxígeno

El oxígeno, aunque es indispensable para la vida de los organismos aerobios, a altas concentraciones o bajo ciertas condiciones llega a ser tóxico. La toxicidad del oxígeno se puede explicar por la aparición de las ROS, que se forman de manera natural como subproducto del metabolismo normal del oxígeno. Son generalmente moléculas muy pequeñas altamente reactivas debido a la presencia de una capa de electrones desapareados. Las principales ROS son:

- a) Las que se producen por la ruptura o excitación del oxígeno molecular: oxígeno atómico ( $O$ ), ozono ( $O_3$ ) y oxígeno singlete ( $^1O_2$ ).
- b) Las parcialmente reducidas: anión superóxido ( $O_2^{--}$ ), peróxido de hidrógeno ( $H_2O_2$ ) y radical hidroxilo ( $^{\cdot}OH$ ).

Las especies parcialmente reducidas de oxígeno se producen por la adición sucesiva de electrones a la molécula de oxígeno en un proceso que se conoce como reducción univalente (**Figura 10**). Para su total reducción a agua, el oxígeno es capaz de aceptar uno a uno, hasta cuatro electrones.

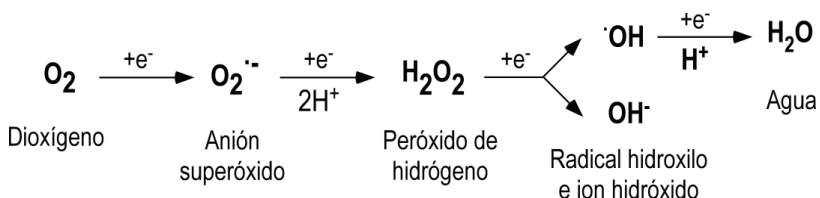
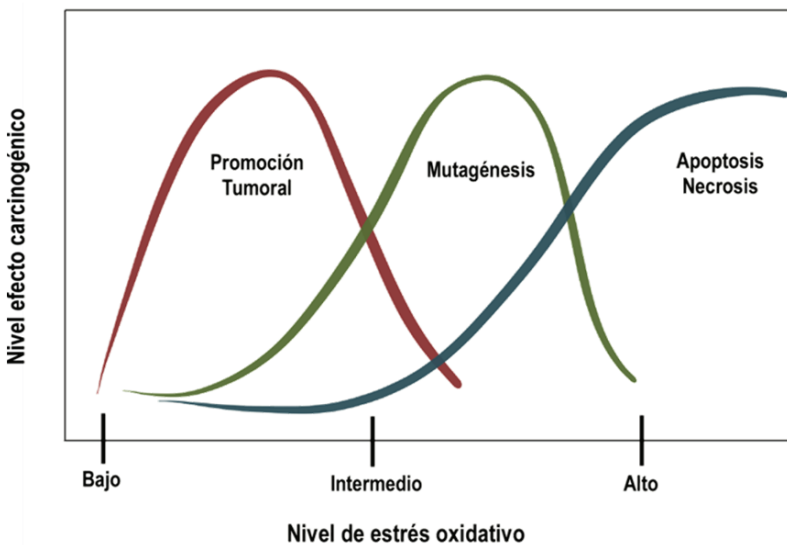


Figura 10. Reducción univalente del oxígeno.

A pesar de la capacidad de los compuestos bioactivos de proteger a las células del estrés oxidativo, existe una evidencia cada vez mayor de su poder prooxidante y por tanto de su posible citotoxicidad [31]. El mismo compuesto podría comportarse como antioxidante o prooxidante, dependiendo de la concentración y la fuente de ROS [31-33].

El tratamiento de células con dichos compuestos puede venir acompañado de un aumento de niveles de ROS intracelular, por la apertura de los poros de la transición de la permeabilidad mitocondrial (mPTP), la liberación de citocromo C, la activación de caspasas, el aumento de p21 y de muerte por apoptosis [31, 34-40], aumento de la peroxidación lipídica y muerte por necrosis [41, 42]. Por lo tanto, mientras que niveles bajos de ROS pueden provocar la aparición de mutaciones y neoplasias, niveles altos de ROS pueden provocar el efecto inverso, provocando una inhibición del crecimiento, senescencia, apoptosis o necrosis (**Figura 11**) [43-45].



**Figura 11.** Relación dosis-efecto dependiente entre el nivel de estrés oxidativo y la promoción del proceso de tumoración, mutagénesis y el proceso de apoptosis/necrosis (extraída y adaptada de Valko, 2006).

### Mecanismos de defensa antioxidante

Las células han desarrollado programas dinámicos para luchar contra el estrés oxidativo causado por las moléculas oxidantes y electrófilas. Los mecanismos de defensa se pueden clasificar principalmente en dos grupos: **endógenos** y **exógenos**. En el grupo de los mecanismos endógenos cabe destacar los sistemas antioxidantes enzimáticos, la superóxido dismutasa (SOD), la glutatión peroxidasa (GPx) y la catalasa (CAT) y como no enzimático destaca el glutatión (GSH). Respecto a los antioxidantes exógenos, que ingresan al organismo solo a través de la dieta, destacarían compuestos como la vitamina C, vitamina E, carotenoides y polifenoles [46].

Recientemente se ha observado que algunas enzimas antioxidantes forman parte de las reacciones de fase II utilizadas en biotransformación de agentes xenobióticos para su excreción:

- En la **fase I**, en la cual participan enzimas que metabolizan carcinógenos y xenobióticos (principalmente enzimas de la familia de los citocromos P450) se llevan a cabo reacciones de

óxido-reducción que introducen o exponen grupos funcionales en dichas moléculas, para hacerlas un poco más polares [47].

- Por otro lado, las reacciones de **fase II** son las que continúan con las acciones que ocurrieron durante la fase I, reducen la electrofilicidad de los metabolitos carcinógenos y xenobióticos modificados mediante su conjugación enzimática con ligandos endógenos, como pueden ser el glutatión (GSH) y el ácido glucurónico [48] y convierten estas moléculas en polares para que puedan ser excretadas. El glutatión (GSH) es un tripeptido de ácido glutámico, cisteína y glicina, y sirve como antioxidante al ser susceptible de reaccionar con radicales libres o ROS debido a su grupo sulfhidrilo.

### El elemento de respuesta antioxidante ARE

La inducción coordinada de los genes que codifican las enzimas de fase II protege a las células contra el daño generado por el estrés oxidativo. El análisis genómico de las secuencias de los promotores de genes de fase II ha revelado que coinciden en una secuencia específica de unión llamada Elemento de Respuesta Antioxidante, **ARE** (del inglés, *Antioxidant Response Element*), que puede ser activada por diversos compuestos oxidantes de naturaleza química diversa.

### Factor de transcripción Nrf2

El factor de transcripción Nrf2 (del inglés, *nuclear factor-erythroid 2-related factor-2*) regula la expresión inducible de numerosos genes relacionados con enzimas detoxificantes y antioxidantes, mediante su unión al elemento de respuesta antioxidante ARE. La activación del factor Nrf2 se encuentra constitutivamente reprimida debido a su unión con una proteína citoplasmática llamada Keap1 (del inglés, *Kelch-like ECH associated protein 1*) y al citoesqueleto (**Figura 12**).

Investigaciones más recientes ponen en evidencia que la activación de Nrf2 ocurre mediante mecanismos más complejos que su simple liberación de Keap1. En el modelo más aceptado actualmente, denominado “Modelo de cierre y bisagra”, se determinó que en ausencia de estrés celular la vida media de Nrf2 es muy corta (10-30 minutos), por lo que sus niveles en los tejidos son bajos. El uso de inhibidores del proteasoma indica que la degradación de Nrf2 ocurre mediante la vía de la ubiquitina-proteasoma [47].

La primera evidencia del papel de Nrf2 en protección contra estrés oxidativo proviene del estudio de Venugopal y Jaiswal en 1996, en el que se demostró que la sobreexpresión del cADN de Nrf1 y Nrf2 aumentaba la expresión de NQO1 en respuesta a antioxidantes y xenobióticos [49]. El papel de Nrf2 se confirmó cuando se obtuvieron los primeros ratones genéticamente modificados y carentes de este factor (Nrf2-/-). Los ratones Nrf2-/- tuvieron un desarrollo aparentemente normal, por lo que se descartó que Nrf2 fuera esencial para la eritropoyesis murina, el crecimiento o el desarrollo. Sin embargo, estos ratones no podían inducir la expresión de los genes responsables de la detoxificación de agentes carcinógenos y de protección contra el estrés oxidativo, en particular los genes de fase II antes mencionados, como los que codifican para las enzimas NQO1 (quinona oxidoreductasa 1), GCL (glutamato-cisteína ligasa), GST (glutatión S-transferasa) y HO-1 (hemo oxigenasa 1) [50].

En estudios recientes se ha demostrado que Nrf2 también contribuye a la actividad del proteasoma 26S, lo cual confirma la importante participación de este factor Nrf2 en la protección contra el estrés oxidativo y los xenobióticos.

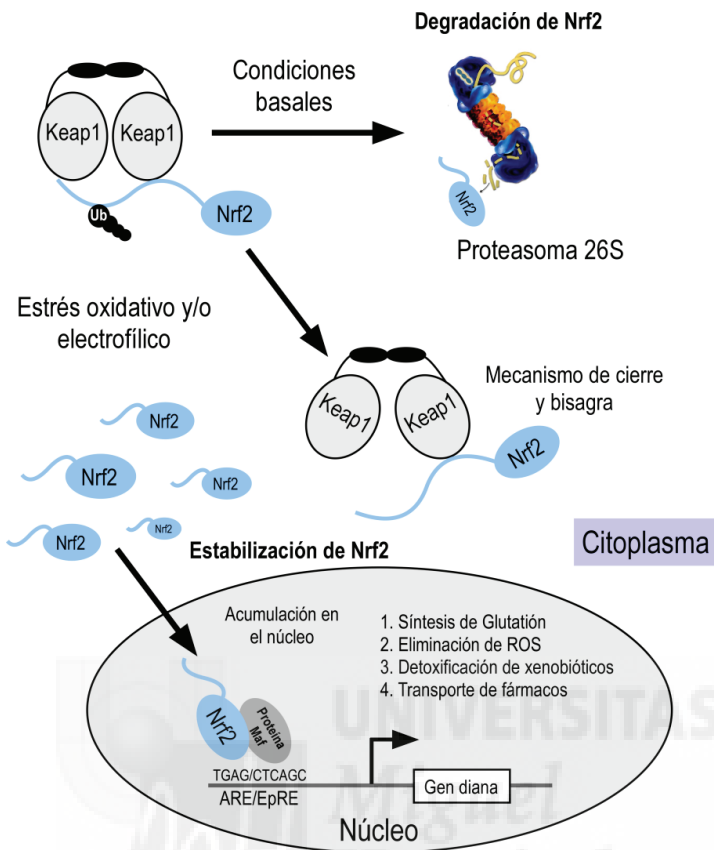


**Figura 12.** La vía Nrf2-Keap1. El factor de transcripción Nrf2 juega un papel central en la expresión de genes citoprotectores en respuesta al estrés oxidativo presente en las células.

Keap1 (del inglés, Kelch-like ECH-associated protein 1) es una proteína citoplasmática esencial para la regulación de Nrf2. En condiciones basales, Nrf2 se asocia a la proteína Keap1, que lo marca para degradación por la vía ubiquitina-proteasoma (extraída y adaptada de Taguchi, Matohashi y Yamamoto, 2011).

## 1.7. Potencial de Membrana Mitochondrial ( $\Delta\Psi_m$ ).

Las mitocondrias son orgánulos intracelulares presentes en todas las células eucariotas.

Están encargados de suministrar la mayor parte de la energía necesaria para la actividad celular, sintetizan ATP a expensas de glucosa, ácidos grasos y aminoácidos por medio de la fosforilación oxidativa [51]. Poseen un sistema de doble membrana, una externa y una interna, que separan tres espacios bien definidos: el *citosol*, el *espacio intermembrana* y la *matriz mitocondrial* (Figura 13).

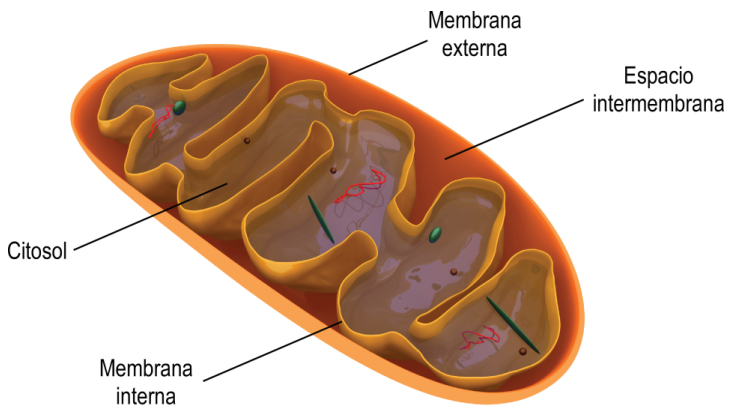


Figura 13. Estructura y principales compartimentos de una mitocondria.

El potencial de membrana mitocondrial se define como el gradiente electroquímico de protones a través de la membrana mitocondrial interna, provocado por la energía que se obtiene mediante la transferencia de electrones a lo largo de la cadena transportadora para bombear protones desde la matriz mitocondrial hacia el espacio intermembrana. La alteración de la cadena de transporte de electrones, dando lugar a la pérdida de potencial de membrana mitocondrial es un mecanismo responsable en la generación de ROS [52]. Por este motivo, la mitocondria se considera una fuente muy importante de ROS y juega un importante papel en la regulación del estrés oxidativo intracelular.

El daño oxidativo mitocondrial juega un papel crítico en la muerte celular y en la regulación, tanto de la apoptosis como de la necrosis [53]. La permeabilización de la membrana mitocondrial y liberación de proteínas al espacio intermembrana son características importantes de estos dos mecanismos.

## 1.8. Biodisponibilidad de los compuestos bioactivos.

Los compuestos bioactivos que han demostrado un posible papel en la prevención de ciertas enfermedades en estudios llevados a cabo *in vitro*, sólo podrán ser efectivos si alcanzan los tejidos donde han de ejercer su acción en concentraciones suficientes para tener un efecto biológico. Es por tanto esencial conocer la absorción, la distribución y el metabolismo de estos compuestos en el organismo mediante estudios de su biodisponibilidad en modelos *in vivo*.

Según la FDA, biodisponibilidad se define como la velocidad y cantidad a la cual un fármaco o compuesto activo, absorbido a partir de la forma de dosificación que lo contiene, se hace disponible en el lugar de acción.

### Absorción y metabolismo

Además de la estructura química que presentan los compuestos bioactivos y la naturaleza de la matriz donde se encuentran, otros factores que influyen en la actividad biológica, es su absorción y metabolismo tras la ingesta [54].

La mayoría de estos compuestos se encuentran en los alimentos en forma de ésteres, glucósidos o polímeros que no pueden ser absorbidos directamente en el intestino. Para ello deben ser previamente hidrolizados por enzimas intestinales o por la microflora del colon. De todos los compuestos, sólo las agliconas son capaces de atravesar las membranas biológicas por ser altamente lipofílicas, por lo tanto, los compuestos bioactivos son conjugados en el intestino e hígado mediante reacciones de metilación, glucuronidación, sulfatación, o sus combinaciones [55].

## Transporte en sangre de compuestos fenólicos

Los compuestos conjugados son transportados en el plasma a los distintos tejidos y órganos, principalmente unidos a albúmina. Como consecuencia de estos procesos, las formas que se encuentran en el plasma y en los tejidos son muy distintas de las que están presentes en los alimentos, y esto dificulta la tarea de identificación de los metabolitos y la evaluación de su actividad biológica [56].

Muchos estudios han llegado a la conclusión de que la biodisponibilidad de la mayoría de dichos compuestos no es excesivamente alta debido a factores tales como baja absorción, la inestabilidad, el metabolismo o la transformación sufrida por la microbiota intestinal [57]. A pesar de su escasa biodisponibilidad, hay estudios que demuestran que muchos compuestos bioactivos presentan actividad a bajas concentraciones en plasma [58].

### 1.9. Extracto de *Rosmarinus officinalis* L. como fuente de compuestos bioactivos

La planta *Rosmarinus officinalis* L., el romero, fue identificada por Linneo en 1753. Etimológicamente, se piensa que el origen del término proviene de la unión de las palabras griegas, “rhos”, arbusto y “myrinos”, arómático, las cuales concuerdan perfectamente con las características de la planta. Por otra parte, el origen del nombre específico “*officinalis*” pone de manifiesto su aplicación como planta medicinal.

Es una especie del género *Rosmarinus* de la familia *Lamiaceae*, cuyo hábitat natural es la región mediterránea, sur de Europa y norte de África [59]. Es un arbusto aromático, leñoso, de hojas perennes, muy ramificado y puede llegar a medir dos metros de altura. Sus flores son de unos 5 mm de largo, aromáticas y tienen un color violeta pálido, rosa o blanco. Se suelen localizar en la cima de las ramas (**Figuras 14 y 15**).



**Figura 14.** Planta de romero en floración.

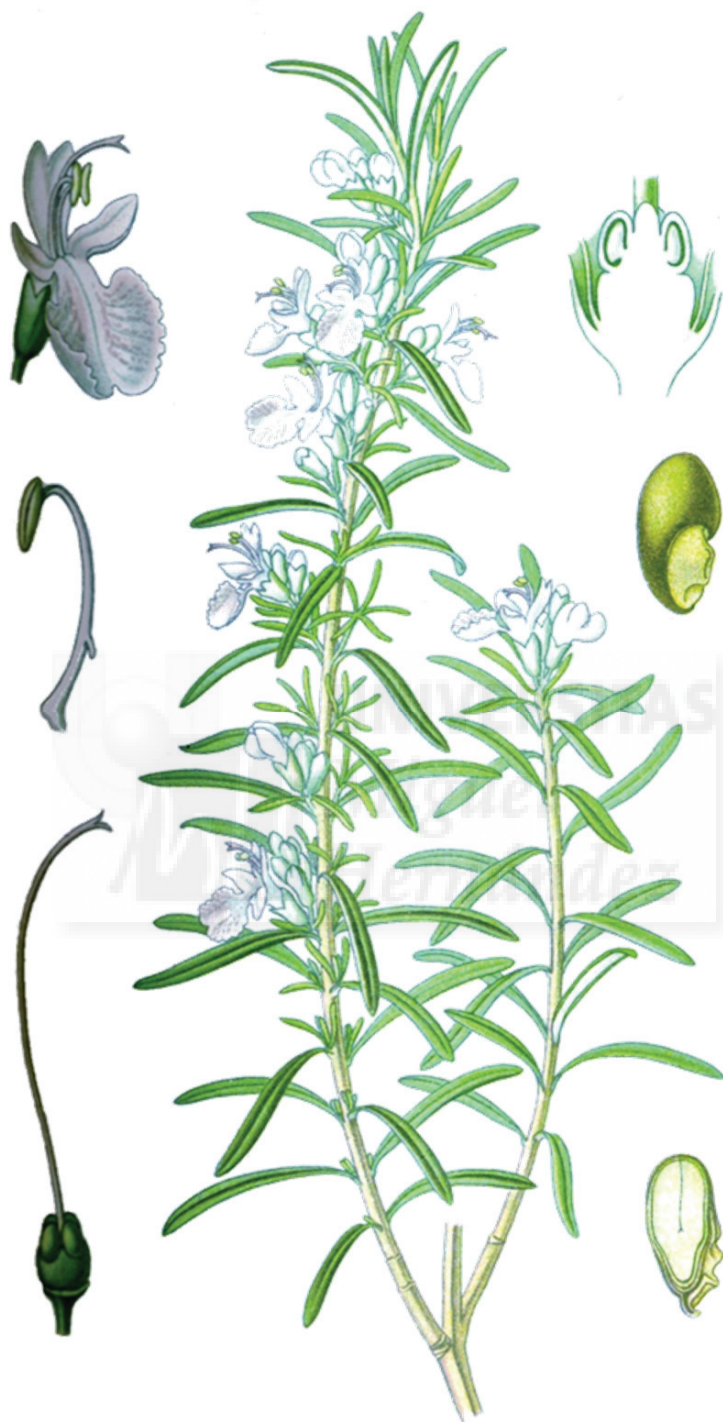
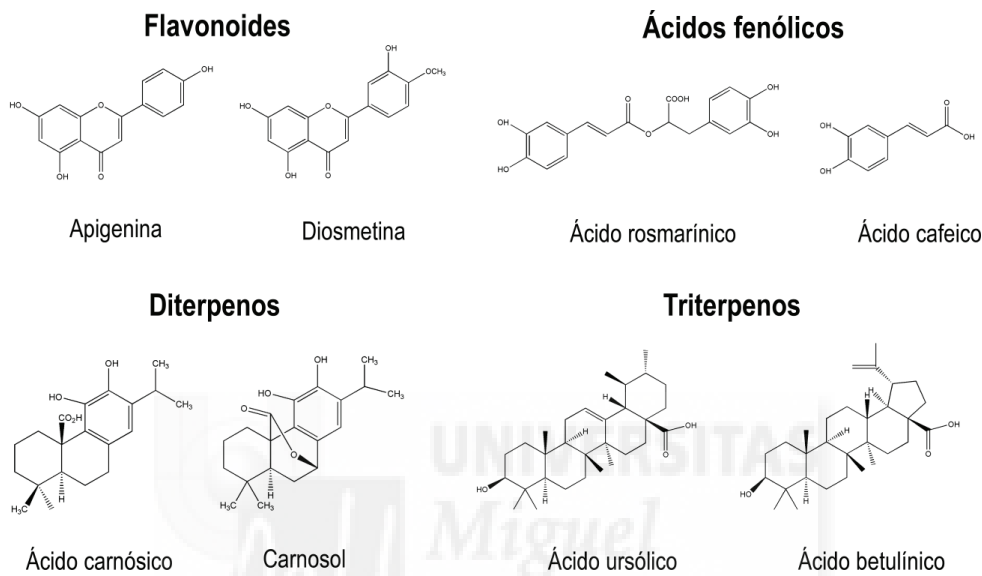


Figura 15. Detalle del tallo, flor y hoja de *Rosmarinus officinalis* L.

Respecto a su composición química, cabe destacar la presencia de **flavonoides** (apigenina, diosmetina, diosmina, hispidulina, luteolina y cirsimartina), **ácidos fenólicos** (cafeico, clorogénico, labiático, neoclorogénico y rosmarínico), **diterpenos** (ácido carnósico, carnosol, rosmanol y rosmadial) y **triterpenos** (ácido ursólico y betulínico) (**Figura 16**) [59, 60].



**Figura 16.** Principales familias de compuestos presentes en el extracto de romero.

En las últimas décadas, la investigación ha confirmado el potencial farmacológico del romero y de sus principales compuestos. Se ha demostrado que extractos de dicha planta presentan un efecto preventivo para el cáncer [61], además de propiedades hepatoprotectoras [62], antimicrobianas [63, 64], antitumorales [59, 65, 66] y un alto poder antioxidante [23].

Respecto a sus principales compuestos, cabe destacar la actividad biológica del diterpeno ácido carnósico, el cual presenta actividad antitumoral inhibiendo la proliferación, migración y adhesión en células de cáncer colorrectal [67], induciendo apoptosis en células de cáncer renal [68] e inhibiendo la transición epitelio-mesenquimal en melanoma [69].

Los estudios llevados a cabo por Kim *et al.* demostraron que el tratamiento con ácido carnósico provoca una disminución en la viabilidad celular de la línea celular humana de cáncer colorrectal HCT116, mediada por la apoptosis causada por la generación excesiva de ROS, la inducción de los genes p53 y Bax y la activación de caspasas 3 y 9. Además, se produjo la escisión de PARP (del inglés, Poly (ADP-Ribose) Polymerase) y la inhibición de la vía de señalización STAT3 (del inglés, *Signal Transducer and Activator of Transcription 3*) [70]. Dicho grupo de investigación, también demostró que el ácido carnósico inhibe la proliferación celular de la línea celular de cáncer de colon HT-29 en co-cultivo con adipocitos 3T3-L1, bloqueando el ciclo celular e induciendo apoptosis [71].

Por otra parte, el diterpeno carnosol además presenta un efecto preventivo en la formación del cáncer [72]. Varios estudios han demostrado que dicho diterpeno muestra un efecto citostático y citotóxico, bloqueando el ciclo celular e induciendo apoptosis, respectivamente [73, 74]. Dentro del grupo de los triterpenos cabe destacar la actividad antitumoral del ácido ursólico, inhibiendo la proliferación celular por apoptosis, aumentando los niveles de ROS intracelular y alterando el potencial de membrana mitocondrial en células de cáncer de mama [75].

#### **1.10. Extracción por Fluidos Supercríticos (FSC), una técnica optimizada para la obtención de extractos enriquecidos en compuestos bioactivos.**

En los últimos años, se han empleado diferentes técnicas de extracción para obtener extractos de romero con una alta actividad biológica, entre las que destacan las extracciones con disolventes convencionales [76, 77] y por ultrasonidos [78]. Otros métodos de extracción tales como la hidrodestilación o la hidrodifusión por microondas también se han aplicado para obtener aceite esencial de romero [79]. A pesar de que estas técnicas son capaces de proporcionar extractos con un alto contenido en compuestos bioactivos, actualmente, se prefieren tecnologías más respetuosas con el medio ambiente y más selectivas.

Entre ellas destaca la extracción por fluidos supercríticos (FSC), la cual se caracteriza por una tecnología innovadora, limpia y respetuosa con el medio ambiente que suscita un gran interés por la extracción de aceites esenciales o compuestos bioactivos a partir de una matriz vegetal [80]. Un fluido supercrítico se define como cualquier sustancia que se encuentra en condiciones de presión y temperatura superiores a su punto crítico, es decir, que puede difundir como un gas y disolver sustancias como un líquido (**Figura 17**).

El FSC más utilizado es el dióxido de carbono ( $\text{CO}_2$ ) por poseer una serie de ventajas como una presión crítica (72,90 bar) y temperatura crítica ( $31,05^\circ\text{C}$ ) moderadas, un alto poder disolvente, no ser tóxico ni inflamable, ser relativamente económico y, particularmente en las aplicaciones alimentarias, por ser un fluido permitido en los alimentos y ser reconocido como GRAS (del inglés, *Generally Recognized as Safe*). El principal inconveniente que presenta el empleo de  $\text{CO}_2$  en FSC es su baja polaridad, lo que dificulta la solubilización de las sustancias polares. Diversos autores han estudiado las diferencias entre los extractos de romero extraídos por fluidos supercríticos, los extractos obtenidos mediante disolventes convencionales (etanol y hexano) y/o mediante hidrodestilación, concluyendo que los extractos supercríticos, en general, presentan mejores actividades biológicas que los obtenidos por técnicas convencionales [81].

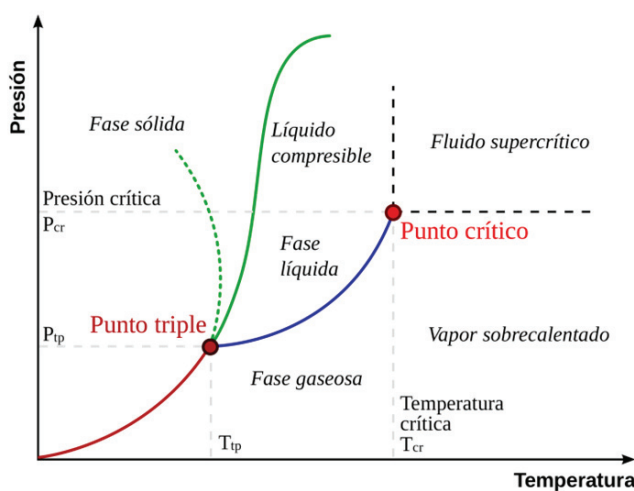


Figura 17. Diagrama de fases de una sustancia.

Respecto a los usos más frecuentes de dicha técnica se encuentra el sector de la industria alimentaria, principalmente para la obtención de compuestos naturales, extracción de aceites y aromas esenciales.

El potencial de la técnica de extracción por FSC para extraer compuestos bioactivos de matrices naturales ya se ha demostrado con diferentes plantas [82, 83]. Existen varios estudios que demuestran que dicha técnica permite obtener extractos con alto poder antioxidante [84-87], con actividad antimicrobiana [88, 89], efecto antiinflamatorio [90] e incluso actividad antitumoral [59, 91].



## **2. HIPÓTESIS DE PARTIDA Y OBJETIVOS**



Estudios preliminares realizados por el grupo de investigación donde se ha desarrollado la presente Tesis Doctoral han evidenciado el efecto antiproliferativo/citotóxico de extractos de romero enriquecidos en terpenoides y obtenidos por fluidos supercríticos en modelos de células de adenocarcinoma de colon [92]. Estos resultados motivan a profundizar en el estudio tanto del efecto antiproliferativo como de su mecanismo acción con el objetivo de desarrollar ingredientes con capacidad quimiopreventiva con posibles aplicaciones en los sectores de la alimentación funcional, los nutracéuticos y el sector farmacéutico. Dado lo comentado anteriormente, se plantea como objetivo principal de la presente Tesis Doctoral **el estudio de la capacidad antiproliferativa de un extracto de romero enriquecido en compuestos bioactivos, utilizando modelos *in vitro* e *in vivo* de cáncer colorrectal humano.** Para el desarrollo de este objetivo principal se han planteado los siguientes objetivos específicos:

1. Comparar el efecto antiproliferativo/citotóxico del extracto de romero en líneas tumorales de cáncer de colon frente al de sus compuestos más abundantes.
2. Identificar los compuestos del extracto de romero potencialmente responsables de la actividad antiproliferativa/citotóxica en los modelos celulares objeto de estudio.
3. Caracterizar los mecanismos que median la muerte celular inducida por el extracto de romero en líneas tumorales humanas de colon.
4. Determinar la actividad del extracto de romero en un modelo *in vivo* basado en xenotransplantes de células de adenocarcinoma de colon humano en ratones inmunodeprimidos y determinar su toxicidad oral aguda en ratas.
5. Estudiar la absorción y la permeabilidad *in vitro* de los compuestos del extracto de romero administrado de forma libre y liposomado empleando monocapas de células intestinales Caco-2.



### **3. METODOLOGÍA**



### 3.1. Líneas celulares.

En este trabajo se han empleado diferentes líneas celulares de adenocarcinoma de colon. Para determinar el efecto antitumoral se emplearon las líneas celulares HGUE-C-1, HT-29 y SW480. Además, se empleó la línea de cáncer colorrectal Caco-2 para realizar ensayos de absorción *in vitro*.

#### Línea celular HGUE-C-1

La línea celular HGUE-C-1 es una línea establecida a partir de cultivo primario, que presenta quimiorresistencia a los fármacos 5-fluorouracilo e Irinotecán. Las células fueron obtenidas en el año 2003 a partir de derrame ascítico de un paciente de 76 años con cáncer de colon [93] en el Hospital General Universitario de Elche.

#### Línea celular HT-29

La línea celular HT-29 es una línea establecida a partir de un tumor extirpado procedente de una mujer caucásica de 44 años que presentaba fenotipo de adenocarcinoma de colon humano moderadamente diferenciado de grado II. Esta línea presenta morfología epitelial, una mutación en el gen p53, es positiva para la expresión de los oncogenes c-myc, K-ras, H-ras, N-ras y Myb y no expresa p21.

#### Línea celular SW480

La línea celular SW480 fue aislada de un tumor primario de colon de un hombre caucásico de 50 años. Presenta morfología epitelial y mutaciones en los oncogenes c-myc, K-ras, H-ras, N-ras, myb, sis y fos.

## Línea celular Caco-2

La línea celular Caco-2 proviene de células epiteliales humanas de adenocarcinoma colorrectal de un hombre caucásico de 72 años. Presenta morfología epitelial y mutaciones en los oncogenes p53 y K-ras.

### 3.2. Condiciones de cultivo.

Para todas las líneas celulares excepto para la línea Caco-2 el medio de cultivo utilizado fue DMEM (del inglés, *Dulbecco's Modified Eagle's Medium*) suplementado con glutamina estable, 5% de suero fetal bovino (SFB) y 50 U/mL de penicilina/estreptomicina. Para la línea celular Caco-2, el medio de cultivo fue suplementado con un 10% de SFB, 1% de HEPES y 1% de aminoácidos no esenciales (reactivos obtenidos de Gibco).

### 3.3. Extracto de romero.

El extracto de romero (ER) se obtuvo a partir de las hojas secas de la planta de romero adquiridas de la Herboristería Murciana (Murcia, España). La extracción se realizó mediante un sistema de fluidos supercríticos (FSC) (Suprex Prep Master, Suprez Corporation, Pittsburg, PA, USA). El flujo de CO<sub>2</sub> fue de 60 g/min y las condiciones de extracción fueron 150 bares y 40°C con un 7% de etanol [94]. A continuación, el disolvente se evaporó utilizando un Rotavapor R-210 (Buchi Labortechnik AG, Flawil, Suiza). Para la realización de los experimentos *in vitro* se preparó una disolución madre o stock en el disolvente más apropiado, en este caso, dimetilsulfóxido (DMSO) para biología molecular (Sigma-Aldrich, España). A partir de la disolución madre se obtuvieron las concentraciones empleadas en los ensayos y como condición control (0) se utilizaron cultivos celulares en presencia de la máxima concentración de disolvente requerido para los compuestos o extracto de romero (0,2% de DMSO).

### **3.4. Aislamiento y purificación de compuestos presentes en el extracto de romero mediante cromatografía semi-preparativa.**

La purificación de los compuestos presentes en el extracto de romero se realizó mediante un sistema de cromatografía líquida de alta resolución (HPLC) semi-preparativa. Para ello, se utilizó un sistema HPLC Gilson GX 281 (Gilson, Middleton, Estados Unidos), equipado con una bomba binaria modelo 331/332, un inyector automático, un detector DAD modelo 171/172 y un colector de fracciones modelo GX-281. El extracto de romero se disolvió en DMSO a una concentración de 50 mg/mL y filtrado a través de filtros de 0,45 µm de tamaño de poro. La separación se llevó a cabo mediante una columna Supelco Ascentis C-18, 10 µm de tamaño de partícula, y dimensiones 21,2 x 250 mm.

Las fases móviles utilizadas fueron como fase A, 0,1% de ácido fórmico en agua, y B, acetonitrilo. El gradiente empleado fue: 0 min, 5% de B; 10 min, 45% de B; 20 min, 55% de B; 26 min, 60% de B; 46 min, 73% de B; 50 min, 80% de B; 55 min, 100% de B; y 60 min, 5% de B. La velocidad de flujo fue de 15 mL/min y el volumen de inyección 1 mL. Los compuestos aislados se monitorizaron mediante UV-Vis a una longitud de onda de 280 nm. Las fracciones se colectaron en intervalos de tiempo de 1 minuto, obteniendo un total de 60 fracciones, las cuales se secaron mediante nitrógeno gaseoso ( $N_2$ ) y en oscuridad y conservadas a -80°C hasta su posterior análisis por HPLC-MS.

### **3.5. Análisis del extracto de romero y sus fracciones mediante HPLC-ESI-QTOF-MS.**

El extracto de romero y las fracciones obtenidas por HPLC semi-preparativa se analizaron mediante HPLC-ESI-QTOF-MS. El extracto se disolvió en etanol a una concentración de 0,8 y 5 mg/mL mientras que las fracciones se disolvieron en DMSO a una concentración de 0,1 mg/mL. A continuación, todas las muestras se filtraron a través de filtros de jeringa de acetato de celulosa de 0,45 µm de tamaño de poro.

Para el análisis de estas muestras se utilizó un cromatógrafo de líquidos UPLC Acquity (Waters, Milford, MA, Estados Unidos) equipado con un compartimento de muestras termostatizado, una bomba binaria y un desgasificador, acoplado a un espectrómetro de masas microTOF Q-II (Bruker Daltonik, Bremen, Alemania). La columna empleada para la separación de los compuestos fue una Zorbax Eclipse Plus C-18, de dimensiones 4,6x150 mm y tamaño de partícula de 1,8 µm. Las fases móviles utilizadas fueron como fase A 0,1% de ácido fórmico en agua y como fase B acetonitrilo. El gradiente empleado fue: 0 min, 5% de B; 5 min, 40% de B; 10 min, 60% de B; 30 min, 95% de B; y 32,5 min, 5% de B. La velocidad de flujo fue de 0,8 mL/min y el volumen de inyección 5 µL.

La detección mediante espectrometría de masas se realizó en modo de ionización negativo con un rango de masas de 50-1100 m/z y con un voltaje capilar de +4 kV. Los parámetros óptimos para el análisis por ESI-QTOF fueron los siguientes: temperatura, 210°C; flujo gas nebulizador, 9 L/min; presión gas nebulizador, 2 bar; funnel 1 RF, 150 Vpp; funnel 2 RF, 200 Vpp; Hexapolo RF, 100 Vpp; tiempo de transferencia, 70 µs; y almacenamiento pre-pulso, 7 µs. La cuantificación de los compuestos se llevó a cabo con los siguientes patrones comerciales: carnosol, diosmetina, apigenina y ácidos carnósico, ursólico y rosmarínico. El resto de compuestos fueron cuantificados a partir de compuestos con alta similitud estructural. Los compuestos rosmanol y sus isómeros epiisorrosmanol y epirrosmanol, la miltipolona, el rosmadial y el rosmaridifenol fueron cuantificados a partir del patrón carnosol. La hinoquiona y el ácido 12-metoxicarnósico fueron cuantificados con ácido carnósico. La anemosapogenina y los ácidos augústico, bentámico, micromérico y betulínico fueron cuantificados como ácido ursólico. Finalmente, la cirsimaritina fue cuantificada con la genkwanina, el (9)-shogaol mediante el ácido rosmarínico y la hispidulina y el crisiliol fueron cuantificados con la diosmetina. La adquisición y análisis de los datos se llevó a cabo mediante el programa informático Data Analysis 4.0 (Bruker Daltonik, Bremen, Alemania).

### 3.6. Determinación de la viabilidad celular.

Para determinar el efecto que ejercen los compuestos puros o el extracto de romero en la viabilidad celular se realizó el ensayo de MTT (bromuro de 3-(4,5-dimetiltiazol-2-il)-2,5-difeniltetrazolio). Este método se basa en la reducción de la sal de tetrazolio MTT de color amarillo y soluble en agua, en cristales de formazán púrpura insolubles en agua. Esta reacción sólo ocurre en células viables y es catalizada por la enzima mitocondrial succinato deshidrogenasa (**Figura 18**). El formazán es solubilizado en DMSO y la densidad óptica del material resultante se mide espectrofotométricamente, siendo la absorbancia proporcional a la concentración de la tinción y correlacionándose esta con el número de células metabólicamente viables en el cultivo.

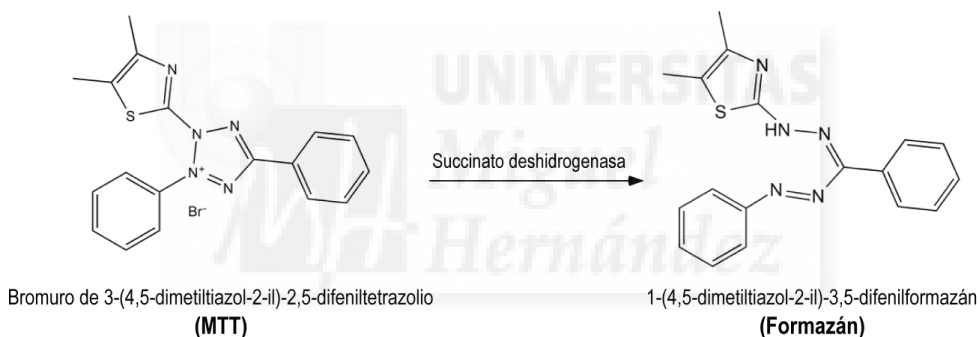


**Figura 18.** Reducción del reactivo MTT mediante la enzima mitocondrial succinato deshidrogenasa a formazán.

Las células fueron sembradas a una densidad de  $5 \times 10^3$  células por pocillo en placas de 96 pocillos y tratadas con los diferentes compuestos o el extracto de romero según las condiciones del ensayo. Una vez finalizado el tratamiento se agregó una solución del reactivo MTT disuelto en medio de cultivo completo (250 µg/mL) y se incubó durante 3-5 horas a 37°C y 5% de CO<sub>2</sub>. Pasado este tiempo, se retiró el contenido de los pocillos y se añadieron 100 µL de DMSO por pocillo para resuspender los cristales de formazán. Las placas se mantuvieron durante 15 minutos en agitación a temperatura ambiente y posteriormente se midió la absorbancia a 570 nm

en un lector de placas SPECTROstar Omega (BMG LabTech GmbH, Offenburg, Alemania), empleando la absorbancia a 620 nm como referencia.

### 3.7. Análisis del ciclo celular.

El análisis del ciclo celular se realizó mediante el estudio del contenido de ADN de las células, ya que éste varía en función de la fase del ciclo celular en la que se encuentren. Para ello se marcó el ADN con la sonda fluorescente yoduro de propidio, la cual se intercala entre los ácidos nucleicos de las células, emitiendo distinta intensidad de fluorescencia en función de su contenido de ADN. Las células que se encuentran en la fase G<sub>2</sub>/M del ciclo celular y, por lo tanto, han duplicado su material genético, dan lugar a una señal de fluorescencia cuya intensidad duplica a la de las células que se encuentran en fase G<sub>1</sub>. La señal de las células que se encuentran en fase S (síntesis) se encuentra comprendida entre las que emiten las células de G<sub>1</sub> y G<sub>2</sub>/M. Por otra parte, las células apoptóticas (fase Sub-G<sub>1</sub>) presentan fragmentación del ADN y emiten menor fluorescencia que las que tienen el ADN íntegro (Figura 19).

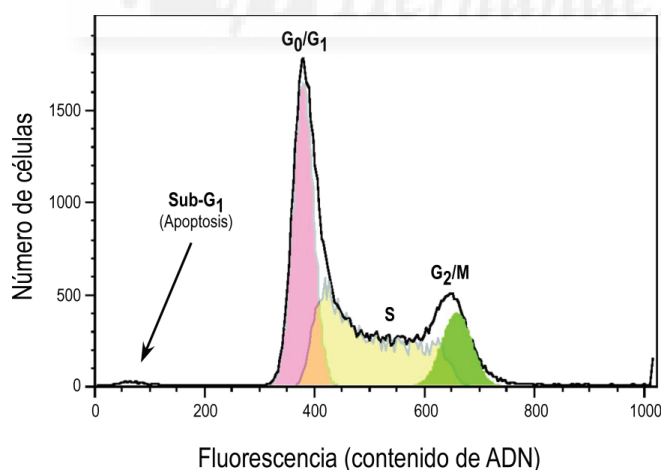


Figura 19. Perfil del ciclo celular obtenido mediante el marcaje de ADN con sondas fluorescentes.

Las células fueron sembradas a una densidad de  $1,5 \times 10^5$  células por pocillo en placas de 6 pocillos y tratadas con el extracto de romero a diferentes concentraciones (10-40  $\mu\text{g/mL}$ ) durante 24 horas. Una vez finalizado el tratamiento, las células se tripsinizaron, se lavaron con tampón fosfato salino (PBS) y se fijaron con etanol frío al 75% al menos 1 hora a -20°C. Tras la fijación, las células se lavaron con PBS, se centrifugaron y se procedió al marcaje fluorescente del ADN añadiendo 200  $\mu\text{L}$  del reactivo *Muse Cell Cycle Kit* (Millipore, Hayward, CA, Estados Unidos), incubando durante 30 minutos a temperatura ambiente y en oscuridad. A continuación, se determinó la distribución de las fases del ciclo celular mediante la adquisición de los datos de fluorescencia empleando la tecnología del equipo *Muse Cell Analyzer* (Millipore, Hayward, CA, Estados Unidos) (**Figura 20**).



Figura 20. Equipo *Muse Cell Analyzer*.

### 3.8. Detección de apoptosis mediante Anexina-V.

La pérdida de la asimetría de membrana es un fenómeno esencial en el proceso apoptótico. Las células que están sufriendo apoptosis se pueden detectar marcando las células con Anexina-V, ya que esta proteína se une a los restos de fosfatidilserina (FS), que en situación normal no son accesibles, pero que, durante el proceso de apoptosis, son expuestos al exterior por la pérdida de asimetría de la membrana celular.

Para distinguir las células de una situación necrótica, que también serían marcadas con la Anexina-V, se añade la sonda 7-aminoactinomicina D (7-AAD), la cual entra en las células que han perdido la integridad de la membrana tal y como ocurre en las células necróticas. Si observamos un gráfico de resultados tipo, en el eje X aparece la fluorescencia de la Anexina-V y en el eje Y aparece la fluorescencia correspondiente a la sonda 7-AAD. De esta manera, según el cuadrante en el que se encuentre la población celular, se presentará una de las siguientes situaciones:

- **Cuadrante inferior izquierdo:** células viables (no unen Anexina-V y excluyen 7-AAD).
- **Cuadrante inferior derecho:** células en apoptosis temprana (unen Anexina-V y excluyen 7-AAD).
- **Cuadrante superior derecho:** células en apoptosis tardía o necróticas (unen Anexina-V e incorporan 7-AAD).
- **Cuadrante superior izquierdo:** células necróticas o en necrosis secundaria (no unen Anexina-V e incorporan 7-AAD) (**Figura 21**).

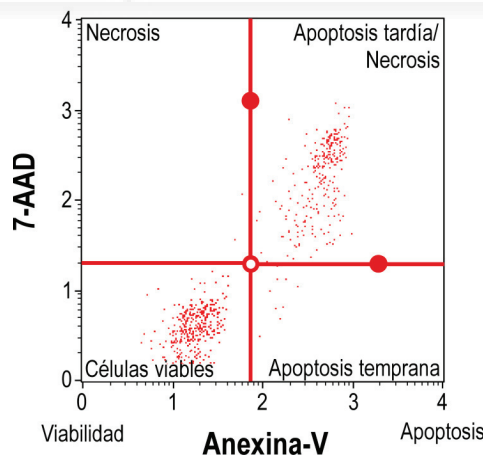


**Figura 21.** Distribución de la población celular según el ensayo Anexina V-7-AAD.

Las células fueron sembradas a una densidad de  $1,5 \times 10^5$  células por pocillo en placas de 6 pocillos y tratadas con el extracto de romero a diferentes concentraciones (10-40  $\mu\text{g/mL}$ ) durante 24 horas. Una vez finalizado el tratamiento, las células se tripsinizaron, se lavaron con PBS, se añadieron 200  $\mu\text{L}$  del reactivo *Muse Annexin V & Dead Cell Kit* (Millipore, Hayward, CA, Estados Unidos) y se incubaron durante 20 minutos a temperatura ambiente y en oscuridad. A continuación, se determinó el porcentaje de apoptosis mediante la adquisición de los datos de fluorescencia empleando la tecnología del equipo *Muse Cell Analyzer* (Millipore, Hayward, CA, Estados Unidos).

### 3.9. Determinación de la integridad de la membrana plasmática.

La muerte celular o citotoxicidad fue determinada mediante la evaluación de la actividad de la enzima lactato deshidrogenasa (LDH), una enzima estable, presente normalmente en el citosol de todas las células, la cual es liberada rápidamente al exterior cuando existe daño celular [95]. Para ello, se empleó el kit de citotoxicidad LDH (Roche Diagnostics GmbH, Mannheim, Alemania), que permite la medición de la actividad de la enzima LDH utilizando una mezcla de reactivos que contiene L-lactato, NAD<sup>+</sup>, diaforasa y la sal de tetrazolio INT (cloruro de iodo-nitrotrifenil tetrazolio). Como muestra la **Figura 22** la LDH cataliza la reducción de NAD<sup>+</sup> a NADH en presencia de L-lactato. Esta formación de NADH se puede medir mediante una reacción acoplada, en la que la sal de tetrazolio INT se reduce a un producto de formazán rojo, que se puede medir por espectrofotometría [96].

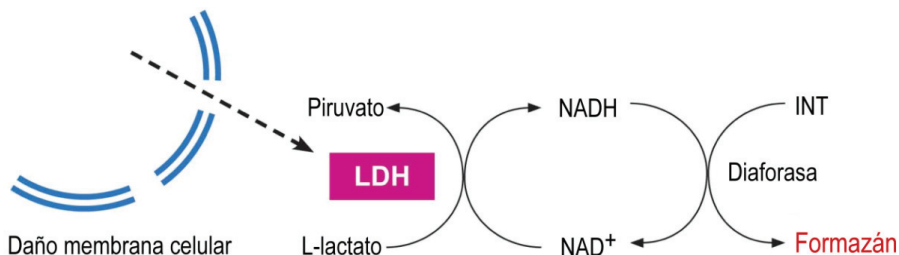


**Figura 22.** Reducción de NAD<sup>+</sup> a NADH mediante la enzima LDH.

Las células fueron sembradas a una densidad de  $5 \times 10^3$  células por pocillo en placas de 96 pocillos y tratadas con el extracto de romero a diferentes concentraciones (10-40  $\mu\text{g/mL}$ ) durante 24 horas. Una vez finalizado el tratamiento, se aspiraron 100  $\mu\text{L}$  de sobrenadante y se transfirieron a otra placa. A continuación, se realizó el ensayo de actividad LDH según el protocolo descrito por el fabricante. Las placas se mantuvieron durante 15 minutos en oscuridad y posteriormente se midió la absorbancia en un lector de placas *SPECTROstar Omega* (BMG LabTech GmbH, Offenburg, Alemania) a 492 nm, empleando la absorbancia a 600 nm como referencia. El porcentaje de citotoxicidad fue calculado mediante la siguiente fórmula:

$$\text{Citotoxicidad (\%)} = \frac{\text{valor experimental} - \text{control negativo}}{\text{control positivo} - \text{control negativo}} \cdot 100$$

Los datos fueron analizados, tomando como 100% de liberación de LDH los pocillos tratados con 1% de Tritón X-100 (control positivo) y como 0% de muerte celular los pocillos tratados con el vehículo (control negativo).

### **3.10. Determinación de necroptosis y autofagia.**

Para determinar el tipo de muerte celular provocada por el extracto de romero, se empleó la necrostatina-1 (inhibidor de la necroptosis) y la cloroquina (inhibidor de la autofagia).

Las células fueron sembradas a una densidad de  $5 \times 10^3$  células por pocillo en placas de 96 pocillos y pretratadas con 10  $\mu\text{M}$  de necrostatina-1 y 10  $\mu\text{M}$  de cloroquina, de manera independiente, durante las dos horas previas al tratamiento realizado con el extracto de romero (10-40  $\mu\text{g/mL}$ ) durante 24 horas. Una vez finalizado el tratamiento, se cuantificó la viabilidad celular mediante el ensayo de MTT.

### 3.11. Cuantificación de Especies Reactivas de Oxígeno (ROS).

La generación de ROS fue detectada con la sonda fluorescente 2',7'-dclorofluoresceína diacetato ( $H_2DCF\text{-DA}$ ). Esta sonda es un compuesto no fluorescente al que la célula es permeable; una vez dentro de la célula, es desesterificado y se vuelve fluorescente por oxidación (DCF), siendo la fluorescencia proporcional a la producción de ROS (Figura 23).

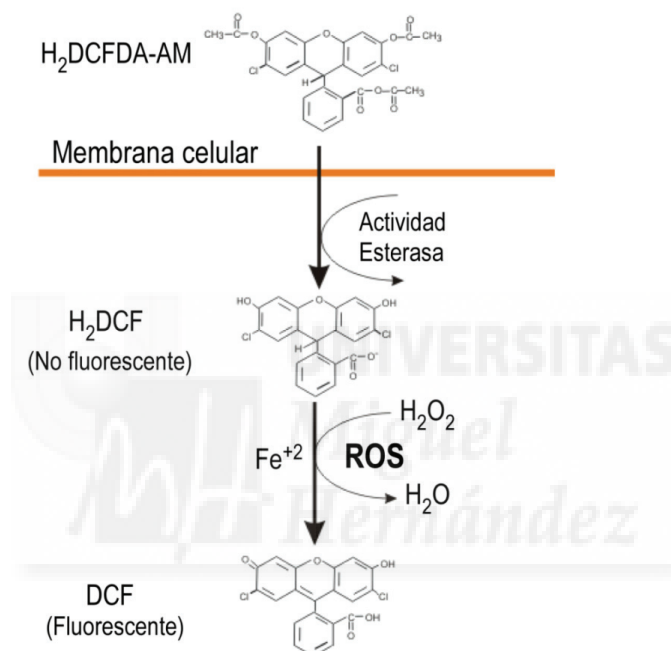


**Figura 23.** Desesterificación de la sonda  $H_2DCF\text{-DA}$  y posterior oxidación dando lugar al compuesto DCF (fluorescente).

Las células fueron sembradas a una densidad de  $5 \times 10^3$  células por pocillo en placas de 96 pocillos y tratadas con el extracto de romero a diferentes concentraciones (10-40  $\mu\text{g/mL}$ ). Además, se utilizó como control positivo de generación de ROS la irradiación de las células con luz ultravioleta B a  $800 \text{ J/m}^2$  [97]. Una vez finalizado el tratamiento, las células se incubaron con 10  $\mu\text{g/mL}$  de  $H_2DCF\text{-DA}$  en medio de cultivo completo durante 20 minutos a  $37^\circ\text{C}$  y 5% de  $\text{CO}_2$ . Pasado este tiempo, se aspiró el contenido de los pocillos, se lavaron con PBS y se procedió a

medir la fluorescencia a una longitud de onda de excitación de 485 nm y de emisión de 535 nm en un lector de placas *POLARstar Omega* (BMG LabTech GmbH, Offenburg, Alemania). La señal de fluorescencia fue normalizada mediante el ensayo de viabilidad celular MTT.

### **3.12. Estudio del Potencial de Membrana Mitocondrial (PMM).**

La pérdida del potencial de membrana mitocondrial fue analizada mediante dos métodos:

(a) *Muse Cell Analyzer* (Millipore, Hayward, CA, Estados Unidos) y (b) microscopía de fluorescencia.

#### ***Muse Cell Analyzer***

Para determinar el PMM las células fueron sembradas a una densidad de  $1,5 \times 10^5$  células por pocillo en placas de 6 pocillos y tratadas con el extracto de romero a diferentes concentraciones (10-40  $\mu\text{g/mL}$ ). Una vez finalizado el tratamiento, se tripsinizaron, se lavaron con PBS y se añadieron 195  $\mu\text{L}$  del reactivo *Muse Mitopotential Kit* (Millipore, Hayward, CA, USA), una sonda catiónica lipofílica, durante 20 minutos a 37°C y 5% de CO<sub>2</sub>. Una vez transcurrido este tiempo, se añadieron 5  $\mu\text{L}$  de la sonda 7-AAD, un marcador de muerte celular, durante 5 minutos a temperatura ambiente. A continuación, se determinó el porcentaje de células despolarizadas mediante la adquisición de los datos de fluorescencia empleando la tecnología del equipo *Muse Cell Analyzer* (Millipore, Hayward, CA, USA).

#### **Microscopía de fluorescencia**

El compuesto fluorescente MitoTracker Red CMXRos (Molecular Probes, Invitrogen, Europa) se introduce en las células y queda retenido en las mitocondrias activas que conservan el PMM. El compuesto fluorescente MitoTracker Green FM tiñe las mitocondrias de las células vivas independientemente del potencial de membrana mitocondrial. De esta manera, pueden

distinguirse por microscopía de fluorescencia las células que no sufrieron una pérdida del PMM de aquellas que sí lo hicieron.

Las células fueron sembradas a una densidad de  $5 \times 10^3$  células por pocillo en placas de 96 pocillos y tratadas con el extracto de romero a diferentes concentraciones (10-40  $\mu\text{g/mL}$ ). Una vez finalizado el tratamiento, las células se lavaron con PBS y se incubaron con 200 nM de MitoTracker Red CMXRos y 200 nM de MitoTracker Green en medio de cultivo completo durante 30 minutos a 37°C y 5% de CO<sub>2</sub>. Finalmente, la fluorescencia se cuantificó mediante el equipo *Cytation 3 Cell Imaging Multi-mode* (BioTek, Alemania) (**Figura 24**).



**Figura 24.** *Cytation 3 Cell Imaging Multi-mode*.

### 3.13. Transfección siRNA.

Para la transfección se utilizó un pequeño ARN de interferencia, siRNA (del inglés, *small interfering*) específico para Nrf2 (Santa Cruz, Europa). Las células fueron sembradas a una densidad de  $5 \times 10^3$  células por pocillo y se transfecaron mediante el reactivo *Lipofectamine 2000 Transfection Reagent* (Invitrogen, Europa), un compuesto catiónico que forma liposomas y cuya eficiencia en la introducción de este tipo de material genético en los distintos tipos celulares es muy alta. Transcurridas 24 horas desde la transfección, las células fueron tratadas con el extracto de romero a 20 y 40  $\mu\text{g/mL}$  durante 24 horas. Al finalizar el tratamiento, se realizó un

ensayo de viabilidad celular mediante el reactivo MTT y se midieron las especies reactivas de oxígeno mediante la sonda H<sub>2</sub>DCF-DA.

### 3.14. Expresión de proteínas mediante *Dot-Blot*.

Para confirmar el silenciamiento del factor de transcripción Nrf2, se estudió la expresión de la proteína mediante el ensayo de *Dot-Blot*. Las células fueron transfectadas mediante el protocolo descrito previamente y sembradas a una densidad de 1,5x10<sup>5</sup> células por pocillo en placas de 6 pocillos.

#### Extracción de proteínas

Una vez finalizado el ensayo, las células se tripsinizaron y se lavaron con PBS. A continuación, se centrifugaron y se resuspendieron en tampón de lisis (50 mM Tris pH 7,4, 1% Igepal CA-630, 150 mM de NaCl, 5 mM de EDTA y 10 mg/mL de inhibidor de proteasas Pefabloc, (Sigma, Europa)). Las células se sometieron posteriormente a tres ciclos de congelación/descongelación y se centrifugaron a 12.000 rpm durante 5 minutos. El precipitado celular se eliminó y la concentración de proteína correspondiente a los extractos celulares (sobrenadante) se determinó mediante el equipo *NanoDrop 1000c* (Thermo Scientific, Europa).

#### Inmunodetección

La detección de proteínas se realizó mediante el equipo *Dot-Blot* (BioRad). Para ello se preparó una membrana de nitrocelulosa del tamaño correspondiente al equipo y se procedió al montaje de todas las piezas del mismo (**Figura 25**). De cada extracto proteico, en función de su concentración, se tomó el volumen correspondiente a 10 µg de proteína y se añadieron las muestras a los pocillos seleccionados. La absorción de la muestra mediante vacío durante 10 minutos provocó la adhesión de la proteína a la membrana, quedando en forma de mancha o *dot*. A continuación, se lavó la membrana de nitrocelulosa tres veces con tampón de lavado

(0,05% de Tween 20 en PBS 1x) y se bloqueó con tampón de bloqueo (5% de leche desnatada en polvo en tampón de lavado) durante 1 hora a temperatura ambiente y en agitación. Una vez bloqueada la membrana, se añadieron los anticuerpos primarios correspondientes para las proteínas  $\beta$ -actina (normalización) y Nrf2, en una dilución 1:500 en tampón de lavado durante 1 hora a temperatura ambiente y en agitación.

Terminado dicho proceso, se procedió a lavar la membrana tres veces con tampón de lavado. Seguidamente, se añadieron los anticuerpos secundarios en una dilución 1:1000 en tampón de lavado durante 1 hora a temperatura ambiente y agitación. Por último, se lavó la membrana tres veces con tampón de lavado y se añadió el reactivo de revelado *WesternSure Premium* (Li-COR, Estados Unidos) durante 5 minutos. La membrana se reveló mediante el sistema de imagen C-Digit-3600 (Li-COR, Estados Unidos).

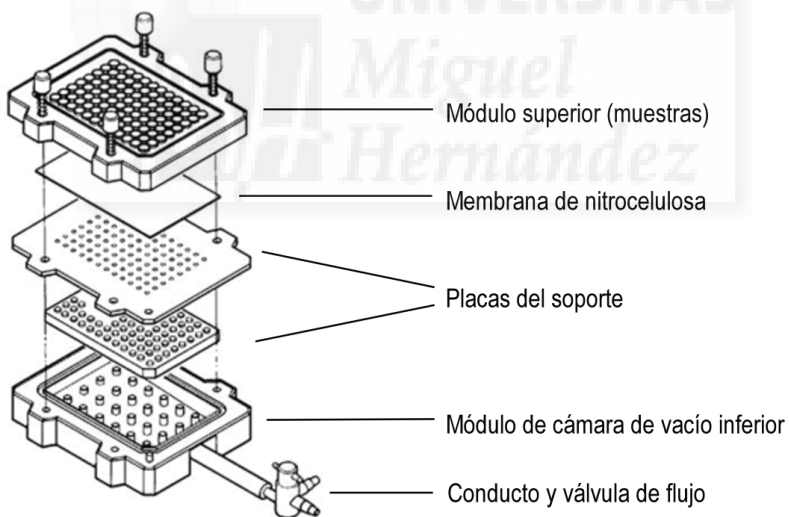


Figura 25. Piezas principales del equipo *Dot-Blot* de BioRad.

### 3.15. Ensayos de proliferación y migración.

Los diferentes aspectos relacionados con la proliferación y migración celular se determinaron mediante tres métodos: el equipo *xCelligence Real Time Cell Analysis*, el ensayo de capacidad clonogénica o de formación de colonias y el ensayo de cierre de herida o *wound healing*.

#### Determinación de la proliferación celular mediante *xCelligence Real Time Cell Analysis (RTCA)*

La proliferación celular se determinó mediante el equipo *RTCA* (Roche Diagnostics GmbH, Alemania) (**Figura 26**), situado en un incubador a 37°C, 5% de CO<sub>2</sub> y ambiente húmedo. El equipo mide cambios en la impedancia eléctrica cuando las células se adhieren y proliferan en una placa de cultivo, cubierta con una matriz de microelectrodos de oro. La impedancia se muestra como un parámetro denominado índice celular (IC), que es directamente proporcional a la superficie cubierta por las células [98-100].

Las células fueron sembradas a una densidad de  $7,5 \times 10^3$  células por pocillo para la línea celular SW480,  $1,5 \times 10^4$  para la línea HGUE-C-1 y  $4,0 \times 10^4$  para la línea HT-29 en las propias placas del equipo. Transcurridas 24 horas, las células fueron tratadas con el extracto de romero a diferentes concentraciones (20 y 40 µg/mL) durante 72 horas. El índice celular (IC) fue registrado cada hora por el programa informático del equipo RTCA.



**Figura 26.** Equipo *xCELLigence RTCA DP* para determinar proliferación, migración e invasión celular.

### Ensayo de capacidad clonogénica: formación de colonias

Para determinar el efecto antiproliferativo del extracto de romero se realizó un ensayo de formación de colonias. Para ello, las células fueron sembradas a una densidad de  $5 \times 10^3$  células por pocillo en placas de 6 pocillos y tratadas con el extracto de romero a diferentes concentraciones (20 y 40  $\mu\text{g}/\text{mL}$ ) durante 24 horas. Una vez finalizado el tratamiento, las células se incubaron con medio de cultivo completo durante 7 días. A continuación, las células se lavaron dos veces con PBS y se fijaron las colonias con etanol al 95% durante 10 minutos. A continuación, las colonias fueron teñidas con cristal violeta al 0,1% durante 10 minutos y lavadas tres veces con PBS. Como criterio de recuento se estableció que una colonia estaba formada a partir de 50 células y el recuento se realizó mediante el equipo *Cytation 3 Cell Imaging Multi-mode* (BioTek, Alemania).

### Ensayo de migración celular: *wound healing*

Para determinar la capacidad de migración de las células se realizó el ensayo de cierre de herida (*wound healing*). Para ello, las células fueron sembradas en placas de 96 pocillos y se esperó a que llegasen al 100% de confluencia. Se realizó una herida mediante una punta de micropipeta de 10  $\mu\text{L}$  en el centro del pocillo y se lavaron todos los pocillos con PBS. A continuación, las células se incubaron con la sonda fluorescente Hoechst 33342 a 10  $\mu\text{g}/\text{mL}$  en medio de cultivo completo durante 20 minutos a 37°C y 5% de CO<sub>2</sub>. Transcurrido este periodo, las células fueron tratadas con el extracto de romero a diferentes concentraciones (10-40  $\mu\text{g}/\text{mL}$ ) durante 72 horas. El porcentaje de cierre de la herida se determinó a través de imágenes obtenidas por el equipo *Cytation 3 Cell Imaging Multi-mode* (BioTek, Alemania) con un objetivo 20x. La intensidad de la fluorescencia se cuantificó con el programa informático Image J 1.48v.

### 3.16. Ensayo de toxicidad oral aguda en ratas.

El ensayo de toxicidad oral aguda se llevó a cabo según la guía 420 de la Organización para la Cooperación y Desarrollo Económico (OCDE). Para el ensayo de toxicidad oral aguda se utilizaron ratas macho Wistar. El vehículo utilizado para disolver el extracto de romero fue aceite de girasol. En primer lugar, se administró a una rata una dosis de 300 mg/kg peso corporal (n=1). Una vez confirmado que no existía mortalidad o signos de toxicidad, se administró a otra rata una dosis de 2000 mg/kg de peso corporal. Como no se detectó ningún signo aparente de toxicidad, se procedió a la administración de más animales con la dosis de 2000 mg/kg (n=5). Como controles se utilizaron un animal sin tratamiento y otro con el vehículo utilizado, en este caso, aceite de girasol (n=2). Los animales se mantuvieron con pienso y agua *ad libitum*, a una temperatura de  $22^{\circ}\text{C} \pm 2^{\circ}\text{C}$ , un fotoperíodo de 12 horas y una humedad relativa de  $70 \pm 5\%$ .

Durante el periodo de valoración toxicológica de los animales, se pesaron cada 4-5 días, ya que la bajada de peso evidenciaría un claro efecto tóxico [101]. Una vez terminado dicho periodo, los animales se sacrificaron mediante asfixia por CO<sub>2</sub> seguida de dislocación cervical. A continuación, se extrajeron los siguientes órganos: bazo, corazón, pulmón, riñones e hígado y se fijaron en formaldehido al 4%. Los órganos se incluyeron en bloques de parafina y se obtuvieron secciones transversales de 5 µm de espesor que se tiñeron con hematoxilina y eosina para su posterior examen histológico por el servicio de Anatomía Patológica perteneciente al Hospital General Universitario de Alicante, mediante microscopía óptica (Olympus BX50, Barcelona, España).

En todo momento se siguieron las prerrogativas incluidas en el Real Decreto 53/2013 y los consejos del personal del Servicio de Experimentación Animal (SEA) de la Universidad Miguel Hernández de Elche (UMH). El ensayo contó además con la aprobación del Órgano Evaluador de Proyectos (Órgano Habilitado) de la UMH.

### 3.17. Ensayo antitumoral en ratones inmunodeprimidos.

Para determinar la actividad antitumoral *in vivo* del extracto de romero se emplearon ratones macho atípicos desnudos BALB/c proporcionados por Harlan Interfauna Ibérica (Barcelona, España). Debido a la inmunodeficiencia que presentan estos animales, el cuidado, tratamiento y seguimiento se llevó a cabo en condiciones de esterilidad y dentro de las instalaciones de barrera del SEA de la UMH. En este caso, la inoculación de los xenotransplantes se llevó a cabo con la línea celular de cáncer colorrectal, HT-29, con una cantidad total de  $2 \times 10^6$  células por ratón resuspendidas en 200  $\mu\text{L}$  de PBS e inyectadas de manera subcutánea (**Figura 27**).

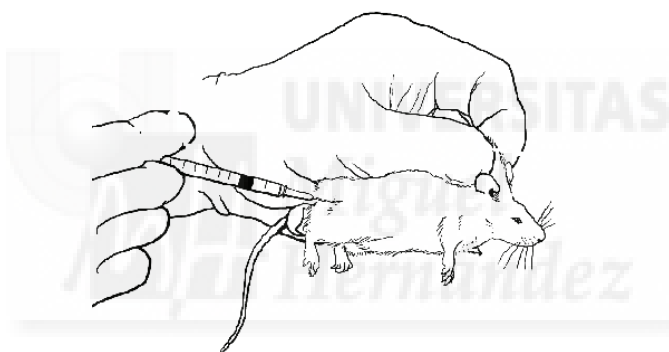


**Figura 27.** Inoculación subcutánea de las células HT-29 en ratones inmunodeprimidos.

Los animales se dividieron en tres grupos para su posterior estudio (10-12 ratones/grupo). En el primer grupo, a los animales se les administró mediante sonda gástrica el vehículo utilizado para disolver el extracto de romero (control), un vehículo formado por 50% de PBS, 40% de PEG400 y 10% de Tween 80. En el segundo grupo, los animales fueron pretratados con el extracto de romero dos semanas antes de la inoculación de las células tumorales con una dosis de 200 mg/kg de peso corporal (3 veces a la semana). Y, por último, en el tercer grupo los animales fueron tratados con la misma dosis, 200 mg/kg de peso corporal (3 veces a la semana), una vez que el volumen del tumor alcanzó aproximadamente 100  $\text{mm}^3$ . El volumen del tumor se

midio dos veces a la semana mediante un calibre pie de rey y la evolución del peso corporal se tuvo en cuenta para valorar un posible efecto tóxico. Los animales se mantuvieron con pienso y agua *ad libitum*, a una temperatura de  $22^{\circ}\text{C} \pm 2^{\circ}\text{C}$ , un fotoperiodo de 12 horas y una humedad relativa de  $70 \pm 5\%$ .

En todo momento se siguieron las prerrogativas incluidas en el Real Decreto 53/2013 y los consejos del personal del SEA de la UMH. El ensayo contó además con la aprobación del Órgano Evaluador de Proyectos (Órgano Habilitado) de la UMH.

### 3.18. Preparación de liposomas (LUVs).

La preparación de liposomas se llevó a cabo mediante dos tipos de lípidos: fosfatidilserina de yema de huevo (80%) y colesterol (20%) (Avanti Polar Lipids Inc., Alabaster, AL, Estados Unidos). Las soluciones madre se prepararon disolviendo las cantidades requeridas de los diferentes lípidos en cloroformo/metanol, 1:1 (v/v). La cantidad apropiada de lípidos y de extracto de romero se secó bajo una corriente de  $\text{N}_2$ . Las últimas trazas de disolvente se eliminaron manteniendo las muestras a vacío durante 3 horas. Una vez seca dicha mezcla, se disolvió en un tampón de hidratación (100 mM de NaCl, 0,1 mM de EDTA y 10 mM de HEPES a pH 7,4) durante 30 minutos a  $37^{\circ}\text{C}$  en agitación. Para la formación de liposomas unilamelares grandes (LUVs), se procedió a la extrusión de la solución durante 25 ciclos a través de una membrana de policarbonato de 100 nm mediante un *LiposoFast extruder* (Avestin, Europa). Para la separación de los liposomas del extracto de romero libre, la mezcla se centrifugó en tubos AMICON (Millipore, Europa) a 3800 rpm (2 ciclos de 30 minutos).

### 3.19. Absorción *in vitro* de los compuestos del extracto de romero.

Para determinar la absorción de los principales compuestos presentes en el extracto de romero se utilizó la línea celular Caco-2. El ensayo de absorción intestinal *in vitro* mediante esta línea celular es un modelo ampliamente aceptado y utilizado [102].

Las células fueron sembradas en insertos de policarbonato (Millipore, España) a una densidad de  $5 \times 10^5$  células por pocillo y en placas de 6 pocillos. El medio de cultivo se reemplazó cada 2-3 días tanto en la cámara apical (AP) como en la cámara basolateral (BL) (**Figura 28**).

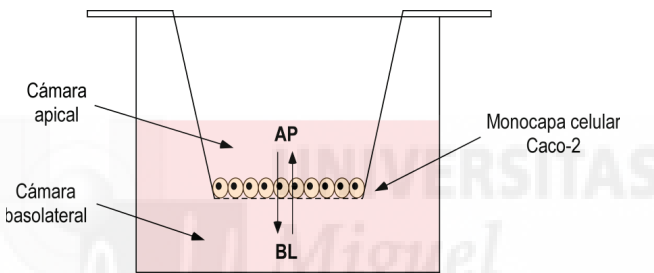


**Figura 28.** Esquema del pocillo formado por el inserto y la monocapa de células Caco-2.

Una vez alcanzados los 19-21 días post-siembra, la integridad de la monocapa se determinó midiendo la resistencia eléctrica transepitelial (TEER) mediante un micro-polímetro (Millicell-ERS, Millipore, España), que mide el potencial de membrana y la resistencia de las células en cultivo (**Figura 29**). A continuación, las células se trataron con extracto de romero libre a una concentración de 200  $\mu\text{g}/\text{mL}$  y extracto de romero encapsulado en liposomas (1,5 mM) disueltos en tampón HBSS a pH 7,4 (del inglés, *Hank's Balanced Salt Solution*).



Figura 29. Representación de la medida de la resistencia eléctrica transepitelial (TEER).

La monocapa celular se lavó dos veces con HBSS precalentado y se incubó con dicha disolución a 37°C durante 30 minutos. El extracto de romero de forma libre y liposomada se añadió al compartimento correspondiente para la cámara AP (2,2 mL) y para la cámara BL (3,2 mL). Se recogieron muestras a diferentes tiempos (0, 30, 60, 90 y 120 minutos) en la cámara receptora y se repuso el mismo volumen de muestra recogida. La incubación durante todo el experimento se realizó a 37°C durante 120 minutos a 50 rpm. Al final del ensayo se recuperó la monocapa y las células se lisaron mediante 3 ciclos de congelación/descongelación seguidos de 10 minutos de sonicación.

Las muestras se centrifugaron a 14.000 rpm durante 15 minutos a 4°C y se obtuvieron dos fracciones: (a) los sobrenadantes (fracción citoplasmática) y (b) los precipitados (membranas). Las muestras se conservaron a -80°C hasta su posterior análisis por cromatografía líquida de alta resolución (HPLC).

### 3.20. Análisis de las muestras procedentes del ensayo de permeabilidad en la línea celular Caco-2 mediante HPLC-MS.

Las muestras procedentes del ensayo de permeabilidad realizado en monocapas de células Caco-2 se analizaron mediante un cromatógrafo UPLC Agilent 1260 (Agilent Technologies, Palo Alto, CA, Estados Unidos). El cromatógrafo de líquidos estaba equipado con una bomba binaria, un desgasificador, un automuestrador, un compartimento termostatizado de columna y un detector DAD. La columna empleada para la separación de los compuestos fue una columna Agilent Zorbax Eclipse Plus C-18, de dimensiones 4,6x150 mm y tamaño de partícula de 1,8 µm. Las fases móviles utilizadas fueron como fase A 0,1% de ácido fórmico en agua y como fase B acetonitrilo. El gradiente empleado fue: 0 min, 5% de B; 5 min, 62% de B; 10 min, 68% de B; 19 min, 80% de B; 34 min, 95% de B; y 37 min, 5% de B. La velocidad de flujo fue de 0,8 mL/min y el compartimento de las muestras se refrigeró a 4°C para evitar la degradación de las muestras. La detección se realizó mediante un espectrómetro de masas Agilent 6540 de Ultra Alta Definición (UHD) QTOF con una interfase ESI. La detección mediante espectrometría de masas se realizó en modo de ionización negativo con un rango de masas de 100-1700 m/z.

Los parámetros óptimos fueron los siguientes: temperatura, 400°C, flujo de gas, 12 L/min; nebulizador, 20 psig; capilar, 4000 V; fragmentador, 130 V; voltaje, 500 V; skimmer, 45 V y octopolo 1 Vpp RF, 750 V. La cuantificación de los compuestos se llevó a cabo con los siguientes patrones comerciales: carnosol, ácido carnósico, ácido ursólico, ácido rosmarínico, genkwanina y diosmetina, todos ellos resuspendidos en HBSS (compuestos obtenidos de Sigma-Aldrich, Steinheim, Alemania y Extrasynthese, Genay, Francia). La adquisición y análisis de los datos se llevó a cabo mediante el programa informático Masshunter B.06.00 (Agilent Technologies, Estados Unidos).

### 3.21. Determinación de la Permeabilidad Aparente ( $P_{app}$ ).

Una vez cuantificadas las concentraciones de todos los compuestos identificados en las muestras derivadas de la cámara AP y BL, se utilizaron dichos valores para calcular el coeficiente de permeabilidad aparente ( $P_{app}$ ). Dicho parámetro fue calculado mediante la siguiente fórmula:

$$P_{app} \text{ (cm/s)} = \frac{dQ}{dt} \cdot \frac{1}{A \cdot C_0 \cdot 60}$$

Donde  $P_{app}$  es la permeabilidad aparente (cm/s),  $dQ/dt$  representa la velocidad de paso ( $\mu\text{M/s}$ ),  $A$  es el área de difusión de la monocapa ( $\text{cm}^2$ ),  $C_0$  es la concentración inicial del compuesto en la cámara dadora ( $\mu\text{M}$ ) y 60 es un factor de conversión [103].

### 3.22. Análisis estadístico.

Los datos obtenidos se analizaron mediante el programa informático *GraphPad Prism* versión 5.01 (GraphPad Software Inc., CA, Estados Unidos) para realizar un análisis de la varianza (ANOVA) con un nivel de confianza del 95% ( $p<0,05$ ) con el fin de identificar diferencias significativas entre las condiciones estudiadas. Los valores se representaron como la media  $\pm$  desviación estándar, SD (del inglés, *Standard Deviation*) de 5-12 réplicas, dependiendo del ensayo. El cálculo de las  $IC_{50}$  se llevó a cabo mediante un análisis de regresión no lineal (curva sigmoidea).

## **4. RESULTADOS**



## **Capítulo primero**

**Fraccionamiento e identificación de los compuestos bioactivos de un  
extracto de romero que contribuyen al efecto antiproliferativo en células  
humanas de cáncer de colon**



## 1. Caracterización cuantitativa del extracto de romero.

En el presente capítulo se realizó la caracterización cuantitativa de los principales compuestos presentes en el extracto de romero. Para este propósito se procedió a cuantificar el extracto por HPLC-ESI-QTOF-MS, utilizando los estándares adecuados, tal y como se menciona en la sección de Metodología. Dada la inexistencia a nivel comercial de todos los compuestos del extracto, se escogieron varios compuestos que se utilizaron como estándares puros, y que estaban disponibles comercialmente, los cuales tenían una estructura química muy similar a los compuestos presentes en el extracto. Los patrones elegidos fueron los siguientes: apigenina, diosmetina, genkwanina, carnosol, ácido carnósico, ácido ursólico, ácido rosmarínico y luteolina.

La **Figura 30** muestra el cromatograma de pico base del extracto de romero, en el cual se han enumerado los picos principales según el orden de elución. Dicho extracto fue caracterizado cualitativamente en un trabajo anterior [104], sin embargo, en dicho trabajo no se realizó el análisis cuantitativo, el cual se ha desarrollado durante la presente Tesis Doctoral.

La cuantificación realizada muestra dos grandes familias de compuestos bioactivos. Por un lado, la familia de los triterpenos (49,5% en peso del total de compuestos identificados), compuesta por la anemosapogenina y los ácidos micromérico, betulínico, ursólico, augústico y bentámico. Por otro lado, se encuentra la familia de los diterpenos (44,3% en peso), compuesta por los ácidos carnósico y 12-metoxicarnósico, carnosol, rosmanol, rosmadial, epiisorrosmanol, epirrosmanol, miltipolona, rosmaridifenol e hinoquiona. A estas dos grandes familias hay que añadir la formada por los flavonoides (2,1% en peso), compuesta por la genkwanina, apigenina, hispidulina, cirsiliol, diosmetina y cirsimaritina (**Figura 31**). Respecto al peso seco, los diterpenos representaron un 10,87%, los triterpenos un 12,16%, y por último, los flavonoides un 0,52% (**Tabla 3**).

Teniendo en cuenta los compuestos de manera individual, el ácido carnósico fue el compuesto más abundante (83 mg/g de extracto seco) seguido de los triterpenos ácidos micromérico, betulínico y ursólico (47, 38 y 21,5 mg/g, respectivamente). El diterpeno carnosol también fue relevante en la cuantificación (10 mg/g).

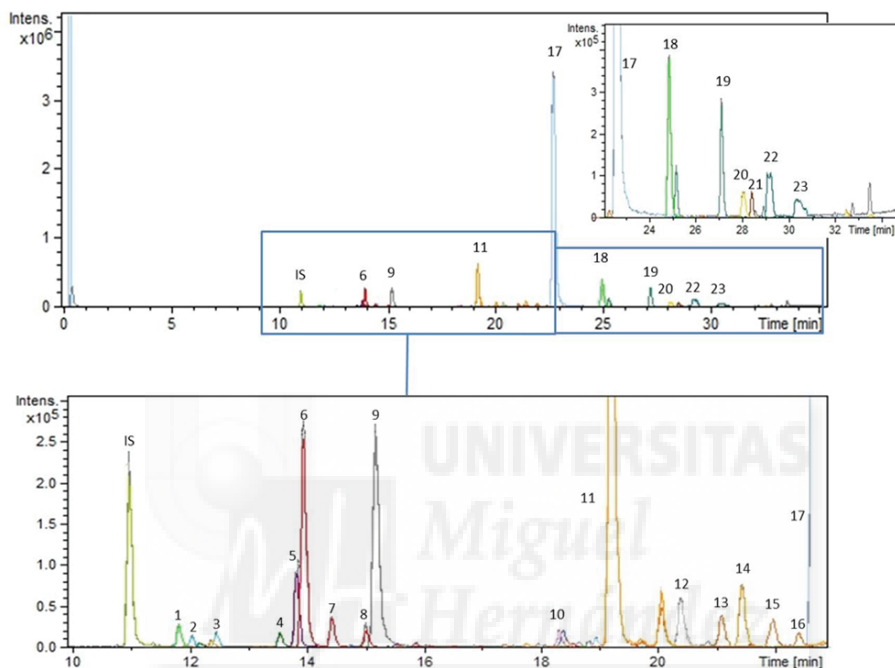


**Figura 30.** Cromatograma de pico base obtenido por HPLC-ESI-QTOF-MS del extracto de romero. Los números de los picos identificados corresponden con su orden de elución.

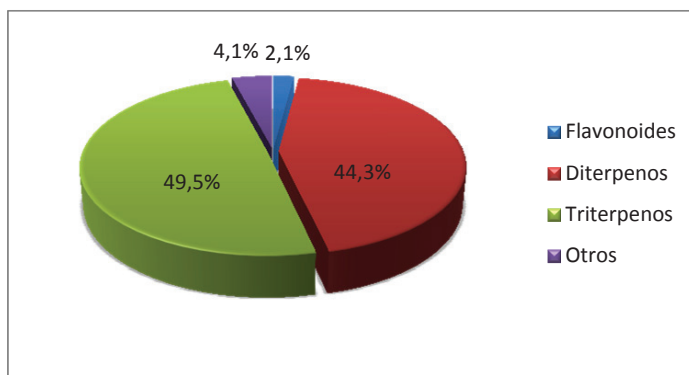


**Figura 31.** Gráfico circular con los porcentajes (%) en peso de las familias de compuestos presentes en el extracto de romero.

Tabla 3. Cuantificación de los compuestos identificados en el extracto de romero.

Pico	TR (min)	m/z experimental	m/z calculada	Fórmula molecular	Compuesto	Concentración (mg/g) ± SD	Peso seco (%)
1	11,84	269,0461	269,0455	C <sub>15</sub> H <sub>10</sub> O <sub>5</sub>	Apigenina	0,50 ± 0,02	0,05
2	12,18	299,0565	299,0561	C <sub>16</sub> H <sub>12</sub> O <sub>6</sub>	Hispidulina	0,31 ± 0,01	0,03
3	12,40	329,0665	329,0667	C <sub>17</sub> H <sub>13</sub> O <sub>7</sub>	Cirsiliol	0,34 ± 0,01	0,03
4	13,55	299,0553	299,0561	C <sub>16</sub> H <sub>12</sub> O <sub>6</sub>	Diosmetina	0,62 ± 0,04	0,06
5	13,83	313,0721	313,0718	C <sub>17</sub> H <sub>14</sub> O <sub>6</sub>	Cirsimartina	0,78 ± 0,07	0,08
6	13,94	345,1714	345,1707	C <sub>20</sub> H <sub>26</sub> O <sub>5</sub>	Rosmanol	4,40 ± 0,10	0,44
7	14,43	345,1709	345,1707	C <sub>20</sub> H <sub>26</sub> O <sub>5</sub>	Epiisorosmanol	0,80 ± 0,05	0,08
8	15,01	345,1709	345,1707	C <sub>20</sub> H <sub>26</sub> O <sub>5</sub>	Epirosmanol	0,38 ± 0,02	0,04
9	15,16	283,0620	283,0612	C <sub>16</sub> H <sub>12</sub> O <sub>5</sub>	Genkwanina	2,61 ± 0,05	0,26
10	18,36	299,1652	299,1653	C <sub>19</sub> H <sub>24</sub> O <sub>3</sub>	Miltipolona	0,32 ± 0,04	0,03
11	19,18	329,1770	329,1758	C <sub>20</sub> H <sub>26</sub> O <sub>4</sub>	Carnosol	10,00 ± 1,00	1,00
12	20,35	343,1548	343,1551	C <sub>20</sub> H <sub>24</sub> O <sub>5</sub>	Rosmadial	1,36 ± 0,06	0,14
13	21,04	471,3471	471,3480	C <sub>30</sub> H <sub>48</sub> O <sub>4</sub>	Anemosapogenina	6,50 ± 0,50	0,65
14	21,38	315,1960	315,1966	C <sub>20</sub> H <sub>28</sub> O <sub>3</sub>	Rosmaridfenol	0,25 ± 0,05	0,02
15	21,91	471,3471	471,3480	C <sub>30</sub> H <sub>48</sub> O <sub>4</sub>	Ácido augústico	6,50 ± 0,50	0,65
16	22,35	471,3474	471,3480	C <sub>30</sub> H <sub>48</sub> O <sub>4</sub>	Ácido bentámico	2,10 ± 0,20	0,21
17	22,65	331,1935	331,1915	C <sub>20</sub> H <sub>28</sub> O <sub>4</sub>	Ácido camósico	83,00 ± 4,00	8,30
18	24,89	345,2083	345,2071	C <sub>21</sub> H <sub>30</sub> O <sub>4</sub>	Ácido 12-metoxicamósico	7,20 ± 0,01	0,72
19	27,11	317,2128	317,2122	C <sub>20</sub> H <sub>30</sub> O <sub>3</sub>	(9)-shogaol	10,10 ± 0,30	1,01
20	28,04	453,3356	453,3374	C <sub>30</sub> H <sub>46</sub> O <sub>3</sub>	Ácido micromérico	47,00 ± 2,00	4,70
21	28,40	299,2015	299,2017	C <sub>20</sub> H <sub>28</sub> O <sub>2</sub>	Hinoquiona	0,95 ± 0,08	0,09
22	29,19	455,3519	455,3531	C <sub>30</sub> H <sub>48</sub> O <sub>3</sub>	Ácido betulínico	38,00 ± 3,00	3,80
23	30,20	455,3519	455,3531	C <sub>30</sub> H <sub>48</sub> O <sub>3</sub>	Ácido ursólico	21,50 ± 0,60	2,15
					Tota flavonoides	5,16	0,52
					Total diterpenos	108,66	10,87
					Total triterpenos	121,60	12,16
					Total otros	10,10	1,01

## 2. Fraccionamiento y análisis de los compuestos del extracto de romero.

El fraccionamiento de los compuestos principales presentes en el extracto de romero se llevó a cabo mediante cromatografía semi-preparativa para determinar el efecto antiproliferativo individual de cada una de las fracciones obtenidas. Se seleccionaron las 10 fracciones que según el análisis por cromatografía se correspondían con los compuestos mayoritarios del extracto de romero. No obstante, algunas de las fracciones contenían más de un compuesto. La composición de estas fracciones (**Tabla 4**) se analizó por HPLC-QTOF y la pureza para todas las fracciones fue de 72% en peso o superior, excepto para las fracciones 4 (formada por 3 compuestos), 9 (2 compuestos) y 10 (2 compuestos).

**Tabla 4.** Composición y pureza (%) de las fracciones seleccionadas para los ensayos posteriores de proliferación celular.

Número fracción	m/z experimental	Fórmula molecular	Compuesto propuesto	Pureza (%)
F1	345,1715	C <sub>20</sub> H <sub>26</sub> O <sub>5</sub>	Rosmanol	82,6
F2	345,1714	C <sub>20</sub> H <sub>26</sub> O <sub>5</sub>	Epiisorrosmanol	83,6
F3	283,0616	C <sub>16</sub> H <sub>12</sub> O <sub>5</sub>	Genkwanina	99,3
	299,1655	C <sub>19</sub> H <sub>24</sub> O <sub>3</sub>	Miltipolona	40,0
F4	457,3325	C <sub>29</sub> H <sub>46</sub> O <sub>4</sub>	Notohamosina B	30,1
	471,3483	C <sub>30</sub> H <sub>48</sub> O <sub>4</sub>	Anemosapogenina	13,1
F5	329,1755	C <sub>20</sub> H <sub>26</sub> O <sub>4</sub>	Carnosol	82,6
F6	343,1556	C <sub>20</sub> H <sub>24</sub> O <sub>5</sub>	Rosmadial	72,0
F7	331,1922	C <sub>20</sub> H <sub>28</sub> O <sub>4</sub>	Ácido carnósico	98,7
F8	345,2070	C <sub>21</sub> H <sub>30</sub> O <sub>4</sub>	Ácido 12-metoxicarnósico	98,6
F9	313,1819	C <sub>20</sub> H <sub>26</sub> O <sub>3</sub>	Taxodiona	44,0
	317,2137	C <sub>20</sub> H <sub>30</sub> O <sub>3</sub>	(9)-shogaol	50,0
F10	299,2021	C <sub>20</sub> H <sub>28</sub> O <sub>2</sub>	Hinoquiona	13,8
	455,3518	C <sub>30</sub> H <sub>48</sub> O <sub>3</sub>	Ácido betulínico	81,0

### 3. Efecto antiproliferativo del extracto de romero y de sus fracciones.

La actividad antiproliferativa/citotóxica del extracto de romero y sus compuestos se analizó en las líneas celulares HGUE-C-1, HT-29 y SW480 durante 24 y 48 horas. El tratamiento con el extracto de romero mostró una disminución dosis-dependiente en la viabilidad celular en todas las líneas de cáncer de colon (**Figura 32**).

A las 24 horas de tratamiento, la línea celular HGUE-C-1 presentó un comportamiento más sensible al tratamiento ( $IC_{50}$ : 12,7  $\mu\text{g/mL}$ ) que SW480 ( $IC_{50}$ : 18,1  $\mu\text{g/mL}$ ) y HT-29 ( $IC_{50}$ : 20,4  $\mu\text{g/mL}$ ). Sin embargo, a las 48 horas de tratamiento las líneas HGUE-C-1 y SW480 mostraron un comportamiento muy similar ( $IC_{50}$ : 9,2  $\mu\text{g/mL}$  y 8,1  $\mu\text{g/mL}$ , respectivamente), manteniendo la línea celular HT-29 la menor sensibilidad al tratamiento ( $IC_{50}$ : 14,8  $\mu\text{g/mL}$ ) (**Tabla 5**).



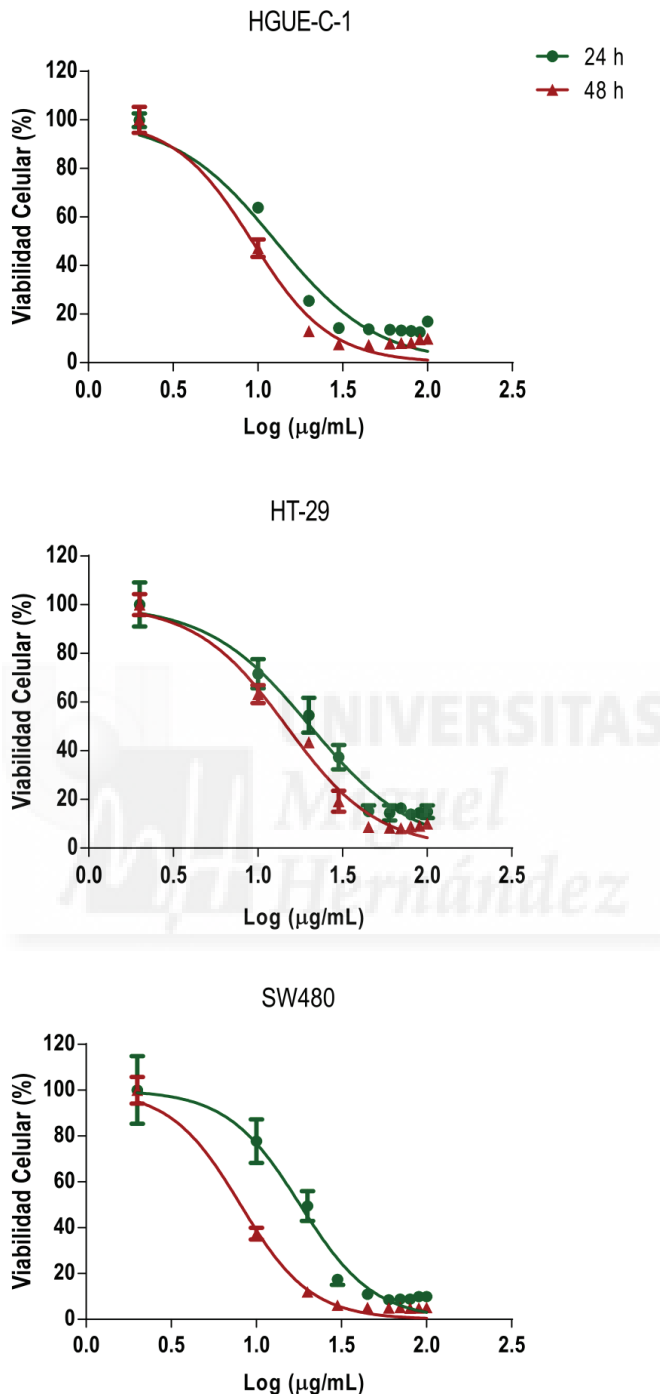


**Figura 32.** Curvas de inhibición de la proliferación celular del extracto de romero en las tres líneas celulares de colon, HGUE-C-1, HT-29 y SW480.

Las células se trataron con diferentes concentraciones del extracto de romero (10-100  $\mu\text{g/mL}$ ) durante 24 y 48 horas. Una vez finalizado el tratamiento se determinó la viabilidad mediante el ensayo de MTT. Los valores se presentan como porcentaje de viabilidad celular (%).

**Tabla 5.** Valores de IC<sub>50</sub> del extracto de romero en las tres líneas celulares de cáncer de colon a 24 y 48 horas de tratamiento.

Valores de IC <sub>50</sub> ( $\mu\text{g/mL}$ ) $\pm$ SD					
HGUE-C-1		HT-29		SW480	
24 h	48 h	24 h	48 h	24 h	48 h
12,7 $\pm$ 1,0	9,2 $\pm$ 1,0	20,4 $\pm$ 2,0	14,8 $\pm$ 1,0	18,1 $\pm$ 1,0	8,1 $\pm$ 0,6

La capacidad antiproliferativa de las fracciones del extracto de romero fue comparada con la capacidad del extracto completo. Para ello se trataron las células a diferentes concentraciones (30 y 60  $\mu\text{g/mL}$ ) durante 24 y 48 horas (**Figura 33**). El extracto de romero mostró un mayor efecto antiproliferativo o muy similar a las fracciones más activas ensayadas.

En la mayoría de las líneas celulares, las fracciones 5, 7, 9 y 10 presentaron un efecto antiproliferativo muy similar al extracto de romero, mientras que las fracciones 2, 3, 4 y 6 mostraron un menor efecto que el extracto completo. Por el contrario, las fracciones 1 y 8 mostraron una actividad similar a la del extracto de romero en la línea celular HGUE-C-1 y SW480, respectivamente.

En general, la mayoría de las fracciones mostraron una mayor actividad antiproliferativa en las células HGUE-C-1, en relación con las otras dos líneas celulares utilizadas y, en todos los casos, el extracto de romero presentó una inhibición de la proliferación celular igual o superior al ser comparado con las fracciones.

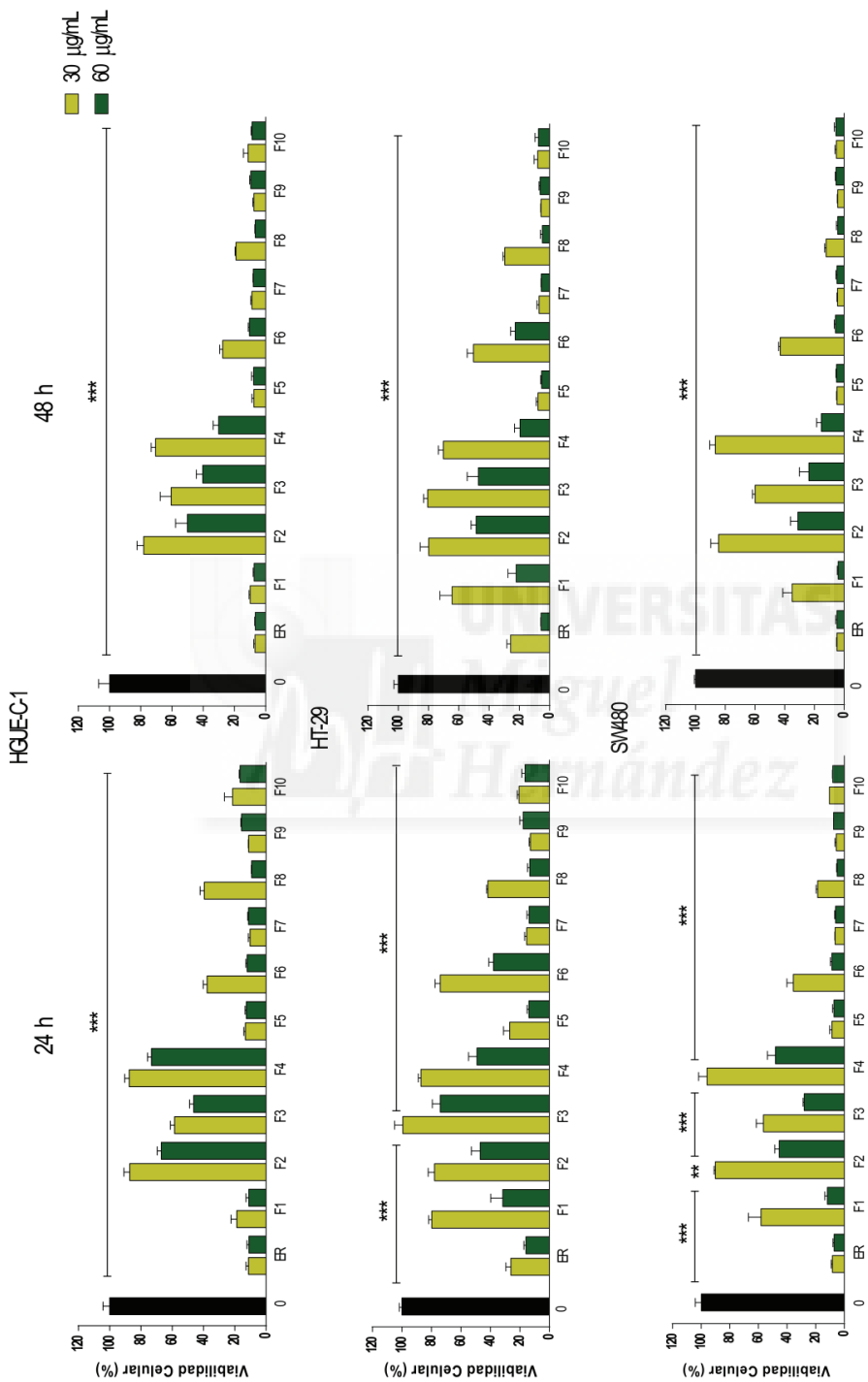


**Figura 33.** Efecto del extracto de romero y sus fracciones en la viabilidad celular de las tres líneas celulares de cáncer de colon, HGU-E-C1, HT-29 y SW480. Las células se trataron con diferentes concentraciones del extracto de romero y sus fracciones (30 y 60 µg/ml) durante 24 y 48 horas. Una vez finalizado el tratamiento se determinó la viabilidad celular mediante el ensayo de MTT. Los valores se presentan como porcentaje de viabilidad celular (%). \*\* ( $p<0.01$ ) y \*\*\* ( $p<0.001$ ) indican diferencias estadísticamente significativas.

## **Capítulo segundo**

**Actividad antiproliferativa y posibles mecanismos de acción del extracto de  
romero en modelos *in vitro* e *in vivo* de CCR**



## 1. Estudio del mecanismo de acción por el cual el ER inhibe la proliferación celular.

Una vez comparada la actividad antiproliferativa del extracto de romero frente a sus fracciones, se procedió al estudio del mecanismo de acción de dicho extracto. En primer lugar, se procedió a estudiar el ciclo celular en células tratadas con diferentes concentraciones del extracto de romero (10-40  $\mu\text{g/mL}$ ) durante 24 horas. Como se observa en la **Figura 34**, el extracto de romero provocó alteraciones en las fases del ciclo celular en todas las líneas estudiadas.

En la línea celular HGUE-C-1 se observó una disminución en la fase  $G_1/G_0$  y un incremento significativo de la fase Sub- $G_1$  a las máximas concentraciones estudiadas, llegando hasta un 12,8% a 40  $\mu\text{g/mL}$ . Por otro lado, en las líneas HT-29 y SW480 se observó una disminución en la fase  $G_1/G_0$  y un incremento significativo en la fase  $G_2/M$ . En las células HT-29 se observó un incremento del 14% a la máxima concentración estudiada, mientras que en las células SW480 se observaron diferencias estadísticamente significativas con un incremento del 12% a 30  $\mu\text{g/mL}$ .

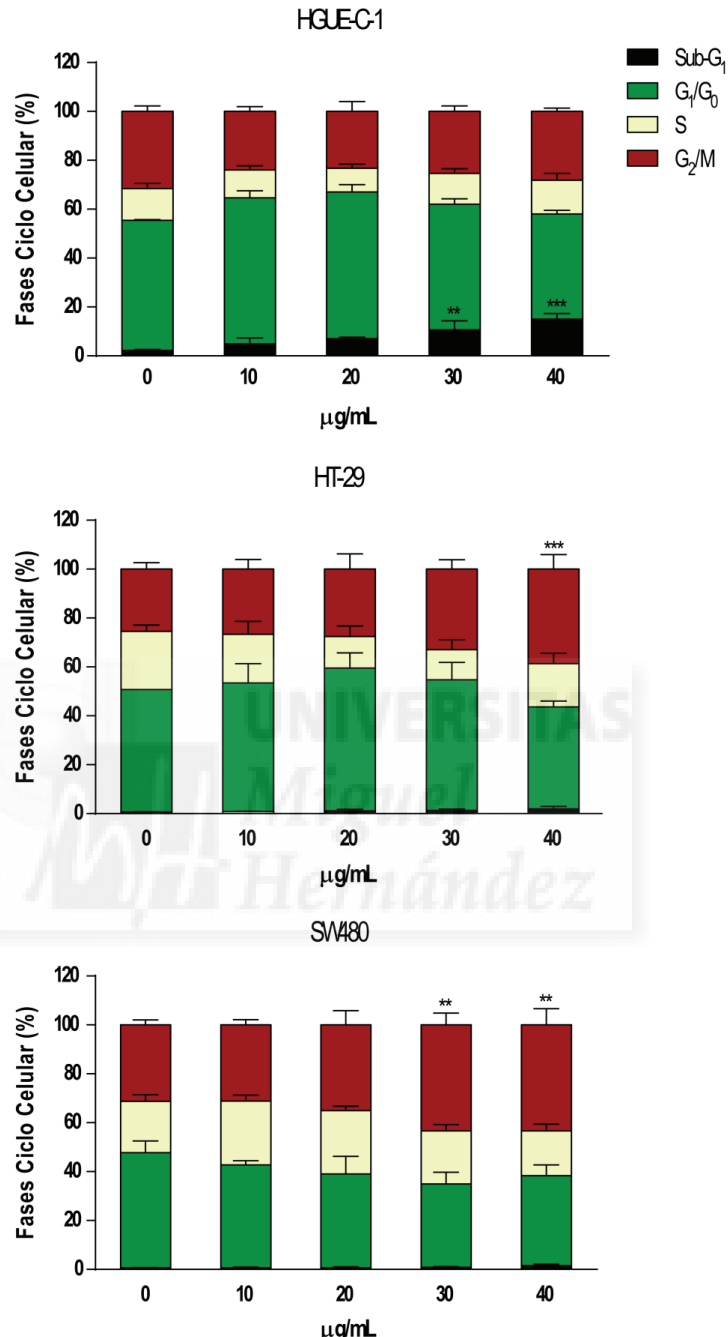


**Figura 34.** Efecto del extracto de romero en el ciclo celular en las tres líneas celulares de cáncer de colon, HGUE-C-1, HT-29 y SW480.

Las células se trataron con diferentes concentraciones del extracto de romero (10-40  $\mu\text{g/mL}$ ) durante 24 horas. Una vez finalizado el tratamiento, el ciclo celular se determinó mediante el equipo *Muse Cell Analyzer*. Los valores se presentan como porcentaje de las fases del ciclo celular. \*\* ( $p<0,01$ ) y \*\*\* ( $p<0,001$ ) indican diferencias estadísticamente significativas.

La siguiente etapa consistió en llevar a cabo la detección de apoptosis mediante Anexina-V en las tres líneas celulares. Las células se trataron con diferentes concentraciones del extracto de romero (10-40 µg/mL) durante 24 horas. El porcentaje de apoptosis se cuantificó tanto a nivel basal como tras la adición de los tratamientos. Como se puede observar en la **Figura 35**, a nivel basal existe un pequeño porcentaje de células apoptóticas que se corresponde con la muerte que las células sufren normalmente en cultivo. El tratamiento con el extracto de romero aumentó el porcentaje de células positivas en Anexina V-7-AAD (cuadrante superior derecho), lo que indica que una población de células se encontraba en situación de apoptosis tardía/necrosis en todas las líneas celulares. La línea celular HGUE-C-1 presentó los niveles más altos de apoptosis tardía, lo que se correlaciona con los resultados obtenidos en la **Figura 34** (estudio del ciclo celular). Las otras dos líneas celulares, HT-29 y SW480, presentaron niveles significativamente menores a los hallados en la línea HGUE-C-1.

De manera complementaria, se determinó la liberación de la enzima intracelular LDH, ya que la permeabilización de la membrana plasmática es una característica de procesos que comprometen la integridad de la membrana como la necrosis y que a veces puede ser confundida con la apoptosis [96]. El tratamiento con el extracto de romero provocó una mayor liberación de la enzima LDH al sobrenadante de manera dosis-dependiente respecto al control de células no tratadas (**Figura 36**), lo que es indicativo de un aumento de la necrosis dependiente de la dosis. Transcurridas 24 horas y a la máxima dosis empleada, las líneas celulares HGUE-C-1 y SW480 mostraron el mayor incremento (32,6 y 20,0%, respectivamente), mientras que la línea HT-29 experimentó un aumento de 14,3%.

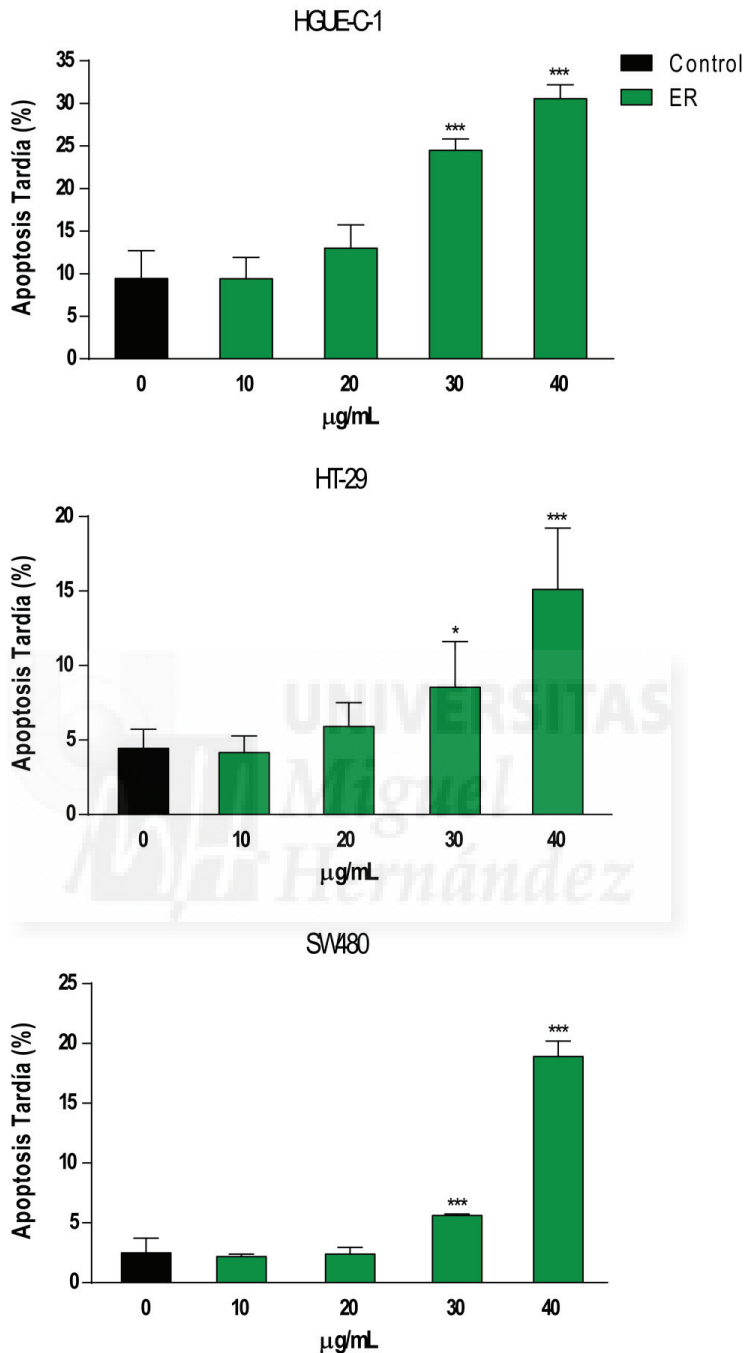


**Figura 35.** Determinación de apoptosis mediante Anexina-V en las tres líneas celulares de cáncer de colon, HGUE-C-1, HT-29 y SW480.

Las células se trataron con diferentes concentraciones del extracto de romero (10-40  $\mu\text{g/mL}$ ) durante 24 horas. Una vez finalizado el tratamiento, el porcentaje de células apoptóticas se determinó mediante el equipo *Muse Cell Analyzer*. Los valores se presentan como porcentaje de apoptosis tardía (%). \* ( $p<0,05$ ) y \*\*\* ( $p<0,001$ ) indican diferencias estadísticamente significativas.

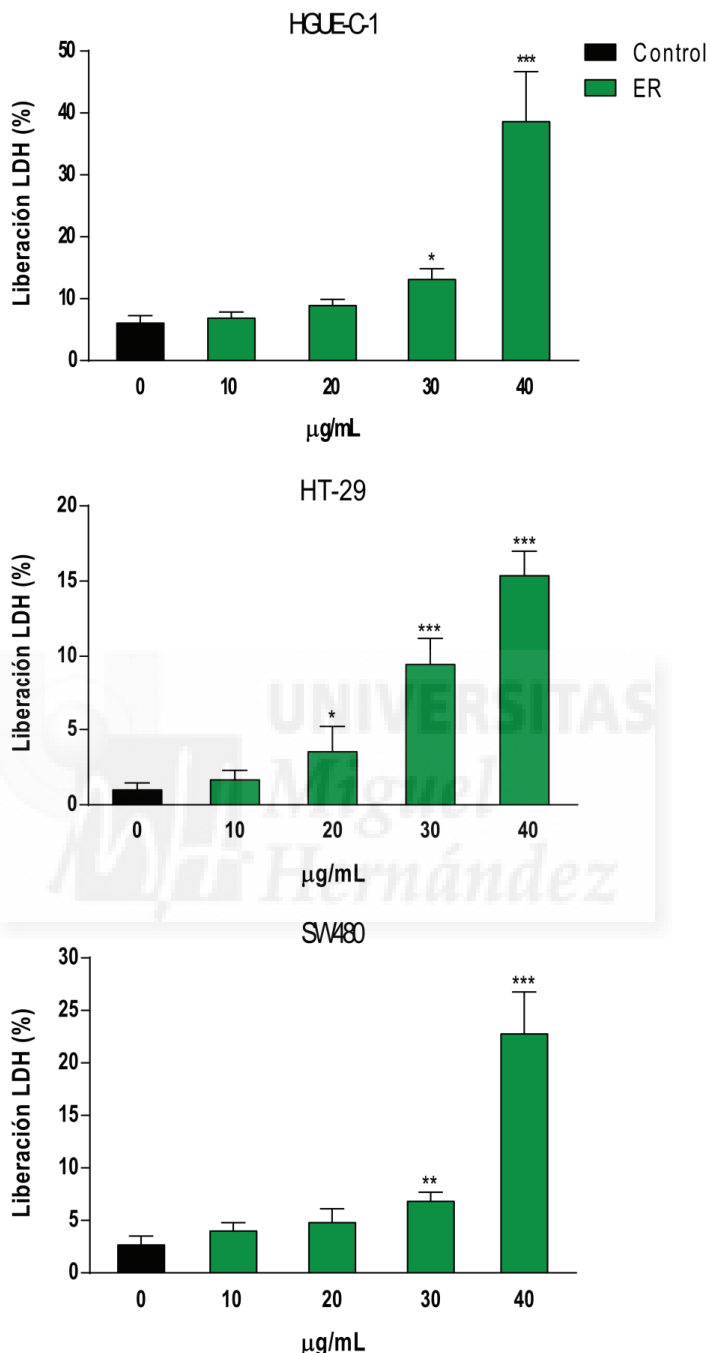


**Figura 36.** Efecto del extracto de romero en la liberación de la enzima intracelular LDH en las tres líneas celulares de cáncer de colon, HGUE-C-1, HT-29 y SW480.

Las células se trataron con diferentes concentraciones del extracto de romero (10-40  $\mu\text{g/mL}$ ) durante 24 horas. Una vez finalizado el tratamiento, el porcentaje de células necróticas se determinó mediante el kit de citotoxicidad LDH. Los valores se presentan como porcentaje de enzima liberada (%). \* ( $p<0,05$ ), \*\* ( $p<0,01$ ) y \*\*\* ( $p<0,001$ ) indican diferencias estadísticamente significativas.

Para profundizar en los posibles mecanismos de acción del extracto de romero se realizó un ensayo de viabilidad celular empleando inhibidores de la necroptosis y la autofagia, la necrostatina-1 y la cloroquina, respectivamente. Como muestra la **Figura 37**, la incubación de las tres líneas celulares con dichos compuestos no produjo cambios en la viabilidad celular al ser tratadas con el extracto de romero. Estos resultados descartaron tanto la necroptosis como la autofagia como posibles mecanismos de acción del extracto de romero.

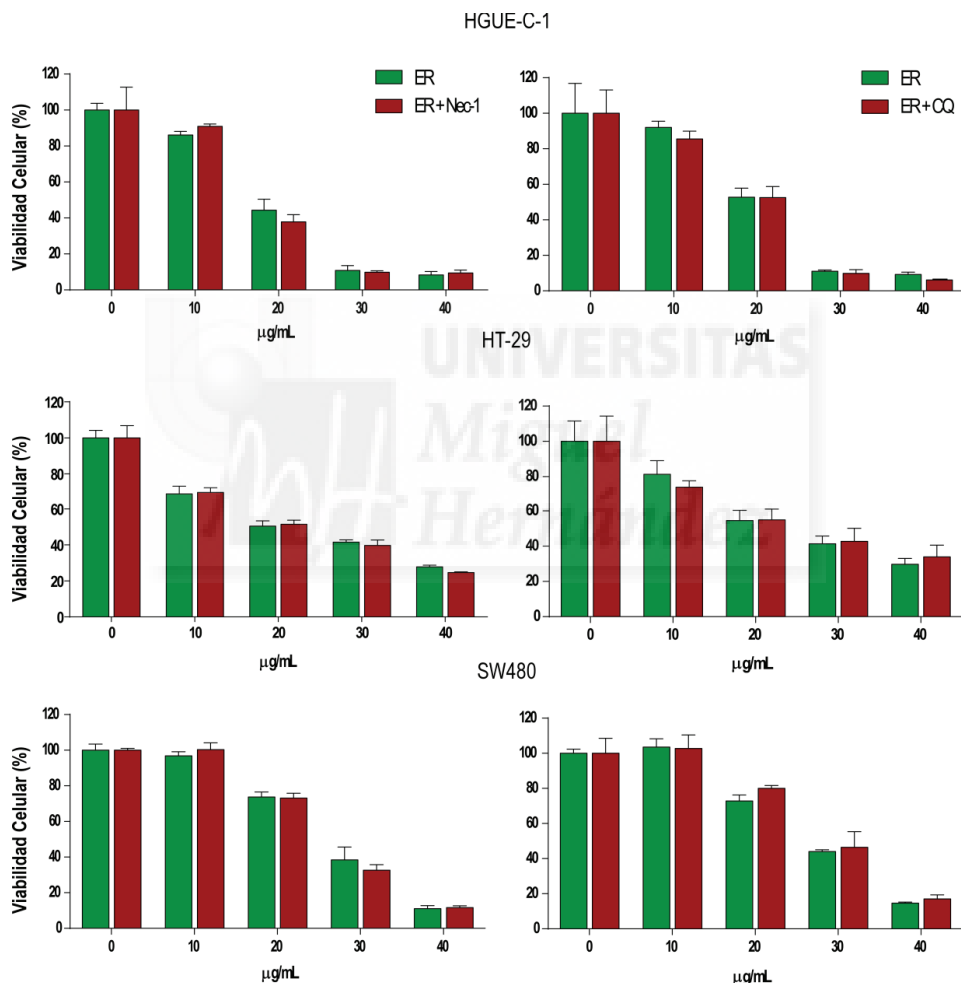


**Figura 37.** Efecto del extracto de romero en la viabilidad celular en las tres líneas celulares de cáncer de colon, HGUE-C-1, HT-29 y SW480.

Las células se pretrataron con necrostatina-1 y cloroquina y con diferentes concentraciones del extracto de romero (10-40  $\mu\text{g/mL}$ ) durante 24 horas. Una vez finalizado el tratamiento se determinó la viabilidad celular mediante el ensayo de MTT. Los valores se presentan como porcentaje de viabilidad celular (%).

## 2. Cuantificación de especies reactivas de oxígeno y potencial de membrana mitocondrial en las líneas de cáncer de colon.

Dado que la presencia de ROS posee un papel primordial en la apoptosis y en la necrosis, se determinó la acumulación de ROS en las tres líneas celulares, HGUE-C-1, HT-29 y SW480, una vez finalizado el tratamiento durante 24 horas con el extracto de romero a diferentes concentraciones (10-40 µg/mL). Como muestra la **Figura 38**, el extracto de romero indujo la generación intracelular de ROS de manera dosis-dependiente en las tres líneas utilizadas.

Para determinar la existencia de cambios en el potencial de membrana mitocondrial (PMM), hecho que podría estar relacionado con la generación de ROS, se utilizó el equipo *Muse Cell Analyzer* y la microscopía de fluorescencia. Las células se trataron con diferentes concentraciones del extracto de romero (10-40 µg/mL) durante 24 horas. Al finalizar el tratamiento, el porcentaje de células despolarizadas aumentó en las tres líneas de cáncer de colon. La línea celular HT-29 presentó un mayor porcentaje de células despolarizadas, seguida de la línea HGUE-C-1 y finalmente, la línea SW480, la cual mostró el menor porcentaje de células despolarizadas (**Figura 39**).

Para corroborar los resultados obtenidos mediante el equipo *Muse Cell Analyzer*, se emplearon dos sondas fluorescentes de manera combinada, MitoTracker Red CMXRos y MitoTracker Green, las cuales determinan mitocondrias viables y masa mitocondrial total, respectivamente. En este caso, se confirmó el resultado anterior, ya que la relación entre la fluorescencia roja y verde disminuyó en todas las líneas celulares, indicando que el porcentaje de células despolarizadas aumentó en todas las líneas celulares con el aumento de concentración del extracto de romero (**Figura 40**).

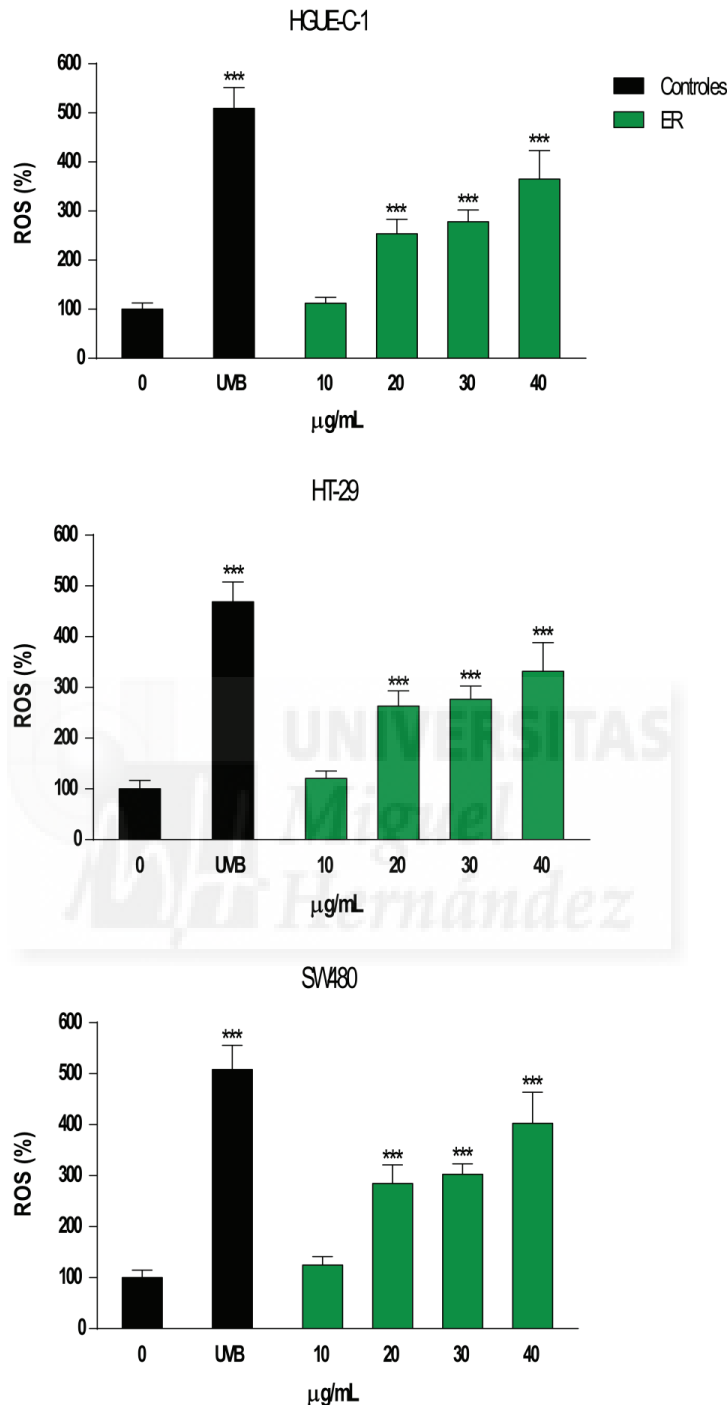


**Figura 38.** Efecto del extracto de romero en la generación de ROS en las tres líneas celulares de cáncer de colon, HGUE-C-1, HT-29 y SW480.

Las células se trataron con diferentes concentraciones del extracto de romero (10-40  $\mu\text{g/mL}$ ) durante 24 horas. Una vez finalizado el tratamiento se determinó la generación de ROS intracelular mediante la sonda H<sub>2</sub>DCF-DA. Los valores se presentan como porcentaje de ROS (%). \*\*\* ( $p < 0,001$ ) indica diferencias estadísticamente significativas.

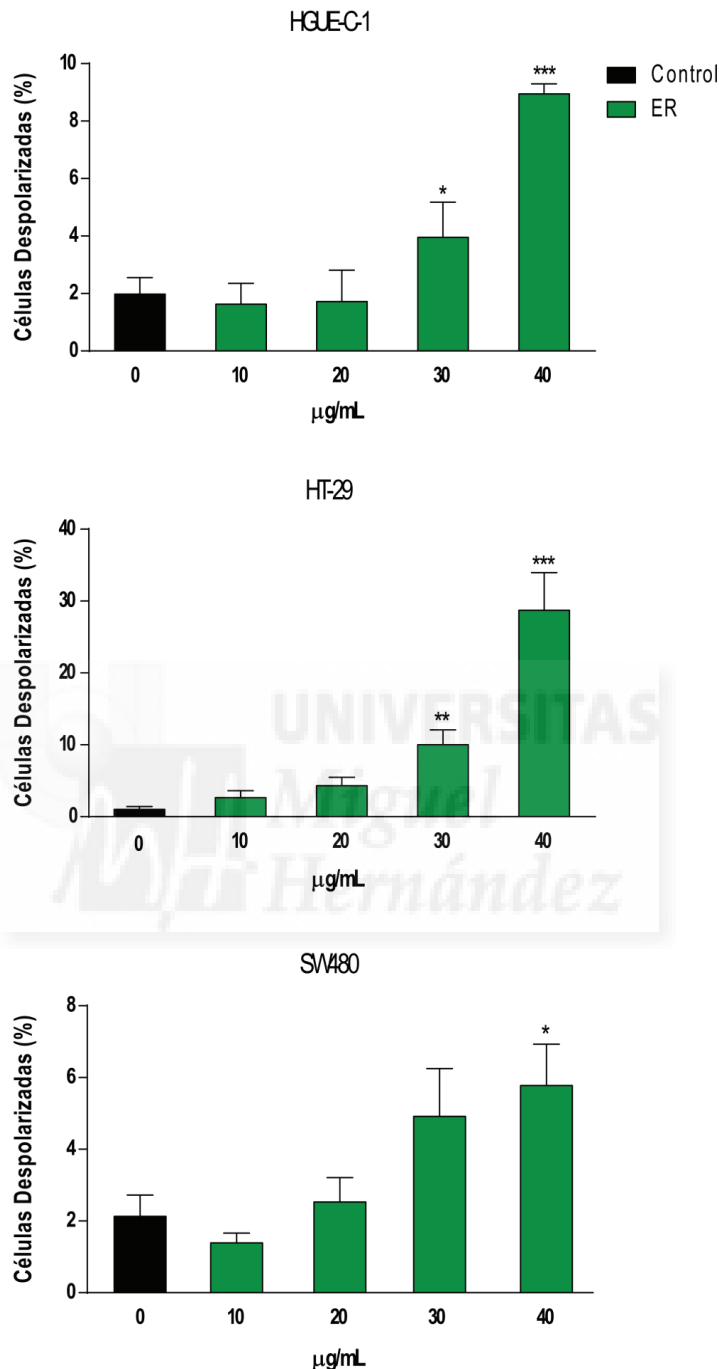


**Figura 39.** Efecto del extracto de romero en el potencial de membrana mitocondrial en las tres líneas celulares de cáncer de colon, HGUE-C-1, HT-29 y SW480.

Las células se trataron con diferentes concentraciones del extracto de romero (10-40  $\mu\text{g/mL}$ ) durante 24 horas. Una vez finalizado el tratamiento, el porcentaje de células despolarizadas se determinó mediante el equipo *Muse Cell Analyzer*. Los valores se presentan como porcentaje de células despolarizadas (%). \* ( $p<0,05$ ), \*\* ( $p<0,01$ ) y \*\*\* ( $p<0,001$ ) indican diferencias estadísticamente significativas.

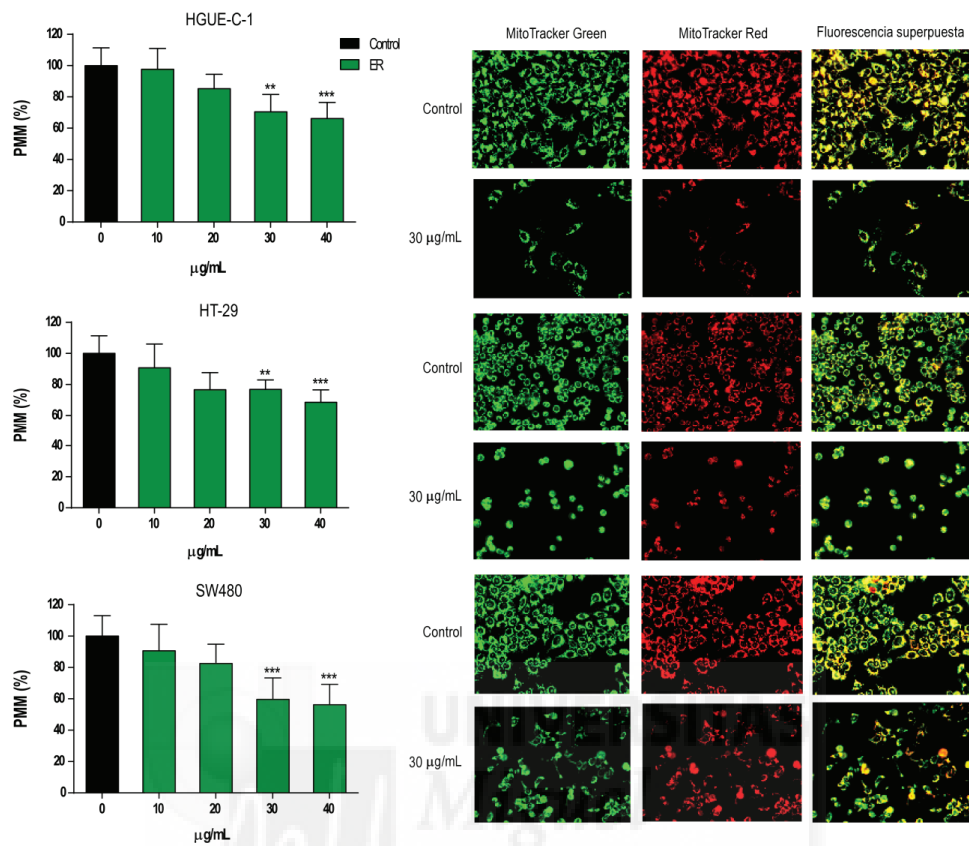


**Figura 40.** Efecto del extracto de romero en el potencial de membrana mitocondrial en las tres líneas celulares de cáncer de colon, HGUE-C-1, HT-29 y SW480 mediante el uso de sondas fluorescentes.

Las células se trataron con diferentes concentraciones del extracto de romero (10-40  $\mu\text{g/mL}$ ) durante 24 horas. Una vez finalizado el tratamiento, se determinó el potencial de membrana mitocondrial mediante la relación de fluorescencia rojo/verde con el equipo *Cytation 3 Cell Imaging Multi-mode*. Los valores se presentan como porcentaje del potencial de membrana mitocondrial (%). \*\* ( $p<0,01$ ) y \*\*\* ( $p<0,001$ ) indican diferencias estadísticamente significativas.

### 3. La implicación del factor de transcripción Nrf2 en el efecto del extracto de romero sobre las células de cáncer colorrectal.

El estrés oxidativo provocado por la generación intracelular de ROS afecta a múltiples factores de transcripción sensibles a un estado redox determinado y conlleva la regulación de genes con acción antioxidante. La vía de señalización Nrf2/Keap1-ARE controla la expresión de los genes relacionados con enzimas antioxidantes (actividad protectora). Como muestra la **Figura 38**, el tratamiento con el extracto de romero provocó un aumento de ROS, por lo que se consideró oportuno el estudio del factor de transcripción Nrf2 y su posible implicación en el mecanismo de defensa frente al efecto prooxidante del extracto de romero. Como muestra la **Figura 41**, el silenciamiento del gen correspondiente a Nrf2 en HGUE-C-1, HT-29 y SW480, utilizando su respectivo ARN de interferencia, modificó significativamente el estado redox intracelular, aumentando los niveles de ROS en células tratadas con el extracto de romero y con ello, disminuyendo la viabilidad celular.

La línea celular SW480 mostró un aumento muy significativo en la producción de ROS en las células transfectadas, alcanzando un 112% por encima de las células no transfectadas a 40 µg/mL. La línea HGUE-C-1 también mostró un aumento significativo de un 96%, seguida de la línea HT-29 que tuvo un comportamiento más resistente, aumentando el nivel de ROS un 60% respecto a las células no transfectadas. Dichos niveles de ROS, causados por el tratamiento de romero, afectaron a la viabilidad celular en todas las líneas estudiadas. En concordancia con la generación de ROS, la línea celular SW480 disminuyó significativamente la viabilidad celular un 27,6% a la concentración de 40 µg/mL, respecto a las células no transfectadas. La línea HGUE-C-1 mostró una disminución de la viabilidad celular de un 16,8% para la concentración más alta estudiada, mientras que la línea HT-29 presentó un descenso del 17,7% respecto a las células no transfectadas.

Una vez estudiada la implicación de este factor de transcripción, se determinó mediante el ensayo de *Dot-Blot* la expresión de Nrf2 en las células transfectadas y no transfectadas, con el fin de confirmar el silenciamiento de dicho gen. Como muestra la **Figura 42**, el nivel de expresión de Nrf2 normalizado con la proteína  $\beta$ -actina fue silenciado parcialmente en las tres líneas celulares estudiadas.

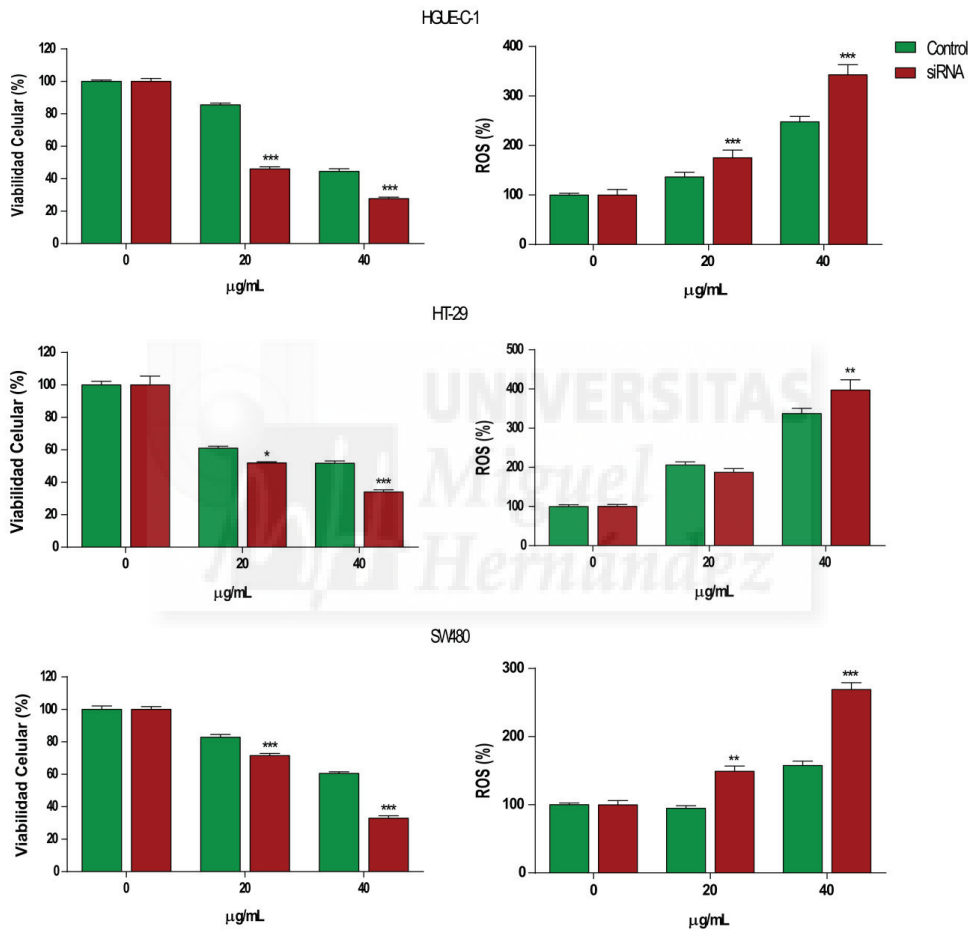


**Figura 41.** Efecto del extracto de romero en la viabilidad celular y la generación de ROS tras el silenciamiento de Nrf2 en las tres líneas celulares de cáncer de colon, HGU-C-1, HT-29 y SW480.

Las células se trataron con diferentes concentraciones del extracto de romero (20 y 40  $\mu\text{g/mL}$ ) durante 24 horas. Una vez finalizado el tratamiento, se determinó la generación de ROS intracelular mediante la sonda  $\text{H}_2\text{DCF-DA}$  y la viabilidad celular mediante el ensayo de MTT. Los valores se presentan como porcentaje de viabilidad celular (%) y porcentaje de ROS (%). \* ( $p<0,05$ ), \*\* ( $p<0,01$ ) y \*\*\* ( $p<0,001$ ) indican diferencias estadísticamente significativas.

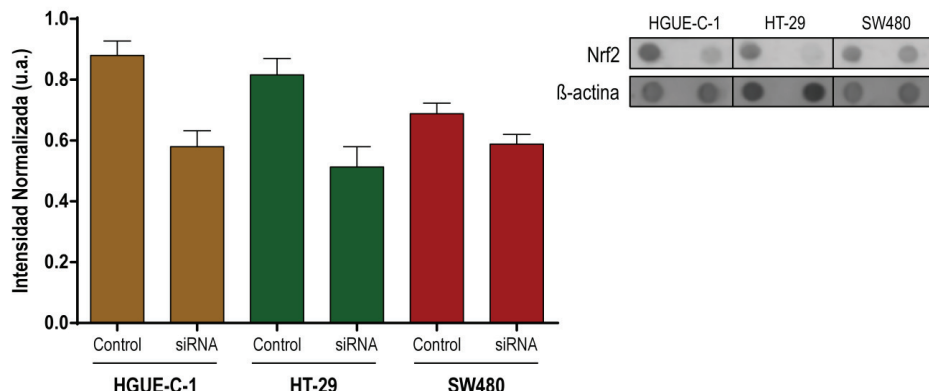


**Figura 42.** Nivel de expresión de Nrf2 tras su silenciamiento en las tres líneas celulares de cáncer de colon, HGUE-C-1, HT-29 y SW480 cuantificado por densitometría y normalizado con la proteína  $\beta$ -actina.

Los valores se presentan como intensidad normalizada en unidades arbitrarias (u.a.). Imágenes representativas de los dots formados en el ensayo de Dot-Blot correspondientes a la  $\beta$ -actina y Nrf2.

#### 4. Efecto del ER en la proliferación y migración celular en las líneas de cáncer de colon.

La actividad antiproliferativa del extracto de romero se determinó de forma alternativa mediante el equipo *xCELLigence RTCA*, el cual realizó un seguimiento del crecimiento celular a tiempo real durante 72 horas. Como se puede observar (**Figura 43**), el tratamiento con el extracto de romero provocó una inhibición de la proliferación celular de manera dosis-dependiente respecto al control de células no tratadas. Las líneas celulares HGUE-C-1 y SW480 presentaron un comportamiento muy similar, inhibiéndose la proliferación celular a la dosis de 20  $\mu\text{g/mL}$ , mientras que la línea HT-29 mostró un comportamiento más resistente.

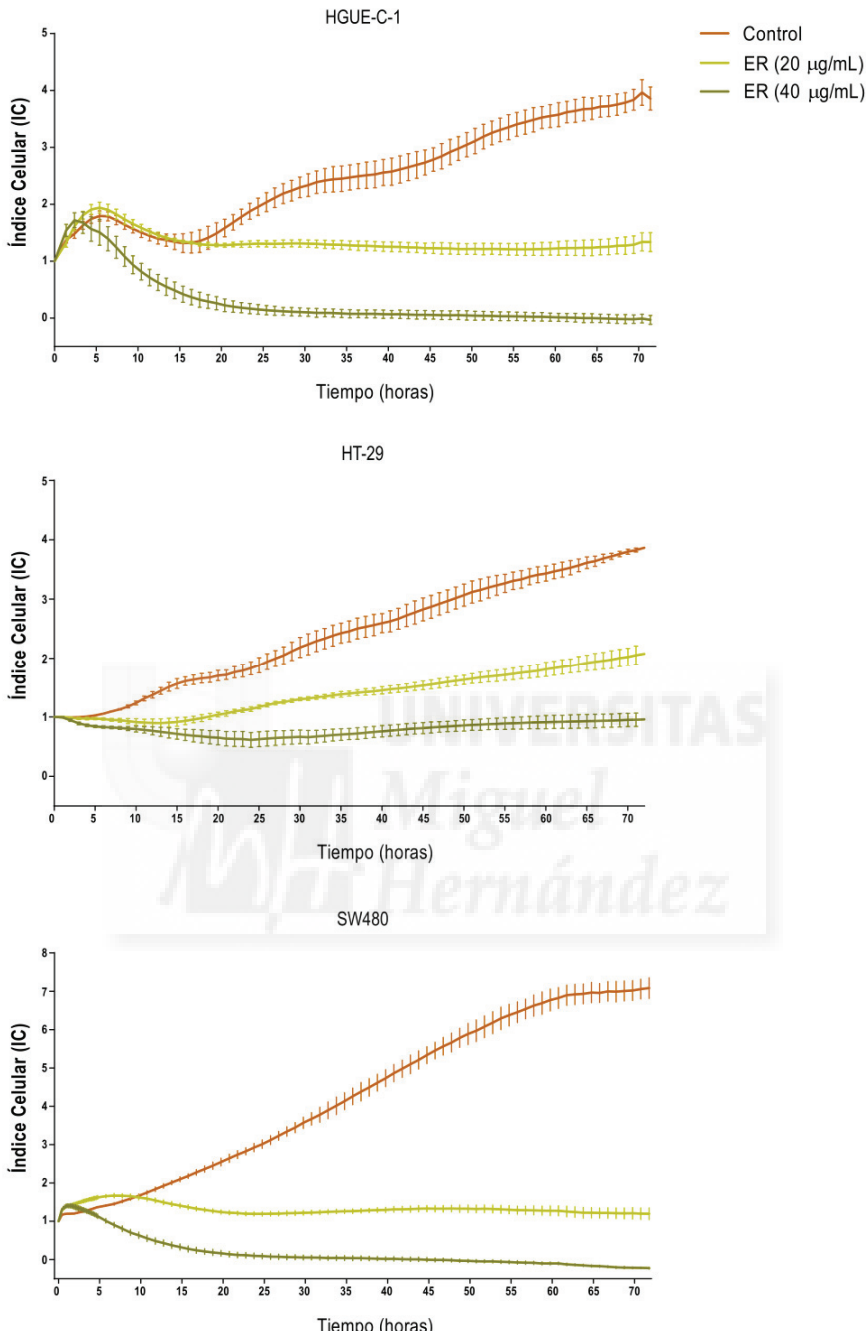


**Figura 43.** Curso temporal de la proliferación celular en las tres líneas celulares de cáncer de colon, HGUE-C-1, HT-29 y SW480.

Las células se trataron con diferentes concentraciones del extracto de romero (20 y 40 µg/mL) durante 72 horas. Durante el tratamiento se registró el índice celular (IC) mediante el equipo *xCELLigence RTCA*. Los valores se presentan como IC en función del tiempo (horas).

Para profundizar en el efecto del extracto de romero en la proliferación celular de las tres líneas estudiadas se realizó un ensayo de formación de colonias, con el objetivo de determinar la capacidad del mismo para reducir la proliferación de las células tumorales de colon. Como muestra la **Figura 44**, el extracto de romero inhibió la formación de colonias de manera dosis-dependiente en las tres líneas celulares.

Las líneas celulares HGUE-C-1 y SW480 fueron las más sensibles al tratamiento con el extracto de romero, mientras que la línea HT-29 mostró un comportamiento más resistente. En las líneas HGUE-C-1 y SW480 se observó una inhibición en la formación de colonias a la mayor concentración utilizada de un 92,3% y 87,1%, respectivamente. Finalmente, en la línea HT-29 se alcanzó una inhibición del 84,5% a 40 µg/mL.

Para determinar el efecto del extracto de romero sobre la capacidad de migración de las líneas celulares HGUE-C-1, HT-29 y SW480, se realizó el ensayo de “cierre de herida” o *wound healing*. Como se muestra en la **Figura 45**, el tratamiento con extracto de romero disminuyó significativamente la migración celular de manera dosis-dependiente en las tres líneas celulares. En la línea celular HGUE-C-1 el extracto de romero inhibió la migración celular un 28,8% y un 66,1% a las concentraciones de 30 y 40 µg/mL, respectivamente. En la línea SW480, se observó una inhibición del 76,7% a 40 µg/mL, mientras que la línea HT-29 presentó una inhibición del 92,5% a esta misma concentración.

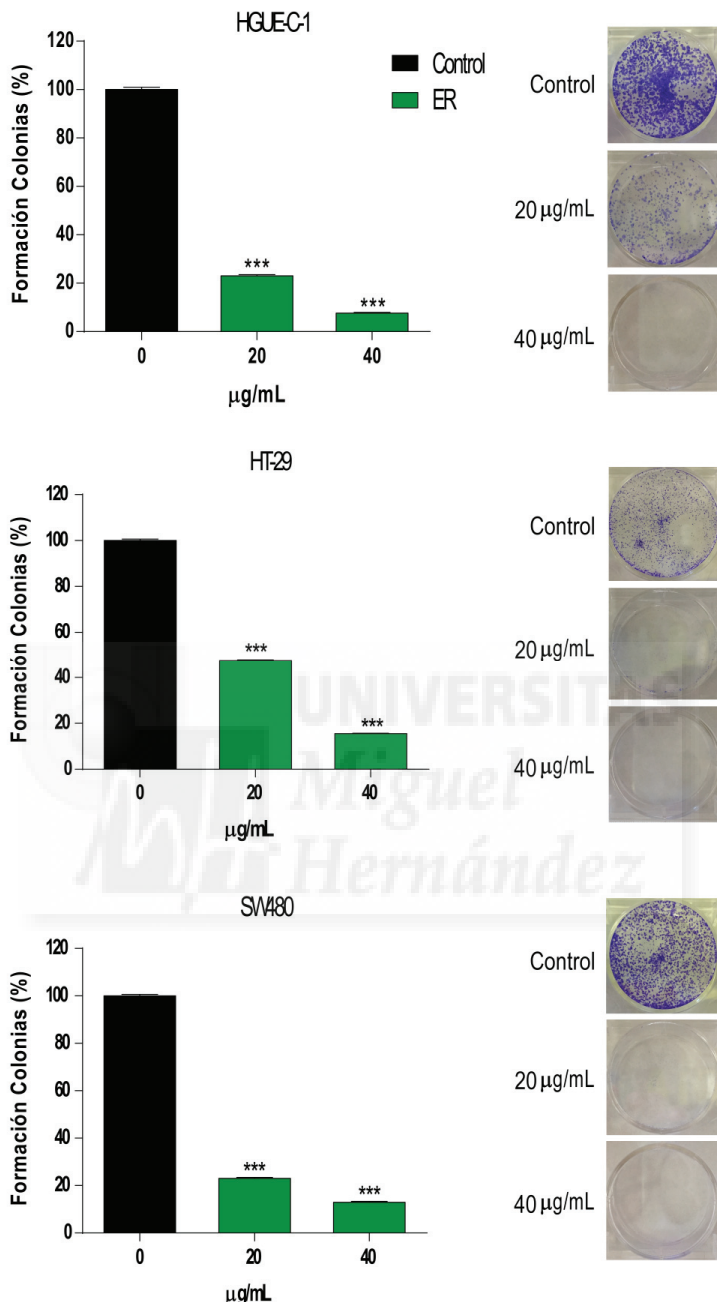


**Figura 44.** Efecto del extracto de romero en la formación de colonias en las tres líneas celulares de cáncer de colon, HGUE-C-1, HT-29 y SW480.

Las células se trataron con diferentes concentraciones del extracto de romero (20 y 40  $\mu\text{g/mL}$ ) durante 24 horas. Una vez finalizado el tratamiento, las células se incubaron con medio de cultivo completo durante 7 días y se determinó la capacidad de formación de colonias mediante el equipo *Cytation 3 Cell Imaging Multi-mode*. Los valores se presentan como porcentaje de formación de colonias (%). \*\*\* ( $p<0,001$ ) indica diferencias estadísticamente significativas.

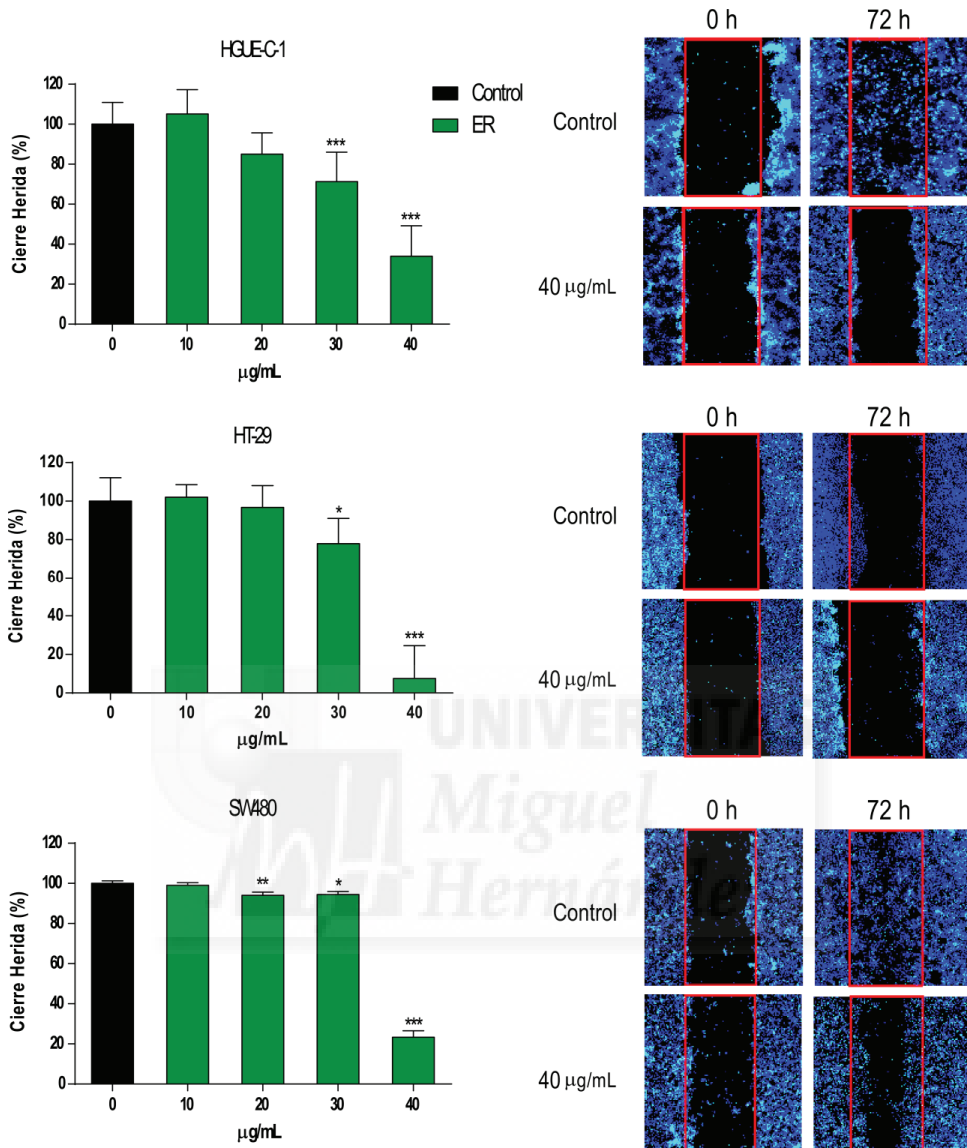


**Figura 45.** Estudio del efecto del extracto de romero en la migración celular mediante el ensayo de *wound healing* en las tres líneas celulares de cáncer de colon, HGUE-C-1, HT-29 y SW480.

Las células se trataron con diferentes concentraciones del extracto de romero (10-40  $\mu\text{g/mL}$ ) durante 72 horas. Durante el tratamiento se realizaron fotografías a diferentes tiempos mediante el equipo *Cytation 3 Cell Imaging Multi-mode*. Los valores se presentan como porcentaje de área cerrada (%). \* ( $p<0,05$ ), \*\* ( $p<0,01$ ) y \*\*\* ( $p<0,001$ ) indican diferencias estadísticamente significativas.

## 5. Toxicidad oral aguda del extracto de romero en ratas.

Se estudió la toxicidad oral aguda del extracto de romero en un modelo animal para determinar la idoneidad del uso oral de dicho extracto. El estudio de toxicidad oral aguda se llevó a cabo de acuerdo con las directrices de la guía 420 de la OCDE. Según esta guía, los compuestos se pueden clasificar en cinco categorías: no clasificado, peligroso, tóxico, muy tóxico y altamente tóxico (**Tabla 6**).

**Tabla 6.** Clasificación de sustancias, según la guía 420 de la Organización para la Cooperación y el Desarrollo Económicos (OCDE).

Rangos DL <sub>50</sub> (mg/kg)	ATC	Clasificación
DL <sub>50</sub> > 2000 mg/kg	ATC 5	No clasificado
300 < DL <sub>50</sub> ≤ 2000 mg/kg	ATC 4	Peligroso
50 < DL <sub>50</sub> ≤ 300 mg/kg	ATC 3	Tóxico
5 < DL <sub>50</sub> ≤ 50 mg/kg	ATC 2	Muy tóxico
DL <sub>50</sub> < 5 mg/kg	ATC 1	Altamente tóxico

La variación en el peso corporal de los animales es uno de los primeros signos de toxicidad, siendo el indicador más sensible a un posible efecto adverso [101]. Se registró el peso corporal de cada animal y no se observó ninguna diferencia entre los grupos estudiados, mostrando en todos ellos un incremento de peso normal durante el ensayo (**Figura 46**).

Además, no hubo cambios significativos en el comportamiento de los animales tales como apatía, hiperactividad o morbilidad. Al finalizar del ensayo, no se observaron efectos letales o signos de toxicidad en ningún grupo estudiado.

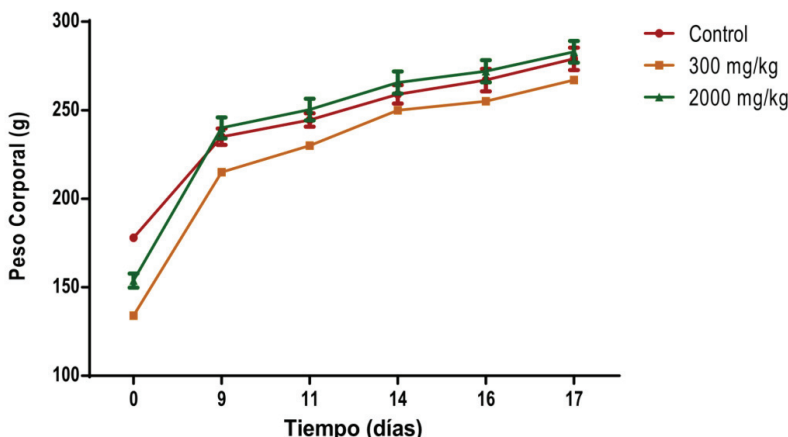


**Figura 46.** Evolución del peso corporal de los distintos grupos de animales no tratados (control) y tratados con el extracto de romero durante la realización del ensayo.

Los valores se presentan como la media del peso corporal de cada uno de los grupos estudiados (g) en función del tiempo (días).

Finalmente, se abordó un análisis histopatológico en el que se analizaron los siguientes órganos: bazo, corazón, hígado, pulmón y riñón. Dichos cortes histológicos fueron evaluados mediante una colaboración con el servicio de Anatomía Patológica, perteneciente al Hospital General Universitario de Alicante, y no se observaron signos de toxicidad en ningún grupo de animales estudiados (**Figura 47**).

Por lo tanto, según estos resultados, el extracto de romero se enmarca en la categoría de no clasificado de acuerdo con la guía 420 de la OCDE ya que no se observó mortalidad ni signos tóxicos atribuibles a la administración de dicho extracto a las dosis de 300 y 2000 mg/kg.

De acuerdo con el Sistema Globalmente Armonizado (GHS) de clasificación y etiquetado de productos químicos, los compuestos que presentan un valor de  $DL_{50}$  superior a 2000 mg/kg se consideran relativamente seguros [105].

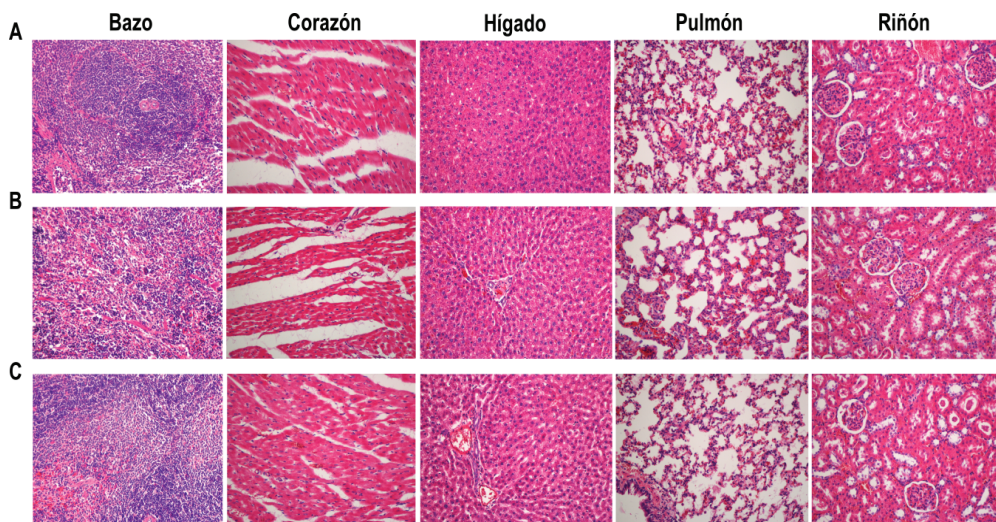


**Figura 47.** Estudio de la toxicidad oral aguda del extracto de romero en un modelo *in vivo*. Imágenes representativas de los cortes histológicos de órganos vitales de animales (A) control y tratados con el extracto de romero a (B) 300 mg/kg y (C) 2000 mg/kg.

## 6. Efecto del extracto de romero en un modelo *in vivo* de cáncer de colon.

Una vez caracterizada la capacidad antiproliferativa *in vitro* del extracto de romero, se abordó la capacidad antitumoral en un modelo *in vivo*, mediante el empleo de un modelo de xenotransplantes de cáncer de colon en ratones inmunodeprimidos. Para evaluar el bienestar animal se llevaron a cabo los siguientes controles:

1. Se registró el peso corporal una vez por semana y no se observó ninguna alteración en la tendencia creciente del peso de los animales (**Figura 48**).
2. Se evaluó el bienestar animal mediante una hoja de valoración de diferentes aspectos (comportamiento, aparición de heridas y aspecto general y de la piel), la cual fue aprobada dentro del procedimiento solicitado al órgano responsable de la ética y el bienestar en la experimentación animal de la UMH.

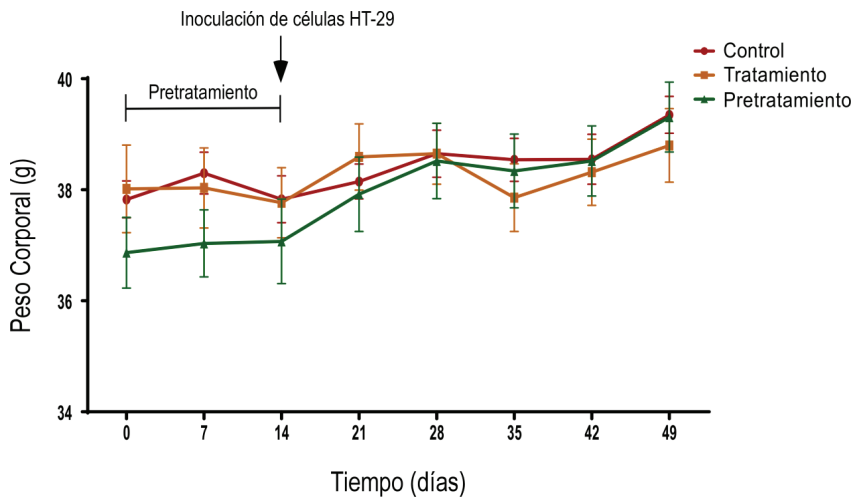
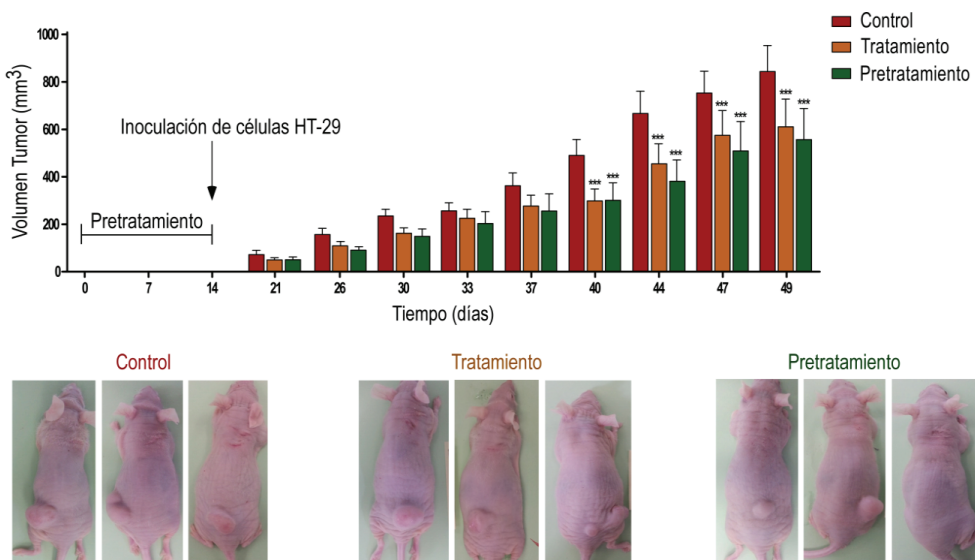


**Figura 48.** Evolución del peso corporal de los distintos grupos de animales no tratados (control) y tratados con el extracto de romero durante la realización del ensayo.

Los valores se presentan como la media del peso corporal de cada uno de los grupos estudiados (g) en función del tiempo (días).

Como medida de la eficacia de los tratamientos, se midió el volumen de los tumores tal y como se detalla en el apartado de Metodología. En el grupo de animales pretratados con el extracto de romero, a 200 mg/kg durante 14 días, se observó una inhibición del crecimiento del tumor a tiempo final de un 34,1%, mientras que en el grupo de animales tratados a partir de la formación del tumor se observó una inhibición de un 27,5%. Aunque entre las dos condiciones estudiadas no se determinaron diferencias estadísticamente significativas, sí se puede observar una tendencia clara, la cual indica que el efecto antitumoral del pretratamiento es levemente superior al del tratamiento (**Figura 49**).



## **Capítulo tercero**

**Estudio de la permeabilidad del extracto de romero en monocapas de células**

**intestinales Caco-2**



## 1. Análisis de las muestras por HPLC ESI-UHD-Qq-TOF-MS.

La caracterización cualitativa y cuantitativa mediante HPLC ESI-UHD-Qq-TOF-MS de las muestras procedentes del ensayo de absorción en el modelo celular Caco-2 se realizó en colaboración con el Centro de Investigación y Desarrollo del Alimento Funcional (CIDAF), bajo la dirección del Dr. Antonio Segura Carretero. En los ensayos de absorción se utilizó el extracto de romero de forma libre y vehiculizado en un sistema de vesículas fosfolipídicas o liposomas.

## 2. Determinación de los valores $P_{app}$ .

Una vez determinadas las concentraciones de los compuestos previamente identificados en las muestras procedentes de la cámara apical (AP) y basolateral (BL), tal y como se describe en el apartado de Metodología, dichos valores se emplearon para obtener los valores de permeabilidad aparente ( $P_{app}$ ). En la **Tabla 7** se muestran los valores para las dos condiciones estudiadas (extracto de romero libre y encapsulado en liposomas) y ambas direcciones analizadas, AP-BL y BL-AP. Algunos compuestos no pudieron cuantificarse ya que su concentración fue inferior a los valores del límite de cuantificación (LOQ), en algunos casos en ambas direcciones y en otros sólo para una de ellas.

## 3. Resultados de permeabilidad según familia de compuestos.

### Flavonoides y derivados de ácidos fenólicos

Los derivados fenólicos, (9)-shogaol y su isómero, se encontraron presentes en todas las muestras analizadas pero los valores de concentración de ambos compuestos se encontraron por debajo del LOQ, por lo que no se pudieron obtener resultados de dichos compuestos. Posteriormente, un análisis más profundo de las muestras reveló que ambos compuestos fueron parcialmente retenidos por la monocapa de células Caco-2, sin ningún tipo de transporte hacia la cámara receptora.

En cuanto a los flavonoides, a pesar de que en el extracto de romero su presencia es menos abundante como muestra su caracterización previa [59], su posible absorción y la importante actividad biológica que éstos poseen justificó un análisis exhaustivo de dichos compuestos. Los flavonoides presentes en el extracto de romero fueron apigenina, hispidulina, diosmetina, genkwanina y cirsimartina. La apigenina, no se pudo cuantificar, ya que la concentración detectada se encontraba por debajo de su límite de cuantificación (LOQ).

Respecto a los otros cuatro flavonoides, no se detectó absorción en ninguna de las dos direcciones estudiadas cuando el extracto de romero se encontraba encapsulado en liposomas. Sin embargo, se detectó una absorción significativa en ambas direcciones cuando el extracto se encontraba de forma libre. Los valores más altos obtenidos fueron para la cirsimartina y la genkwanina (dirección AP-BL), sin diferencias estadísticamente significativas entre ellos ( $p>0,05$ ). Este estudio supone la primera contribución al conocimiento de la permeabilidad de estos flavonoides.

La diosmetina y la hispidulina presentaron valores de permeabilidad inferiores, mostrando diferencias estadísticamente significativas respecto a la cirsimartina ( $p<0,001$  y  $p<0,01$ , respectivamente), pero sin mostrar diferencias entre ellos ( $p>0,05$ ).

Respecto a la dirección BL-AP, la cirsimartina, la genkwanina y la hispidulina mostraron valores de permeabilidad muy similares, sin diferencias significativas entre ellos ( $p>0,05$ ), seguidos por la diosmetina con el valor más bajo de permeabilidad ( $p<0,001$ ) (**Tabla 7**).

## Diterpenos

Los diterpenos, junto a los triterpenos, son el grupo principal de compuestos presentes en el extracto de romero, en el cual se incluyen hasta 10 compuestos [59]. Los diterpenos presentes en el extracto de romero son los ácidos carnósico y 12-metoxicarnósico, carnosol, rosmanol y sus isómeros (epiisorrosmanol y epirrosmanol), rosmadial, rosmaridifenol, hinoquiona y miltipolona.

El valor de permeabilidad más alto en la dirección AP-BL y para el extracto de forma libre se obtuvo para el compuesto ácido carnósico seguido del epiisorrosmanol con una diferencia estadísticamente significativa entre ellos ( $p<0,001$ ). Los siguientes compuestos por orden de permeabilidad fueron, el epirrosmanol y el rosmanol, que no mostraron diferencias significativas entre ellos ( $p>0,05$ ), pero sí con respecto al anterior, el epiisorrosmanol ( $p<0,001$ ). El compuesto carnosol y su isómero, el rosmadial, el ácido 12-metoxicarnósico y la miltipolona mostraron valores de  $P_{app}$  entre 1,46 y  $2,10 \times 10^{-5}$  cm/s. Por otro lado, el rosmaridifenol mostró valores inferiores ( $P_{app}$  en el rango de  $10^{-6}$  cm/s), mientras que para el compuesto hinoquiona no se observó absorción.

Respecto a la dirección BL-AP, el ácido carnósico también presentó el valor más alto de permeabilidad ( $p<0,001$ ), seguido por el resto de compuestos sin diferencias significativas entre ellos ( $p>0,05$ ), excepto para la miltipolona que no fue absorbida.

En el estudio del extracto de romero encapsulado en la dirección AP-BL, el rosmanol mostró la permeabilidad más alta, seguido del epiisorrosmanol, rosmadial, epirrosmanol y carnosol. Sin embargo, la encapsulación de dichos compuestos provocó una disminución en los valores de permeabilidad.

En general, para todos los diterpenos presentes en el extracto de romero, los valores de permeabilidad de los compuestos fueron inferiores en la forma encapsulada que en la libre (**Tabla 7**).

### Triterpenos

Los triterpenos son la familia de compuestos más abundante en el extracto de romero según su caracterización previa [59], la cual incluye 6 compuestos: la anemosapogenina y los ácidos augústico, betulínico, micromérico, bentámico y ursólico.

Respecto al extracto de romero encapsulado en liposomas, no se observó absorción en ninguna de las dos direcciones estudiadas de los compuestos mencionados anteriormente.

En el estudio del extracto de romero de forma libre, se observó que dicho grupo de compuestos presentó valores de  $P_{app}$  bajos (en el rango de  $10^{-6}$  cm/s). En la dirección AP-BL, los ácidos betulínico y ursólico no presentaron absorción, pero sí se encontraban presentes en la monocapa celular. En cuanto a los otros triterpenos, el valor de permeabilidad más alto se obtuvo con el ácido augústico, seguido por el ácido micromérico, bentámico y la anemosapogenina, sin presentar diferencias estadísticamente significativas entre ellos ( $p>0,05$ ). Respecto a la dirección BL-AP, cabe destacar que los seis triterpenos fueron absorbidos, pero mostraron valores de permeabilidad bajos (**Tabla 7**).

**Tabla 7.** Valores de  $P_{app}$  de los compuestos (cm/s) en el ER libre y ER liposomado y en ambas direcciones estudiadas. Los valores representan la media ( $n=6$ )  $\pm$  desviación estándar (SD). N.C. (no calculado, LOQ), N.E. (no error) cuando solo una de las réplicas se utilizó para obtener el valor y N.A. (no absorbida) indica  $P_{app}=0$ .

Compuesto	Familia	Extracto de romero libre				Extracto de romero liposomado			
		Dirección AP-BL		Dirección BL-AP		Dirección AP-BL		Dirección BL-AP	
		$P_{app}$ (cm/s)	$\pm$ SD	$P_{app}$ (cm/s)	$\pm$ SD	$P_{app}$ (cm/s)	$\pm$ SD	$P_{app}$ (cm/s)	$\pm$ SD
Apigenina	Flavonoide	N.C.		N.C.		N.C.		N.C.	
Cirsimartina	Flavonoide	3,33x10 <sup>-5</sup>	1,17x10 <sup>-6</sup>	3,07x10 <sup>-5</sup>	6,29x10 <sup>-6</sup>	3,18x10 <sup>-8</sup>	4,03x10 <sup>-8</sup>	3,18x10 <sup>-8</sup>	4,03x10 <sup>-8</sup>
Diosmetina	Flavonoide	2,50x10 <sup>-6</sup>	N.E.	4,13x10 <sup>-6</sup>	1,38x10 <sup>-6</sup>	N.A.	N.A.	N.A.	N.A.
Hispidulina	Flavonoide	9,05x10 <sup>-6</sup>	3,04x10 <sup>-6</sup>	1,31x10 <sup>-5</sup>	9,60x10 <sup>-7</sup>	N.A.	N.A.	N.A.	N.A.
Genkwanina	Flavonoide	1,49x10 <sup>-5</sup>	2,47x10 <sup>-6</sup>	1,62x10 <sup>-5</sup>	3,42x10 <sup>-6</sup>	N.A.	N.A.	N.A.	N.A.
Carnosol	Diterpeno	1,46x10 <sup>-5</sup>	2,11x10 <sup>-6</sup>	1,35x10 <sup>-5</sup>	5,15x10 <sup>-6</sup>	4,03x10 <sup>-8</sup>	3,18x10 <sup>-8</sup>	2,61x10 <sup>-7</sup>	2,72x10 <sup>-8</sup>
Carnosol isómero	Diterpeno	2,15x10 <sup>-5</sup>	3,30x10 <sup>-6</sup>	2,13x10 <sup>-5</sup>	5,73x10 <sup>-6</sup>	4,03x10 <sup>-8</sup>	3,18x10 <sup>-8</sup>	4,03x10 <sup>-8</sup>	3,18x10 <sup>-8</sup>
Ácido camósico	Diterpeno	1,27x10 <sup>-4</sup>	1,55x10 <sup>-5</sup>	9,04x10 <sup>-5</sup>	1,09x10 <sup>-5</sup>	N.A.	N.A.	N.A.	N.A.
Ácido 12-metoxicarmósico	Diterpeno	1,85x10 <sup>-5</sup>	4,04x10 <sup>-6</sup>	2,77x10 <sup>-5</sup>	5,12x10 <sup>-6</sup>	N.A.	N.A.	N.A.	N.A.
Rosmádial	Diterpeno	1,90x10 <sup>-5</sup>	2,84x10 <sup>-6</sup>	1,59x10 <sup>-5</sup>	1,20x10 <sup>-6</sup>	2,67x10 <sup>-6</sup>	6,43x10 <sup>-7</sup>	1,24x10 <sup>-5</sup>	9,19x10 <sup>-7</sup>
Rosmanol	Diterpeno	4,59x10 <sup>-5</sup>	7,48x10 <sup>-6</sup>	4,42x10 <sup>-5</sup>	3,53x10 <sup>-6</sup>	2,91x10 <sup>-5</sup>	9,45x10 <sup>-6</sup>	3,33x10 <sup>-5</sup>	N.E.
Epirosmanol	Diterpeno	5,51x10 <sup>-5</sup>	2,79x10 <sup>-5</sup>	1,21x10 <sup>-5</sup>	7,90x10 <sup>-6</sup>	1,92x10 <sup>-6</sup>	4,17x10 <sup>-7</sup>	2,63x10 <sup>-6</sup>	6,02x10 <sup>-7</sup>
Epiisrosmandal	Diterpeno	1,04x10 <sup>-4</sup>	1,79x10 <sup>-5</sup>	9,23x10 <sup>-6</sup>	6,55x10 <sup>-6</sup>	8,18x10 <sup>-6</sup>	3,02x10 <sup>-6</sup>	1,30x10 <sup>-5</sup>	3,52x10 <sup>-6</sup>
Miltipolona	Diterpeno	1,76x10 <sup>-5</sup>	1,97x10 <sup>-6</sup>	N.A.	N.A.	N.A.	N.A.	1,68x10 <sup>-7</sup>	8,91x10 <sup>-8</sup>
Hinoquiona	Diterpeno	N.A.		1,36x10 <sup>-5</sup>	1,22x10 <sup>-6</sup>	N.A.	N.A.	N.A.	N.A.
Rosmaridifenol	Diterpeno	2,43x10 <sup>-6</sup>	6,44x10 <sup>-7</sup>	2,68x10 <sup>-6</sup>	1,28x10 <sup>-6</sup>	N.A.	N.A.	N.A.	N.A.
Ácido augústico	Triterpeno	7,35x10 <sup>-6</sup>	3,64x10 <sup>-6</sup>	7,93x10 <sup>-6</sup>	4,12x10 <sup>-6</sup>	N.A.	N.A.	N.A.	N.A.
Ácido betulínico	Triterpeno	N.A.		6,30x10 <sup>-6</sup>	5,66x10 <sup>-7</sup>	N.A.	N.A.	N.A.	N.A.
Anemosapogenina	Triterpeno	3,27x10 <sup>-6</sup>	1,79x10 <sup>-6</sup>	6,17x10 <sup>-6</sup>	2,99x10 <sup>-6</sup>	N.A.	N.A.	N.A.	N.A.
Ácido microméricico	Triterpeno	7,20x10 <sup>-6</sup>	2,26x10 <sup>-6</sup>	2,45x10 <sup>-6</sup>	1,63x10 <sup>-6</sup>	N.A.	N.A.	N.A.	N.A.
Ácido bentámico	Triterpeno	5,20x10 <sup>-6</sup>	2,40x10 <sup>-6</sup>	7,03x10 <sup>-6</sup>	3,25x10 <sup>-6</sup>	N.A.	N.A.	N.A.	N.A.
Ácido ursólico	Triterpeno	N.A.		7,20x10 <sup>-6</sup>	2,26x10 <sup>-6</sup>	N.A.	N.A.	N.C.	N.C.
(9)-shogaol	Fenilpropanoide	N.C.		N.C.	N.C.	N.C.	N.C.	N.C.	N.C.
(9)-shogaol isómero	Fenilpropanoide	N.C.		N.C.	N.C.	N.C.	N.C.	N.C.	N.C.



## **5. DISCUSIÓN**



**1. El extracto de romero produce un efecto antiproliferativo muy similar a sus compuestos aislados en líneas celulares de cáncer de colon.**

En diversos estudios se ha demostrado la actividad citotóxica de diferentes extractos de romero y de sus principales compuestos en varios tipos de modelos de cáncer, como leucemia, próstata, mama, piel y colon [61, 106-108]. Al analizar la composición del extracto de romero, se observa que los diterpenos junto a los triterpenos, podrían ser los compuestos más activos en la inhibición de la proliferación celular. En la bibliografía se pueden encontrar estudios que postulan que el ácido carnósico podría ser el principal compuesto en la actividad citotóxica del extracto de romero.

Esta hipótesis corrobora los resultados obtenidos en el presente trabajo, en el cual la fracción 7, correspondiente al ácido carnósico, fue una de las más activas en la mayoría de líneas celulares a la concentración más baja ensayada (30 µg/mL). Las fracciones 5 (compuesta por carnosol) y 9 (taxodiona) mostraron una actividad citotóxica muy similar a la del extracto de romero completo, lo que demuestra el gran poder antiproliferativo de los diterpenos. La fracción 1 (rosmanol) mostró un gran efecto antiproliferativo en la línea HGUE-C-1 respecto a las otras líneas celulares. Además, la fracción 8 (compuesta por ácido 12-metoxicarnósico) presentó una gran inhibición de la proliferación celular en la línea SW480 respecto a las otras dos líneas. En concordancia con los resultados obtenidos, diversos estudios han demostrado la actividad antiproliferativa del ácido 12-metoxicarnósico en líneas celulares de cáncer de hígado [109].

Sin embargo, la fracción 10 (compuesta principalmente por el triterpeno ácido betulínico), demostró que este grupo de compuestos también podría contribuir significativamente a la actividad citotóxica del extracto de romero.

Respecto a los valores de IC<sub>50</sub>, en la bibliografía se pueden encontrar valores para el ácido carnósico, betulínico y ursólico de 48,5, 32,7 y 26,0 µM respectivamente, los cuales corresponden a 24 horas de tratamiento en la línea celular HT-29 [67, 110, 111]. En trabajos realizados por el grupo de investigación se han obtenido valores de IC<sub>50</sub> similares a los encontrados en la bibliografía, 31,9, 10,3 y 9,49 µM para el ácido carnósico, betulínico y ursólico respectivamente. El ácido ursólico presenta un valor de IC<sub>50</sub> en SW480 después de 48 horas de tratamiento de 23,9 µM [102]. En el caso de otros diterpenos y triterpenos, no se han encontrado valores de IC<sub>50</sub> relativos a dichos compuestos, por lo tanto, de acuerdo con los resultados obtenidos, se postula que el valor de IC<sub>50</sub> para estos compuestos es inferior a la concentración más baja probada (30 µg/mL).

Estudios recientes han demostrado la actividad antitumoral de los compuestos del romero, tanto en modelos *in vitro* como en modelos animales [61]. Según los resultados obtenidos en el presente trabajo, el ácido carnósico y el carnosol se proponen como los compuestos más activos de la hoja de romero, responsables de la actividad antiproliferativa en las células de cáncer de colon, con la posible contribución de algún triterpeno como el ácido betulínico.

A pesar de que los diterpenos ácido carnósico y carnosol presentaron una alta actividad citotóxica y/o citostática, otros diterpenos como el rosmanol y el triterpeno ácido ursólico han mostrado en diversos estudios que inducen apoptosis en células tumorales [112, 113]. Los diterpenos ácido carnósico y carnosol han demostrado alterar múltiples vías asociadas con la inflamación y el cáncer, en las cuales se incluye el factor de transcripción nuclear kappa B (NF-κB), proteínas relacionadas con la apoptosis, la vía de señalización de la fosfatidilinositol-3-kinasa (PI3K/Akt), receptores de andrógenos y estrógenos y, actividad antiangiogénica [14, 107]. Dentro de los triterpenos, el ácido betulínico se ha propuesto como un prometedor compuesto antitumoral por su actividad antiproliferativa en una gran variedad de líneas celulares de cáncer

[114-116]. Este compuesto presenta actividad antiangiogénica, induce apoptosis, actúa como inmunomodulador y además posee capacidad para inducir la diferenciación celular [117]. En el extracto de romero completo, el ácido betulínico es bastante abundante, un 3,8%, siendo el compuesto principal de la fracción 10, una de las fracciones más activas en la línea celular SW480. Además, la fracción contenía de forma minoritaria el diterpeno hinoquiona, que podría derivar de la degradación del compuesto carnosol.

La fracción 9 también presentó una gran actividad antitumoral, formada por (9)-shogaol, gingerol y taxodiona. Otros compuestos estructuralmente relacionados con el shogaol han demostrado capacidad para inducir apoptosis en células de cáncer de colon y la taxodiona procedente de especies del género *Salvia* ha mostrado poseer efecto antiproliferativo en células de leucemia [118, 119].

Finalmente, los resultados obtenidos demostraron que el extracto de romero presenta una actividad antiproliferativa igual o superior a las fracciones purificadas del mismo. Dicha actividad podría deberse a los diterpenos ácido carnósico y carnosol, además de la contribución de triterpenos con el ácido betulínico y ursólico. Este comportamiento podría deberse a un efecto aditivo o sinérgico entre los compuestos presentes en el extracto, el cual debería ser comprobado en estudios futuros. Se puede concluir que no procede avanzar en la obtención de una fracción purificada o incluso de un compuesto puro ya que no mejora la actividad antiproliferativa del extracto completo y sí aumentaría los costes de su producción. Por estas razones, los estudios posteriores fueron realizados con el extracto de romero completo.

## 2. El extracto de romero posee un efecto antiproliferativo en modelos de cáncer de colon debido principalmente a una muerte celular por necrosis y a un bloqueo del ciclo celular.

En el presente trabajo se ha podido determinar el mecanismo de acción por el cual el extracto de romero inhibe la proliferación celular. En primer lugar, mediante el análisis del ciclo celular se determinó que el extracto de romero provocaba un efecto citostático en las líneas HT-29 y SW480, bloqueando de manera significativa las células en la fase G<sub>2</sub>/M. Por otra parte, en la línea HGUE-C-1 se observó un efecto citotóxico, aumentando la fase Sub-G<sub>1</sub> (apoptosis).

Estudios previos han demostrado que extractos de romero bloquean el ciclo celular en la fase G<sub>2</sub>/M en células de melanoma humano [65]. Por otro lado, al ser un extracto Enriquecido en diterpenos (ácido carnósico y carnosol), dichos compuestos podrían ser responsables del efecto citostático del extracto de romero. En la bibliografía existen diversos estudios en los cuales se demuestra la capacidad del ácido carnósico y del carnosol de bloquear el ciclo celular en la fase G<sub>2</sub>/M en células de leucemia [120]. Dentro de los triterpenos, el ácido betulínico también ha demostrado ejercer un bloqueo en la fase G<sub>2</sub>/M en células de cáncer de mama [121].

Respecto a la cuantificación de la apoptosis, se observó una acumulación de la población celular en el cuadrante de Anexina V/7-AAD doble positivo de manera dependiente de la dosis, lo que sugiere una muerte celular por apoptosis tardía o bien por necrosis. A pesar de la presencia de la población celular en dicho cuadrante, la ausencia de células en apoptosis temprana sugiere que el mecanismo por el cual el extracto de romero ejerce su efecto antiproliferativo es la necrosis en lugar de la apoptosis. Para confirmar este efecto, se estudió la liberación de la enzima LDH, hecho que se relaciona con la permeabilización de la membrana plasmática y, por consiguiente, con una muerte por necrosis [122-124]. En este caso, tanto la cuantificación de la Anexina-V como la liberación de LDH coincidieron en los resultados obtenidos, lo que refuerza la hipótesis de una muerte celular mediada por necrosis.

Dado que la muerte celular por necroptosis comparte características fundamentales con la necrosis, una muerte celular regulada e independiente de caspasas [125, 126], se estimó oportuno el estudio de dicha muerte mediante el inhibidor específico necrostatina-1 [127]. El pretratamiento de las células con este compuesto no inhibió la muerte celular, por lo que se descarta este mecanismo de muerte. Otra hipótesis planteada como posible causa de muerte celular fue la inducción de autofagia producida por el extracto de romero. Para valorar esta posibilidad, las células fueron pretratadas con el compuesto cloroquina, un inhibidor de la autofagia [128]. Los resultados obtenidos parecen descartar la autofagia en las tres líneas celulares estudiadas.

El análisis del ciclo celular, la cuantificación de la apoptosis mediante Anexina-V, la liberación de la enzima LDH al medio de cultivo y el estudio de la necroptosis y autofagia proporcionan resultados contundentes de que el extracto de romero no induce una muerte celular por los mecanismos mencionados anteriormente. Por el contrario, todos los resultados obtenidos revelan que la actividad antitumoral del extracto de romero en las líneas celulares de cáncer de colon se debe principalmente a un efecto citotóxico, a través de muerte por necrosis, y en menor medida a un efecto citostático, bloqueando el ciclo celular en la fase G<sub>2</sub>/M.

### **3. El tratamiento con el extracto de romero induce la generación intracelular de ROS y afecta a la viabilidad mitocondrial.**

Existen evidencias de que las ROS juegan un papel importante tanto en la muerte celular por apoptosis como en la necrosis. Los resultados obtenidos demuestran que el tratamiento con el extracto de romero eleva los niveles de ROS intracelular en todas las líneas utilizadas. Niveles fisiológicos de ROS pueden regular la transcripción de múltiples genes, actuar como moléculas de señalización y como defensa contra la infección por patógenos. Por otra parte, la producción excesiva de ROS conduce a un estado exacerbado de estrés oxidativo y puede dañar irreversiblemente moléculas vitales y orgánulos, lo que puede desembocar en una muerte celular por necrosis.

Conocidas estas afirmaciones y con el fin de determinar la influencia de las ROS en el mecanismo de muerte mediado por el ER, se determinó el nivel de estrés oxidativo intracelular y sus posibles efectos en el potencial de membrana mitocondrial. En general, los resultados obtenidos demuestran que, tras el tratamiento con el extracto de romero, existe un porcentaje significativo de células con el potencial mitocondrial despolarizado, hecho que podría estar relacionado con la muerte por necrosis en las células de cáncer colorrectal.

Existen estudios que demuestran que los compuestos bioactivos pueden actuar como antioxidantes o como prooxidantes [31]. Diversos autores han comprobado que los diterpenos ácido carnósico, carnosol y rosmanol alteran la funcionalidad de la mitocondria en células humanas de cáncer hepático, mama y colorrectal, respectivamente [73, 129]. Otro compuesto como el triterpeno ácido ursólico también ha demostrado alterar el potencial de membrana mitocondrial y poseer efecto prooxidante en células humanas de cáncer de mama [130].

**4. El tratamiento de las células de cáncer de colon con ER activa la vía del factor de transcripción Nrf2 en correlación con el aumento de ROS. El silenciamiento del gen aumenta los niveles de ROS y disminuye la viabilidad celular.**

Estudios recientes han demostrado que el factor de transcripción Nrf2 es fundamental en la respuesta de defensa celular tanto en células normales como tumorales frente a gran variedad de compuestos y agentes como las ROS [131]. Para confirmar este hecho, se procedió al silenciamiento del gen de Nrf2 mediante la transfección con un siRNA. En el estudio realizado, la transfección aumentó los niveles de las especies reactivas de oxígeno de las células transfectadas frente a las no transfectadas y, además, disminuyó significativamente la viabilidad celular.

Este resultado indica que el silenciamiento del gen acelera el daño celular debido al aumento masivo de las ROS, lo que conlleva una disminución considerable de la viabilidad en las células transfectadas, provocada probablemente por una muerte por necrosis. Por lo tanto, se confirmó que el silenciamiento de Nrf2 sensibilizó a las líneas celulares frente al tratamiento con el extracto de romero. La posible supresión de enzimas antioxidantes y citoprotectoras, mecanismos de protección activados en la vía Nrf2, podría ser una de las causas del aumento de ROS y, por consiguiente, del aumento de la citotoxicidad.

En estudios anteriores se comprobó que el tratamiento de células HT-29 con dicho extracto de romero aumentó los niveles de expresión de Nrf2 y de otras proteínas reguladas por este factor de transcripción, como son las involucradas en la generación de NADPH, detoxificantes y antioxidantes [132]. Como consecuencia, es previsible que en el modelo celular estudiado en el presente trabajo y bajo el tratamiento con el extracto de romero, las células de cáncer de colon activen la vía del factor Nrf2 simplemente como mecanismo de protección y como respuesta al aumento en los niveles de ROS.

Diversos autores postulan que los compuestos inductores de Nrf2 son eficaces en el ámbito de la prevención del cáncer [133, 134], mientras que otros investigadores afirman que su activación continuada en ciertos tipos de cáncer favorece la proliferación celular y la quimiorresistencia [135, 136]. Por lo tanto, el sistema regulador Nrf2-Keap1 puede jugar un “doble papel” en el organismo, ya que diversos compuestos (inductores o inhibidores) pueden ser beneficiosos o perjudiciales según las condiciones en las que se encuentren.

## 5. El tratamiento de modelos celulares de colon con ER inhibe tanto la proliferación como la migración celular.

Dentro de las características principales de las células tumorales destacan la capacidad proliferativa, invasiva, de supervivencia y de formación de tumores a través de la metástasis. Evidentemente, los sistemas *in vitro* poseen muchas limitaciones para abordar estos aspectos dado que la tumorogénesis y la metástasis son el resultado de la interacción entre los diversos tipos celulares en el tumor y las células del tejido.

Estudios previos han demostrado la capacidad de diversos extractos de romero de inhibir la proliferación celular en varias líneas tumorales de colon [92], páncreas [137], mama [108, 138], leucemia [108, 139], próstata [108], hígado [108, 140] y pulmón [108]. En el presente trabajo, además de determinar la capacidad antiproliferativa del ER mediante técnicas convencionales, como la determinación de células viables por MTT, se utilizaron técnicas adicionales para elucidar los efectos del extracto sobre otros aspectos mencionados como la proliferación, la capacidad de supervivencia y la migración celular.

Se abordó el análisis de la proliferación celular a tiempo real mediante el equipo xCelligence RTCA en las tres líneas de cáncer de colon durante 72 horas de tratamiento con el extracto de romero, obteniendo así el índice celular en los intervalos de tiempo establecidos. Este ensayo proporcionó un resultado muy fiable sobre los cambios acontecidos en la viabilidad celular a tiempo real y durante un periodo de tiempo más amplio, indicando que el ER realmente

produce una fuerte inhibición en la proliferación de las tres líneas celulares, sobre todo en las líneas HGUE-C-1 y SW480.

Uno de los aspectos con mayor relevancia en el desarrollo del cáncer es la capacidad de supervivencia que poseen las células tumorales frente a los fármacos utilizados para su tratamiento. Uno de los métodos más empleados para determinar la citotoxicidad en modelos celulares es el ensayo clonogénico o de formación de colonias. Es un estudio a largo plazo que permite analizar la supervivencia celular a partir de la capacidad que tiene la célula de regenerarse tras haber sido expuesta a un agente tóxico, de tal manera que la evaluación *in vitro* nos permite estimar el posible tipo de respuesta del agente a nivel *in vivo* [141-143]. Los resultados obtenidos en este ensayo demostraron una inhibición de la supervivencia por el extracto de manera dosis-dependiente en las tres líneas estudiadas, que se demostró de manera más intensa a 20 µg/mL, sobre todo en las células HGUE-C-1 y SW480. Diversos autores han demostrado la capacidad de extractos de romero de inhibir la formación de colonias en células tumorales de colon y pulmón [144, 145]. Los diterpenos ácido carnósico y carnosol también han demostrado inhibir la formación de colonias en cáncer cervical y de mama [73, 146]. Dentro de los triterpenos, cabe destacar que el tratamiento de células de melanoma con ácido betulínico en combinación con la radioterapia posee un efecto aditivo en el ensayo clonogénico respecto a los tratamientos individuales [147]. En la misma línea se encuentra el ácido ursólico, el cual ha demostrado que su combinación con el ácido zoledrónico (ZOL), fármaco para el tratamiento del osteosarcoma, potencia el efecto de los compuestos de forma aislada en este tipo de cáncer [148].

El estudio de la migración celular en la investigación del cáncer es de gran interés, ya que la principal causa de muerte en los pacientes con cáncer es la capacidad de las células de migrar e invadir otros tejidos u órganos. Entre los diversos métodos para el estudio de la migración celular cabe destacar el ensayo de “cierre de herida” o *wound healing*. Estudios

recientes han demostrado la capacidad del ácido carnósico, compuesto principal del extracto de romero, de inhibir significativamente la proliferación celular y la capacidad de migración en células de cáncer de colon y cáncer cervical [67, 146]. Dichos resultados apoyan los obtenidos en la presente Tesis Doctoral, los cuales demuestran que el extracto de romero presenta una gran capacidad de inhibir la migración celular, principalmente en la línea celular HGUE-C-1, seguida de las líneas HT-29 y SW480.

## **6. El extracto de romero no presenta signos de toxicidad oral aguda en ratas Wistar.**

El uso de plantas medicinales está ampliamente extendido, sin embargo, es pertinente estudiar sus posibles efectos secundarios si se piensa en el desarrollo de nuevos fármacos a partir de extractos procedentes de dichas plantas [149]. La toxicidad de un extracto puede deberse a los compuestos presentes en él, a una sobredosis, a un uso prolongado o a la interacción con otros compuestos [150]. Por estos motivos, se debe evaluar la toxicidad oral del extracto y, con ello, establecer la seguridad del producto.

A pesar de que la guía 420 de la OCDE fija las dosis en 5, 50, 300 y 2000 mg/kg, se debe fijar como dosis inicial aquella a la cual se espera que exista algún signo de toxicidad o mortalidad; en este caso, se consideró oportuno comenzar el ensayo con el extracto de romero a una dosis de 300 mg/kg de peso corporal, dados los antecedentes sobre el uso de este tipo de extractos. La administración de una dosis límite de 2000 mg/kg de peso corporal no provocó mortalidad ni signos de toxicidad aparente en ningún animal estudiado. Los resultados del estudio histopatológico realizado al finalizar el ensayo también corroboraron la ausencia de toxicidad. Además, la evolución del peso corporal respecto al tiempo, indicador de toxicidad, mostró una tendencia positiva. De acuerdo con las normas internacionales para la clasificación de sustancias, los resultados de la exposición oral aguda del extracto de romero en ratas indican que éste podría considerarse como un extracto relativamente seguro. De hecho, estos resultados

se encuentran en concordancia con el estudio realizado por Anadón *et al.*, en el cual también se determinó que la ingesta aguda de un extracto de romero similar no provocó alteraciones en los parámetros comentados anteriormente, por lo que es considerado un extracto que presenta baja toxicidad oral [151].

## 7. El extracto de romero disminuye la tumorogénesis en un modelo *in vivo* de xenotransplantes de cáncer de colon.

La implantación de xenotransplantes en ratones inmunodeprimidos permitió estudiar la progresión y la evolución de los tumores de colon humano durante el tratamiento de los animales con el extracto de romero por vía oral.

Existen antecedentes de la capacidad de los compuestos del romero de inhibir el crecimiento de tumores de diverso origen. Kim *et al.* comprobaron que los ratones tratados con ácido carnósico frente a los no tratados presentaron un menor número de tumores de colon [71]. Un estudio reciente realizado por Wang *et al.* en un modelo de ratón con leucemia inducida por la línea celular K562/A02 demostró que el tratamiento de los animales con ácido carnósico y adriamicina aumentó el número de células apoptóticas en comparación con los animales tratados sólo con adriamicina [152]. Estos resultados demuestran que el ácido carnósico posee actividad antitumoral de forma individual o en combinación con otros compuestos en modelos *in vivo*. Además, se ha descrito un posible efecto preventivo de este compuesto, a 10 mg/kg en un modelo de hámster dorado (Golden Hamster) con cáncer bucal inducido por 7,12-dimetilbenzo(a)antraceno, inhibiendo casi por completo la implantación de estos tumores respecto al grupo control [153]. Esto podría deberse a la absorción intestinal del ácido carnósico o a posibles metabolitos derivados de este compuesto con efecto antitumoral. De hecho, Doolaege *et al.* demostraron que el ácido carnósico se absorbe después de la administración oral en ratas y existen trazas en intestino, abdomen, hígado, piernas y tejido muscular [154].

Otro diterpeno presente en el ER, el carnosol, ha demostrado capacidad por vía oral para disminuir de manera significativa el volumen de tumores de fibrosarcoma implantados en ratones atípicos BALB/c [155]. Además, existen estudios que demuestran que el carnosol administrado por vía oral a una dosis de 30 mg/kg reduce el crecimiento de tumores de próstata en ratones immunodeprimidos un 36% respecto al control no tratado [156]. Cabe destacar que extractos de romero similares al estudiado en el presente trabajo presentaron efecto antitumoral en modelos *in vivo* de cáncer de colon y páncreas [137].

Los resultados comentados anteriormente confirman los datos obtenidos en el presente trabajo, los cuales demuestran que el tratamiento con el extracto de romero enriquecido en diterpenos y triterpenos podría tener un efecto preventivo en la formación de tumores y que, además, inhibe el desarrollo del tumor una vez formado.

#### **8. La absorción de los compuestos del ER en forma libre y liposomada en modelos de monocapas de células intestinales es moderada y se produce principalmente por difusión pasiva.**

La absorción intestinal de compuestos bioactivos en el modelo celular Caco-2 ha sido ampliamente estudiada por diversos autores [157-161]. Sin embargo, existe una escasa información sobre la absorción de los compuestos cuando se encuentran presentes en extractos complejos.

A pesar del bajo porcentaje de flavonoides y derivados de ácidos fenólicos presentes en el extracto de romero, estos compuestos merecen el estudio de su absorción por la importante actividad biológica que suelen presentar. El compuesto (9)-shogaol y su isómero se encontraban por debajo de su límite de detección, por lo que no se pudo obtener el valor de permeabilidad, sin embargo, el análisis de las muestras mediante HPLC desveló que estos compuestos se encontraban parcialmente retenidos en la membrana celular y en la fracción citoplasmática de la línea Caco-2. A pesar de no existir en la bibliografía datos sobre la absorción del compuesto (9)-

shogaol, los datos sobre un compuesto similar, el (6)-shogaol, podrían confirmar dicha teoría, sugiriendo que dicho compuesto podría sufrir una biotransformación a través de la monocapa celular o bien quedado retenido en ella [162].

Según los resultados obtenidos, puede concluirse que los flavonoides presentes en el extracto de romero no mostraron diferencias en la absorción entre los dos sentidos estudiados cuando el extracto se encontraba en forma libre, lo que sugiere un transporte de absorción por difusión pasiva [163, 164]. Por otra parte, cabe resaltar que la encapsulación del extracto en liposomas no mejoró la absorción de esta familia de compuestos. En cuanto al flavonoide apigenina, no se pudo cuantificar ya que se encontraba por debajo del límite de cuantificación. Sin embargo, existe un estudio en el cual se determina su absorción de forma individual, obteniendo un valor de permeabilidad de  $1,38 \times 10^{-5}$  cm/s [165]. Los valores de permeabilidad más elevados pertenecen a la cirsimaritina y la genkwanina, siendo el primer estudio en determinar dichos valores a partir del extracto completo en el modelo celular Caco-2.

La diosmetina y la hispidulina mostraron los valores de permeabilidad más bajos, sin embargo, un estudio demuestra que la diosmetina de forma pura presenta valores de permeabilidad más altos [159]. Esta diferencia con los resultados obtenidos en el presente trabajo podría deberse a la baja presencia del compuesto en el extracto de romero y/o a la competencia con otros polifenoles y terpenos presentes en el extracto.

Respecto al grupo de los diterpenos, el ácido carnósico fue el que presentó la mayor permeabilidad, seguido del epiisorrosmanol, epirosmanol y el rosmanol. En general, la encapsulación en liposomas del extracto no mejoró la absorción de ninguno de los compuestos estudiados en este grupo. También se puede concluir, que ligeras modificaciones en la estructura de estos compuestos podrían ser cruciales en los valores de permeabilidad.

Por último, en el grupo de los triterpenos también se observó absorción cuando el extracto se encontraba de forma libre y no cuando se encontraba de forma liposomada. El ácido augústico y el ácido micromérico presentaron los valores de permeabilidad más altos, sin embargo, de manera global fue el grupo de compuestos que mostró menor absorción. La alta hidrofobicidad de estos compuestos podría ser la causa de quedar retenidos en los fosfolípidos de los liposomas o por la interacción con la membrana plasmática y otras estructuras lipídicas en el interior celular. Hechos que, sin duda, necesitan ensayos futuros para ser ratificados.

Dado que la absorción de todos los compuestos se analizó en el contexto del extracto completo, se pueden producir mecanismos de interacción como competencia entre los compuestos, en particular entre los que presentan estructuras químicas muy similares. Los resultados también indican que la mayoría de compuestos son moderadamente absorbidos y el principal mecanismo de absorción para los compuestos es la difusión pasiva. Por otra parte, el uso de liposomas para mejorar la absorción de los compuestos no resultó ser una estrategia eficiente, ya que de manera contraria a otros estudios, no mejoró la permeabilidad [166].

Finalmente, los resultados obtenidos en la presente memoria justifican la realización de ensayos preclínicos adicionales con el objetivo de corroborar los efectos observados con el extracto de romero y de profundizar en el mecanismo molecular de la acción potencialmente antitumoral del extracto. En la actualidad se está realizando un estudio transcriptómico, proteómico y metabolómico de los tumores procedentes del ensayo animal con el objetivo de esclarecer qué genes modulan su expresión y cuáles son las rutas metabólicas afectadas por la acción del extracto utilizado por vía oral. Por otro lado, también se hace necesario realizar estudios de metabolómica en modelos animales o en ensayos de intervención en humanos con el propósito de conocer los metabolitos potencialmente responsables de la actividad observada.

## **6. CONCLUSIONES**



1. La caracterización y cuantificación del extracto de romero (ER), revela que los compuestos mayoritarios en el extracto son los triterpenos, seguidos de los diterpenos y, por último, en menor medida los flavonoides. Los ensayos de citotoxicidad en las tres líneas de cáncer de colon utilizadas mostraron una actividad antiproliferativa del extracto de romero muy similar o superior, en la mayoría de los casos, a la que presentaron las fracciones aisladas del mismo. Después de comparar los resultados obtenidos con aquellos previamente publicados en la bibliografía, se propone a los diterpenos, ácido carnósico y carnosol, junto con algún triterpeno como el ácido betulínico, como responsables de los efectos observados.
2. Las causas principales de la inhibición de la proliferación celular en modelos *in vitro* de cáncer de colon por parte del extracto de romero son el bloqueo del ciclo celular (efecto citostático) y, en mayor medida, la muerte celular por necrosis (efecto citotóxico). Esta capacidad antiproliferativa viene acompañada por un aumento de la generación intracelular de ROS que conlleva la pérdida del potencial de membrana mitocondrial, hechos que podrían ser los responsables de dicha capacidad antiproliferativa.
3. El silenciamiento del gen correspondiente al factor de transcripción Nrf2 sensibiliza a las células de carcinoma de colon frente al tratamiento con el extracto de romero, aumentando los niveles de ROS intracelular y disminuyendo la viabilidad celular, probablemente por un aumento de la necrosis. Este efecto podría deberse a la disminución de la expresión de enzimas antioxidantes y otros mecanismos de protección activados en la vía Nrf2 que protegen a las células de un elevado estrés oxidativo.



4. El tratamiento de células de cáncer de colon con el extracto de romero muestra una fuerte actividad antiproliferativa a medio-largo plazo. El extracto de romero también disminuye la capacidad migratoria de grupos de células en las tres líneas de cáncer de colon utilizadas.
5. La administración oral aguda del extracto de romero en ratas, 2000 mg/kg, no reveló ningún signo de toxicidad ni mortalidad en los animales estudiados. Según los resultados obtenidos, el extracto de romero se clasifica según la guía 420 de la OCDE como una sustancia no clasificada, por lo que su ingesta se considera segura.
6. La administración oral del extracto de romero a 200 mg/kg, en un modelo de xenotransplantes de células de carcinoma de colon HT-29 en ratones inmunodeprimidos muestra una inhibición significativa del tamaño de los tumores, sin observar pérdida de peso corporal ni signos de toxicidad en los animales. Estos hechos justifican la utilización de dicho extracto en nuevos ensayos preclínicos para corroborar su eficacia.
7. Se han obtenido datos de permeabilidad y de absorción de un total de 24 compuestos presentes en el extracto de romero de forma libre y encapsulada en liposomas en un modelo de monocapas de células intestinales, determinados por primera vez en un extracto complejo. El mecanismo principal propuesto para la absorción de estos compuestos es la difusión pasiva. La encapsulación del extracto de romero en liposomas no mejoró en ningún caso la absorción de los compuestos presentes en el extracto. Los diterpenos mostraron valores de permeabilidad superiores que los triterpenos y los flavonoides, siendo el ácido carnósico y el epiisorrosmanol los que presentaron los valores de permeabilidad más altos. Se propone a los diterpenos y a algún triterpeno como los compuestos que contribuyen a los efectos observados en el modelo animal.





## 7. BIBLIOGRAFÍA



1. Torre, L.A., et al., *Global cancer statistics, 2012*. CA Cancer J Clin, 2015. **65**(2): p. 87-108.
2. Todd, R., et al., *Cell cycle dysregulation in oral cancer*. Crit Rev Oral Biol Med, 2002. **13**(1): p. 51-61.
3. Stewart, Z.A., M.D. Westfall, and J.A. Pietenpol, *Cell-cycle dysregulation and anticancer therapy*. Trends Pharmacol Sci, 2003. **24**(3): p. 139-45.
4. Elmore, S., *Apoptosis: a review of programmed cell death*. Toxicol Pathol, 2007. **35**(4): p. 495-516.
5. Ouyang, L., et al., *Programmed cell death pathways in cancer: a review of apoptosis, autophagy and programmed necrosis*. Cell Prolif, 2012. **45**(6): p. 487-98.
6. MacFarlane, M. and A.C. Williams, *Apoptosis and disease: a life or death decision*. EMBO Rep, 2004. **5**(7): p. 674-8.
7. Franklin, J.L., *Redox regulation of the intrinsic pathway in neuronal apoptosis*. Antioxid Redox Signal, 2011. **14**(8): p. 1437-48.
8. Golstein, P. and G. Kroemer, *Cell death by necrosis: towards a molecular definition*. Trends Biochem Sci, 2007. **32**(1): p. 37-43.
9. Fulda, S., et al., *Cellular stress responses: cell survival and cell death*. Int J Cell Biol, 2010. **2010**: p. 214074.
10. Wu, W., P. Liu, and J. Li, *Necroptosis: an emerging form of programmed cell death*. Crit Rev Oncol Hematol, 2012. **82**(3): p. 249-58.
11. Zhao, H., et al., *Role of necroptosis in the pathogenesis of solid organ injury*. Cell Death Dis, 2015. **6**: p. e1975.
12. Chen, D., et al., *EGCG, green tea polyphenols and their synthetic analogs and prodrugs for human cancer prevention and treatment*. Adv Clin Chem, 2011. **53**: p. 155-77.
13. Weng, C.J. and G.C. Yen, *Chemopreventive effects of dietary phytochemicals against cancer invasion and metastasis: phenolic acids, monophenol, polyphenol, and their derivatives*. Cancer Treat Rev, 2012. **38**(1): p. 76-87.
14. Kuriyama, S., et al., *Green tea consumption and mortality due to cardiovascular disease, cancer, and all causes in Japan: the Ohsaki study*. JAMA, 2006. **296**(10): p. 1255-65.
15. Mursu, J., et al., *Flavonoid intake and the risk of ischaemic stroke and CVD mortality in middle-aged Finnish men: the Kuopio Ischaemic Heart Disease Risk Factor Study*. Br J Nutr, 2008. **100**(4): p. 890-5.
16. Jeong, W.Y., et al., *Determination of polyphenols in three Capsicum annuum L. (bell pepper) varieties using high-performance liquid chromatography-tandem mass spectrometry: their contribution to overall antioxidant and anticancer activity*. J Sep Sci, 2011. **34**(21): p. 2967-74.
17. Ogunleye, A.A., F. Xue, and K.B. Michels, *Green tea consumption and breast cancer risk or recurrence: a meta-analysis*. Breast Cancer Res Treat, 2010. **119**(2): p. 477-84.

18. Liu, L., et al., *The antiatherogenic potential of oat phenolic compounds*. Atherosclerosis, 2004. **175**(1): p. 39-49.
19. Mulvihill, E.E. and M.W. Huff, *Antiatherogenic properties of flavonoids: implications for cardiovascular health*. Can J Cardiol, 2010. **26 Suppl A**: p. 17A-21A.
20. Beara, I.N., et al., *Phenolic profile, antioxidant, anti-inflammatory and cytotoxic activities of black (*Tuber aestivum* Vittad.) and white (*Tuber magnatum* Pico) truffles*. Food Chem, 2014. **165**: p. 460-6.
21. Zimmer, A.R., et al., *Antioxidant and anti-inflammatory properties of Capsicum baccatum: from traditional use to scientific approach*. J Ethnopharmacol, 2012. **139**(1): p. 228-33.
22. Silva, J.C., et al., *Antimicrobial activity, phenolic profile and role in the inflammation of propolis*. Food Chem Toxicol, 2012. **50**(5): p. 1790-5.
23. Perez-Fons, L., M.T. Garzon, and V. Micol, *Relationship between the antioxidant capacity and effect of rosemary (*Rosmarinus officinalis* L.) polyphenols on membrane phospholipid order*. J Agric Food Chem, 2010. **58**(1): p. 161-71.
24. Mondal, H., et al., *Central-stimulating and analgesic activity of the ethanolic extract of Alternanthera sessilis in mice*. BMC Complement Altern Med, 2014. **14**: p. 398.
25. Abourashed, E.A., *Bioavailability of Plant-Derived Antioxidants*. Antioxidants (Basel), 2013. **2**(4): p. 309-25.
26. Ververidis, F., et al., *Biotechnology of flavonoids and other phenylpropanoid-derived natural products. Part I: Chemical diversity, impacts on plant biology and human health*. Biotechnol J, 2007. **2**(10): p. 1214-34.
27. Lindsay, D.G. and S.B. Astley, *European research on the functional effects of dietary antioxidants - EUFEDA*. Mol Aspects Med, 2002. **23**(1-3): p. 1-38.
28. Myburgh, K.H., *Polyphenol supplementation: benefits for exercise performance or oxidative stress?* Sports Med, 2014. **44 Suppl 1**: p. S57-70.
29. Porter, J.W.S., S. L., *Biosynthesis of Isoprenoid Compounds*, ed. W.-I. Publication. Vol. I. 1981, New York.
30. Schiestl, F.P., et al., *Sex pheromone mimicry in the early spider orchid (*ophrys sphegodes*): patterns of hydrocarbons as the key mechanism for pollination by sexual deception*. J Comp Physiol A, 2000. **186**(6): p. 567-74.
31. Galati, G. and P.J. O'Brien, *Potential toxicity of flavonoids and other dietary phenolics: significance for their chemopreventive and anticancer properties*. Free Radic Biol Med, 2004. **37**(3): p. 287-303.
32. Cao, G., E. Sofic, and R.L. Prior, *Antioxidant and prooxidant behavior of flavonoids: structure-activity relationships*. Free Radic Biol Med, 1997. **22**(5): p. 749-60.
33. Day, B.W., et al., *Peroxidase-catalyzed pro- versus antioxidant effects of 4-hydroxytamoxifen: enzyme specificity and biochemical sequelae*. Chem Res Toxicol, 1999. **12**(1): p. 28-37.

34. Yoon, H.S., et al., *Genistein induces apoptosis of RPE-J cells by opening mitochondrial PTP*. Biochem Biophys Res Commun, 2000. **276**(1): p. 151-6.
35. Bolton, J.L., et al., *Role of quinones in toxicology*. Chem Res Toxicol, 2000. **13**(3): p. 135-60.
36. Morin, D., et al., *Curcumin induces the mitochondrial permeability transition pore mediated by membrane protein thiol oxidation*. FEBS Lett, 2001. **495**(1-2): p. 131-6.
37. Inayat-Hussain, S.H., S.L. Winski, and D. Ross, *Differential involvement of caspases in hydroquinone-induced apoptosis in human leukemic hl-60 and jurkat cells*. Toxicol Appl Pharmacol, 2001. **175**(2): p. 95-103.
38. Salvi, M., et al., *Interaction of genistein with the mitochondrial electron transport chain results in opening of the membrane transition pore*. Biochim Biophys Acta, 2002. **1556**(2-3): p. 187-96.
39. Mouria, M., et al., *Food-derived polyphenols inhibit pancreatic cancer growth through mitochondrial cytochrome C release and apoptosis*. Int J Cancer, 2002. **98**(5): p. 761-9.
40. Shen, S.C., et al., *Structurally related antitumor effects of flavanones in vitro and in vivo: involvement of caspase 3 activation, p21 gene expression, and reactive oxygen species production*. Toxicol Appl Pharmacol, 2004. **197**(2): p. 84-95.
41. Sergediene, E., et al., *Prooxidant toxicity of polyphenolic antioxidants to HL-60 cells: description of quantitative structure-activity relationships*. FEBS Lett, 1999. **462**(3): p. 392-6.
42. Dickancaite, E., et al., *Prooxidant character of flavonoid cytotoxicity: structure-activity relationships*. Biochem Mol Biol Int, 1998. **45**(5): p. 923-30.
43. Boonstra, J. and J.A. Post, *Molecular events associated with reactive oxygen species and cell cycle progression in mammalian cells*. Gene, 2004. **337**: p. 1-13.
44. Frippiat, C., et al., *Signal transduction in H2O2-induced senescence-like phenotype in human diploid fibroblasts*. Free Radic Biol Med, 2002. **33**(10): p. 1334-46.
45. Fiers, W., et al., *More than one way to die: apoptosis, necrosis and reactive oxygen damage*. Oncogene, 1999. **18**(54): p. 7719-30.
46. Bouayed, J. and T. Bohn, *Exogenous antioxidants--Double-edged swords in cellular redox state: Health beneficial effects at physiologic doses versus deleterious effects at high doses*. Oxid Med Cell Longev, 2010. **3**(4): p. 228-37.
47. Kobayashi, A., et al., *Oxidative and electrophilic stresses activate Nrf2 through inhibition of ubiquitination activity of Keap1*. Mol Cell Biol, 2006. **26**(1): p. 221-9.
48. Lee, J.M. and J.A. Johnson, *An important role of Nrf2-ARE pathway in the cellular defense mechanism*. J Biochem Mol Biol, 2004. **37**(2): p. 139-43.
49. Venugopal, R. and A.K. Jaiswal, *Nrf1 and Nrf2 positively and c-Fos and Fra1 negatively regulate the human antioxidant response element-mediated expression of NAD(P)H:quinone oxidoreductase1 gene*. Proc Natl Acad Sci U S A, 1996. **93**(25): p. 14960-5.
50. Jaiswal, A.K., *Nrf2 signaling in coordinated activation of antioxidant gene expression*. Free Radic Biol Med, 2004. **36**(10): p. 1199-207.

51. Granata, S., et al., *Mitochondria: a new therapeutic target in chronic kidney disease*. Nutr Metab (Lond), 2015. **12**: p. 49.
52. Szeto, H.H., *Mitochondria-targeted peptide antioxidants: novel neuroprotective agents*. AAPS J, 2006. **8**(3): p. E521-31.
53. Bai, J. and A.I. Cederbaum, *Mitochondrial catalase and oxidative injury*. Biol Signals Recept, 2001. **10**(3-4): p. 189-99.
54. Manach, C., et al., *Polyphenols: food sources and bioavailability*. Am J Clin Nutr, 2004. **79**(5): p. 727-47.
55. Scalbert, A. and G. Williamson, *Dietary intake and bioavailability of polyphenols*. J Nutr, 2000. **130**(8S Suppl): p. 2073S-85S.
56. Natsume, M., et al., *Structures of (-)-epicatechin glucuronide identified from plasma and urine after oral ingestion of (-)-epicatechin: differences between human and rat*. Free Radic Biol Med, 2003. **34**(7): p. 840-9.
57. Cherubini, A., M.F. Beal, and B. Frei, *Black tea increases the resistance of human plasma to lipid peroxidation in vitro, but not ex vivo*. Free Radic Biol Med, 1999. **27**(3-4): p. 381-7.
58. Nifli, A.P., et al., *Polyphenol interaction with the T47D human breast cancer cell line*. J Dairy Res, 2005. **72 Spec No**: p. 44-50.
59. Borras-Linares, I., et al., *A bioguided identification of the active compounds that contribute to the antiproliferative/cytotoxic effects of rosemary extract on colon cancer cells*. Food Chem Toxicol, 2015. **80**: p. 215-22.
60. Borras-Linares, I., et al., *Rosmarinus officinalis leaves as a natural source of bioactive compounds*. Int J Mol Sci, 2014. **15**(11): p. 20585-606.
61. Ngo, S.N., D.B. Williams, and R.J. Head, *Rosemary and cancer prevention: preclinical perspectives*. Crit Rev Food Sci Nutr, 2011. **51**(10): p. 946-54.
62. Raskovic, A., et al., *Antioxidant activity of rosemary (*Rosmarinus officinalis L.*) essential oil and its hepatoprotective potential*. BMC Complement Altern Med, 2014. **14**: p. 225.
63. Bozin, B., et al., *Antimicrobial and antioxidant properties of rosemary and sage (*Rosmarinus officinalis L.* and *Salvia officinalis L.*, Lamiaceae) essential oils*. J Agric Food Chem, 2007. **55**(19): p. 7879-85.
64. Del Campo, J., M.J. Amiot, and C. Nguyen-The, *Antimicrobial effect of rosemary extracts*. J Food Prot, 2000. **63**(10): p. 1359-68.
65. Cattaneo, L., et al., *Anti-Proliferative Effect of Rosmarinus officinalis L. Extract on Human Melanoma A375 Cells*. PLoS One, 2015. **10**(7): p. e0132439.
66. Singletary, K., C. MacDonald, and M. Wallig, *Inhibition by rosemary and carnosol of 7,12-dimethylbenz[a]anthracene (DMBA)-induced rat mammary tumorigenesis and in vivo DMBA-DNA adduct formation*. Cancer Lett, 1996. **104**(1): p. 43-8.

67. Barni, M.V., et al., *Carnosic acid inhibits the proliferation and migration capacity of human colorectal cancer cells*. Oncol Rep, 2012. **27**(4): p. 1041-8.
68. Min, K.J., K.J. Jung, and T.K. Kwon, *Carnosic Acid Induces Apoptosis Through Reactive Oxygen Species-mediated Endoplasmic Reticulum Stress Induction in Human Renal Carcinoma Caki Cells*. J Cancer Prev, 2014. **19**(3): p. 170-8.
69. Park, S.Y., et al., *Carnosic acid inhibits the epithelial-mesenchymal transition in B16F10 melanoma cells: a possible mechanism for the inhibition of cell migration*. Int J Mol Sci, 2014. **15**(7): p. 12698-713.
70. Kim, D.H., et al., *Carnosic acid inhibits STAT3 signaling and induces apoptosis through generation of ROS in human colon cancer HCT116 cells*. Mol Carcinog, 2016. **55**(6): p. 1096-110.
71. Kim, Y.J., et al., *Carnosic acid suppresses colon tumor formation in association with antiadipogenic activity*. Mol Nutr Food Res, 2014. **58**(12): p. 2274-85.
72. Chun, K.S., et al., *Carnosol: a phenolic diterpene with cancer chemopreventive potential*. J Cancer Prev, 2014. **19**(2): p. 103-10.
73. Al Dhaheri, Y., et al., *Carnosol induces ROS-mediated beclin1-independent autophagy and apoptosis in triple negative breast cancer*. PLoS One, 2014. **9**(10): p. e109630.
74. Johnson, J.J., et al., *Carnosol, a dietary diterpene, displays growth inhibitory effects in human prostate cancer PC3 cells leading to G2-phase cell cycle arrest and targets the 5'-AMP-activated protein kinase (AMPK) pathway*. Pharm Res, 2008. **25**(9): p. 2125-34.
75. Mishra, T., et al., *Isolation, Characterization and Anticancer Potential of Cytotoxic Triterpenes from Betula utilis Bark*. PLoS One, 2016. **11**(7): p. e0159430.
76. Doolaege, E.H., et al., *Characterization of two unknown compounds in methanol extracts of rosemary oil*. J Agric Food Chem, 2007. **55**(18): p. 7283-7.
77. Almela, L., et al., *Liquid chromatographic-mass spectrometric analysis of phenolics and free radical scavenging activity of rosemary extract from different raw material*. J Chromatogr A, 2006. **1120**(1-2): p. 221-9.
78. Paniwnyk, L., et al., *The enhancement and scale up of the extraction of anti-oxidants from Rosmarinus officinalis using ultrasound*. Ultrason Sonochem, 2009. **16**(2): p. 287-92.
79. Presti, M.L., et al., *A comparison between different techniques for the isolation of rosemary essential oil*. J Sep Sci, 2005. **28**(3): p. 273-80.
80. Fornari, T., et al., *Isolation of essential oil from different plants and herbs by supercritical fluid extraction*. J Chromatogr A, 2012. **1250**: p. 34-48.
81. Ibanez, E., et al., *Subcritical water extraction of antioxidant compounds from rosemary plants*. J Agric Food Chem, 2003. **51**(2): p. 375-82.
82. Garcia-Perez, J.S., et al., *Identification of Bioactivity, Volatile and Fatty Acid Profile in Supercritical Fluid Extracts of Mexican arnica*. Int J Mol Sci, 2016. **17**(9).

83. Li, J., J. Zhang, and M. Wang, *Extraction of Flavonoids from the Flowers of Abelmoschus manihot (L.) Medic by Modified Supercritical CO<sub>2</sub>) Extraction and Determination of Antioxidant and Anti-Adipogenic Activity*. *Molecules*, 2016. **21**(7).
84. Cheng, M.C., et al., *Antioxidant Properties of Essential Oil Extracted from Pinus morrisonicola Hay Needles by Supercritical Fluid and Identification of Possible Active Compounds by GC/MS*. *Molecules*, 2015. **20**(10): p. 19051-65.
85. Zugic, A., et al., *Evaluation of Anticancer and Antioxidant Activity of a Commercially Available CO<sub>2</sub> Supercritical Extract of Old Man's Beard (*Usnea barbata*)*. *PLoS One*, 2016. **11**(1): p. e0146342.
86. Chauhan, R., et al., *Characterization of *Linum usitatissimum L.* oil obtained from different extraction technique and in vitro antioxidant potential of supercritical fluid extract*. *J Pharm Bioallied Sci*, 2015. **7**(4): p. 284-8.
87. Mohammed, N.K., et al., *The Effects of Different Extraction Methods on Antioxidant Properties, Chemical Composition, and Thermal Behavior of Black Seed (*Nigella sativa L.*) Oil*. *Evid Based Complement Alternat Med*, 2016. **2016**: p. 6273817.
88. Valle, D.L., Jr., et al., *Antimicrobial Activities of Methanol, Ethanol and Supercritical CO<sub>2</sub> Extracts of Philippine Piper betle L. on Clinical Isolates of Gram Positive and Gram Negative Bacteria with Transferable Multiple Drug Resistance*. *PLoS One*, 2016. **11**(1): p. e0146349.
89. Tremonte, P., et al., *Antimicrobial Effect of Malpighia Punicifolia and Extension of Water Buffalo Steak Shelf-Life*. *J Food Sci*, 2016. **81**(1): p. M97-105.
90. Justo, O.R., et al., *Evaluation of in vitro anti-inflammatory effects of crude ginger and rosemary extracts obtained through supercritical CO<sub>2</sub> extraction on macrophage and tumor cell line: the influence of vehicle type*. *BMC Complement Altern Med*, 2015. **15**: p. 390.
91. Moon, J.Y., H. Kim, and S.K. Cho, *Auraptene, a Major Compound of Supercritical Fluid Extract of Phalsak (*Citrus Hassaku Hort ex Tanaka*), Induces Apoptosis through the Suppression of mTOR Pathways in Human Gastric Cancer SNU-1 Cells*. *Evid Based Complement Alternat Med*, 2015. **2015**: p. 402385.
92. Valdes, A., et al., *Effect of rosemary polyphenols on human colon cancer cells: transcriptomic profiling and functional enrichment analysis*. *Genes Nutr*, 2013. **8**(1): p. 43-60.
93. Grasso, S., et al., *HGUE-C-1 is an atypical and novel colon carcinoma cell line*. *BMC Cancer*, 2015. **15**: p. 240.
94. Herrero, M., et al., *Green processes for the extraction of bioactives from Rosemary: Chemical and functional characterization via ultra-performance liquid chromatography-tandem mass spectrometry and in-vitro assays*. *J Chromatogr A*, 2010. **1217**(16): p. 2512-20.
95. Saad, B., et al., *Evaluation of medicinal plant hepatotoxicity in co-cultures of hepatocytes and monocytes*. *Evid Based Complement Alternat Med*, 2006. **3**(1): p. 93-8.

96. Chan, F.K., K. Moriwaki, and M.J. De Rosa, *Detection of necrosis by release of lactate dehydrogenase activity*. Methods Mol Biol, 2013. **979**: p. 65-70.
97. Perez-Sanchez, A., et al., *Protective effects of citrus and rosemary extracts on UV-induced damage in skin cell model and human volunteers*. J Photochem Photobiol B, 2014. **136**: p. 12-8.
98. Tiruppathi, C., et al., *Electrical method for detection of endothelial cell shape change in real time: assessment of endothelial barrier function*. Proc Natl Acad Sci U S A, 1992. **89**(17): p. 7919-23.
99. Whipple, R.A., et al., *Epithelial-to-mesenchymal transition promotes tubulin detyrosination and microtentacles that enhance endothelial engagement*. Cancer Res, 2010. **70**(20): p. 8127-37.
100. Boyd, J.M., et al., *A cell-microelectronic sensing technique for profiling cytotoxicity of chemicals*. Anal Chim Acta, 2008. **615**(1): p. 80-7.
101. Aleman, C.L., et al., *Reference data for the principal physiological indicators in three species of laboratory animals*. Lab Anim, 2000. **34**(4): p. 379-85.
102. van Breemen, R.B. and Y. Li, *Caco-2 cell permeability assays to measure drug absorption*. Expert Opin Drug Metab Toxicol, 2005. **1**(2): p. 175-85.
103. Lin, H., et al., *Enhancing effect of surfactants on fexofenadine.HCl transport across the human nasal epithelial cell monolayer*. Int J Pharm, 2007. **330**(1-2): p. 23-31.
104. Borras Linares, I., et al., *Comparison of different extraction procedures for the comprehensive characterization of bioactive phenolic compounds in Rosmarinus officinalis by reversed-phase high-performance liquid chromatography with diode array detection coupled to electrospray time-of-flight mass spectrometry*. J Chromatogr A, 2011. **1218**(42): p. 7682-90.
105. Winder, C., R. Azzi, and D. Wagner, *The development of the globally harmonized system (GHS) of classification and labelling of hazardous chemicals*. J Hazard Mater, 2005. **125**(1-3): p. 29-44.
106. Einbond, L.S., et al., *Carnosic acid inhibits the growth of ER-negative human breast cancer cells and synergizes with curcumin*. Fitoterapia, 2012. **83**(7): p. 1160-8.
107. Johnson, J.J., *Carnosol: a promising anti-cancer and anti-inflammatory agent*. Cancer Lett, 2011. **305**(1): p. 1-7.
108. Yesil-Celiktas, O., et al., *Inhibitory effects of rosemary extracts, carnosic acid and rosmarinic acid on the growth of various human cancer cell lines*. Plant Foods Hum Nutr, 2010. **65**(2): p. 158-63.
109. Peng, C.H., et al., *Supercritical fluid extracts of rosemary leaves exhibit potent anti-inflammation and anti-tumor effects*. Biosci Biotechnol Biochem, 2007. **71**(9): p. 2223-32.
110. Ding, W., et al., *A 3D QSAR study of betulinic acid derivatives as anti-tumor agents using topomer CoMFA: model building studies and experimental verification*. Molecules, 2013. **18**(9): p. 10228-41.
111. Shan, J.Z., et al., *Ursolic acid inhibits proliferation and induces apoptosis of HT-29 colon cancer cells by inhibiting the EGFR/MAPK pathway*. J Zhejiang Univ Sci B, 2009. **10**(9): p. 668-74.
112. Meng, Y., et al., *Ursolic Acid Induces Apoptosis of Prostate Cancer Cells via the PI3K/Akt/mTOR Pathway*. Am J Chin Med, 2015. **43**(7): p. 1471-86.

113. Cheng, A.C., et al., *Rosmanol potently induces apoptosis through both the mitochondrial apoptotic pathway and death receptor pathway in human colon adenocarcinoma COLO 205 cells*. Food Chem Toxicol, 2011. **49**(2): p. 485-93.
114. Potze, L., et al., *Betulinic Acid Kills Colon Cancer Stem Cells*. Curr Stem Cell Res Ther, 2015.
115. Ali-Seyed, M., et al., *Betulinic Acid: Recent Advances in Chemical Modifications, Effective Delivery, and Molecular Mechanisms of a Promising Anticancer Therapy*. Chem Biol Drug Des, 2016. **87**(4): p. 517-36.
116. An, N., H.Y. Li, and X.M. Zhang, *Growth inhibitive effect of betulinic acid combined with tripterine on MSB-1 cells and its mechanism*. Poult Sci, 2015. **94**(12): p. 2880-6.
117. Laszczyk, M.N., *Pentacyclic triterpenes of the lupane, oleanane and ursane group as tools in cancer therapy*. Planta Med, 2009. **75**(15): p. 1549-60.
118. Fu, J., et al., *Cysteine-conjugated metabolites of ginger components, shogaols, induce apoptosis through oxidative stress-mediated p53 pathway in human colon cancer cells*. J Agric Food Chem, 2014. **62**(20): p. 4632-42.
119. Tayarani-Najaran, Z., et al., *Cytotoxic and apoptogenic properties of three isolated diterpenoids from Salvia chorassanica through bioassay-guided fractionation*. Food Chem Toxicol, 2013. **57**: p. 346-51.
120. Visanji, J.M., D.G. Thompson, and P.J. Padfield, *Induction of G2/M phase cell cycle arrest by carnosol and carnosic acid is associated with alteration of cyclin A and cyclin B1 levels*. Cancer Lett, 2006. **237**(1): p. 130-6.
121. Mertens-Talcott, S.U., et al., *Betulinic acid decreases ER-negative breast cancer cell growth in vitro and in vivo: role of Sp transcription factors and microRNA-27a:ZBTB10*. Mol Carcinog, 2013. **52**(8): p. 591-602.
122. Nzaramba, M.N., et al., *Antiproliferative activity and cytotoxicity of Solanum jamesii tuber extracts on human colon and prostate cancer cells in vitro*. J Agric Food Chem, 2009. **57**(18): p. 8308-15.
123. Szliszka, E., et al., *Ethanol Extract of Polish Propolis: Chemical Composition and TRAIL-R2 Death Receptor Targeting Apoptotic Activity against Prostate Cancer Cells*. Evid Based Complement Alternat Med, 2013. **2013**: p. 757628.
124. Bronikowska, J., et al., *The combination of TRAIL and isoflavones enhances apoptosis in cancer cells*. Molecules, 2010. **15**(3): p. 2000-15.
125. Vandenebeele, P., et al., *Molecular mechanisms of necroptosis: an ordered cellular explosion*. Nat Rev Mol Cell Biol, 2010. **11**(10): p. 700-14.
126. Galluzzi, L., et al., *Molecular definitions of cell death subroutines: recommendations of the Nomenclature Committee on Cell Death 2012*. Cell Death Differ, 2012. **19**(1): p. 107-20.
127. Degterev, A., et al., *Identification of RIP1 kinase as a specific cellular target of necrostatins*. Nat Chem Biol, 2008. **4**(5): p. 313-21.

128. Chen, P., et al., *Synergistic inhibition of autophagy and neddylation pathways as a novel therapeutic approach for targeting liver cancer*. Oncotarget, 2015. **6**(11): p. 9002-17.
129. Xiang, Q., et al., *Carnosic acid induces apoptosis associated with mitochondrial dysfunction and Akt inactivation in HepG2 cells*. Int J Food Sci Nutr, 2015. **66**(1): p. 76-84.
130. Lewinska, A., et al., *Ursolic acid-mediated changes in glycolytic pathway promote cytotoxic autophagy and apoptosis in phenotypically different breast cancer cells*. Apoptosis, 2017.
131. Wang, X.J., et al., *Nrf2 enhances resistance of cancer cells to chemotherapeutic drugs, the dark side of Nrf2*. Carcinogenesis, 2008. **29**(6): p. 1235-43.
132. Valdes, A., et al., *Comprehensive Proteomic Study of the Antiproliferative Activity of a Polyphenol-Enriched Rosemary Extract on Colon Cancer Cells Using Nanoliquid Chromatography-Orbitrap MS/MS*. J Proteome Res, 2016. **15**(6): p. 1971-85.
133. Giudice, A. and M. Montella, *Activation of the Nrf2-ARE signaling pathway: a promising strategy in cancer prevention*. Bioessays, 2006. **28**(2): p. 169-81.
134. Surh, Y.J., J.K. Kundu, and H.K. Na, *Nrf2 as a master redox switch in turning on the cellular signaling involved in the induction of cytoprotective genes by some chemopreventive phytochemicals*. Planta Med, 2008. **74**(13): p. 1526-39.
135. Jaramillo, M.C. and D.D. Zhang, *The emerging role of the Nrf2-Keap1 signaling pathway in cancer*. Genes Dev, 2013. **27**(20): p. 2179-91.
136. Ganan-Gomez, I., et al., *Oncogenic functions of the transcription factor Nrf2*. Free Radic Biol Med, 2013. **65**: p. 750-64.
137. Gonzalez-Vallinas, M., et al., *Expression of microRNA-15b and the glycosyltransferase GCNT3 correlates with antitumor efficacy of Rosemary diterpenes in colon and pancreatic cancer*. PLoS One, 2014. **9**(6): p. e98556.
138. Gonzalez-Vallinas, M., et al., *Modulation of estrogen and epidermal growth factor receptors by rosemary extract in breast cancer cells*. Electrophoresis, 2014. **35**(11): p. 1719-27.
139. Shabtay, A., et al., *Synergistic antileukemic activity of carnosic acid-rich rosemary extract and the 19-nor Gemini vitamin D analogue in a mouse model of systemic acute myeloid leukemia*. Oncology, 2008. **75**(3-4): p. 203-14.
140. Vicente, G., et al., *Isolation of carnosic acid from rosemary extracts using semi-preparative supercritical fluid chromatography*. J Chromatogr A, 2013. **1286**: p. 208-15.
141. Franken, N.A., et al., *Clonogenic assay of cells in vitro*. Nat Protoc, 2006. **1**(5): p. 2315-9.
142. Hirschhaeuser, F., et al., *Multicellular tumor spheroids: an underestimated tool is catching up again*. J Biotechnol, 2010. **148**(1): p. 3-15.
143. Katt, M.E., et al., *In Vitro Tumor Models: Advantages, Disadvantages, Variables, and Selecting the Right Platform*. Front Bioeng Biotechnol, 2016. **4**: p. 12.

144. Slamenova, D., et al., *Rosemary-stimulated reduction of DNA strand breaks and FPG-sensitive sites in mammalian cells treated with H<sub>2</sub>O<sub>2</sub> or visible light-excited Methylene Blue*. Cancer Lett, 2002. **177**(2): p. 145-53.
145. Moore, J., et al., *Rosemary extract reduces Akt/mTOR/p70S6K activation and inhibits proliferation and survival of A549 human lung cancer cells*. Biomed Pharmacother, 2016. **83**: p. 725-732.
146. Su, K., et al., *The inhibitory effects of carnosic acid on cervical cancer cells growth by promoting apoptosis via ROS-regulated signaling pathway*. Biomed Pharmacother, 2016. **82**: p. 180-91.
147. Selzer, E., et al., *Effects of betulinic acid alone and in combination with irradiation in human melanoma cells*. J Invest Dermatol, 2000. **114**(5): p. 935-40.
148. Wu, C.C., et al., *Combined Use of Zoledronic Acid Augments Ursolic Acid-Induced Apoptosis in Human Osteosarcoma Cells through Enhanced Oxidative Stress and Autophagy*. Molecules, 2016. **21**(12).
149. Neergheen-Bhujun, V.S., *Underestimating the toxicological challenges associated with the use of herbal medicinal products in developing countries*. Biomed Res Int, 2013. **2013**: p. 804086.
150. Ko, R., *Adverse reactions to watch for in patients using herbal remedies*. West J Med, 1999. **171**(3): p. 181-6.
151. Anadon, A., et al., *Acute oral safety study of rosemary extracts in rats*. J Food Prot, 2008. **71**(4): p. 790-5.
152. Wang, L.Q., et al., *The anti-leukemic effect of carnosic acid combined with adriamycin in a K562/A02/SCID leukemia mouse model*. Int J Clin Exp Med, 2015. **8**(7): p. 11708-17.
153. Manoharan, S., et al., *Carnosic acid: a potent chemopreventive agent against oral carcinogenesis*. Chem Biol Interact, 2010. **188**(3): p. 616-22.
154. Doolaeghe, E.H., et al., *Absorption, distribution and elimination of carnosic acid, a natural antioxidant from Rosmarinus officinalis, in rats*. Plant Foods Hum Nutr, 2011. **66**(2): p. 196-202.
155. Rahnama, M., et al., *Evaluation of anti-cancer and immunomodulatory effects of carnosol in a Balb/c WEHI-164 fibrosarcoma model*. J Immunotoxicol, 2015. **12**(3): p. 231-8.
156. Johnson, J.J., et al., *Disruption of androgen and estrogen receptor activity in prostate cancer by a novel dietary diterpene carnosol: implications for chemoprevention*. Cancer Prev Res (Phila), 2010. **3**(9): p. 1112-23.
157. Borras-Linares, I., et al., *Permeability Study of Polyphenols Derived from a Phenolic-Enriched Hibiscus sabdariffa Extract by UHPLC-ESI-UHR-Qq-TOF-MS*. Int J Mol Sci, 2015. **16**(8): p. 18396-411.
158. Seiquer, I., et al., *Assessing the bioavailability of polyphenols and antioxidant properties of extra virgin argan oil by simulated digestion and Caco-2 cell assays. Comparative study with extra virgin olive oil*. Food Chem, 2015. **188**: p. 496-503.

159. Serra, H., et al., *Prediction of intestinal absorption and metabolism of pharmacologically active flavones and flavanones*. Bioorg Med Chem, 2008. **16**(7): p. 4009-18.
160. Tarko, T., A. Duda-Chodak, and N. Zajac, *Digestion and absorption of phenolic compounds assessed by in vitro simulation methods. A review*. Roczniki Państwowych Zakładów Higieny, 2013. **64**(2): p. 79-84.
161. Soler-Rivas, C., et al., *Testing and enhancing the in vitro bioaccessibility and bioavailability of Rosmarinus officinalis extracts with a high level of antioxidant abietanes*. J Agric Food Chem, 2010. **58**(2): p. 1144-52.
162. Mukkavilli, R., et al., *Modulation of cytochrome P450 metabolism and transport across intestinal epithelial barrier by ginger biophenolics*. PLoS One, 2014. **9**(9): p. e108386.
163. Mangas-Sanjuan, V., et al., *Innovative in vitro method to predict rate and extent of drug delivery to the brain across the blood-brain barrier*. Mol Pharm, 2013. **10**(10): p. 3822-31.
164. Moradi-Afrapoli, F., et al., *Validation of UHPLC-MS/MS methods for the determination of kaempferol and its metabolite 4-hydroxyphenyl acetic acid, and application to in vitro blood-brain barrier and intestinal drug permeability studies*. J Pharm Biomed Anal, 2016. **128**: p. 264-74.
165. Teng, Z., et al., *Intestinal absorption and first-pass metabolism of polyphenol compounds in rat and their transport dynamics in Caco-2 cells*. PLoS One, 2012. **7**(1): p. e29647.
166. Mignet, N., J. Seguin, and G.G. Chabot, *Bioavailability of polyphenol liposomes: a challenge ahead*. Pharmaceutics, 2013. **5**(3): p. 457-71.



**ANEXO I: Artículos científicos relacionados con la temática de la  
Tesis Doctoral**





## A bioguided identification of the active compounds that contribute to the antiproliferative/cytotoxic effects of rosemary extract on colon cancer cells

Isabel Borrás-Linares <sup>a,c,1</sup>, Almudena Pérez-Sánchez <sup>b,1</sup>, Jesús Lozano-Sánchez <sup>a,c</sup>, Enrique Barrajón-Catalán <sup>b</sup>, David Arráez-Román <sup>a,c,\*</sup>, Alejandro Cifuentes <sup>d</sup>, Vicente Micó <sup>b,e,2</sup>, Antonio Segura Carretero <sup>a,c,2</sup>

<sup>a</sup> Department of Analytical Chemistry, Faculty of Sciences, University of Granada, Avda Fuentenueva s/n, Granada 18071, Spain

<sup>b</sup> Institute of Molecular and Cellular Biology, Miguel Hernández University, Avda. Universidad s/n, Elche 03202, Spain

<sup>c</sup> Research and Development of Functional Food Centre (CIDAF), Health Science Technological Park, Avda. del Conocimiento s/n, Granada 18100, Spain

<sup>d</sup> Laboratory of Foodomics, CIAL (CSIC), Nicolas Cabrera 9, Madrid 28049, Spain

<sup>e</sup> CIBER (CB12/03/30038, Fisiopatología de la Obesidad y la Nutrición, CIBERobn, Instituto de Salud Carlos III)



### ARTICLE INFO

#### Article history:

Received 27 January 2015

Accepted 13 March 2015

Available online 20 March 2015

#### Keywords:

Antiproliferative activity

Cytotoxicity

Colon cancer

HPLC-ESI-QTOF-MS

Rosemary

Terpenoids

### ABSTRACT

Rosemary extracts have exhibited potential cytostatic or cytotoxic effects in several cancer cell models but their bioactive compounds are yet to be discovered. In this work, the anticancer activity of a rosemary-leaf extract and its fractions were assayed to identify the phenolic compounds responsible for their antiproliferative/cytotoxic effects on a panel of human colon cancer cell lines. Bioguided fractionation of the rosemary-leaf extract was achieved by semi-preparative chromatography. The rosemary extract and the compounds in the fractions were characterized and quantified by HPLC-ESI-QTOF-MS. Cellular viability in the presence of these fractions and the whole extract was determined after 24 or 48 h incubations by using an MTT assay. Fractions containing diterpenes or triterpenes were the most active but not as much as the whole extract. In conclusion, carnosic acid, carnosol, 12-methoxycarnosic acid, taxodione, hinokione and betulinic acid were the putative candidates that contributed to the observed antiproliferative activity of rosemary in human colon cancer cells. Whether the effects of the extract and fractions are only cytostatic or cytotoxic needs to be elucidated. Nevertheless, the comparative antiproliferative study on the fractions and whole extract revealed potential synergistic effects between several components in the extract that may deserve further attention.

© 2015 Elsevier Ltd. All rights reserved.

### 1. Introduction

At present, cancer is a major health problem in many developed countries and a leading cause of death worldwide, accounting for 8.2 million deaths in 2012 (World Health Organization (WHO), 2014). Colorectal cancer is the fourth most common cause of death from cancer, causing approximately 700,000 deaths per year. The risk of developing this particular malignancy increases with age and some environmental factors, with diet being one of the most closely related factors. An inverse relation between high consumption of fruit and vegetables and the colon cancer incidence in a population

has been reported, and therefore proper nutrition seems to play an important role in colorectal cancer prevention (Franceschi et al., 1998; Pan et al., 2011; Pauwels, 2011).

Plants and herbs are a source of compounds with potential anticancer activity that are able to prevent, reverse and/or inhibit carcinogenesis at different stages. Among these compounds, polyphenols have attracted interest because of the pleiotropic properties that target different inflammatory, redox-sensitive and energy-sensing metabolic pathways by modulating the activity of different transcription factors (Barrajón-Catalán et al., 2014; Menéndez et al., 2013), which is consistent with the multifactorial character of cancer. The potential use of several individual polyphenols such as quercetin, ellagic acid or chlorogenic acid, or different vegetable matrices, e.g., green tea or olive oil, to treat colorectal cancer has been reported (Hosokawa et al., 1990; Kim et al., 2010; Pahlke et al., 2006; Shan et al., 2009a; Xavier et al., 2009).

Rosemary (*Rosmarinus officinalis* L.) is a shrub from the family Labiateae (Lamiaceae) that is mostly distributed throughout the Mediterranean area. Diterpenes such as carnosic acid (CA) and carnosol

\* Corresponding author. Department of Analytical Chemistry, Faculty of Sciences, University of Granada, Avda Fuentenueva s/n, 18071, Granada, Spain. Tel.: +34958248409; fax: +34958243328.

E-mail address: [darraez@ugr.es](mailto:darraez@ugr.es) (D. Arráez-Román).

<sup>1</sup> These authors contributed equally to this work.

<sup>2</sup> These authors share co-senior authorship.

(CAR) are abundant in rosemary leaves, in addition to the caffeoyl derivative rosmarinic acid. A wide variety of biological activities have been attributed to this plant, namely hepatoprotective (Sotelo-Félix et al., 2002), antimicrobial (Bozin et al., 2007; Del Campo et al., 2000), antithrombotic (Yamamoto et al., 2005), diuretic (Haloui et al., 2000), antidiabetic (Bakirel et al., 2008), anti-inflammatory (Altinier et al., 2007), antioxidant (Pérez-Fons et al., 2010) and anti-cancer (Dörrie et al., 2001; Huang et al., 2005; Lo et al., 2002; Visanji et al., 2006). Accordingly, the inhibitory effects of rosemary extracts and their isolated components on the growth of breast, liver, prostate, lung and leukemia cancer cells have been reported (Johnson, 2011; Yesil-Celiktas et al., 2010). By using transcriptomic and metabolomic analyses, we recently showed that CA and CAR exert antiproliferative/cytotoxic effects on colon cancer cells by activating nuclear receptor factor 2 (NRF2)-dependent pathways and ROS metabolism, which is accompanied by elevated levels of glutathione and decreased levels of N-acetyl putrescine (Valdés et al., 2014). This finding is consistent with the activation of genes related to the antioxidant phase II enzymes observed in a transcriptomic analysis on the effects of a diterpenenriched rosemary extract on colon cancer cells (Valdés et al., 2013). Nevertheless, the whole extract seems to exert additional changes on the expression of genes related to cell cycle progression and the endoplasmic reticulum stress response. This result suggests the potential synergistic effects of the whole extract because of the presence of additional compounds at a lower concentration in combination with diterpenes, which deserves further attention.

Therefore, the aims of our study were to perform a bioguided isolation of the bioactive fractions of rosemary extract by semi-preparative chromatography, to characterize them by high-performance liquid chromatography with electrospray ionization coupled with quadrupole-time-of-flight mass spectrometry (HPLC-ESI-QTOF-MS), and to study the comparative antiproliferative or cytotoxic activity of the whole extract and the fractions against several colon cancer cell lines to search for potential synergistic effects.

## 2. Materials and methods

### 2.1. Chemicals

All chemicals were analytical reagent grade and used as received. Formic acid and acetonitrile used for analytical and semi-preparative chromatography were purchased from Fluka, Sigma-Aldrich (Steinheim, Germany) and Fisher Scientific (Madrid, Spain), respectively. Water was purified by a Milli-Q system from Millipore (Bedford, MA, USA). Ursolic acid (UA), rosmarinic acid, genkwanin, diosmetin and luteolin were obtained from Extrasynthese (Genay, France). Carnosol (CAR), carnosic acid (CA) and apigenin were obtained from Fluka, Sigma-Aldrich. The stock solutions containing these analytes were prepared in dimethyl sulfoxide (DMSO) and methanol (Fisher Scientific, Madrid, Spain) and stored at -80 °C until use.

### 2.2. Rosemary-leaf extract

The rosemary extract (RE) was obtained from dried rosemary leaves that were acquired from Herboristería Murciana (Murcia, Spain) as described by Herrero et al. (2010). In brief, a supercritical fluid extraction system (Suprex Prep Master, Suprex Corporation, Pittsburgh, PA, USA) was used, the flow of neat CO<sub>2</sub> was set at 60 g/min, and the extraction conditions were 150 bar and 40 °C with 6.6% ethanol as a modifier. The extraction time was 5 hours to ensure high recovery efficiency. For solvent evaporation, a Rotavapor R-210 (Buchi Labortechnik AG, Flawil, Switzerland) was employed.

### 2.3. The isolation and purification of rosemary compounds

For the isolation of the rosemary compounds, the SFE extract obtained as described above was dissolved in DMSO up to a concentration of 50 mg/ml. Prior to injection, the extract solution was filtered with a single-use filter (0.45 µm). The fractionation of the rosemary-leaf extract was achieved by using a Gilson preparative HPLC system (Gilson, Middleton, USA) equipped with a binary pump (model 331/332), automated liquid handling solutions (model GX-271) and UV-Vis detector (model UV-VIS 156). The compounds were fractionated with an Ascentis C18 column (10 µm, 250 × 212 mm) at room temperature. The mobile phases used for the separation consisted of water plus 0.1% formic acid as eluent A, and acetonitrile as eluent B. The following multi-step linear gradient was applied: 0 min, 5% B; 10 min, 45% B; 20 min,

55% B; 26 min, 60% B; 46 min, 73% B; 50 min, 80% B; 55 min, 100% B; and 60 min, 5% B. The initial conditions were held for 15 min. The flow rate was 15 ml/min and the injection volume was 1 ml.

The separated compounds were monitored by UV-Vis at a wavelength of 280 nm. The fraction collection step consisted of UV-based purification, and this step determined the elution time window for collecting each fraction. Finally, a total of 10 fractions were collected and the solvent was evaporated in darkness under a nitrogen stream. The residue of each fraction was weighed and stored at -80 °C until use.

### 2.4. HPLC-ESI-QTOF-MS analysis

The rosemary-leaf extract and the collected fractions obtained by semi-preparative chromatography were analyzed by HPLC-ESI-QTOF-MS. The extract was dissolved in ethanol at concentrations of 800 and 5000 µg/ml. The collected fractions were then dissolved in an appropriate volume of DMSO up to a concentration of 100 µg/ml. Finally, the solutions were passed through a 0.25 µm filter before HPLC analysis. The samples were analyzed by using a UPLC Acuity (Waters, Milford, MA, USA) coupled with a micrOTOF-Q II mass spectrometer (Bruker Daltonik, Bremen, Germany). The column was a Zorbax Eclipse Plus C18 (4.6 × 150 mm, 1.8 µm). The mobile phases consisted of water plus 0.1% formic acid as eluent A and acetonitrile as eluent B. The separation was performed at room temperature with a gradient elution programmed at a flow rate of 0.8 ml/min. The multi-step linear gradient was as follows: 0 min, 5% B; 5 min, 40% B; 10 min, 60% B; 30 min, 95% B; and 32.5 min, 5% B. The initial conditions were maintained for 5 minutes. The injection volume in the HPLC system was 5 µl.

The UPLC system was coupled to the mass spectrometer via an ESI interface operating in negative ion mode with a capillary voltage of +4 kV. Because the flow rate under chromatographic conditions was set at 0.8 ml/min to obtain a stable spray and consequently reproducible results, the effluent from the HPLC had to be split. A "T"-type splitter was employed to reduce the flow from 0.8 to 0.2 ml/min. For all the experiments, detection was performed by considering a mass range of 50–1100 m/z, and by using nitrogen as nebulizing and drying gas. The optimum values of the ESI-QTOF parameters were as follows: drying gas temperature, 210 °C; drying gas flow, 9 l/min, nebulizing gas pressure, 2 bar; funnel 1 RF, 150.0 Vpp; funnel 2 RF, 200.0 Vpp; hexapole RF, 100.0 Vpp; transfer time, 70 µs; and pre-pulse storage, 7 µs.

The instrument was calibrated externally with a 74900-00-05 Cole Palmer syringe pump (Vernon Hills, IL, USA) that was directly connected to the interface and contained a 1 mM sodium formate cluster solution. The calibration solution was prepared as follows: 10 µl of 1 M sodium hydroxide was mixed with 990 µl of 0.1% formic acid in water:isopropanol (1:1, v/v). The mixture was injected at the beginning of each run and all the spectra were calibrated prior to compound identification. Due to the compensation of temperature drifts achieved inside the instrument, this external calibration provided accurate mass values that were better than 5 ppm. The accurate mass data of the molecular ions were processed with Data Analysis 4.0 software (Bruker Daltonik), which provides a list of possible elemental formulas via Generate Molecular Formula Editor.

### 2.5. Cell lines and cultures

Colon adenocarcinoma HT-29 and SW480 cells were obtained from the IMIM (Institut Municipal d'Investigació Médica, Barcelona, Spain) and ATCC (American Type Culture Collection, LGC Promochem, UK), respectively, and HGUE-C-1 was an established cell line derived from a primary colon cancer cell line from Hospital General Universitario de Elche. The cells were grown in DMEM supplemented with 5% heat-inactivated fetal bovine serum, 2 mM L-glutamine, 50 U/ml penicillin G, and 50 µg/ml streptomycin at 37 °C in a humidified atmosphere with 5% CO<sub>2</sub>. The cells were trypsinized every three days according to the manufacturer's instructions, and they were seeded in 96-well plates.

### 2.6. Antiproliferative activity assays

To study the rosemary extract effect on the proliferation of HGUE-C-1, HT-29 and SW480 cell lines, the cells were seeded at a density of 5 × 10<sup>3</sup> cells/well, permitted to adhere overnight at 37 °C, and exposed to rosemary extract and the isolated fractions containing 30 or 60 µg/ml for 24 or 48 h. To obtain the concentration of rosemary extract that inhibited 50% of the cell growth (IC<sub>50</sub> value), the cells were treated with various concentrations of extract (0–100 µg/ml), and cell proliferation was estimated by MTT assay. After incubations in the presence of the extract or the fractions for 24 or 48 h, the cells were washed with PBS and incubated with MTT (3-(4,5-dimethylthiazol-2-yl)-2,5-diphenyltetrazolium bromide) for 3–4 h at 37 °C and 5% CO<sub>2</sub>. The medium was removed, and 100 µl of DMSO per well was added to dissolve the formazan crystals. The plates were shaken for 15 min and analyzed by using a microplate reader (SPECTROstar Omega, BMG LabTech GmbH, Offenburg, Germany) at 570 nm.

### 2.7. Statistical analysis

The values are represented as the means ± SD of 4–6 determinations, depending on the assay. The values were subjected to statistical analysis (one-way ANOVA to compare between different treatments, Student's t-test for unpaired samples and

Tukey's test for multiple comparisons). Dose response curves and IC<sub>50</sub> values were obtained by non-linear regression analysis (sigmoidal dose responses with variable slopes) and compared by using two-way ANOVA with a Bonferroni post-test. The IC<sub>50</sub> values are expressed as the means of three experiments. All the calculations and adjustments were performed by using Graph Pad Prism version 5.01 software (Graph Pad Software Inc., CA, USA).

### 3. Results

### 3.1. Quantitative characterization of the rosemary-leaf extract

**Figure 1** shows the base peak chromatogram (BPC) of the extract that was analyzed as described in the Materials and Methods section in which the main peaks have been numbered according to their elution order. The rosemary-leaf extract under study was qualitatively characterized in a previous work (Borrás Linares et al., 2011); however, quantitative data were not reported. **Table 1** summarizes the quantitative results obtained by HPLC-ESI-QTOF-MS for the major compounds in the extract.

For quantitative purposes, standard calibration graphs of CAR, CA, UA, rosmarinic acid, genkwanin, diosmetin and apigenin were prepared by using luteolin at a concentration of 5 ppm as an internal standard. The validation of the proposed method was performed with linearity, sensitivity, and precision parameters. Table 2 shows the limits of detection (LODs) and quantification (LOQs), calibration range, calibration equations, and regression coefficient ( $r^2$ ) for all the standards used. All calibration curves

showed good linearity between different concentrations depending on the analytes studied. The LODs and LOQs for individual compounds in standard solutions were also calculated as S/N = 3 and S/N = 10, respectively, where S/N is the signal-to-noise ratio. The repeatability of the method was measured as the relative standard deviation (RSD %) in terms of concentration. The rosemary-leaf extract was injected several times ( $n = 6$ ) on the same day (intraday precision) and 3 times on 2 consecutive days (interday precision,  $n = 12$ ). The intraday repeatability of the developed method for all analytes ranged from 0.09 to 3.67%, whereas the interday repeatability ranged from 0.16 to 4.21%.

The compound concentrations were determined by using the corrected area for each individual compound (three replicates) and by interpolating in the corresponding calibration curve. Apigenin, diosmetin, genkwanin, CAR, CA and UA were quantified by using the calibration curves obtained from their respective commercial standards. The other compounds were tentatively quantified on the basis of calibration curves from other compounds with structural similarities. Rosmanol, its isomers epirosmosmanol and epirosmanol, miltipolone, rosmadial and rosmardiphenol were quantified with CAR standard. Hinokione and 12-methoxycarnosic acid were expressed as CA. The UA was used to quantify augustic, benthamic, micromeric and betulinic acids, in addition to anemosapogenin. Finally, a genkwanin standard was used for cirsimarin quantification. [9]-shogaol was expressed as rosmarinic acid, and diosmetin was used to estimate the hispidulin and cirsiliol contents. Despite

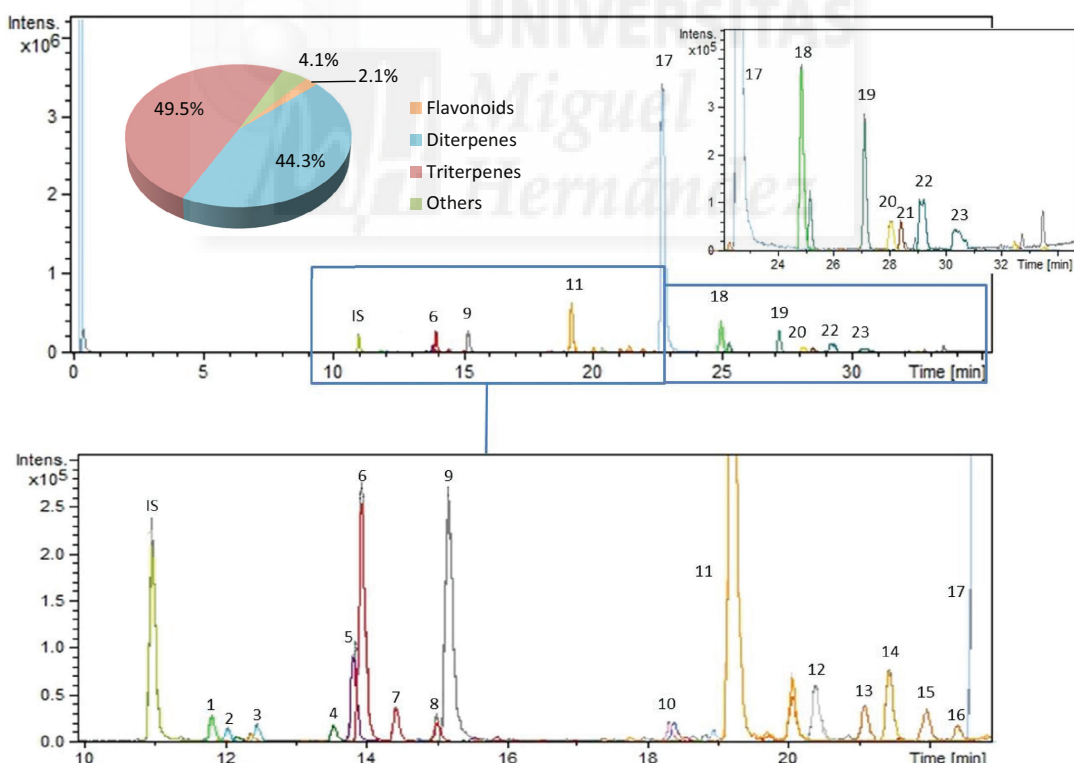


**Fig. 1.** A base peak chromatogram obtained by performing a UPLC-ESI-QTOF-MS analysis of the rosemary-leaf extract, in which the peaks are identified with numbers according to their elution order. The insert indicates the relative percentage of compounds in the extract as distributed by families.

**Table 1**  
The quantitative results for compounds identified in the RE (value =  $X \pm SD$ ).

Peak	Rt (min)	m/z experimental	m/z calculated	Error (ppm)	mSigma	Molecular formula	Analyte	Concentration (mg/g)	% dry weight (w/w)
1	11.84	269.0461	269.0455	2.2	17.7	C <sub>15</sub> H <sub>10</sub> O <sub>5</sub>	Apigenin	0.50 ± 0.02	0.05
2	12.18	299.0655	299.0561	-1.2	36.8	C <sub>16</sub> H <sub>12</sub> O <sub>6</sub>	Hippuridin	0.31 ± 0.01	0.03
3	12.40	329.0665	329.0667	0.6	7.2	C <sub>17</sub> H <sub>13</sub> O <sub>7</sub>	Cirsiliol	0.34 ± 0.01	0.03
4	13.55	299.0553	299.0561	2.8	7.3	C <sub>16</sub> H <sub>20</sub> O <sub>6</sub>	Diosmetin	0.62 ± 0.04	0.06
5	13.83	313.0721	313.0718	0.9	8.5	C <sub>17</sub> H <sub>14</sub> O <sub>6</sub>	Cirsamaritin	0.78 ± 0.07	0.08
6	13.94	345.1714	345.1707	1.9	7.9	C <sub>20</sub> H <sub>26</sub> O <sub>5</sub>	Rosmanol	4.4 ± 0.1	0.44
7	14.43	345.1709	345.1707	0.5	7.6	C <sub>20</sub> H <sub>26</sub> O <sub>5</sub>	Epirosmanol	0.80 ± 0.05	0.08
8	15.01	345.1709	345.1707	0.5	7.6	C <sub>20</sub> H <sub>26</sub> O <sub>5</sub>	Epirosmanol	0.38 ± 0.02	0.04
9	15.16	283.0622	283.0612	2.7	15.7	C <sub>16</sub> H <sub>12</sub> O <sub>5</sub>	Genkwanin	2.61 ± 0.05	0.26
10	18.36	299.1633	299.1633	0.3	5.5	C <sub>19</sub> H <sub>24</sub> O <sub>3</sub>	Miltipolone	0.32 ± 0.04	0.03
11	19.18	329.1758	329.1758	3.5	10	C <sub>20</sub> H <sub>26</sub> O <sub>4</sub>	Carnosol	10 ± 1	1.00
12	20.35	343.1548	343.1551	0.9	12.1	C <sub>20</sub> H <sub>24</sub> O <sub>5</sub>	Rosmaridol	1.36 ± 0.06	0.14
13	21.04	471.3471	471.348	1.9	24.8	C <sub>30</sub> H <sub>48</sub> O <sub>4</sub>	Arenosapogenin	6.5 ± 0.5	0.65
14	21.38	315.1960	315.1966	1.8	13.9	C <sub>20</sub> H <sub>28</sub> O <sub>3</sub>	Rosmaridphenol	0.25 ± 0.05	0.02
15	21.91	471.3471	471.3480	1.8	34.4	C <sub>30</sub> H <sub>48</sub> O <sub>4</sub>	Augustinic acid	6.5 ± 0.5	0.65
16	22.35	471.3474	471.3480	1.3	25.1	C <sub>30</sub> H <sub>48</sub> O <sub>4</sub>	Benthamic acid	2.1 ± 0.2	0.21
17	22.65	331.1935	331.1915	6.2	12.6	C <sub>20</sub> H <sub>28</sub> O <sub>4</sub>	Carnosic acid	83 ± 4	8.30
18	24.89	345.2083	345.2071	3.3	13.6	C <sub>21</sub> H <sub>30</sub> O <sub>4</sub>	12-methoxyarnosic acid	7.20 ± 0.01	0.72
19	27.11	317.2128	317.2122	1.7	27.7	C <sub>20</sub> H <sub>30</sub> O <sub>3</sub>	[9]-Shogaol	10.1 ± 0.3	1.01
20	28.04	453.3356	453.3374	4.0	10.5	C <sub>30</sub> H <sub>46</sub> O <sub>3</sub>	Microstemic acid	47 ± 2	4.70
21	28.40	299.2015	299.2017	0.4	2.3	C <sub>20</sub> H <sub>28</sub> O <sub>3</sub>	Hinokione	0.95 ± 0.08	0.09
22	29.19	455.3519	455.3531	2.5	18.6	C <sub>20</sub> H <sub>40</sub> O <sub>3</sub>	Berulinic acid	38 ± 3	3.80
23	30.20	455.3519	455.3531	2.5	18.6	C <sub>30</sub> H <sub>48</sub> O <sub>3</sub>	Ursolic acid	21.5 ± 0.6	2.15
						Flavonoids	5.16	0.52	
						Diterpenes	108.66	10.87	
						Triterpenes	12.16	1.26	
						Others	10.1	1.01	

**Table 2**  
Analytical parameters for the standards used for quantification purposes.

Analyte	LOD ( $\mu\text{g/ml}$ )	LOQ ( $\mu\text{g/ml}$ )	Calibration range ( $\mu\text{g/ml}$ )	Calibration equations	$r^2$
Carnosol	0.019	0.06	0.1–25	$y = 84.476 x + 0.3537$	0.989
Carnosic acid	0.018	0.06	0.5–70	$y = 94.036 x + 0.0152$	0.9907
Ursolic acid	0.070	0.22	0.5–50	$y = 10^6 x + 56483$	0.9763
Rosmarinic acid	0.035	0.09	0.5–15	$y = 40352 x - 0.0142$	0.9909
Genkwanin	0.014	0.04	0.1–15	$y = 147.37 x - 0.0399$	0.9803
Diosmetin	0.028	0.09	0.1–5	$y = 51.106 x - 0.0386$	0.9906
Apigenin	0.016	0.05	0.5–5	$y = 62.358 x + 0.0308$	0.9912

the fact that the response of the standards may differ from those of the analytes, the concentration of each compound present in the whole extract was estimated ([Table 1](#)).

### 3.2. Isolation and analysis of fractions from rosemary-leaf extract

The major compounds present in the rosemary-leaf extract were isolated by semi-preparative chromatography to study their individual anticancer activity. A total of 10 fractions that contained almost pure compounds were collected and selected for their bioactivity evaluation based on the UV chromatogram registered in the semi-preparative system, which corresponded to the major compounds of the extract. The composition of these fractions ([Table 3](#)) was analyzed and quantitated by HPLC-QTOF as previously described. Except for fractions F4 (3 compounds), F9 (2 compounds) and F10 (2 compounds), the purity of the fractions were of 72% (w/w) and above.

### 3.3. The effects of rosemary-leaf extract and isolated fractions on cell proliferation

The antiproliferative/cytotoxic activity of the rosemary extract and the isolated fractions was assayed on HT-29, SW480 and HGUE-C-1 cell lines at 24 and 48 h. The incubation of the cells with rosemary extract yielded a dose-dependent decrease in cell viability for all colon cancer cell lines and treatment time lapse ([Fig. 2](#)). The comparison of the IC<sub>50</sub> values derived from [Fig. 2](#) is summarized in [Fig. 3](#). At 24 h, the HGUE-C-1 cells were more sensitive to rosemary extract (IC<sub>50</sub> = 12.7  $\mu\text{g/ml}$ ) than SW480 (IC<sub>50</sub> = 18.1  $\mu\text{g/ml}$ ) or HT29 cells (20.4  $\mu\text{g/ml}$ ). By contrast, the HGUE-C-1 and SW480 cells were almost equally sensitive after 48 h treatments (IC<sub>50</sub> = 9.2  $\mu\text{g/ml}$  and 8.1  $\mu\text{g/ml}$ , respectively) and the HT29 cells were less sensitive (14.8  $\mu\text{g/ml}$ ). Significant differences between 24 and 48 h treatments were found in all cell lines ( $p < 0.001$ ), indicating that the longer the treatment the lower the IC<sub>50</sub> values. The reduced IC<sub>50</sub> value after 48 hours of treatment was more dramatic for SW480 cells ([Figs. 2 and 3](#)).

The capacity to reduce the cell proliferation of all the RE fractions was compared with that of the whole extract at two different concentrations (30 and 60  $\mu\text{g/ml}$ ) ([Fig. 4](#)). The RE treatment exhibited the best results for all the tested conditions and cell lines or at least showed a similar level of inhibition to that of the most active fractions. In most cell lines, fractions 5, 7, 9 and 10 showed a similar level of antiproliferative activity than RE. However, fractions 2, 3, 4 and 6 exhibited less capacity to reduce cancer cell viability than RE. On the contrary, fractions 1 and 8 exhibited similar activity to that observed for RE in the HGUE-C-1 and SW480 cell lines, respectively. In general, most fractions showed higher antiproliferative/cytotoxic activity in HGUE-C-1 relative to the other two cell lines ([Figs. 2 and 3](#)).

**Table 3**

The composition of the selected purified fractions used for the antiproliferative assays.

Fraction number	m/z experimental	Molecular formula	Error (ppm)	mSigma	Proposed compound	Purity (% dw)
F 1	345.1715	C <sub>20</sub> H <sub>26</sub> O <sub>5</sub>	-2.2	12.1	Rosmanol	82.6
F 2	345.1714	C <sub>20</sub> H <sub>26</sub> O <sub>5</sub>	-1.7	5.6	Epiisorosmanol	83.6
F 3	283.0616	C <sub>16</sub> H <sub>22</sub> O <sub>5</sub>	-1.3	12.2	Genkwanin	99.3
F 4	299.1655	C <sub>19</sub> H <sub>24</sub> O <sub>3</sub>	-0.7	21.7	Miltipolone	40.0
	457.3325	C <sub>29</sub> H <sub>46</sub> O <sub>4</sub>	-0.4	20.9	Notohamosin B	30.1
	471.3483	C <sub>30</sub> H <sub>48</sub> O <sub>4</sub>	-0.7	31.8	Anemosapogenin	13.1
F 5	329.1755	C <sub>20</sub> H <sub>26</sub> O <sub>4</sub>	1.1	15.7	Carnosol	82.6
F 6	343.1556	C <sub>20</sub> H <sub>24</sub> O <sub>5</sub>	-1.6	7.8	Rosmadial	72.0
F 7	331.1922	C <sub>20</sub> H <sub>28</sub> O <sub>4</sub>	-2.1	25.8	Carnosic acid	98.7
F 8	345.2070	C <sub>21</sub> H <sub>30</sub> O <sub>4</sub>	0.2	6.6	12-methoxycarnosic acid	98.6
F 9	313.1819	C <sub>20</sub> H <sub>26</sub> O <sub>3</sub>	-3.0	7.5	Taxodione	44.0
	317.2137	C <sub>20</sub> H <sub>30</sub> O <sub>3</sub>	-4.6	19.3	[9]-Shogaol	50.0
F 10	299.2021	C <sub>20</sub> H <sub>28</sub> O <sub>2</sub>	-1.5	1.5	Hinokione	13.8
	455.3518	C <sub>30</sub> H <sub>48</sub> O <sub>3</sub>	2.8	1.1	Betulinic acid	81.0

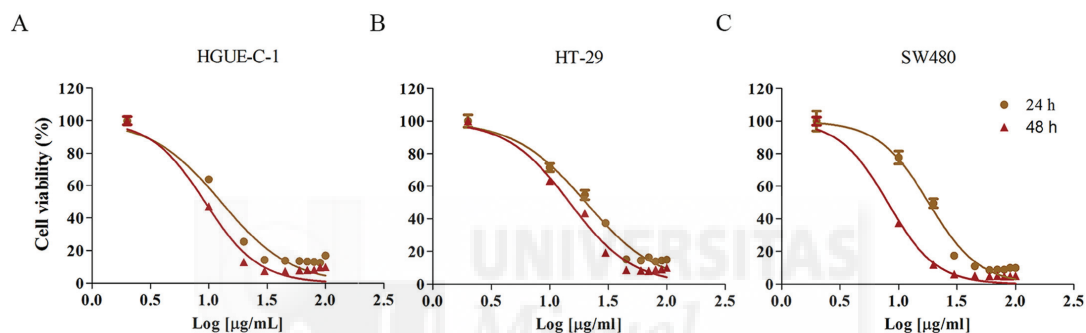


**Fig. 2.** The sigmoidal dose–response curves of cell viability for the following three different colon cancer cell lines: HGUE-C-1, HT-29 or SW480 (A, B and C) in the presence of the RE. The cells were treated with different concentrations (0–100 μg/ml) of RE for 24 or 48 h. After the treatments, cell viability was measured by MTT assay. The data are expressed as the means of 6 replicates ± SD.

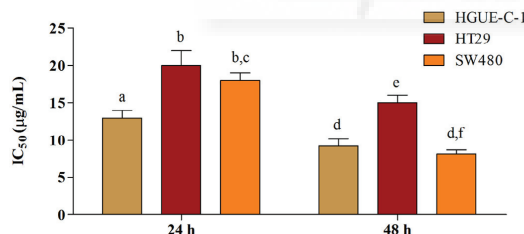


**Fig. 3.** IC<sub>50</sub> values derived from cell viability plots with treatments of three colon cancer cell lines in the presence of RE after 24 and 48 hours. Different letters above the bars indicate statistically significant differences ( $p < 0.001$ ) between samples after two-way ANOVA analysis.

#### 4. Discussion

Triterpenes were the most abundant compounds in RE (49.5% of the total identified compounds), followed by diterpenes (44.3%) and minor quantities of flavonoids (2.1%) (Fig. 1). Diterpenes accounted for almost 11% of the total dry weight (dw) and triterpenes for approximately 12% dw (Table 1). Considering the individual compounds, the diterpene CA was the most abundant one (83 mg/g) followed by the triterpenes micromeric, betulinic and ursolic acids (47, 38 and 21.5 mg/g, respectively), which were previously described in rosemary (Laszczyk, 2009). CAR, the δ-lactone derivative

of CA, was also relevant (10 mg/g), and other diterpenes (rosmanol, rosmadial, and 12-methoxycarnosic acid), triterpenes (anemosapogenin, augistic acid, and benthamic acid), flavonoids (genkwanin) and [9]-shogaol were present at concentrations ranging from 1.36 to 10.1 mg/g extract. The rest of the compounds were all below 1 mg/g extract.

The growth conditions (geographical and pedoclimatic factors), extraction and conservation procedures may significantly influence the phenolic composition of a botanical extract. Indeed, the phenolic diterpenes present in RE have been shown to be thermal and photo-degradable (Schwarz and Ternes, 1992). Solid-liquid extraction (SLE), pressurized-liquid extraction (PLE) and supercritical fluid extraction (SFE) have been used to extract phenolic compounds from rosemary. The studied rosemary-leaf extract exhibited a high CA content compared to the data previously reported in literature for PLE and SFE rosemary extracts (Herrero et al., 2010; Yesil-Celiktas et al., 2007). This result could be explained due to the use of ethanol as co-solvent in SFE performed in this research. Concerning the presence of intermediate phenolic diterpenes derived from CA, these compounds were found in lower amount compared to other extraction processes (Herrero et al., 2010; Kontogianni et al., 2013). This fact suggests a low degradation level for some compounds, especially for CA, during the extraction procedure used in this research. In addition, regarding the flavonoid content, this extract showed slightly lower concentrations in comparison to various rosemary extracts obtained with SLE (Kontogianni et al., 2013).

All the compounds present in the RE were identified in the purified fractions, except notohamosin B and taxodione, which appeared

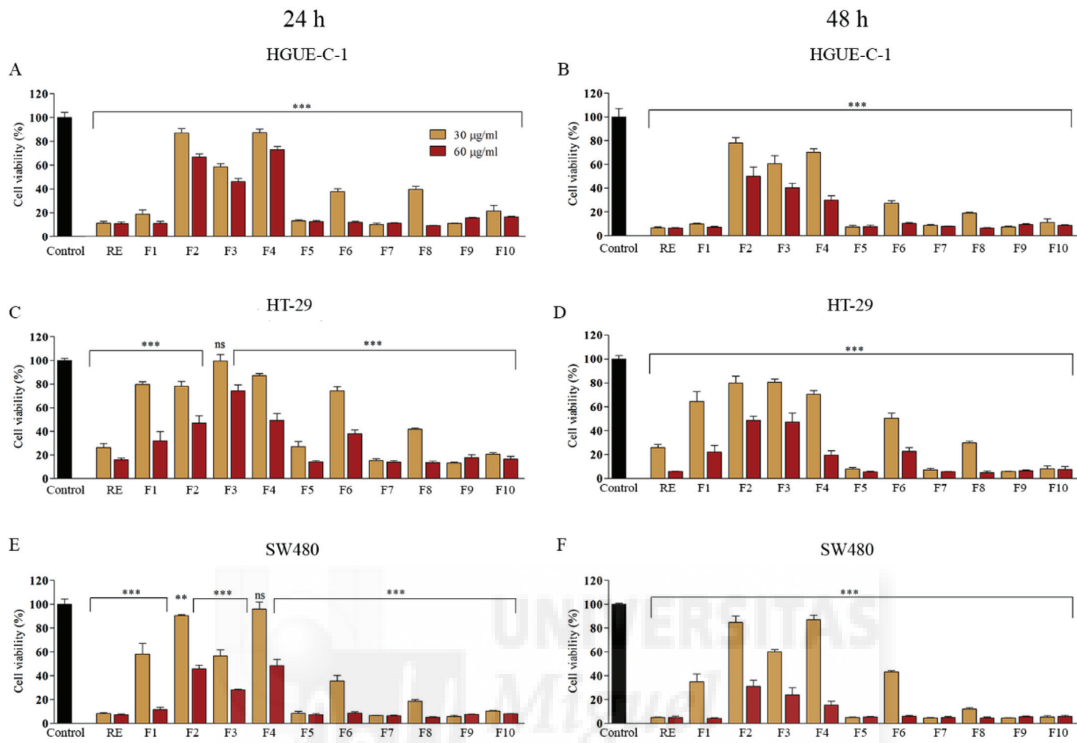


**Fig. 4.** The effects of RE and its isolated fractions on the cell viability of the three colon cancer cell lines HGUE-C-1, HT-29 or SW480. The cells were treated with different concentrations (30 or 60 µg/ml) for 24 or 48 h. After the treatment, cell viability was measured by MTT assay. The values are represented as the percentage of viable cells (100% viability corresponds to non-treated control cells). The data are expressed as the means of 4 replicates ± SD. \*\* (p < 0.01) and \*\*\* (p < 0.001) indicate statistically significant differences in comparison with control cells.

as newly identified compounds in fractions F4 and F9, respectively, and were most likely present at a very low concentration in the extract. After fractionating the RE, fractions 1, 2, 3, 5, 6, 7 and 8 (**Table 3**) were pure and only presented single compounds in each one, namely rosmanol, episorosmanol, genkwanin, CAR, rosmadial, CA and 12-methoxycarnosic acid, respectively. The phenolic diterpenes CAR, CA, rosmadial, rosmanol and its isomer episorosmanol, and the flavonoid genkwanin, have been previously described in this plant source (**Almeida et al., 2006; Chen et al., 2005, 2006; Pérez-Fons et al., 2010; Señorans et al., 2000**). Unfortunately, it was not possible to purify the compounds miltipolone, notohamosin B and anemosapogenin to homogeneity, and they were found to be mixed into fraction number 4. Miltipolone is a diterpenoid tropolone that was first identified in *Salvia miltiorrhiza* (**Regasini et al., 2008**). Notohamosin B is a nortriterpenoid isolated from methanol extracts of *Notochaepta hamosa* Benth. and it has been identified in rosemary extract (**Borrás Linares et al., 2011; Fujita et al., 1988**). In addition, anemosapogenin is a triterpene, which is also called 23-hydroxybetulinic acid, and it was isolated from the aerial parts of rosemary (**Mahmoud et al., 2005**). Fractions 9 and 10 yielded 2 compounds each with taxodione and [9]-shogaol for the first fraction, and hinokione and betulinic acid in the second. [9]-shogaol, hinokione and betulinic acid were previously identified in different rosemary-leaf extracts, whereas taxodione has been

detected in the stems of this plant (**Bai et al., 2010; El-Lakany, 2004; Kontogianni et al., 2013; Nakasugi, 1996**).

The antiproliferative or cytotoxic activity of different rosemary compounds and extracts on various cancer cell lines and *in vivo* models have been previously reported including leukemia, prostate, breast, skin and colon cancers (**Einbond et al., 2012; Johnson, 2011; Kar et al., 2012; Ngo et al., 2011; Yesil-Celiktas et al., 2010**). A compositional analysis of all these extracts indicates that phenolic diterpenes are thought to be the most active compounds against cancer cell proliferation followed by triterpenoids, which have shown lower activity. Consistent with this finding, the above-mentioned studies postulate that CA may be the major contributor to the antiproliferative activity exhibited by rosemary extract. This finding is consistent with our results from fraction F7, which was almost composed of pure CA, and it was one of the most active in most cell lines at the lowest concentration assayed (i.e., 30 µg/ml). In addition, fractions F5 (containing CAR), F9 (containing taxodione) and F10 (containing hinokione + betulinic acid) were almost as antiproliferative as the whole extract on most cell lines, which is consistent with the strongest activity of diterpenes. Nevertheless, the high percentage of betulinic acid in F10 (81.0%) indicates that triterpenes may also significantly contribute to decreased cancer cell viability. F8, which contained almost pure 12-methoxycarnosic acid, also presented stronger antiproliferative activity in SW480 cells,

in comparison with the other two cell lines, and F1 (rosmanol) had a similar differential effect on HGUE-C-1 colon cancer cells. The antiproliferative activity of 12-methoxycarnosic acid has also been reported in hepatoma cell lines (Peng et al., 2007). Depending on the cell type, this preferential effect may indicate that further modifications of the pharmacophore nucleus of diterpenes would lead to the design of more selective drugs against different colon cancer cell phenotypes. In any case, due to the complexity of the terpenoid composition of the rosemary extract, the coexistence of antiproliferative and cytotoxic effects in colon cancer cells may take place. The nature of this effect may deserve further attention.

Reported IC<sub>50</sub> values for carnosic acid, betulinic acid and ursolic acid were 48.5, 32.7 and 26 μM, respectively, after 24 h treatments of HT-29 colon cancer cells (Barni et al., 2012; Ding et al., 2013; Shan et al., 2009b), whereas ursolic acid IC<sub>50</sub> value on SW480 colon cancer cells after 48 h treatments was 23.9 μM (Wang et al., 2013). No values were found for other diterpenes or triterpenes from rosemary on colon cancer cells in the literature. In agreement to our results, the reported IC<sub>50</sub> values would be slightly under the lowest concentration used in this study for pure fractions, i.e. 30 μg/ml. The anticancer activity of rosemary compounds both *in vitro* and in animal models has been recently reviewed (Ngo et al., 2011). Consistent with our results, CA and CAR are proposed as the most active constituents of rosemary leaves that are responsible for antiproliferative effects on colon cancer cells with the contribution of some triterpenes such as UA. Whereas most diterpenes such as CA and CAR seemed to display antiproliferative or cytostatic activity, other diterpenes such as rosmanol and the triterpene UA exhibited apoptotic effects. CAR and CA have been shown to target multiple pathways associated with inflammation and cancer, which include nuclear factor kappa B (NF-κB), apoptosis-related proteins, the phosphatidylinositol-3-kinase (PI3K)/Akt proliferation pathway, androgen and estrogen receptors and antiangiogenic activity (Johnson, 2011; López-Jiménez et al., 2013). Studies performed in other cancer cell models show that their mechanism of action is unlikely to be tissue-specific. In our study, the F1 fraction that contained rosmanol (an oxidative degradation product derived from CA or CAR) was also very active in the HGUE-C-1 colon cancer cell line derived from the *primary* tumor, which may require further research in relation to the specific phenotype of this cell line. In any case, the low abundance of diterpenes in RE (11%) does not justify its strong antiproliferative activity in comparison with that of almost pure fractions containing diterpenes such as F1, F2, F5, F6, F7 or F8 (72–98%).

Like other pentacyclic triterpenes, betulinic acid has been suggested as a promising anticancer lead compound with broad anticancer activity in a series of cancer cell lines. This compound has demonstrated antiangiogenic, apoptotic, and immunomodulatory effects in addition to differentiation-inducing effects, which are believed to be related to the lupane moiety (Laszczyk, 2009). Betulinic acid was fairly abundant in RE (3.8%) and was the primary compound in F10 (81%), one of the most active fractions especially in SW480 colon cancer cells. This fraction also contained minor quantities of the diterpene hinokione, which most likely derives from CAR degradation. However, the abundance of betulinic acid and that of other triterpenes (12%) in the extract is not in accordance with the strong antiproliferative activity of the whole extract. Fraction 9 also exhibited strong activity and contained [9]-shogaol, a gingerol-like phenol, and the diterpene taxodiene. Shogaol-related compounds have shown apoptotic capacity in human colon cancer cells and taxodiene from *Salvia* species exhibited cytotoxicity in leukemia cancer cells (Fu et al., 2014; Tayarani-Najaran et al., 2013).

As a general consideration, the results pointed out that the extract, which contained approximately 11% diterpenes and 12% triterpenes, exhibited higher antiproliferative/cytotoxic properties than any of the purified fractions, which contained almost pure compounds at

percentages over 72% purity (dry weight). This finding may reveal potential synergistic behavior between the different compounds in the extract. This polypharmacological behavior of the RE would also reduce the possible emergence of drug-resistant phenotypes. We propose that the antiproliferative/cytotoxic activity of RE may be based on the complementary concurrence of diterpenes and triterpenes. The identification of the specific combinations of diterpenes and triterpenes that exhibit maximum anticancer activity and the character of this effect (cytostatic, cytotoxic or both) will inevitably demand additional research.

## 5. Conclusions

A bioactive rosemary-leaf extract obtained by SFE and bearing strong antiproliferative/cytotoxic capacity was first quantitatively characterized by HPLC-ESI-QTOF-MS, and CA proved to be the most abundant compound, followed by the triterpenes micromeric, betulinic and ursolic acids. Bioguided fractionation by semipreparative chromatography of the extract to obtain pure compounds showed that CA, CAR, 12-methoxycarnosic acid, taxodiene, hinokione and betulinic acid were the putative candidates for the antiproliferative activity in a panel of human colon cancer cells including a cancer cell line derived from a *primary* tumor. Nevertheless, the comparative antiproliferative study of the fractions and the whole extract revealed the potential synergistic effect between several components in the extract.

## Conflict of interest

The authors declare that there are no conflicts of interest.

## Transparency document

The Transparency document associated with this article can be found in the online version.

## Acknowledgements

This work was supported by projects AGL2011-29857-C03-02 and AGL2011-29857-C03-03 (Spanish Ministry of Science and Innovation), in addition to P10-FQM-6563 and P11-CTS-7625 (Andalusian Regional Government Council of Innovation and Science), PROMETEO/2012/007 and ACOMP/2013/093 (Generalitat Valenciana), and CIBER (CB12/03/30038, Fisiopatología de la Obesidad y la Nutrición, CIBERObn, Instituto de Salud Carlos III). The authors are grateful to the Spanish Ministry of Science and Innovation for grants FPU (AP2007-03246) and FPI (BES-2009-028128), and the Spanish Ministry of Economy and Competitiveness (MINECO) for the projects BFU2014-52433-C3-1-R, BFU2014-52433-C3-2-R and in association with the European Social Fund (FSE) for the contract PTQ-13-06429.

## References

- Almela, L., Sánchez-Muñoz, B., Fernández-López, J.A., Roca, M.J., Rabe, V., 2006. Liquid chromatographic-mass spectrometric analysis of phenolics and free radical scavenging activity of rosemary extract from different raw material. *J. Chromatogr. A* 1120, 221–229.
- Altinier, G., Sosa, S., Aquino, R.P., Mencherini, T., Loggia, R.D., Tubaro, A., 2007. Characterization of topical antiinflammatory compounds in *Rosmarinus officinalis* L. *J. Agric. Food Chem.* 55, 1718–1723.
- Bai, N., He, K., Rollier, M., Lai, C., Shao, X., Pan, M., et al., 2010. Flavonoids and phenolic compounds from *Rosmarinus officinalis*. *J. Agric. Food Chem.* 58, 5363–5367.
- Bakirel, T., Bakirel, U., Keleş, O.U., Ülgen, S.G., Yardibi, H., 2008. *In vivo* assessment of antidiabetic and antioxidant activities of rosemary (*Rosmarinus officinalis*) in alloxan-diabetic rabbits. *J. Ethnopharmacol.* 116, 64–73.
- Barni, M.V., Carlini, M.J., Cafferata, E.G., Puricelli, L., Moreno, S., 2012. Carnosic acid inhibits the proliferation and migration capacity of human colorectal cancer cells. *Oncol. Rep.* 27, 1041–1048.

- Barrajón-Catalán, E., Herranz-López, M., Joven, J., Segura-Carretero, A., Alonso-Villaverde, C., Menéndez, J.A., et al., 2014. Molecular promiscuity of plant polyphenols in the management of age-related diseases: far beyond their antioxidant properties. *Adv. Exp. Med. Biol.* 824, 141–159.
- Borrás Linares, I., Arráez-Román, D., Herrero, M., Ibáñez, E., Segura-Carretero, A., Fernández-Gutiérrez, A., 2011. Comparison of different extraction procedures for the comprehensive characterization of bioactive phenolic compounds in *Rosmarinus officinalis* by reversed-phase high-performance liquid chromatography with diode array detection coupled to electrospray time-of-flight mass spectrometry. *J. Chromatogr. A* 1218, 7682–7690.
- Bozin, B., Mimica-Dukic, N., Samojlik, I., Jovin, E., 2007. Antimicrobial and antioxidant properties of rosemary and sage (*Rosmarinus officinalis* L. and *Salvia officinalis* L., Lamiaceae) essential oils. *J. Agric. Food Chem.* 55, 7879–7885.
- Chen, J., Li, S., Li, P., Song, Y., Chai, X., Ma, D., 2005. Qualitative and quantitative analysis of active flavonoids in *Flos Lonicerae* by capillary zone electrophoresis coupled with solid-phase extraction. *J. Sep. Sci.* 28, 365–372.
- Chen, X., Hu, L., Su, X., Kong, L., Ye, M., Zou, H., 2006. Separation and detection of compounds in honeysuckle by integration of ion-exchange chromatography fractionation with reversed-phase liquid chromatography-atmospheric pressure chemical ionization mass spectrometer and matrix-assisted laser desorption/ionization time-of-flight mass spectrometry analysis. *J. Pharm. Biomed. Anal.* 40, 559–570.
- Del Campo, J., Amiot, M., Nguyen-The, C., 2000. Antimicrobial effect of rosemary extracts. *J. Food Prot.* 63, 1359–1368.
- Ding, W., Sun, M., Luo, S., Xu, T., Cao, Y., Yan, X., et al., 2013. A 3D QSAR study of betulinic acid derivatives as anti-tumor agents using topomer CoMFA model building studies and experimental verification. *Molecules* 18, 10228–10241.
- Dörrie, J., Sapala, K., Zunino, S.J., 2001. Carnosol-induced apoptosis and downregulation of Bcl-2 in B-lineage leukemia cells. *Cancer Lett.* 170, 33–39.
- Einbond, L.S., Wu, H., Kashiwazaki, R., He, K., Roller, M., Su, T., et al., 2012. Carnosic acid inhibits the growth of ER-negative human breast cancer cells and synergizes with curcumin. *Fitoterapia* 83, 1160–1168.
- El-Lakany, A.M., 2004. Chlorosmaridione; a novel chlorinated diterpene quinone methide from *Rosmarinus officinalis* L. *Nat. Prod. Sci.* 10, 59–62.
- Franceschi, S., Parpinel, M., La Vecchia, C., Favero, A., Talamini, R., Negri, E., 1998. Role of different types of vegetables and fruit in the prevention of cancer of the colon, rectum, and breast. *Epidemiology* 9, 338–341.
- Fu, J., Chen, H., Soroka, D.N., Warin, R.F., Sang, S., 2014. Cysteine-conjugated metabolites of ginger components, shogaols, induce apoptosis through oxidative stress-mediated p53 pathway in human colon cancer cells. *J. Agric. Food Chem.* 62, 4632–4642.
- Fujita, T., Takeda, Y., Han-dong, S., Minami, Y., Marunaka, T., Takeda, S., et al., 1988. Cytotoxic and antitumor activities of *Rabdiosa* diterpenoids. *Planta Med.* 54, 414–417.
- Haloui, M., Louedec, L., Michel, J., Iyounni, B., 2000. Experimental diuretic effects of *Rosmarinus officinalis* and *Centaurium erythraea*. *J. Ethnopharmacol.* 71, 465–472.
- Herrero, M., Plaza, M., Cifuentes, A., Ibanez, E., 2010. Green processes for the extraction of bioactives from rosemary: chemical and functional characterization via ultra-performance liquid chromatography-tandem mass spectrometry and *in-vitro* assays. *J. Chromatogr. A* 1217, 2512–2520.
- Hosokawa, N., Hosokawa, Y., Sakai, T., Yoshida, M., Marui, N., Nishino, H., et al., 1990. Inhibitory effect of quercentin on the synthesis of a possibly cell-cycle-related 17-kDa protein, in human colon cancer cells. *Int. J. Cancer* 45, 1119–1124.
- Huang, S., Ho, C., Lin-Shiau, S., Lin, J., 2005. Carnosol inhibits the invasion of B16/F10 mouse melanoma cells by suppressing metalloproteinase-9 through down-regulating nuclear factor- $\kappa$ B and c-Jun. *Biochem. Pharmacol.* 69, 221–232.
- Johnson, J.J., 2011. Carnosol: a promising anti-cancer and anti-inflammatory agent. *Cancer Lett.* 305, 1–7.
- Kar, S., Palit, S., Ball, W.B., Das, P.K., 2012. Carnosic acid modulates Akt/IKK/NF- $\kappa$ B signaling by PP2A and induces intrinsic and extrinsic pathway mediated apoptosis in human prostate carcinoma PC-3 cells. *Apoptosis* 17, 735–747.
- Kim, H., Kim, S., Kim, B., Lee, S., Park, Y., Park, B., et al., 2010. Apoptotic effect of quercentin on HT-29 colon cancer cells via the AMPK signaling pathway. *J. Agric. Food Chem.* 58, 8643–8650.
- Kontogianni, V.G., Tomic, G., Nikolic, I., Nerantzaki, A.A., Sayyad, N., Stosic-Grujicic, S., et al., 2013. Phytochemical profile of *Rosmarinus officinalis* and *Salvia officinalis* extracts and correlation to their antioxidant and anti-proliferative activity. *Food Chem.* 136, 120–129.
- Laszczyk, M.N., 2009. Pentacyclic triterpenes of the lupane, oleanane and ursane group as tools in cancer therapy. *Planta Med.* 75, 1549–1560.
- Lo, A., Liang, Y., Lin-Shiau, S., Ho, C., Lin, J., 2002. Carnosol, an antioxidant in rosemary, suppresses inducible nitric oxide synthase through down-regulating nuclear factor- $\kappa$ B in mouse macrophages. *Carcinogenesis* 23, 983–991.
- López-Jiménez, A., García-Caballero, M., Medina, M.Á., Quesada, A.R., 2013. Anti-angiogenic properties of carnosol and carnosic acid, two major dietary compounds from rosemary. *Eur. J. Nutr.* 52, 85–95.
- Mahmoud, A.A., Al-Shihry, S.S., Son, B.W., 2005. Diterpenoid quinones from rosemary (*Rosmarinus officinalis* L.). *Phytochemistry* 66, 1685–1690.
- Menéndez, J.A., et al., 2013. Xenohormetic and anti-aging activity of secoiridoid polyphenols present in extra virgin olive oil: a new family of geroprotector agents. *Cell Cycle* 12, 555–578.
- Nakasugi, T., 1996. Antimutagens involving in the leaves of *Rosmarinus officinalis* L. *Nat. Med. Mol.* 50, 354–357.
- Ngo, S.N.T., Williams, D.B., Head, R.J., 2011. Rosemary and cancer prevention: preclinical perspectives. *Crit. Rev. Food Sci. Nutr.* 51, 946–954.
- Pahlke, G., Ngiewih, Y., Kern, M., Jakobs, S., Marko, D., Eisenbrand, G., 2006. Impact of quercentin and EGCG on key elements of the Wnt pathway in human colon carcinoma cells. *J. Agric. Food Chem.* 54, 7075–7082.
- Pan, M., Lai, C., Wu, J., Ho, C., 2011. Molecular mechanisms for chemoprevention of colorectal cancer by natural dietary compounds. *Mol. Nutr. Food Res.* 55, 32–45.
- Pauwels, E.K.J., 2011. The protective effect of the mediterranean diet: focus on cancer and cardiovascular risk. *Med. Princ. Pract.* 20, 103–111.
- Peng, C., Su, J., Chyau, C., Sung, I., Ho, S., Peng, C., et al., 2007. Supercritical fluid extracts of rosemary leaves exhibit potent anti-inflammation and anti-tumor effects. *Biosci. Biotech. Bioch.* 71, 2223–2232.
- Pérez-Fons, L., Garzón, M.T., Micó, V., 2010. Relationship between the antioxidant capacity and effect of rosemary (*Rosmarinus officinalis* L.) polyphenols on membrane phospholipid order. *J. Agric. Food Chem.* 58, 161–171.
- Regasini, L.O., Velosa, J.C.R., Silva, D.H.S., Furlan, M., de Oliveira, O.M.M., Khalil, N.M., et al., 2008. Flavonols from *Pterogyne nitens* and their evaluation as myeloperoxidase inhibitors. *Phytochemistry* 69, 1739–1744.
- Schwarz, K., Terres, W., 1992. Antioxidative constituents of *Rosmarinus officinalis* and *Salvia officinalis*. I. Determination of phenolic diterpenes with antioxidative activity amongst tocopherol using HPLC. *Z. Lebensm. Unters. Forsch.* 195, 95–98.
- Señorans, F.J., Ibáñez, E., Cavero, S., Tabera, J., Reglero, G., 2000. Liquid chromatographic-mass spectrometric analysis of supercritical-fluid extracts of rosemary plants. *J. Chromatogr. A* 870, 491–499.
- Shan, B., Wang, M., Li, R., 2009a. Quercetin inhibit human SW480 colon cancer growth in association with inhibition of cyclin D1 and survivin expression through Wnt/ $\beta$ -catenin signaling pathway. *Cancer Invest.* 27, 604–612.
- Shan, J.Z., Xuan, Y.Y., Zheng, S., Dong, Q., Zhang, S.Z., 2009b. Ursolic acid inhibits proliferation and induces apoptosis of HT-29 colon cancer cells by inhibiting the EGFR/MAPK pathway. *J. Zhejiang Univ. Sci. B* 10, 668–674.
- Sotelo-Félix, J.I., Martínez-Fong, D., Muriel, P., Santillán, R.L., Castillo, D., Yahuaca, P., 2002. Evaluation of the effectiveness of *Rosmarinus officinalis* (Lamiaceae) in the alleviation of carbon tetrachloride induced acute hepatotoxicity in the rat. *J. Ethnopharmacol.* 81, 145–154.
- Tayarani-Najaran, Z., Mousavi, S.H., Tajfarid, F., Asili, J., Soltani, S., Hatamipour, M., et al., 2013. Cytotoxic and apoptotic properties of three isolated diterpenoids from *Salvia chorassanica* through bioassay-guided fractionation. *Food Chem.* Toxicol. 75, 346–351.
- Valdés, A., García-Cañas, V., Rocamora-Reverte, L., Gómez-Martínez, Á., Ferragut, J.A., Cifuentes, A., 2013. Effect of rosemary polyphenols on human colon cancer cells: transcriptomic profiling and functional enrichment analysis. *Genes Nutr.* 8, 43–60.
- Valdés, A., García-Cañas, V., Simó, C., Ibáñez, C., Micó, V., Ferragut, J.A., et al., 2014. Comprehensive foodomics study on the mechanisms operating at various molecular levels in cancer cells in response to individual rosemary polyphenols. *Anal. Chem.* 86, 9807–9815.
- Visanji, J., Thompson, D.G., Padfield, P.J., 2006. Induction of G2/M phase cell cycle arrest by carnosol and carnosic acid is associated with alteration of cyclin A and cyclin B1 levels. *Cancer Lett.* 237, 130–136.
- Wang, J., Guo, W., Chen, W., Yu, W., Tian, Y., Fu, L., et al., 2013. Melatonin potentiates the antiproliferative and pro-apoptotic effects of ursolic acid in colon cancer cells by modulating multiple signaling pathways. *J. Pineal Res.* 54, 406–416.
- World Health Organization (WHO), 2014. Cancer prevention. Available from <http://www.who.int/cancer/en/>.
- Xavier, C.P.R., Lima, C.F., Preto, A., Seruca, R., Fernandes-Ferreira, M., Pereira-Wilson, C., 2009. Luteolin, quercentin and ursolic acid are potent inhibitors of proliferation and inducers of apoptosis in both KRAS and BRAF mutated human colorectal cancer cells. *Cancer Lett.* 281, 162–170.
- Yamamoto, J., Yamada, K., Naemura, A., Yamashita, T., Arai, R., 2005. Testing various herbs for antithrombotic effect. *Nutrition* 21, 580–587.
- Yesil-Celiktas, O., Girgin, G., Orhan, H., Wicher, H.J., Bedir, E., Vardar-Sukan, F., 2007. Screening of free radical scavenging capacity and antioxidant activities of *Rosmarinus officinalis* extracts with focus on location and harvesting times. *Eur. Food Res. Technol.* 224, 443–451.
- Yesil-Celiktas, O., Sevimli, C., Bedir, E., Vardar-Sukan, F., 2010. Inhibitory effects of rosemary extracts, carnosic acid and rosmarinic acid on the growth of various human cancer cell lines. *Plant Food. Hum. Nutr.* 65, 158–163.

## RESEARCH ARTICLE

# Evaluation of the intestinal permeability of rosemary (*Rosmarinus officinalis* L.) extract polyphenols and terpenoids in Caco-2 cell monolayers

Almudena Pérez-Sánchez<sup>1\*</sup>, Isabel Borrás-Linares<sup>2,3\*</sup>, Enrique Barrajón-Catalán<sup>1,4,5</sup>, David Arráez-Román<sup>2,3</sup>, Isabel González-Álvarez<sup>4</sup>, Elena Ibáñez<sup>6</sup>, Antonio Segura-Carretero<sup>2,3</sup>, Marival Bermejo<sup>4</sup>, Vicente Micol<sup>1,7\*</sup>



## OPEN ACCESS

**Citation:** Pérez-Sánchez A, Borrás-Linares I, Barrajón-Catalán E, Arráez-Román D, González-Álvarez I, Ibáñez E, et al. (2017) Evaluation of the intestinal permeability of rosemary (*Rosmarinus officinalis* L.) extract polyphenols and terpenoids in Caco-2 cell monolayers. PLoS ONE 12(2): e0172063. doi:10.1371/journal.pone.0172063

**Editor:** Miguel Angel Medina, Universidad de Málaga, SPAIN

**Received:** October 19, 2016

**Accepted:** January 30, 2017

**Published:** February 24, 2017

**Copyright:** © 2017 Pérez-Sánchez et al. This is an open access article distributed under the terms of the [Creative Commons Attribution License](#), which permits unrestricted use, distribution, and reproduction in any medium, provided the original author and source are credited.

**Data Availability Statement:** All relevant data are within the paper and its Supporting Information files.

**Funding:** This work was supported by projects AGL2011-29857-C03-02, AGL2011-29857-C03-03, AGL2015-67995-C3-1-R, and AGL2015-67995-C3-2-R, and FPU grant (AP2007-03246) from Spanish Ministry of Science and Innovation; Torres Quevedo grants PTQ-13-06429 and PTQ-14-07243 from the Spanish Ministry of Economy

**1** Institute of Molecular and Cell Biology, Miguel Hernández University, Avda. Universidad s/n, Elche, Spain, **2** Department of Analytical Chemistry, Faculty of Sciences, University of Granada, Avda Fuentenueva s/n, Granada, Spain, **3** Research and Development of Functional Food Centre (CIDAF), Health Science Technological Park, Avda. del Conocimiento n° 37, Armilla, Spain, **4** Pharmacokinetics and Pharmaceutical Technology Area, Engineering Department, Universidad Miguel Hernández, San Juan de Alicante, Alicante, Spain, **5** INVROTECNIA S.L., Santiago Grisolía 2, Tres Cantos, Madrid, Spain, **6** Laboratory of Foodomics, Institute of Food Science Research-CIAL (CSIC-UAM), Nicolás Cabrera 9, Campus Cantoblanco, Madrid, Spain, **7** CIBER, Fisiopatología de la Obesidad y la Nutrición, CIBERObn, Instituto de Salud Carlos III (CB12/03/30038), Spain

\* These authors contributed equally to this work.

\* [vmicol@umh.es](mailto:vmicol@umh.es)

## Abstract

Rosemary (*Rosmarinus officinalis*) is grown throughout the world and is widely used as a medicinal herb and to season and preserve food. Rosemary polyphenols and terpenoids have attracted great interest due to their potential health benefits. However, complete information regarding their absorption and bioavailability in Caco-2 cell model is scarce. The permeation properties of the bioactive compounds (flavonoids, diterpenes, triterpenes and phenylpropanoids) of a rosemary extract (RE), obtained by supercritical fluid extraction, was studied in Caco-2 cell monolayer model, both in a free form or liposomed. Compounds were identified and quantitated by liquid chromatography coupled to quadrupole time-of-flight with electrospray ionization mass spectrometry analysis (HPLC-ESI-QTOF-MS), and the apparent permeability values ( $P_{app}$ ) were determined, for the first time in the extract, for 24 compounds in both directions across cell monolayer. For some compounds, such as triterpenoids and some flavonoids,  $P_{app}$  values found were reported for the first time in Caco-2 cells. Our results indicate that most compounds are scarcely absorbed, and passive diffusion is suggested to be the primary mechanism of absorption. The use of liposomes to vehiculize the extract resulted in reduced permeability for most compounds. Finally, the biopharmaceutical classification (BCS) of all the compounds was achieved according to their permeability and solubility data for bioequivalence purposes. BCS study reveal that most of the RE compounds could be classified as classes III and IV (low permeability); therefore, RE itself should also be classified into this category.

and Competitiveness (MINECO); grant P11-CTS-7625 from Andalusian Regional Government Council of Innovation and Science; PROMETEO/2016/006, ACOMP/2013/093 and ACIF/2013/064 from Generalitat Valenciana; CIBER (CB12/03/30038, Fisiopatología de la Obesidad y la Nutrición, CIBERObn, Instituto de Salud Carlos III). The authors are also thankful to ChemAxon for providing a free academic license of Marvin for structure handling and other toolkits. The funder Invitrotecnia S.L. provided support in the form of salaries for author EBC.

**Competing interests:** The funder Invitrotecnia S.L. provided support in the form of salaries for author EBC, but did not have any additional role in the study design, data collection and analysis, decision to publish, or preparation of the manuscript. This does not alter author's adherence to PLOS ONE policies on sharing data and materials. The other authors declare that there are no conflicts of interest.

## Introduction

Rosemary (*Rosmarinus officinalis* L.) is a shrub from the *Labiatae* (*Lamiaceae*) family that is primarily distributed throughout the Mediterranean area. It has been demonstrated that rosemary and its major compounds, the diterpenes carnosic acid (CA) and carnosol (CAR) and the caffeoyl derivative rosmarinic acid, exert various beneficial effects on health, including potent antioxidant capacity [1, 2] and hepatoprotective [3], antimicrobial [4, 5], anti-inflammatory [6, 7], anti-cancer [8–13] and antidiabetic effects [14].

We have previously reported the antiproliferative effects of a polyphenol-enriched rosemary extract (RE) obtained via supercritical extraction in several colon cancer cell models [13]. Transcriptomic and metabolomic analysis suggested that the extract activated genes related to antioxidant phase II enzymes and cell cycle progression [12]. This result was consistent with the activation of nuclear receptor factor 2 (NRF2)-dependent pathways, ROS and glutathione metabolism by CA as determined using a comprehensive Foodomics approach [11]. However, bioguided purification of the extract revealed potential synergistic antiproliferative effects between diterpenes and triterpenes [13].

The rosemary polyphenols (di- and triterpenes) are considered promising drug candidates in the pharmaceutical, cosmetic, and nutritional fields. However, these compounds exhibit physicochemical characteristics that result in unfavorable transcellular transport across epithelial barriers. Several attempts have been made to evaluate the absorption of the active compounds from rosemary extract in cell and animal models. The bioavailability of major diterpenoids derived from rosemary extract in different tissues in a rat model of obesity has been reported [15]. Moreover, the absorption, distribution and elimination of carnosic acid have been evaluated in rats [16]. However, complete information regarding the absorption and bioavailability of a full range of rosemary bioactive compounds (flavonoids, diterpenes and triterpenes) in Caco-2 cell monolayers is not available. Studies examining the permeation of carnosic acid and carnosol in Caco-2 cells are present in the literature, but permeation was either insufficiently characterized [17] or was found to be almost negligible [18]. In addition, no comparative data regarding the permeation and potential absorption mechanisms of all compounds present in rosemary extract have been generated so far.

Liposomes have been utilized to improve solubility and selectivity and to improve bioavailability of poorly soluble drugs by modifying drug absorption, reducing metabolism, prolonging biological half-life or reducing toxicity. Phospholipid bilayers of liposomes are very similar to the structure of cell membranes; therefore, liposomes can deliver encapsulated drugs, peptides and natural compounds by fusing with target cell membranes, and their specificity can be improved by antibody coupling [19–22]. Several plant polyphenols and bioactive compounds, such as catechins [23], anthraquinones [24], phenylpropanoids [25], and diterpenes [1], have been shown to possess the capacity to interact with phospholipid membranes.

In the present paper, a Caco-2 cell monolayer model, which is a well-accepted model of human intestinal absorption [26], was used to comprehensively study and compare the permeation properties of different bioactive compounds (flavonoids, diterpenes, triterpenes and phenylpropanoids) identified in a rosemary extract (RE) by HPLC-ESI-QTOF-MS and obtained via supercritical fluid extraction [27]. The permeation behaviors of the compounds were compared when the extract was in a free form or encapsulated into liposomes. Moreover, all compounds were biopharmaceutically classified based on their permeability and solubility data for bioequivalence purposes.

## Materials and methods

### Chemicals and cell culture materials

All chemicals were of analytical reagent grade and were used as received. For mobile phase preparation, formic acid and acetonitrile were purchased from Sigma-Aldrich (Steinheim, Germany) and Fisher Scientific (Madrid, Spain), respectively. Water was purified using a Milli-Q system from Millipore (Bedford, MA, USA). The standard compounds ursolic acid, rosmarinic acid, genkwanin, diosmetin and luteolin were obtained from Extrasynthese (Genay, France). Carnosol, carnosic acid and apigenin were obtained from Fluka, Sigma-Aldrich (Steinheim, Germany). Egg yolk phosphatidylcholine was purchased from Lipoid GmbH (Ludwigshafen, Germany), and cholesterol was obtained from Avanti Polar Lipids (Alabaster, AL, USA). Methanol and dimethyl sulfoxide (DMSO) from Fisher Scientific (Madrid, Spain) were used to prepare the stock solutions utilized for quantitation purposes. Hank's balanced culture medium (HBSS), Dulbecco's Modified Eagle's Medium (DMEM), fetal bovine serum (FBS), 100 U/mL penicillin/streptomycin, MEM Non-Essential Amino Acids Solution (100x) and 1 M HEPES were obtained from Gibco/Thermo Fisher Scientific (Waltham, MA, USA). The human colon adenocarcinoma cell line Caco-2 was obtained from the American Type Culture Collection. Caco-2 cells were cultured in DMEM containing D-glucose (4.5 g/L) and supplemented with 10% FBS, 1% NEAA, 1% HEPES, penicillin (100 U/mL) and streptomycin (100 µg/mL) at 37°C in a humidified atmosphere with 5% CO<sub>2</sub>.

### Cell viability assay

The cytotoxic effects of free and encapsulated RE extract on Caco-2 cells were tested using the 3-(4,5-dimethylthiazol-2-yl)-2,5-diphenyltetrazolium bromide (MTT) assay. Caco-2 cells were plated in 96-well plates (Costar, Fisher Scientific, Pittsburgh, PA, USA) until cell monolayers were obtained. Then, the medium was aspirated, and cells were treated with different concentrations of RE for 2 h. The medium was removed, and cells were washed with PBS and incubated with MTT for 3–4 h at 37°C and 5% CO<sub>2</sub>. The medium was removed, and 100 µL of DMSO per well was added to dissolve the formazan crystals. The plates were shaken for 15 min, and absorbance was measured using a microplate reader (SPECTROstar Omega, BMG LabTech GmbH, Germany) at 570 nm.

### Caco-2 monolayer transport studies

Caco-2 cells are a well-established *in vitro* model for the investigation of intestinal permeabilities of different compounds or drugs [28–30]. Cells were seeded at a density of  $5.0 \times 10^5$  cells on 6-well transwell polycarbonate filters (Millipore, Spain). Cell culture was maintained at 37°C under 90% humidity and 5% CO<sub>2</sub>. The medium was replaced every 2–3 days for both the apical (AP) and basal (BL) sides of the transwell filters. Cell monolayers were used 19–21 days after seeding, once confluence and differentiation were achieved. The integrity of each cell monolayer was checked by measuring the trans-epithelial electrical resistance (TEER) before and after the experiments with an epithelial voltoohmmeter (Millicell-ERS®) (see results on S3 Table). Permeability studies were performed by adding the RE at a concentration of 200 µg/mL or the liposomal RE formulation.

The liposomal formulation was prepared using the conventional thin film hydration technique. Egg yolk phosphatidylcholine and cholesterol (80:20 w/w) and 10% (w/w) RE with respect to total phospholipids were dissolved in a 1:1 mixture of chloroform/methanol. A lipid film was obtained by evaporating the organic solvent under a stream of nitrogen (N<sub>2</sub>) and then further vacuum-dried for 3–4 h to remove any residual organic solvent. The film was hydrated

with HEPES buffer (100 mM NaCl, 0.1 mM EDTA, 10 mM HEPES, pH 7.4) via vigorous vortexing for 30 min at 37°C. The multilamellar liposomal suspension was filter-extruded through a 100-nm polycarbonate Track-Etch Nuclepore membrane (Whatman, UK) to obtain large unilamellar vesicles (LUVs). Size reduction was carried out with 15 extrusion cycles performed by hand with a Liposofast™ syringe extruder (Avestin Inc., Canada). The resulting suspension was centrifuged at 4,000 rpm for 30 min (2 cycle) using an Amicon® Ultra (Millipore, Hayward, CA, USA) to separate the liposomes from non-encapsulated drug. The liposomal suspension was diluted to a concentration of 1.5 mM with HBSS for absorption experiments in the receiving chamber.

The transport experiment was initiated by removing the culture medium from the AP and BL sides of the transwell filters. The Caco-2 monolayers were rinsed twice with pre-warmed HBSS medium (pH 7.4) and incubated with the same solution at 37°C for 30 min. The test compounds were added to the AP (2.2 mL) or BL side (3.2 mL), while the receiving chamber contained the corresponding volume of HBSS. Incubation was performed at 37°C for 120 min, with shaking at 50 rpm.

To follow transport across the cell monolayer, several culture medium samples of 0.2 mL were collected at different time points (0, 30, 60, 90 and 120 min) from the AP or BL sides during the permeability assay. The volume of the samples taken at each time point was replaced with the same volume of HBSS to maintain the total volume in the chamber throughout the experiment.

Before HPLC-ESI-QTOF-MS analysis, samples were centrifuged for 15 min at 12,000 rpm and 4°C. The supernatant was spiked with 5 µg/mL of an internal standard (luteolin) to ensure the reproducibility of the results between analyses, and samples were stored at -80°C until analysis was complete. At the end of the transport study, the Caco-2 cell monolayers were also collected, and the cells were lysed with 3 subsequent freeze-thaw cycles (10 min each) followed by bath sonication. The samples were centrifuged for 15 min at 14,000 rpm and 4°C, and the supernatants (cytoplasmic fraction) and the pellets (cell membranes) were spiked with 5 µg/mL luteolin as an internal standard. Then, the samples were subjected to protein precipitation using methanol, vortex-mixed, maintained at -20°C for 2 h and centrifuged at 12,000 rpm for 15 min at 4°C. Finally, the supernatants were evaporated in a vacuum concentrator, re-dissolved in 100 µL of HBSS culture medium and stored at -80°C until analysis was performed.

Apparent permeability values ( $P_{app}$ ) for each compound were calculated according to the following equation:

$$P_{app} = \frac{dQ}{dt} \cdot \frac{1}{A \cdot C_0 \cdot 60}$$

where  $P_{app}$  is the apparent permeability (cm/s),  $dQ/dt$  is the steady state flux, A is the diffusion area of the monolayers (cm<sup>2</sup>),  $C_0$  is the initial concentration of the drug in the donor compartment (µM) and 60 is a conversion factor [31].

### Analytical methodology

HPLC analyses were performed on an Agilent 1260 HPLC instrument (Agilent Technologies, Palo Alto, CA, USA) equipped with a binary pump, an online degasser, an auto-sampler, a thermostatically controlled column compartment, and diode array detectors. The samples were separated on an Agilent Zorbax Eclipse Plus C18 column (1.8 µm, 4.6 × 150 mm). The mobile phases consisted of water plus 0.1% formic acid as mobile phase A and acetonitrile as mobile phase B, using a gradient elution based on the following profile: 0 min, 5% B; 5 min, 62% B; 10 min, 68% B; 19 min, 80% B; 34 min, 95% B; 37 min, 5% B and finally a conditioning

cycle of 5 min under the initial conditions before the next analysis. The flow rate was 0.8 mL/min, the column temperature set at 25°C and the auto-sampler compartment was refrigerated at 4°C to avoid sample degradation.

Detection was performed using an Agilent 6540 Ultra High Definition (UHD) Accurate-Mass Q-TOF mass spectrometer equipped with a Jet Stream dual ESI interface, which increases LC/MS sensitivity by improving the spatial focusing of electrospray droplets. Mass spectra were recorded in negative ionization mode over a mass range from 100–1700 m/z. Ultrahigh pure nitrogen was used as the drying and nebulizing gas. The operating parameters were as follows: drying gas flow rate, 10 L/min; drying gas temperature, 325°C; sheath gas temperature, 400°C; sheath gas flow, 12 L/min; nebulizer, 20 psig; capillary, 4000 V; fragmentor, 130 V, nozzle voltage, 500 V; skimmer, 45 V and octopole 1 RF Vpp, 750 V. Continuous infusion of the reference ions m/z 112.985587 (trifluoroacetate anion) and 1033.988109 (adduct of hexakis (<sup>1</sup>H,<sup>1</sup>H,<sup>3</sup>H-tetrafluoropropoxy) phosphazine or HP-921) in negative ion mode were used to correct each spectrum to achieve accurate mass measurements, typically better than 2 ppm. All operations, acquisition and analysis of data were controlled using Masshunter workstation software version B.06.00 (Agilent Technologies, USA).

### Statistical analysis

Two-way ANOVA and statistical comparisons of the different treatments were performed using Tukey's post-test in GraphPad Prism version 5.00 (GraphPad Software, San Diego, CA, USA). Differences were considered statistically significant at  $p < 0.05$ . Statistical significance is detailed in figures using the following symbols: \*  $p < 0.05$ , \*\*  $p < 0.01$  and \*\*\*  $p < 0.001$ .

## Results and discussion

We recently reported the composition of the rosemary leaf extract (RE) under study as determined by HPLC-ESI-QTOF-MS analysis [13]. In that study, bioguided purification of the most active fractions was undertaken to identify the compounds bearing the highest antiproliferative capacities in a colon cancer cell model. The aim of the present study was to compare the intestinal absorption and permeability behavior of all compounds in the RE, both when the extract was in a free or in an encapsulated formulation, using the Caco-2 model system. To achieve this, the quantitation of bioactive compounds and absorption results will be discussed by grouping the different bioactive compounds into families (flavonoids, diterpenes, triterpenes and phenylpropanoid derivatives).

### HPLC ESI-UHD-Qq-TOF-MS analysis

For quantitative purposes, six standard calibration graphs were prepared using HBSS culture medium to quantify the major compounds in the rosemary extract using the following commercial standards: carnosol, carnosic acid, ursolic acid, rosmarinic acid, genkwanin, and diosmetin.

Variability of peak area produced by mass data change over time may be a limitation for quantification by mass spectrometry, depending on the instrument. Thus, an internal standard (luteolin) was used at a concentration of 5 µg/mL to improve reproducibility. This compound met all requirements in terms of structural similarity compared with the analytes, retention time (which did not interfere with other compounds) and compensation for potential variations in instrumental analysis. Moreover, to avoid ion suppression or signal enhancement of signals due to interference derived from the matrix, the calibration solutions were prepared in HBSS culture medium, which was the same matrix containing the samples in the permeability assay. Therefore, compound concentrations were determined using the corrected area for each

individual compound (three replicates) and by interpolating the corresponding calibration curve. The limit of detection (LOD) ranged from  $0.0008 \pm 0.0002$  (diosmetin) to  $0.04 \pm 0.01$  (ursolic acid)  $\mu\text{g}/\text{mL}$ . The limit of quantification (LOQ) ranged from  $0.003 \pm 0.001$  (diosmetin) to  $0.14 \pm 0.03$  (ursolic acid)  $\mu\text{g}/\text{mL}$ .

Quantification was performed using available commercial standards for carnosol, diosmetin, apigenin, genkwanin and carnosic, ursolic and rosmarinic acids. Compounds that had no commercially available standards were tentatively quantified on the basis of calibration curves for other compounds with similar structures. Thus, rosmanol, its isomers epiisorosmanol and epirosmanol, miltipolone, rosmadial and rosmaridiphenol were quantified with the carnosol standard. Hinokione and 12-methoxycarnosic acid were expressed as carnosic acid. The ursolic acid calibration curve was used to quantify augistic, benthamic, micromeric and betulinic acids, in addition to anemosapogenin. Finally, the genkwanin standard was used for cirsimarin quantification; [9]-shogaol was expressed as rosmarinic acid, and diosmetin was used to estimate the hispidulin content.

### Determination of $P_{app}$ values

After quantifying the concentrations of all identified compounds in samples derived from the apical and basolateral compartments, as described in the previous section, concentration values were used to obtain  $P_{app}$  values based on the formula described in the Materials section. Values are shown in [Table 1](#) for both the AB and BA directions and for free and encapsulated formulations. Some compounds could not be quantified because their concentrations fell below LOQ values, sometimes for both directions or formulations (free or encapsulated) and occasionally for one of these. Detailed explanations for clustering compounds in families are provided in the following sections.

**Flavonoids and phenylpropanoid derivatives.** The phenylpropanoid derivative (9)-shogaol (a gingerol-like compound) and its isomer ([Fig 1D](#)) were present in all the samples but were below their respective LOQs; thus, no conclusions could be drawn for these compounds. A deeper analysis of the samples revealed that both compounds were partly retained by Caco-2 cells without any transport to the receptor chamber because amounts of these compounds below their LOQs were also detected in the cytoplasmic fractions of Caco-2 cells, as previously reported for (6)-shogaol [[32](#)].

Despite the fact that flavonoids were less frequently represented in the extract based on our previous quantitative characterization [[13](#)], their potential absorption and biological activity are worthy of analysis. Flavonoids present in the RE were apigenin, hispidulin, diosmetin, genkwanin and cirsimarin ([Fig 1A](#)). Conclusions regarding apigenin in the context of the whole extract could not be reached because the concentration fell below its LOQ. However, several studies have reported apigenin absorption in the Caco-2 cell model [[33–37](#)]. For the other four flavonoids, no permeation was detected in either of the directions when the RE sample was encapsulated into liposomes. However, significant permeation was detected for the RE in its free form in both the AB and BA directions. The highest values for AB were obtained for cirsimarin and genkwanin, with no significant differences between them ( $p > 0.05$ ); this is the first report of cirsimarin and genkwanin values in Caco-2 cells. Diosmetin and hispidulin exhibited lower permeation values that demonstrated statistically significant differences compared to cirsimarin ( $p < 0.001$  and  $0.01$ , respectively), but there was no difference between them ( $p > 0.05$ ). Higher values than those observed in our study have been reported for pure diosmetin in both flux directions [[38](#)], but it must be noted that competition with other polyphenols and terpenoids may take place in the whole extract. Absorption values for hispidulin and apigenin in the whole extract were in agreement with those reported for the pure compounds [[39, 40](#)].

Table 1.  $P_{app}$  values.

Compound	Family	Non encapsulated RE				Encapsulated RE			
		AB direction		BA direction		AB direction		BA direction	
		$P_{app}$	SD	$P_{app}$	SD	$P_{app}$	SD	$P_{app}$	SD
Apigenin	Flavonoid	N.C.		N.C.		N.C.		N.C.	
Cirsimarinin	Flavonoid	3.33E-05	1.17E-06	3.07E-05	6.29E-06	N.A.	N.A.	N.A.	N.A.
Diosmetin	Flavonoid	2.50E-06	N.E.	4.13E-06	1.38E-06	N.A.	N.A.	N.A.	N.A.
Hispidulin	Flavonoid	9.05E-06	3.04E-06	1.31E-05	9.60E-07	N.A.	N.A.	N.A.	N.A.
Genkwanin	Flavonoid	1.49E-05	2.47E-06	1.62E-05	3.42E-06	N.A.	N.A.	N.A.	N.A.
Carnosol	Diterpene	1.46E-05	2.10E-06	1.35E-05	5.15E-06	4.03E-08	3.18E-08	2.61E-07	2.72E-08
Carnosol isomer	Diterpene	2.15E-05	3.30E-06	2.13E-05	5.73E-06	4.03E-08	3.18E-08	4.03E-08	3.18E-08
Carnosic acid	Diterpene	1.27E-04	1.55E-05	9.04E-05	1.09E-05	N.A.	N.A.	N.A.	N.A.
12-Methoxycarnosic acid	Diterpene	1.85E-05	4.04E-06	2.77E-05	5.12E-06	N.A.	N.A.	N.A.	N.A.
Rosmadial	Diterpene	1.90E-05	2.84E-06	1.59E-05	1.20E-06	2.67E-06	6.43E-07	1.24E-05	9.19E-07
Rosmanol	Diterpene	4.59E-05	7.48E-06	4.42E-05	3.53E-06	2.91E-05	9.45E-06	3.33E-05	N.C.
Epirosmanol	Diterpene	5.51E-05	2.79E-05	1.21E-05	7.90E-06	1.92E-06	4.17E-07	2.63E-06	6.02E-07
Epiisorosmanol	Diterpene	1.04E-04	1.79E-05	9.23E-06	6.55E-06	8.18E-06	3.02E-06	1.30E-05	3.52E-06
Miltipolone	Diterpene	1.76E-05	1.97E-06	N.A.	N.A.	N.A.	N.A.	1.68E-07	8.91E-08
Hinokione	Diterpene	N.A.	N.A.	1.36E-05	1.22E-06	N.A.	N.A.	N.A.	N.A.
Rosmaridiphenol	Diterpene	2.43E-06	6.44E-07	2.68E-06	1.28E-06	N.A.	N.A.	N.A.	N.A.
Augustic acid	Triterpene	7.35E-06	3.64E-06	7.93E-06	4.12E-06	N.A.	N.A.	N.A.	N.A.
Betulinic acid	Triterpene	0.00E+00	0.00E+00	6.30E-06	5.66E-07	N.A.	N.A.	N.A.	N.A.
Anemosapogenin	Triterpene	3.27E-06	1.79E-06	6.17E-06	2.99E-06	N.A.	N.A.	N.A.	N.A.
Micromeric acid	Triterpene	7.20E-06	2.26E-06	2.45E-06	1.63E-06	N.A.	N.A.	N.A.	N.A.
Benthamic acid	Triterpene	5.20E-06	2.40E-06	7.03E-06	3.25E-06	N.A.	N.A.	N.A.	N.A.
Ursolic acid	Triterpene	0.00E+00	0.00E+00	7.20E-06	2.26E-06	N.A.	N.A.	N.A.	N.A.
(9)-Shogaol	Phenylpropanoid	N.C.		N.C.		N.C.		N.C.	
(9)-Shogaol Isomer	Phenylpropanoid	N.C.		N.C.		N.C.		N.C.	

$P_{app}$  values in cm/s for all the compounds quantitated in the free and encapsulated formulations of RE in both AB and BA directions. Values represent the mean of six independent replicates  $\pm$  standard deviation (SD). N.C., non-calculated (see text for further explanations). N.E., no error was obtained as only one of the replicates was used as the other presented values below LOQ. N.A. indicates  $P_{app} = 0$  (non-absorbed).

doi:10.1371/journal.pone.0172063.t001

Regarding the basal-apical direction, cirsimarinin, genkwanin and hispidulin demonstrated similar permeation values with no significant differences between them ( $p > 0.05$ ), followed by diosmetin, which had the lowest value ( $p < 0.001$ ).

Based on our results, we can conclude that rosemary flavonoids did not exhibit differences when comparing the two flux directions (AB and BA) for the free-form extract, which suggests a passive diffusion transport mechanism. No transport at all was observed when these compounds were incorporated into liposomes.

**Diterpenoids.** Diterpenoids (10.87% w/w of the extract) together with triterpenoids constitute the major group of compounds in the extract and comprise up to 10 compounds (Fig 1B and Table 1) [13]. The diterpenoids present in the RE were carnosic acid, carnosol, rosmadial and its isomers (epiisorosmanol and epirosmanol), 12-methoxycarnosic acid, rosmadial, rosmaridiphenol, hinokione and miltipolone.

Among all the diterpenes and the non-encapsulated RE, the highest permeability in the AB direction was obtained for carnosic acid (with  $p < 0.001$ ), followed by epirosmanol and rosmadial, which did not demonstrate statistically significant differences between them ( $p > 0.05$ ). A carnosol isomer, rosmadial, 12-methoxy carnosic acid, miltipolone and carnosol exhibited

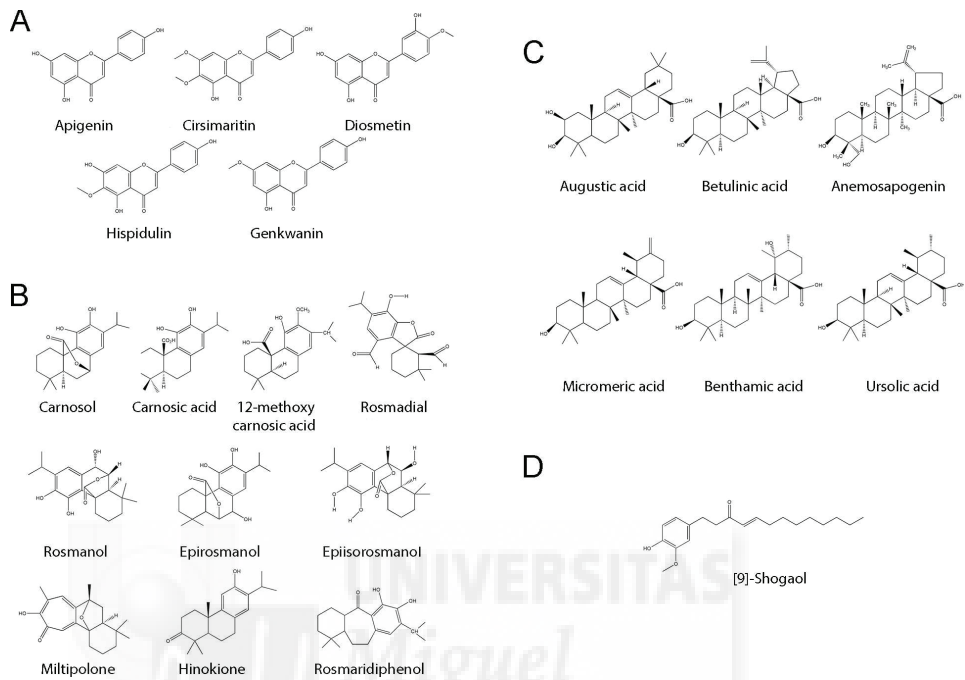


**Fig 1. Chemical structures of all the compounds identified in RE.** A: Flavonoids, B: diterpenes, C: triterpenes, D: phenylpropanoid derivatives.

doi:10.1371/journal.pone.0172063.g001

Papp values ranging from 2.1 to 1.46E-05. In contrast, the diterpenoid rosmaridiphenol demonstrated lower absorption ( $P_{app}$  in the E-06 range), while hinokione showed no absorption. For the BA direction, the highest permeability value was obtained for carnosic acid ( $p<0.001$ ) followed by the rest of the compounds, with no relevant differences between them ( $p>0.05$ ) with the exception of miltipolone, which was not absorbed.

In general, absorption values of the compounds were lower for the encapsulated form than for the free extract. When absorption for the encapsulated form in the AB direction was studied, rosmanol demonstrated the highest permeability followed by epiisorosmanol, rosmadial and epirosmanol. The encapsulated formulation dramatically decreased the permeability for epirosmanol, epiisorosmanol (both at  $p<0.001$ ) and rosmanol ( $p<0.05$ ) in the AB direction, with no changes in the BA direction compared with the free formulation. As there is no difference in polarity between these compounds (see Log P in Table 2), it can be assumed that the few differences in their structures must be crucial for their absorption. Both isomers of carnosol showed significantly lower absorption values than those previously reported. The rest of the compounds showed no absorption in the encapsulated extract (12-methoxy carnosic acid, carnosic acid, rosmaridiphenol, miltipolone and hinokione). For the BA direction, identical behavior for the abovementioned compounds was observed.

It can be concluded that among all the diterpenes, rosmanol and its isomers epiisorosmanol and epirosmanol exhibited the highest permeabilities for both formulations, particularly in the AB direction. Rosmadial and rosmanol demonstrated similar absorption values when the free

**Table 2.** Chemical family, physicochemical and permeation data and BCS classification.

Compound	Family	D (M)	S (mg/mL)	Vs	D <sub>0</sub>	Solubility	Log P	Permeability	BCS Class
								Based on Log P	Based on Log P
								Based on P <sub>app</sub>	Based on P <sub>app</sub>
Apigenin	Flavonoid	3.70E-02	4.47E-03	8.28	3.31E-02	High	1.90	Low	III
								N.C.	N.C.
Cirsimarinin	Flavonoid	3.18E-02	2.57E-04	123.79	4.95E-01	High	2.04	Low	III
								Low	III
Diosmetin	Flavonoid	3.33E-02	4.27E-03	7.81	3.12E-02	High	1.78	Low	III
								Low	III
Hispidulin	Flavonoid	3.33E-02	1.58E-03	21.01	8.41E-02	High	1.78	Low	III
								Low	III
Genkwanin	Flavonoid	3.52E-02	4.17E-04	84.39	3.38E-01	High	2.17	Low	III
								Low	III
Carnosol	Diterpene	3.03E-02	2.57E-05	1177.43	4.71	Low	4.58	High	II
								Low	IV
Carnosol Isomer	Diterpene	3.03E-02	2.57E-05	1177.43	4.71	Low	4.58	High	II
								Low	IV
Carnosic acid	Diterpene	3.01E-02	1.51E-02	1.99	7.95E-03	High	5.14	High	I
								Low	III
12-methoxycarnosic acid	Diterpene	2.89E-02	5.50E-03	5.25	2.10E-02	High	5.4	High	I
								Low	III
Rosmadial	Diterpene	2.90E-02	9.12E-05	318.37	1.27	Low	3.74	High	II
								Low	IV
Rosmanol	Diterpene	2.89E-02	5.75E-05	501.65	2.01	Low	3.70	High	II
								Low	IV
Epirosmanol	Diterpene	2.89E-02	5.75E-05	501.65	2.01	Low	3.70	High	II
								Low	IV
Epiisorosmanol	Diterpene	2.89E-02	5.75E-05	501.65	2.01	Low	3.70	High	II
								High	II
Miltipolone	Diterpene	3.33E-02	3.55E-05	938.23	3.75	Low	1.02	Low	IV
								Low	IV
Hinokione	Diterpene	3.33E-02	2.19E-05	1521.42	6.09	Low	5.85	High	II
								N.C.	N.C.
Rosmaridiphenol	Diterpene	3.16E-02	1.55E-06	20404.08	81.62	Low	4.89	High	II
								Low	IV
Augustic acid	Triterpene	2.11E-02	1.15E-04	184.25	7.37E-01	High	6.52	High	I
								Low	III
Betulinic acid	Triterpene	2.19E-02	2.04E-05	1072.43	4.29	Low	7.38	High	II
								N.C.	N.C.
Anemosapogenin	Triterpene	2.12E-02	1.20E-04	175.96	7.04E-01	High	6.32	High	I
								Low	III
Micromeric acid	Triterpene	2.20E-02	1.23E-04	178.77	7.15E-01	High	6.91	High	I
								Low	III
Benthamic acid	Triterpene	2.12E-02	5.89E-04	35.93	1.44E-01	High	6.13	High	I
								Low	III
Ursolic acid	Triterpene	2.19E-02	1.51E-05	1446.66	5.79	Low	7.33	High	II
								N.C.	N.C.

(Continued)

**Table 2.** (Continued)

Compound	Family	D (M)	S (mg/mL)	Vs	D <sub>0</sub>	Solubility	Log P	Permeability	BCS Class
								Based on Log P	Based on Log P
								Based on P <sub>app</sub>	Based on P <sub>app</sub>
[9]-Shogaol	Phenylpropanoid	3.14E-02	1.29E-06	24375.88	97.50	Low	5.26	High	II
								N.C.	N.C.
[9]-Shogaol Isomer	Phenylpropanoid	3.14E-02	1.29E-06	24375.88	97.50	Low	5.26	High	II
								N.C.	N.C.

Chemical family, physicochemical and permeation data and BCS classification for all the compounds of RE studied in the absorption assay in the free form and considering 10 mg dose scenario.

doi:10.1371/journal.pone.0172063.t002

and encapsulated formulations were compared. In contrast, epirosmanol and epiiserosmanol showed higher absorption values in the AB direction when encapsulated ( $p < 0.001$  for both). Finally, miltipolone exhibited interesting behavior: no absorption was observed in the BA direction for the free formulation, whereas no absorption was observed in the opposite direction (AB) for the encapsulated form.

Interestingly, certain facts should be noted for individual compounds. Diterpenoids, such as carnosol and its isomer, demonstrated less absorption when encapsulated, regardless of the direction analyzed. In the case of both carnosol isomers, the  $P_{app}$  values for the AB direction and for the BA direction were significantly higher for the free formulation (carnosol ( $p < 0.01$ ) and carnosol isomer ( $p < 0.001$ )) than for the encapsulated formulation. The carnosol isomer exhibited a higher  $P_{app}$  value than carnosol in the free formulation (both directions), but no significant differences were observed for these compounds when the AB and BA directions were compared ( $p > 0.05$ ). For the encapsulated extract, no significant differences were observed between the isomers in the AB direction, but carnosol demonstrated a higher permeability than its isomer in the BA direction. These results contradict the generally accepted notion that hydrophobic diterpenes are better absorbed when encapsulated into phospholipid vesicles and thus may deserve further study.

Another interesting issue is related to the influence of certain moieties present in the compounds on absorption behavior. For carnosic and 12-methoxycarnosic acids,  $P_{app}$  values could be obtained only for the free formulation. Permeation in the AB direction was higher than in the BA direction for both compounds, but only for carnosic acid was statistically significant ( $p < 0.001$ ). The presence of the methoxy moiety increases the permeability by almost one order of magnitude in the AB direction but reduces the permeability in the opposite direction. This result indicates that the increase in hydrophobicity attributable to the methoxy group increases absorption and concomitantly enhances retention once the compound is absorbed by reducing BA permeability. However, further studies should be undertaken to elucidate the absorption mechanism.

Considering previous data reported in the literature, it appears that the absorption observed in the present work for most of the compounds was higher than absorption values previously reported. For example, the absorption of carnosic acid and carnosol has previously been studied in a Caco-2 cell model, but no permeation was observed in certain cases [18], or longer periods of time were required to achieve permeation into the basolateral chamber [17]. No information regarding the other diterpenoids is available in the literature, either for individual compounds or complex mixtures or extracts.

**Triterpenoids.** Triterpenoids were the most abundant family in the rosemary extract (12.16% w/w) according to our previous analysis [13] and comprised six compounds ([Fig 1C](#)): augustic, betulinic, micromeric, benthamic and ursolic acids and anemosapogenin.

No absorption data for the triterpenoids could be determined based on the concentrations of the compounds in the basolateral and apical chambers when the extract was applied in the encapsulated formulation ([Table 1](#)). Augustic acid and anemosapogenin were detected only in the donor chamber but at levels below their LOQs. A similar result was obtained for ursolic, micromeric and benthamic acids; however, their concentrations could be measured in the donor chamber because they surpassed LOQs. Betulinic acid was detected both in the donor chamber and also inside the cells but was not detected in the receptor chamber. These data indicate that none of the triterpenoids are absorbed from the encapsulated formulation, independent of their chemical structure. It is likely that the high hydrophobicities of these compounds, which demonstrate high Log P values ([Table 2](#)), favor their retention in phospholipid vesicles or their association with the plasmatic membrane and other lipophilic structures inside cells.

In contrast, all triterpenoids were absorbed with low  $P_{app}$  values in the free formulation, although important differences were observed ([Table 1](#)). Ursolic acid, which showed a  $P_{app}$  values similar to that one previously reported [41] and betulinic acid were not absorbed in the AB direction and were partly retained by the Caco-2 cells. The other four triterpenoids were absorbed in the AB direction, with no significant differences ( $p > 0.05$ ) between them. All six triterpenoids were absorbed in the BA direction, also with low  $P_{app}$  values and with no significant differences between them ( $p > 0.05$ ). This indicates that the slight differences between the chemical structures of these compounds do not result in different absorption behaviors. As mentioned for the diterpenoids, encapsulation into phospholipid vesicles did not appear to be a good approach to increase triterpenoid bioavailability. As with most of the diterpenoids analyzed in the previous section, data regarding the absorption of rosemary triterpenoids are presented in this study for the first time.

The absorption of natural polyphenols has been widely studied in the Caco-2 model [36–38, 42–44]. However, scant information regarding the absorption of these compounds is available for complex mixtures such as botanical extracts. In some absorption studies, no identification of rosemary compounds was performed, and only total polyphenolic content was determined [42]. Other studies have reported the permeabilities of only a few compounds within a studied extract, employing a semiquantitative approach [17, 18, 44]. In the present study, the permeabilities of all compounds identified in the rosemary extract via HPLC ESI-UHD-Qq-TOF-MS analysis were studied in both the AB and BA directions and, additionally, were compared with an encapsulated formulation of the extract. Given that the absorptions of all compounds were analyzed in the context of the whole RE, several mechanisms of interaction, such as competition and inhibition of potentiation, between compounds may occur, particularly between compounds sharing similar chemical structures. The analyses performed in this study indicate that the permeabilities of complex botanical extracts can be fully analyzed by employing high sensitivity mass spectrometry and improved purification techniques.

Our results indicate that most compounds are scarcely absorbed, and passive diffusion is suggested to be the major mechanism of absorption for most compounds, as the AB and BA directions both yielded similar results. Further mechanistic studies must be carried out to elucidate this mechanism. In contrast, we confirmed that contrary to previous observations for other compounds, the use of liposomes to encapsulate RE compounds is not a good approach to improve their permeability because  $P_{app}$  values were reduced or negligible for the majority of the compounds. According to Fick's Law, absorption depends on the permeability/diffusion

constant and concentration of the compound. If the solubility of a compound demonstrating low absorption is increased due to encapsulation into liposomes and its concentration is enhanced in the donor chamber, an increase in the absorption may occur to compensate for its reduced absorption, as reported for other hydrophobic natural compounds [45]. This does not appear to be the case for the diterpenoids and triterpenoids in RE, but further studies must be carried out to clarify these observations.

### Biopharmaceutical classification

The Biopharmaceutical Classification System (BCS) was developed by Amidon and coworkers twenty years ago to classify drugs for a waiver of *in vivo* bioequivalence studies [46]. This system classifies drugs into four categories based on their intestinal permeability and solubility (see [S1 Table](#)), and currently this system is accepted worldwide by researchers and governmental institutions such as the FDA and EMA. In addition to its regulatory use, BCS is a tool for drug development because it helps identify the limiting factors in the absorption process [47]. In this work, the 24 compounds identified from RE were classified individually according to this system to obtain relevant information regarding their absorbed oral fraction. For this purpose, only data derived from the free extract permeation were used.

**Permeability values.** Log P values were obtained for all compounds using ChemDraw software® Ultra version 8.0 (CambridgeSoft Corp. USA) and are shown in [Table 2](#). The Log P value is a widely accepted parameter to express the lipophilicities of biological drugs in medicinal and agro chemistry. According to BCS, compounds are divided into high permeability (Class I: high permeability, high solubility; Class II: high permeability, low solubility) or low permeability (Class III: low permeability, high solubility; Class IV: low permeability, low solubility) categories by comparing with the Log P value (2.18) of the standard metoprolol, which is the reference compound employed for this purpose [48, 49]. Based on this parameter, the permeabilities of all compounds derived from RE were tabulated as high or low ([Table 2](#)). Moreover, the  $P_{app}$  value of this reference drug ( $0.6 \times 10^{-4}$  cm/s) was also available, which allowed us to establish another classification for the permeabilities of RE compounds based on this parameter, using the  $P_{app}$  values of the compounds obtained in the AB direction only for the free formulations ([Table 2](#)). Therefore, the Log P and  $P_{app}$  values were used in [Table 2](#) to classify compounds as high- or low-solubility drugs for permeability, providing two different classifications based on the partition coefficient and the intestinal permeability.

### Solubility values

Together with permeability, water solubility is another parameter that is required to classify drugs or compounds according BCS. For this purpose, the dose number value,  $D_0$ , must be obtained from the following equation:

$$D_0 = \frac{\text{maximum administered dose}}{S_w \cdot 250}$$

where  $S_w$  is the minimum solubility of each compound in water (in the pH range from 1.2 to 6.8) and the 250 value indicates the volume of a glass of water. A value of  $D_0 \leq 1$  indicates that the maximum administered dose can be dissolved in a glass of water; thus, the compound is classified as a high-solubility drug. Unfortunately, natural compounds such as polyphenols and terpenoids exhibit poor solubility. No experimental data regarding the solubilities of the 24 compounds identified from RE in this study are available. This problem was overcome using Marvin Suite software (version 16.1.11.0, ChemAxon Ltd.), which provides several

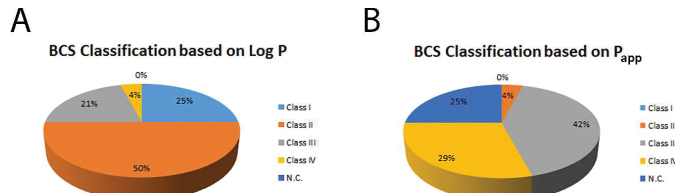


**Fig 2. BCS classification.** Plots show the BCS classification of all compounds in RE using the 10 mg dose scenario according LogP (A) y  $P_{app}$  (B) values.

doi:10.1371/journal.pone.0172063.g002

physicochemical properties, including a prediction of water solubility ( $S_w$ ). [Table 2](#) includes the  $S_w$  values for all 24 compounds.

As no information was available regarding the maximum doses of these compounds, two putative scenarios were selected to simulate a high-activity drug, dosed as a 10-mg tablet, or a low-activity drug, dosed as a 100-mg tablet. [Table 2](#) shows the results for the high-activity drug (10-mg dose), and [S2 Table](#) includes results from the second option (100-mg dose). In the present study, all compounds were classified for BCS by considering the experimental data for absorption ( $P_{app}$ ) and the calculated Log P value ([Table 2](#)). According to the Log P value, most compounds belong to the high-permeability classes (I and II), with class II being the most numerous ([Fig 2A](#)), except in the case of the flavonoids. However, when experimental  $P_{app}$  values were used for classification, the results changed dramatically, and low-permeability classes (III and IV) became the most abundant ([Fig 2B](#)). This classification was nearly independent of the solubility scenario and considered dose (compare [Fig 2](#) and [S1 Fig](#)). Moreover, the different families of compounds also exhibited different behaviors in terms of BCS classification. Most flavones in RE were classified as class III (low permeability, high solubility) and class IV (low permeability, low solubility) with the exception of apigenin, for which no experimental  $P_{app}$  could be determined and, consequently, no BCS classification was proposed. This result was in agreement with recently reported data and reinforces the notion that the limited bioavailabilities of most polyphenols may be improved by strategies focused on increasing drug solubilities and dissolution rates in the gastrointestinal fluid [50]. The phenylpropanoid derivatives shogaol and shogaol isomer (gingerol-like compounds) were classified as class II (high permeability, low solubility), which is in agreement with the presence of a long saturated carbon chain in their structure that confers a certain degree of hydrophobicity to these compounds.

Conversely, most terpenoids demonstrated different classes depending on the use of Log P or  $P_{app}$  for their classification (see [Table 2](#)). Both diterpenoids and triterpenoids were primarily classified as class II (high permeability, low solubility) or class IV (low permeability, low solubility) when Log P or  $P_{app}$  was utilized, respectively, for the classification. A regulatory classification of any compound must be based on experimental data, but the Log P approach has previously been used for screening purposes [48, 49]. Based on our results, we confirm that important differences may arise when experimental  $P_{app}$  values are used to classify compounds versus Log P approximation. It can be concluded that the  $P_{app}$  value, when available, is a more appropriate alternative to establish BCS classification because this value is derived from data determined in a living cellular model, which provides results with greater biological significance than those obtained from calculations based on physicochemical characteristics.

It must be noted that in this study,  $S_w$  was obtained for the individual compounds. However, the solubilities of the compounds in the complex RE mixture may be affected by the presence of other compounds, and this will exert an undeniable impact on the absorption of the compound. This feature deserves further investigation.

In conclusion, BCS classification of the 24 compounds present in the RE extract was achieved by considering the aforementioned limitations and using experimental  $P_{app}$  rather than Log P when available. This revealed that most of the compounds in RE were classified as classes III and IV. Based on this, RE enriched in diterpenes and triterpenes should also be classified as class III or IV (low permeability), which is in agreement with the low bioavailabilities of rosemary compounds reported in the literature. However, this statement should be interpreted with caution due to the complexity of the extract, and further research may be required before a final classification is given. The results obtained here represent a significant contribution to our knowledge of the oral absorptions and bioavailabilities of rosemary compounds and their biopharmaceutical classifications and will aid in the development of delivery strategies to improve solubility and bioavailability. In addition, as rosemary compounds have demonstrated their influence in microbiota in previous studies [51–53] this point must be also addressed in future studies.

## Conclusions

Rosemary is widely used as a medicinal herb and to season and preserve food, and its bioactive compounds (terpenoids and polyphenols) possess demonstrated potential health benefits related to chronic human diseases. Although most studies have been performed in cell models, recent evidence for such effects is emerging in animal models. However, only a few studies have explored the intestinal absorption of these compounds to determine their permeability and the metabolites responsible for such effects. In this study, we provide data regarding the permeabilities of 24 compounds derived from a rosemary extract in Caco-2 cell monolayers (flavonoids, diterpenes, triterpenes and phenylpropanoids) by comparing the extract in both free and encapsulated form. Flavonoids demonstrated a passive diffusion transport mechanism, with cirsimarin and genkwanin having the highest permeation values. Among the diterpenes, carnosic acid, rosmanol and its isomers episisorosmanol and epirosmanol exhibited the highest permeability values. Triterpenoids exhibited lower permeability values than diterpenes and flavonoids. Most compounds demonstrated poor or negligible permeation when RE was incorporated into phospholipid vesicles. For some of the aforementioned compounds, this study is the first report of their permeability. In this study, we also performed biopharmaceutical classification (BCS) for all the compounds based on their permeability and solubility data for bioequivalence purposes, which may represent a basis for future studies focused on the development of rosemary-based nutraceuticals or drugs. Most of the RE compounds were classified as classes III and IV (low permeability); therefore, RE should also be classified into this category.

## Supporting information

**S1 Fig. BCS classification.** Plots show the BCS classification of all compounds in RE using the 100 mg dose scenario according LogP (A) y  $P_{app}$  (B) values.  
(DOCX)

**S1 Table. BCS classification.**  
(DOCX)

**S2 Table. Chemical family, physicochemical and permeation data and BCS classification.**  
Chemical family, physicochemical and permeation data and BCS classification for all the compounds of RE studied in the absorption assay in the free form and considering 100 mg dose scenario.  
(DOCX)

**S3 Table. TEER values.** Trans-epithelial electrical resistance (TEER) obtained in  $\Omega \cdot \text{cm}^2$  units by using an epithelial voltohmmeter (Millicell-ERS®). Each well (6 wells were used for each condition) was measured three independents times before sample addition (initial value) and at the end of the incubation time (final value).  
(DOCX)

## Acknowledgments

This work was supported by projects AGL2011-29857-C03-02, AGL2011-29857-C03-03, AGL2015-67995-C3-1-R, and AGL2015-67995-C3-2-R, and FPU grant (AP2007-03246) from Spanish Ministry of Science and Innovation; Torres Quevedo grants PTQ-13-06429 and PTQ-14-07243 from the Spanish Ministry of Economy and Competitiveness (MINECO); grant P11-CTS-7625 from Andalusian Regional Government Council of Innovation and Science; PROMETEO/2016/006, ACOMP/2013/093 and ACIF/2013/064 from Generalitat Valenciana; CIBER (CB12/03/30038, Fisiopatología de la Obesidad y la Nutrición, CIBERobn, Instituto de Salud Carlos III). The authors are also thankful to ChemAxon for providing a free academic license of Marvin for structure handling and other toolkits.

## Author Contributions

**Conceptualization:** VM MB EI ASC.

**Formal analysis:** EBC.

**Funding acquisition:** VM ASC DAR MB.

**Investigation:** APS IGA IBL EBC VM DAR ASC.

**Methodology:** EBC APS IBL DAR IGA MB.

**Project administration:** VM MB ASC.

**Resources:** EI VM ASC.

**Supervision:** VM.

**Validation:** DAR EBC MB.

**Visualization:** APS EBC.

**Writing – original draft:** EBC.

**Writing – review & editing:** EBC APS IGA IBL VM DAR MB ASC.

## References

1. Perez-Fons L, Aranda FJ, Guillen J, Villalain J, Micol V. Rosemary (*Rosmarinus officinalis*) diterpenes affect lipid polymorphism and fluidity in phospholipid membranes. *Arch Biochem Biophys.* 2006; 453 (2):224–36. doi: [10.1016/j.abb.2006.07.004](https://doi.org/10.1016/j.abb.2006.07.004) PMID: [16949545](https://pubmed.ncbi.nlm.nih.gov/16949545/)
2. Perez-Fons L, Garzon MT, Micol V. Relationship between the antioxidant capacity and effect of rosemary (*Rosmarinus officinalis* L.) polyphenols on membrane phospholipid order. *J Agric Food Chem.* 2010; 58(1):161–71. doi: [10.1021/jf9026487](https://doi.org/10.1021/jf9026487) PMID: [19924866](https://pubmed.ncbi.nlm.nih.gov/19924866/)
3. Sotelo-Felix JL, Martinez-Fong D, Muriel P, Santillan RL, Castillo D, Yahuaca P. Evaluation of the effectiveness of *Rosmarinus officinalis* (Lamiaceae) in the alleviation of carbon tetrachloride-induced acute hepatotoxicity in the rat. *J Ethnopharmacol.* 2002; 81(2):145–54. PMID: [12065145](https://pubmed.ncbi.nlm.nih.gov/12065145/)
4. Bozin B, Mimica-Dukic N, Samoilik I, Jovin E. Antimicrobial and antioxidant properties of rosemary and sage (*Rosmarinus officinalis* L. and *Salvia officinalis* L., Lamiaceae) essential oils. *J Agric Food Chem.* 2007; 55(19):7879–85. doi: [10.1021/jf0715323](https://doi.org/10.1021/jf0715323) PMID: [17708648](https://pubmed.ncbi.nlm.nih.gov/17708648/)

5. Del Campo J, Amiot MJ, Nguyen-The C. Antimicrobial effect of rosemary extracts. *J Food Prot.* 2000; 63(10):1359–68. PMID: [11041135](#)
6. Altinier G, Sosa S, Aquino RP, Mencherini T, Della Loggia R, Tubaro A. Characterization of topical anti-inflammatory compounds in *Rosmarinus officinalis* L. *J Agric Food Chem.* 2007; 55(5):1718–23. doi: [10.1021/jf062610+](#) PMID: [17288440](#)
7. Tsai TH, Chuang LT, Lien TJ, Liung YR, Chen WY, Tsai PJ. *Rosmarinus officinalis* extract suppresses *Propionibacterium acnes*-induced inflammatory responses. *J Med Food.* 2013; 16(4):324–33. doi: [10.1089/jmf.2012.2577](#) PMID: [23514231](#)
8. Dorrie J, Sapala K, Zunino SJ. Carnosol-induced apoptosis and downregulation of Bcl-2 in B-lineage leukemia cells. *Cancer Lett.* 2001; 170(1):33–9. PMID: [11448532](#)
9. Huang SC, Ho CT, Lin-Shiau SY, Lin JK. Carnosol inhibits the invasion of B16/F10 mouse melanoma cells by suppressing metalloproteinase-9 through down-regulating nuclear factor-kappa B and c-Jun. *Biochem Pharmacol.* 2005; 69(2):221–32. doi: [10.1016/j.bcp.2004.09.019](#) PMID: [15627474](#)
10. Lo AH, Liang YC, Lin-Shiau SY, Ho CT, Lin JK. Carnosol, an antioxidant in rosemary, suppresses inducible nitric oxide synthase through down-regulating nuclear factor-kappaB in mouse macrophages. *Carcinogenesis.* 2002; 23(6):983–91. PMID: [12082020](#)
11. Valdes A, Garcia-Canas V, Simo C, Ibanez C, Micol V, Ferragut JA, et al. Comprehensive foodomics study on the mechanisms operating at various molecular levels in cancer cells in response to individual rosemary polyphenols. *Anal Chem.* 2014; 86(19):9807–15. doi: [10.1021/ac502401j](#) PMID: [25188358](#)
12. Valdes A, Garcia-Canas V, Rocamora-Reverte L, Gomez-Martinez A, Ferragut JA, Cifuentes A. Effect of rosemary polyphenols on human colon cancer cells: transcriptomic profiling and functional enrichment analysis. *Genes & nutrition.* 2013; 8(1):43–60.
13. Borrás-Linares I, Pérez-Sánchez A, Lozano-Sánchez J, Barrajón-Catalán E, Arraez-Roman D, Cifuentes A, et al. A bioguided identification of the active compounds that contribute to the antiproliferative/cytotoxic effects of rosemary extract on colon cancer cells. *Food Chem Toxicol.* 2015; 80:215–22. doi: [10.1016/j.fct.2015.03.013](#) PMID: [25801906](#)
14. Bakirel T, Bakirel U, Keles OU, Ulgen SG, Yardibi H. In vivo assessment of antidiabetic and antioxidant activities of rosemary (*Rosmarinus officinalis*) in alloxan-diabetic rabbits. *J Ethnopharmacol.* 2008; 116(1):64–73. doi: [10.1016/j.jep.2007.10.039](#) PMID: [18063331](#)
15. Romo Vaquero M, Garcia Villalba R, Larrosa M, Yanez-Gascon MJ, Fromentin E, Flanagan J, et al. Bioavailability of the major bioactive diterpenoids in a rosemary extract: metabolic profile in the intestine, liver, plasma, and brain of Zucker rats. *Molecular nutrition & food research.* 2013; 57(10):1834–46.
16. Doolaege EH, Raes K, De Vos F, Verhe R, De Smet S. Absorption, distribution and elimination of carnosic acid, a natural antioxidant from *Rosmarinus officinalis*, in rats. *Plant Foods Hum Nutr.* 2011; 66(2):196–202. doi: [10.1007/s11130-011-0233-5](#) PMID: [21751091](#)
17. Arranz E, Mes J, Wicheris HJ, Jaime L, Mendiola JA, Reglero G, et al. Anti-inflammatory activity of the basolateral fraction of Caco-2 cells exposed to a rosemary supercritical extract. *Journal of Functional Foods.* 2015; 13:384–90.
18. Cristina SR, Marín FR, Susana S, García-Risco MR, Javier S, Guillermo R. Testing and enhancing the in vitro bioaccessibility and bioavailability of *Rosmarinus officinalis* extracts with a high level of antioxidant abietanes. *Journal of Agricultural and Food Chemistry.* 2010; 58(2):1144–52. doi: [10.1021/jf902087q](#) PMID: [20038145](#)
19. Sharma A SU. Liposomes in drug delivery: progress and limitations. *Int J Pharm.* 1997; 154(2):123–40.
20. Lian T, Ho RJ. Trends and developments in liposome drug delivery systems. *J Pharm Sci.* 2001; 90(6):667–80. PMID: [11357170](#)
21. Barrajón-Catalán E, Menéndez-Gutiérrez MP, Falco A, Carrato A, Saceda M, Micol V. Selective death of human breast cancer cells by lytic immunoliposomes: Correlation with their HER2 expression level. *Cancer Lett.* 2010; 290(2):192–203. doi: [10.1016/j.canlet.2009.09.010](#) PMID: [19896266](#)
22. Catania A, Barrajón-Catalán E, Nicolosi S, Cicirata F, Micol V. Immunoliposome encapsulation increases cytotoxic activity and selectivity of curcumin and resveratrol against HER2 overexpressing human breast cancer cells. *Breast Cancer Res Treat.* 2013; 141:55–65. doi: [10.1007/s10549-013-2667-y](#) PMID: [23959397](#)
23. Caturla N, Vera-Samper E, Villalain J, Mateo CR, Micol V. The relationship between the antioxidant and the antibacterial properties of galloylated catechins and the structure of phospholipid model membranes. *Free Radic Biol Med.* 2003; 34(6):648–62. PMID: [12633742](#)
24. Alves DS, Perez-Fons L, Estepa A, Micol V. Membrane-related effects underlying the biological activity of the anthraquinones emodin and barbaloin. *Biochem Pharmacol.* 2004; 68(3):549–61. doi: [10.1016/j.bcp.2004.04.012](#) PMID: [15242821](#)

25. Funes L, Laporta O, Cerdán-Calero M, Micol V. Effects of verbascoside, a phenylpropanoid glycoside from lemon verbena, on phospholipid model membranes. *Chem Phys Lipids*. 2010; 163(2):190–9. doi: [10.1016/j.chemphyslip.2009.11.004](https://doi.org/10.1016/j.chemphyslip.2009.11.004) PMID: [19925782](#)
26. van Breemen RB, Li Y. Caco-2 cell permeability assays to measure drug absorption. *Expert Opin Drug Metab Toxicol*. 2005; 1(2):175–85. doi: [10.1517/17425255.1.2.175](https://doi.org/10.1517/17425255.1.2.175) PMID: [16922635](#)
27. Herrero M, Plaza M, Clí Fuente A, Ibáñez E. Green processes for the extraction of bioactives from Rosemary: Chemical and functional characterization via ultra-performance liquid chromatography-tandem mass spectrometry and in-vitro assays. *J Chromatogr A*. 2010; 1217(16):2512–20. doi: [10.1016/j.jchroma.2009.11.032](https://doi.org/10.1016/j.jchroma.2009.11.032) PMID: [19945706](#)
28. Artursson P, Karlsson J. Correlation between oral drug absorption in humans and apparent drug permeability coefficients in human intestinal epithelial (Caco-2) cells. *Biochem Biophys Res Commun*. 1991; 175(3):880–5. PMID: [1673839](#)
29. Artursson P, Palm K, Luthman K. Caco-2 monolayers in experimental and theoretical predictions of drug transport. *Adv Drug Deliv Rev*. 2001; 46(1–3):27–43. PMID: [11259831](#)
30. Artursson P. Epithelial transport of drugs in cell culture. I: A model for studying the passive diffusion of drugs over intestinal absorptive (Caco-2) cells. *J Pharm Sci*. 1990; 79(6):476–82. PMID: [1975619](#)
31. Lin H, Gebhardt M, Bian S, Kwon KA, Shim CK, Chung SJ, et al. Enhancing effect of surfactants on fexofenadine-HCl transport across the human nasal epithelial cell monolayer. *Int J Pharm*. 2007; 330(1–2):23–31. doi: [10.1016/j.ijpharm.2006.08.043](https://doi.org/10.1016/j.ijpharm.2006.08.043) PMID: [16997520](#)
32. Mukkavilli R, Gundala SR, Yang C, Donthamsetty S, Cantuaria G, Jadhav GR, et al. Modulation of cytochrome P450 metabolism and transport across intestinal epithelial barrier by ginger biophenolics. *PLoS ONE*. 2014; 9(9):e108386. doi: [10.1371/journal.pone.0108386](https://doi.org/10.1371/journal.pone.0108386) PMID: [25251219](#)
33. Falé PL, Ascensão L, Serralheiro MLM. Effect of luteolin and apigenin on rosmarinic acid bioavailability in Caco-2 cell monolayers. *Food and Function*. 2013; 4(3):426–31. doi: [10.1039/c2fo30318c](https://doi.org/10.1039/c2fo30318c) PMID: [23223784](#)
34. Teng Z, Yuan C, Zhang F, Huan M, Cao W, Li K, et al. Intestinal absorption and first-pass metabolism of polyphenol compounds in rat and their transport dynamics in caco-2 cells. *PLoS ONE*. 2012; 7(1).
35. D'Antuono I, Garbett A, Linsalata V, Minervini F, Cardinale A. Polyphenols from artichoke heads (*Cynara cardunculus* (L.) subsp. *scolymus* Hayek): In vitro bio-accessibility, intestinal uptake and bioavailability. *Food and Function*. 2015; 6(4):1268–77. doi: [10.1039/c5fo00137d](https://doi.org/10.1039/c5fo00137d) PMID: [25758164](#)
36. Tian XJ, Yang XW, Yang X, Wang K. Studies of intestinal permeability of 36 flavonoids using Caco-2 cell monolayer model. *Int J Pharm*. 2009; 367(1–2):58–64. doi: [10.1016/j.ijpharm.2008.09.023](https://doi.org/10.1016/j.ijpharm.2008.09.023) PMID: [18848870](#)
37. Yang Y, Bai L, Li X, Xiong J, Xu P, Guo C, et al. Transport of active flavonoids, based on cytotoxicity and lipophilicity: An evaluation using the blood-brain barrier cell and Caco-2 cell models. *Toxicology in Vitro*. 2014; 28(3):388–96. doi: [10.1016/j.tiv.2013.12.002](https://doi.org/10.1016/j.tiv.2013.12.002) PMID: [24362044](#)
38. Serra H, Mendes T, Bronze MR, Simplicio AL. Prediction of intestinal absorption and metabolism of pharmacologically active flavones and flavanones. *Bioorg Med Chem*. 2008; 16(7):4009–18. doi: [10.1016/j.bmc.2008.01.028](https://doi.org/10.1016/j.bmc.2008.01.028) PMID: [18249545](#)
39. Wang Y, Wu Q, Yang XW, Yang X, Wang K. The membrane transport of flavonoids from *Crossostephium chinense* across the Caco-2 monolayer. *Biopharm Drug Dispos*. 2011; 32(1):16–24. doi: [10.1002/bdd.735](https://doi.org/10.1002/bdd.735) PMID: [21162116](#)
40. Falé PL, Ascensão L, Serralheiro ML. Effect of luteolin and apigenin on rosmarinic acid bioavailability in Caco-2 cell monolayers. *Food Funct*. 2013; 4(3):426–31. doi: [10.1039/c2fo30318c](https://doi.org/10.1039/c2fo30318c) PMID: [23223784](#)
41. Qiang Z, Ye Z, Hauck C, Murphy PA, McCoy JA, Widrlechner MP, et al. Permeability of rosmarinic acid in *Prunella vulgaris* and ursolic acid in *Salvia officinalis* extracts across Caco-2 cell monolayers. *J Ethnopharmacol*. 2011; 137(3):1107–12. doi: [10.1016/j.jep.2011.07.037](https://doi.org/10.1016/j.jep.2011.07.037) PMID: [21798330](#)
42. Seiquer I, Rueda A, Ollalla M, Cabrera-Vique C. Assessing the bioavailability of polyphenols and antioxidant properties of extra virgin argan oil by simulated digestion and Caco-2 cell assays. Comparative study with extra virgin olive oil. *Food Chemistry*. 2015; 188:496–503. doi: [10.1016/j.foodchem.2015.05.006](https://doi.org/10.1016/j.foodchem.2015.05.006) PMID: [26041223](#)
43. Tarko T, Duda-Chodak A, Zajac N. Digestion and absorption of phenolic compounds assessed by in vitro simulation methods. A review. *Roczniki Państwowego Zakładu Higieny*. 2013; 64(2):79–84. PMID: [23987074](#)
44. Borrás-Linares I, Herranz-López M, Barrajón-Catalán E, Arráez-Román D, González-Álvarez I, Bermejo M, et al. Permeability study of polyphenols derived from a phenoic-enriched hibiscus sabdariffa extract by UHPLC-ESI-UHR-Qq-TOF-MS. *International journal of molecular sciences*. 2015; 16(8):18396–411. doi: [10.3390/ijms160818396](https://doi.org/10.3390/ijms160818396) PMID: [26262611](#)

45. Barrajón-Catalán E, Funes L, Herranz-López M, González-Álvarez I, Bermejo M, V. M. Differential absorption of curcuminoids between free and liposomal curcumin formulations. In: Curcumin: clinical uses, health effects and potential complications: Nova Publishers; 2016. p. 99–110.
46. Amidon GL, Lennernas H, Shah VP, Crison JR. A theoretical basis for a biopharmaceutic drug classification: the correlation of in vitro drug product dissolution and in vivo bioavailability. *Pharm Res*. 1995; 12(3):413–20. PMID: [7617530](#)
47. Benet LZ. The Role of BCS (Biopharmaceutics Classification System) and BDDCS (Biopharmaceutics Drug Disposition Classification System) in Drug Development. *J Pharm Sci*. 2013; 102(1):34–42. doi: [10.1002/jps.23359](#) PMID: [23147500](#)
48. Kasim NA, Whitehouse M, Ramachandran C, Bermejo M, Lennernas H, Hussain AS, et al. Molecular properties of WHO essential drugs and provisional biopharmaceutical classification. *Mol Pharm*. 2004; 1(1):85–96. PMID: [15832504](#)
49. Takagi T, Ramachandran C, Bermejo M, Yamashita S, Yu LX, Amidon GL. A provisional biopharmaceutical classification of the top 200 oral drug products in the United States, Great Britain, Spain, and Japan. *Molecular Pharmaceutics*. 2006; 3(6):631–43. doi: [10.1021/mp0600182](#) PMID: [17140251](#)
50. Kaur H, Kaur G. A Critical Appraisal of Solubility Enhancement Techniques of Polyphenols. *Journal of pharmaceutics*. 2014; 2014:180845. doi: [10.1155/2014/180845](#) PMID: [26556188](#)
51. Anabousi S, Bakowsky U, Schneider M, Huwer H, Lehr CM, Ehrhardt C. In vitro assessment of transferrin-conjugated liposomes as drug delivery systems for inhalation therapy of lung cancer. *Eur J Pharm Sci*. 2006; 29(5):367–74. doi: [10.1016/j.ejps.2006.07.004](#) PMID: [16952451](#)
52. Ambrosini MV, Bruschelli G, Mariucci G, Mandile P, Giuditta A. Post-trial sleep in old rats trained for two-way active avoidance task. *Physiol Behav*. 1997; 62(4):773–8. PMID: [9284496](#)
53. Anilkumar AP, Kumari V, Mehrotra R, Aasen I, Mitterschiffthaler MT, Sharma T. An fMRI study of face encoding and recognition in first-episode schizophrenia. *Acta neuropsychiatrica*. 2008; 20(3):129–38. doi: [10.1111/j.1601-5215.2008.00280.x](#) PMID: [25385522](#)

**ANEXO II: Otros artículos científicos relacionados con la temática  
de la Tesis Doctoral**





ELSEVIER

Contents lists available at SciVerse ScienceDirect

Phytomedicine

journal homepage: [www.elsevier.de/phymed](http://www.elsevier.de/phymed)



## Synergism of plant-derived polyphenols in adipogenesis: Perspectives and implications

María Herranz-López<sup>a,1</sup>, Salvador Fernández-Arroyo<sup>b,1</sup>, Almudena Pérez-Sánchez<sup>a</sup>, Enrique Barrajón-Catalán<sup>a</sup>, Raúl Beltrán-Debón<sup>c</sup>, Javier Abel Menéndez<sup>d</sup>, Carlos Alonso-Villaverde<sup>e</sup>, Antonio Segura-Carretero<sup>b</sup>, Jorge Joven<sup>c</sup>, Vicente Micol<sup>a,\*</sup>

<sup>a</sup> Instituto de Biología Molecular y Celular (IBMC), Universidad Miguel Hernández, Elche, Alicante, Spain

<sup>b</sup> Department of Analytical Chemistry, Faculty of Sciences, University of Granada, Av/Fuentenueva, 18071 Granada, Spain

<sup>c</sup> Centre de Recerca Biomèdica, Hospital Universitari de Sant Joan, IISPV, Universitat Rovira i Virgili, C/Sant Joan s/n, 43201 Reus, Spain

<sup>d</sup> Catalan Institute of Oncology (ICO), Girona, Catalonia, Spain

<sup>e</sup> Servei de Medicina Interna, Hospital Son Llàtzer, Palma, Illes Balears, Spain

### ARTICLE INFO

#### Keywords:

Adipogenesis

*Hibiscus sabdariffa*

Leptin

MCP-1

Polyphenols

Synergism

### ABSTRACT

Dietary polyphenols may exert their pharmacological effect via synergistic interactions with multiple targets. Putative effects of polyphenols in the management of obesity should be primarily evaluated in adipose tissue and consequently in well-documented cell model. We used *Hibiscus sabdariffa* (HS), a widely recognised medicinal plant, as a source of polyphenols with a number of salutary effects previously reported. We present here the full characterisation of bioactive components of HS aqueous extracts and document their effects in a model of adipogenesis from 3T3-L1 cells and in hypertrophic and insulin-resistant adipocytes. Aqueous extracts were up to 100 times more efficient in inhibiting triglyceride accumulation when devoid of fibre and polysaccharides. Significant differences were also observed in reactive oxygen species generation and adipokine secretion. We also found that, when polyphenols were fractionated and isolated, the benefits of the whole extract were greater than the sum of its parts, which indicated a previously unnoticed synergism. In conclusion, polyphenols have interactive and complementary effects, which suggest a possible application in the management of complex diseases and efforts to isolate individual components might be irrelevant for clinical medicine and/or human nutrition.

© 2012 Elsevier GmbH. All rights reserved.

### Introduction

Obesity-associated metabolic, oxidative and inflammatory disturbances are a growing epidemic and are associated with at least six of the top ten causes of death (McGeer and McGeer 2004). Adipocytes store excess energy, but when overloaded they become resistant to insulin, which compromises their ability to accumulate

lipids and facilitates alterations in structure and metabolism in remote tissues, such as the pancreas, liver and muscle (Yu and Zhu 2004; Jernas et al. 2006; Rull et al. 2010). Excessive oxidation in adipose cells is common and triggers cellular stress (Furukawa et al. 2004; Yeop Han et al. 2010). The resulting sequence of events remains poorly understood in humans but tends to self-perpetuate if untreated. Initially, there is a complex process of cellular adaptation, monitored by tissue-resident macrophages. When failure and malfunction become extreme, a chronic inflammatory response is unleashed (Rull et al. 2010).

If assumptions are accurate, it is conceivable that antioxidant and/or anti-inflammatory therapies that act on adipose tissue may have potential benefits in the amelioration of obesity-related diseases. However, current available drugs have not been assayed yet. The only validated therapeutic measure consists of preventing hypertrophy in adipocytes via caloric restriction or increased caloric expenditure, but changes in lifestyle are difficult to achieve. Plant-derived polyphenols may provide a similar effect without restricting caloric intake (Lamming et al. 2004; Howitz and Sinclair 2008). Polyphenols are antioxidant and anti-inflammatory

**Abbreviations:** HS, *Hibiscus sabdariffa*; AHS, aqueous extract of *H. sabdariffa*; PEHS, phenolic extract of *H. sabdariffa*; FBS, foetal bovine serum; TNF- $\alpha$ , tumour necrosis factor-alpha; IGF1, insulin-like growth factor-1; IL-6, interleukin-6; VEGF, vascular endothelial growth factor; IL-1 $\alpha$ , interleukin-1 alpha; IL-1 $\beta$ , interleukin-1 beta; MCP-1, monocyte chemoattractant protein-1; IBMX, 3-isobutyl-1-methylxanthine.

\* Corresponding author at: Instituto de Biología Molecular y Celular, Universidad Miguel Hernández, Avda. de la Universidad S/N., 03202 Elche, Alicante, Spain.  
Tel.: +34 96 6658430; fax: +34 96 6658758.

E-mail address: [vmicol@umh.es](mailto:vmicol@umh.es) (V. Micol).

<sup>1</sup> These authors have equally contributed to this research and are listed in random order.

molecules that interact in humans with molecular targets involved in stress response pathways, and increased ingestion of dietary polyphenols could be helpful. However, plant-derived polyphenols are secondary metabolites that are synthesised in response to a major stress event; consequently, the expected amount of polyphenols in our commonly consumed food is very low. We reasoned that tropical plant-derived products could be a potential source of polyphenol concentrate and could be used to design dietary supplements. Recent data indicate that aqueous extracts of *Hibiscus sabdariffa* (HS) might ameliorate metabolic disturbances (Carvajal-Zarrabal et al. 2005; Alarcon-Aguilar et al. 2007; Kim et al. 2007), but human trials have been generally unsatisfactory, due to an incomplete characterisation of the essential bioactive components (Beltrán-Debón et al. 2009; Mozaffari-Khosravi et al. 2009; Kuriyan et al. 2010). In this study, we address this issue, document the effects of polyphenols on mouse adipocytes and provide data that support multi-target action in the same signalling cascades or response networks.

## Materials and methods

### Materials

3T3-L1 cells were purchased from the American Type Culture Collection (Manassas, VA, USA). Dexamethasone, 3-isobutyl-1-methylxanthine, insulin, crystal violet, Ascentis C18 preparative reverse phase column, formic acid, acetonitrile and ethanol were obtained from Sigma-Aldrich (Madrid, Spain). Dulbecco's modified Eagle's medium, calf serum, foetal bovine serum, and an antibiotic mixture (penicillin-streptomycin) were purchased from PAA Laboratories (Linz, Austria). Sodium pyruvate and trypsin-EDTA were obtained from Invitrogen (Carlsbad, CA). Polyvinylidifluoride (PVDF) filters, 0.22 µm, were obtained from Millipore (Bedford, MA). AdipoRed™ Assay Reagent was obtained from Lonza (Walkersville, MD USA). The resin used for the preparative chromatography was Amberlite™ FPX66 (Rohm and Haas, Philadelphia, USA). The standards for the calibration curves, chlorogenic acid, quercetin-3-rutinoside, quercetin-3-glucoside, kaempferol-3-O-rutinoside, kaempferol 3-(*p*-coumaroylglucoside), quercetin, 4-hydroxycoumarin and delphinidin-3-sambubioside were purchased either from Fluka, Extrasynthese (Genay, France) or Polyphenols Laboratories (Hanaveien, Norway).

### Methods of extraction and fractionation of polyphenols

Primary aqueous extract (AHS) was obtained from sun-dried calyces from plants harvested by investigators in Senegal with an approximate plant-to-extract ratio of 5:1 as previously described (Beltrán-Debón et al. 2009). The purified extract (PEHS) was prepared by removing fibre and polysaccharides by precipitation in 85% ethanol (v/v). Extracts were reconstituted in water at 170 mg/ml and loaded onto a 1.5 cm × 25 cm chromatographic column containing Amberlite™ FPX66. The retained phenolic fraction was finally eluted with 95% ethanol and 0.01% trifluoroacetic acid, rotary evaporated and freeze-dried. Total phenolic content in AHS and PEHS was measured with the Folin-Ciocalteu method (Huang et al. 2005). To further characterise the bioactive components, PEHS was dissolved in distilled water to a concentration of 230 mg/ml, filtered through a 0.45 µm PVDF filter and fractionated using a WellChrom preparative HPLC system (Merck-Knauer, Berlin, Germany). We used an Ascentis C18 preparative reverse phase column (10 µm, 25 cm × 21.2 mm), and elution was performed using acetonitrile as a mobile phase in a multistep linear gradient at room temperature with a flow rate of 19 ml/min. The preparative version of EuroChrom® software, version 3.01, was

used for data acquisition and analysis. We obtained 35 fractions representing distinct combinations of components, which were identified and quantified. We then lyophilised the resulting fractions for assays described below.

### Characterisation and quantification of polyphenols

Analysis was performed in a Rapid Resolution Liquid Chromatography 1200 (Agilent Technologies, Palo Alto, CA) using a Zorbax Eclipse Plus C<sub>18</sub>, 4.6 mm × 150 mm, 1.8 µm column at room temperature with a flow rate of 0.5 ml/min and an injection volume of 10 µl (Rodríguez-Medina et al. 2009). The chromatographic system was coupled to a time-of-flight (TOF) mass spectrometer (MS) (Bruker Daltonic Bremen, Germany) that was equipped with an orthogonal electrospray interface (ESI; model G1607A from Agilent Technologies, Palo Alto, CA, USA) that operated in negative and positive modes of ionisation. Compound identification was made by comparing the retention times and mass spectra obtained by TOF-MS with those of authentic standards or interpreted according to previously obtained mass spectra. Quantification of the major compounds in AHS, PEHS and the isolated fractions was carried out using commercially available standards when available or previously reported structurally similar compounds (Fernandez-Arroyo et al., 2011).

### In vitro experimental models

The 3T3-L1 preadipocytes were propagated and differentiated according to described procedures (Green and Kehinde 1975) (see also supporting information). Differential effects on adipogenesis were assayed by adding extracts and fractions in pre-designed concentrations to the media at the beginning of the induction period; these conditions were maintained until cells were harvested. The absence of cytotoxicity was ascertained by the crystal violet method. In all experiments, more than 90% of the cells were mature adipocytes after 8–10 days of incubation. For other experiments, we used hypertrophied, insulin-resistant adipocytes obtained by increasing the time of incubation (22 days) in 25 mM glucose (Yeop Han et al. 2010). In these cases, extracts and fractions were added at day 18 and allowed to incubate for 4 days before harvesting. We assessed triglyceride accumulation with AdipoRed™; extracts and fractions were added either at day 8 (mature adipocytes) or at day 18 (hypertrophied adipocytes) after induction and were incubated for 2 or 4 additional days, respectively. Fat droplets were analysed with a Nikon Eclipse TE 2000U fluorescence microscope controlled by NIS-Elements software.

### Measurement of intracellular reactive oxygen species (ROS) and secreted adipokines

Measurements were performed on hypertrophied adipocytes in 25 mM glucose to assess the effect of proposed extracts. These extracts were added to adipocytes at day 18 after inducing differentiation, and incubation proceeded for four additional days under the same conditions. ROS generation was assessed with 2',7'-dichlorodihydrofluorescein diacetate as described (Yeop Han et al. 2010), and fluorescence was measured in a multiwell plate reader (POLARstar Omega microplate) with excitation at 485 nm and emission at 520 nm. In separate experiments, several cytokines (leptin, tumour necrosis factor-alpha (TNF-α), insulin-like growth factor-1 (IGF-1), interleukin-6 (IL-6), vascular endothelial growth factor (VEGF), interleukin-1 alpha (IL-1α), interleukin-1 beta (IL-1β) and monocyte chemoattractant protein-1 (MCP-1)) were measured by ELISA (Signosis, Inc., Sunnyvale, CA, USA) in resulting supernatants following the manufacturer's instructions.

### Statistical analyses

Values were represented as means  $\pm$  standard deviation. Differences between two or more groups were compared using non-parametric tests and were considered statistically significant when  $p < 0.05$ . The means of quantitative variables were analysed using one-way ANOVA, the Student *t*-test for unpaired samples and Tukey test for multiple comparisons. All statistical analyses were performed with the Statistical Package for Social Science version 17.0 (SPSS, Chicago, IL, USA).

### Results

#### Relative composition of candidate bioactive components

There were no major qualitative differences in polyphenol content between AHS and PEHS; therefore, the precipitation procedures used to remove other soluble material did not result in selective losses in benefit (Fig. 1A and B and Table 1). However, such manipulations resulted in immediately apparent quantitative differences and subsequent changes in relative contribution (Table 2). The phenolic content of AHS, as expressed in gallic acid equivalents, was significantly ( $p < 0.001$ ) lower ( $2.26 \pm 0.11$  g/100 g) than that of PEHS ( $28.42 \pm 0.33$  g/100 g). Relative differences were observed in organic acids and all families of phenolic compounds: organic acid derivatives (hydroxycitric and hibiscus acids), anthocyanins (delphinidin-3-sambubioside and cyanidin-3-sambubioside), phenolic acid derivatives (chlorogenic acid and 5-O-caffeoyleshikimic acid), and several flavonol derivatives (quercetin, myricetin and kaempferol glycosides) (Table 2). PEHS was fractionated into 35 different fractions, and only fractions 6, 9 and 14 (Fig. 1C–E

and Table 2) significantly inhibited adipogenesis at concentrations ranging from 10 to 40  $\mu$ g/ml. For clarity, negative results for the remaining fractions are not shown. During the fractionation procedure and the subsequent concentration, significant peaks were additionally detected and identified in PEHS (hibiscus acid dimethyl ester, coumaroylquinic acid, leucoside (kaempferol-3-O-sambubioside)) and several unidentified compounds. At least six new identified peaks (numbers 32–37) appeared only in isolated fractions. The composition of these fractions differed notably. The major component of fraction 6 was delphinidin-3-sambubioside, fraction 9 contained cyanidin-3-sambubioside, chlorogenic acid and tetra-O-methylleiediflavanone as major components, and fraction 14 was especially rich in glycosylated flavonols, such as quercetin-3-sambubioside and myricetin-3-glucoside (Table 2).

#### Phenolic compounds inhibited adipogenic differentiation of 3T3-L1 cells: fibre and/or polysaccharides were either inactive or interfered in the model

We found that AHS significantly inhibited lipid accumulation and adipogenic differentiation of pre-adipocytes but only at concentrations  $\geq 500$   $\mu$ g/ml, which are not likely to be achieved *in vivo*. However, the relative activity of PEHS was much higher and evident even at concentrations  $< 10$   $\mu$ g/ml. Both extracts showed a significant reduction in the number of differentiated cells when compared with the control, as well as a dose-dependent response in the reduction in the accumulation of triglycerides (Fig. 2A–E). Cells differentiated in the presence of adipogenic agents plus 1000  $\mu$ g/ml AHS or 40  $\mu$ g/ml PEHS extracts accumulated 44.4% and 19.3% of triglyceride, respectively, as compared to levels normally observed

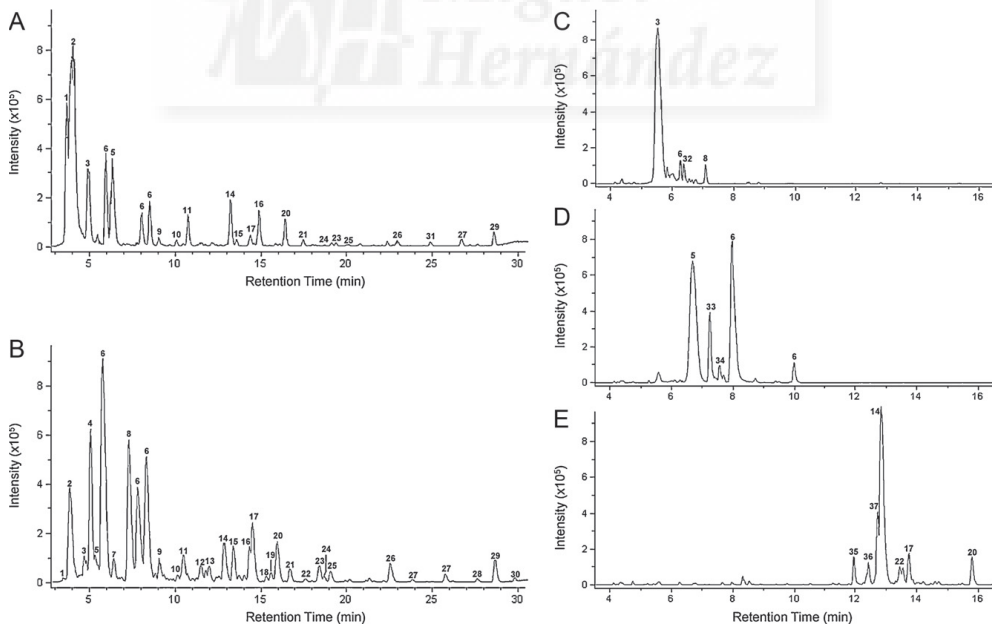


**Fig. 1.** Representative base peak chromatograms obtained by HPLC-ESI-TOF-MS of *Hibiscus sabdariffa* AHS (A) and PEHS (B) extracts at 50 mg/ml and 5 mg/ml, respectively. Qualitative differences between AHS and PEHS were deemed negligible, but quantitative differences were evident, especially with respect to the content of phenolic acids, anthocyanins and flavonols. Fractionation of PEHS, obtained through semipreparative liquid chromatography, showed that only a few fractions (C–E) were active in adipocytes.

**Table 1**

Relevant analytical data for components isolated in AHS and PEHS (see also Fig. 1). Note that peaks 31–37 were only identified after a further process of purification.

Peak number	Compound	Retention time (min)	Molecular formula	[M-H] <sup>-</sup>	UV-Vis (nm)
1	Hydroxycitric acid	4.35	C <sub>6</sub> H <sub>8</sub> O <sub>8</sub>	207.0140	—
2	Hibiscus acid	4.72	C <sub>6</sub> H <sub>6</sub> O <sub>7</sub>	189.0035	—
3	Delphinidin-3-sambubioside	5.50	C <sub>26</sub> H <sub>30</sub> O <sub>16</sub>	595.1446	280, 520
4	Unknown	5.86	C <sub>8</sub> H <sub>12</sub> O <sub>8</sub>	235.0461	278, 334
5	Cyanidin-3-sambubioside	6.11	C <sub>26</sub> H <sub>30</sub> O <sub>15</sub>	579.1493	280, 520
6	Chlorogenic acid	6.52/8.41/8.92	C <sub>16</sub> H <sub>18</sub> O <sub>9</sub>	353.0891	297, 324
7	Unknown	7.13	—	230.0127	272, 298
8	Hibiscus acid dimethyl ester	7.91	C <sub>8</sub> H <sub>10</sub> O <sub>7</sub>	217.0354	292
9	Methyl digallate	9.62	C <sub>15</sub> H <sub>12</sub> O <sub>9</sub>	335.0409	278
10	2-O-Trans-caffeooyl-hydroxicitic acid	10.60	C <sub>15</sub> H <sub>14</sub> O <sub>11</sub>	369.0463	285, 330
11	Myricetin-3-arabinogalactoside	10.91	C <sub>26</sub> H <sub>28</sub> O <sub>17</sub>	611.1254	260, 354
12	Coumaroylquinic acid	11.86	C <sub>16</sub> H <sub>18</sub> O <sub>8</sub>	337.0929	310
13	Unknown	12.34	C <sub>11</sub> H <sub>11</sub> NO <sub>5</sub>	236.0564	272
14	Quercetin-3-sambubioside	13.11	C <sub>26</sub> H <sub>28</sub> O <sub>16</sub>	595.1309	345
15	Unknown	13.63	C <sub>16</sub> H <sub>20</sub> O <sub>10</sub>	371.0984	278
16	Quercetin-3-rutinoside	14.50	C <sub>27</sub> H <sub>30</sub> O <sub>16</sub>	609.1462	255, 353
17	5-O-Caffeoylshikimic acid	14.69	C <sub>16</sub> H <sub>16</sub> O <sub>8</sub>	335.0768	296, 326
18	Leucoside (kaempferol-3-O-sambubioside)	15.44	C <sub>26</sub> H <sub>28</sub> O <sub>15</sub>	579.1355	278, 505
19	Unknown	15.69	C <sub>17</sub> H <sub>22</sub> O <sub>10</sub>	385.1140	270
20	Quercetin-3-glucoside	16.04	C <sub>21</sub> H <sub>20</sub> O <sub>12</sub>	463.0873	253, 356
21	Kaempferol-3-O-rutinoside	16.71	C <sub>27</sub> H <sub>30</sub> O <sub>15</sub>	593.1512	265, 350
22	Unknown	17.58	C <sub>18</sub> H <sub>22</sub> O <sub>9</sub>	381.1191	278
23	Unknown	18.33	C <sub>21</sub> H <sub>30</sub> O <sub>11</sub>	457.1715	—
24	Methyl-epigallocatechin	18.60	C <sub>16</sub> H <sub>16</sub> O <sub>7</sub>	319.0823	268, 336
25	Unknown	18.93	—	503.1759	278
26	Myricetin	22.19	C <sub>15</sub> H <sub>10</sub> O <sub>8</sub>	317.0298	372
27	N-Feruloyltyramine	23.40/25.19	C <sub>18</sub> H <sub>20</sub> NO <sub>4</sub>	312.1234	286, 316
28	Unknown	26.94	—	307.0726	288, 353, 414
29	Quercetin	28.67	C <sub>15</sub> H <sub>10</sub> O <sub>7</sub>	301.0339	253, 372
30	Unknown	29.89	C <sub>18</sub> H <sub>34</sub> O <sub>5</sub>	329.2333	—
31	Prodelphinidin B3	24.82	C <sub>30</sub> H <sub>26</sub> O <sub>14</sub>	609.1250	312
32	Tetra-O-methyljdeediflavanone	4.30	C <sub>34</sub> H <sub>30</sub> O <sub>11</sub>	613.1715	341
33	Unknown	6.11	C <sub>26</sub> H <sub>30</sub> O <sub>16</sub>	597.1461	338
34	Caffeoylglucose	6.46	C <sub>15</sub> H <sub>18</sub> O <sub>9</sub>	341.0878	314
35	Unknown	11.37	C <sub>26</sub> H <sub>44</sub> O <sub>16</sub>	611.2557	277
36	Unknown	11.93	C <sub>27</sub> H <sub>32</sub> O <sub>17</sub>	627.1567	278
37	Myricetin-3-glucoside	12.25	C <sub>21</sub> H <sub>20</sub> O <sub>13</sub>	479.0831	355

in control cells. The extract concentration that led to 50% of inhibition of triglyceride accumulation ( $IC_{50}$ ) was  $799 \pm 225 \mu\text{g/ml}$  for AHS and  $9.1 \pm 2.8 \mu\text{g/ml}$  for PEHS, respectively. This result revealed that PEHS was approximately 90–100 times more effective in reducing triglyceride accumulation. This difference was around 10 times higher than that expected for actual polyphenol concentrations, which indicated that the absence of polysaccharides and other soluble material improved the inhibition of triglyceride cellular uptake in this model.

#### Anti-adipogenic activity of polyphenols was no longer conserved in most isolated fractions

Only 3 of 35 polyphenolic fractions (numbers 6, 9 and 14; Fig. 1C–E) significantly inhibited adipogenesis. The efficacy of these fractions was dose-dependent; fraction 14 was the most active throughout the dosing range (Fig. 2F). None of these fractions at  $40 \mu\text{g/ml}$  achieved the effectiveness that was obtained with the total mixture of polyphenols (PEHS). Changes in activity with combinations of these fractions at different concentrations were negligible. None of the binary combinations (20 or  $30 \mu\text{g/ml}$  of each fraction) achieved higher activities than the individual fractions. Moreover, the strong inhibitory action of fraction 14 was maintained when using pairs 6/14 and 9/14. Finally, the combination of three of the fractions (20  $\mu\text{g/ml}$  of each) also failed to improve the anti-adipogenic activity, as compared with both isolated fractions and combinations. Taking all results into account, the presence of all polyphenols was necessary in order to achieve maximum efficacy, and the relative proportion was potentially a relevant factor.

#### Phenolic compounds were active in mature as well as hypertrophied and insulin-resistant adipocytes

When extracts were assayed in mature adipocytes, the addition of AHS did not significantly affect triglyceride content, even at  $1000 \mu\text{g/ml}$ , but  $40 \mu\text{g/ml}$  of PEHS decreased triglyceride content by 20–30% when assayed at  $40 \mu\text{g/ml}$  (Supporting Information; Fig. 2). These novel findings prompted the exploration of the effects of PEHS in a cell model of adipocyte hypertrophy in the context of insulin resistance, similar to that observed in the adipose tissue of obese patients (Yu and Zhu 2004; Jernas et al. 2006; Takahashi et al. 2008; Yeop Han et al. 2010). Surprisingly, we found significant effects with AHS and that both AHS and PEHS were more efficient at reducing triglyceride accumulation in insulin-resistant adipocytes than in mature adipocytes ( $1000 \mu\text{g/ml}$  AHS: 19% mean values reduction;  $40 \mu\text{g/ml}$  PEHS: 38% mean values reduction) (Fig. 3). It appeared that the PEHS-mediated reduction in triglyceride accumulation was significantly higher during the adipogenesis process than in mature or hypertrophic adipocytes but we found a differential response with both extracts. The generation of endogenous ROS was not affected by AHS (Fig. 4A and B), but the effect of PEHS was significant and dose-dependent, achieving a 30% reduction, which indicated that the removed material might have deleterious effects on either the diffusibility or the intrinsic antioxidant activity of phenolic compounds. These deleterious effects were not observed with their putative anti-inflammatory properties. We observed that both extracts at the tested concentrations significantly decreased the amount of secreted adipokines with respect to controls (Fig. 4C). This result indicated that the effect of fibre and/or saccharides could be specific. For most of the adipokines assayed,

**Table 2**  
Quantitative data in ppm (m/m) for major components found in extracts and fractions with significant biological activity.

Peak number	Compound	Quantification technique	AHS	PEHS	Fraction 6	Fraction 9	Fraction 14
1	Hydroxycitric acid	MS-TOF ( <i>m/z</i> 207)	8288.0 ± 397.6	—	—	—	—
2	Hibiscus acid	MS-TOF ( <i>m/z</i> 189)	31.122.0 ± 1128.4	128.134.2 ± 9486.9	—	—	—
3	Delphinidin-3-sambubioside	DAD-UV (520 nm)	207.312. ± 165.6	207.315.5 ± 1807.6	415.227.9 ± 18.558.3	—	—
5	Cyanidin-3-sambubioside	DAD-UV (520 nm)	19392 ± 39.3	87.143.1 ± 393.1	193.354.1 ± 3119.0	—	—
6	Chlorogenic acid	DAD-UV (355 nm)	57200 ± 39.4	106.469.9 ± 1182.0	5381.5 ± 173.9	137.219.1 ± 1425.8	—
8	Hibiscus acid dimethyl ester	MS-TOF ( <i>m/z</i> 217)	—	5300.5 ± 325.9	—	—	—
9	Methyl digalate	DAD-UV (270 nm)	57.3 ± 2.5	2802.3 ± 46.6	—	—	—
11	Myricetin-3- <i>α</i> -arabinoglucoside	DAD-UV (350 nm)	—	4755.5 ± 53.8	—	—	—
12	Comaratoxylinic acid	DAD-UV (310 nm)	—	772.9 ± 10.4	—	—	—
14	Quercetin-3-sambubioside	DAD-UV (350 nm)	3040.0 ± 5.9	7673.8 ± 424.6	—	—	—
16	Quercetin-3-rutinoside	DAD-UV (350 nm)	4957.4 ± 4.3	4953.2 ± 47.9	—	—	—
17	5-O-Caffeoylshikimic acid	DAD-UV (325 nm)	171.5 ± 6.9	3526.7 ± 49.2	—	—	—
18	Leucoside	DAD-UV (350 nm)	—	1123.0 ± 25.4	—	—	—
20	Quercetin-3-glucoside	DAD-UV (350 nm)	143.7 ± 2.2	3071.6 ± 15.9	—	—	—
21	Kaempferol-3-O-rutinoside	DAD-UV (350 nm)	91.9 ± 2.3	2185.5 ± 15.5	—	—	—
24	Methyl- <i>ε</i> -pigallocatechin	DAD-UV (270 nm)	—	310.9 ± 5.5	—	—	—
26	Myricetin	DAD-UV (370 nm)	—	4765.9 ± 49.1	—	—	—
27	<i>N</i> -Feruloyltyramine	DAD-UV (325 nm)	99.0 ± 1.8	867.9 ± 8.6	—	—	—
29	Quercetin	DAD-UV (370 nm)	121.2 ± 2.0	5795.2 ± 61.7	—	—	—
31	Prodelphinidin B3	DAD-UV (310 nm)	1839.2 ± 25.3	322.0 ± 2.9	—	—	—
32	Tetra-O-methylquidediflavonone	DAD-UV (350 nm)	—	—	13.515.7 ± 125.8	—	—
34	Caffeoylglucose	MS-TOF ( <i>m/z</i> 341)	—	—	—	2902.1 ± 67.5	—
37	Myricetin-3-glucoside	DAD-UV (350 nm)	—	—	—	29.383.6 ± 1245.1	—

both extracts showed the same quantitative efficacy. A differential response, higher for PEHS than for AHS, was only observed with the secretion of leptin and MCP-1.

## Discussion

The efficacy of phytotherapy is currently under intense debate (Wagner 2011). To firmly establish beneficial effects that may yield valuable nutritional advice or dietary supplements, human studies demand (Mozaffari-Khosravi et al. 2009; Kuriyan et al. 2010) full chemical characterisation of the source of polyphenols and the effect of further manipulation in the relative composition. Our novel findings suggested that the previous removal of fibre and polysaccharides, which represent up to 60% of the total weight of soluble extracts (Müller and Franz 1992), might significantly increase the activity of a polyphenolic mixture. Adipogenesis was substantially inhibited by a standardised *Hibiscus sabdariffa* extract, and the effect of the full extract was higher than the sum of its parts, which provided further evidence that a combination of bioactive components was superior to isolated constituents. In essence, the assayed extracts are a complex mixture of anthocyanins, organic acids, phenolic acids and flavonols (Rodríguez-Medina et al. 2009). Nevertheless, our results revealed that some compounds can have a higher contribution to the observed effects, which suggested the importance of relative composition and that different formulations might yield different outcomes. For instance, the putative hypolipidemic effects of polyphenolic mixtures have been mainly associated with the presence of organic acids (Carvajal-Zarrabal et al. 2005). In contrast, the described effects of PEHS in adipogenesis were obtained in a scenario in which the proportion of phenolic compounds was higher than that of organic acids. From data obtained from isolated fractions, it could be concluded that glycosylated flavonols were the most active compounds amongst individual components, but this finding seemed irrelevant when compared to the action of the full mixture. Although other isolated phenolic compounds (apigenin, epigallocatechin gallate, resveratrol and quercetin) have also shown to inhibit adipogenesis in 3T3-L1 adipocytes in similar concentrations (10–50 µg/ml, Lin et al. 2005; Bandopadhyay et al. 2006; Yang et al. 2008), cytotoxicity was readily observed. This point is extremely important because plant-derived polyphenols are a complex mixture that interacts with numerous endogenous molecular targets in humans but are surprisingly safe even at high doses (Corson and Crews 2007; Goel et al. 2008; Efferth and Koch 2011).

Another novel finding was that PEHS also actively diminished triglyceride accumulation in mature and even insulin-resistant hypertrophied adipocytes, which suggested an induction in the lipolysis rate (Yu and Zhu 2004; Takahashi et al. 2008). This effect could be important in the management of metabolic disturbances because the uninhibited release of fatty acids from hypertrophied adipocytes might lead to systemic lipotoxicity and insulin resistance (Unger 1995). It was also established that excess triglyceride accumulation in adipocytes generated an excess of ROS that triggered inflammation (Yeop Han et al. 2010). Although the differential abilities observed between AHS and PEHS deserve further consideration, PEHS clearly possesses antioxidative and anti-inflammatory actions in mature and hypertrophied adipocytes. These properties might also have therapeutic implications because these are important processes in 3T3-L1 adipocytes that are directly related to the accumulation of fat and with potential regulation via JNK/NF-κB pathways as described (Furukawa et al. 2004; Takahashi et al. 2008; Yeop Han et al. 2010). Once again we highlight the importance of a particular formulation of phenolic compounds because PEHS was particularly active in inhibiting the secretion of leptin and MCP-1, which are important adipokines

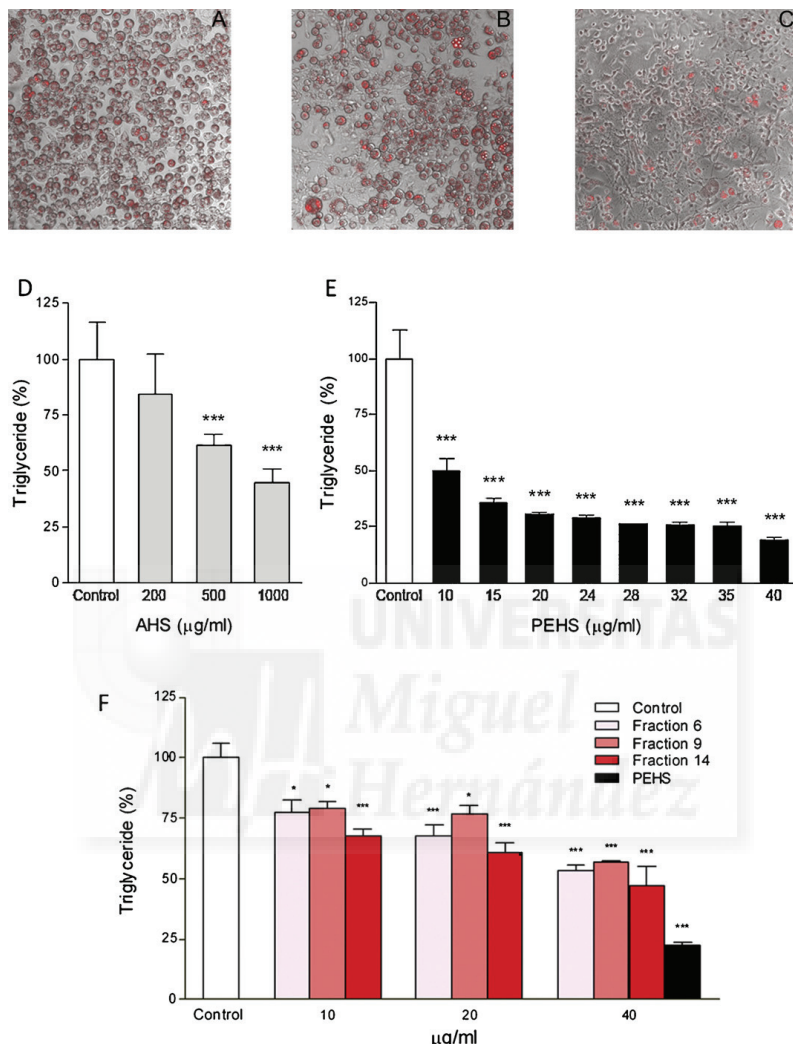


**Fig. 2.** Polyphenols from *Hibiscus sabdariffa* significantly inhibited the accumulation of triglycerides in 3T3-L1 preadipocytes and programmed adipogenesis. Representative microphotographs of cells stained with AdipoRed<sup>TM</sup> (treatment groups: control, 1000  $\mu\text{g/ml}$  AHS or 40  $\mu\text{g/ml}$  PEHS; A–C), demonstrate that the number of mature adipocytes was substantially decreased in cells treated with extracts. The quantitative effects of different doses on the final content of triglyceride are also shown (D–E). The effect of selected fractions in the accumulation of triglycerides in 3T3-L1 preadipocytes is shown in (F). Cell viability was unaffected even at higher concentrations. \* $p < 0.05$  and \*\*\* $p < 0.001$  versus control.

that regulate the migration of non-resident macrophages to the adipose tissue and overall systemic metabolism (Furukawa et al. 2004). This anti-inflammatory effect has also been observed with resveratrol or alpha lipoic acid (Szkudelska et al. 2009; Prieto-Hontoria et al. 2011).

The apparently additive, synergistic or even antagonistic action of each polyphenol and the intrinsic complications of understanding adipocyte metabolism without knowledge of genetic and proteomic kinetics impede efforts to describe the possible biological reactions and metabolic networks involved. Polyphenol reaction and diffusion rates also confound these efforts. Moreover,

the process of transformation and regeneration in these particular cells, and the effects that we described strongly suggested the presence of repeat-pattern mechanisms (Gierer and Meinhardt 1972), which is a self-organising, self-repairing, reaction-diffusion system (Turing 1990).

We speculate that this relationship can be applied to every combination of polyphenols with medicinal effects, but at least two major points should be highlighted. Leptin production correlates positively with insulin resistance, fat mass and adipocyte volume in response to metabolic stress (Frederich et al. 1995). The observed benefit with PEHS was comparatively higher than that observed

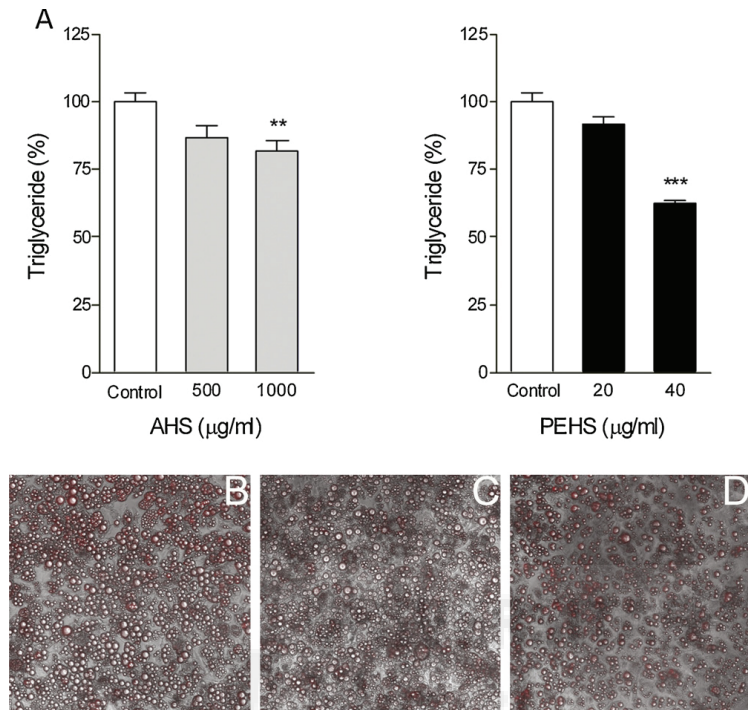


**Fig. 3.** Polyphenols from *Hibiscus sabdariffa* significantly decreased the accumulation of triglycerides in 3T3-L1 hypertrrophied/insulin-resistant adipocytes (A). Effects are shown for AHS (500–1000 µg/ml) (left panel) and PEHS (20–40 µg/ml) (right panel). (B)–(D) are representative microphotographs of cells stained with AdipoRed™; treatment groups: control, 1000 µg/ml AHS or 40 µg/ml PEHS, respectively. The number of fat droplets per cell was decreased in the experiments with PEHS. Cell viability was unaffected even at higher concentrations. \*\* $p < 0.01$  and \*\*\* $p < 0.001$  versus control.

with triglyceride accumulation, which suggested that leptin gene expression was a possible pharmacologic target, although this is effect obviously modulated by actions on a variety of other targets (Frederich et al. 1995; Rupnick et al. 2002; Tilg and Moschen 2006; Samuni et al. 2010). Results with MCP-1 excretion were expected. We have previously reported in humans that these polyphenolic extracts significantly reduce the concentration of circulating MCP-1, which is relevant because MCP-1 has been proposed as a biomarker and therapeutic target in the management of obesity and its related complications (Beltrán-Debón et al. 2009).

We should express caution, however, when interpreting *in vitro* data to actual actions of polyphenols in the body, especially if no data have been collected regarding the action of physiological metabolites of tested polyphenols on the same cell systems. First, the intestinal flora is likely to metabolise some of these compounds. Once the glucoside cleaved, the released aglycone is subjected to the action of specific enzymes in the wall of the small intestine leading to glucuronide, sulphated, and methylated metabolites, which may reach their target tissues and organs. Obviously, our *in vitro* assays do not take into account the *in vivo* bioavailability issue and can lead to false positive interpretations. To date, there is no data about human or animal studies on metabolites deriving from HS polyphenols. Although some bioavailability studies on phenolic acids, anthocyanins and flavonols are available, these are contained in very different food matrixes what may radically modify the interaction amongst these compounds in the gastrointestinal tract and therefore their absorption. Whilst human

absorption and bioavailability studies have revealed that phenolic acids and anthocyanins can be retrieved in plasma and urine in their intact form after food consumption (Paredes-López et al. 2010; Williamson et al. 2011), flavonols and flavanols seem to be found in various forms, free or conjugated with glucuronic, sulphate or methyl groups (Day et al. 2001; Williamson et al. 2011).

Because in studies with green tea polyphenols, the metabolites mostly had reduced biological activity, it might be tempting to suggest that conversion of HS polyphenols into less-active metabolites would compromise the cellular effects denoted in the present study. In some systems, however, polyphenols-derived metabolites were found to have the equivalent or even greater activity than the parental polyphenols (Lambert et al. 2007). In the present study, PEHS contains up to thirty identifiable phenolic compounds by HPLC-MS. Accepting that absorption of many of these compounds is negligible; still several of them will be conjugated and will interact with multiple metabolic targets. Thus, to study the effects of all possible metabolites becomes an enormous and fascinating target, which will be undoubtedly matter for future research.

In conclusion, we propose that this particular formulation of polyphenols should be assayed in clinical trials because of its observed regulation of adipogenesis, its regulation of oxidative stress signalling pathways in mature and/or hypertrophied adipocytes and its subsequent ability to alter the expression of adipokines. In regards to the preparation of phytopharmaceuticals or dietary supplements, we propose that the separation of soluble material other than polyphenols prior to use will increase

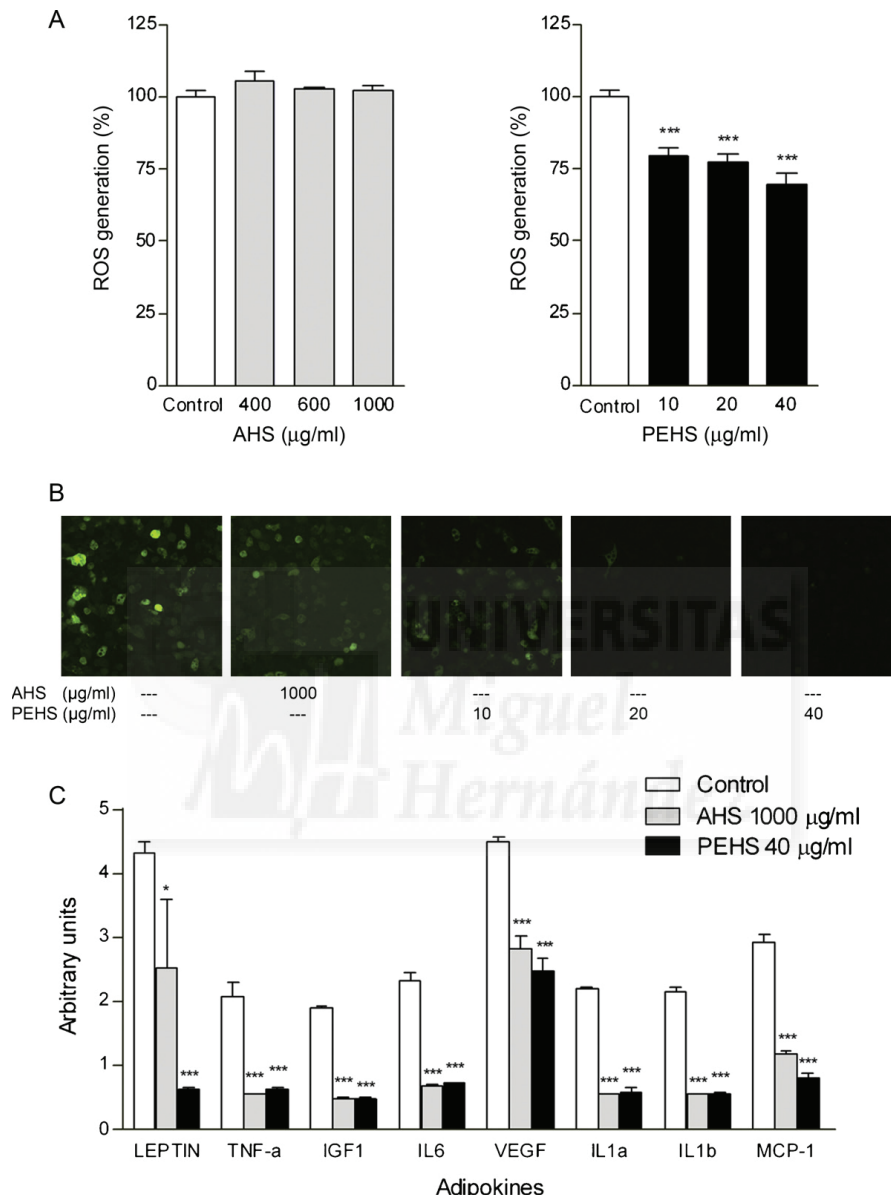


**Fig. 4.** The phenolic fraction from *Hibiscus sabdariffa* inhibited ROS generation and modulated the concentration of secreted adipokines in hypertrophied 3T3-L1 adipocytes (A). Cells were incubated with different doses of AHS (400–1000 μg/ml) (left panel) or PEHS (10–40 μg/ml) (right panel) and ROS generation was measured by H<sub>2</sub>DCFDA labelling. Whereas PEHS affected ROS generation in a dose-dependent manner, AHS did not. Representative fluorescence microphotographs of cells stained with H<sub>2</sub>DCFDA are shown in (B). Although the secretion of assayed adipokines was efficiently decreased with both extracts, a differential response was obtained with leptin and MCP-1 (C). \*p < 0.05 and \*\*\*p < 0.001 versus control.

the possibility of safely obtaining synergistic effects. Although bioavailability and safety issues require further studies, we have demonstrated the potential pharmacological and therapeutic superiority of a combination of polyphenols with respect to their

individual components. The existence of synergistic efficacy of binary combinations of compounds has been evaluated and verified by Berenbaum's isobole method (Berenbaum 1989; Wagner 2011). Unfortunately, this method cannot be applied in our case at

this stage due to the complexity of the polyphenol mixture. It is possible that the benefits of polyphenols are the result of mere additive effects or simple combinatory actions, but the data suggest a synergistic effect at least in the sense of that described by Mark Twain: "a bonus achieved when things work together harmoniously".

### Conflict of interest statement

The authors declare that there are no conflicts of interest.

### Acknowledgements

We thank MONTELOEDER, SL for providing raw plant material and for advice on the extraction and purification procedures. RBD and MHL were the recipients of fellowships from the Comissionat per a Universitat i Recerca del Departament d'Innovació, Universitats i Empresa de la Generalitat de Catalunya and Programa Vali+d from Generalitat Valenciana, respectively. We thank Andalusian Regional Government Council of Innovation and Science for granted Excellence Project.

### Appendix A. Supplementary data

Supplementary data associated with this article can be found, in the online version, at doi:10.1016/j.phymed.2011.12.001.

### References

- Alcaron-Aguilar, F.J., Zamilpa, A., Perez-Garcia, M.D., Almanza-Perez, J.C., Romero-Nuñez, E., Campos-Sepulveda, E.A., Vazquez-Carrillo, L.I., Roman-Ramos, R., 2007. Effect of Hibiscus sabdariffa on obesity in MSG mice. *J. Ethnopharmacol.* 114, 66–71.
- Bandyopadhyay, S., Lion, J.M., Mentaverri, R., Ricupero, D.A., Kamei, S., Romero, J.R., Chattopadhyay, N., 2006. Attenuation of osteoclastogenesis and osteoclast function by apigenin. *Biochem. Pharmacol.* 72, 184–197.
- Beltrán-Debón, R., Alonso-Villaverde, C., Aragón, C., Rodríguez-Medina, I., Rull, A., Micó, V., Segura-Carretero, A., Fernández-Gutiérrez, A., Camps, J., Joven, J., 2009. The aqueous extract of Hibiscus sabdariffa calices modulates the production of monocyte chemoattractant protein-1 in humans. *Phytomedicine* 17, 186–191.
- Berenbaum, M.C., 1989. What is synergy? *Pharmacol. Rev.* 41, 93–141.
- Carvajal-Zarrabal, O., Waliszewski, S.M., Barradas-Dermitz, D.M., Orta-Flores, Z., Hayward-Jones, P.M., Nolasco-Hipólito, C., Angulo-Guerrero, O., Sanchez-Ricano, R., Infanzón, R.M., Trujillo, P.R., 2005. The consumption of Hibiscus sabdariffa dried calyx ethanolic extract reduced lipid profile in rats. *Plant Foods Hum. Nutr.* 60, 153–159.
- Corson, T.W., Crews, C.M., 2007. Molecular understanding and modern application of traditional medicines: triumphs and trials. *Cell* 130, 769–774.
- Day, A.J., Mellon, F., Barron, D., Sarrazin, G., Morgan, M.R., Williamson, G., 2001. Human metabolism of dietary flavonoids: identification of plasma metabolites of quercetin. *Free Radic. Res.* 35, 941–952.
- Efferth, T., Koch, E., 2011. Complex interactions between phytochemicals. The multi-target therapeutic concept of phytotherapy. *Curr. Drug Targets* 12, 122–132.
- Fernandez-Arroyo, S., Rodriguez-Medina, I.C., Beltrán-Debón, R., Pasini, F., Joven, J., Micó, V., Segura-Carretero, A., Fernandez-Gutierrez, A., 2011. Quantification of the polyphenolic fraction and in vitro antioxidant and in vivo anti-hyperlipemic activities of Hibiscus sabdariffa aqueous extract. *Food Res. Int.* 44, 1490–1495.
- Frederich, R.C., Hamann, A., Anderson, S., Lollmann, B., Lowell, B.B., Flier, J.S., 1995. Leptin levels reflect body lipid content in mice: evidence for diet-induced resistance to leptin action. *Nat. Med.* 1, 1311–1314.
- Furukawa, S., Fujita, T., Shimabukuro, M., Iwaki, M., Yamada, Y., Nakajima, Y., Nakayama, O., Makishima, M., Matsuda, M., Shimomura, I., 2004. Increased oxidative stress in obesity and its impact on metabolic syndrome. *J. Clin. Invest.* 114, 1752–1761.
- Gierer, A., Meinhardt, H., 1972. A theory of biological pattern formation. *Kybernetik* 12, 30–39.
- Goel, A., Jhurani, S., Aggarwal, B.B., 2008. Multi-targeted therapy by curcumin: how spicy is it? *Mol. Nutr. Food Res.* 52, 1010–1030.
- Green, H., Kehinde, O., 1975. An established preadipose cell line and its differentiation in culture. II. Factors affecting the adipose conversion. *Cell* 5, 19–27.
- Howitz, K.T., Sinclair, D.A., 2008. Xenohormesis: sensing the chemical cues of other species. *Cell* 133, 387–391.
- Huang, D., Boxin, O.U., Prior, R.L., 2005. The chemistry behind antioxidant capacity assays. *J. Agric. Food Chem.* 53, 1841–1856.
- Jernas, M., Palming, J., Sjöholm, K., Jennische, E., Svensson, P.-A., Gabrielsson, B.G., Levin, M., Sjögren, A., Rudemo, M., Lystig, T.C., Carlsson, B., Carlson, L.M.S., Lonn, M., 2006. Separation of human adipocytes by size: hypertrophic fat cells display distinct gene expression. *FASEB J.* 20, 1540–1542.
- Kim, J.K., So, H., Youn, M.J., Kim, H.J., Kim, Y., Park, C., Kim, S.J., Ha, Y.A., Chai, K.Y., Kim, S.M., Kim, K.Y., Park, R., 2007. Hibiscus sabdariffa L. water extract inhibits the adipocyte differentiation through the PI3-K and MAPK pathway. *J. Ethnopharmacol.* 114, 260–267.
- Kuriyan, R., Kumar, D.R., R.R., Kurpad, A.V., 2010. An evaluation of the hypolipidemic effect of an extract of Hibiscus sabdariffa leaves in hyperlipidemic Indians: a double blind, placebo controlled trial. *BMC Complement. Altern. Med.* 10, 27.
- Lambert, J.D., Sang, S., Yang, C.S., 2007. Biotransformation of green tea polyphenols and the biological activities of those metabolites. *Mol. Pharm.* 4, 819–825.
- Lamming, D.W., Wood, J.G., Sinclair, D.A., 2004. Small molecules that regulate lifespan: evidence for xenohormesis. *Mol. Microbiol.* 53, 1003–1009.
- Lin, J., Della-Fera, M.A., Baile, C.A., 2005. Green tea polyphenol epigallocatechin gallate inhibits adipogenesis and induces apoptosis in 3T3-L1 adipocytes. *Obes. Res.* 13, 982–990.
- McGeer, P.L., McGeer, E.G., 2004. Inflammation and the degenerative diseases of aging. *Ann. N.Y. Acad. Sci.* 1035, 104–116.
- Mozaffari-Khosravi, H., Jalali-Khanabadi, B.A., Afkhami-Ardekani, M., Fatehi, F., 2009. Effects of sour tea (Hibiscus sabdariffa) on lipid profile and lipoproteins in patients with type II diabetes. *J. Altern. Complement. Med.* 15, 899–903.
- Müller, B.M., Franz, G., 1992. Chemical structure and biological activity of polysaccharides from Hibiscus sabdariffa. *Planta Med.* 58, 60–67.
- Paredes-Lopez, O., Cervantes-Cejá, M.L., Vigna-Perez, M., Hernández-Perez, T., 2010. Berries: improving human health and healthy aging, and promoting quality life – a review. *Plant Foods Hum. Nutr.* 65, 299–308.
- Prieto-Hontoria, P.L., Perez-Matute, P., Fernandez-Galilea, M., Martinez, J.A., Moreno-Alvaga, M.J., 2011. Lipoic acid inhibits leptin secretion and Sp1 activity in adipocytes. *Mol. Nutr. Food Res.* 55, 1–11.
- Rodríguez-Medina, I.C., Beltrán-Debón, R., Micó, V., Alonso-Villaverde, C., Joven, J., Menéndez, J.A., Segura-Carretero, A., Fernández-Gutiérrez, A., 2009. Direct characterization of aqueous extract of *Hibiscus sabdariffa* using HPLC with diode array detection coupled to ESI and ion trap MS. *J. Sep. Sci.* 32, 3441–3448.
- Rull, A., Camps, J., Alonso-Villaverde, C., Joven, J., 2010. Insulin resistance, inflammation, and obesity: role of monocyte chemoattractant protein-1 (or CCL2) in the regulation of metabolism. *Mediators Inflamm.* 2010, 326580.
- Rupnick, M.A., Panigrahy, D., Zhang, C.Y., Dallabrida, S.M., Lowell, B.B., Langer, R., Folkman, M.J., 2002. Adipose tissue mass can be regulated through the vasculature. *Proc. Natl. Acad. Sci. U.S.A.* 99, 10730–10735.
- Samuni, Y., Cook, J.A., Choudhuri, D., DeGraff, W., Sowers, A.L., Krishna, M.C., Mitchell, J.B., 2010. Inhibition of adipogenesis by Tempol in 3T3-L1 cells. *Free Radic. Biol. Med.* 49, 667–673.
- Szkudelska, K., Nogowska, L., Szkudelski, T., 2009. The inhibitory effect of resveratrol on leptin secretion from rat adipocytes. *Eur. J. Clin. Invest.* 39, 899–905.
- Takahashi, K., Yamaguchi, S., Shimoyama, T., Seki, H., Miyokawa, K., Katsuta, H., Tanaka, T., Yoshimoto, K., Ohno, H., Nagamatsu, S., Ishida, H., 2008. JNK- and I(kappa)B-dependent pathways regulate MCP-1 but not adipoletin release from artificially hypertrophied 3T3-L1 adipocytes preloaded with palmitate in vitro. *Am. J. Physiol. Endocrinol. Metab.* 294, E898–E909.
- Tilg, H., Moschen, A.R., 2006. Adipocytokines: mediators linking adipose tissue, inflammation and immunity. *Nat. Rev. Immunol.* 6, 772–783.
- Turing, A.M., 1990. The chemical basis of morphogenesis. 1953. *Bull. Math. Biol.* 52, 153–197 (discussion 119–152).
- Unger, R.H., 1995. Lipotoxicity in the pathogenesis of obesity-dependent NIDDM. Genetic and clinical implications. *Diabetes* 44, 863–870.
- Wagner, H., 2011. Synergy research: approaching a new generation of phytopharmaceuticals. *Fitoterapia* 82, 34–37.
- Williamson, G., Dionisi, F., Renouf, M., 2011. Flavanols from green tea and phenolic acids from coffee: critical quantitative evaluation of the pharmacokinetic data in humans after consumption of single doses of beverages. *Mol. Nutr. Food Res.* 55, 864–873.
- Yang, J.Y., Della-Fera, M.A., Rayalam, S., Ambati, S., Hartzell, D.L., Park, H.J., Baile, C.A., 2008. Enhanced inhibition of adipogenesis and induction of apoptosis in 3T3-L1 adipocytes with combinations of resveratrol and quercetin. *Life Sci.* 82, 1032–1039.
- Yeop Han, C., Kargi, A.Y., Omer, M., Chan, C.K., Wabitsch, M., O'Brien, K.D., Wight, T.N., Chait, A., 2010. Differential effect of saturated and unsaturated fatty acids on the generation of monocyte adhesion and chemotactic factors by adipocytes: dissociation of adipocyte hypertrophy from inflammation. *Diabetes* 59, 386–396.
- Yu, Y.H., Zhu, H., 2004. Chronological changes in metabolism and functions of cultured adipocytes: a hypothesis for cell aging in mature adipocytes. *Am. J. Physiol. Endocrinol. Metab.* 286, E402–E410.





## Use of advanced techniques for the extraction of phenolic compounds from Tunisian olive leaves: Phenolic composition and cytotoxicity against human breast cancer cells

Amani Taamalli <sup>a,b,c</sup>, David Arráez-Román <sup>b,c</sup>, Enrique Barrajón-Catalán <sup>e</sup>, Verónica Ruiz-Torres <sup>e</sup>, Almudena Pérez-Sánchez <sup>e</sup>, Miguel Herrero <sup>d</sup>, Elena Ibañez <sup>d</sup>, Vicente Micó <sup>e</sup>, Mokhtar Zarrouk <sup>a</sup>, Antonio Segura-Carretero <sup>b,c,\*</sup>, Alberto Fernández-Gutiérrez <sup>b,c</sup>

<sup>a</sup> Laboratoire Caractérisation et Qualité de l'Huile d'Olive, Centre de Biotechnologie de Borj Cedria, BP 901, 2050 Hammam-Lif, Tunisia

<sup>b</sup> Department of Analytical Chemistry, Faculty of Sciences, University of Granada, Granada 18071, Spain

<sup>c</sup> Research and Development of Functional Food Centre (CIDAF), Health Science Technological Park, Avda. DelConocimiento s/n, 18100 Granada, Spain

<sup>d</sup> Department of Bioactivity and Food Analysis, Institute of Food Science Research-CIAL (CSIC-UAM), Nicolás Cabrera 9, Campus Cantoblanco, 28049 Madrid, Spain

<sup>e</sup> Institute of Molecular and Cell Biology, University Miguel Hernández, Avda. Universidad s/n, 30202 Elche, Spain

### ARTICLE INFO

#### Article history:

Received 1 December 2011

Accepted 26 February 2012

Available online 13 March 2012

#### Keywords:

Phenolic compounds  
Supercritical fluid extraction  
Pressurized liquid extraction  
Microwave-assisted extraction  
Breast cancer cells  
HPLC-ESI-TOF-MS/IT-MS<sup>2</sup>

### ABSTRACT

A comparison among different advanced extraction techniques such as microwave-assisted extraction (MAE), supercritical fluid extraction (SFE) and pressurized liquid extraction (PLE), together with traditional solid–liquid extraction, was performed to test their efficiency towards the extraction of phenolic compounds from leaves of six Tunisian olive varieties. Extractions were carried out at the best selected conditions for each technique; the obtained extracts were chemically characterized using high-performance liquid chromatography (HPLC) coupled to electrospray time-of-flight mass spectrometry (ESI-TOF-MS) and electrospray ion trap tandem mass spectrometry (ESI-IT-MS<sup>2</sup>). As expected, higher extraction yields were obtained for PLE while phenolic profiles were mainly influenced by the solvent used as optimum in the different extraction methods. A larger number of phenolic compounds, mostly of a polar character, were found in the extracts obtained by using MAE. Best extraction yields do not correlate with highest cytotoxic activity against breast cancer cells, indicating that cytotoxicity is highly dependent on the presence of certain compounds in the extracts, although not exclusively on a single compound. Therefore, a multifactorial behavior is proposed for the anticancer activity of olive leaf compounds.

© 2012 Elsevier Ltd. All rights reserved.

### 1. Introduction

In the search of new bioactive compounds from natural raw materials, food by-products have gained a considerable attention for their high potential as a source of phytochemicals, low cost and high environmental impact of such residues. For instance, in the olive oil industry, one of the most promising source of bioactives are olive leaves obtained as biomass after pruning of olive trees (Erbay and Icier, 2010). This residue is a very abundant vegetable material and it supposes a potential source of polyphenols (De Leonardi et al., 2008). Constituents of olive leaves have shown antiviral (Lee-Huang et al., 2003), antimicrobial (Markin et al., 2003), antioxidant, anti-inflammatory (Bouaziz et al., 2008; Briante et al., 2002), and anti-carcinogenic (Abaza et al., 2007; Bouallgui et al., 2011) activities.

Different extraction techniques have been used to extract bioactives from olive leaves; among them, conventional solid–liquid extraction with ethanol (Rada et al., 2007) or methanol: water (Bouaziz et al., 2008) and ultrasound assisted extraction (Cárcel et al., 2010). Considering the importance of the extraction process as a way to isolate and purify interesting compounds from natural raw materials, testing different extraction procedures is mandatory. One of the main needs in the development of extraction processes is to substitute inefficient and long extraction processes, usually requiring high volumes of toxic organic solvents, for non-conventional extraction procedures such as microwave-assisted extraction (MAE), supercritical fluid extraction (SFE) or pressurized liquid extraction (PLE), that require considerably less amounts of toxic solvents while providing higher extraction efficiencies and lower environmental impact (Herrero et al., 2010a,b; Mendiola et al., 2007). These modern extraction techniques can be regarded as a possible tool not only from a laboratory point of view but also for the natural products and food industries. In fact, industrial applications of SFE have experienced a strong development since the early 1990s in terms of patents (Schütz, 2007). It was reported

\* Corresponding author at: Research Group FQM-297, Department of Analytical Chemistry, Faculty of Sciences, University of Granada, C/Fuentenueva s/n, 18071 Granada, Spain. Tel.: +34 958243296; fax: +34 958243328.

E-mail address: [ansegura@ugr.es](mailto:ansegura@ugr.es) (A. Segura-Carretero).

that a large-scale commercial (3 ton/h) MAE is available for industrial use (Pangarkar, 2008). Although few reports can be found considering pilot scale units (Terigai et al., 2011; Boonkird et al., 2008), in view of the advantages of MAE and the development of equipment for large-scale commercial operation, MAE has a bright future. Thus lab scale studies can be used to determine factors required for scale-up the extraction process and equipments.

Recently, olive compounds have shown significant anti-carcinogenic effects by directly modulating the activities of various types of receptor tyrosine kinases, including the human epidermal growth factor receptor (HER2) (García-Villalba et al., 2010; Menéndez et al., 2007, 2009). Although secoiridoids seem to contribute importantly to such activity, the main responsible compounds have not been identified yet (Fu et al., 2010; Lozano-Sánchez et al., 2010). A recent review has highlighted the chemoprevention of doxorubicin toxicity (doxorubicin is a key of chemotherapeutic agent in different types of cancer treatment with chronic and acute associated toxic side effect) making use of natural antioxidants among them antioxidants from virgin olive oil (Granados-Principal et al., 2010).

Therefore, the goal of the present study was to compare different extraction processes (conventional extraction, MAE, SFE and PLE), performed under certain conditions reported in the literature, towards the selective extraction of phenolic components from olive leaves deriving from six Tunisian olive varieties. To fully characterize their phenolic composition, a new method was used based on HPLC coupled to ESI-TOF-MS and ESI-IT-MS<sup>2</sup>. Moreover, the cytotoxicity of the different extracts against the JIMT-1 breast cancer cell line, a trastuzumab-resistant human cell line, was assayed. The possible correlation between the phenolic composition of the extracts and their cytotoxic activity was also studied.

## 2. Experimental

### 2.1. Chemicals and reagents

HPLC-grade acetonitrile (ACN) methanol and ethanol were purchased from Labscan (Dublin, Ireland). Acetic acid was of an analytical grade (assay >99.5%) and purchased from Fluka (Switzerland). Water was purified by using a Milli-Q system (Millipore, Bedford, USA). The carbon dioxide liquefied at high pressure used in supercritical extraction was supplied by Praxair Inc. (Danbury, CT, USA).

Standard compounds such as hydroxytyrosol, luteolin, apigenin, quercetin, taxifolin, vanillin and quinic acid were purchased from Sigma-Aldrich (St. Louis, MO, USA). (+)-pinoresinol was acquired from Arbo Nova (Turku, Finland), oleuropein and rutin from Extrasynthèse (Lyon, France).

### 2.2. Plant material and treatment

Leaves used in this study were obtained from six Tunisian olive varieties: 'Oueslati' (1), 'Chetoui' (2), 'Chemlali' (3), 'El Hor' (4), 'Jarboui' (5) and 'Chemchali' (6). Olive leaves were collected from different parts of the tree, so as to minimize the sun exposure effect. After collection, fresh leaves were immediately transferred to the laboratory, washed with distilled water and ground under liquid Nitrogen.

### 2.3. Apparatus and instruments

#### 2.3.1. MAE apparatus

MAE experiments were carried out with a START E Milestone Microwave Laboratory System (Milestone S.r.l, Sorisole (BG) Italy). The apparatus was equipped with a single magnetron system with

rotating diffuser for homogeneous microwave distribution in the cavity, delivered microwave power was 1.200 W, controlled via microprocessor, allowing rapid heating of high-throughput rotors, output power up to 1200 W in 1 W increments, a fiber-optic automatic temperature control (ATC-FO) System which allows direct continuous monitoring and control of a reference vessel up to 300 °C, a MPR-600/12S medium pressure segmented rotor containing 12 vessels for operating pressure up to 30 bar (435 psi). The microwave was operated via a compact control terminal 260 interface with bright, touch-screen display.

#### 2.3.2. SFE apparatus

The SFE system was based on a Suprex Prep Master (Suprex Corporation, Pittsburgh, PA, USA) with several modifications. A thermostatic oven heated by air convection was used to set the extraction cell (8 mL) containing the sample. An HPLC pump Waters 510 (Waters Corporation, Milford, MA, USA) was used to introduce the modifier in the extraction system. A pre-heater system was employed by placing a heating coil inside a glycerine bath (JP Selecta Agimatic N, JP Selecta S.A., Abrera, Spain) to guarantee that the fluid employed in all the experiences reaches the extraction cell at the target temperature. After the modifier pump, a check valve (Swagelok SS-CHS2-BU-10, Swagelok Corporation, Solon, OH, USA) was used. A micrometering valve (Hoke SS-SS4-BU-VH, Hoke Incorporated, Spartanburg, SC, USA) was placed after the extraction cell to manually control the flow. A computer-controlled mass flowmeter (EL-FLOW® Mass Flow Meter/Controller F-111C, Bronkhorst High-Tech BV, Almelo, The Netherlands) was used to adjust the carbon dioxide flow rate at the values selected for each experiment. After depressurization, the extracts were collected in a collection vessel previously described (Ibañez et al., 1999). Inside the collection vessel, 30 mL volume glass vials were placed to recover the extracts.

#### 2.3.3. PLE apparatus

The PLE system consisted in a home-made device described elsewhere (Ramos et al., 2007). Basically, it consisted of an extraction cell housed in an oven provided with temperature control and regulation, a Hewlett-Packard 1050 series isocratic pump (Palo Alto, USA) to deliver and pressurize the solvent in the extraction cell and two six-port Rheodyne valves (model 7000, Rheodyne L.P., Rohnert Park, CA, USA) connected to the inlet and outlet ends of the extraction cell. The temperature and the heating rate were set by varying the energy applied to the heating resistances. The temperature programme was manually started at the beginning of each experiment and stopped at the selected extraction time. The extraction cell (8 mL) consisted in a stainless steel holder (100 × 4.6 mm i.d. × 6.6 mm o.d.) sealed with 5 µm stainless steel frits (Supelco, Bellefonte, USA).

#### 2.3.4. HPLC apparatus

Separation of phenolic compounds from olive leaf extracts was performed on an Agilent 1200 series Rapid Resolution LC (Agilent Technologies, CA, USA) consisting of vacuum degasser, autosampler, and a binary pump equipped with a C18 Eclipse Plus analytical column (4.6 × 150 mm, 1.8 µm) from Agilent Technologies. The mobile phases used were water with acetic acid (0.5%) (mobile phase A) and acetonitrile (mobile phase B) and the solvent gradient changed according to the following conditions: from 0 to 10 min, 95% A to 70% A; from 10 to 12 min, 70% A to 67% A; from 12 to 17 min, 67% A to 62% A; from 17 to 20 min, 62% A to 50% A; from 20 to 23 min, 50% A to 5% A; from 23 to 25 min, 5% A to 95% A; from 25 to 35 min, 95% A. The flow rate used was set at 0.80 mL/min throughout the gradient. The effluent from the HPLC column was splitted using a T-type phase separator before being introduced into the mass spectrometer. Flow entering into the ESI-TOF-MS

or ESI-IT-MS detector was 0.2 mL/min. The column temperature was maintained at 25 °C and the injection volume was 10 µL.

#### 2.3.5. ESI-TOF-MS analysis

The HPLC system was coupled to a micrOTOF (BrukerDaltonics, Bremen, Germany), an orthogonal-accelerated TOF mass spectrometer (oaTOFMS), using an electrospray interface (model G1607A from Agilent Technologies, Palo Alto, CA, USA). Parameters for analysis were set using negative ion mode with spectra acquired over a mass range from 50 to 1000 *m/z*. The optimum values of the ESI-MS parameters were: capillary voltage,+4.5 kV; drying gas temperature, 190 °C; drying gas flow, 9.0 L/min; and nebulizing gas pressure, 2 bar.

The accurate mass data of the molecular ions were processed through the newest software Data Analysis 3.4 (BrukerDaltonics, Bremen, Germany), which provided a list of possible elemental formulae by using the Generate Molecular Formula™ editor. The Editor uses a CHNO algorithm, which provides standard functionalities such as minimum/maximum elemental range, electron configuration, and ring-plus double bonds equivalents, as well as a sophisticated comparison of the theoretical with the measured isotope pattern (sigma value) for increased confidence in the suggested molecular formula. The widely accepted accuracy threshold for confirmation of elemental compositions has been established at 5 ppm.

During the development of the HPLC method, external instrument calibration was performed using a Cole Palmer syringe pump (Vernon Hills, Illinois, USA) directly connected to the interface, passing a solution of sodium formate cluster containing 5 mM sodium hydroxide in the sheath liquid of 0.2% formic acid in water/isopropanol 1:1 (v/v). Using this method, an exact calibration curve based on numerous cluster masses, each differing by 68 Da ( $\text{Na}-\text{CHO}_2$ ) was obtained. Due to the compensation of temperature drift in the micrOTOF, this external calibration provided accurate mass values (better 5 ppm) for a complete run without the need for a dual sprayer setup for internal mass calibration.

#### 2.3.6. IT- $\text{MS}^2$ analysis

An identical HPLC system was coupled to a BrukerDaltonics Esquire 2000 ion trap mass spectrometer (BrukerDaltonics, Bremen, Germany) equipped with an electrospray interface (Agilent Technologies, CA, USA) operating in the negative ionization mode. The ion trap scanned at the 50–1000 *m/z* range at 13,000 u/s during the separation and detection. The maximum accumulation time for the ion trap was set at 200 ms, the target count at 20,000 and compound stability was set at 50%. The optimum values of the ESI-MS parameters were: capillary voltage,+3.0 kV; drying gas temperature, 300 °C; drying gas flow, 7.0 L/min; and nebulizing gas pressure, 21.7 psi. The instrument was controlled by Esquire NT software from BrukerDaltonics.

### 2.4. Extraction methods and conditions

#### 2.4.1. Conventional solvent extraction (CM)

10 mL of a mixture of methanol and water (80:20, v/v) was added to 1 g of fresh milled olive leaves and the sample was maintained 24 h in the dark at room temperature. The extracts were filtered through a 0.45 µm syringe filter prior to analysis (Abaza et al., 2011).

#### 2.4.2. Microwave-assisted extraction procedure (MAE)

1.25 g of milled fresh olive leaves were transferred into the microwave extraction vessel and suspended in 10 mL of a mixture of methanol and water (80:20, v/v). Then extraction was carried out for 6 min, considering an irradiation temperature equal to 80 °C. After extraction, the vessel was cooled down to room tem-

perature before opening, using the ventilation option of the system. The extracts were filtered through a 0.45 µm syringe filter prior to analysis.

#### 2.4.3. Supercritical fluid extraction procedure (SFE)

Prior to the extraction process, 1 g of milled olive leaves was homogenized with 1 g of sea sand, that was selected as inert material to hold the sample inside the extraction cell and to improve efficiency while avoiding formation of preferential flow paths. This mixture was introduced into the extraction cell and packed with glass wool. Extractions were carried out at 150 bar and 40 °C; once reached the experimental conditions, the extraction solvent (consisting on a mixture of  $\text{CO}_2$  plus 6.6% of ethanol as modifier) passed through the extraction cell for 2 h.

#### 2.4.4. Pressurized liquid extraction procedure (PLE)

One gram of grinded olive leaves was placed in the extraction cell that was subsequently filled with 5 g of sea sand. Once the cell was mounted in the device, the selected solvent (either ethanol or water) was pumped into the cell and the lines from the pump to the outer valve. Then, the solvent was pressurized up to the selected pressure (ca. 100 bar), which was controlled via the pump recorder. Simultaneously, the temperature programme was started to heat both, sample and extraction solvent at the selected temperature (150 °C) for a given time (20 min). After the static time, the upper valve was switched to allow the pressurized solvent leave the cell. Blank samples were run after each extraction to avoid any contamination or memory effect.

#### 2.4.5. Cytotoxicity assays

The human breast carcinoma cell line JIMT-1, which derives from a breast cancer clinically resistant to trastuzumab (Tanner et al., 2004) was kindly provided by Institut Català d’Oncologia (Girona, Spain). Cells were routinely grown in DMEM + GlutaMAX medium supplemented with 10% of heat-inactivated foetal bovine serum (GIBCO) containing 50 U/ml penicillin and 50 mg/mL of streptomycin (GIBCO). Cells were incubated at 37 °C in a humidified 5%  $\text{CO}_2$  air atmosphere. Cell viability was determined through the MTT assay (Fu et al., 2010). Briefly, cells were plated in 96-well plates at a density yielding 70–80% confluence when the cytotoxicity assay was performed. Complete medium was refreshed and cultures were treated with different doses of the extracts for 72 h. All the results corresponding to MTT experiments were expressed as the mean of a minimum of 6–8 replicates  $\pm$  SD. The 50% cytotoxic concentration values (CC50) were determined from the survival plots using GraphPad PRISM 5 (GraphPad Software).

### 2.5. Statistical analysis

Two-way ANOVA test at a confidence level of 95% was performed using SPSS 13.0 for windows software.

## 3. Results and discussion

Extraction conditions were established for each extraction process considering previous results published in the literature for phenolics extraction using SFE, PLE and MAE in different matrices, including rosemary and olive leaves (Herrero et al., 2010a,b; Herrero et al., 2011; Taamalli et al., 2012).

PLE and SFE are considered green technologies to produce bioactives from natural sources such as plants and algae (Herrero et al., 2010a,b; Plaza et al., 2009), as GRAS-qualified solvents such as  $\text{CO}_2$ , ethanol or water are frequently used in these technologies. In this study, PLE and SFE extraction processes were carried out under optimum conditions using only GRAS-qualified solvents. These

have been compared to MAE and conventional solid–liquid extraction, which used a mixture of methanol and water (80:20). Hydroalcoholic extraction is the choice of solvent for optimum phenolic's extraction due to the high extraction yield of a wide range of phenolic compounds from diverse types of samples including fruit, vegetables and olive oil (Tura and Robards, 2002). Our main target was to find out advantages and drawbacks between the different extraction processes in relation to the extraction of phenolics from olive leaves.

First of all, it is worth to mention that extraction processes assisted by temperature, such as PLE and MAE, have shorter extraction times than conventional technologies and SFE; this is mainly due to the increase of the analytes solubility in the extraction media when surface tension and solvent viscosity decreases, which, at the end, improves extraction efficiency. MAE extraction temperature was selected at 80 °C because, as previously reported (Taamalli et al., 2012), higher temperatures provide lower extraction efficiencies. Regarding PLE, 150 °C was selected as optimum temperature for phenolics extraction when ethanol was used as extracting solvent, since this condition has been reported to achieve the highest phenolic content and antioxidant capacity (Herrero et al., 2011). Although previous results obtained in our research group suggested the use of 200 °C for PLE water extractions, in this study we selected 150 °C in order to avoid the generation of compounds deriving from thermal dehydration of saccharides such as 5-hydroxymethylfurfural (Plaza et al., 2010). On the other hand, these conditions were also optimum in terms of phenolics content, antioxidant activity and extraction yield (Herrero et al., 2011).

Table 1 shows the yield obtained for the different extraction processes using six different varieties of Tunisian olive leaves. A two-way analysis of variance has been carried out and the results showed that the yield was significantly influenced by the extraction method ( $p < 0.05$ ), the olive variety ( $p < 0.05$ ). The interaction of extraction method and the olive variety was also significant ( $p < 0.05$ ). As observed, the use of PLE with ethanol as extraction solvent produced the highest yield for all the studied varieties. In this sense, the highest yield was obtained from the Chemchali (6) variety. MAE also produced high extraction yields, but significantly lower than those obtained by PLE using ethanol. The only exception was the case of Jarboui (5) variety for which MAE was the less efficient extraction technique in terms of total extracted yield. Lastly, PLE using water as solvent, conventional extraction (MeOH: H<sub>2</sub>O), as well as SFE using CO<sub>2</sub> and ethanol as cosolvent produced comparable yields. It is important to remark that the extraction yield strongly depends on the solvent employed. Nevertheless, extracts with similar yields, but produced under different extraction techniques, would show completely different chemical composition. Therefore, the phenolic composition of the extracts was studied in detail to evaluate the potential of the different extraction techniques.

In a recent study, we have optimized the MAE extraction conditions for phenolics' extraction from olive leaves and also identified, via HPLC-ESI-TOF-MS/IT-MS<sup>2</sup>, the main phenolic compounds present in MAE extracts (Taamalli et al., 2012). This information and

the data previously reported in literature (Briante et al., 2002; Fu et al., 2010; Arráez-Román et al., 2008; Meirinhos et al., 2005; Mylonaki et al., 2008) have been used as a basis for identifying the compounds detected in the different olive leaf extracts in the present study through the comparison of their relative retention time values, TOF-MS and IT-MS<sup>2</sup> data in addition to the comparison with authentic standard solutions when available. Representative base peak chromatograms (BPCs) of a mass range (50–1000 m/z), for the extracts under the optimum extraction conditions for MAE, PLE, SFE and conventional extraction are presented in Fig. 1 (only BPCs of samples showing the highest cytotoxic activity in each extraction method are shown). Peak identification is shown in Table 2.

As can be seen in Table 2, hydroxytyrosol glucoside was not detected in 'Oueslati', 'Chetoui', 'Chemlali' and 'El Hor' varieties whereas its aglycon form (hydroxytyrosol), in addition to elenolic acid glucoside isomer 2, and luteolin rutinoside isomer 2, were not found in 'Chemchali' variety. On the other hand, secologanaside, luteolin rutinoside isomer, syringaresinol and luteolin diglucoside isomer 2 were not detected in the 'Jarboui' extract. Among the different extraction techniques used, extracts obtained under MAE conditions showed the largest number of identified phenolic compounds (Table 2). Hydroxytyrosol glucoside, secologanaside, hydroxytyrosol, elenolic acid glucoside isomer 2, vanillin and taxifolin were not detected in SFE samples from different olive leaf varieties, although non-polar compounds were extracted in a higher extent, as expected. Vanillin was not detected in the extracts obtained by PLE using ethanol as extracting solvent (PLE-E), whereas quercetin was not detected in PLE using water as solvent (PLE-W).

Quantitatively, the total phenolic contents (TPCs), expressed as the total peak areas of the identified compounds, showed variation among the different extracts according to the variety and the extraction method employed. As Fig. 2A shows, MAE samples showed the highest TPCs in comparison to the other extraction methods, being 'Chemlali' (MAE 3) and 'El Hor' (MAE 4) the varieties having the highest TPCs. MAE technique was followed by CM and PLE techniques, being PLE-W and SFE those achieving the lowest TPC values.

Fig. 2B, C and D shows the content of selected secoiridoid and flavonoid compounds, expressed as peak area, of the samples obtained with different processes and olive varieties.

Results showed that 2"-methoxyoleuropein was not well extracted with either PLE (using water or ethanol as solvent) or SFE (using CO<sub>2</sub> + 6.6% ethanol) as compared to the other extraction methods (Fig. 2B). SFE and PLE (using water as solvent) did not show a good efficiency either for extracting oleuropein. Besides, SFE was the best extraction procedure for apigenin and diosmetin isolation. In contrast, MAE showed the best recoveries for oleuropein, 10-hydroxy-oleuropein and 2"-methoxyoleuropein (isomer 1 and 2), being these values higher than those of 10-hydroxy-oleuropein in all the extracts, except for those extracted with PLE (Fig. 2B). Therefore, most oleuropein derivatives seemed to be more efficiently extracted with the use of MAE or CM, being SFE

**Table 1**

Values of extraction yield (expressed as % of fresh weight) obtained for the six different Tunisian olive leaf varieties using different extraction processes (SFE, PLE, MAE, conventional) performed at the mentioned conditions.

Extraction process (conditions: solvent, T, time, pressure)	Oueslati (1) yield (%)	Chetoui (2) yield (%)	Chemlali (3) yield (%)	El Hor (4) yield (%)	Jarboui (5) yield (%)	Chemchali (6) yield (%)
SFE (CO <sub>2</sub> + ethanol, 40 °C, 1 h, 150 bar)	9.5	8.9	5.8	8.2	9.7	5.8
PLE (ethanol, 150 °C, 20 min, 100 bar)	19.9	19.5	14.8	19.6	16.7	22.4
PLE (water, 150 °C, 20 min, 100 bar)	10.4	7.5	8.4	8.9	11.2	11.0
MAE (methanol:water 80:20, 80 °C, 6 min)	16.7	10.6	11.2	11.6	5.2	12.1
Conventional (methanol:water 80:20, room T, 24 h)	9.4	8.1	8.2	8.2	9.1	16.8

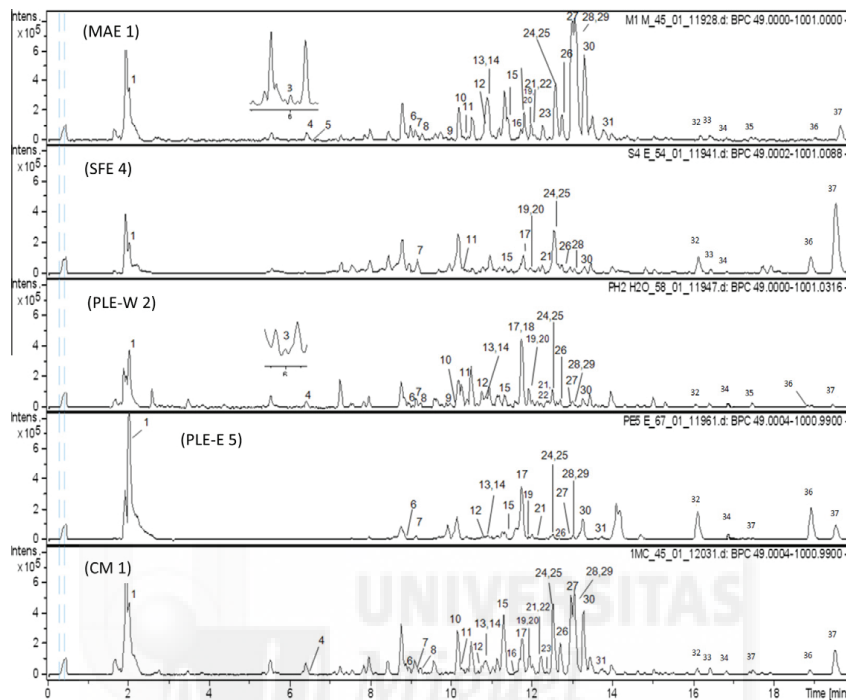


**Fig. 1.** Base Peak chromatograms (BPCs) of olive leaf extracts obtained with different extraction methods that showed highest cytotoxic activity on human breast cancer cells: MAE 1, SFE 4, PLE-W 2 and CM 1: microwave-assisted extraction (MAE), supercritical fluid extraction (SFE), pressurized liquid extraction using water as solvent (PLE-W), pressurized liquid extraction using ethanol as solvent (PLE-E) and conventional extraction method (CM). Numbers correspond to the different varieties according to Table 1. Peak identification as in Table 2.

the worst behaving technique. It was generally observed that considering the great chemical variability of the samples, each technique seemed to be more adequate than others for the extraction of each particular class of compounds.

Abundance of the phenolic compounds was also dependent on the variety. Among all the analyzed samples, 'El Hor' olive leaf extract obtained by SFE (SFE 4) was the richest in diosmetin (Fig. 2C), whereas, when extracted by MAE, 'El Hor' olive leaf extract (MAE 4) was the richest in oleuropein. 'Chemlali' and 'Chemchali' extracts obtained by SFE (SFE 3 and SFE 6, respectively) were the richest in apigenin (Fig. 2C) and luteolin (Fig. 2D), respectively. The 'Chetoui' olive leaf extract (sample 2) was the richest in apigenin rutinoside regardless the extraction technique utilized, indicating that this variety may be especially enriched in this flavone. Besides 'Chetoui' extracts, 'El Hor' extracts obtained by using CM extraction and 'Jarboui' extracts obtained by MAE and CM were also rich in apigenin rutinoside.

Olive leaf derived compounds have demonstrated their cytotoxic activity against different cancers such as leukemia, colon and breast cancer (Abaza et al., 2007; Fu et al., 2010; Hashim et al., 2008). Their cytotoxic activity is especially relevant in HER2 positive breast cancers where olive extracts reduce the over-expression of HER2 and diminish the resistance to trastuzumab, a monoclonal anti-HER2 antibody clinically used in the therapy of these cancers (Menendez et al., 2007). JIMT-1 cells derive from a HER2 positive breast carcinoma but resistant to trastuzumab and then, constitute an adequate model to test the cytotoxic activity

of olive extracts. A recent study on *Cistaceae* extracts showed a notorious capacity to inhibit the proliferation of JIMT-1 breast cancer cells (Barrajón-Catalána et al., 2010). In our study, all the extracts obtained through the different techniques were tested for their cytotoxicity on JIMT-1 cells after incubation during 72 h. Table 3 shows the CC<sub>50</sub> values obtained. Olive leaf extracts showing CC<sub>50</sub> values higher than 800 µg/mL were considered as non active (NA). Most of the extracts obtained by PLE (water and ethanol) or CM extraction methods showed a low cytotoxic activity with the exception of PLE-E 5. In contrast, MAE extracts showed a significant cytotoxic activity against JIMT-1 cells, especially that one deriving from 'Queslati' variety (MAE 1). In general, the highest potency was obtained with extracts obtained by SFE. The highest cytotoxic activity corresponded to 'El Hor' olive leaf extract obtained by SFE (SFE 4), which showed a CC<sub>50</sub> as low as 7 µg/mL. Only in a few cases, higher cytotoxicity correlated to higher extraction yield (MAE 1 and PLE-E 5) (Table 1). In general, extraction yield did not correlate with the total phenolic content, revealing that other compounds different than phenolics were extracted in the processes. Whereas highest yield was obtained using PLE followed by MAE, highest phenolic content was obtained with MAE followed by CM. Therefore, cytotoxicity seemed to be more related with phenolic compounds than with total yield. Nevertheless, most SFE extracts, which showed the lowest extraction yields i.e. <10%, and a low total phenolic content, presented high cytotoxic activity. Thus, this activity might be due to a particular class of phenolic compounds.

**Table 2**

Table 2 Characterized compounds in olive leaf extracts obtained by the different extraction methods using HPLC-ESI-TOF-MS/IT-MS<sup>2</sup> (selected ion: [M-H]<sup>-</sup>).

peak	Compound	MAE						SFE						PLE-W						PLE-E						Conventional extraction						Ref.
		1	2	3	4	5	6	1	2	3	4	5	6	1	2	3	4	5	6	1	2	3	4	5	6	1	2	3	4	5	6	
1	Quinic acid	+	+	+	+	+	+	+	+	+	+	+	+	+	+	+	+	+	+	+	+	+	+	+	+	+	+	+	+	+	+	Taamalli et al. (2012)
2	Hydroxytyrosol-glucoside	-	-	-	-	+	-	-	-	-	-	-	-	-	-	-	-	-	-	-	-	-	-	-	-	-	-	-	-	-	Fu et al. (2010)	
3	Secologanoside	+	-	+	-	-	-	-	-	-	-	-	-	-	-	-	-	-	-	-	-	-	-	-	-	-	-	-	-	-	Fu et al. (2010) and Taamalli et al. (2012)	
4	Vanillin	+	+	+	+	+	-	-	-	-	-	-	-	-	-	-	-	-	-	-	-	-	-	-	-	-	-	-	-	-	Benavente-García et al. (2000) and Taamalli et al. (2012)	
5	Hydroxytyrosol	+	+	+	+	+	-	-	-	-	-	-	-	-	-	-	-	-	-	-	-	-	-	-	-	-	-	-	-	-	Benavente-García et al. (2000), Briante et al. (2002), Fu et al. (2010) and Arráez-Román et al. (2008)	
6	Elenolic acid glucoside isomer 1	+	+	+	+	+	+	-	-	-	-	-	-	-	-	-	-	-	-	-	-	-	-	-	-	-	-	-	-	-	Fu et al. (2010) and Taamalli et al. (2012)	
7	Oleuropein aglycone derivative	+	+	+	+	+	+	+	+	+	+	+	+	+	+	+	+	+	+	+	+	+	+	+	+	+	+	+	+	+	Fu et al. (2010) and Taamalli et al. (2012)	
8	Luteolin diglucoside isomer 1	+	+	+	+	-	-	-	-	-	-	-	-	-	-	-	-	-	-	-	-	-	-	-	-	-	-	-	-	-	Fu et al. (2010) and Taamalli et al. (2012)	
9	Elenolic acid glucoside isomer 2	+	-	+	+	-	-	-	-	-	-	-	-	-	-	-	-	-	-	-	-	-	-	-	-	-	-	-	-	-	Fu et al. (2010) and Taamalli et al. (2012)	
10	Luteolin diglucoside isomer 2	+	+	+	+	-	-	-	-	-	-	-	-	-	-	-	-	-	-	-	-	-	-	-	-	-	-	-	-	-	Fu et al. (2010) and Taamalli et al. (2012)	
11	2-(2-Et-Hy-6-propionylcyclohexyl) acetic acid glucoside	+	+	+	+	+	+	+	+	+	+	+	+	+	+	+	+	+	+	+	+	+	+	+	+	+	+	+	+	+	Fu et al. (2010) and Taamalli et al. (2012)	
12	Rutin	+	+	+	+	+	+	+	-	-	-	-	-	-	-	-	-	-	-	-	-	-	-	-	-	-	-	-	-	-	Benavente-García et al. (2000), Mylonaki et al. (2008), Fu et al. (2010) and Taamalli et al. (2012)	
13	Luteolin-rutinoside isomer 1	+	+	+	+	+	+	-	-	-	-	-	-	-	-	-	-	-	-	-	-	-	-	-	-	-	-	-	-	-	Mylonaki et al. (2008) and Taamalli et al. (2012)	
14	10-hydroxy-oleuropein	+	+	+	+	+	+	+	+	-	-	-	-	-	-	-	-	-	-	-	-	-	-	-	-	-	-	-	-	-	Fu et al. (2010) and Taamalli et al. (2012)	
15	Luteolin glucoside isomer 1	+	+	+	+	+	+	+	+	+	+	+	+	+	+	+	+	+	+	+	+	+	+	+	+	+	+	+	+	+	Fu et al. (2010) and Taamalli et al. (2012)	
16	Oleuropein diglucoside	+	+	+	+	+	-	-	-	-	-	-	-	-	-	-	-	-	-	-	-	-	-	-	-	-	-	-	-	-	Fu et al. (2010) and Taamalli et al. (2012)	
17	Apigenin rutinoside	+	+	+	+	+	+	+	+	+	+	+	+	+	+	+	+	+	+	+	+	+	+	+	+	+	+	+	+	+	Meirinhos et al. (2005), Mylonaki et al. (2008) and Taamalli et al. (2012)	
18	Syringaresinol	+	+	+	+	-	-	-	-	-	-	-	-	-	-	-	-	-	-	-	-	-	-	-	-	-	-	-	-	-	Fu et al. (2010) and Taamalli et al. (2012)	
19	Diosmin isomer 1	+	+	+	+	+	+	+	+	+	+	+	+	+	+	+	+	+	+	+	+	+	+	+	+	+	+	+	+	+	Campanero et al. (2010) and Taamalli et al. (2012)	
20	Luteolin rutinoside isomer 2	+	+	+	+	-	-	-	-	-	-	-	-	-	-	-	-	-	-	-	-	-	-	-	-	-	-	-	-	-	Mylonaki et al. (2008) and Taamalli et al. (2012)	
21	Diosmin isomer 2	+	+	+	+	+	+	+	+	+	+	+	+	+	+	+	+	+	+	+	+	+	+	+	+	+	+	+	+	+	Campanero et al. (2010) and Taamalli et al. (2012)	
22	Taxifolin	+	+	+	+	+	-	-	-	-	-	-	-	-	-	-	-	-	-	-	-	-	-	-	-	-	-	-	-	-	Fu et al. (2010) and Taamalli et al. (2012)	
23	Luteolin glucoside isomer 2	+	+	-	+	+	-	-	-	-	-	-	-	-	-	-	-	-	-	-	-	-	-	-	-	-	-	-	-	-	Fu et al. (2010) and Taamalli et al. (2012)	
24	Apigenin-7-o-glucoside	+	+	+	+	+	+	+	+	+	+	+	+	+	+	+	+	+	+	+	+	+	+	+	+	+	+	+	+	+	Benavente-García et al. (2000), Meirinhos et al. (2005), Fu et al. (2010) and Taamalli et al. (2012)	
25	Luteolin glucoside isomer 3	+	+	+	+	+	+	+	+	+	+	+	+	+	+	+	+	+	+	+	+	+	+	+	+	+	+	+	+	+	Fu et al. (2010) and Taamalli et al. (2012)	
26	Chryseryl-7-o-glucoside	+	+	+	+	+	+	+	+	+	+	+	+	+	+	+	+	+	+	+	+	+	+	+	+	+	+	+	+	+	Fu et al. (2010) and Taamalli et al. (2012)	
27	2'-MethoxyOleuropein isomer 1	+	+	+	+	+	+	+	+	-	-	-	-	-	-	-	-	-	-	-	-	-	-	-	-	-	-	-	-	-	Tanahashi et al. (1999) and Taamalli et al. (2012)	
28	Luteolin glucoside isomer 4	+	+	+	+	+	+	+	+	+	-	-	-	-	-	-	-	-	-	-	-	-	-	-	-	-	-	-	-	-	Fu et al. (2010) and Taamalli et al. (2012)	
29	2'-Methoxyoleuropein isomer 2	+	+	+	+	+	+	+	-	-	-	-	-	-	-	-	-	-	-	-	-	-	-	-	-	-	-	-	-	-	Tanahashi et al. (1999) and Taamalli et al. (2012)	
30	Oleuropein	+	+	+	+	+	+	+	+	+	+	+	+	+	+	+	+	+	+	+	+	+	+	+	+	+	+	+	+	+	Benavente-García et al. (2000), Briante et al. (2002) and Taamalli et al. (2012)	
31	Oleuropein isomer	+	+	+	+	+	+	+	+	+	+	+	+	-	-	-	-	-	-	-	-	-	-	-	-	-	-	-	-	-	Fu et al. (2010) and Taamalli et al. (2012)	
32	Luteolin	+	+	+	+	+	+	+	+	+	+	+	+	+	+	+	+	+	+	+	+	+	+	+	+	+	+	+	+	+	Benavente-García et al. (2000), Meirinhos et al. (2005), Arráez-Román et al. (2008) and Fu et al. (2010)	
33	Quercetin	+	+	+	+	+	-	-	-	-	-	-	-	-	-	-	-	-	-	-	-	-	-	-	-	-	-	-	-	-	Fu et al. (2010) and Taamalli et al. (2012)	
34	Pinoresinol	+	+	+	+	+	+	+	+	+	+	+	+	+	+	+	+	+	+	+	+	+	+	+	+	+	+	+	+	+	Taamalli et al. (2012)	
35	Acetoxy-pinoresinol	+	+	+	+	+	+	+	+	+	+	+	+	+	+	+	+	+	+	+	+	+	+	+	+	+	+	+	+	+	Taamalli et al. (2012)	
36	Apigenin	+	+	+	+	+	+	+	+	+	+	+	+	+	+	+	+	+	+	+	+	+	+	+	+	+	+	+	+	+	Benavente-García et al. (2000), Meirinhos et al. (2005), Arráez-Román et al. (2008) and Taamalli et al. (2012)	
37	Diosmetin	+	+	+	+	+	+	+	+	+	+	+	+	+	+	+	+	+	+	+	+	+	+	+	+	+	+	+	+	+	Benavente-García et al. (2000), Meirinhos et al. (2005), Arráez-Román et al. (2008) and Taamalli et al. (2012)	

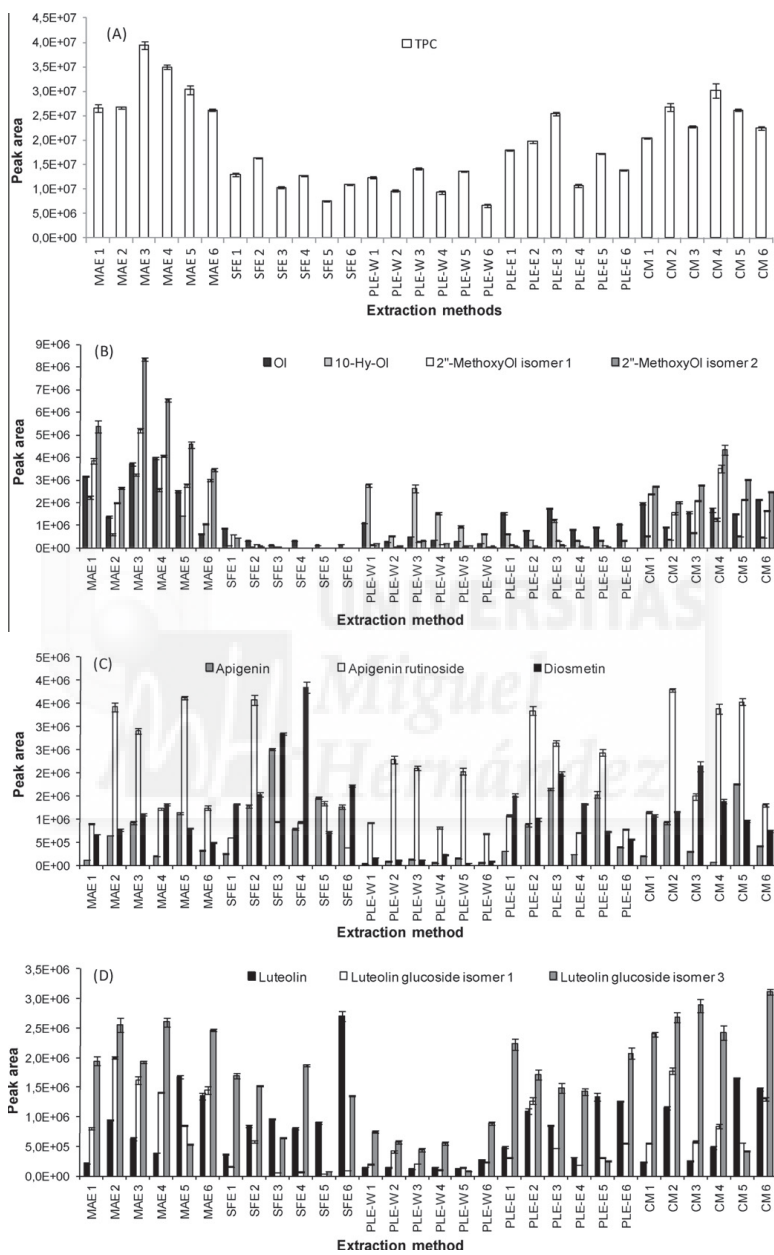


**Fig. 2.** Extraction efficiency of the different extraction methods for total phenolic content (TPC) (A), for main identified secoiriodoids (B) and flavonoids (C, D); microwave-assisted extraction (MAE), supercritical fluid extraction (SFE), pressurized liquid extraction using water as solvent (PLE-W), pressurized liquid extraction using ethanol as solvent (PLE-E) and conventional extraction method (CM), numbers correspond to the different varieties according to Table 1.

As mentioned, SFE extracts were poor in oleuropein derivatives and especially abundant in flavones such as luteolin and diosmetin. Consequently, the possible influence of these compounds on can-

cer cell cytotoxicity deserves further attention in future studies. Anyhow, the strong cytotoxic activity observed for some extracts (SFE 4, MAE 1, and PLE-E 5) does not rely on the abundance of a

**Table 3**

CC50 values obtained after treating JIMT-1 breast cancer cells with the different phenolic extracts deriving from six Tunisian olive leaf varieties NA: CC50 higher than 800 µg/mL.

Olive leaf sample	MAE CC50 (µg/mL)	SFE CC50 (µg/mL)	PLE-W CC50 (µg/mL)	PLE-E CC50 (µg/mL)	Conventional extraction CC50 (µg/mL)
Oueslati (1)	188 ± 24.5	633.5 ± 260.3	NA	NA	550.5 ± 92.2
Chetoui (2)	415.9 ± 14.2	NA	729.2 ± 86.5	NA	796.1 ± 395.4
Chemlali (3)	481.1 ± 49.5	560.1 ± 66.6	NA	NA	NA
El Hor (4)	515.8 ± 69.1	7.0 ± 5.5	NA	NA	NA
Jarboui (5)	435.8 ± 42.6	364.0 ± 25.0	NA	135.6 ± 31.9	NA
Chemchali (6)	711.9 ± 178.9	284.9 ± 78.7	NA	NA	636.7 ± 57.6

single compound so the interaction of different compounds with different cellular targets is postulated to exist. In this regard, several authors have recently pointed out that dietary polyphenols may exert their pharmacological effect through their synergistic interactions by interacting with multiple targets (Efferth and Koch, 2011; Wagner, 2011). It is also plausible that the cytotoxic effect is dependent on additional compounds that were not identified in this study.

#### 4. Conclusions

The development of new extraction processes to obtain bioactives, such as phenolic compounds, from food by-products is raising the attention of researchers and industries. A comparison has been carried out among non-conventional extraction techniques, such as MAE, SFE and PLE, and traditional solid-liquid extraction. Although the non-conventional techniques have shown important advantages, it is worth to mention that the main compositional differences among techniques depend on the type of solvent used to carry out the extraction. Thus, fast processes could be obtained using MAE and PLE, temperature-driven extraction processes, while greener processes could be achieved using SFE and PLE with water. Therefore, the optimum conditions for each process should be selected depending on the target compound to be isolated and other considerations (such as environmental impact, bioactivity, final use, etc.). In general, MAE and CM seem to be the choice for extracting more polar compounds such as oleuropein derivatives, apigenin rutinoside and luteolin glucoside isomer 3. As expected, SFE or PLE were more efficient to extract compounds with less polarity such as apigenin, luteolin, or diosmetin. The cytotoxic activity of the different olive leaf extracts against breast cancer cells does not correlate either with olive variety, process extraction yield, or amount of phenolic compounds. Highest cytotoxic effect was observed with SFE extracts, which were richer in flavones such as diosmetin or luteolin, but this biological activity does not rely on the abundance of a single compound or a family of compounds. Anyhow, the potential anticancer activity of these compounds and their extracts, especially that of the 'El Hor' variety, deserves further attention.

#### Conflict of Interest

The authors declare that there are no conflicts of interest.

#### Acknowledgments

The authors are grateful to the Tunisian Ministry of Higher Education and Scientific Research, to the Spanish Ministry of Education and Science for the project AGL2011-29857-C03-02 and to Andalusian Regional Government Council of Innovation and Science for the excellence projects P09-CTS-4564, P10-FQM-6563, and P11-CTS-7625, and to the University of Granada for the GREIB project GREIB.PYR-2011-02. M.H. and E.B.C. thank the Spanish Science

and Innovation Ministry (MICINN) for their "Ramón y Cajal" and "Torres Quevedo" (PTQ-08-03-08076) research contracts.

#### References

- Abaza, L., Talorette, T.P.N., Yamada, P., Kurita, Y., Zarrouk, M., Isoda, H., 2007. Tunisian Gerboui olive leaf extract induces growth inhibition and differentiation of human leukemia HL-60 cells. *J. Biosci. Biotechnol. Biochem.* 71, 1306–1312.
- Abaza, L., Ben Youssef, N., Manai, H., Mahjoub Haddada, F., Methenni, K., Zarrouk, M., 2011. Chétoui olive leaf extracts: influence of the solvent type on phenolics and antioxidant activities. *Grasas y Aceites* 62, 96–104.
- Arráez-Román, D., Sawalha, S., Segura-Carretero, A., Menéndez, J., Fernández-Gutiérrez, A., 2008. Identification of phenolic compounds in olive leaves using CE-ESI-TOF-MS. *Food Eng. hi-tec.* 19, 18–22.
- Barrajón-Catalána, E., Fernández-Arroyo, S., Saura, D., Guillén, E., Fernández-Gutiérrez, A., Segura-Carretero, A., Micó, V., 2010. Cistaceae aqueous extracts containing ellagitannins show antioxidant and antimicrobial capacity, and cytotoxic activity against human cancer cells. *Food Chem. Toxicol.* 48, 2273–2282.
- Benavente-García, O., Castillo, J., Lorente, J., Ortuño, A., Del Rio, J.A., 2000. Antioxidant activity of phenolics extracted from *Olea europaea* L. leaves. *Food Chem.* 68, 457–462.
- Boonkirk, S., Phisalaphong, C., Phisalaphong, M., 2008. Ultrasound-assisted extraction of capsaicinoids from *Capsicum frutescens* on a lab- and pilot-plant scale. *Ultrasonics Sonochemistry* 15, 1075–1079.
- Bouallagui, Z., Han, J., Isoda, H., Sayadi, S., 2011. Hydroxytyrosol rich extract from olive leaves modulates cell cycle progression in MCF-7 human breast cancer cells. *Food Chem. Toxicol.* 49, 179–184.
- Bouaziz, M., Fki, I., Jemai, H., Ayadi, M., Sayadi, S., 2008. Effect of storage on refined and husk olive oils composition: Stabilization by addition of natural antioxidants from Chemlali olive leaves. *Food Chem.* 108, 253–262.
- Briante, R., Patumi, M., Terenziani, S., Bismuto, E., Febbraio, F., Nucci, R., 2002. *Olea europaea* L. leaf extract and derivatives: antioxidant properties. *J. Agric. Food. Chem.* 50, 4934–4940.
- Campanero, M.A., Escobar, M., Pérez, G., García-Quetglas, E., Sadaba, B., Ramón Azanza, J., 2010. Simultaneous determination of diosmin and diosmetin in human plasma by ion trap liquid chromatography-atmospheric pressure chemical ionization tandem mass spectrometry: application to a clinical pharmacokinetic study. *J. Pharm. Biomed. Anal.* 51, 875–881.
- Cárcel, J.A., García-Pérez, J.V., Mulet, A., Rodríguez, L., Riera, E., 2010. Ultrasonic assisted antioxidant extraction from grape stalks and olive leaves. *Physics Procedia* 3, 147–152.
- De Leonards, A., Aretini, A., Alfano, G., Macciola, V., Ranalli, G., 2008. Isolation of a hydroxytyrosol-richextract from olive leaves (*Olea Europaea* L.) and evaluation of its antioxidant properties and bioactivity. *Eur. Food Res. Technol.* 226, 653–659.
- Efferth, T., Koch, E., 2011. Complex interactions between phytochemicals. The multi-target therapeutic concept of phytotherapy. *Curr. Drug Targets* 12, 122–132.
- Erbay, Z., Icier, F., 2010. The importance and potential uses of olive leaves. *Food Rev. Int.* 26 (4), 319–334.
- Fu, S., Arráez-Roman, D., Segura-Carretero, A., Menéndez, J.A., Menéndez-Gutiérrez, M.P., Micó, V., Fernández-Gutiérrez, A., 2010. Qualitative screening of phenolic compounds in olive leaf extracts by hyphenated liquid chromatography and preliminary evaluation of cytotoxic activity against human breast cancer cells. *Anal. Bioanal. Chem.* 397 (2), 643–654.
- García-Villalba, R., Carrasco-Pancorbo, A., Oliveras-Ferraro, C., Vázquez-Martín, A., Menéndez, J.A., Segura-Carretero, A., Fernández-Gutiérrez, A., 2010. Characterization and quantification of phenolic compounds of extra-virgin olive oils with antioxidant properties by a rapid and resolute LC-ESI-TOF MS method. *J. Pharm. Biomed. Anal.* 51, 416–429.
- Granados-Principial, S., Quiles, J.L., Ramírez-Tortosa, C.L., Sanchez-Rovira, P., Ramírez-Tortosa, M.C., 2010. New advances in molecular mechanisms and the prevention of adriamycin toxicity by antioxidant nutrients. *Food Chem. Toxicol.* 48, 1425–1438.
- Hashim, Y.Z., Rowland, I.R., McGlynn, H., Servili, M., Selvaggini, R., Taticchi, A., Esposto, S., Montedoro, G., Kaisalo, L., Wähälä, K., Gill, C.I., 2008. Effects of olive

- oil phenolics on invasion in human colon adenocarcinoma cells in vitro. *Int. J. Cancer.* 122 (3), 495–500.
- Herrero, M., Mendiola, J.A., Cifuentes, A., Ibáñez, E., 2010a. Supercritical fluid extraction: recent advances and applications. *J. Chromatogr. A* 1217, 2495–2511.
- Herrero, M., Plaza, M., Cifuentes, A., Ibáñez, E., 2010b. Green processes for extraction of bioactives from Rosemary. Chemical and functional characterization via UPLC-MS/MS and in-vitro assays. *J. Chromatogr. A* 1217, 2512–2520.
- Herrero, M., Temirzoda, T.N., Segura-Carretero, A., Quirantes, R., Plaza, M., Ibáñez, E., 2011. New possibilities for the valorization of olive oil by-products. *J. Chromatogr. A* 1218 (42), 7511–7520.
- Ibáñez, E., Oca, A., De Murga, G., López-Sébastián, S., Tabera, J., Reglero, G., 1999. Supercritical fluid extraction and fractionation of different pre-processed rosemary plants. *J. Agric. Food Chem.* 47, 1400–1404.
- Lee-Huang, S., Zhang, L., Huang, P.L., Chang, Y.T., Huang, P.L., 2003. Anti-HIV activity of olive leaf extract (OLE) and modulation of host cell gene expression by HIV-1 infection and OLE treatment. *Biochem. Biophys. Res. Commun.* 307, 1029–1037.
- Lozano-Sánchez, J., Segura-Carretero, A., Menéndez, J.A., Oliveras-Ferraro, C., Cerretani, L., Fernández-Gutiérrez, A., 2010. Prediction of extra virgin olive oil varieties through their phenolic profile. Potential cytotoxic activity against human breast cancer cells. *J. Agric. Food Chem.* 58 (18), 9942–9955.
- Markin, D., Duek, L., Berdicevsky, I., 2003. In vitro antimicrobial activity of olive leaves. *Mycoses* 46, 132–136.
- Mendiola, J.A., Herrero, M., Cifuentes, A., Ibáñez, E., 2007. Sample treatments prior to capillary electrophoresis-mass spectrometry. *J. Chromatogr. A* 1152, 234–246.
- Meirinhos, J., Silva, B.M., Valentao, P., Seabra, R.M., Pereira, J.A., Dias, A., Andrade, P.B., Ferreres, F., 2005. Analysis and quantification of flavonoidic compounds from Portuguese Olive (*Olea europaea* L.) leaf cultivars. *Nat. Prod. Res.* 19, 189–195.
- Menéndez, J.A., Vazquez-Martin, A., Colomer, R., brunet, J., Carrasco-Pancorbo, A., García-Villalba, R., Fernandez-Gutierrez, A., Segura-Carretero, A., 2007. Olive oil's bitter principle reverses acquired autoresistance to trastuzumab (Herceptin) in HER2-overexpressing breast cancer cells. *BMC Cancer* 7, 80.
- Menéndez, J.A., Vazquez-Martin, A., Oliveras-Ferraro, C., García-Villalba, R., Carrasco-Pancorbo, A., Fernandez-Gutierrez, A., Segura-Carretero, A., 2009. Extra-virgin olive oil polyphenols inhibit HER2 (erbB-2)-induced malignant transformation in human breast epithelial cells: relationship between the chemical structures of extra-virgin olive oil secoiridoids and lignans and their inhibitory activities on the tyrosine kinase activity of HER2. *Int. J. Oncol.* 34, 43–51.
- Mylonaki, S., Klassos, E., Dimitris, P., Makris, Panagiotis K., 2008. Optimisation of the extraction of olive (*Olea europaea*) leaf phenolics using water/ethanol-based solvent systems and response surface methodology. *Anal. Bioanal. Chem.* 392, 977–985.
- Pangarkar, V. G. 2008. Microdistillation, Thermomicrodistillation and Molecular Distillation Techniques. In Extraction technologies for medicinal and aromatic plants. Eds. Sukhdev Swami Handa, Suman Preet, Singh Khanuja, Gennaro Longo, Dev Dutt Rakesh. International centre for science and high technology, Trieste, 129–143.
- Plaza, M., Herrero, M., Cifuentes, A., Ibáñez, E., 2009. Innovative natural functional ingredients from microalgae. *J. Agric. Food Chem.* 57, 7159–7170.
- Plaza, M., Amigo-Benavent, M., del Castillo, M.D., Ibáñez, E., Herrero, M., 2010. Facts about the formation of new antioxidants in natural samples after subcritical water extraction. *Food Res. Int.* 43, 2341–2348.
- Rada, M., Guinda, A., Cayuela, J. 2007. Solid/liquid extraction and isolation by molecular distillation of hydroxytyrosol from *Olea europaea* L. leaf. *Eur. J. Lipid. Sci. Technol.* 109, 1071–1076.
- Ramos, J.J., Dietz, C., González, M.J., Ramos, L., 2007. Miniaturised selective pressurised liquid extraction of polychlorinated biphenyls from food stuffs. *J. Chromatogr. A* 1152, 254–261.
- Schütz, E., 2007. Supercritical fluids and applications – a patent review. *Chem. Eng. Technol.* 30, 685–688.
- Taamalli, A., Arráez-Román, D., Ibáñez, E., Zarrouk, M., Segura-carretero, A., Fernández-Gutiérrez, A., 2012. Optimization of microwave-assisted extraction for the characterization of olive leaf phenolic compounds by using HPLC-ESI-TOF-MS/IT-MS2. *J. Agric. Food Chem.* 60, 791–798.
- Tanahashi, T., Sakai, T., Takenaka, Y., Nagakura, N., Chen, C.C., 1999. Structure elucidation of two secoiridoid glucosides from *Jasminum officinale* L. var. *grandiflorum* (L.) Kobuski. *Chem. Pharm. Bull.* 47, 1582–1586.
- Tanner, M., Kapanen, A.I., Junnila, T., Raheem, O., Grennan, S., Elo, J., Elenius, K., Isola, J., 2004. Characterization of a novel cell line established from a patient with Herceptin-resistant breast cancer. *Mol. Cancer Ther.* 3, 1585–1.
- Terigar, B.G., Balasubramanian, S., Sabliov, C.M., Lima, M., Boldor, D., 2011. Soybean and rice bran oil extraction in a continuous microwave system: from laboratory- to pilot-scale. *J. Food Eng.* 104, 208–217.
- Tura, D., Robards, K., 2002. Sample handling strategies for the determination of biophenols in food and plants. *J. Chromatogr. A* 975, 71–93.
- Wagner, H., 2011. Synergy research: approaching a new generation of phytopharmaceuticals. *Fitoterapia* 82, 34–37.



## Xenohormetic and anti-aging activity of secoiridoid polyphenols present in extra virgin olive oil

A new family of gerosuppressant agents

Javier A. Menendez,<sup>1,2,†,‡,\*</sup> Jorge Joven,<sup>3,†,‡,\*</sup> Gerard Aragonès,<sup>3</sup> Enrique Barrajón-Catalán,<sup>4</sup> Raúl Beltrán-Debón,<sup>3</sup> Isabel Borrás-Linares,<sup>5,6</sup> Jordi Camps,<sup>3</sup> Bruna Corominas-Faja,<sup>1,2</sup> Sílvia Cuñí,<sup>1,2</sup> Salvador Fernández-Arroyo,<sup>5,6</sup> Anabel García-Heredia,<sup>3</sup> Anna Hernández-Aguilera,<sup>3</sup> María Herranz-López,<sup>4</sup> Cecilia Jiménez-Sánchez,<sup>5,6</sup> Eugeni López-Bonet,<sup>2,7</sup> Jesús Lozano-Sánchez,<sup>5,6</sup> Fedra Luciano-Mateo,<sup>3</sup> Begoña Martín-Castillo,<sup>2,8</sup> Vicente Martín-Paredero,<sup>3</sup> Almudena Pérez-Sánchez,<sup>4</sup> Cristina Oliveras-Ferraro,<sup>1,2</sup> Marta Riera-Borrull,<sup>3</sup> Esther Rodríguez-Gallego,<sup>3</sup> Rosa Quirantes-Piné,<sup>5,6</sup> Anna Rull,<sup>3</sup> Laura Tomás-Menor,<sup>4</sup> Alejandro Vazquez-Martín,<sup>1,2</sup> Carlos Alonso-Villaverde,<sup>3</sup> Vicente Micol<sup>4</sup> and Antonio Segura-Carretero<sup>5,6,‡,\*</sup>

<sup>1</sup>Metabolism and Cancer Group; Translational Research Laboratory; Catalan Institute of Oncology, Girona, Spain; <sup>2</sup>Girona Biomedical Research Institute; Girona, Spain; <sup>3</sup>Unitat de Recerca Biomèdica (URB-CRB); Institut d'Investigació Sanitària Pere Virgili (IISPV); Universitat Rovira i Virgili; Reus, Spain; <sup>4</sup>Molecular and Cellular Biology Institute (IBMC); Miguel Hernández University; Elche, Spain; <sup>5</sup>Department of Analytical Chemistry; Faculty of Sciences; University of Granada; Granada, Spain; <sup>6</sup>Research and Development of Functional Food Centre (CIDAF); Health Science Technological Park; Granada, Spain; <sup>7</sup>Department of Anatomical Pathology; Dr Josep Trueta University Hospital; Girona, Spain; <sup>8</sup>Clinical Research Unit; Catalan Institute of Oncology; Girona, Spain

<sup>†</sup>These authors contributed equally to this work.

<sup>‡</sup>These authors share co-senior authorship.

**A**ging can be viewed as a quasi-programmed phenomenon driven by the overactivation of the nutrient-sensing mTOR gerogene. mTOR-driven aging can be triggered or accelerated by a decline or loss of responsiveness to activation of the energy-sensing protein AMPK, a critical gerosuppressor of mTOR. The occurrence of age-related diseases, therefore, reflects the synergistic interaction between our evolutionary path to sedentarism, which chronically increases a number of mTOR activating gero-promoters (e.g., food, growth factors, cytokines and insulin) and the “defective design” of central metabolic integrators such as mTOR and AMPK. Our laboratories at the Bioactive Food Component Platform in Spain have initiated a systematic approach to molecularly elucidate and clinically explore whether the “xenohormesis hypothesis,” which states that stress-induced synthesis of plant polyphenols and many other phytochemicals provides an environmental chemical signature that upregulates stress-resistance pathways in plant consumers, can be explained in terms of the reactivity of the AMPK/mTOR-axis

to so-called xenohormetins. Here, we explore the AMPK/mTOR-xenohormetic nature of complex polyphenols naturally present in extra virgin olive oil (EVOO), a pivotal component of the Mediterranean style diet that has been repeatedly associated with a reduction in age-related morbid conditions and longer life expectancy. Using crude EVOO phenolic extracts highly enriched in the secoiridoids oleuropein aglycon and decarboxymethyl oleuropein aglycon, we show for the first time that: (1) The anticancer activity of EVOO secoiridoids is related to the activation of anti-aging/cellular stress-like gene signatures, including endoplasmic reticulum (ER) stress and the unfolded protein response, spermidine and polyamine metabolism, sirtuin-1 (SIRT1) and NRF2 signaling; (2) EVOO secoiridoids activate AMPK and suppress crucial genes involved in the Warburg effect and the self-renewal capacity of “immortal” cancer stem cells; (3) EVOO secoiridoids prevent age-related changes in the cell size, morphological heterogeneity, arrayed cell arrangement and senescence-associated β-galactosidase staining of normal diploid human

**Keywords:** hormesis, xenohormesis, olive oil, cancer, aging, mTOR, AMPK, resveratrol, gerogenes, gerosuppression

Submitted: 01/09/13

Accepted: 01/23/13

<http://dx.doi.org/10.4161/cc.23756>

\*Correspondence to: Javier A. Menendez, Jorge Joven and Antonio Segura-Carretero; Email: jmenendez@idibgi.org or jmenendez@iconologia.net, jjoven@grupsagessa.com, jorge.joven@urv.cat and ansegura@ugr.es

fibroblasts at the end of their proliferative lifespans. EVOO secoiridoids, which provide an effective defense against plant attack by herbivores and pathogens, are bona fide xenohormetins that are able to activate the gerosuppressor AMPK and trigger numerous resveratrol-like anti-aging transcriptomic signatures. As such, EVOO secoiridoids constitute a new family of plant-produced gerosuppressant agents that molecularly “repair” the aimless (and harmful) AMPK/mTOR-driven quasi-program that leads to aging and aging-related diseases, including cancer.

Plants have been used for medicinal purposes for thousands of years. A third of the 20 most widely sold drugs on the market are plant-derived, and new molecules that may be beneficial for health are rapidly being discovered.<sup>1-4</sup> The global economy and human health both depend in part on the discovery of new and effective medicines. Surprisingly, little effort has been focused on plants that are known to synthesize molecules beneficial to the health of other organisms. One of the reasons for this lack of attention is the ease of patenting new synthetic drugs (known as “new chemical entities”); another is the “impurity” (non-specificity) of plant-derived biocompounds. A compound is considered “non-specific” if it interacts with a number of endogenous proteins. A priori, a plant-derived compound that interacts with several molecular targets may have an imperceptible effect (or even an adverse effect) compared with a pure molecule that interacts specifically with a particular protein.<sup>1-4</sup> However, a number of plant molecules interact with enzymes and receptors in ways that are not harmful. By the 5th century B.C.E., Hippocrates had described salicylic acid as “a bitter powder extracted from the willow that relieves pain and reduces fevers.”<sup>5,6</sup> In 1763, Reverend Edward Stone experimented with the bark of the white willow (*Salix alba*) to treat fever and concluded that it was “a very effective remedy.”<sup>6,7</sup> Since then, a variety of salicylates have been isolated from plants and used in the treatment of goiter, rheumatic fever, pain and arthritis. Today, 45,000 t of aspirin, an acetylated salicylic acid derivative, is produced each year.

Aspirin is just one example of the dozens of plant-derived compounds that are now known to be beneficial to human health and that, furthermore, interact with more than one molecular target. Curiously, salicylate has been shown to activate adenosine monophosphate-activated protein kinase (AMPK),<sup>8,9</sup> which is a key therapeutic target for the treatment of obesity, type 2 diabetes and cancer due to its role as a central regulator of lipid and glucose metabolism<sup>10-12</sup> and as a critical modulator of aging through its interactions with mTOR, SIRT1 and the sestrins.<sup>13-24</sup>

### Hormesis

Living organisms continually face adverse situations or harmful stimuli. Adaptation to these external aggressors, whether chemical, physical, biological or social, is paramount to survival. In addition, mild exposure to a stimulus that could be harmful at high concentrations might confer subsequent resistance or tolerance to some aggression, even one brought about by the stimulus itself. This adaptive response to stress has been identified as an evolutionarily conserved process. In toxicology, the term hormesis is used to define a two-phase nonlinear biological response in which exposure to a low dose of or weak stimulus by an environmental toxin or harmful substance produces a potentially beneficial effect, while a high dose leads to adverse effects.<sup>25-30</sup> In the biomedical field, hormesis refers to an adaptive response of cells and organisms to a moderate or intermittent stressor.<sup>31-34</sup> Thus, hormesis could be defined as a process in which exposure to a low dose of an environmental factor or chemical compound that is harmful at high concentrations has a beneficial and adaptive effect on the cell or organism. Furthermore, hormesis represents an essential concept in evolution, because it offers a possible explanation for how life on this planet has adapted to an environment that is at times particularly aggressive. To overcome environmental stresses, organisms might have developed a variety of cell signaling pathways that mediate hormetic responses.<sup>35-38</sup> These include transcription factors and the kinases that regulate them, which modulate the expression of genes that encode cytoprotective

and stress-response proteins such as chaperones and antioxidant and detoxifying enzymes, among others.

Many animal studies involving dietary restriction (DR) regimens such as caloric restriction (CR), total-nutrient restriction, alternate-day fasting and short-term fasting have shown that DR can increase the resistance of the cells of these animals to various types of stress.<sup>39-50</sup> For example, mortality due to natural causes or induced by temperature or specific toxins is significantly reduced in animals subjected to CR compared with animals consuming a normal diet. Reduced caloric intake may also protect animals from various types of cancer, including pancreatic, mammary and prostate cancer.<sup>51-57</sup> In humans, alternate-day fasting improves symptoms and reduces markers of inflammation and oxidative stress in asthma patients, retards the growth of tumors and sensitizes a range of cancer cell types to chemotherapy.<sup>58-60</sup> By considering CR without malnutrition to be a “mild dietary stress,” the ability of CR to prevent or lessen the severity of cancer, stroke, coronary heart disease, autoimmune disease, allergy, Parkinson disease and Alzheimer disease has been largely considered to represent an “overcompensation” resulting from hormetic mechanisms.<sup>61</sup>

### Xenohormesis

Another well-known example of a hormetic process is exposure to low concentrations of certain phytochemicals. Organisms appear to have evolved the ability to detect stress markers produced by other species in their habitats. In this way, organisms might prepare themselves in anticipation of potential adverse environmental conditions. This inter-species hormesis is known as xenohormesis, the phenomenon in which an organism detects the chemical signals of another species regarding the state of the immediate environment or the availability of food.<sup>62-66</sup> This hormetic process generates beneficial effects for the organism. The existence of xenohormesis might explain how chemical compounds produced by plants and other autotrophs to defend against adverse environmental conditions can produce beneficial effects in the heterotrophs (animals and fungi) that consume them. Animals take

advantage of the information contained in specific compounds produced by plants in response to stress. In fact, the majority of the known beneficial health effects of edible plants are attributed to molecules produced in response to stress.

Plant stress responses have evolved over millions of years. Because most plants cannot move physically, they must tolerate environmental stresses that may appear at any moment. This type of "sedentary lifestyle" may explain the complexity of the stress response in plants. Plants produce toxins to protect themselves against fungi, insects and predators. Plants cultivated for consumption contain fewer natural toxins than their wild counterparts. When plants grow under aggressive conditions, one observes an increase in the production of natural pesticides (biopesticides) that can produce acute intoxication in humans. Some studies have estimated that more than 90% of pesticides present in the human diet are chemical compounds that are produced by plants to protect themselves. Therefore, xenohormesis could explain how the sophisticated stress response that has evolved as a result of the stationary lifestyle of plants can confer stress resistance and survival benefits to animals that consume bioactive compounds produced by environmentally stressed plants.<sup>63</sup> While xenohormetic compounds are harmful to insects and microorganisms, the sub-toxic levels at which humans ingest them appear to result in moderate cellular stress responses. This, in turn, might activate stress-response adaptation pathways, leading to increased expression of genes that encode cytoprotective proteins such as antioxidant enzymes, chaperones, growth factors, phase 2 detoxification enzymes and mitochondrial proteins. In this scenario, the ability of a combination of anti-oxidant/anti-inflammatory polyphenols found in many fruits and vegetables to slow aging<sup>67</sup> can be explained by molecular mechanisms that are largely unrelated to any potential antioxidant properties. For example, dietary flavonoids such as quercetin and blueberry polyphenols, among others, have been shown to modulate the lifespan of simple model organisms by activating molecular mechanisms independent of their antioxidant capacity.<sup>68-74</sup>

Polyphenols found in tea and curcumin interact with dozens of molecular targets, providing many health benefits unrelated to their antioxidant properties.<sup>75-85</sup> In this regard, the natural polyphenolic compound resveratrol (3,5,4'-trihydroxystilbene) has emerged as a still-debatable mediator of longevity that certainly delays or attenuates many age-related chronic diseases in animal models.<sup>86-106</sup> Currently, activation of AMPK<sup>15,107-110</sup> rather than activation of the deacetylase SIRT1 seems to be a/the major effect of resveratrol, providing a plausible explanation for many of the health benefits of this compound that have been reported to date.

### **Extra Virgin Olive Oil (EVOO) Polyphenols And Xenohormesis: A Forgotten Scenario**

We are beginning to accumulate epidemiological, clinical and experimental evidence suggesting that consumption of phenolic-enriched fruits, vegetables and herbs might reduce the risk of chronic diseases, including human malignancies.<sup>111-113</sup> In this regard, it has been repeatedly suggested that the ability of the so-called "Mediterranean diet" (i.e., the dietary patterns found in olive-growing areas of the Mediterranean basin) to significantly reduce the incidence of atherosclerosis and cardiovascular disease and decrease the risk of several types of human carcinomas, including breast cancer,<sup>114-118</sup> can be largely attributed to the unique characteristics of extra virgin olive oil (EVOO), which is an integral ingredient of the traditional Mediterranean diet and is the juice of the olive obtained solely by mechanical means and consumed without any further refining process other than washing, filtration, decantation or centrifugation. Apart from the health benefits that can be expected from EVOO as the richest source of the monounsaturated fatty acid (MUFA) oleic acid (OA; 18:1n-9),<sup>119</sup> cold-pressed EVOO includes minor components such as aliphatic and triterpenic alcohols, sterols, hydrocarbons, volatile compounds and several antioxidants.<sup>120-126</sup> Although tocopherols and carotenoids are also present, hydrophilic phenolics represent the most abundant family of bioactive EVOO compounds.

As for many plant-derived polyphenols, it has been largely assumed that EVOO-derived complex phenols such as lignans, flavonoids and secoiridoids<sup>127-130</sup> provide health benefits, primarily due to their antioxidant activity.<sup>131-133</sup> However, the antioxidant capacity of EVOO polyphenols does not directly correlate with their efficacy in terms of bioactivity (e.g., toxicity against cultured cancer cells). Moreover, when EVOO is provided in the diet, plasma concentrations of polyphenols are often lower than the levels required for protection against oxidation. Although the metabolites of EVOO polyphenols may reach concentrations in the bloodstream that are several-fold higher than that found in EVOO, EVOO polyphenol-derived compounds tend to have significantly decreased antioxidant activity compared with the parental compounds.<sup>63,134</sup> As an alternative to general mechanisms related to the antioxidant and/or trapping activity of oxygen radicals commonly observed with many plant-derived phenolics, recent studies have demonstrated that complex polyphenols can exert anti-carcinogenic effects by directly modulating the activities of various types of oncoproteins.<sup>135-140</sup> The results from our laboratory support the idea that EVOO-derived complex polyphenols constitute a previously unrecognized family of anticancer phytochemicals that have a significant impact on the proliferation and survival of cancer cells, at least in part through the specific suppression of protein activities, gene expression and/or signal transduction events closely related to the malignant phenotype.<sup>129,141-149</sup>

Although a Mediterranean diet and, more specifically, EVOO consumption have both been associated with increased longevity in the human population,<sup>150-156</sup> few studies have attempted to explore in depth the ultimate molecular mechanisms by which EVOO may influence longevity; for the most part, it has been assumed that these effects are the result of the antioxidant potential of its phenolic compounds and other free-radical scavengers, such as vitamin E.<sup>157</sup> However, if it is accepted that aging is not caused by reactive oxygen species (ROS), which are instead associated with longevity,<sup>40,158-178</sup> why have scientists not yet rejected the commonly accepted

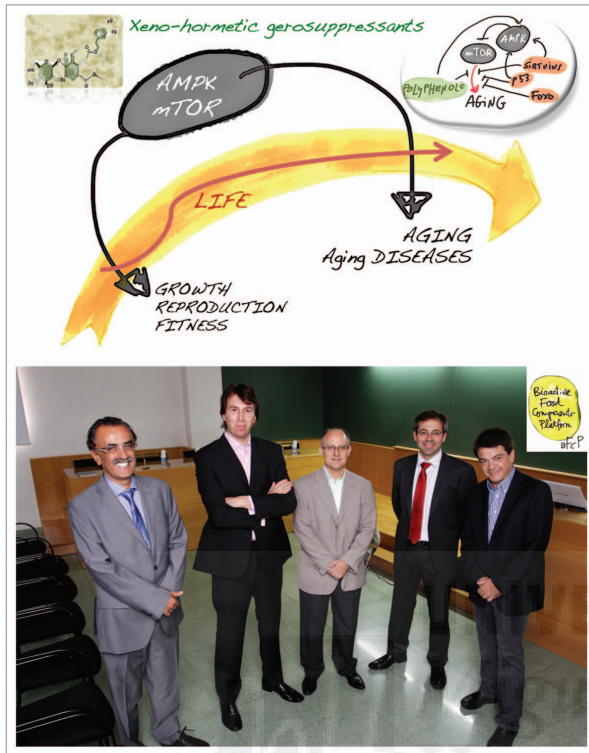


**Figure 1.** The Bioactive Food Component Platform (BFCP), Spain. The Spanish BFCP has two main goals: first, to molecularly elucidate the cellular and physiological abilities of humans to take advantage of the health benefits chemically encrypted within plant-derived biocompounds; second, to translate the sophisticated stress response of plants, which has evolved as a result of their stationary lifestyle, to the clinical arena to combat human aging and age-related diseases. Both goals of the BFCP revolve around the assumption that age-related diseases (e.g., atherosclerosis, diabetes, cancer, and others) reflect the synergistic interaction between our evolutionary path to sedentarism, which chronically increases a number of mTOR activating gero-promoting factors (e.g., nutrients, growth factors, cytokines, insulin), and the “defective design” of central metabolic integrators such as mTOR and AMPK. Design defects in the metabolic nature of the antagonistic pleiotropy model of aging involve both the ability of the mTOR gerogene to continue, in an aimless (and harmful) manner, a developmental program that was beneficial early in life but was not switched off upon its completion, and the necessary weakness of gerosuppressor genes such as AMPK that antagonize the gerogenic mTOR pathway (i.e., the responsiveness of AMPK signaling should clearly decline with aging, because robust, continuous activation of AMPK in response to cellular stresses will result in accelerated aging).<sup>354,355</sup> The BFCP therefore aims to revisit the xeno-hormesis hypothesis in terms of clinically valuable plant-produced gerosuppressant agents that molecularly “repair” the aimless (and harmful) AMPK/mTOR-driven quasi-program of aging and aging-related diseases (top panel). The BFCP integrates five multidisciplinary teams of biologists, biochemists, chemists, pharmacists, physicians, and engineers to research, design, and develop anti-aging biomedical strategies based on plant-derived gerosuppressants. From left to right in the bottom photograph are Dr Jorge Joven (Universitat Rovira i Virgili, Reus, Spain), Dr Javier A. Menendez (Catalan Institute of Oncology, Girona, Spain), Dr Vicente Micol (Miguel Hernández University, Elche, Spain), Dr Antonio Segura-Carretero (University of Granada, Granada, Spain), and Dr Carlos Alonso-Villaverde (Universitat Rovira i Virgili, Reus, Spain). (The original painting in the top panel is from Dr Jorge Joven based on Fig. 3, ref. 311 by Dr Mikhail V. Blagosklonny; the BFCP team photograph in the bottom panel is by photographer Pere Ferré, Tarragona, Spain).

view that the anti-aging benefits of EVOO phenolics are simply due to their antioxidant potential? Even more intriguing is the fact that, despite the structural resemblance of EVOO complex polyphenols to some of the hormetic polyphenols mentioned above (e.g., resveratrol), none of the phenolic components naturally present in EVOO have been characterized in terms of their potential to extend lifespan. An exception is a recently published study by Cafueño and colleagues<sup>179</sup> suggesting that tyrosol, a phenol present in EVOO, may increase lifespan and stress resistance in *Caenorhabditis elegans*, likely through the activation of hormetic mechanisms.

Our laboratories at the Bioactive Food Component Platform (BFCP) in Spain (Fig. 1) have recently begun a systematic approach to evaluate for the first time whether secoiridoids, a family of complex phenols found in Oleaceae plants that structurally resemble well-known anti-aging molecules such as resveratrol, are bona fide xeno-hormetic compounds that significantly impact pivotal signal-transduction pathway(s) (i.e., gerogenes and/or gerosuppressors) that drive(s) most, if not all, aging-related diseases. Dr Blagosklonny has recently proposed that “hormesis does not make sense except in the light of TOR-driven aging.”<sup>180</sup> Instead of purposely reconciling hormesis with the conventional view on aging (i.e., aging is a decline and/or a deterioration due to the accumulation of random molecular and cellular damage), Dr Blagosklonny proposes that, because aging is an aimless quasi-programmed phenomenon that is driven by overactivated gerogenes belonging to the nutrient-sensing mTOR (mammalian target of rapamycin) pathway (e.g., mTOR, S6K), the mTOR pathway limits lifespan by accelerating age-related diseases (Fig. 1). Therefore, in humans (and other mammals), age-related diseases represent hyperfunctional phenotypes of mTOR-driven aging that actually limit lifespan. Understandably, if mTOR gerogene activity limits lifespan by accelerating the progression of age-related diseases, such as atherosclerosis or cancer, direct or indirect pharmacological suppression of mTOR-driven aging via the activation of mTOR gerosuppressors such as AMPK would be expected to increase healthy lifespan. In this scenario,

Dr Blagosklonny differentiates two types of hormesis, namely, “increasing aging tolerance” or “hormesis B,” which does not affect the aging process itself, and “slowing-down aging” or “hormesis A,” which does affect the aging process by directly inhibiting mTOR activity (e.g., CR, rapamycin, resveratrol, metformin) or by imitating mTOR inhibition (e.g., heat shock). We obviously rejected the idea that EVOO secoiridoids could increase aging tolerance, which may allow an organism to survive catastrophes caused by aging-related diseases. In a “hormesis A” scenario, we hypothesized the following: (1) The anticancer activity of EVOO secoiridoid polyphenols results from the activation of anti-aging-like gene signatures in cancer cells (i.e., the enhancement of cellular stress mechanisms suppresses the hyperfunctional phenotype of immortal cells). (2) EVOO-derived secoiridoids activate the energy-sensing AMPK gerosuppressor (i.e., EVOO secoiridoids operates as AMPK-activating low-energy mimickers). (3) Chronic exposure to EVOO secoiridoid polyphenols efficiently delays the senescence phenotype in normal diploid human fibroblasts (i.e., the agonistic activity of EVOO secoiridoids toward the AMPK gerosuppressor improves the structural and functional integrity of normal cells without promoting their entrance into a potentially deleterious hyperproliferative mode).

In this paper, we present the first body of experimental evidence suggesting that EVOO secoiridoid polyphenols, by acting as biocompounds that belong to the recently defined group of “hormesis A” compounds, can efficiently promote cytotoxicity in human cancer cells through the paradoxical activation of anti-aging/cellular stress-like gene signatures, which, in turn, significantly weaken age-related effects (e.g., cellular senescence) in normal human diploid fibroblasts.

### **Secoiridoid-Rich EVOO Phenolic Fractions Activate Resveratrol-Like Anti-Aging Transcriptomic Signatures in Cancer Cells**

We previously reported that the cytotoxic potencies of individual phenolic extracts (PE) from a variety of EVOO

monovarietals were positively related to the relative content of secoiridoids, a group of complex polyphenols.<sup>145,146</sup> Highly active EVOO PEs were notably enriched in secoiridoids (Fig. 2), whereas substitution of secoiridoids by other complex polyphenols, such as lignans, in PE mixtures was related to a loss of tumoricidal activity. To identify the key pathways and functions associated with the anti-tumoral activity of crude PE isolated from individual EVOO monovarietals, we performed genome-wide analyses in which we compared the global transcriptomic profiles of JIMT1 breast cancer cells using whole human genome microarrays. RNA was extracted and prepared from metastatic JIMT1 breast cancer cells that had been cultured for 6 h at 70% confluence in the absence or presence of four different EVOO PEs exhibiting the following cytotoxic potencies: EVOO-PE7 > EVOO-PE3 > EVOO-PE10 > > EVOO-PE12, as determined by MTT-based cell viability assays after 5 d exposure to EVOO PEs.<sup>145,146</sup> After RNA hybridization to an Agilent 44K (double-density) Whole Human Genome Oligo Microarray containing 45,220 features (probes) representing 41,000 unique human genes and transcripts, the normalized and filtered data from all experimental groups were analyzed simultaneously using the SAM algorithm. We set the significance cut-off at a median FDR of < 5.0%. When we used a 2.0-fold change cut-off relative to the transcriptome of untreated control cells to identify specific effects of EVOO PEs on gene expression, we observed that JIMT1 cancer cells treated with the EVOO PE with the lowest secoiridoid content (PE12) had the lowest number of altered genes (Fig. 3). Of note, while the total number of altered genes was similar (~400 to 600) after exposure to EVOO PEs with higher secoiridoid content (EVOO-PE7, EVOO-PE3 and EVOO-PE10), there was a trend toward enhanced levels of transcripts of more genes in response to EVOO PEs with higher secoiridoid contents. Intriguingly, the majority of the altered genes (~84%) were upregulated following treatment with EVOO-PE7, the phenolic extract with the highest relative secoiridoid content (Fig. 2; Table S1) and the highest anti-tumoral activity.<sup>146</sup>

When we previously screened the Kyoto Encyclopedia of Genes and Genomes (KEGG) pathway database by performing Gene Set Enrichment Analysis (GSEA) to identify key pathways and functions potentially associated with the anti-tumoral activity of EVOO PEs, we observed that the highly active EVOO-PE7 had a dramatic differential impact on the expression of the *GADD45* stress-response gene family; by contrast, the expression of this family of genes remained largely unchanged upon treatment with EVOO-PE3 or EVOO-PE10.<sup>146</sup> We thus speculated that naturally occurring phenolic mixtures highly enriched in the complex polyphenols oleuropein aglycon (OA) and decarboxymethyl oleuropein aglycon (DOA) (Fig. 2) could lead to enhanced transcript levels of genes that are upregulated by stress. To test this hypothesis, we utilized the “core analysis” function included in the analysis software package Ingenuity pathway analysis (IPA, Ingenuity Systems Inc.) to interpret EVOO-PE7-induced global transcriptomic profiles in the context of biological processes, networks and pathways. The IPA software algorithmically generates networks of up- and downregulated functionally related annotated genes based on their connectivity and assigns a score (i.e., a numerical value that takes into consideration both the number of focus genes in a network and the size of the network to approximate how relevant each network is to the original list of focus genes). Figure 4 illustrates graphically the two gene network functions that were most significantly (score ≥ 3) upregulated (red) and downregulated (green) within the EVOO secoiridoid-induced stress transcriptomic signature in human breast cancer cells.

EVOO secoiridoids activate endoplasmic reticulum (ER) stress chaperones and unfolded protein response (UPR) genes. The primary function of the gene networks that were upregulated by EVOO secoiridoids was related to “cellular function and maintenance and cellular compromise” (score = 49). These gene networks include numerous genes encoding isoforms of constitutively expressed and stress-induced 70-kDa heat shock proteins (Hsp70s), which are chaperones

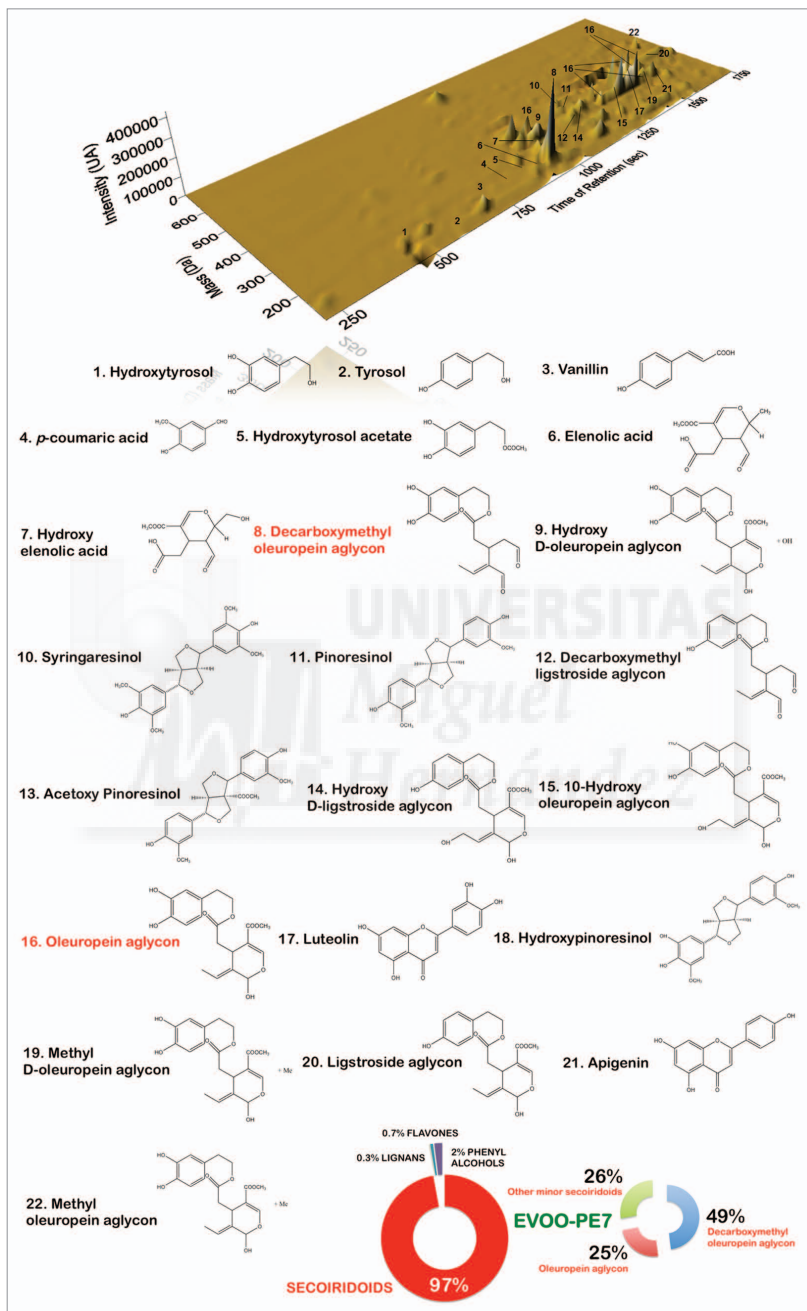


**Figure 2.** Main phenolic compounds identified in EVOO phenolic extracts by HPLC-DAD-ESI-TOF. The figure shows the chemical structures of the main phenolic compounds identified in secoiridoids-rich Picual EVOO variety following protocols described in reference 147. The figure shows also the percent distribution of the main phenolic families identified in the Picual EVOO-PE7.

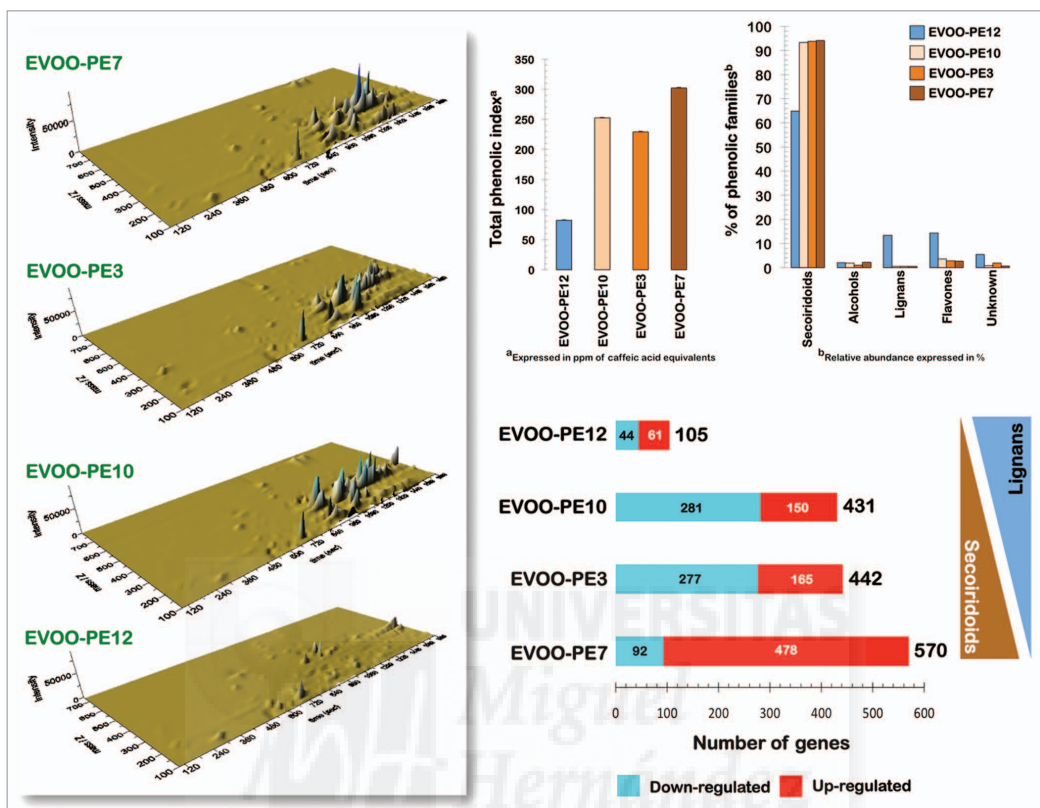


**Figure 3.** Relationship between the distribution of phenolic families in EVOO-PEs and their impact on the whole-genome transcription profile of human breast cancer cells. Total RNA isolated from JIMT1 cells grown in the absence or presence of EVOO-PE12, EVOO-PE10, EVOO-PE3 or EVOO-PE7 (2 µg/mL) for 6 h was extracted with TRIzol reagent (Invitrogen) according to the manufacturer's instructions. RNA quantity and quality were determined using the RNA 6000 Nano Assay kit on an Agilent 2100 BioAnalyzer (Agilent Technologies) as recommended. Whole Human Genome Oligo Microarrays (G4112F) were then hybridized. Briefly, 500 ng of total RNA from each sample was amplified by Oligo-dT-T7 reverse transcription and labeled by in vitro transcription with T7 RNA polymerase in the presence of Cy5-CTP or Cy3-CTP using the Quick And Labeling Kit (Agilent) and purified using RNAeasy columns (Qiagen). After fragmentation, 825 ng of labeled cRNA from each of the two samples were co-hybridized in situ hybridization buffer (Agilent) for 17 h at 65°C and washed at room temperature for 1 min in Gene Expression Wash Buffer 1 (Agilent) and 1 min at 37°C in Gene Expression Wash Buffer 2 (Agilent). The images were generated on a confocal microarray scanner (G2565BA, Agilent) at 5 µm resolution and quantified using GenePix 6.0 (Molecular Dynamics). Spots with signal intensities of at least twice the local background that were not saturated and not flagged by GenePix were considered reliable. Extracted intensities were background-corrected, and the log2 ratios were normalized in an intensity-dependent fashion by the global LOWESS method (intra-chip normalization). Normalized log2 ratios were scaled between arrays to make all data comparable. Raw data were processed using MMARGE, a web implementation of LIMMA, a microarray analysis library developed within the Bioconductor project in the R statistical environment. To identify genes that are differentially expressed, the multiclass SAM procedure (significance analysis of microarrays) was applied. Genes with a q-value (FDR) below 5% and a fold change exceeding 2.0 in absolute value were selected as relevant (see also Table S2).

involved in crucial cellular functions in all kingdoms of life.<sup>181-184</sup> While constitutively expressed Hsp70 chaperones have housekeeping functions (e.g., folding of nascent polypeptides, protein translocation between cellular compartments and degradation of unstable and misfolded proteins), stress-induced Hsp70s prevent

the accumulation of proteins that have become denatured in response to various cellular stresses (e.g., heat stress, radiation, ischemia, heavy metals or other stimuli that activate stress transcription factors). Treatment with the secoiridoid-rich EVOO-PE7 extract markedly (~11-fold) upregulated the expression of the *HSPA6* (Hsp70B') gene, which is strictly inducible with no detectable basal expression.<sup>185,186</sup> Indeed, HSPA6 protein induction is a sensitive biomarker of cellular stress that appears transiently in response to heat stress, whereas levels of *HSPA1A* (Hsp72), which was also induced by EVOO-PE7, persist for days.<sup>187</sup> EVOO-PE7

(*Hsp70B'*) gene, which is strictly inducible with no detectable basal expression.<sup>185,186</sup> Indeed, HSPA6 protein induction is a sensitive biomarker of cellular stress that appears transiently in response to heat stress, whereas levels of *HSPA1A* (Hsp72), which was also induced by EVOO-PE7, persist for days.<sup>187</sup> EVOO-PE7

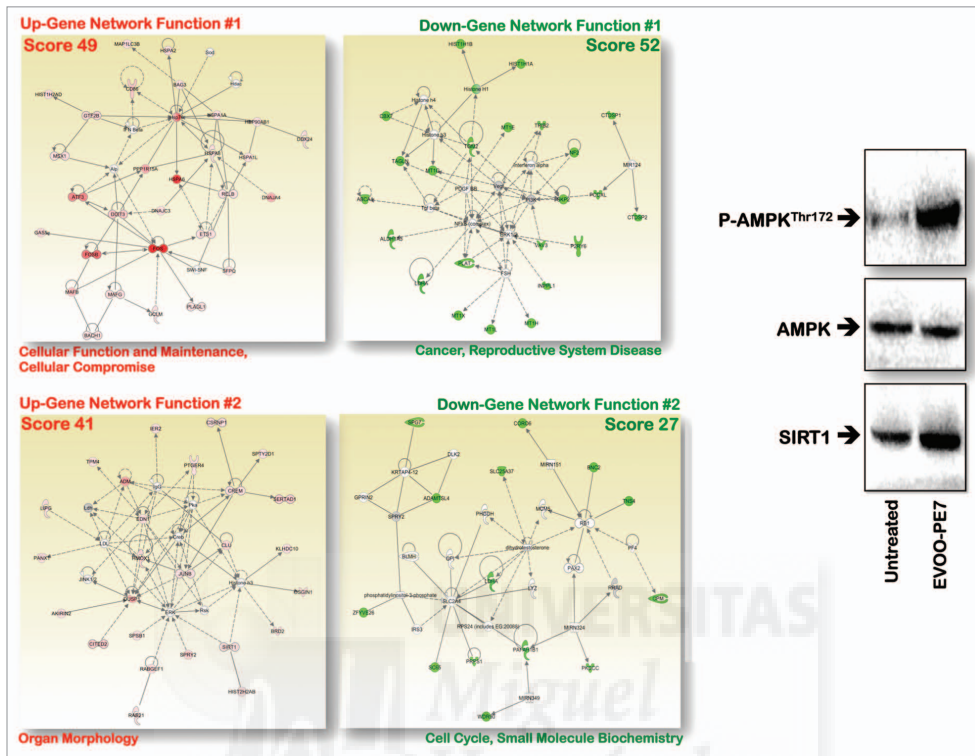


**Figure 4.** Network analysis of EVOO secoiridoids-regulated genes in human breast cancer cells. Left: Gene networks were constructed using ingenuity pathway analysis (Ingenuity® Systems). Data sets containing identifiers of genes with > 2.0-fold up- or downregulatory changes were uploaded into the application. These “focus genes” were overlaid onto a global molecular network developed from information contained in the Ingenuity pathway knowledge base. Networks of these “focus genes” (nodes) are algorithmically generated based on the principle that highly connected gene networks are most biologically meaningful. All edges are supported by at least one reference from the literature stored in the Ingenuity pathway knowledge base (the IPA interaction database is manually curated by scientists and updated quarterly). Briefly, the user-input or “focus genes” gene list is compared with the “global molecular network” (GMN) database, which consists of thousands of genes and interactions. The focus genes are sorted based on highest to lowest connectivity within the GMN; networks of approximately 35 genes are then constructed beginning with the most highly connected focus gene. IPA assigns a p value for a network of size  $n$  and an input focus gene list of size  $f$  by calculating the probability of identifying  $f$  or more focus genes in a randomly selected set of  $n$  genes from the GMN. The intensity of the node color indicates the degree of expression (green scale for downregulated nodes; red scale for upregulated nodes). The score indicates the likelihood that the genes in a network are found together by random chance. Using a 99% confidence interval, scores of  $\geq 3$  are significant. Nodes are displayed using various shapes that represent the functional class of the gene product (diamonds, enzymes; ovals, transcription factors; triangles, kinases; circles, others). A solid line indicates a direct interaction; a dashed line indicates an indirect interaction. A line without an arrowhead indicates binding, and a plus sign indicates that other networks contain this gene product. Figure shows up- and downregulated networks with the two highest IPA score (a composite measure that indicates statistical significance that molecules depicted in the network are interconnected). Right: Representative western blot analyses of SIRT1, total AMPK, and phosphorylated AMPK (fosfo-AMPK $\alpha$ Thr172) in EVOO untreated (control) and secoiridoids-treated JIMT1 breast cancer cells.

secoiridoids enhanced the expression of the *HSPA1L* gene (*Hsp70-hom* or *Hsp70t*), which encodes a constitutively expressed, non-inducible cytosolic protein that is highly abundant in testis,<sup>189,190</sup> and of *HSPA2* (*Hsp70-2*), a constitutively expressed gene that is expressed at high levels in testis, is essential for the maturation of male gametocytes and is linked

to male infertility.<sup>191-194</sup> Importantly, EVOO-PE7 secoiridoids also upregulated the transcriptional expression of the *DNAJA4* and *DNAJC3* genes, which encodes the endoplasmic reticulum (ER)-localized DnaJ family of proteins (ERdj proteins).<sup>195</sup> The induced transcription of DNAJ genes is part of a specific pathway that is collectively termed the “unfolded

protein response” (UPR) and is evoked when unfolded proteins accumulate in the ER.<sup>196-199</sup> The UPR ultimately leads to reduced import of proteins into the ER and upregulation of genes encoding ER chaperones and other components of the ER-associated degradation pathway.<sup>200</sup>

The previously unrecognized ability of EVOO secoiridoids to upregulate a set of

genes involved in the ER stress response to unfolded proteins may appear to conflict with the demonstrated ability of these compounds to strongly inhibit the growth of highly aggressive breast cancer cells.<sup>145,146</sup> The UPR is the major protective and compensatory mechanism that enables cells to survive during ER stress. While UPR induction initially results in a general decrease in protein synthesis, which reduces the influx of nascent proteins into the ER, activation of the UPR also results in the enhanced transcription of ER resident chaperones, folding enzymes and other components of the protein degradation machinery, thus preventing aggregation of the accumulating misfolded proteins. This cell protective mechanism, which is also elicited upon induction of Hsp70s,<sup>201,202</sup> results in a transient induction of cell cycle arrest and in the accumulation of molecular chaperones that bind and recover unfolded proteins. However, prolonged exposure of cells to ER stress can induce a switch from cell survival to cell death, because the protective function of these mechanisms appears to be temporally restricted.<sup>203,204</sup> In this scenario, it is reasonable to suggest that exposure to EVOO secoiridoids promotes cell death-UPR branch signaling by impeding the alleviation of ER stress. Moreover, the coupling of EVOO secoiridoid-activated ER stress and UPR with EVOO secoiridoid-induced cytotoxicity in cancer cells appears to recapitulate the molecular mechanism by which the well-known defense molecule resveratrol simultaneously exerts anti-proliferative and chemopreventive effects.<sup>205,206</sup> First, induction of *GADD153/CHOP (DDIT3)*, one of the pivotal components of the ER stress pathway that is significantly upregulated by EVOO secoiridoids, has been shown to be involved in resveratrol-induced cell death in cancer cells.<sup>207</sup> Second, resveratrol has been shown to upregulate genes involved in the ER stress response to unfolded proteins.<sup>208</sup> Third, because resveratrol can trigger ER stress-induced cell death, UPR could be a potential mechanism of resveratrol cytotoxicity.<sup>206,209</sup> EVOO secoiridoids and resveratrol could also share mechanism(s) through which they activate ER stress-like responses. Like resveratrol, EVOO

secoiridoid polyphenols paradoxically have a propensity to stimulate the formation of ROS,<sup>210-213</sup> which can cause oxidation of nascent proteins, leading to misfolding of proteins and ER stress.<sup>214</sup> In addition, EVOO secoiridoid polyphenols can operate in a resveratrol-like manner to molecularly mimic a CR-like situation involving ATP deficiency.<sup>15,107-110,215-217</sup>

**EVOO secoiridoids induce c-Fos and modify the expression of genes related to polyamine metabolism.** The most prominent EVOO secoiridoid-activated “cellular function and maintenance and cellular compromise” gene network involves not only the chaperone genes *HSPA6* and *Hsp70*, but also *c-Fos*, a key resveratrol-targeted proto-oncogene.<sup>218,219</sup> Indeed, the gene whose expression was most enhanced after treatment with EVOO secoiridoids was *c-Fos* (FOS; ~20-fold). *FOSB*, another member of the Fos family of transcription factors, which includes *c-Fos*, *FosB*, *Fra1* and *Fra2*, was also one of the 10 most upregulated genes (~11-fold). The Fos family proteins heterodimerize with Jun family proteins (c-Jun, JunB and JunD) to form active AP-1 (activator protein-1) transcription factors, which bind to AP-1 sites present in the promoters of certain genes and regulate their transcription. Of note, treatment of human breast cancer cells with EVOO secoiridoids significantly (~3-fold) upregulated the expression of *JUNB*. There is increasing evidence that the AP-1 complex plays an important role not only in the proliferation but also in the differentiation of several cell types; several chemopreventive agents (e.g., 1,25-dihydroxyvitamin D3 and butyrate) stimulate cell differentiation in an AP-1-dependent manner.<sup>220,221</sup> Resveratrol also stimulates the AP-1 constituents c-Fos and c-Jun to inhibit cancer cell growth.<sup>218</sup> The data imply that EVOO secoiridoid-induced upregulation of AP-1 is not associated with tumorigenesis, but rather with growth inhibition and/or differentiation of breast cancer cells.

Because resveratrol-induced *c-Fos* is functionally related to resveratrol's ability to modify polyamine metabolism,<sup>218</sup> we speculated that the previously unrecognized ability of EVOO secoiridoids to induce *c-Fos* might involve changes in the expression of genes associated with

polyamine synthesis and/or polyamine catabolism. Similar to resveratrol, EVOO secoiridoids significantly upregulated (~4-fold) the expression of spermidine/spermine N<sup>1</sup>-acetyltransferase (*SSAT*), the rate-limiting enzyme in polyamine catabolism (Table S1). This enzyme converts spermine to spermidine and the latter to putrescine in cooperation with polyamine oxidase (*PAOX*). Increased polyamine catabolism in response to EVOO secoiridoids was also suggested by the significant upregulation of the spermine oxidase (*SMO*) gene. Unlike resveratrol, EVOO secoiridoids downregulated *PAOX* gene expression, whereas they upregulated some genes involved in polyamine biosynthesis, such as arginase (*ARG2*) and ornithine decarboxylase (*ODC*). Although we lacked experimental approaches for measuring the intracellular levels of spermine, spermidine, putrescine and acetyl-spermidine following exposure to EVOO secoiridoids, our data indicate that the mechanism of the growth inhibitory action of EVOO-derived complex polyphenols likely involves an increase in polyamine catabolism with simultaneous induction of *c-Fos* and its AP-1-related DNA binding activity.

The previously unrecognized ability of EVOO secoiridoids to upregulate key genes directly involved in the conversion of arginine to ornithine (i.e., arginase) and in the conversion of ornithine to putrescine (i.e., ornithine decarboxylase) suggests that the augmentation of polyamine catabolism observed after exposure of cells to EVOO secoiridoids could be related to growth inhibition processes, whereas the augmentation of polyamine synthesis could be related to bona fide anti-aging effects. This appears likely, because polyamine levels decline continuously with age and polyamine (spermidine or high-polyamine diet) supplementation increases life span in model organisms.<sup>101,222-231</sup> Because autophagy is required for the cytoprotective and/or anti-aging effects of resveratrol and spermidine, experiments are currently underway in our laboratories at the Bioactive Food Component Platform in Spain to determine if regulation of polyamine metabolism by EVOO-derived secoiridoids differentially impacts the fitness of cancer vs. normal cells undergoing

metabolic stress. Because pro-autophagic polyphenols have been shown to reduce the acetylation of cytoplasmic proteins,<sup>232</sup> we are also investigating whether EVOO secoiridoids might impact the activation status of autophagy while differentially affecting the acetylproteome of cancer vs. normal cells.

**EVOO secoiridoids upregulate SIRT1 and inhibit cancer-promoting genes.** In the above-mentioned transcriptome scenario and considering that resveratrol and spermidine increase lifespan by activating the histone deacetylase Sirtuin 1 (SIRT1) and inhibiting histone acetylases, respectively,<sup>101</sup> we determined if the resveratrol-like actions of EVOO secoiridoids involve changes in the expression of the *SIRT1* gene. Of note, not only was *SIRT1* significantly upregulated by EVOO secoiridoids, *SIRT1* was also part of the second most significant gene network activated by EVOO secoiridoids, the “organ morphology” gene network (score = 41) (Fig. 4). Although *SIRT1* has long been thought to play a role in cancer, the debate regarding its role as an oncogene or tumor suppressor continues.<sup>19,232,233</sup> As an inducer of cell survival, it might appear reasonable to suggest that *SIRT1* fits the definition of an oncogene; conversely, because *SIRT1* is considered important in organism survival, a tumor suppressor function might also be anticipated. Genetic and drug-induced activation of *SIRT1* has been shown to inhibit growth and/or induce apoptosis in certain cancer models,<sup>234,235</sup> while super-*SIRT1* mice exhibiting moderate *SIRT1* overexpression (a ~3-fold increase) are generally healthier than control mice and are partially protected from certain solid tumors.<sup>236-239</sup>

Because neoplastic cells are thought to recapitulate many stem cell characteristics, including metabolic ones,<sup>17,20,240-245</sup> the oncogenic vs. tumor-suppressive activities of *SIRT1* can be viewed in terms of the specific contribution of *SIRT1* to maintaining or impeding “stemness-like” status in cell populations involved in tissue regeneration or cancer tissue heterogeneity, respectively. To preliminarily assess whether EVOO secoiridoid-induced upregulation of *SIRT1* is related to the activation of onco-suppressive transcriptional events in highly aggressive cancer

cells, we evaluated whether well-known oncogenes were among the 92 genes that were significantly downregulated by EVOO secoiridoids (Table S1; Fig. 4). Interestingly, the EVOO secoiridoids most frequently downregulated gene networks related to “cancer and reproductive system disease” (score = 52), including numerous metallothionein (MT) gene isoforms (*MT1E*, *MT1G*, *MT1X*, *MT1L*, *MT1H*). MT belongs to a family of metal-binding proteins whose roles range from heavy metal detoxification to the promotion of tumorigenesis. MT has been reported to be highly expressed in many tumors, including breast cancer, and is known to regulate key processes such as cell proliferation, apoptosis and even chemoresistance.<sup>246-250</sup> Because the role of MT in metal ion homeostasis is fundamental for controlling the activation of stem/progenitor cells, we speculated that MT downregulation by EVOO secoiridoids might be part of a broader genetic network involving key cancer stem cell (CSC)-related genes. Consistent with this hypothesis, the “cancer and reproductive system disease” gene network downregulated by EVOO secoiridoids includes the *ALDH1A3* gene, a biomarker of primitive normal human mammary luminal cells that shows high activity specifically in breast carcinomas. In such tumors, expression of the *ALDH1A3* gene identifies the tumorigenic cell fraction that is capable of self-renewal and of generating tumors by recapitulating the heterogeneity of the parental tumor (i.e., breast CSCs).<sup>251-254</sup> We are currently investigating whether treatment with EVOO secoiridoids impedes the propensity of breast CSCs to form multicellular “microtumors” under non-adherent and non-differentiating conditions (i.e., mammospheres).

In addition to the CSC marker *ALDH1A3*, treatment with EVOO secoiridoids notably downregulated the expression of *SKP2*, the gene that encodes the F-box protein S-phase kinase-associated protein 2 (Skp2). Skp2 belongs to the ubiquitin-proteasome system (UPS), which plays a vital role in regulating many biological processes by controlling the timely turnover of proteins. Because Skp2 is responsible for the degradation of several tumor suppressor proteins

(e.g., p27, p57, p21, p130, FOXO1), it is thought to function as an oncoprotein that interacts with other major signaling pathways (e.g., PI3K/Akt, mTOR, PPAR $\gamma$ , ERK, FoxP3 and IGF) in breast cancer.<sup>255-259</sup> As such, there is renewed interest in developing Skp2 inhibitors as a general approach for cancer prevention and therapy.<sup>259</sup> Although specific drugs that inactivate Skp2 in cancer cells have not been identified, it is noteworthy that several naturally occurring compounds (1,2,3,4,6-penta-O-galloyl- $\beta$ -D-glucose [PGG], gallic acid, epigallocatechin-gallate [EGCG], quercetin, curcumin, and lycopene) downregulate Skp2 expression in human cancers, including breast cancer.<sup>260-262</sup> We now add the complex polyphenols secoiridoids to the growing list of natural polyphenols that can function as potent inhibitors of Skp2.

The function of the second most downregulated gene network in response to EVOO secoiridoids is related to “cell cycle, amino acid metabolism and small molecule biochemistry” (score = 27) and was identified based on *LDHA*, a gene that was also overrepresented in the most downregulated gene network described above (Fig. 4). Lactate dehydrogenase (LDH) acts at a critical branch point in the metabolism of major nutrients; it is also active in the tricarboxylic acid (TCA) cycle and in determining tumor pH.<sup>263</sup> Glucose and glutamine are the major carbon sources for rapidly proliferating tumors and provide precursors for nucleic acids, proteins and lipids as well as reducing capability (NADPH). Pyruvate is largely derived from glucose and glutamine metabolism; it can be converted to lactate by the LDH complex and/or enter the TCA cycle for conversion to CO<sub>2</sub> and ATP. The conversion of pyruvate to lactate is also catalyzed by LDH in a reversible reaction that results in the formation of NAD<sup>+</sup>, which is necessary for further glycolysis. LDH is a tetrameric enzyme containing two major subunits (A and B) that are coded by the *LDHA* and *LDHB* genes; together, these subunits form five different isoenzymes.<sup>264</sup> Although all five isoenzymes can catalyze the forward and backward conversion of pyruvate and lactate, LDHA kinetically favors the conversion of pyruvate to lactate, whereas LDHB

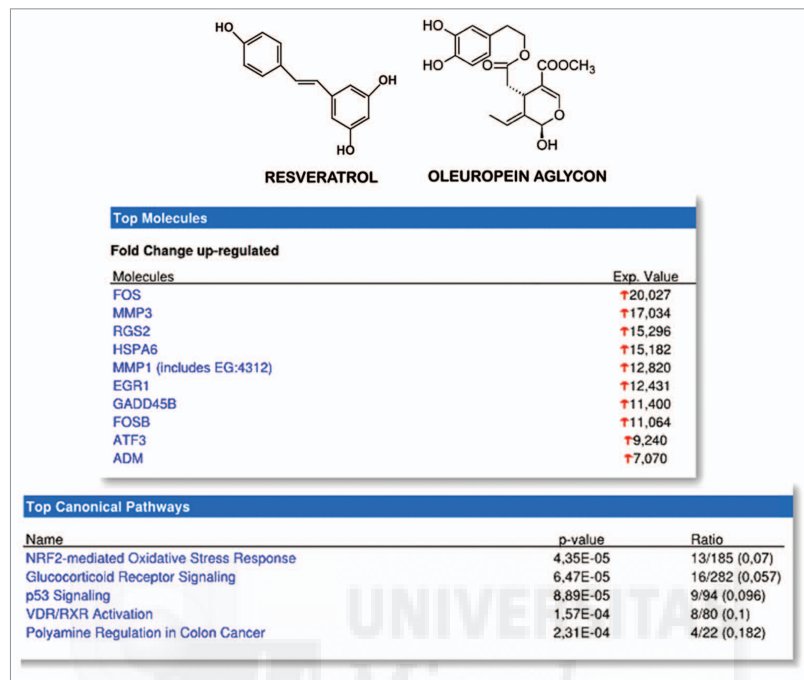


**Figure 5.** Top: Structural similarities between resveratrol and the EVOO secoiridoid oleuropein aglycon. Bottom: IPA-identified top individual genes and top canonical pathways affected by EVOO secoiridoids.

predominantly converts lactate to pyruvate, which is further oxidized through the TCA cycle. Serum LDH levels are often increased in cancer patients, and *LDHA* protein expression is often upregulated in tumors.<sup>265-273</sup> Like high lactate levels, which are a key feature of the aerobic glycolysis (Warburg effect) in tumor cells and are associated with the subsequent development of metastases,<sup>274,275</sup> the presence of high LDH levels in tumors has been linked to poor prognosis and greater metastatic potential. Because the LDHA protein is required for the maintenance and progression of many tumors, it also represents a potential target for cancer therapy.<sup>276</sup> Our findings suggest a potential inhibitory role of EVOO secoiridoids against the Warburg effect in tumor cells.

EVOO secoiridoids are resveratrol transcriptional mimickers that activate the energy sensor AMPK. Previous studies have shown that resveratrol efficiently induces changes in the transcriptional

profiles of key metabolic tissues that closely resemble the changes induced by CR.<sup>91,277</sup> The data presented here demonstrate that EVOO secoiridoids appear to mimic key features of resveratrol-induced gene expression patterns to inhibit the growth of cancer cells, whose aberrant bioenergetic and biosynthetic metabolism is unambiguously required for proliferation and/or survival. To further confirm that administration of EVOO secoiridoids functionally mimics resveratrol via activation of AMPK-related stress signaling pathways, we employed two additional complementary approaches. First, systematic and integrative analyses of EVOO secoiridoid-regulated gene lists were conducted using the DAVID (Database for Annotation, Visualization and Integrated Discovery) bioinformatics resource (National Institute of Allergy and Infectious Diseases, NIH), a web-based public database capable of uncovering biological features and meaning

associated with large gene lists, regardless of which genomic platform or software package was used to generate the list (<http://david.abcc.ncifcrf.gov/>). DAVID uses a set of fuzzy classification algorithms to group genes based on their co-occurrence in annotation terms and ranks the gene groups using an internal (EASE) score.<sup>278,279</sup> DAVID was used to evaluate the enrichment distribution across the “biological processes” in the gene ontology (GO) tree. The threshold value of the enrichment score was set at 1.0 instead of 1.3, thereby avoiding the loss of important information. The gene list was organized and condensed into biologically meaningful modules using the DAVID gene functional classification tool at the medium level of statistical stringency. When ranking the importance of annotation groups with enrichment scores  $\geq 1.0$ , DAVID term-centric modular enrichment analysis revealed that the “biological modules” significantly enhanced by EVOO

secoiridoids paradoxically included positive regulation of “developmental and biological processes,” “response to stress,” “organ morphogenesis,” “response to chemical stimulus (unfolded protein),” “response to wounding” and “chromatin assembly,” among others (Table S2). The activation of anti-aging biological modules was concomitant with the significant downregulation of “hexose catabolic processes,” “cell cycle” and “cellular carbohydrate metabolic processes,” among others (Table S2). Therefore, highly aggressive cancer cells appear to react to EVOO secoiridoid-triggered cellular stress signals by evoking cell survival programs that ultimately result in cancer cell death.

Second, to unambiguously determine whether the crucial signaling pathways that are significantly altered in the presence of EVOO secoiridoids are similar to those previously recognized for resveratrol, we used the “canonical pathway analysis” function included in the IPA analysis software. This analysis associates probe sets with the canonical pathways included in Ingenuity’s Knowledge Base and returns two measures of association: (1) the ratio of the number of genes from the list that map to the pathway to the total number of genes that map to the same pathway, and (2) a p value based on Fisher’s exact test to ascertain enrichment. Notably, when the canonical pathways induced by EVOO secoiridoids were ordered by p value ( $p < 0.05$ ; the ratio value is also shown), all of the molecular mechanisms underlying resveratrol’s recognized anti-aging effects were over-represented in the five canonical pathways that were most significantly upregulated by EVOO secoiridoids in cancer cells (Fig. 5). First, the above-mentioned resveratrol-induced FOS-dependent inhibition of polyamine synthesis and increased polyamine catabolism<sup>218,219</sup> was mirrored in the EVOO secoiridoid-induced “polyamine regulation in colon cancer” pathway ( $p = 2.31E-04$ ). Second, the resveratrol-related vitamin-D/retinoic acid-like differentiation-induced effects<sup>280-284</sup> were mirrored in the EVOO secoiridoid-induced “VDR/RXR activation” pathway ( $p = 1.57E-04$ ). Third, the resveratrol-induced p53-related engagement of cell cycle arrest and/or apoptotic signals<sup>285-290</sup> was mirrored

in the EVOO secoiridoid-induced “p53 signaling” pathway ( $p = 8.89E-05$ ). Fourth, resveratrol’s anti-inflammatory effects related to epigenetic and chaperone-dependent activation of the glucocorticoid receptor<sup>134,291-294</sup> were mirrored in the EVOO secoiridoid-induced “glucocorticoid receptor signaling” pathway ( $p = 6.47E-05$ ). Fifth, resveratrol’s ability to protect against oxidative stress damage by modulating nuclear redox factor 2 (NRF2) signaling<sup>295-302</sup> was mirrored in the EVOO secoiridoid-induced “NRF2-mediated oxidative stress response” pathway ( $p = 4.35E-05$ ). Considering that most of the beneficial effects of CR on the carcinogenic process are likely mediated by NRF2<sup>303,304</sup> and that recent studies have shown that a diet rich in EVOO phenolics (e.g., hydroxytyrosol, which is mainly formed from the hydrolysis of the secoiridoid oleuropein aglycone) induces SIRT1 and NRF2-dependent gene expression of anti-stress targets [e.g., glutathione-S-transferase (GST),  $\gamma$ -glutamyl cysteine synthetase ( $\gamma$ -GCS), nicotinamide adenine dinucleotide phosphate [NAD(P)H]:quinone oxidoreductase (NQO1) and paraoxonase-2 (PON2) mRNAs as well as paraoxonase-1 (PON1) activity] in senescence-accelerated (SAMP8) mice,<sup>305</sup> our findings strongly support the idea that the ability of secoiridoids to activate NRF2 signaling in somatic cells constitutes a mechanism through which EVOO complex polyphenols could lead to a delay in or the prevention of the onset of some forms of human cancers (e.g., breast cancer) and subsequently contribute to improved human health and lifespan.

Finally, we sought to investigate the unexplored possibility that EVOO secoiridoids might attenuate the adaptable aging-accelerating mTOR signaling pathway in cancer cells. Incubation of JIMT1 breast cancer cells (Fig. 4) and PC9 lung carcinoma cells (data not shown) with increasing concentrations of an EVOO PE rich in secoiridoids resulted in increasing activation of the mTOR gerosuppressor AMPK.<sup>306</sup> Activation of AMPK was associated with phosphorylation of the  $\alpha$ -catalytic subunit of the enzyme at Thr-172, as assessed using a phosphospecific antibody. Minimal changes in total AMPK protein levels were detected with

anti- $\alpha$ 1/- $\alpha$ 2 AMPK antibodies. When EVOO phenolic extracts highly enriched with secoiridoids were replaced by EVOO phenolic extracts with a similar content of total polyphenols but enriched with lignans, we observed a drastic decrease in the ability of the EVOO PEs to activate AMPK (data not shown). These results demonstrate for the first time that AMPK becomes significantly activated by EVOO-derived phenolic extracts when the amount of complex polyphenol secoiridoids but not lignans exceeds a critical threshold.

### EVOO Secoiridoid Polyphenols Induce Senescence Delay in Human Diploid Fibroblasts

Well-accepted hormetic strategies such as repeated mild heat stress (RMHS) significantly affect several age-related phenomena in human skin fibroblasts, e.g., cell size and cell morphology, but do not modify the proliferative capacity of these cells.<sup>32,33,78</sup> We decided to investigate whether repeated exposure to non-cytotoxic concentrations of EVOO secoiridoids might improve the structural and functional integrity of skin fibroblasts *in vitro* without promoting entrance of these cells into a potentially deleterious hyperproliferative mode. Thus, using the well-established *in vitro* senescence model of human diploid fibroblasts (HDFs), we determined for the first time whether senescence-associated changes occur in response to chronic exposure to crude EVOO PEs. Cell viability (MTT assays) confirmed that, at the concentration employed in our studies, EVOO secoiridoids did not exhibit highly toxic effects. Compared with untreated control fibroblasts, we observed almost no cell death of young HDFs after 72 h of incubation with 200 ng/mL EVOO-PE7. After 10 d of treatment, however, 20–25% of the cells cultured in the presence of the secoiridoid-rich EVOO PE were metabolically nonviable (data not shown).

Low-passage p16<sup>INK4a</sup>-positive WI-38 fetal lung HDFs and p16<sup>INK4a</sup>-negative BJ-1 neonatal foreskin HDFs were exposed to low concentrations of EVOO secoiridoids or to the same volume of vehicle twice a week during serial

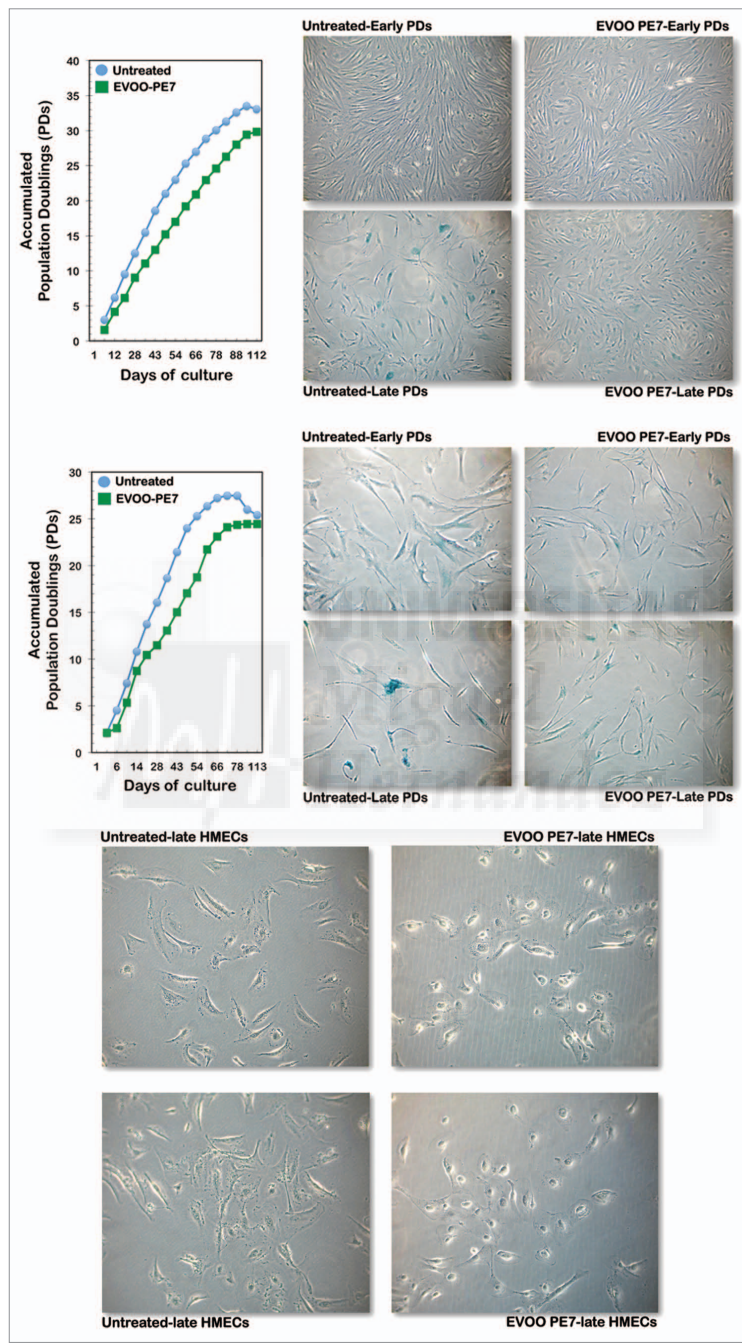


**Figure 6.** For figure legend, see page 568.

**Figure 6 (See previous page).** Impact of chronic exposure to EVOO secoiridoids in age-related changes of cultured human diploid fibroblasts (HDFs) and human mammary epithelial cells (HMECs). Left: Graphs showing cumulative population doubling for BJ-1 (top) and WI-38 (bottom) HDFs continuously cultured in the absence or presence of 200 ng/mL EVOO-PE7. Representative microphotographs illustrate the differential acquisition of age-related biomarkers including changes in cell morphology and SA- $\beta$ -gal activity (blue staining) in response to EVOO secoiridoids. Right: Representative microphotographs illustrate the impact of short-term treatment (3 d) with EVOO secoiridoids in the vacuolization and abundant accumulation of cell debris in pre-senescent HMECs.

passaging throughout their entire replicative life spans. Chronic exposure to EVOO secoiridoids failed to lengthen the proliferative lifespans of WI-38 and BJ-1 HDFs (Fig. 6). However, whereas the growth rates, population doubling rates and cumulative population doubling (PD) levels of the cells were mostly unaffected by repeated exposure to EVOO secoiridoids, age-related changes in cell size, cellular morphology and senescence-associated  $\beta$ -galactosidase (SA- $\beta$ -gal) staining were significantly altered. Age-related alterations in the morphology of fibroblasts, which is one of the most obvious changes that occurs during cellular aging, was significantly reduced in EVOO secoiridoid-treated HDFs. At the end of their proliferative lifespans, untreated control cultures underwent a significant increase in cell size, taking on a flattened appearance; their morphological heterogeneity also increased, and they suffered a complete loss of arrayed arrangement and accumulated significant amounts of intracellular and extracellular debris, with concomitant increases in the sizes of their nuclei and nucleoli (Fig. 6, left). Indeed, a short-term treatment (3 d) with EVOO secoiridoids notably ameliorated the intense vacuolization and abundant accumulation of cell debris in nearly senescent human mammary epithelial cells (HMECs) (Fig. 6, right). Moreover, we noted significantly higher proportions of  $\beta$ -gal-positive WI-38 and BJ-1 cells in old HDF cultures than in young HDF cultures. At the end of their proliferative lifespans, HDF cultures grown continuously in the presence of EVOO secoiridoids demonstrated significantly reduced age-related morphological alterations and displayed relatively young-like morphologies. Old HDF cultures chronically exposed to EVOO secoiridoids did not undergo significant cell enlargement and largely maintained the thin, long, spindle shapes observed in younger HDF cell populations. In

contrast to control cultures, EVOO secoiridoid-treated HDFs maintained an arrayed arrangement of morphologically homogeneous cells (Fig. 6), with reduced accumulation of lysosomal residual bodies and an almost complete absence of multinucleated cells. When the proliferation rate of the untreated control cultures began to decrease as cellular senescence approached, SA- $\beta$ -gal activity was measured; we notably observed significantly fewer  $\beta$ -gal-positive cells in EVOO secoiridoid-treated HDFs than in vehicle-treated HDFs (Fig. 6).

Taken together, these findings demonstrate for the first time that complex mixtures of crude EVOO PEs antagonize cellular senescence without modifying the proliferative capacity of HDFs. Katsiki and colleagues<sup>307</sup> previously reported that oleuropein-treated cultures of normal human fibroblasts exhibited a significant delay in the appearance of senescence morphology. In their hands, however, oleuropein treatment of human embryonic fibroblasts conferred a life-span extension of approximately 15%. It is plausible that the presence of numerous phenolic molecules within a crude EVOO PE would not preclude the ability of “diluted” secoiridoids to suppress senescence as efficiently as a single purified secoiridoid (e.g., oleuropein) and that, at concentrations such as those used in our experiment, the slightly cytotoxic effects of the crude EVOO phenolic mixture would prevent a plausible anti-aging (preservation of proliferative capacity) effect. Of note, when older HDFs chronically cultured in the presence of 200 ng/mL EVOO-PE7 were challenged with higher concentrations of the same PE, they were notably refractory to the cytotoxic effects observed when EVOO secoiridoid-naïve young HDFs were treated with the same high dose of polyphenols (data not shown). This finding supports the idea that continuous exposure to hormetic stresses (e.g., low-dose

secoiridoids) can protect cells from stronger stresses (e.g., high-dose secoiridoids) but that these stronger stresses do not cause aging, as aging is not caused by any stress.<sup>180</sup>

### EVOO Secoiridoid Polyphenols: A New Family of “Xenohormetic” Compounds

The previously unrecognized ability of EVOO secoiridoids to activate endogenous cellular defense pathways (e.g., the evolutionarily conserved NAD-dependent deacetylase sirtuin-1 and NRF2 pathways) that integrate the adaptive stress response and positively control the expression of a battery of stress response proteins in human cells support the original “xenohormesis hypothesis” of Howitz and Sinclair<sup>63,89,154</sup> invoking the interspecies communication of stress signals. The literature on sirtuin focuses on pharmacological activators of SIRT1 (e.g., resveratrol, SRT1720), which have been proposed as therapeutics for diabetes, neurodegeneration, inflammation and other diseases. However, many compounds may have been identified as SIRT1 activators due to artifacts in the assay methodology (i.e., the use of fluorescently tagged substrates). By performing the first comprehensive analysis of gene expression and transcriptome dynamics of human breast cancer cells grown in the presence of crude phenolic EVOO extracts, we present compelling data that suggest that the stress response of Oleacea plants, which has evolved as a result of their stationary lifestyle, might confer stress resistance and “anti-aging benefits” to animals such as humans that consume bioactive secoiridoids produced by Oleacea.

In highly proliferative cancer cells that possess aberrant bioenergetic and biosynthetic metabolism, EVOO secoiridoid-imposed metabolic reprogramming would be expected to promote growth inhibition and cell death; however, the ability of

relatively non-toxic secoiridoids to upregulate a variety of transcriptomic programs involved in regulating stress responses should result in increased longevity of normal cells. This apparent metabolic paradox can easily be resolved in the context of an evolutionary view of the “AMPK/mTOR-xenohormetic” model. AMPK, whose ancestral role may have been related to the response to starvation for the preferred carbon source, glucose, appears to have arisen very early during eukaryotic evolution. Rapid cell growth requires the active synthesis of proteins, rRNA and lipids, all of which are switched off by the activation of AMPK (and, likely, by downstream inactivation of mTOR). Indeed, one reason for the high glycolytic rate of rapidly proliferating cells, including tumor cells, is that the TCA cycle ceases to be a purely catabolic pathway and becomes at least partially anabolic, actively providing precursors for biosynthesis, particularly citrate for lipid synthesis.<sup>275</sup> Accordingly, both tumor cells and viruses (and likely other pathogens) appear to have developed mechanisms to downregulate the energy sensor AMPK and escape from its restraining influence on growth and biosynthesis.<sup>9,10,107</sup> In an “AMPK/mTOR-xenohormetic” model, there is no need to assume that animals and fungi have retained an ability to be activated by certain plant stress molecules, because they provide useful advance warning of a deteriorating environment or food supply. Soil bacteria do not produce the macrocyclic lactone rapamycin as an anticancer drug or a pro-longevity medicine but as an antibiotic that inhibits the growth of fungal competitors. The French lilac or goat’s rue (*Galega officinalis*) produces galegine, the bioactive starting material from which metformin was developed, as a defense compound to deter grazing by herbivores, not as a gerosuppressant that delays aging and suppresses tumorigenesis. Grapes produce resveratrol in response to fungal infection but not as a longevity nutrient with anticancer properties. Similarly, upon activation and conversion to oleuropein aglycone by deglycosylation, phenolic secoiridoid glycosides such as oleuropein can induce a loss of nutritive value via the loss of lysine and inactivation of enzymes by functioning as a unique multivalent

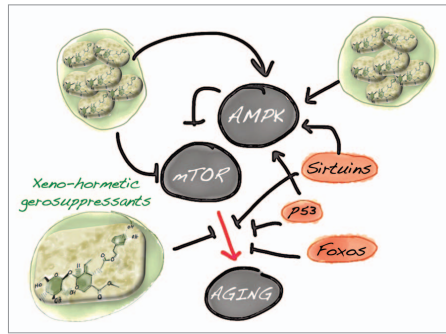


**Figure 7.** EVOO secoiridoids: A new family of plant-produced gerosuppressant agents that molecularly “repair” the aimless (and harmful) AMPK/mTOR-driven quasi-program that leads to aging and aging-related diseases, including cancer.

alkylator that acts as a protein crosslinker, providing plants with an effective defense against attack by herbivores and possibly by pathogens.<sup>307-310</sup> The fact that numerous and apparently unrelated “nutraceuticals,” “xenobiotics” and other biocompounds derived from traditional herbal medicines act as xenohormetic compounds merely reflects their common ability to inhibit the aging-driven activity of mTOR gerogenes and/or to activate key gerosuppressors of the mTOR pathway (i.e., AMPK).<sup>180,311-322</sup> Considering that mitochondria became the main cellular power source during the evolutionary development of eukaryotes,<sup>323</sup> AMPK plausibly arose very early during eukaryotic evolution due to the requirement for sensing energy status in the cytoplasm and providing a signal to modulate mitochondrial function. Indeed, the ancestral function of AMPK in plants and animals was likely to orchestrate resistance responses to the effects of carbohydrate starvation (e.g., to trigger a switch back to oxidative metabolism in response to deprivation of the preferred carbon source, glucose). Of note, most of the potent activators of AMPK are plant defense compounds that inhibit mitochondrial ATP synthesis. Forthcoming studies should definitively elucidate whether EVOO secoiridoids and other xenohormetic compounds impact both mitochondrial functionality and AMPK-like metabolic sensors across different species (e.g., olive and human) during times of stress; in this scenario, xenohormesis should be viewed as providing a shared

ability to molecularly connect mitochondria and AMPK during evolution. Curiously, SIRT1 has been shown to play an essential role in the ability of moderate doses of resveratrol to stimulate AMPK and improve mitochondrial function both *in vitro* and *in vivo*.<sup>324</sup>

#### EVOO Secoiridoid Polyphenols: A New Family of “Gerosuppressant” Compounds

Despite the high degree of structural resemblance between EVOO-derived complex polyphenols and well-recognized CR-like polyphenols that are known to experimentally extend lifespan (i.e., resveratrol), no studies have explored the actual molecular function of EVOO secoiridoids in retarding human aging. As for many other polyphenols, it has been erroneously assumed that EVOO-derived complex phenols provide health benefits, including higher longevity, largely because of their antioxidant activity. Our laboratories at the Spanish BFCP have been studying for the first time whether secoiridoids, a family of complex phenolics characteristic of Oleaceae plants, by functioning as biocompounds belonging to the recently defined group of “hormesis A” compounds (i.e., inhibitors of the pro-aging activity of mTOR gerogenes and/or activators of mTOR gerosuppressors such as AMPK) can, like resveratrol, affect anti-aging signaling pathways in ways that significantly promote cytotoxicity in immortal tumor cells and that weaken

age-related pro-senescence effects in normal cells. Because changes in the expression of significant numbers of genes have been linked to the anticancer and lifespan effects of all known lifespan interventions (CR- and the so-called CR-mimetics), we hypothesized that global changes in the human transcriptome detectable by the use of high-density microarrays could be used for the preliminary identification of candidate EVOO secoiridoids-induced anti-aging/anticancer gene signatures. The strength of evidence supporting the xenohormetic activity of EVOO secoiridoids was tested by assuming that their tumocidal activity results from the paradoxical activation of cellular stress-like, anti-aging transcriptomic signatures in cancer cells. By following this genome-wide analysis approach in highly aggressive human breast cancer cells that were briefly exposed to crude EVOO phenolic extracts highly enriched in the secoiridoids oleuropein aglycone and decarboxymethyl oleuropein aglycone, we demonstrated that Oleacea plant defense molecules, which are able to exert strong protein-denaturing/protein-crosslinking/lysine-alkylating activities against herbivores, can efficiently induce in human cells intracellular signaling pathways that may respond to biological stress at the molecular/cellular level. We confirmed that the stress pathways activated by EVOO secoiridoids might defend cells and tissues in a hormetic-like manner, because they regulate energy metabolism in a way that would be expected to enhance cellular survival during times of stress. Thus, the anticancer activity of EVOO secoiridoids was found to be related to the activation of anti-aging/cellular stress-like gene signatures, including endoplasmic reticulum (ER) stress and the unfolded protein response, spermidine and polyamine metabolism, sirtuin-1 (SIRT1),<sup>325-351</sup> and NRF2 signaling. EVOO secoiridoids activated the gerosuppressor AMPK and inhibited crucial metabolic genes involved in the Warburg effect and the self-renewal capacity of “immortal” cancer stem cells and EVOO secoiridoids significantly prevented age-related changes in cell size, morphological heterogeneity, arrayed arrangement and senescence-associated  $\beta$ -galactosidase staining of normal diploid

human fibroblasts at the end of their proliferative lifespan.

Aging can be viewed as a quasi-programmed phenomenon driven by the overactivation of the nutrient-sensing mTOR gerogene. Complementing this idea, emerging studies indicate that the responsiveness of AMPK signaling clearly declines with aging.<sup>306</sup> The loss of sensitivity of AMPK activation to cellular stress impairs metabolic regulation, increases oxidative stress and reduces autophagic clearance. Not surprisingly, very recent studies have illuminated the central role that loss of the AMPK gerosuppressor plays in dictating the unique metabotype that drives tumorigenesis.<sup>352,353</sup> Given that AMPK is a crucial gerosuppressor and tumor-suppressor that suppresses mTOR-driven geroconversion (as well as mTOR oncogenic transformation), age-related diseases reflect a synergistic interaction between our evolutionary path to sedentarism, which chronically increases a number of gero-promoting factors, e.g., mTOR activators such as nutrients (glucose, amino acids, fatty acids), growth factors, cytokines and insulin and the “defective design” of central metabolic integrators such as AMPK and mTOR. In this scenario, xenohormesis should be viewed in terms of plant-produced gero-suppressants that molecularly “repair” the aimless (and harmful) AMPK/mTOR-driven quasi-program of aging and aging-related diseases (Fig. 7).

#### Disclosure of Potential Conflicts of Interest

No potential conflicts of interest were disclosed.

#### Acknowledgments

This work was financially supported by the Instituto de Salud Carlos III (Ministerio de Sanidad y Consumo, Fondo de Investigación Sanitaria (FIS), Spain, grants CP05-00090, PI06-0778 and RD06-0020-0028), the Fundación Científica de la Asociación Española Contra el Cáncer (AECC, Spain) and the Ministerio de Ciencia e Innovación (SAF2009-11579, Plan Nacional de I+D+I, MICINN, Spain). Alejandro Vazquez-Martín received the Sara Borrell post-doctoral contract (CD08/00283, Ministerio de Sanidad y Consumo, Fondo

de Investigación Sanitaria -FIS-, Spain). Silvia Cuffí received a research fellowship (Formación de Personal Investigador, FPI) from the Ministerio de Ciencia e Innovación (MICINN, Spain).

#### Supplemental Materials

Supplemental materials may be found here:  
[www.landesbioscience.com/journals/cc/article/23756](http://www.landesbioscience.com/journals/cc/article/23756)

#### References

- Koehn FE, Carter GT. The evolving role of natural products in drug discovery. *Nat Rev Drug Discov* 2005; 4:206-20; PMID:15729362; <http://dx.doi.org/10.1038/nrd1657>
- McChesney JD, Venkataraman SK, Henri JT. Plant natural products: back to the future or into extinction? *Phytochemistry* 2007; 68:2015-22; PMID:17574638; <http://dx.doi.org/10.1016/j.phytoc.2007.04.032>
- Molinari G. Natural products in drug discovery: present status and perspectives. *Adv Exp Med Biol* 2009; 655:13-27; PMID:20047031; [http://dx.doi.org/10.1007/978-1-4419-1132-2\\_2](http://dx.doi.org/10.1007/978-1-4419-1132-2_2)
- Li JW, Vedera JC. Drug discovery and natural products: end of an era or an endless frontier? *Science* 2009; 325:161-5; PMID:19589993; <http://dx.doi.org/10.1126/science.1168243>
- Lévesque H, Lafont O. Aspirin throughout the ages: a historical review. *Rev Med Interne* 2000; 21(Suppl 1):8s-17s; PMID:10763200
- Vane JR. The fight against rheumatism: from willow bark to COX-1 sparing drugs. *J Physiol Pharmacol* 2000; 51:573-86; PMID:11192932
- Hedner T, Everts B. The early clinical history of salicylates in rheumatology and pain. *Clin Rheumatol* 1998; 17:222-36; PMID:9586674; <http://dx.doi.org/10.1007/BF01450953>
- Hawley SA, Fullerton MD, Ross FA, Schertzer JD, Chevzoff C, Walker KJ, et al. The ancient drug salicylate directly activates AMP-activated protein kinase. *Science* 2012; 336:918-22; PMID:22517326; <http://dx.doi.org/10.1126/science.1215327>
- Hardie DG, Ross FA, Hawley SA. AMP-activated protein kinase: a target for drugs both ancient and modern. *Chem Biol* 2012; 19:1222-36; PMID:23102217; <http://dx.doi.org/10.1016/j.chembiol.2012.08.019>
- Hardie DG, Ross FA, Hawley SA. AMPK: a nutrient and energy sensor that maintains energy homeostasis. *Nat Rev Mol Cell Biol* 2012; 13:251-62; PMID:22436748; <http://dx.doi.org/10.1038/nrm3311>
- Xu J, Ji J, Yan XH. Cross-talk between AMPK and mTOR in regulating energy balance. *Crit Rev Food Sci Nutr* 2012; 52:373-81; PMID:22369257; <http://dx.doi.org/10.1080/10408398.2010.500245>
- Salminen A, Kaarniranta K. AMP-activated protein kinase (AMPK) controls the aging process via an integrated signaling network. *Ageing Res Rev* 2012; 11:230-41; PMID:22186033; <http://dx.doi.org/10.1016/j.arr.2011.12.005>
- Mousa SA, Gallari C, Simone T, Dier E, Yalcin M, Dyskin E, et al. Dual targeting of the antagonistic pathways mediated by Sirt1 and TXNIP as a putative approach to enhance the efficacy of anti-aging interventions. *Aging (Albany NY)* 2009; 1:412-24; PMID:20195491
- Lee JH, Bodmer R, Bier E, Karin M. Sestrins at the crossroad between stress and aging. *Aging (Albany NY)* 2010; 2:369-74; PMID:20606249

15. Vakana E, Platania LC. AMPK in BCR-ABL expressing leukemias. Regulatory effects and therapeutic implications. *Oncotarget* 2011; 2:1322-8; PMID:22249159
16. Steelman LS, Chappell WH, Abrams SL, Kempf RC, Long J, Laipler P, et al. Roles of the Raf/MEK/ERK and PI3K/PTEN/Akt/mTOR pathways in controlling growth and sensitivity to therapy-implications for cancer and aging. *Aging (Albany NY)* 2011; 3:192-222; PMID:21422497
17. Del Barco S, Vazquez-Martin A, Cufi S, Oliveras-Ferraro C, Bosch-Barrera J, Joven J, et al. Metformin: multi-faceted protection against cancer. *Oncotarget* 2011; 2:896-917; PMID:22203527
18. Leonteva OV, Blagosklonny MV. Yeast-like chronological senescence in mammalian cells: phenomenon, mechanism and pharmacological suppression. *Aging (Albany NY)* 2011; 3:1078-91; PMID:22156391
19. Calvaneo V, Fraga MF. Sirt1 brings stemness closer to cancer and aging. *Aging (Albany NY)* 2011; 3:162-7; PMID:21307403
20. Menendez JA, Cufi S, Oliveras-Ferraro C, Martin-Castillo B, Joven J, Vellon L, et al. Metformin and the ATM DNA damage response (DDR): accelerating the onset of stress-induced senescence to boost protection against cancer. *Aging (Albany NY)* 2011; 3:1063-77; PMID:22170748
21. Pardo PS, Boriek AM. The physiological roles of Sirt1 in skeletal muscle. *Aging (Albany NY)* 2011; 3:430-7; PMID:21483036
22. Coroninas-Faja B, Quirantes-Piné R, Oliveras-Ferraro C, Vazquez-Martin A, Cufi S, Martin-Castillo B, et al. Metabolic fingerprint reveals that metformin impairs one-carbon metabolism in a manner similar to the antifolate class of chemotherapy drugs. *Aging (Albany NY)* 2012; 4:480-98; PMID:22837425
23. Iglesias-Bartolome R, Gurkina SJ. Exploiting the mTOR paradox for disease prevention. *Oncotarget* 2012; 3:1061-3; PMID:23165441
24. Timmers S, Auwerx J, Schrauwen P. The journey of resveratrol from yeast to human. *Aging (Albany NY)* 2012; 4:146-58; PMID:22436213
25. Richardson RB. Ionizing radiation and aging: rejuvenating an old idea. *Aging (Albany NY)* 2009; 1:887-902; PMID:19757573
26. Calabrese EJ. Hormesis is central to toxicology, pharmacology and risk assessment. *Hum Exp Toxicol* 2010; 29:249-61; PMID:20332169; http://dx.doi.org/10.1177/0960327109363973
27. Kendig EL, Le HH, Belcher SM. Defining hormesis: evaluation of a complex concentration-response phenomenon. *Int J Toxicol* 2010; 29:235-46; PMID:20448256; http://dx.doi.org/10.1177/1091581810363012
28. Calabrese V, Cornelius C, Cuzzocrea S, Iavicoli I, Rizzarelli E, Calabrese EJ. Hormesis, cellular stress response and vitagenes as critical determinants in aging and longevity. *Mol Aspects Med* 2011; 32:279-304; PMID:22020144; http://dx.doi.org/10.1016/j.mam.2011.10.007
29. Martins I, Galluzzi L, Kroemer G. Hormesis, cell death and aging. *Aging (Albany NY)* 2011; 3:821-8; PMID:21931183
30. Calabrese EJ, Iavicoli I, Calabrese V. Hormesis: why it is important to biogerontologists. *Biogerontology* 2012; 13:215-35; PMID:22270337; http://dx.doi.org/10.1007/s10522-012-9374-7
31. Radak Z, Chung HY, Gore S. Exercise and hormesis: oxidative stress-related adaptation for successful aging. *Biogerontology* 2005; 6:71-5; PMID:15834665; http://dx.doi.org/10.1007/s10522-004-7386-7
32. Rattan SIS. Anti-ageing strategies: prevention or therapy? Showing ageing from within. *EMBO Rep* 2005; 6(Spec No):S25-9; PMID:15995657; http://dx.doi.org/10.1038/sj.emboj.7400401
33. Rattan SI. Hormetic modulation of aging and longevity by mild heat stress. *Dose Response* 2005; 3:533-46; PMID:18648625; http://dx.doi.org/10.2203/dose-response.003.04.008
34. Masoro EJ. Role of hormesis in life extension by caloric restriction. *Dose Response* 2007; 5:163-73; PMID:18648602; http://dx.doi.org/10.2203/dose-response.006-005.Masoro
35. Mattson MP. Hormesis defined. *Ageing Res Rev* 2008; 7:1-7; PMID:18162444; http://dx.doi.org/10.1016/j.arr.2007.08.007
36. Yashin AI. Hormesis against aging and diseases: using properties of biological adaptation for health and survival improvement. *Dose Response* 2009; 8:41-7; PMID:20221287; http://dx.doi.org/10.2203/dose-response.09-024.Yashin
37. Calabrese V, Cornelius C, Dinkova-Kostova AT, Iavicoli I, Di Paola R, Koverech A, et al. Cellular stress responses, hormetic phytochemicals and vitagenes in aging and longevity. *Biochim Biophys Acta* 2012; 1822:753-83; PMID:22108204; http://dx.doi.org/10.1016/j.bbadiis.2011.11.002
38. Calabrese EJ. Hormesis: Toxicological foundations and role in aging research. [Epub ahead of print]. *Exp Gerontol* 2012; PMID:22525590
39. Safdie FM, Dorff T, Quinn D, Fontana L, Wei M, Lee C, et al. Fasting and cancer treatment in humans: A case series report. *Aging (Albany NY)* 2009; 1:988-1007; PMID:20157582
40. Ristow M, Schmeisser S. Extending life span by increasing oxidative stress. *Free Radic Biol Med* 2011; 51:327-36; PMID:21619928; http://dx.doi.org/10.1016/j.freeradbiomed.2011.05.010
41. Weiss EP, Fontana L. Caloric restriction: powerful protection for the aging heart and vasculature. *Am J Physiol Heart Circ Physiol* 2011; 301:H1205-19; PMID:21841020; http://dx.doi.org/10.1152/ajph-heat.00685.2011
42. Raffaghello L, Safdie F, Bianchi G, Dorff T, Fontana L, Longo VD. Fasting and differential chemotherapy protection in patients. *Cell Cycle* 2010; 9:4474-6; PMID:21088487; http://dx.doi.org/10.4161/cc.9.22.13954
43. Blagosklonny MV. Rapamycin-induced glucose intolerance: hunger or starvation diabetes. *Cell Cycle* 2011; 10:2249-55; PMID:22157190; http://dx.doi.org/10.4161/cc.10.24.18595
44. Blagosklonny MV. Once again on rapamycin-induced insulin resistance and longevity: despite of or owing to. *Aging (Albany NY)* 2012; 4:350-8; PMID:22683661
45. Zhang D, Liu Y, Chen D. SIRT-ain relief from age-inducing stress. *Aging (Albany NY)* 2011; 3:158-61; PMID:21307404
46. Khanna A, Muthusamy S, Liang R, Sarojini H, Wang E. Gain of survival signaling by down-regulation of three key miRNAs in brain of calorie-restricted mice. *Aging (Albany NY)* 2011; 3:223-36; PMID:21415464
47. Soare A, Cangemi R, Omodei D, Holloszy JO, Fontana L. Long-term calorie restriction, but not endurance exercise, lowers core body temperature in humans. *Aging (Albany NY)* 2011; 3:374-9; PMID:21483032
48. Longo VD, Fontana L. Intermittent supplementation with rapamycin as a dietary restriction mimetic. *Aging (Albany NY)* 2011; 3:1039-40; PMID:22147496
49. Lee C, Longo VD. Fasting vs dietary restriction in cellular protection and cancer treatment: from model organisms to patients. *Oncogene* 2011; 30:3305-16; PMID:21516129; http://dx.doi.org/10.1038/onc.2011.91
50. Chung JH. Using PDE inhibitors to harness the benefits of calorie restriction: lessons from resveratrol. *Aging (Albany NY)* 2012; 4:144-5; PMID:22388573
51. Longo VD, Fontana L. Calorie restriction and cancer prevention: metabolic and molecular mechanisms. *Trends Pharmacol Sci* 2010; 31:89-98; PMID:20097433; http://dx.doi.org/10.1016/j.tips.2009.11.004
52. Yamaza H, Komatsu T, Wakita S, Kijogi C, Park S, Hayashi H, et al. FoxO1 is involved in the anti-neoplastic effect of calorie restriction. *Aging Cell* 2010; 9:372-82; PMID:20222901; http://dx.doi.org/10.1111/j.1474-9726.2010.00563.x
53. Anisimov VN. Metformin for aging and cancer prevention. *Aging (Albany NY)* 2010; 2:760-74; PMID:21084729
54. Hursting SD, Smith SM, Lashinger LM, Harvey AE, Perkins SN. Calories and carcinogenesis: lessons learned from 30 years of calorie restriction research. *Carcinogenesis* 2010; 31:83-9; PMID:1996554; http://dx.doi.org/10.1093/carcin/bgp280
55. Longo VD, Fontana L. Calorie restriction and cancer prevention: metabolic and molecular mechanisms. *Trends Pharmacol Sci* 2010; 31:89-98; PMID:20097433; http://dx.doi.org/10.1016/j.tips.2009.11.004
56. Martín-Montalvo A, Villalba JM, Navas P, de Cabo R, Nrf2, cancer and calorie restriction. *Oncogene* 2011; 30:505-20; PMID:21057541; http://dx.doi.org/10.1038/onc.2010.492
57. Thompson HJ, McTiernan A. Weight cycling and cancer: weighing the evidence of intermittent caloric restriction and cancer risk. *Cancer Prev Res (Phila)* 2011; 4:1736-42; PMID:21982873; http://dx.doi.org/10.1158/1940-6207.CAPR-11-0133
58. Erkelk FO, Celik GE, Keskin O, Güllü E, Mungan D, Misirdigil Z. Fasting: an important issue in asthma management compliance. *Ann Allergy Asthma Immunol* 2006; 97:370-4; PMID:17042144; http://dx.doi.org/10.1016/S1081-1206(10)60803-4
59. Lee C, Raffaghello L, Brandhorst S, Safdie FM, Bianchi G, Martin-Montalvo A, et al. Fasting cycles retard growth of tumors and sensitize a range of cancer cell types to chemotherapy. *Sci Transl Med* 2012; 4:24ra27; PMID:22323820; http://dx.doi.org/10.1126/scitranslmed.3003293
60. Safdie F, Brandhorst S, Wei M, Wang W, Lee C, Hwang S, et al. Fasting enhances the response of glioma to chemo- and radiotherapy. *PLoS One* 2012; 7:e44603; PMID:22984531; http://dx.doi.org/10.1371/journal.pone.0044603
61. Kouda K, Iki M. Beneficial effects of mild stress (hormetic effects): dietary restriction and health. *J Physiol Anthropol* 2010; 29:127-32; PMID:20686325; http://dx.doi.org/10.2114/jpa.2.29.127
62. Lamming DW, Wood IG, Sinclair DA. Small molecules that regulate lifespan: evidence for xenohormesis. *Mol Microbiol* 2004; 53:1003-9; PMID:15306006; http://dx.doi.org/10.1111/j.1365-2958.2004.04209.x
63. Howitz KT, Sinclair DA. Xenohormesis: sensing the chemical cues of other species. *Cell* 2008; 133:387-91; PMID:18455976; http://dx.doi.org/10.1016/j.cell.2008.04.019
64. Hooper PL, Hooper PL, Tytell M, Vigh L. Xenohormesis: health benefits from an eat of plant stress response evolution. *Cell Stress Chaperones* 2010; 15:761-70; PMID:20524162; http://dx.doi.org/10.1007/s12192-010-0206-x
65. Son TG, Camandoli S, Mattson MP. Hormetic dietary phytochemicals. *Neuromolecular Med* 2008; 10:236-46; PMID:18543123; http://dx.doi.org/10.1007/s12107-008-8037-y
66. Surh YJ. Xenohormesis mechanisms underlying chemopreventive effects of some dietary phytochemicals. *Ann N Y Acad Sci* 2011; 1229:1-6; PMID:21793832; http://dx.doi.org/10.1111/j.1749-6632.2011.06097.x

67. Joseph JA, Shukitt-Hale B, Casadesus G. Reversing the deleterious effects of aging on neuronal communication and behavior: beneficial properties of fruit polyphenolic compounds. *Am J Clin Nutr* 2005; 81(Suppl):313S-6S; PMID:15640496
68. Benavente-Garcia O, Castillo J. Update on uses and properties of citrus flavonoids: new findings in anticancer, cardiovascular, and anti-inflammatory activity. *J Agric Food Chem* 2008; 56:6185-205; PMID:18593176; <http://dx.doi.org/10.1021/jf8006568>
69. Seelinger G, Merfort I, Schemp CM. Anti-oxidant, anti-inflammatory and anti-allergic activities of luteolin. *Planta Med* 2008; 74:1667-77; PMID:18937165; <http://dx.doi.org/10.1055/s-0028-1088314>
70. Chondrogianni N, Kapeta S, Chinou I, Vassilatou K, Papasideri I, Ginos ES. Anti-ageing and rejuvenating-effects of quercetin. *Exp Gerontol* 2010; 45:763-71; PMID:20619334; <http://dx.doi.org/10.1016/j.exger.2010.07.001>
71. Klappan AK, Hones S, Mylonas I, Brüning A. Proteasome inhibition by quercetin triggers macroautophagy and blocks mTOR activity. *Histochem Cell Biol* 2012; 137:25-36; PMID:21993664; <http://dx.doi.org/10.1007/s00418-011-0869-0>
72. Armour SM, Baur JA, Hsieh SN, Land-Bracha A, Thomas SM, Sinclair DA. Inhibition of mammalian S6 kinase by resveratrol suppresses autophagy. *Aging* (Albany NY) 2009; 1:515-28; PMID:20157535
73. Saul N, Piersch K, Menzel R, Steinberg CE. Quercetin-mediated longevity in Caenorhabditis elegans: is DAF-16 involved? *Mech Ageing Dev* 2008; 129:611-3; PMID:18692520; <http://dx.doi.org/10.1016/j.mad.2008.07.001>
74. Wilson MA, Shukitt-Hale B, Kalf W, Ingram DK, Joseph JA, Wolfow CA. Blueberry polyphenols increase lifespan and thermostolerance in Caenorhabditis elegans. *Aging Cell* 2006; 5:59-68; PMID:16441844; <http://dx.doi.org/10.1111/j.1474-9726.2006.00192.x>
75. Speciale A, Chirafisi J, Saia A, Cimino F. Nutritional antioxidants and adaptive cell responses: an update. *Curr Mol Med* 2011; 11:770-89; PMID:21999148; <http://dx.doi.org/10.2174/156652411798062395>
76. Rockenfeller P, Madeo F. Ageing and eating. *Biochim Biophys Acta* 2010; 1803:499-506; PMID:20079384; <http://dx.doi.org/10.1016/j.bbamcr.2010.01.001>
77. Zaveri NT. Green tea and its polyphenolic catechins: medicinal uses in cancer and noncancer applications. *Life Sci* 2006; 78:2073-80; PMID:16445946; <http://dx.doi.org/10.1016/j.lfs.2005.12.006>
78. Rattan SI, Ali RE. Hormetic prevention of molecular damage during cellular aging of human skin fibroblasts and keratinocytes. *Ann N Y Acad Sci* 2007; 1100:424-30; PMID:17460207; <http://dx.doi.org/10.1196/annals.1395.047>
79. Mattson MP. Dietary factors, hormesis and health. *Ageing Res Rev* 2008; 7:43-8; PMID:17913594; <http://dx.doi.org/10.1016/j.arr.2007.08.004>
80. Xiang L, Nakamura Y, Lim YM, Yamasaki Y, Kurokawa-Nose Y, Maruyama W, et al. Tetrahydrocurcumin extends life span and inhibits the oxidative stress response by regulating the FOXO forkhead transcription factor. *Aging* (Albany NY) 2011; 3:1098-109; PMID:22156377
81. Pramanik D, Campbell NR, Das S, Gupta S, Chenna V, Bish S, et al. A composite polymer nanoparticle overcomes multidrug resistance and ameliorates doxorubicin-associated cardiomyopathy. *Oncotarget* 2012; 3:640-50; PMID:22791660
82. Petrovski G, Das DK. Does autophagy take a front seat in lifespan extension? *J Cell Mol Med* 2010; 14:2543-51; PMID:21114762; <http://dx.doi.org/10.1111/j.1582-4934.2010.01196.x>
83. Chung S, Yao H, Caito S, Hwang JW, Arunachalam G, Rahman I. Regulation of SIRT1 in cellular functions: role of polyphenols. *Arch Biochem Biophys* 2010; 501:79-90; PMID:20450879; <http://dx.doi.org/10.1016/j.abb.2010.05.003>
84. Sikora E, Bielak-Zmijewska A, Mosieniak G, Piwocka K. The promise of slow down ageing may come from curcumin. *Curr Pharm Des* 2010; 16:884-92; PMID:20388102; <http://dx.doi.org/10.2174/138161210709883507>
85. Queen BL, Tollesbol TO. Polyphenols and aging. *Curr Aging Sci* 2010; 3:34-42; PMID:20298168
86. Baur JA, Sinclair DA. Therapeutic potential of resveratrol: the in vivo evidence. *Nat Rev Drug Discov* 2006; 5:493-506; PMID:16732220; <http://dx.doi.org/10.1038/nrd2060>
87. Liu BL, Zhang X, Zhang W, Zhen HN. New enlightenment of French Paradox: resveratrol's potential for cancer chemoprevention and anti-cancer therapy. *Cancer Biol Ther* 2007; 6:1833-6; PMID:18087218; <http://dx.doi.org/10.4161/cbt.6.12.5161>
88. Jiang M, Cai L, Udeani GO, Slowing KV, Thomas CF, Beecher CW, et al. Cancer chemopreventive activity of resveratrol, a natural product derived from grapes. *Science* 1997; 275:218-20; PMID:8985016; <http://dx.doi.org/10.1126/science.275.5297.218>
89. Howitz KT, Bitmaner KJ, Cohen HY, Lamming DW, Lavo S, Wood JG, et al. Small molecule activators of sirtuins extend Saccharomyces cerevisiae lifespan. *Nature* 2003; 425:191-6; PMID:12939617; <http://dx.doi.org/10.1038/nature01960>
90. Baur JA, Pearson KJ, Price NL, Jamieson HA, Lerin C, Kalra A, et al. Resveratrol improves health and survival of mice on a high-calorie diet. *Nature* 2006; 444:337-42; PMID:16786191; <http://dx.doi.org/10.1038/nature05354>
91. Pearson KJ, Baur JA, Lewis KN, Peshkin L, Price NL, Labinsky N, et al. Resveratrol delays age-related deterioration and mimics transcriptional aspects of dietary restriction without extending life span. *Cell Metab* 2008; 8:157-68; PMID:18599363; <http://dx.doi.org/10.1016/j.cmet.2008.06.011>
92. Lagouge M, Argmann C, Gerhart-Hines Z, Meziane H, Lerin C, Daussin F, et al. Resveratrol improves mitochondrial function and protects against metabolic disease by activating SIRT1 and PGC-1alpha. *Cell* 2006; 127:1109-22; PMID:17112576; <http://dx.doi.org/10.1016/j.cell.2006.11.013>
93. Wood JG, Rogina B, Lava S, Howitz K, Helfand SL, Tatar M, et al. Sirtuin activators mimic caloric restriction and delay ageing in metazoans. *Nature* 2004; 430:686-9; PMID:15254550; <http://dx.doi.org/10.1038/nature02789>
94. Agarwal B, Baur JA. Resveratrol and life extension. *Ann N Y Acad Sci* 2011; 1215:138-43; PMID:21261652; <http://dx.doi.org/10.1111/j.1749-6632.2010.05850.x>
95. Bass TM, Weinke D, Houthooft K, Gems D, Partridge L. Effects of resveratrol on lifespan in *Drosophila melanogaster* and *Caenorhabditis elegans*. *Mech Ageing Dev* 2007; 128:546-52; PMID:17875315; <http://dx.doi.org/10.1016/j.mad.2007.07.007>
96. Valenzano DR, Terzibasi E, Genade T, Cattaneo A, Domenici L, Cellerino A. Resveratrol prolongs lifespan and retards the onset of age-related markers in a short-lived vertebrate. *Curr Biol* 2006; 16:296-300; PMID:16461283; <http://dx.doi.org/10.1016/j.cub.2005.12.038>
97. Blagosklonny MV. Inhibition of S6K by resveratrol: in search of the purpose. *Aging* (Albany NY) 2009; 1:511-4; PMID:20157534
98. Demidenko ZN, Blagosklonny MV. At concentrations that inhibit mTOR, resveratrol suppresses cellular senescence. *Cell Cycle* 2009; 8:1901-4; PMID:19471118; <http://dx.doi.org/10.4161/cc.8.12.8810>
99. Rascón B, Hubbard BP, Sinclair DA, Amdam GV. The lifespan extension effects of resveratrol are conserved in the honey bee and may be driven by a mechanism related to caloric restriction. *Aging* (Albany NY) 2012; 4:499-508; PMID:22868943
100. Timmers S, Auwerx J, Schrauwen P. The journey of resveratrol from yeast to human. *Aging* (Albany NY) 2012; 4:146-58; PMID:22436213
101. Morselli E, Galuzzi L, Kepp O, Criollo A, Maiuri MC, Tavernarakis N, et al. Autophagy mediates pharmacological lifespan extension by spermidine and resveratrol. *Aging* (Albany NY) 2009; 1:961-70; PMID:20157579
102. Hofseth LJ, Singh UP, Singh NP, Nagarkatti M, Nagarkatti PS. Taming the beast within: resveratrol suppresses colitis and prevents colon cancer. *Aging* (Albany NY) 2010; 2:183-4; PMID:20436227
103. Vetterli L, Maechler P. Resveratrol-activated SIRT1 in liver and pancreatic beta-cells: a Janus head looking to the same direction of metabolically homeostasis. *Aging* (Albany NY) 2011; 3:444-9; PMID:21483037
104. Antosh M, Fox D, Helfand SL, Cooper LN, Neretti N. New comparative genomics approach reveals a conserved health span signature across species. *Aging* (Albany NY) 2011; 3:576-83; PMID:21775776
105. Chung JH. Using PDE inhibitors to harness the benefits of calorie restriction: lessons from resveratrol. *Aging* (Albany NY) 2012; 4:144-5; PMID:22388573
106. Vang O, Ahmad N, Baile CA, Baur JA, Brown K, Csizsar A, et al. What is new for an old molecule? Systematic review and recommendations on the use of resveratrol. *PLoS One* 2011; 6:e19881; PMID:21698226; <http://dx.doi.org/10.1371/journal.pone.0019881>
107. Hardie DG. Sensing of energy and nutrients by AMP-activated protein kinase. *Am J Clin Nutr* 2011; 93:891S-6; PMID:21325438; <http://dx.doi.org/10.3945/jcn.110.001925>
108. Do GM, Jung UJ, Park HJ, Kwon EY, Jeon SM, McGregor RA, et al. Resveratrol ameliorates diabetes-related metabolic changes via activation of AMP-activated protein kinase and its downstream targets in db/db mice. *Mol Nutr Food Res* 2012; 56:1282-91; PMID:22715031; <http://dx.doi.org/10.1002/mnfr.20100067>
109. Chen S, Xiao X, Feng X, Li W, Zhou N, Zheng L, et al. Resveratrol induces Sirt1-dependent apoptosis in 3T3-L1 preadipocytes by activating AMPK and suppressing AKT activity and survivin expression. *J Nutr Biochem* 2012; 23:1100-12; PMID:22137261; <http://dx.doi.org/10.1016/j.jn.2011.06.003>
110. Timmers S, Konings E, Biley L, Houtkooper RH, van de Weijer T, Goossens GH, et al. Calorie restriction-like effects of 30 days of resveratrol supplementation on energy metabolism and metabolic profile in obese humans. *Cell Metab* 2011; 14:612-22; PMID:21555504; <http://dx.doi.org/10.1016/j.cmet.2011.10.002>
111. Hsu CL, Yen GC. Phenolic compounds: evidence for inhibitory effects against obesity and their underlying molecular signaling mechanisms. *Mol Nutr Food Res* 2008; 52:53-61; PMID:18081207; <http://dx.doi.org/10.1002/mnfr.20070039>
112. Crozier A, Jaganathan IB, Clifford MN. Dietary phenolics: chemistry, bioavailability and effects on health. *Nat Prod Rep* 2009; 26:1001-43; PMID:19636448; <http://dx.doi.org/10.1039/b802662a>
113. Cicerele S, Conlan XA, Sinclair AJ, Keast RS. Chemistry and health of olive oil phenolics. *Crit Rev Food Sci Nutr* 2009; 49:218-36; PMID:19093267; <http://dx.doi.org/10.1080/10408390701856223>
114. Colomer R, Menéndez JA. Mediterranean diet, olive oil and cancer. *Clin Transl Oncol* 2006; 8:15-21; PMID:16632435; <http://dx.doi.org/10.1007/s12094-006-0090-0>

115. Menendez JA, Lupu R. Mediterranean dietary traditions for the molecular treatment of human cancer: anti-oncogenic actions of the main olive oil's monounsaturated fatty acid oleic acid (18:1n-9). *Curr Pharm Biotechnol* 2006; 7:495-502; PMID:17168666; <http://dx.doi.org/10.2174/138920106779116900>
116. Escrich E, Moral R, Grau L, Costa I, Solanas M. Molecular mechanisms of the effects of olive oil and other dietary lipids on cancer. *Mol Nutr Food Res* 2007; 51:1279-92; PMID:17879998
117. Colomer R, Lupu R, Papadimitropoulou A, Vellón L, Vázquez-Martín A, Brunet J, et al. Giacomo Castelvetro's salads. Anti-HER2 oncogene nutraceuticals since the 17th century? *Clin Transl Oncol* 2008; 10:30-4; PMID:18208790; <http://dx.doi.org/10.1007/s12094-008-0151-7>
118. López-Miranda J, Pérez-Jiménez F, Ros E, De Caterina R, Badimon L, Covas MI, et al. Olive oil and health: summary of the II international conference on olive oil and health consensus report, Jaén and Córdoba (Spain) 2008. *Nutr Metab Cardiovasc Dis* 2010; 20:284-94; PMID:20303720; <http://dx.doi.org/10.1016/j.numecd.2009.12.007>
119. Escrich E, Solanas M, Moral R, Costa I, Grau L. Are the olive oil and other dietary lipids related to cancer? Experimental evidence. *Clin Transl Oncol* 2006; 8:868-83; PMID:17169760; <http://dx.doi.org/10.1007/s12094-006-0105-5>
120. Galli C, Visioli F. Antioxidant and other activities of phenolics in olives/olive oil, typical components of the Mediterranean diet. *Lipids* 1999; 34:23-6; PMID:10188593; <http://dx.doi.org/10.1007/BF02562224>
121. Owen RW, Giacosa A, Hull WE, Haubner R, Spiegelhalder B, Bartsch H. The antioxidant/anticancer potential of phenolic compounds isolated from olive oil. *Eur J Cancer* 2000; 36:1235-47; PMID:10882862; [http://dx.doi.org/10.1016/S0959-8049\(00\)00103-9](http://dx.doi.org/10.1016/S0959-8049(00)00103-9)
122. Owen RW, Mier W, Giacosa A, Hull WE, Spiegelhalder B, Bartsch H. Identification of lignans as major components in the phenolic fraction of olive oil. *Clin Chem* 2000; 46:976-88; PMID:10894841
123. Visioli F, Galli C. Phenolics from olive oil and its waste products. Biological activities in vitro and in vivo studies. *World Rev Nutr Diet* 2001; 88:233-7; PMID:11935962; <http://dx.doi.org/10.1159/0000059757>
124. Visioli F, Poli A, Galli C. Antioxidant and other biological activities of phenols from olives and olive oil. *Med Sci Rev* 2002; 22:65-75; PMID:11746176; <http://dx.doi.org/10.1002/med.1028>
125. Visioli F, Galli C. Biological properties of olive oil phytochemicals. *Crit Rev Food Sci Nutr* 2002; 42:209-21; PMID:12058980; <http://dx.doi.org/10.1080/10408690209825529>
126. Beauchamp GK, Keast RS, Morel D, Lin J, Pika J, Han Q, et al. Phytochemistry: ibuprofen-like activity in extra-virgin olive oil. *Nature* 2005; 437:45-6; PMID:16136122; <http://dx.doi.org/10.1038/437045a>
127. Carrasco-Pancorbo A, Cerretani L, Bendini A, Segura-Carretero A, Gallina-Toschi T, Fernández-Gutiérrez A. Analytical determination of polyphenols in olive oils: a survey of their sensory properties, health effects, antioxidant activity and analytical methods. An overview of the last decade. *Molecules* 2007; 12:1679-719; PMID:17960082; <http://dx.doi.org/10.3390/12081679>
129. García-Villalba R, Carrasco-Pancorbo A, Oliveras-Ferraro C, Vázquez-Martín A, Menéndez JA, Segura-Carretero A, et al. Characterization and quantification of phenolic compounds of extra-virgin olive oils with anticancer properties by a rapid and resolute LC-ESI-TOF MS method. *J Pharm Biomed Anal* 2010; 51:416-29; PMID:19596535; <http://dx.doi.org/10.1016/j.jpba.2009.06.021>
130. García-Villalba R, Carrasco-Pancorbo A, Vázquez-Martín A, Oliveras-Ferraro C, Menéndez JA, Segura-Carretero A, et al. A 2-D-HPLC-CE platform coupled to ESI-TOF-MS to characterize the phenolic fraction in olive oil. *Electrophoresis* 2009; 30:2688-701; PMID:19650044; <http://dx.doi.org/10.1002/elps.200800807>
131. Owen RW, Giacosa A, Hull WE, Haubner R, Würtele G, Spiegelhalder B, et al. Olive-oil consumption and health: the possible role of antioxidants. *Lancet Oncol* 2000; 1:107-12; PMID:11905662; [http://dx.doi.org/10.1016/S1470-2045\(00\)00015-2](http://dx.doi.org/10.1016/S1470-2045(00)00015-2)
132. Servili M, Espósito S, Fabiani R, Urbani S, Tatichai A, Mariucci F, et al. Phenolic compounds in olive oil: antioxidant, health and organoleptic activities according to their chemical structure. *Inflammopharmacology* 2009; 17:76-84; PMID:19234678; <http://dx.doi.org/10.1007/s10787-008-8014-y>
133. Raederstorff D. Antioxidant activity of olive polyphenols in humans: a review. *Int J Vitam Nutr Res* 2009; 79:152-65; PMID:20209466; <http://dx.doi.org/10.1024/0300-9831.79.3.152>
134. Sinclair DA. Toward a unified theory of caloric restriction and longevity regulation. *Mech Ageing Dev* 2005; 126:987-1002; PMID:15893363; <http://dx.doi.org/10.1016/j.mad.2005.03.019>
135. Way TD, Kao MC, Lin JK. Apigenin induces apoptosis through proteasomal degradation of HER2/neu in HER2/neu-overexpressing breast cancer cells via the phosphatidylinositol 3-kinase/Akt-dependent pathway. *J Biol Chem* 2004; 279:4479-89; PMID:14602723; <http://dx.doi.org/10.1074/jbc.M305529200>
136. Way TD, Kao MC, Lin JK. Degradation of HER2/neu by apigenin induces apoptosis through cytochrome c release and caspase-3 activation in HER2/neu-overexpressing breast cancer cells. *FEBS Lett* 2005; 562:145-52; PMID:16052074; <http://dx.doi.org/10.1016/j.febslet.2004.11.061>
137. Shimizu M, Deguchi A, Joe AK, McKoy JF, Moriwaki H, Weinstein IB. EGCG inhibits activation of HER3 and expression of cyclooxygenase-2 in human colon cancer cells. *J Exp Ther Oncol* 2005; 5:69-78; PMID:16416603
138. Shimizu M, Deguchi A, Hara Y, Moriwaki H, Weinstein IB. EGCG inhibits activation of the insulin-like growth factor-1 receptor in human colon cancer cells. *Biochem Biophys Res Commun* 2005; 334:947-53; PMID:16053920; <http://dx.doi.org/10.1016/j.bbrc.2005.06.182>
139. Shimizu M, Deguchi A, Lim JT, Moriwaki H, Kopelovich L, Weinstein IB. (-)-Epigallocatechin gallate and polyphenon E inhibit growth and activation of the epidermal growth factor receptor and human epidermal growth factor receptor-2 signaling pathways in human colon cancer cells. *Clin Cancer Res* 2005; 11:2735-46; PMID:15814656; <http://dx.doi.org/10.1158/1078-0432.CCR-04-2014>
140. Chiang CT, Way TD, Lin JK. Sensitizing HER2-overexpressing cancer cells to luteolin-induced apoptosis through suppressing p21(WAF1/CIP1) expression with rapamycin. *Mol Cancer Ther* 2007; 6:2127-38; PMID:17620442; <http://dx.doi.org/10.1158/1535-7163.MCT-07-0107>
141. Menendez JA, Vazquez-Martín A, Colomer R, Brunet J, Carrasco-Pancorbo A, García-Villalba R, et al. Olive oil's bitter principle reverses acquired autoresistance to trastuzumab (Herceptin) in HER2-overexpressing breast cancer cells. *BMC Cancer* 2007; 7:80; PMID:17490486; <http://dx.doi.org/10.1186/1471-2407-7-80>
142. Menendez JA, Vazquez-Martín A, Oliveras-Ferraro C, García-Villalba R, Carrasco-Pancorbo A, Fernández-Gutiérrez A, et al. Analyzing effects of extra-virgin olive oil polyphenols on breast cancer-associated fatty acid synthase protein expression using reverse-phase protein microarrays. *Int J Mol Med* 2008; 22:433-9; PMID:18813848
143. Menendez JA, Vazquez-Martín A, Oliveras-Ferraro C, García-Villalba R, Carrasco-Pancorbo A, Fernández-Gutiérrez A, et al. Extra-virgin olive oil polyphenols inhibit HER2 (erbB-2)-induced malignant transformation in human breast epithelial cells: relationship between the chemical structures of extra-virgin olive oil secoiridoids and lignans and their inhibitory activities on the tyrosine kinase activity of HER2. *Int J Oncol* 2009; 34:43-51; PMID:19082476
144. Menendez JA, Vazquez-Martín A, García-Villalba R, Carrasco-Pancorbo A, Oliveras-Ferraro C, Fernández-Gutiérrez A, et al. abAnti-HER2 (erbB-2) oncogene effects of phenolic compounds directly isolated from commercial Extra-Virgin Olive Oil (EVOO). *BMC Cancer* 2008; 8:377; PMID:19094209; <http://dx.doi.org/10.1186/1471-2407-8-377>
145. Lozano-Sánchez J, Segura-Carretero A, Menendez JA, Oliveras-Ferraro C, Cerretani L, Fernández-Gutiérrez A. Prediction of extra virgin olive oil varieties through their phenolic profile. Potential cytotoxic activity against human breast cancer cells. *J Agric Food Chem* 2010; 58:9942-55; PMID:20795736; <http://dx.doi.org/10.1021/jf1015024>
146. Oliveras-Ferraro C, Fernández-Arroyo S, Vazquez-Martín A, Lozano-Sánchez J, Cuffi S, Joven J, et al. Crude phenolic extracts from extra virgin olive oil circumvent de novo breast cancer resistance to HER1/HER2-targeting drugs by inducing GADD45-sensed cellular stress, G2/M arrest and hyperacetylation of Histone H3. *Int J Oncol* 2011; 38:1533-47; PMID:21455577
147. Vazquez-Martín A, Fernández-Arroyo S, Cuffi S, Oliveras-Ferraro C, Lozano-Sánchez J, Vellón L, et al. Phenolic secoiridoids in extra virgin olive oil impede fibrogenic and oncogenic epithelial-to-mesenchymal transition: extra virgin olive oil as a source of novel antiaging phytochemicals. *Rejuvenation Res* 2012; 15:3-21; PMID:22229524; <http://dx.doi.org/10.1089/rej.2011.21203>
148. García-Villalba R, Carrasco-Pancorbo A, Oliveras-Ferraro C, Menéndez JA, Segura-Carretero A, Fernández-Gutiérrez A. Uptake and metabolism of olive oil polyphenols in human breast cancer cells using nano-liquid chromatography coupled to electrospray ionization-time of flight-mass spectrometry. *J Chromatogr B Anal Technol Biomed Life Sci* 2012; 898:69-77; PMID:22608806; <http://dx.doi.org/10.1016/j.jchromb.2012.04.021>
149. Roldán C, de la Torre A, Mota S, Morales-Soto A, Menéndez J, Segura-Carretero A. Identification of active compounds in vegetal extracts based on correlation between activity and HPLC-MS data. *Food Chem* 2013; 136:392-9; PMID:23122076; <http://dx.doi.org/10.1016/j.foodchem.2012.08.027>
150. Buckland G, Agudo A, Travier N, Huerta JM, Cirera L, Tormo MJ, et al. Adherence to the Mediterranean diet reduces mortality in the Spanish cohort of the European Prospective Investigation into Cancer and Nutrition (EPIC-Spain). *Br J Nutr* 2011; 106:1581-91; PMID:21736834; <http://dx.doi.org/10.1017/S0007114511002078>
151. Lagiou P, Trichopoulos D, Sandin S, Lagiou A, Mucci L, Wolk A, et al. Mediterranean dietary pattern and mortality among young women: a cohort study in Sweden. *Br J Nutr* 2006; 96:384-92; PMID:16923235; <http://dx.doi.org/10.1079/BJN20061824>

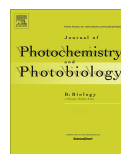
152. Trichopoulou A, Orfanos P, Norat T, Bueno-de-Mesquita B, Ocké MC, Peeters PH, et al. Modified Mediterranean diet and survival: EPIC-elderly prospective cohort study. *BMJ* 2005; 330:991; PMID:15820966; <http://dx.doi.org/10.1136/bmj.38415.641558F>
153. Trichopoulou A, Dilis V. Olive oil and longevity. *Mol Nutr Food Res* 2007; 51:1275-8; PMID:17879997
154. Trichopoulou A. Traditional Mediterranean diet and longevity in the elderly: a review. *Public Health Nutr* 2004; 7:943-7; PMID:15482622; <http://dx.doi.org/10.1079/PHN2004558>
155. Trichopoulou A, Critiselis E. Mediterranean diet and longevity. *Eur J Cancer Prev* 2004; 13:453-6; PMID:15452459; <http://dx.doi.org/10.1097/0000469-200410000-00014>
156. Trichopoulou A, Costacou T, Bania C, Trichopoulos D. Adherence to a Mediterranean diet and survival in a Greek population. *N Engl J Med* 2003; 348:2599-608; PMID:12826634; <http://dx.doi.org/10.1056/NEJMoa025039>
157. Frankel EN. Nutritional and biological properties of extra virgin olive oil. *J Agric Food Chem* 2011; 59:785-92; PMID:21210703; <http://dx.doi.org/10.1021/jf103813t>
158. Blagosklonny MV. Aging: ROS or TOR. *Cell Cycle* 2008; 7:3344-54; PMID:18971624; <http://dx.doi.org/10.4161/cc.7.21.6965>
159. Hunt PR, Son TG, Wilson MA, Yu QS, Wood WH, Zhang Y, et al. Extension of lifespan in *C. elegans* by naphthoquinones that act through stress hormesis mechanisms. *PLoS One* 2011; 6:e21922; PMID:21765926; <http://dx.doi.org/10.1371/journal.pone.0021922>
160. Hwang AB, Lee SJ. Regulation of life span by mitochondrial respiration: the HIF-1 and ROS connection. *Aging (Albany NY)* 2011; 3:304-10; PMID:21389351
161. Keane M, Matthijssen F, Sharpe M, Vanfleteren J, Gems D. Superoxide dismutase mimetics elevate superoxide dismutase activity in vivo but do not retard aging in the nematode *Caenorhabditis elegans*. *Free Radic Biol Med* 2004; 37:239-50; PMID:15203195; <http://dx.doi.org/10.1016/j.freeradbiomed.2004.04.005>
162. Doonan R, McElwee JJ, Matthijssen F, Walker GA, Hourhoofd K, Back P, et al. Against the oxidative damage theory of aging: superoxide dismutases protect against oxidative stress but have little or no effect on life span in *Caenorhabditis elegans*. *Genes Dev* 2008; 22:3236-41; PMID:19056880; <http://dx.doi.org/10.1101/gad.504808>
163. Van Raamsdonk JM, Hekimi S. Deletion of the mitochondrial superoxide dismutase sod-2 extends lifespan in *Caenorhabditis elegans*. *PLoS Genet* 2009; 5:e1000361; PMID:19197346; <http://dx.doi.org/10.1371/journal.pgen.1000361>
164. Gems D, Doonan R. Antioxidant defense and aging in *C. elegans*: is the oxidative damage theory of aging wrong? *Cell Cycle* 2009; 8:1681-7; PMID:19411855; <http://dx.doi.org/10.4161/cc.8.11.8595>
165. Lapointe J, Hekimi S. When a theory of aging ages badly. *Cell Mol Life Sci* 2010; 67:1-8; PMID:19730800; <http://dx.doi.org/10.1007/s00018-009-0138-8>
166. Edman U, Garcia AM, Busuttil RA, Sorensen D, Lundell M, Kapahi P, et al. Lifespan extension by dietary restriction is not linked to protection against somatic DNA damage in *Drosophila melanogaster*. *Aging Cell* 2009; 8:331-8; PMID:19627272; <http://dx.doi.org/10.1111/j.1474-9726.2009.00480.x>
167. Van Raamsdonk JM, Meng Y, Camp D, Yang W, Jia X, Bénard C, et al. Decreased energy metabolism extends life span in *Caenorhabditis elegans* without reducing oxidative damage. *Genetics* 2010; 185:559-71; PMID:20382831; <http://dx.doi.org/10.1534/genetics.110.115378>
168. Van Raamsdonk JM, Hekimi S. Reactive Oxygen Species and Aging in *Caenorhabditis elegans*: Causal or Casual Relationship? *Antioxid Redox Signal* 2010; 13:1911-53; PMID:20568954; <http://dx.doi.org/10.1089/ars.2010.3215>
169. Yang W, Li J, Hekimi S. A Measurable increase in oxidative damage due to reduction in superoxide detoxification fails to shorten the life span of long-lived mitochondrial mutants of *Caenorhabditis elegans*. *Genetics* 2007; 177:2063-74; PMID:18073424; <http://dx.doi.org/10.1534/genetics.107.078078>
170. Guachalla LM, Rudolph KL. ROS induced DNA damage and checkpoint responses influences on aging? *Cell Cycle* 2010; 9:4058-60; PMID:20935491; <http://dx.doi.org/10.4161/cc.9.20.13577>
171. Yang W, Hekimi S. A mitochondrial superoxide signal triggers increased longevity in *Caenorhabditis elegans*. *PLoS Biol* 2010; 8:e1000556; PMID:2151885; <http://dx.doi.org/10.1371/journal.pbio.1000556>
172. Hekimi S, Lapointe J, Wen Y. Taking a "good" look at free radicals in the aging process. *Trends Cell Biol* 2011; 21:569-76; PMID:21824781; <http://dx.doi.org/10.1016/j.tcb.2011.06.008>
173. Sanz A, Fernández-Ayala DJ, Stefanatos RK, Jacobs HT. Mitochondrial ROS production correlates with, but does not directly regulate lifespan in *Drosophila*. *Aging (Albany NY)* 2010; 2:200-23; PMID:20453260
174. Pani G, P66SHC and ageing: ROS and TOR? *Aging (Albany NY)* 2010; 2:514-8; PMID:20689155
175. Cabreira F, Ackerman D, Doonan R, Araiz C, Back P, Papp D, et al. Increased life span from overexpression of superoxide dismutase in *Caenorhabditis elegans* is not caused by decreased oxidative damage. *Free Radic Biol Med* 2011; 51:1575-82; PMID:21839827; <http://dx.doi.org/10.1016/j.freeradbiomed.2011.07.020>
176. Speakman JR, Selman C. The free-radical damage theory: Accumulating evidence against a simple link of oxidative stress to ageing and lifespan. *Bioessays* 2011; 33:255-9; PMID:21290398; <http://dx.doi.org/10.1002/bies.201000132>
177. Lee SJ, Hwang AB, Kenyon C. Inhibition of respiration extends *C. elegans* life span via reactive oxygen species that increase HIF-1 activity. *Curr Biol* 2010; 20:2131-6; PMID:21093262; <http://dx.doi.org/10.1016/j.cub.2010.10.057>
178. Rodriguez KA, Wywial E, Perez VI, Lambert AJ, Edrey YH, Lewis KN, et al. Walking the oxidative stress tightrope: a perspective from the naked mole-rat, the longest-living rodent. *Curr Pharm Des* 2011; 17:2290-307; PMID:21736541; <http://dx.doi.org/10.2147/cpd.1316121179705247>
179. Cañuelo A, Gilbert-López B, Pacheco-Lifán P, Martínez-Lara E, Siles E, Miranda-Vizcute A. Tyrosol, a main phenol present in extra virgin olive oil, increases lifespan and stress resistance in *Caenorhabditis elegans*. *Mech Ageing Dev* 2012; 133:563-74; PMID:22842366; <http://dx.doi.org/10.1016/j.mad.2012.07.004>
180. Blagosklonny MV. Hormesis does not make sense except in the light of TOR-driven aging. *Aging (Albany NY)* 2011; 3:1051-62; PMID:22166724
181. Mayer MP, Bukau B. Hsp70 chaperones: cellular functions and molecular mechanism. *Cell Mol Life Sci* 2005; 62:670-84; PMID:15770419; <http://dx.doi.org/10.1007/s00018-004-4464-6>
182. Broochieri L, Conway de Macario E, Macario AJ. hsp70 genes in the human genome: Conservation and differentiation patterns predict a wide array of overlapping and specialized functions. *BMC Evol Biol* 2008; 8:19; PMID:18215318; <http://dx.doi.org/10.1186/1471-2148-8-19>
183. Daugaard M, Rohde M, Jäättälä M. The heat shock protein 70 family: Highly homologous proteins with overlapping and distinct functions. *FEBS Lett* 2007; 581:3702-10; PMID:17544402; <http://dx.doi.org/10.1016/j.febslet.2007.05.039>
184. Neznanov N, Komarov AP, Neznanova L, Stanhope-Baker P, Gudkov AV. Proteotoxic stress targeted therapy (PSTT): induction of protein misfolding enhances the antitumor effect of the proteasome inhibitor bortezomib. *Oncotarget* 2011; 2:209-21; PMID:21444945
185. Leung TKC, Rajendran MY, Monfries C, Hall C, Lim L. The human heat-shock protein family: Expression of a novel heat-inducible HSP70 (HSP70B) and isolation of its cDNA and genomic DNA. *Biochem J* 1990; 267:125-32; PMID:2327978
186. Leung TKC, Hall C, Rajendran M, Spurr NK, Lim L. The human heat-shock genes HSPA6 and HSPA7 are both expressed and localize to chromosome 1. *Genomics* 1992; 12:74-9; PMID:1346391; [http://dx.doi.org/10.1016/0888-7543\(92\)90409-L](http://dx.doi.org/10.1016/0888-7543(92)90409-L)
187. Noonan EJ, Place RF, Giardina C, Hightower LE. Hsp70' regulation and function. *Cell Stress Chaperones* 2007; 12:219-29; PMID:17915554; <http://dx.doi.org/10.1379/CSC.278.1>
188. Rohde M, Daugaard M, Jensen MH, Helin K, Nylandsted J, Jäättälä M. Members of the heat-shock protein 70 family promote cancer cell growth by distinct mechanisms. *Genes Dev* 2005; 19:570-72; PMID:15741319; <http://dx.doi.org/10.1101/gad.305405>
189. Milner CM, Campbell RD. Structure and expression of the three MHC-linked HSP70 genes. *Immunogenetics* 1990; 32:242-51; PMID:1700760; <http://dx.doi.org/10.1007/BF00187095>
190. Sargent CA, Dunham I, Trowsdale J, Campbell RD. Human major histocompatibility complex contains genes for the major heat shock protein HSP70. *Proc Natl Acad Sci U S A* 1989; 86:1968-72; PMID:2538825; <http://dx.doi.org/10.1073/pnas.86.6.1968>
191. Son WY, Hwang SH, Han CT, Lee JH, Kim S, Kim YC. Specific expression of heat shock protein HspA2 in human male germ cells. *Mol Hum Reprod* 1999; 5:1122-6; PMID:10587366; <http://dx.doi.org/10.1093/molehr/5.12.1122>
192. Govin J, Caron C, Escoffier E, Ferro M, Kuhn L, Rousseau S, et al. Post-meiotic shifts in HSP2A/HSP70.2 chaperone activity during mouse spermatogenesis. *J Biol Chem* 2006; 281:37888-92; PMID:1703236; <http://dx.doi.org/10.1074/jbc.M608147200>
193. Zhu D, Dix DJ, Eddy EM. HSP70-2 is required for CDC2 kinase activity in meiosis I of mouse spermatocytes. *Development* 1997; 124:3007-14; PMID:9247342
194. Feng HL, Sandlow JI, Sparks AET. Decreased expression of the heat shock protein hsp70-2 is associated with the pathogenesis of male infertility. *Fertil Steril* 2001; 76:1136-9; PMID:11703740; [http://dx.doi.org/10.1016/S0015-0282\(01\)02892-8](http://dx.doi.org/10.1016/S0015-0282(01)02892-8)
195. Svärd M, Bitterová E, Bourhis JM, Guy JE, The crystal structure of the human co-chaperone P58(IPK). *PLoS One* 2011; 6:e22337; PMID:21799829; <http://dx.doi.org/10.1371/journal.pone.0022337>
196. Yan W, Frank CL, Korth MJ, Sophie BL, Novoa I, Ron D, et al. Control of PERK eIF2alpha kinase activity by the endoplasmic reticulum stress-induced molecular chaperone P58IPK. *Proc Natl Acad Sci U S A* 2002; 99:15920-5; PMID:12446838; <http://dx.doi.org/10.1073/pnas.252341799>
197. Wiseman RL, Haynes CM, Ron D. SnapShot: The unfolded protein response. *Cell* 2010; 140:590-590.e2; PMID:20178750; <http://dx.doi.org/10.1016/j.cell.2010.02.006>
198. Ron D, Walter P. Signal integration in the endoplasmic reticulum unfolded protein response. *Nat Rev Mol Cell Biol* 2007; 8:519-29; PMID:1756364; <http://dx.doi.org/10.1038/nrm2199>
199. Zhang K, Kaufman RJ. The unfolded protein response: a stress signaling pathway critical for health and disease. *Neurology* 2006; 66(Suppl 1):S102-9; PMID:16432136; <http://dx.doi.org/10.1212/01.wnl.0000192306.98198.ec>

200. Kroemer G, Mariño G, Levine B. Autophagy and the integrated stress response. *Mol Cell* 2010; 40:280-93; PMID:20965422; <http://dx.doi.org/10.1016/j.molcel.2010.09.023>
201. Endo S, Hiramatsu N, Hayakawa K, Okamura M, Kasai A, Tagawa Y, et al. Geranylgeranylacetone, an inducer of the 70-kDa heat shock protein (HSP70), elicits unfolded protein response and coordinates cellular fate independently of HSP70. *Mol Pharmacol* 2007; 72:1337-48; PMID:17702888; <http://dx.doi.org/10.1124/mol.107.039164>
202. Haynes CM, Ron D. The mitochondrial UPR - protecting organelle protein homeostasis. *J Cell Sci* 2010; 123:3849-55; PMID:21048161; <http://dx.doi.org/10.1242/jcs.075119>
203. Lin JH, Li H, Yasumura D, Cohen HR, Zhang C, Panning B, et al. IRE1 signaling affects cell fate during the unfolded protein response. *Science* 2007; 318:944-9; PMID:17791856; <http://dx.doi.org/10.1126/science.1146361>
204. Debnath J, Baehrecke EH, Kroemer G. Does autophagy contribute to cell death? *Autophagy* 2005; 1:66-74; PMID:16874022; <http://dx.doi.org/10.4161/auto.1.2.1738>
205. Liu BQ, Gao YY, Niu XF, Xie JS, Meng X, Guan Y, et al. Implication of unfolded protein response in resveratrol-induced inhibition of K562 cell proliferation. *Biochem Biophys Res Commun* 2010; 391:778-82; PMID:19944671; <http://dx.doi.org/10.1016/j.bbrc.2009.11.137>
206. Yan Y, Gao YY, Liu BQ, Niu XF, Zhuang Y, Wang HQ. Resveratrol-induced cytotoxicity in human Burkitt's lymphoma cells is coupled to the unfolded protein response. *BMC Cancer* 2010; 10:445; PMID:2073265; <http://dx.doi.org/10.1186/1471-2407-10-445>
207. Woo KJ, Lee TJ, Lee SH, Lee JM, Seo JH, Jeong YJ, et al. Elevated gadd153/chop expression during resveratrol-induced apoptosis in human colon cancer cells. *Biochem Pharmacol* 2007; 73:68-76; PMID:17049495; <http://dx.doi.org/10.1016/j.bcp.2006.09.015>
208. Viswanathan M, Kim KM, Berdichevsky A, Guarante L. A role for SIR-2.1 regulation of ER stress response genes in determining *C. elegans* life span. *Dev Cell* 2005; 9:605-15; PMID:16256736; <http://dx.doi.org/10.1016/j.devcel.2005.09.017>
209. Chinta SJ, Poksay KS, Kaundinya G, Hart M, Bredesen DE, Andersen JK, et al. Endoplasmic reticulum stress-induced cell death in dopaminergic cells: effect of resveratrol. *J Mol Neurosci* 2009; 39:157-68; PMID:19145491; <http://dx.doi.org/10.1007/s12031-008-9170-7>
210. Hwang JT, Kwak DW, Lin SK, Kim HM, Kim YM, Park OJ. Resveratrol induces apoptosis in chemoresistant cancer cells via modulation of AMPK signaling pathway. *Ann N Y Acad Sci* 2007; 1095:441-8; PMID:17404056; <http://dx.doi.org/10.1196/annals.1397.047>
211. Heiss EH, Schilder YD, Dirsch VM. Chronic treatment with resveratrol induces redox stress- and ataxia telangiectasia-mutated (ATM)-dependent senescence in p53-positive cancer cells. *J Biol Chem* 2007; 282:26759-66; PMID:17626009; <http://dx.doi.org/10.1074/jbc.M703229200>
212. Low IC, Chen ZX, Pervaiz S. Bel-2 modulates resveratrol-induced ROS production by regulating mitochondrial respiration in tumor cells. *Antioxid Redox Signal* 2010; 13:807-19; PMID:20367277; <http://dx.doi.org/10.1089/ars.2009.3050>
213. Hussain AR, Uddin S, Bu R, Khan OS, Ahmed SO, Ahmed M, et al. Resveratrol suppresses constitutive activation of AKT via generation of ROS and induces apoptosis in diffuse large B cell lymphoma cell lines. *PLoS One* 2011; 6:e24703; PMID:21931821; <http://dx.doi.org/10.1371/journal.pone.0024703>
214. Malhotra JD, Kaufman RJ. Endoplasmic reticulum stress and oxidative stress: a vicious cycle or a double-edged sword? *Antioxid Redox Signal* 2007; 9:2277-93; PMID:17979528; <http://dx.doi.org/10.1089/ars.2007.1782>
215. Khanal P, Oh WK, Yun HJ, Namgoong GM, Ahn SG, Kwon SM, et al. p-HPEA-EDA, a phenolic compound of virgin olive oil, activates AMP-activated protein kinase to inhibit carcinogenesis. *Carcinogenesis* 2011; 32:545-53; PMID:21216846; <http://dx.doi.org/10.1093/carcin/bgq001>
216. Hao J, Shen W, Yu G, Jin H, Li X, Feng Z, et al. Hydroxytyrosol promotes mitochondrial biogenesis and mitochondrial function in 3T3-L1 adipocytes. *J Nutr Biochem* 2010; 21:634-44; PMID:19576748; <http://dx.doi.org/10.1016/j.jnutbio.2009.03.012>
217. Smith JJ, Kenney RD, Gagne DJ, Frushour BP, Ladd W, Galonelk HL, et al. Small molecule activators of SIRT1 replicate signaling pathways triggered by caloric restriction in vivo. *BMC Syst Biol* 2009; 3:31; PMID:19284563; <http://dx.doi.org/10.1186/1752-0509-3-31>
218. Wolter F, Turchanowicz L, Stein J. Resveratrol-induced modification of polyamine metabolism is accompanied by induction of c-Fos. *Carcinogenesis* 2003; 24:469-74; PMID:12663506; <http://dx.doi.org/10.1093/carcin/24.3.469>
219. Arthur M, Back JH, Kopelovich L, Bickers DR, Kim AL. Multiple molecular targets of resveratrol: Anticarcinogenic mechanisms. *Arch Biochem Biophys* 2009; 486:95-102; PMID:19514131; <http://dx.doi.org/10.1016/j.abb.2009.01.018>
220. Chen A, Davis BH, Bisognette M, Scaglione-Sewell B, Brusatis TA. 25-Dihydroxyvitamin D(3) stimulates activator protein-1-dependent Caco-2 cell differentiation. *J Biol Chem* 1999; 274:35505-13; PMID:10585423; <http://dx.doi.org/10.1074/jbc.274.35505>
221. Souleimani A, Asselin C. Regulation of C-fos expression by sodium butyrate in the human colon carcinoma cell line Caco-2. *Biochem Biophys Res Commun* 1993; 193:330-6; PMID:8503924; <http://dx.doi.org/10.1006/bbrc.1993.1628>
222. Minoia N, Carmona-Gutierrez D, Madeo F. Polyamines in aging and disease. *Aging* (Albany NY) 2011; 3:102-32; PMID:21869457
223. Eisenberg T, Knauer H, Schaeuer A, Büttner S, Ruckenstein C, Carmona-Gutierrez D, et al. Induction of autophagy by spermidine promotes longevity. *Nat Cell Biol* 2009; 11:1305-14; PMID:19801973; <http://dx.doi.org/10.1038/ncb1973>
224. Madeo F, Eisenberg T, Büttner S, Ruckenstein C, Kroemer G. Spermidine: a novel autophagy inducer and longevity elixir. *Autophagy* 2010; 6:160-2; PMID:2010777; <http://dx.doi.org/10.4161/auto.6.1.10600>
225. Madeo F, Tavernarakis N, Kroemer G. Can autophagy promote longevity? *Nat Cell Biol* 2010; 12:842-6; PMID:2081357; <http://dx.doi.org/10.1038/ncb0910-842>
226. Morselli E, Maríño G, Bennetzen MV, Eisenberg T, Megalou E, Schroeder S, et al. Spermidine and resveratrol induce autophagy by distinct pathways converging on the acetylproteome. *J Cell Biol* 2011; 192:615-29; PMID:21339330; <http://dx.doi.org/10.1083/jcb.201008167>
227. Maríño G, Morselli E, Bennetzen MV, Eisenberg T, Megalou E, Schroeder S, et al. Longevity-relevant regulation of autophagy at the level of the acetylproteome. *Autophagy* 2011; 7:647-9; PMID:21460620; <http://dx.doi.org/10.4161/auto.7.6.15191>
228. Rubinstein DC, Maríño G, Kroemer G. Autophagy and aging. *Cell* 2011; 146:682-95; PMID:21884931; <http://dx.doi.org/10.1016/j.cell.2011.07.030>
229. Bennetzen MV, Maríño G, Pultz D, Morselli E, Fargeman NJ, Kroemer G, et al. Phosphoproteomic analysis of cells treated with longevity-related autophagy inducers. *Cell Cycle* 2012; 11:1827-40; PMID:22517431; <http://dx.doi.org/10.4161/cc.20233>
230. Minoia N, Carmona-Gutierrez D, Bauer MA, Rockenfeller P, Eisenberg T, Brandhorst S, et al. Spermidine promotes stress resistance in Drosophila melanogaster through autophagy-dependent and -independent pathways. *Cell Death Dis* 2012; 3:e401; PMID:23059820; <http://dx.doi.org/10.1038/cddis.2012.139>
231. Bauer MA, Carmona-Gutierrez D, Ruckenstein C, Reisenbichler A, Megalou EV, Eisenberg T, et al. Spermidine promotes mating and fertilization efficiency in model organisms. [Epub ahead of print]. *Cell Cycle* 2012; 12; PMID:23255134
232. Liu T, Liu PY, Marshall GM. The critical role of the class III histone deacetylase SIRT1 in cancer. *Cancer Res* 2009; 69:1702-5; PMID:19244112; <http://dx.doi.org/10.1158/0008-5472.CAN-08-3365>
233. Nelson LE, Valentine RJ, Ciciccedo JM, Gauthier MS, Idzi Y, Ruderman NB. A novel inverse relationship between metformin-triggered AMPK-SIRT1 signaling and p53 protein abundance in high glucose-exposed HepG2 cells. *Am J Physiol Cell Physiol* 2012; 303:C4-13; PMID:22378745; <http://dx.doi.org/10.1152/ajpcell.00296.2011>
234. Wang RH, Sengupta K, Li C, Kim HS, Cao L, Xiaoz C, et al. Impaired DNA damage response, genome instability, and tumorigenesis in SIRT1 mutant mice. *Cancer Cell* 2008; 14:312-23; PMID:18835033; <http://dx.doi.org/10.1016/j.ccr.2008.09.001>
235. Fu M, Liu M, Sauve AA, Jiao X, Zhang X, Wu X, et al. Hormonal control of androgen receptor function through SIRT1. *Mol Cell Biol* 2006; 26:8122-35; PMID:16923962; <http://dx.doi.org/10.1128/MCB.00289-06>
236. Pfluger PT, Herranz D, Velasco-Miguel S, Serrano M, Tschoß M. Sirt1 protects against high-fat diet-induced metabolic damage. *Proc Natl Acad Sci U S A* 2008; 105:9793-8; PMID:18599449; <http://dx.doi.org/10.1073/pnas.0802917105>
237. Herranz D, Serrano M. Impact of Sirt1 on mammalian aging. *Aging* (Albany NY) 2010; 2:315-6; PMID:20562473
238. Herranz D, Muñoz-Martín M, Cañamero M, Mulero F, Martínez-Pastor B, Fernández-Capetillo O, et al. Sirt1 improves healthy ageing and protects from metabolic syndrome-associated cancer. *Nat Commun* 2010; 1:3; PMID:20975665; <http://dx.doi.org/10.1038/ncomms1001>
239. Herranz D, Serrano M. SIRT1: recent lessons from mouse models. *Nat Rev Cancer* 2010; 10:819-23; PMID:21102633; <http://dx.doi.org/10.1038/nrc2962>
240. Sell S. Stem cell origin of cancer and differentiation therapy. *Crit Rev Oncol Hematol* 2004; 51:1-28; PMID:15207251; <http://dx.doi.org/10.1016/j.critrevonc.2004.04.007>
241. Menendez JA, Vellon L, Oliveras-Ferraro C, Cufi S, Vazquez-Martín A. mTOR-regulated senescence and autophagy during reprogramming of somatic cells to pluripotency: a roadmap from energy metabolism to stem cell renewal and aging. *Cell Cycle* 2011; 10:3658-77; PMID:22052357; <http://dx.doi.org/10.4161/cc.10.21.18128>
242. Menendez JA, Cufi S, Oliveras-Ferraro C, Vellon L, Joven J, Vazquez-Martín A. Gerosuppressor metformin: less is more. *Aging* (Albany NY) 2011; 3:348-62; PMID:21483040
243. Cufi S, Vazquez-Martín A, Oliveras-Ferraro C, Quirantes R, Segura-Carretero A, Micó L, et al. Metformin lowers the threshold for stress-induced senescence: a role for the microRNA-200 family and miR-205. *Cell Cycle* 2012; 11:1235-46; PMID:22356767; <http://dx.doi.org/10.4161/cc.11.16.9665>

244. Vazquez-Martin A, Vellon L, Quirós PM, Cuffi S, Ruiz de Galarreta E, Oliveras-Ferraro C, et al. Activation of AMP-activated protein kinase (AMPK) provides a metabolic barrier to reprogramming somatic cells into stem cells. *Cell Cycle* 2012; 11:974-89; PMID:2233578; <http://dx.doi.org/10.4161/cc.11.5.19450>
245. Vazquez-Martin A, Coroninas-Faja B, Cuffi S, Vellon L, Oliveras-Ferraro C, Menendez OJ, et al. The mitochondrial H (+)-ATP synthase and the lipogenic switch: New core components of metabolic reprogramming in induced pluripotent stem (iPS) cells. [Epub ahead of print]. *Cell Cycle* 2012; 12; PMID:23287468
246. Lai Y, Yip GW, Bay BH. Targeting metallothionein for prognosis and treatment of breast cancer. *Recent Pat Anticancer Drug Discov* 2011; 6:178-85; PMID:21449882; <http://dx.doi.org/10.2174/157489211795328495>
247. Bay BH, Jin R, Huang J, Tan PH. Metallothionein as a prognostic biomarker in breast cancer. *Exp Biol Med (Maywood)* 2006; 231:1516-21; PMID:17018874
248. Eckslager T, Adam V, Hrabata J, Figova K, Kizek R. Metallothioneins and cancer. *Curr Protein Pept Sci* 2009; 10:360-75; PMID:19689357; <http://dx.doi.org/10.2174/138920309789822243>
249. Pedersen MØ, Larsen A, Stoltenberg M, Penkowa M. The role of metallothionein in oncogenesis and cancer prognosis. *Prog Histochem Cytochem* 2009; 44:29-64; PMID:19348910; <http://dx.doi.org/10.1016/j.proghi.2008.10.001>
250. Nielsen AE, Bohr A, Penkowa M. The Balance between Life and Death of Cells: Roles of Metallothioneins. *Biomark Insights* 2007; 1:99-111; PMID:18690641
251. Ginesier C, Hur MH, Charafe-Jauffret E, Monville F, Dutcher J, Brown M, et al. ALDH1 is a marker of normal and malignant human mammary stem cells and a predictor of poor clinical outcome. *Cell Stem Cell* 2007; 1:555-67; PMID:18371393; <http://dx.doi.org/10.1016/j.stem.2007.08.014>
252. Eirew P, Kannan N, Knapp DJ, Vaillant F, Emerman JT, Lindeman GJ, et al. Aldehyde dehydrogenase activity is a biomarker of primitive normal human mammary luminal cells. *Stem Cells* 2012; 30:344-8; PMID:22131125; <http://dx.doi.org/10.1002/stem.1001>
253. Marcato P, Dean CA, Pan D, Araslanova R, Gillis M, Joshi M, et al. Aldehyde dehydrogenase activity of breast cancer stem cells is primarily due to isoform ALDH1A3 and its expression is predictive of metastasis. *Stem Cells* 2011; 29:32-45; PMID:21280157; <http://dx.doi.org/10.1002/stem.563>
254. Marcato P, Dean CA, Giacomantonio CA, Lee PW. Aldehyde dehydrogenase: its role as a cancer stem cell marker comes down to the specific isoform. *Cell Cycle* 2011; 10:1378-24; PMID:21552008; <http://dx.doi.org/10.4161/cc.10.9.15486>
255. Herskoff DD. Oncogenic properties and prognostic implications of the ubiquitin ligase Skp2 in cancer. *Cancer* 2008; 112:1415-24; PMID:18260093; <http://dx.doi.org/10.1002/cncr.23317>
256. Chan CH, Lee SW, Wang J, Lin HK. Regulation of Skp2 expression and activity and its role in cancer progression. *ScientificWorldJournal* 2010; 10:1001-15; PMID:20526532; <http://dx.doi.org/10.1100/tsw.2010.89>
257. Wang Z, Fukushima H, Inuzuka H, Wan L, Liu P, Gao D, et al. Skp2 is a promising therapeutic target in breast cancer. *Front Oncol* 2012; 1:18702; PMID:22279619; <http://dx.doi.org/10.3389/fonc.2011.00057>
258. Wang Z, Inuzuka H, Zhong J, Liu P, Sarkar FH, Sun Y, et al. Identification of acetylation-dependent regulatory mechanisms that govern the oncogenic functions of Skp2. *Oncotarget* 2012; 3:1294-300; PMID:23230084
259. Lin HK, Chen Z, Wang G, Nardella C, Lee SW, Chan CH, et al. Skp2 targeting suppresses tumorigenesis by Arf-p53-independent cellular senescence. *Nature* 2010; 464:374-9; PMID:20237562; <http://dx.doi.org/10.1038/nature08815>
260. Huang HC, Lin CL, Lin JK, 1,2,3,4,6-penta-O-galloyl- $\beta$ -D-glucose, quercetin, curcumin and lycopene induce cell-cycle arrest in MDA-MB-231 and BT474 cells through downregulation of Skp2 protein. *J Agric Food Chem* 2011; 59:6765-75; PMID:21598989; <http://dx.doi.org/10.1021/jf201096v>
261. Huang HC, Way TD, Lin CL, Lin JK. EGCG stabilizes p27kip1 in E2-stimulated MCF-7 cells through down-regulation of the Skp2 protein. *Endocrinology* 2008; 149:5972-83; PMID:18719023; <http://dx.doi.org/10.1210/en.2008-0408>
262. Hsu JD, Kao SH, Ou TT, Chen VJ, Li YJ, Wang CJ. Gallic acid induces G2/M phase arrest of breast cancer cell MCF-7 through stabilization of p27(Kip1) attributed to disruption of p27(Kip1)/Skp2 complex. *J Agric Food Chem* 2011; 59:1996-2003; PMID:21299246; <http://dx.doi.org/10.1021/jf103656v>
263. Kroemer G, Pouyssegur J. Tumor cell metabolism: cancer's Achilles' heel. *Cancer Cell* 2008; 13:472-82; PMID:18538731; <http://dx.doi.org/10.1016/j.ccr.2008.05.005>
264. Everse J, Kaplan NO. Lactate dehydrogenases: structure and function. *Adv Enzymol Relat Areas Mol Biol* 1973; 37:61-133; PMID:4140436
265. Fantin VR, St-Pierre J, Leder P. Attenuation of LDH-A expression uncovers a link between glycolysis, mitochondrial physiology, and tumor maintenance. *Cancer Cell* 2006; 9:425-34; PMID:16766262; <http://dx.doi.org/10.1016/j.ccr.2006.04.023>
266. Koukourakis MI, Giatromanolaki A, Simopoulos C, Polychronidis A, Sivridis E. Lactate dehydrogenase 5 (LDH5) relates to up-regulated hypoxia inducible factor pathway and metastasis in colorectal cancer. *Clin Exp Metastasis* 2005; 22:25-30; PMID:16132575; <http://dx.doi.org/10.1007/s10580-005-2343-7>
267. Serganova I, Rizwan A, Ni X, Thakur SB, Vider J, Russell J, et al. Metabolic imaging: a link between lactate dehydrogenase A, lactate, and tumor phenotype. *Clin Cancer Res* 2011; 17:6250-61; PMID:21844011; <http://dx.doi.org/10.1158/1078-0432.CCR-11-0397>
268. Martinez-Outschoorn UE, Prisco M, Ertel A, Tsirigos A, Lin Z, Pavlides S, et al. Ketones and lactate increase cancer cell "stemness," driving recurrence, metastasis and poor clinical outcome in breast cancer: achieving personalized medicine via Metabolo-Genomics. *Cell Cycle* 2011; 10:1271-86; PMID:21512313; <http://dx.doi.org/10.4161/cc.10.8.15330>
269. Whitaker-Menezes D, Martinez-Outschoorn UE, Lin Z, Ertel A, Flomenberg N, Witkiewicz AK, et al. Evidence for a stromal-epithelial "lactate shuttle" in human tumors: MCT4 is a marker of oxidative stress in cancer-associated fibroblasts. *Cell Cycle* 2011; 10:1772-83; PMID:21558814; <http://dx.doi.org/10.4161/cc.10.11.15659>
270. Balliet RM, Capparelli C, Guido C, Pestell TG, Martinez-Outschoorn UE, Lin Z, et al. Mitochondrial oxidative stress in cancer-associated fibroblasts drives lactate production, promoting breast cancer tumor growth: understanding the aging and cancer connection. *Cell Cycle* 2011; 10:4065-73; PMID:22129993; <http://dx.doi.org/10.4161/cc.10.23.18254>
271. Guido C, Whitaker-Menezes D, Capparelli C, Balliet R, Lin Z, Pestell RG, et al. Metabolic reprogramming of cancer-associated fibroblasts by TGF- $\beta$  drives tumor growth: connecting TGF- $\beta$  signaling with "Warburg-like" cancer metabolism and L-lactate production. *Cell Cycle* 2012; 11:3019-35; PMID:22874531; <http://dx.doi.org/10.4161/cc.21384>
272. Guido C, Whitaker-Menezes D, Lin Z, Pestell RG, Howell A, Zimmers TA, et al. Mitochondrial fission induces glycolytic reprogramming in cancer-associated myofibroblasts, driving stromal lactate production, and early tumor growth. *Oncotarget* 2012; 3:798-810; PMID:22878233
273. Carito V, Bonuccelli G, Martinez-Outschoorn UE, Whitaker-Menezes D, Caroleo MC, Cione E, et al. Metabolic remodeling of the tumor microenvironment: migration stimulating factor (MSF) reprograms myofibroblasts toward lactate production, fueling anabolic tumor growth. *Cell Cycle* 2012; 11:3403-14; PMID:22918248; <http://dx.doi.org/10.4161/cc.121701>
274. Walenta S, Mueller-Klieser WF. Lactate: mirror and motor of tumor malignancy. *Semin Radiat Oncol* 2004; 14:267-74; PMID:15254870; <http://dx.doi.org/10.1016/j.semradonc.2004.04.004>
275. Vander Heiden MG, Cantley LC, Thompson CB. Understanding the Warburg effect: the metabolic requirements of cell proliferation. *Science* 2009; 324:1029-33; PMID:19460998; <http://dx.doi.org/10.1126/science.1160809>
276. Le A, Cooper CR, Gouw AM, Dinavahi R, Maitra A, Deck LM, et al. Inhibition of lactate dehydrogenase A induces oxidative stress and inhibits tumor progression. *Proc Natl Acad Sci U S A* 2010; 107:2037-42; PMID:20133848; <http://dx.doi.org/10.1073/pnas.0914433107>
277. Berger JL, Kayo T, Vann JM, Arias EB, Wang J, Hacker TA, et al. A low dose of dietary resveratrol partially mimics caloric restriction and retards aging parameters in mice. *PLoS One* 2008; 3:e2264; PMID:18523577; <http://dx.doi.org/10.1371/journal.pone.0002264>
278. Huang W, Sherman BT, Lempicki RA. Bioinformatics enrichment tools: paths toward the comprehensive functional analysis of large gene lists. *Nucleic Acids Res* 2009; 37:1-13; PMID:19033363; <http://dx.doi.org/10.1093/nar/gkn923>
279. Huang W, Sherman BT, Lempicki RA. Systematic and integrative analysis of large gene lists using DAVID bioinformatics resources. *Nat Protoc* 2009; 4:44-57; PMID:19131956; <http://dx.doi.org/10.1038/nprot.2008.211>
280. Wierusz JA, Welsh J. Phytoestrogen regulation of a Vitamin D3 receptor promoter and 1,25-dihydroxyvitamin D3 actions in human breast cancer cells. *J Steroid Biochem Mol Biol* 2003; 84:149-57; PMID:12710998; [http://dx.doi.org/10.1016/S0960-0760\(03\)00024-4](http://dx.doi.org/10.1016/S0960-0760(03)00024-4)
281. Boissy P, Andersen TL, Abdallah BM, Kassem M, Plesner M, Delaisé JM. Resveratrol inhibits myeloma cell growth, prevents osteoclast formation, and promotes osteoblast differentiation. *Cancer Res* 2005; 65:9943-52; PMID:16267019; <http://dx.doi.org/10.1158/0008-5472.CAN-05-0651>
282. Hayes DP. Resveratrol and vitamin D: significant potential interpretive problems arising from their mutual processes, interactions and effects. *Med Hypotheses* 2011; 77:765-72; PMID:21840648; <http://dx.doi.org/10.1016/j.mehy.2011.07.033>
283. Singh CK, Kumar A, LaVoie HA, DiPette DJ, Singh US. Resveratrol prevents impairment in activation of retinoic acid receptors and MAP kinases in the embryos of a rodent model of diabetic embryopathy. *Reprod Sci* 2012; 19:949-61; PMID:22534330; <http://dx.doi.org/10.1177/1933719112438972>

284. Stefanska B, Salamé P, Bednarek A, Fabianowska-Majewska K. Comparative effects of retinoic acid, vitamin D and resveratrol alone and in combination with adenosine analogues on methylation and expression of phosphatase and tensin homologue tumour suppressor gene in breast cancer cells. *Br J Nutr* 2012; 107:781-90; PMID:21801466; <http://dx.doi.org/10.1017/S0007114511003631>
285. Huang C, Ma WY, Goranson A, Dong Z. Resveratrol suppresses cell transformation and induces apoptosis through a p53-dependent pathway. *Carcinogenesis* 1999; 20:237-42; PMID:10069459; <http://dx.doi.org/10.1093/carcin/20.2.237>
286. Lu J, Ho CH, Ghai G, Chen KY. Resveratrol analog, 3,4,5,4'-tetrahydroxystilbene, differentially induces pro-apoptotic p53/Bax gene expression and inhibits the growth of transformed cells but not their normal counterparts. *Carcinogenesis* 2001; 22:321-8; PMID:11181455; <http://dx.doi.org/10.1093/carcin/22.2.321>
287. She QB, Bode AM, Ma WY, Chen NY, Dong Z. Resveratrol-induced activation of p53 and apoptosis is mediated by extracellular-signal-regulated protein kinases and p38 kinase. *Cancer Res* 2001; 61:1604-10; PMID:11245472
288. Baek SJ, Wilson LC, Eling TE. Resveratrol enhances the expression of non-steroidal anti-inflammatory drug-activated gene (NAG-1) by increasing the expression of p53. *Carcinogenesis* 2002; 23:425-34; PMID:11895857; <http://dx.doi.org/10.1093/carcin/23.3.425>
289. Alkhala M. Resveratrol-induced apoptosis is associated with activation of p53 and inhibition of protein translation in T47D human breast cancer cells. *Pharmacology* 2007; 80:134-43; PMID:17534123; <http://dx.doi.org/10.1159/000103253>
290. Gossau A, Pabbatja S, Knapp S, Chen KY. Trans- and cis-stilbene polyphenols induced rapid perinuclear mitochondrial clustering and p53-independent apoptosis in cancer cells but not normal cells. *Eur J Pharmacol* 2008; 587:25-34; PMID:18486125; <http://dx.doi.org/10.1016/j.ejphar.2008.03.027>
291. Donnelly RE, Newton R, Kennedy GE, Fenwick PS, Leung RH, Itu K, et al. Anti-inflammatory effects of resveratrol in lung epithelial cells: molecular mechanisms. *Am J Physiol Lung Cell Mol Physiol* 2004; 287:L77-83; PMID:15180920; <http://dx.doi.org/10.1152/ajplung.00110.2004>
292. de la Lastra CA, Villegas I. Resveratrol as an anti-inflammatory and anti-aging agent: mechanisms and clinical implications. *Mol Nutr Food Res* 2005; 49:405-50; PMID:15832402; <http://dx.doi.org/10.1002/mnfr.200500022>
293. Amar R, Solanes G, Giralt M, Villarroya F. SIRT1 is involved in glucocorticoid-mediated control of uncoupling protein-3 gene transcription. *J Biol Chem* 2007; 282:34066-76; PMID:17884810; <http://dx.doi.org/10.1074/jbc.M707114200>
294. Das S, Das DK. Anti-inflammatory responses of resveratrol. *Inflamm Allergy Drug Targets* 2007; 6:168-73; PMID:17897053; <http://dx.doi.org/10.2174/iblc.M707114200>
295. Mattson MP, Cheng A. Neurohormetic phytochemicals: Low-dose toxins that induce adaptive neuronal stress responses. *Trends Neurosci* 2006; 29:632-9; PMID:17000014; <http://dx.doi.org/10.1016/j.tins.2006.09.001>
296. Kode A, Rajendrasozhan S, Caio S, Yang SR, Megson IL, Rahman I. Resveratrol induces glutathione synthesis by activation of Nrf2 and protects against cigarette smoke-mediated oxidative stress in human lung epithelial cells. *Am J Physiol Lung Cell Mol Physiol* 2008; 294:L478-88; PMID:18162601; <http://dx.doi.org/10.1152/ajplung.00361.2007>
297. Rubiolo JA, Mithieux G, Vega FV. Resveratrol protects primary rat hepatocytes against oxidative stress damage: activation of the Nrf2 transcription factor and augmented activities of antioxidant enzymes. *Eur J Pharmacol* 2008; 591:66-72; PMID:18616940; <http://dx.doi.org/10.1016/j.ejphar.2008.06.067>
298. Ungvari Z, Bagi Z, Feher A, Recchia FA, Sonntag WE, Pearson K, et al. Resveratrol confers endothelial protection via activation of the antioxidant transcription factor Nrf2. *Am J Physiol Heart Circ Physiol* 2010; 299:H18-24; PMID:20418481; <http://dx.doi.org/10.1152/ajpheart.00260.2010>
299. Bishayee A, Barnes KF, Bhatia D, Darvesh AS, Carroll RT. Resveratrol suppresses oxidative stress and inflammatory response in diethylnitrosamine-initiated rat hepatocarcinogenesis. *Cancer Prev Res (Phila)* 2010; 3:753-63; PMID:20501860; <http://dx.doi.org/10.1158/1940-6207.CAPR-09-0171>
300. Sahin K, Orhan C, Akdemir F, Tuzcu M, Iben C, Sahin N. Resveratrol protects quail hepatocytes against heat stress: modulation of the Nrf2 transcription factor and heat shock proteins. *J Anim Physiol Anim Nutr (Berl)* 2012; 96:66-74; PMID:21244525; <http://dx.doi.org/10.1111/j.1439-0396.2010.01123.x>
301. He X, Wang L, Szklarz G, Bi Y, Ma Q. Resveratrol inhibits paraquat-induced oxidative stress and fibrogenic response by activating the nuclear factor erythroid 2-related factor 2 pathway. *J Pharmacol Exp Ther* 2012; 342:81-90; PMID:22493042; <http://dx.doi.org/10.1124/jpet.112.194142>
302. Cheng AS, Cheng YH, Chiou CH, Chang TL. Resveratrol upregulates Nrf2 expression to attenuate methylglyoxal-induced insulin resistance in Hep G2 cells. *J Agric Food Chem* 2012; 60:9180-7; PMID:22917016; <http://dx.doi.org/10.1021/jf302831d>
303. Pearson KJ, Lewis KN, Price NL, Chang JW, Perez E, Cascajo MV, et al. Nrf2 mediates cancer protection but not prolongevity induced by caloric restriction. *Proc Natl Acad Sci U S A* 2008; 105:2325-30; PMID:18287083; <http://dx.doi.org/10.1073/pnas.0712162105>
304. Martin-Montalvo A, Villalba JM, Navas P, de Cabo R. NRF2, cancer and calorie restriction. *Oncogene* 2011; 30:505-20; PMID:21057541; <http://dx.doi.org/10.1038/onc.2010.492>
305. Bayram B, Ozcelik B, Grimm S, Roeder T, Schrader C, Ernst IM, et al. A diet rich in olive oil phenolics reduces oxidative stress in the heart of SAMP8 mice by induction of Nrf2-dependent gene expression. *Rejuvenation Res* 2012; 15:71-81; PMID:22236145; <http://dx.doi.org/10.1089/rej.2011.1205>
306. Salminen A, Kaarniranta K. AMP-activated protein kinase (AMPK) controls the aging process via an integrated signaling network. *Ageing Res Rev* 2012; 11:230-41; PMID:22186033; <http://dx.doi.org/10.1016/j.arr.2011.12.005>
307. Kartsiki M, Chondrogianni N, Chinou I, Rivett AJ, Gonos ES. The olive constituent oleuropein exhibits proteasome stimulatory properties in vitro and confers life span extension of human embryonic fibroblasts. *Rejuvenation Res* 2007; 10:157-72; PMID:17518699; <http://dx.doi.org/10.1089/rej.2006.0513>
308. Konno K, Hirayama C, Yasui H, Nakamura M. Enzymatic activation of oleuropein: a protein cross-linker used as a chemical defense in the privet tree. *Proc Natl Acad Sci U S A* 1999; 96:9159-64; PMID:10430912; <http://dx.doi.org/10.1073/pnas.96.16.9159>
309. Báñez AG, Gómez P, Del Río JA, Ortúño A. Dysfunctionality of the xylem in *Olea europaea* L. Plants associated with the infection process by *Vorticillium dahliae* Kleb. Role of phenolic compounds in plant defense mechanism. *J Agric Food Chem* 2007; 55:3373-7; PMID:17394331; <http://dx.doi.org/10.1021/jf063166d>
310. Lee OH, Lee BY. Antioxidant and antimicrobial activities of individual and combined phenolics in *Olea europaea* leaf extract. *Bioresour Technol* 2010; 101:3751-4; PMID:20106659; <http://dx.doi.org/10.1016/j.biortech.2009.12.052>
311. Blagosklonny MV. Revisiting the antagonistic pleiotropy theory of aging: TOR-driven program and quasi-program. *Cell Cycle* 2010; 9:3151-6; PMID:20724817; <http://dx.doi.org/10.4161/cc.9.16.13120>
312. Blagosklonny MV. NCI's provocative questions on cancer: some answers to ignite discussion. *Oncotarget* 2011; 2:1352-67; PMID:22267462
313. Anisimov VN, Zabezhinski MA, Popovich IG, Piskunova TS, Semenchenko AV, Tyndyk ML, et al. Rapamycin increases lifespan and inhibits spontaneous tumorigenesis in inbred female mice. *Cell Cycle* 2011; 10:4230-6; PMID:22107964; <http://dx.doi.org/10.4161/cc.10.24.18486>
314. Leontieva OV, Blagosklonny MV. Yeast-like chronological senescence in mammalian cells: phenomenon, mechanism and pharmacological suppression. *Aging (Albany NY)* 2011; 3:1078-91; PMID:22156391
315. Blagosklonny MV. Molecular damage in cancer: an argument for mTOR-driven aging. *Aging (Albany NY)* 2011; 3:1130-41; PMID:22246147
316. Blagosklonny MV. Cell cycle arrest is not senescence, which is not just cell cycle arrest: terminology for TOR-driven aging. *Aging (Albany NY)* 2012; 4:159-65; PMID:22394614
317. Pospelova TV, Leontieva OV, Bykova TV, Zubova SG, Pospelov VA, Blagosklonny MV. Suppression of replicative senescence by rapamycin in rodent embryonic cells. *Cell Cycle* 2012; 11:2402-7; PMID:22672902; <http://dx.doi.org/10.4161/cc.20882>
318. Komarova EA, Antoch MP, Novorotskaya LR, Chernova OB, Paszkiewicz G, Leontieva OV, et al. Rapamycin extends lifespan and delays tumorigenesis in heterozygous p53+/− mice. *Aging (Albany NY)* 2012; 4:709-14; PMID:23123616
319. Comas M, Toshkov I, Kuropatwinski KK, Chernova OB, Polinsky AV, Blagosklonny MV, et al. New nanoformulation of rapamycin Rapatar extends lifespan in homozygous p53−/− mice by delaying carcinogenesis. *Aging (Albany NY)* 2012; 4:715-22; PMID:23117593
320. Leontieva OV, Blagosklonny MV. Hypoxia and geroprotection: the mTOR saga continues. *Cell Cycle* 2012; 11:3926-31; PMID:22987149; <http://dx.doi.org/10.4161/cc.21908>
321. Blagosklonny MV. How to save Medicare: the anti-aging remedy. *Aging (Albany NY)* 2012; 4:547-52; PMID:22915707
322. Blagosklonny MV. Prospective treatment of age-related diseases by slowing down aging. *Am J Pathol* 2012; 181:1142-6; PMID:22841821; <http://dx.doi.org/10.1016/j.ajpath.2012.06.024>
323. Lane N, Martin W. The energetics of genome complexity. *Nature* 2010; 467:929-34; PMID:20962839; <http://dx.doi.org/10.1038/nature09486>
324. Price NL, Gomes AP, Ling AJ, Duarte FV, Martin-Montalvo A, North BJ, et al. SIRT1 is required for AMPK activation and the beneficial effects of resveratrol on mitochondrial function. *Cell Metab* 2012; 15:675-90; PMID:22560220; <http://dx.doi.org/10.1016/j.cmet.2012.04.003>
325. Saunders LR, Sharma AD, Tawney J, Nakagawa M, Okita K, Yamanaka S, et al. miRNAs regulate SIRT1 expression during mouse embryonic stem cell differentiation and in adult mouse tissues. *Aging (Albany NY)* 2010; 2:415-31; PMID:20634564
326. Pardo PS, Boriek AM. An autoregulatory loop reverts the mechanosensitive Sirt1 induction by EGFR in skeletal muscle cells. *Aging (Albany NY)* 2012; 4:456-61; PMID:22820707

327. Purushotham A, Schug TT, Li X. SIRT1 performs a balancing act on the tight-rope toward longevity. *Aging* (Albany NY) 2009; 1:669-73; PMID:20157548
328. Brooks CL, Gu W. Anti-aging protein SIRT1: a role in cervical cancer? *Aging* (Albany NY) 2009; 1:278-80; PMID:20157516
329. Stein S, Schäfer N, Breitenstein A, Besler C, Winnik S, Lohmann C, et al. SIRT1 reduces endothelial activation without affecting vascular function in ApoE<sup>-/-</sup> mice. *Aging* (Albany NY) 2010; 2:353-60; PMID:20606253
330. Lee J, Kemper JK. Controlling SIRT1 expression by microRNAs in health and metabolic disease. *Aging* (Albany NY) 2010; 2:527-34; PMID:20606156
331. Yang Z, Ming XF. The vascular SIRTainity. *Aging* (Albany NY) 2010; 2:331-2; PMID:20606250
332. Bolasco G, Calogero R, Carrara M, Banchaabouchi MA, Bilbao D, Mazzoccoli G, et al. Cardioprotective mIGF-1/SIRT1 signaling induces hypertension, leukocytosis and fear response in mice. *Aging* (Albany NY) 2012; 4:402-16; PMID:22691943
333. Halperin-Sheinfeld M, Gerller A, Okun E, Sredni B, Cohen HY. The Tellurium compound, AS101, increases SIRT1 level and activity and prevents type 2 diabetes. *Aging* (Albany NY) 2012; 4:436-47; PMID:22761194
334. Cantó C, Auwerx J. Interference between PARPs and SIRT1: a novel approach to healthy ageing? *Aging* (Albany NY) 2011; 3:543-7; PMID:21566260
335. Vinciguerra M, Santini MP, Claycomb WC, Ladurner AG, Rosenthal N. Local IGF-1 isoform protects cardiomyocytes from hypertrophic and oxidative stresses via SirT1 activity. *Aging* (Albany NY) 2010; 2:43-62; PMID:20228935
336. Schug TT, Li X. Surprising sirtuin crosstalk in the heart. *Aging* (Albany NY) 2010; 2:129-32; PMID:20375467
337. Ramadori G, Coppari R. Does hypothalamic SIRT1 regulate aging? *Aging* (Albany NY) 2011; 3:325-8; PMID:21464518
338. Hirschey MD, Shimazu T, Capra JA, Pollard KS, Verdin E. SIRT1 and SIRT3 deacetylate homologous substrates: AcCS1L2 and HMGCS1L2. *Aging* (Albany NY) 2011; 3:635-42; PMID:21701047
339. Mai A. Identification of specific and semi-specific SIRT1 inhibitors through computer-aided studies. *Aging* (Albany NY) 2011; 3:819-20; PMID:21937768
340. Schlicker C, Boanca G, Lakshminarayanan M, Steegborn C. Structure-based development of novel sirtuin inhibitors. *Aging* (Albany NY) 2011; 3:852-72; PMID:21937767
341. Banerjee KK, Ayyub C, Sengupta S, Kolthur-Seetharam U. dSir2 deficiency in the fatbody, but not muscles, affects systemic insulin signaling, fat mobilization and starvation survival in flies. *Aging* (Albany NY) 2012; 4:206-23; PMID:22411915
342. Naiman S, Kanfi Y, Cohen HY. Sirtuins as regulators of mammalian aging. *Aging* (Albany NY) 2012; 4:521-2; PMID:22915706
343. Antosh M, Fox D, Helfand SL, Cooper LN, Neretti N. New comparative genomics approach reveals a conserved health span signature across species. *Aging* (Albany NY) 2011; 3:576-83; PMID:21775776
344. Froy O, Misrikian R. Effect of feeding regimens on circadian rhythms: implications for aging and longevity. *Aging* (Albany NY) 2010; 2:7-27; PMID:20228939
345. Borrás C, Monleón D, López-Gruess R, Gambini J, Orlando L, Pallardó FV, et al. RasGrf1 deficiency delays aging in mice. *Aging* (Albany NY) 2011; 3:262-76; PMID:21422498
346. Vendrell A, Posas F. Sir2 plays a key role in cell fate determination upon SAPK activation. *Aging* (Albany NY) 2011; 3:1163-8; PMID:22245992
347. Zhang D, Liu Y, Chen D. SIRT-ain relief from age-inducing stress. *Aging* (Albany NY) 2011; 3:158-61; PMID:21307404
348. Ha CW, Huh WK. The implication of Sir2 in replicative aging and senescence in *Saccharomyces cerevisiae*. *Aging* (Albany NY) 2011; 3:319-24; PMID:21415463
349. Tucci P. Caloric restriction: is mammalian life extension linked to p53? *Aging* (Albany NY) 2012; 4:525-34; PMID:22983298
350. Burks TN, Cohn RD. One size may not fit all: anti-aging therapies and sarcopenia. *Aging* (Albany NY) 2011; 3:1142-53; PMID:22184279
351. Panieri E, Toietta G, Mele M, Labate V, Ranieri SC, Fusco S, et al. Nutrient withdrawal rescues growth factor-deprived cells from mTOR-dependent damage. *Aging* (Albany NY) 2010; 2:487-503; PMID:21397373
352. Vazquez-Martin A, Cufi S, Lopez-Bonet E, Coroninas-Faja B, Oliveras-Ferraro C, Martin-Castillo B, et al. Metformin limits the tumorigenicity of iPS cells without affecting their pluripotency. *Sci Rep* 2012; 2:964; PMID:23236586; <http://dx.doi.org/10.1038/srep00964>
353. Faubert B, Boily G, Izreig S, Griss T, Samborska B, Dong Z, et al. AMPK Is a Negative Regulator of the Warburg Effect and Suppresses Tumor Growth In vivo. *Cell Metab* 2012; In press; PMID:23274086
354. Mariño G, Ugadé AP, Salvador-Montoliu N, Varela I, Quirós PM, Cadíñanos J, et al. Premature aging in mice activates a systemic metabolic response involving autophagy induction. *Hum Mol Genet* 2008; 17:2196-211; PMID:18443001; <http://dx.doi.org/10.1093/hmg/ddn120>
355. Mariño G, López-Otín C. Autophagy and aging: new lessons from progeroid mice. *Autophagy* 2008; 4:807-9; PMID:18612261



## Protective effects of citrus and rosemary extracts on UV-induced damage in skin cell model and human volunteers



A. Pérez-Sánchez <sup>a,1</sup>, E. Barrajón-Catalán <sup>a,1</sup>, N. Caturla <sup>b</sup>, J. Castillo <sup>c,e</sup>, O. Benavente-García <sup>c,e</sup>, M. Alcaraz <sup>d,e</sup>, V. Micol <sup>a,\*</sup>

<sup>a</sup> Skin Research Platform (SRP), Instituto de Biología Molecular y Celular (IBMC), Universidad Miguel Hernández, Avenida de la Universidad s/n, E-03202 Elche, Alicante, Spain

<sup>b</sup> Monteloeder S.L., Miguel Servet 16, nave 17, 03203 Elche, Alicante, Spain

<sup>c</sup> Nutrafur S.A., Camino Viejo de Pliego, km.2, 30820 Alcantarilla, Murcia, Spain

<sup>d</sup> Radiology and Physical Medicine Department, Faculty of Medicine, University of Murcia, 30100 Espinardo, Murcia, Spain

<sup>e</sup> Institute of Research Into Aging, University of Murcia, 30100 Espinardo, Murcia, Spain

### ARTICLE INFO

#### Article history:

Received 24 February 2014

Received in revised form 5 April 2014

Accepted 7 April 2014

Available online 20 April 2014

#### Keywords:

UV radiation

Oral photoprotection

ROS

DNA damage

Rosemary

Citrus

Polyphenols

### ABSTRACT

Ultraviolet radiation absorbed by the epidermis is the major cause of various cutaneous disorders, including photoaging and skin cancers. Although topical sunscreens may offer proper skin protection, dietary plant compounds may significantly contribute to lifelong protection of skin health, especially when unconsciously sun UV exposed. A combination of rosemary and citrus bioflavonoids extracts was used to inhibit UV harmful effects on human HaCaT keratinocytes and in human volunteers after oral intake. Survival of HaCaT cells after UVB radiation was higher in treatments using the combination of extracts than in those performed with individual extracts, indicating potential synergic effects. The combination of extracts also decreased UVB-induced intracellular radical oxygen species (ROS) and prevented DNA damage in HaCaT cells by comet assay and decreased chromosomal aberrations in X-irradiated human lymphocytes. The oral daily consumption of 250 mg of the combination by human volunteers revealed a significant minimal erythema dose (MED) increase after eight weeks (34%,  $p < 0.05$ ). Stronger protection was achieved after 12 weeks (56%,  $p < 0.01$ ). The combination of citrus flavonoids and rosemary polyphenols and diterpenes may be considered as an ingredient for oral photoprotection. Their mechanism of action may deserve further attention.

© 2014 Elsevier B.V. All rights reserved.

### 1. Introduction

UV radiation from the sun induces several harmful responses, including erythema, immunosuppression, edema, sunburn, hyperplasia, hyperpigmentation, premature aging and skin cancer. Only UVA (320–400 nm) and UVB (280–320 nm) are harmful to our skin. UVA accounts for more than 90% of the total UV radiation reaching us and is constant throughout the year, but UVB photons are one thousand times more capable of causing sunburn than UVA and increase considerably in the summer [1]. UVA is thought to play a crucial role in photoaging and causes epidermal hyperplasia, stratum corneum thickening and the synthesis of inflammatory cytokines and metalloproteinases (MMPs) [2,3]. Meanwhile, UVB causes sunburn, sun tanning, pigmented spots and wrinkles and accelerates skin aging.

Both UVA and UVB contribute significantly to photoaging. Photoaging is the superposition of chronic UV-induced damage on intrinsic skin aging and accounts for most age-related changes in skin appearance [4]. The molecular mechanism of photoaging is mostly triggered by ROS-mediated activation of cell surface receptors leading to stimulation of stress-associated kinase pathways, which are mediated by protein 1 (AP-1) nuclear transcription factor [5]. This factor prompts prostaglandin release, keratinocyte proliferation and a loss of collagen synthesis [6]. ROS also lead to the activation of NF-κB transcription factor, which induces the expression of pro-inflammatory cytokines and metalloproteinases (MMPs). Finally, ROS-induced mitochondrial DNA deletions compromise mitochondrial function [4]. All these factors together with direct protein oxidation contribute to accelerate extracellular matrix degradation. Although UVA is suspected to play a major role in photoaging, UVB activates AP-1 and causes direct DNA damage, inflammation, immunosuppression, angiogenesis and elastin degradation.

Major protective systems in human skin cells are the natural pigment melanin, which absorbs and scatters UV radiation, and

\* Corresponding author. Tel.: +34 96 6658430; fax: +34 96 6658758.

E-mail address: [vmicol@um.es](mailto:vmicol@um.es) (V. Micol).

<sup>1</sup> These authors have contributed equally.

skin cells' antioxidant enzymes (catalase, superoxide dismutase and glutathione peroxidase) [4]. Moreover, p53 protein plays a crucial role in UVB protection, acting as a transcription factor that controls genes involved in the cell cycle, apoptosis and DNA repair [7].

Human skin is inadvertently exposed to approximately 2/3 of the cumulative erythema ultraviolet (UV) dose/year when no topical protection is used [8]. Therefore, beyond topical sunscreen protection when consciously exposed [9], photoprotection by dietary compounds via endogenous delivery to the skin may significantly contribute to lifelong protection of skin health. Several plant phytochemicals have been found to be effective in preventing UV-induced DNA oxidative damage through a ROS scavenging mechanism *in vitro* and in animal models [1]. Rosmarinic acid [10–12], a phenolic acid derivative, the isoflavone genistein [13] and silybin from milk thistle [14] have exhibited skin protective effects against UVB-induced ROS on mice and cell models through p53 activation and decreased DNA damage. Chrysin (5,7-dihydroxyflavone) attenuates apoptosis, ROS generation and cyclooxygenase 2 (COX-2) expression and diminishes aquaporin-3 downregulation induced by UVB and UVA [15]. Rosemary diterpenes display strong *in vitro* antioxidant and anti-inflammatory effects, together with *in vivo* skin protective effects [16–18], and forskolin protects keratinocytes from UVB-induced apoptosis independently of melanin content [19].

In the present study, a specific combination of a rosemary extract, enriched in polyphenols and diterpenes, and a citrus bioflavonoid extract, containing flavonoids, was used for the first time to inhibit UVB's harmful effects on human keratinocytes. The capacity of this combination to decrease UVB-mediated cell death, ROS formation and DNA damage in human keratinocytes, and genotoxicity induced by X-rays in human lymphocytes, was assessed. A human intervention study using 250 mg of this combination by oral administration for three months was also established to determine the capacity of the ingredient to increase the minimal erythema dose (MED) of the volunteers upon UV exposure.

## 2. Materials and methods

### 2.1. Materials

The human keratinocytes HaCaT (a spontaneously immortalized cell line) were obtained from CLS Cell Lines Service GmbH (Eppelheim, Germany). Dulbecco's modified Eagle's medium (DMEM), fetal bovine serum (FBS) and penicillin-streptomycin were obtained from Gibco® (Life Technologies Co., Europe). Phytohemagglutinin, cytochalasin B (Cyt B) and the rest of the reagents were purchased from Sigma-Aldrich (Europe).

### 2.2. Extracts

Herbal extracts were kindly provided by Monteloeder, Inc. Citrus extract, obtained from immature grapefruit, was enriched in citrus bioflavonoids as declared by the manufacturer and showed a phenolic content of  $22.57 \pm 2.65$  expressed as GAE (gallic acid equivalents)/100 g dry weight (dw). The rosemary extract contained phenolic compounds and diterpenes, as declared, and a phenolic content of  $57.16 \pm 1.25$  GAE/100 g dw was determined. The combination of extracts (NutroxSun®) used in the cellular assays and the human intervention study contained the two extracts at a 1:1 ratio and had a phenolic content of  $36.32 \pm 3.91$  GAE/100 g dw. Powered extracts were stored at RT under controlled humidity conditions in a desiccator. Rosemary extract was dissolved into sterile distilled water and citrus extract and the combination were dissolved into DMSO at desired concentrations. Solutions were sterile filtered and freshly prepared for every cellular assay.

### 2.3. Keratinocyte cell culture

HaCaT cells were grown in DMEM with 10% (v/v) FBS and 1% (v/v) penicillin-streptomycin (0.1 mg/ml penicillin and 100 U/ml streptomycin) in a humidified atmosphere with CO<sub>2</sub> (5% v/v) at 37 °C. The HaCaT cells were trypsinized every third day, following the manufacturer's instructions, and seeded in 96- or six-well plates, depending on the assay.

### 2.4. Treatment of cells, UVB irradiation and MTT survival assay

Cells were cultured in 96-well plates and maintained in medium for 24 h. For treatments, cells at 50–70% confluence were washed with phosphate-buffered saline (PBS) and treated with PBS containing the selected extract (12.5–100 µg/ml, no toxicity was observed at these concentrations), followed by treatment with UVB light emitted from a Bio-Link Crosslinker BLX-E312 (Vilber Lourmat, France) at 800 or 1200 J/m<sup>2</sup> [20]. Afterward, the PBS was replaced with fresh medium, and the cells were incubated for 72 h for viability assays or for 2 h for comet or ROS assays. The MTT assay was used for determining cellular viability [21]. The cell protection level was calculated as the percentage of cell viability recovered under a certain condition, where 100% was the difference between non-irradiated cells and irradiated cells in the absence of the extract.

### 2.5. Total phenolic content determination

Total polyphenolic content was determined using the Folin-Ciocalteu method, using gallic acid as the standard [22,23].

### 2.6. ROS generation evaluation

2',7'-Dichlorodihydrofluorescein diacetate (H<sub>2</sub>DCFDA) (Molecular probes®, Life Technologies Co., Europe) was used to monitor the intracellular ROS generation induced by UVB radiation [21]. Promptly, cells were cultured in a 96-well black plate until 90–100% confluence was reached. The cells were then treated with a thin layer of PBS containing the combined extract (75–100 µg/ml), followed by treatment with UVB light (800 or 1200 J/m<sup>2</sup>) and labeled with H<sub>2</sub>DCFDA.

### 2.7. Single-cell gel electrophoresis (comet assay)

Comet assay was essentially performed as previously reported [11]. A total of 50 nuclei by duplicate were utilized for determination of Comet score. The gels were analyzed by fluorescence microscopy (Nikon Eclipse TE2000U). DNA damage was quantified as described in Supplementary information section.

### 2.8. Cytokinesis-blocked micronucleus (CBMN) assay and genotoxicity

Human whole blood samples were obtained and treated in the presence and in the absence of the extracts and exposed to 2 Gy doses of X-rays (see Supplementary information for details). After X-irradiation, the micronucleus assay was performed on the irradiated lymphocytes using a reported CBMN method [24,25], adapted by the International Atomic Energy Agency (2011).

### 2.9. Human intervention study

The human intervention assay was developed on 10 healthy human volunteers by EVIC HISPANIA, Centro Experimental de Evaluación Cutánea, S.L. (Spain) to study the protective activity of the combination (NutroxSun®) after oral ingestion by the calculation of MED at different times (reference code 10-0266/0).

The compliance of the product with the European regulations in force was guaranteed after reviewing the procedure, undertaking letter, informed consent and previous documentation on the tested product (see [Supplementary information](#) for details).

### 2.10. Statistical analysis

The data were expressed as the mean  $\pm$  SD of 4–8 determinations, depending on the assay. One-way analysis of variance (ANOVA) and statistical comparisons of the different treatments were performed using Tukey's test in GraphPad Prism version 5.0 (GraphPad Software). In the CBMN study, the degree of dependence and correlation between variables was assessed using ANOVA complemented by a contrast of means ( $p < 0.05$ ). For human intervention study, a Student's *t* test for paired series was used.

## 3. Results and discussion

### 3.1. Effects of the combined extract and its individual components on the viability of HaCaT cells exposed to UVB

To study the protective effects of citrus and rosemary extracts and that of their combination, HaCaT cell viability after UVB irradiation (800 or 1200 J/m<sup>2</sup> dose) in the presence of the extracts, was determined using the MTT assay ([Fig. 1](#)). At 800 J/m<sup>2</sup>, the presence of citrus extract steadily increased cell protection until saturation observed approximately at 50 µg/ml ([Fig. 1A](#)). A level of maximum protection of approximately 40% was reached compared with a control irradiated in the absence of the extract. When the UVB dose was increased to 1200 J/m<sup>2</sup>, protection gradually increased with extract concentration until reaching a similar level of protection, i.e., 50%, but at higher concentrations (100 µg/ml). Rosemary extract exerted a lower level of protection than citrus extract, especially at high radiation dose ([Fig. 1B](#)). Levels of protection of 30% and 13% were observed at 800 and 1200 J/m<sup>2</sup>, respectively, at the maximum extract concentration assayed (100 µg/ml).

The dissimilar polyphenolic compositions of citrus and rosemary extracts might provide with complementary protective mechanisms by reaching different cellular targets. To test this hypothesis, a mixture at a 1:1 ratio was evaluated in UV protection assays, as previously described, in a concentration range of 12.5–100 µg/ml ([Fig. 1C](#)). The combination showed a higher level of protection at all concentrations compared with individual citrus or rosemary extracts. When cells were exposed to 800 J/m<sup>2</sup>, the combined extracts promoted a significant level of protection upon an increase in extract concentration, reaching a protection level of 70% at the highest concentration used. At 1200 J/m<sup>2</sup>, the combination was also extremely potent and reached a nearly 60%

protection level at 100 µg/ml compared with cells irradiated in the absence of it. When protection levels were compared at 800 J/m<sup>2</sup> ([Supplementary Table 1](#)), citrus and rosemary extracts at 50 µg/ml accomplished 40% and 13% protection, respectively (a theoretical additive effect of 53%). However, the combined extract achieved 70% protection at 100 µg/ml (which contained 50 µg/ml of each extract). These results indicate that the combination of citrus and rosemary extracts provided stronger protective effects in the cell model than the sum of the formulation's separate components. An even more striking result was observed when cells were irradiated with a 1200 J/m<sup>2</sup> dose. The combination achieved 60% protection at 100 µg/ml, whereas individual citrus and rosemary extracts at 50 µg/ml accomplished 13% and 5%, respectively. Detailed protection percentages for every concentration and extract are shown in [Supplementary Table 1](#). These results strongly support the hypothesis that both extracts act synergistically in photoprotection since the combination exhibited better protection results than the sum of the effects of the individual components. Synergic effects have been previously described for plant polyphenols in order to explain abnormally enhanced antimicrobial, antioxidant and hypotriglyceridemic activities [[21,26](#)].

The rosemary polyphenols rosmarinic acid, carnosic acid and carnosol have been postulated to be effective agents for attenuating cell-damaging effects against UV radiation and also ionizing radiation [[10–12,27,28](#)]. Moreover, naringenin, a citrus bioflavonoid, was able to increase the survival of UVB-irradiated keratinocytes [[29](#)]. Nevertheless, the current study is the first one to report the synergic effect between these plant compounds. Rosemary and citrus polyphenols show a significant absorption within UVB range, so it seems reasonable to assume that part of their protective effect is based on a direct absorption and scattering of UVB radiation. Nevertheless, since some of these compounds may rapidly reach intracellular targets, we propose that they may be able to scavenge superoxide radical anions (O<sub>2</sub><sup>·</sup>), hydroxyl radicals (·OH) and lipoperoxyl radicals (R-OO<sup>·</sup>), which subsequently generate DNA damage and protein oxidation. Due to these preliminary results in a cell model, the combined extract was selected for further assays in which the formulation's capability to attenuate specific harmful effects related to photoaging, such as ROS generation and DNA damage, were analyzed.

### 3.2. Antioxidant activity and attenuation of ROS generation in UVB-irradiated HaCaT cells by rosemary and citrus combined extract

Intracellular ROS are one of the most damaging effects of both UVB and UVA radiations on skin, with subsequent damage to lipids, proteins and mitochondrial and nuclear DNA. Both citrus bioflavonoids and rosemary compounds have well-documented ROS-scavenging capacity in several models, including human skin cells.

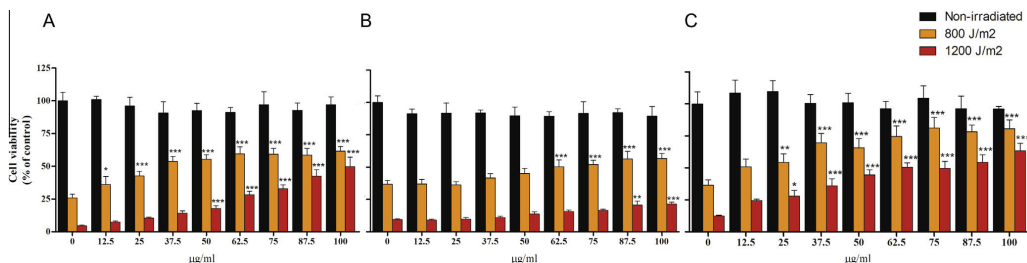


**Fig. 1.** Survival of human keratinocytes after irradiation with 800 or 1200 J/m<sup>2</sup> UVB in the presence of citrus extract (A), rosemary extract (B) or the combination of both (C). The data are expressed as the mean of 6–8 replicates  $\pm$  SD. \* $(p < 0.05)$ , \*\* $(p < 0.01)$  and \*\*\* $(p < 0.001)$  indicate statistically significant differences compared with an irradiated sample in the absence of the extracts.

Naringenin inhibits apoptosis and pyrimidine dimers upon UVB radiation [29]. Several rosemary compounds have shown a potent radical-scavenging capacity, primarily against lipid peroxidation [16], and the prevention of UV-induced ROS generation and MMP expression by carnosic acid has been reported [30].

To study the potential protective effect of the combination of extracts on the intracellular ROS generation induced by UVB radiation, cells were exposed to UVB at an 800 or 1200 J/m<sup>2</sup> dose in the presence of two different concentrations of the combined extract. ROS generation was then measured with H<sub>2</sub>DCFDA, a fluorescent probe that becomes fluorescent when oxidized by free radicals and that is especially sensitive to H<sub>2</sub>O<sub>2</sub>, ·OH and peroxy nitrite at the intracellular level [31]. Fig. 2 shows the ROS generation in HaCaT cells after UVB radiation in the absence and in the presence of various concentrations of the combined extract. As observed, a certain fluorescence signal was observed due to basal metabolism of HaCaT cells in the absence of irradiation and extract supplementation (black bar). When cells were irradiated either with 800 J/m<sup>2</sup> or 1200 J/m<sup>2</sup> in the absence of the extract, fluorescence signal showed a significant increase of 36% and 62%, respectively, compared with basal condition (0%) due to UVB-induced ROS generation ( $p < 0.001$ ). Although UVA is more effective in inducing oxidative damage [4], these results strongly demonstrate that UVB is able to produce ROS species at intracellular level in cell model. In contrast, when cells were irradiated with 800 J/m<sup>2</sup> in the presence of the combined extract, fluorescence intensity decreased significantly ( $p < 0.001$ ) as concentration increased compared to irradiated and non-treated cells, i.e., 42% ROS decrease at 75 µg/ml and 50% ROS decrease at 100 µg/ml of the combined extract. The capacity of the combination to inhibit ROS generation was even stronger at 1200 J/m<sup>2</sup> UVB dose, showing 64% ROS decrease at 75 µg/ml and 71% ROS decrease at 100 µg/ml of the combination compared to irradiated and non-treated cells. Besides the evident UVB absorption capacity of the polyphenols present in the combination, these results clearly indicate that an additional mechanism of the combined extract photoprotective properties may be related to its capacity to decrease the generation of intracellular radical species such as H<sub>2</sub>O<sub>2</sub>, ·OH or peroxy nitrite, which have been directly linked to DNA oxidative damage [32].

### 3.3. Effects of the combined extract on UVB-induced DNA damage

To confirm the hypothesis that inhibition of UV-induced intracellular ROS was concomitant with a certain level of DNA

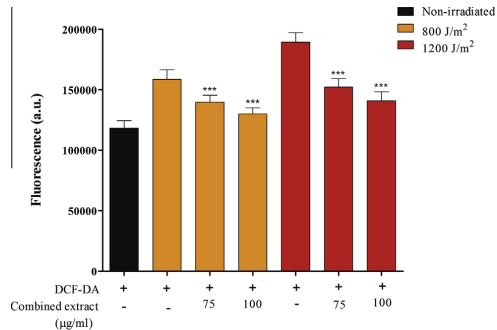


**Fig. 2.** Measurement of UV-induced ROS generation using H<sub>2</sub>DCFDA fluorescent probe. Total fluorescence is expressed as arbitrary units. The data are expressed as the mean ± SD. The black bar indicates the fluorescence signal under basal conditions in the absence of irradiation (0%). \*\*\*( $p < 0.001$ ) indicates significant differences compared with irradiated cells at the same UVB dose in the absence of the extract combination.

protection, we studied the level of nuclear DNA damage in individual cells exposed to UVB using the comet assay. Fig. 3 shows representative pictures of the effect of combined extract on comet electrophoresis gels for HaCaT cells that were either irradiated at 1200 J/m<sup>2</sup> or non-irradiated and the corresponding gels' quantification. The incubation of human keratinocytes with 100 µg/ml of combined extract did not significantly affect the comet score when cells were not irradiated (Fig. 3C) compared with the control (Fig. 3B), indicating the absence of genotoxicity for the extract. When control cells were irradiated, the comet score increased considerably (Fig. 3D) indicating an increased DNA damage. In contrast, the presence of 100 µg/ml of the combined extract (Fig. 3E) significantly reduced the DNA damage ( $p < 0.05$ ), i.e., by 26% compared with irradiated and untreated cells. Therefore, our results reveal that the combination of rosemary and citrus extracts can decrease the number of UV-induced DNA breaks and hence either attenuates the genotoxic effects of UV radiation or protects the DNA repair machinery.

UVB acts on the epidermal basal cell layer of the skin; it is absorbed by chromophores (such as DNA, RNA, proteins and melanin); and has been experimentally demonstrated to cause DNA damage, pyrimidine dimers, 8-OHdG formation, p53 induction, protein oxidation and the generation of ROS [33,34]. Incorrect repair of these lesions leads to mutations, which may cause the development of cancer cells [35]. The excited oxygen electrons of the ROS induced by UVB alter the red/ox state of the cell and also damage mitochondria, inducing apoptosis and tissue injury and contributing to altered cell growth and differentiation or to the development of skin cancer [33,36]. Considering all of the above mentioned *in vitro* evidence, i.e., the cell survival increase and the decrease in intracellular ROS generation and DNA damage by the combined extract, we suggest that the combination of rosemary and citrus extracts may be able to attenuate further major events leading to photoaging and skin cancer.

### 3.4. The genoprotective effects of combined extract against X-ray-induced ROS and DNA damage

Ionizing radiation generates reactive oxygen and nitrogen species within minutes of exposing cells to radiation, leading to compromised mitochondria viability, MAPK pathways activation and DNA damage [37]. Therefore, we have used X-ray as a model to test whether the combination of the extracts would be able to protect against a massive generation of radical species induced by X-ray exposure through micronuclei (MN) measurement.

Human whole-blood samples were X-ray-irradiated in the presence or absence of combined extract, and the number of lymphocytes bearing MN was determined after cell culture. When whole blood was exposed to 2 Gy in the absence of the combined extract, the number of lymphocytes bearing MN increased considerably compared with non-irradiated cells (Fig. 4). In contrast, combined extract caused a significant reduction of MN/500 CB frequency ( $p < 0.001$ ) when administered either before or after irradiation (Fig. 4) compared with irradiated and non-treated cells. The protection factor exhibited a value of 39% protection when the combined extract was utilized before irradiation and 32% protection when the combined extract was used immediately after irradiation. These results agree with those obtained in the comet assay and corroborate the genoprotective and antimutagenic capacity of rosemary and citrus extracts combination against both UV-induced DNA damage and X-ray-induced ROS/RNS formation and subsequent chromosomal damage. The mechanism of this protection is most likely based on the capacity of the compounds present in the combination to scavenge the massive number of free radicals generated by X-ray, which leads to chromosomal aberrations. It has been postulated that both hydrophilic and lipophilic

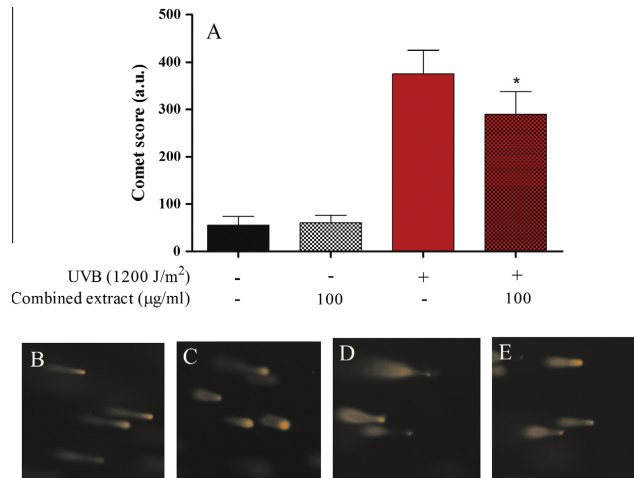


**Fig. 3.** Rosemary and citrus combination decreases UVB-induced DNA strand break formation in HaCaT cells (A). Keratinocytes were treated with the combination (100 µg/ml) and exposed to UVB (1200 J/m<sup>2</sup>). To evaluate DNA damage, 50 cells (nuclei) per slide were analyzed. Total damage was expressed in arbitrary units and determined as described in the materials and methods section. Control consisting of non-irradiated HaCaT cells (B), non-irradiated cells in the presence of the combination (100 µg/ml) (C), irradiated cells at 1200 J/m<sup>2</sup> (D) and irradiated cells in the presence of the combination (100 µg/ml) at 1200 J/m<sup>2</sup> (E). The data are expressed as the mean ± SD. \*(p < 0.05) indicates significant differences compared with irradiated cells in the absence of the combination.

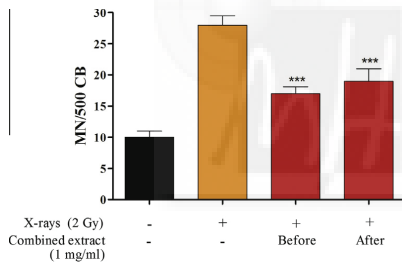


**Fig. 4.** Influence of rosemary and citrus combination administered before or after X-ray irradiation on the frequency of MN in irradiated and non-irradiated human lymphocytes. The number of MN was expressed in arbitrary units and determined as described in the materials and methods section. The data are expressed as the mean ± SD. \*\*\*(p < 0.001) indicates significant differences compared with irradiated and non-treated cells.

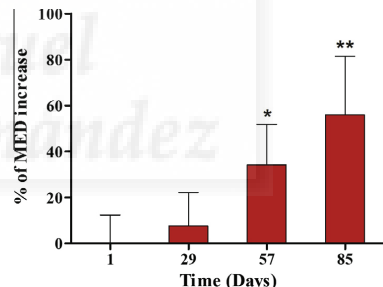


**Fig. 5.** Evaluation of the average MED of human volunteers measured at days 29, 57 and 85 of receiving the dietary supplement containing the combination compared with the starting value. The data are expressed as the mean ± SD. \*(p < 0.05) and \*\*(p < 0.01) indicate significant differences compared with the first day.

antioxidants from rosemary protect human lymphocytes from gamma-radiation when added before irradiation due to their capacity to eliminate the massive generation of superoxide anion and hydroxyl radicals upon irradiation. Interestingly, only oil-soluble antioxidants such as rosemary diterpenes seem to protect after irradiation probably due to their capacity to inhibit lipid peroxidative processes leading to chromosomal oxidative damage [27,28]. Therefore, we propose that the lipophilic antioxidants are the major contributors to DNA protective effect after irradiation, and that both, hydrophilic polyphenols and lipophilic antioxidants, contribute to the increased protection when added before irradiation.

### 3.5. Human intervention study results

To test the photoprotective efficacy of the combined extract, a human intervention study was performed by the oral

administration to volunteers for whom the MED was determined after exposure to UV radiation. Details of the study protocol and MED variation results are described in the materials and Supplementary sections. None of the volunteers discontinued oral administration, so no exclusions were considered. The average results for MED variation during the trial are shown in Fig. 5. No significant differences in the MED value were by day 29th of consumption of combined extract compared with the initial values ( $p = 0.429$ ). In contrast, at the day 57th of treatment, a significant increase in the MED was observed (34%,  $p < 0.05$ ), indicating that after approx. eight weeks of oral ingestion of the combined extract, higher doses of UV radiation were needed to cause an erythematous skin reaction. The MED also increased after 85 days of treatment (56%,  $p < 0.01$ ), indicating that longer oral treatments can improve UV protection effects. Long treatments with the supplement can most likely maintain steady-state systemic concentrations of active metabolites that protect skin cells from the inflammatory reaction appearing after UV radiation.

Several studies have reported the capacity of dietary supplements to prevent UV-induced skin damage in human volunteers. The oral consumption of  $\beta$ -carotene (90 mg/d) for 24 weeks resulted in a modest increase in the MED [38,39], as for high daily doses of  $\alpha$ -tocopherol (1000–3000 IU) and ascorbate (2–3 g) [40,41]. An increase in the MED by 15% after the consumption of a combination of lycopene and a probiotic for six weeks has also been reported [42]. A high dose of squalene (13.5–27 g/day) for 90 days showed significant effects on photoprotection after measurements of skin biopsies [43]. In contrast, a combination of carotenoids, vitamins C and E and proanthocyanidins did not show significant differences in the MED compared with a placebo, but a significant decrease in MMP-1 and MMP-9 was observed in the group receiving the supplement [44]. Considering the reported Folin values, daily dose of total polyphenols in the combination used in the present human trial was approximately 100 mg, which supposes a very reasonable and safe antioxidants dose, and much lower compared to most of the abovementioned studies. In most studies on photoprotection based on nutritional ingredients, there is a time frame of approximately 6–10 weeks until protection against erythema becomes significant [8]. This data that reveals relatively long consumption periods is in agreement with our results, which show that the oral ingestion of a combination of rosemary and citrus extracts for eight weeks provides improved protection against UV-induced erythema. The most likely reason for this behavior seems to be that skin biological turnover requires several weeks to incorporate photoprotective nutrients.

In conclusion, although rosemary and citrus extracts have individually demonstrated cellular protective properties against the damaging radical species induced by UVB radiation, the extract combination used in this study showed a synergistic behavior in increasing the survival of human keratinocytes. The combination drastically decreased the generation of UVB-induced intracellular ROS and was also capable of preventing UV-induced DNA damage in the comet assay, which may contribute to decrease the risk for further skin disorders. Combination also showed genoprotective and antimutagenic properties in a model for massive generation of radical species using ionizing radiation. Finally, the photoprotective properties of this combination were corroborated in human volunteers through a 37% increase in the MED ( $p < 0.05$ ) after eight weeks of oral ingestion, and even stronger MED increase after twelve weeks (56%,  $p < 0.01$ ). This study is the first to show that the oral ingestion of a combination of rosemary and citrus extracts can reduce some molecular events related to skin photodamage, such as intracellular ROS generation and DNA damage. The results may contribute to understand how dietary polyphenols may provide a skin protective effect against UV, further than the daily use of topical sunscreens.

#### 4. Disclosure statement

NC works for Monteloeder, SL-JC and OB-G work for Nutrafur, SA.

#### 5. Abbreviations

UV	ultraviolet
ROS	reactive oxygen species
GAE	gallic acid equivalents
dw	dry weight
H <sub>2</sub> DCFDA	2',7'-dichlorofluorescein diacetate
PBS	phosphate-buffered saline
DMSO	dimethyl sulfoxide
MED	minimal erythema dose
MN	micronuclei

#### Acknowledgements

This work was supported by grants AGL2011-29857-C03-03 (Spanish Ministry of Science and Innovation), PROMETEO/2012/007 and ACOMP/2013/093 from Generalitat Valenciana (GV) and CIBER (CB12/03/30038, Fisiopatología de la Obesidad y la Nutrición, CIBERObn, Instituto de Salud Carlos III). The authors are grateful to GV for VALi+D fellowship ACIF/2013/064. We also thank Monteloeder and Nutrafur for their financial support of the human trial.

#### Appendix A. Supplementary material

Supplementary data associated with this article can be found, in the online version, at <http://dx.doi.org/10.1016/j.jphotobiol.2014.04.007>.

#### References

- [1] A. Svobodova, J. Psotova, D. Walterova, Natural phenolics in the prevention of uv-induced skin damage. A review, *Biomol. Pap. Med. Fac. Univ. Palacky Olomouc Czech Repub.* 147 (2003) 53–56.
- [2] R.M. Lavker, G.F. Gerberick, D. Veres, C.J. Irwin, K.H. Kaidbey, Cumulative effects from repeated exposures to suberythemal doses of uvb and uva in human skin, *J. Am. Acad. Dermatol.* 32 (1995) 53–62.
- [3] M. Wlaschek, G. Heinen, A. Poswig, A. Schwarz, T. Krieg, K. Scharffetter-Kochanek, Uva-induced autocine stimulation of fibroblast-derived collagenase/mmp-1 by interrelated loops of interleukin-1 and interleukin-6, *J. Photochem. Photobiol. B* 59 (1994) 550–556.
- [4] M. Yaar, B.A. Gilchrest, Photoageing: mechanism, prevention and therapy, *Br. J. Dermatol.* 157 (2007) 874–887.
- [5] Y. Xu, Y. Shao, J.J. Voorhees, G.J. Fisher, Oxidative inhibition of receptor-type protein-tyrosine phosphatase kappa by ultraviolet irradiation activates epidermal growth factor receptor in human keratinocytes, *J. Biol. Chem.* 281 (2006) 27389–27397.
- [6] G.J. Fisher, S.C. Datta, H.S. Talwar, Z.Q. Wang, J. Varani, S. Kang, J.J. Voorhees, Molecular basis of sun-induced premature skin ageing and retinoid antagonism, *Nature* 379 (1996) 335–339.
- [7] D. Decraene, The Uvb-Response in Human Skin and its Modulation by the Proto-OncoGenic Als Signaling Pathway, Leuven University Press, 2004.
- [8] H. Sies, W. Stahl, Nutritional protection against skin damage from sunlight, *Ann. Rev. Nutrit.* 24 (2004) 173–200.
- [9] M.S. Lattha, J. Martis, V. Shobha, R. Sham Shinde, S. Bangera, B. Krishnankutty, S. Bellary, S. Varughese, P. Rao, B.R. Naveen Kumar, Sunscreening agents: a review, *J. Clin. Aesthet. Dermatol.* 6 (2007) 16–26.
- [10] J. Vostálová, A. Zdarilová, A. Žďarová, A. Žďarová, *Prunella vulgaris* extract and rosmarinic acid prevent uvb-induced DNA damage and oxidative stress in hacat keratinocytes, *Arch. Dermatol. Res.* 302 (2010) 171–181.
- [11] J. Psotova, A. Svobodova, H. Kolarova, D. Walterova, Photoprotective properties of *prunella vulgaris* and rosmarinic acid on human keratinocytes, *J. Photochem. Photobiol. B* 84 (2006) 167–174.
- [12] M. Sanchez-Campillo, J.A. Gabaldon, J. Castillo, O. Benavente-Garcia, M.J. Del Bano, M. Alcaraz, V. Vicente, N. Alvarez, J.A. Lozano, Rosmarinic acid, a photoprotective agent against uv and other ionizing radiations, *Food Chem. Toxicol.* 47 (2009) 386–392.
- [13] H. Wei, X. Zhang, Y. Wang, M. Lebwohl, Inhibition of ultraviolet light-induced oxidative events in the skin and internal organs of hairless mice by isoflavone genistein, *Cancer Lett.* 185 (2002) 21–29.
- [14] R.P. Singh, R. Agarwal, Mechanisms and preclinical efficacy of silibinin in preventing skin cancer, *Eur. J. Cancer* 41 (2005) 1969–1979.
- [15] N.L. Wu, J.Y. Fang, M. Chen, C.J. Wu, C.C. Huang, C.F. Hung, Chrysins protects epidermal keratinocytes from uva- and uvb-induced damage, *J. Agric. Food Chem.* 59 (2011) 8391–8400.
- [16] P. Sapra, E.H. Moase, J. Ma, T.M. Allen, Improved therapeutic responses in a xenograft model of human b lymphoma (namalwa) for liposomal vincristine versus liposomal doxorubicin targeted via anti-cd19 igg2a or fab' fragments, *Clin. Cancer Res.* 10 (2004) 1100–1111.
- [17] E.A. Offord, J.C. Gautier, O. Avanti, C. Scaletta, F. Runge, K. Kramer, L.A. Applegate, Photoprotective potential of lycopene, beta-carotene, vitamin e, vitamin c and carnosic acid in uva-irradiated human skin fibroblasts, *Free Radic. Biol. Med.* 32 (2002) 1293–1303.
- [18] S. Reuter, S. Eifes, M. Dicato, B.B. Aggarwal, M. Diederich, Modulation of anti-apoptotic and survival pathways by curcumin as a strategy to induce apoptosis in cancer cells, *Biochem. Pharmacol.* 76 (2008) 1340–1351.
- [19] T. Passeron, T. Namiki, H.J. Passeron, E. Le Pape, V.J. Hearing, Forskolin protects keratinocytes from uvb-induced apoptosis and increases DNA repair independent of its effects on melanogenesis, *J. Invest. Dermatol.* 129 (2009) 162–166.

- [20] A.O. Abu-Yousif, K.A. Smith, S. Getsios, K.J. Green, R.T. Van Dross, J.C. Pelling, Enhancement of uvb-induced apoptosis by apigenin in human keratinocytes and organotypic keratinocyte cultures, *Cancer Res.* 68 (2008) 3057–3065.
- [21] M. Herranz-López, S. Fernandez-Arroyo, A. Perez-Sánchez, E. Barrajón-Catalán, R. Beltran-Debon, J.A. Menendez, C. Alonso-Villaverde, A. Segura-Carretero, J. Joven, V. Micol, Synergism of plant-derived polyphenols in adipogenesis: Perspectives and implications, *Phytomedicine* 19 (2012) 253–261.
- [22] D. Huang, O.U. Boxin, R.L. Prior, The chemistry behind antioxidant capacity assays, *J. Agric. Food Chem.* 53 (2005) 1841–1856.
- [23] E. Barrajón-Catalán, S. Fernandez-Arroyo, D. Saura, E. Guillen, A. Fernandez-Gutierrez, A. Segura-Carretero, V. Micol, Cistaceae aqueous extracts containing ellagittannins show antioxidant and antimicrobial capacity, and cytotoxic activity against human cancer cells, *Food Chem. Toxicol.* 48 (2010) 2273–2282.
- [24] M. Fenech, The cytokinesis-block micronucleus technique: a detailed description of the method and its application to genotoxicity studies in human populations, *Mutat. Res.* 285 (1993) 35–44.
- [25] M. Fenech, A.A. Morley, Measurement of micronuclei in lymphocytes, *Mutat. Res.* 147 (1985) 29–36.
- [26] L. Tomás-Menor, A. Morales-Soto, E. Barrajón-Catalán, C. Roldán-Segura, A. Segura-Carretero, V. Micol, Correlation between the antibacterial activity and the composition of extracts derived from various spanish cistus species, *Food Chem. Toxicol.* 55 (2013) 313–322.
- [27] M.J. Del Bano, J. Castillo, O. Benavente-Garcia, J. Lorente, R. Martin-Gil, C. Acevedo, M. Alcaraz, Radioprotective-antimutagenic effects of rosemary phenolics against chromosomal damage induced in human lymphocytes by gamma-rays, *J. Agric. Food Chem.* 54 (2006) 2064–2068.
- [28] M. Alcaraz, C. Acevedo, J. Castillo, O. Benavente-Garcia, D. Armero, V. Vicente, M. Canteras, Liposoluble antioxidants provide an effective radioprotective barrier, *Br J. Radiol.* 82 (2009) 605–609.
- [29] M.A. El-Mahdy, Q. Zhu, Q.E. Wang, G. Wani, S. Patnaik, Q. Zhao, S. Arafa el. B. Barakat, S.N. Mir, A.A. Wani, Naringenin protects hacat human keratinocytes against uvb-induced apoptosis and enhances the removal of cyclobutane pyrimidine dimers from the genome, *Photochem. Photobiol.* 84 (2008) 307–316.
- [30] M. Park, J. Han, C.S. Lee, B.H. Soo, K.M. Lim, H. Ha, Carnosic acid, a phenolic diterpene from rosemary, prevents uv-induced expression of matrix metalloproteinases in human skin fibroblasts and keratinocytes, *Exp. Dermatol.* 22 (2013) 336–341.
- [31] O. Myhre, J.M. Andersen, H. Aarnes, F. Fonnum, Evaluation of the probes 2',7'-dichlorofluorescin diacetate, luminol, and lucigenin as indicators of reactive species formation, *Biochem. Pharmacol.* 65 (2003) 1575–1582.
- [32] M. Ichihashi, M. Ueda, A. Budiyanto, T. Bito, M. Oka, M. Fukunaga, K. Tsuru, T. Horikawa, Uv-induced skin damage, *Toxicology* 189 (2003) 21–39.
- [33] J. Krutmann, P. Humbert, *Nutrition for Healthy Skin: Strategies for Clinical and Cosmetic Practice*, Springer, 2011.
- [34] S. Liardet, C. Scalleta, R. Panizzon, P. Hohlfeld, L. Laurent-Applegate, Protection against pyrimidine dimers, p53, and 8-hydroxy-2'-deoxyguanosine expression in ultraviolet-irradiated human skin by sunscreens: Difference between uvb + uva and uvb alone sunscreens, *J. Invest. Dermatol.* 117 (2001) 1437–1441.
- [35] L. Marrot, J.R. Meunier, Skin DNA photodamage and its biological consequences, *J. Am. Acad. Dermatol.* 58 (2008) S139–S148.
- [36] D.E. Heck, A.M. Vetrano, T.M. Mariano, J.D. Laskin, Uvb light stimulates production of reactive oxygen species: unexpected role for catalase, *J. Biol. Chem.* 278 (2003) 22432–22436.
- [37] J.K. Leach, G. Van Tuyle, P.S. Lin, R. Schmidt-Ullrich, R.B. Mikkelson, Ionizing radiation-induced, mitochondria-dependent generation of reactive oxygen/nitrogen, *Cancer Res.* 61 (2001) 3894–3901.
- [38] M.M. Mathews-Roth, M.A. Pathak, J. Parrish, T.B. Fitzpatrick, E.H. Kiss, K. Toda, W. Clemens, A clinical trial of the effects of oral beta-carotene on the responses of human skin to solar radiation, *J. Invest. Dermatol.* 59 (1972) 349–353.
- [39] J. Lee, S. Jiang, N. Levine, R.R. Watson, Carotenoid supplementation reduces erythema in human skin after simulated solar radiation exposure, *Proc. Soc. Exp. Biol. Med.* 223 (2000) 170–174.
- [40] B. Eberlein-König, M. Placzek, B. Przybilla, Protective effect against sunburn of combined systemic ascorbic acid (vitamin c) and d-alpha-tocopherol (vitamin e), *J. Am. Acad. Dermatol.* 38 (1998) 45–48.
- [41] J. Fuchs, H. Kern, Modulation of uv-light-induced skin inflammation by d-alpha-tocopherol and l-ascorbic acid: a clinical study using solar simulated radiation, *Free Radic. Biol. Med.* 25 (1998) 1006–1012.
- [42] D. Bouilly-Gauthier, C. Jeannet, Y. Maubert, L. Duteil, C. Quelle-Roussel, N. Piccardi, C. Montastier, P. Manissier, G. Pierard, J.P. Ortonne, Clinical evidence of benefits of a dietary supplement containing probiotics and carotenoids on ultraviolet-induced skin damage, *Br J. Dermatol.* 163 (2010) 536–543.
- [43] S. Cho, C.W. Choi, D.H. Lee, C.H. Won, S.M. Kim, S. Lee, M.J. Lee, J.H. Chung, High-dose squalene ingestion increases type I procollagen and decreases ultraviolet-induced DNA damage in human skin *in vivo* but is associated with transient adverse effects, *Clin. Exp. Dermatol.* 34 (2009) 500–508.
- [44] A.K. Greul, J.U. Grundmann, F. Heinrich, I. Pfitzner, J. Bernhardt, A. Ambach, H.K. Biesalski, H. Gollnick, Photoprotection of uv-irradiated human skin: an antioxidative combination of vitamins e and c, carotenoids, selenium and proanthocyanidins, *Skin. Pharmacol. Appl. Skin Physiol.* 15 (2002) 307–315.



# ARTICLE IN PRESS

FRIN-06295; No of Pages 8

Food Research International xxx (2016) xxx–xxx



Contents lists available at ScienceDirect

Food Research International

journal homepage: [www.elsevier.com/locate/foodres](http://www.elsevier.com/locate/foodres)



## Pressurized liquid extraction of *Neochloris oleoabundans* for the recovery of bioactive carotenoids with anti-proliferative activity against human colon cancer cells

M. Castro-Puyana <sup>a,b,1</sup>, A. Pérez-Sánchez <sup>c,1</sup>, A. Valdés <sup>b</sup>, O.H.M. Ibrahim <sup>d</sup>, S. Suarez-Álvarez <sup>e</sup>, J.A. Ferragut <sup>c</sup>, V. Micol <sup>c</sup>, A. Cifuentes <sup>b</sup>, E. Ibáñez <sup>b,\*</sup>, V. García-Cañas <sup>b</sup>

<sup>a</sup> Laboratory of Foodomics, Institute of Food Science Research-CIAL (CSIC-UAM), Nicolás Cabrera 9, Campus Cantoblanco, 28049 Madrid, Spain

<sup>b</sup> Department of Analytical Chemistry, Physical Chemistry and Chemical Engineering, Faculty of Biology, Environmental Science and Chemistry, University of Alcalá, Ctra. Madrid-Barcelona, Km. 33.600, 28871 Alcalá de Henares, Madrid, Spain

<sup>c</sup> Institute of Molecular and Cellular Biology, Miguel Hernández University, Avda. Universidad s/n, 03202 Elche, Alicante, Spain

<sup>d</sup> Horticulture Department, Fac. Agric, Assiut University, Assiut, Egypt

<sup>e</sup> Neiker Tecnalia, Biotechnology Department, Arkatea's Agrifood Campus, 01080 Vitoria-Gasteiz, Alava, Spain

### ARTICLE INFO

#### Article history:

Received 24 February 2016

Received in revised form 23 May 2016

Accepted 30 May 2016

Available online xxxx

#### Keywords:

*Neochloris oleoabundans*

Carotenoids

Pressurized liquid extraction

Colon cancer

Antiproliferative effects

### ABSTRACT

In recent years, the green microalgae *Neochloris oleoabundans* have demonstrated to be an interesting natural source of carotenoids that could be used as potential food additive. In this work, different *N. oleoabundans* extracts obtained by pressurized liquid extraction (PLE) have been analyzed in depth to evaluate the influence of different culture conditions (effect of nitrogen, light intensity or carbon supplied) not only on the total carotenoid content but also on the carotenoid composition produced by these microalgae. Regardless of the cultivation conditions, lutein and carotenoid monoesters were the most abundant carotenoids representing more than 60% of the total content in all extracts. Afterwards, the effect of the different *N. oleoabundans* extracts and the dose-effect of the most potent algae extracts (namely, N9, PS and CO<sub>2</sub> (—)) on the proliferation of human colon cancer cells lines (HT-29 and SW480) and a cell line established from a primary colon cancer cell culture (HGUE-C-1) were evaluated by an MIT assay whereas a stepwise multiple regression analysis was performed to get additional evidences on the relationship between carotenoid content and the antiproliferative activity. Results revealed that, as a general trend, those extracts with high total carotenoid content showed comparably antiproliferative activity being possible to establish a high correlation between the cell proliferation values and the carotenoid constituents. Monoesters showed the highest contribution to cell proliferation inhibition whereas lutein and violaxanthin showed negative correlation and diesters and zeaxanthin showed a positive significant contribution to cell proliferation.

© 2016 Published by Elsevier Ltd.

## 1. Introduction

Nowadays, cancer constitutes one of the leading causes of death. Cancer research has been mainly focused on the search for curative treatments, and few studies have aimed to develop preventive strategies that can be useful in the long period of carcinogenesis of the tumors. This period is suitable for employing chemopreventive strategies based on the use of natural, synthetic or biological substances to reduce the risk of developing a cancer (Talero et al., 2015). In this regard, the exploration of compounds from natural sources with health effects with the

aim of developing a new functional food or nutraceutical is an intense field of research.

Marine environment, which contains a vast array of organisms (bacteria, cyanobacteria, fungi, algae, microalgae or small invertebrates with unique biological properties), represents a huge and underutilized natural source to isolate bioactive compounds to be used in the food and pharmaceutical industries. Among all the marine sources, microalgae have raised an enormous interest. These microorganisms may be used as natural bioreactors since depending on the cultivation conditions they are able to stimulate the synthesis of compounds with health effects, including carotenoids (Herrero, Mendiola, Castro-Puyana, & Ibáñez, 2012; Ibáñez & Cifuentes, 2013). In fact, contents up to 10% carotenoids (w/w) have been described in some microalgae species and may be of high interest as source of pure carotenoids (Guedes, Amaro, & Malcata, 2011). The beneficial effects of carotenoids as antioxidant

\* Corresponding author.

E-mail address: [elena.ibanez@csic.es](mailto:elena.ibanez@csic.es) (E. Ibáñez).

<sup>1</sup> These authors contributed equally to this work.

compounds are well documented. Moreover, they have been also associated with relevant bioactivities such as lower risk of coronary heart diseases and prevention of cancer. Several studies have demonstrated the antiproliferative activity of carotenoids, such as violaxanthin, zeaxanthin, lutein or fucoxanthin, isolated from microalgae against different cancer cells (Cha, Koo, & Lee, 2008; Christaki, Bonos, Giannenas, & Florou-Paneri, 2013; Guedes et al., 2011; Moghadamtousi et al., 2014; Pasquet et al., 2011). A key point to carry out these analyses is obviously the extraction of carotenoids from the microalgae. From the viewpoint of the extraction processes, the new challenges involve the development of green and sustainable processes which enable a fast, selective and efficient extraction and isolation of bioactive compounds from natural matrices (Barba, Grimi, & Vorobiev, 2015; Herrero & Ibáñez, 2015; Roselló-Soto et al., 2015). In this regard, advanced extraction techniques based on the use of compressed fluids (Supercritical Fluid Extraction (SFE), pressurized liquid extraction (PLE)) (Herrero, Castro-Puyana, Mendiola, & Ibáñez, 2013) and the employment of new strategies based on ultrasound-assisted extraction (Parniakov, Apicella, et al., 2015) and pulsed electric field assisted extraction (Parniakov, Barba, et al., 2015a; Parniakov, Barba, et al., 2015b) are among the most promising techniques. These techniques are considered alternative processes to extract nutritionally valuable compounds from microalgae while complying with green chemistry principles and sustainability. Among them, PLE (technique based on the extraction at high temperatures (usually above the boiling point of the solvent) and pressures that maintain the solvent in the liquid state during the extraction) has demonstrated being an interesting alternative to extract carotenoids from different microalgae such as *Haematococcus pluvialis*, *Dunaliella salina*, *Chlorella vulgaris*, *Spirulina platensis*, etc. (Cha et al., 2010; Denery, Dragull, Tang, & Li, 2004; Herrero, Jaime, Martín-Álvarez, Cifuentes, & Ibáñez, 2006; Jaime et al., 2005; Jaime et al., 2010; Plaza et al., 2012). Recently, PLE has also been successfully applied to the extraction of carotenoids from *Neochloris oleoabundans* (Castro-Puyana et al., 2013). Besides the production of lipids, *N. oleoabundans* has recently demonstrated its potential to accumulate relevant amounts of carotenoids when it is grown under certain conditions so that it can be considered as a novel source of natural carotenoids (Castro-Puyana et al., 2013; Chue et al., 2012; Goiris et al., 2012; Urreta et al., 2014).

Considering that microalgae structure has a marked influence in cell disruption and thus in the degree of extraction of intracellular valuable compounds, extraction conditions should be optimized targeting the compounds of interest. In this sense, it is important to focus not only on the family of compounds of interest, for instance carotenoids, but also on the specific compounds responsible for a described bioactivity. Therefore, it is crucial also to perform an in depth chemical characterization, using potent analytical techniques, of the compounds present in the bioactive extracts and to correlate them with the associated bioactivity.

Therefore, the aim of this work was to study the composition and content of carotenoids in different *N. oleoabundans* extracts obtained by PLE in order to evaluate the differences in the type and amount of carotenoids produced when different culture conditions (effect of nitrogen, light intensity or carbon supplied) are employed. Furthermore, the activity of the different *N. oleoabundans* extracts against two colon cancer cell lines and one primary colon cancer cells was also investigated to establish correlations between not only the carotenoid content but also carotenoid constituents and their antiproliferative activity.

## 2. Material and methods

### 2.1. Chemicals and reagents

Ethanol was supplied by Panreac Química (Barcelona, Spain). Methanol, methyl *tert*-butyl ether (MTBE), hexane, and acetone were obtained from LabScan (Gliwice, Poland). Sea sand was from VWR (Leuven, Belgium). Standard samples of β-carotene, lutein, chlorophyll *a* (from

*Anacystis nidulans* algae), and chlorophyll *b* (from spinach) were obtained from Sigma-Aldrich (Madrid, Spain), whereas astaxanthin monopalmitate and astaxanthin dipalmitate were purchased from CaroteNature GmbH (Lupsingen, Switzerland).

### 2.2. Samples

*Neochloris oleoabundans* (UTEX#1185) was obtained from the culture collection of algae at the University of Texas (Austin, TX, USA). Modified Bold's Basal Medium (BBM) was used as medium for cultivation (Andersen, Berges, Harrison, & Watanabe, 2005). Cultures were established in BBM containing 9 mM KNO<sub>3</sub> until cell reached optical density (OD 660 nm) of 5.0. Aliquots of 200 mL were centrifuged (520 × g during 5 min), washed with distilled water once and used as inoculum in three consecutive experiments aimed to study the effect of nitrogen, light and CO<sub>2</sub> in the carotenoid and chlorophyll cellular content.

All the experiments were carried out in a culture chamber at 24 ± 2 °C, under 16-h photoperiod. Cultures were grown in batch mode, using 9-cm wide glass reactors containing a working volume of 1 L and subjected to continuous stirring by bubbling air at a constant flow rate.

To evaluate the effect of nitrogen, cultures were grown in BBM supplemented with KNO<sub>3</sub> (used as nitrogen source) at concentrations of 3, 6 and 9 mM (samples N3, N6 and N9, respectively). Pure CO<sub>2</sub> was supplied automatically to the bubbling air for 30 s every 10 min to maintain the pH below 8 and ensure carbon sufficiency. The incident light intensity on the reactor surface was 400 μmol photons m<sup>-2</sup> s<sup>-1</sup> (Philips TLD 58 W).

To determine the effect of light intensity, cultures were grown in BBM supplemented with 3 mM KNO<sub>3</sub> and subjected to two different incident light intensities on the reactor surface: 240 μmol photons m<sup>-2</sup> s<sup>-1</sup> (sample LL) and of 400 μmol photons m<sup>-2</sup> s<sup>-1</sup> (sample HL). Pure CO<sub>2</sub> was automatically supplied as described above.

The effect of carbon supply was investigated in cultures grown in BBM supplemented with 3 mM KNO<sub>3</sub> and under an incident light intensity of 400 μmol photons m<sup>-2</sup> s<sup>-1</sup> which were cultivated suppressing the CO<sub>2</sub> addition during cultivation (sample CO<sub>2</sub> (-)) or supplementing CO<sub>2</sub> automatically as described above (sample CO<sub>2</sub> (+)).

In all of the above experiments, cells were harvested by centrifugation (520 × g, 5 min) 6 days after reaching the stationary phase of growth, which was induced by the depletion of the initially supplemented nitrogen, as described in Urreta et al. (Urreta et al., 2014). The obtained algal biomass was pre-frozen at -20 °C, lyophilized and stored under dry and dark conditions until further use.

In addition to those samples described above, other two samples were included in this study. The first of them was obtained from cultures grown in MBB medium at 3 mM KNO<sub>3</sub>, using an incident light intensity of 400 μmol photons m<sup>-2</sup> s<sup>-1</sup> and with automatic injection of CO<sub>2</sub> (therefore under similar culture conditions than those used for samples N3, HL and CO<sub>2</sub> (+)). In this case, cells were harvested 10 days after reaching the stationary phase of growth instead of after 6 days (sample D10).

The last sample (sample PS) was collected from a culture operated at pilot plant scale which was used to reproduce the culture conditions corresponding to sample N3, therefore grown with 3 mM KNO<sub>3</sub>, 400 μmol photons m<sup>-2</sup> s<sup>-1</sup> of light intensity and automatic supply of CO<sub>2</sub>, until 6-days after reaching the stationary phase of growth. This culture was grown in a 30-cm wide tubular photo bioreactor with a working volume of 40 L.

### 2.3. Pressurized liquid extraction (PLE)

Before PLE, between 1.2 and 2.5 g of lyophilized algae samples were treated by 3 cycles of cryogenic grinding using a Mixer Mill CryoMill (Retsch, Haan, Germany) to break down the cell wall to obtain the highest extraction yield. Three steps were carried out in each cycle:

# ARTICLE IN PRESS

M. Castro-Puyana et al. / Food Research International xxx (2016) xxx-xxx

3

precooling (frequency 1/s = 5 during 2 min), grinding (frequency 1/s = 20 during 3 min) and intermediate cooling (frequency 1/s = 5 during 1 min), as previously described (Castro-Puyana et al., 2013). PLE extractions of pre-treated samples were performed using an accelerated solvent extractor (ASE 200, Dionex, Sunnyvale, CA, USA). Extractions were carried out using ethanol as solvent at 100 °C and 20 min as static extraction time, as suggested in Castro-Puyana et al. (2013). An extraction cell heating-up was applied during 5 min prior to each extraction (time fixed by the system). All extractions were done (in duplicate) using 11 mL extraction cells at 1500 psi containing 0.6 g of algae mixed homogenously with 2 g of sea sand. In addition, these samples were introduced inside the cell between sand layers in a sandwich-like format. The extracts obtained were protected from light and stored under refrigeration until HPLC analysis.

To carry out the antiproliferative activity assay, the extracts were evaporated with a Rotavapor R-210 (Büchi Labortechnik AG, Flawil, Switzerland). Dry extracts were dissolved in dimethyl sulfoxide (DMSO, Sigma-Aldrich) at 125 mg/mL, and stored as aliquots at -80 °C until use.

## 2.4. Quantification of carotenoids and chlorophylls by LC-DAD

Carotenoid and chlorophylls content in the extracts was determined by HPLC employing an Agilent HP 1100 series liquid chromatograph (Agilent Technologies, CA, USA) equipped with a DAD, and using a YMC-C30 reversed-phase column (250 mm × 4.6 mm id, 5 µm particle size, YMC Europe, Schermbek, Germany). The mobile phase was a mixture of MeOH:MTBE:water (90:7:3 v/v/v) (A) and MeOH:MTBE (10:90 v/v) (B) eluted according to the following gradient: 0 min, 0% B; 20 min, 30% B; 35 min, 50% B; 45 min, 80% B; 50 min, 100% B; 52 min, 0% B. Flow rate was 0.8 mL/min, the injection volume was 10 µL, and detection was at 450 and 660 nm (recorded spectra from 240 to 770 nm by DAD). For the calibration curve, standard solutions of β-carotene (ranging from 0.025 to 1 mg/mL), lutein (from  $1.25 \times 10^{-3}$  to 0.04 mg/mL), astaxanthin monopalmitate and dipalmitate (both ranging from  $6.25 \times 10^{-4}$  to 0.04 mg/mL), chlorophyll a and chlorophyll b (both from  $3.13 \times 10^{-3}$  to 0.2 mg/mL) were prepared by appropriate dilution of the stocks and injected into the LC-DAD instrument. Each standard was dissolved from a stock solution (1–2 mg/mL) with different solvents, i.e. lutein, chlorophyll a, and chlorophyll b were dissolved in ethanol, astaxanthin monopalmitate and astaxanthin dipalmitate in hexane:acetone (1:1 v/v), and β-carotene in hexane. The linear regression equations for each standard curve were obtained by plotting the amount of standard compound injected against the peak area.

## 2.5. Cell culture conditions

Colon adenocarcinoma HT-29 and SW480 cells were obtained from the IMIM (Institut Municipal d'Investigació Médica, Barcelona, Spain) and ATCC (American Type Culture Collection, LGC Promochem, UK), respectively, and HGUE-C-1 was an established cell line derived from a primary colon cancer cell line of a single primary human colon carcinoma at the Hospital General Universitario de Elche (Alicante, Spain). The cells were grown in DMEM supplemented with 5% heat inactivated fetal bovine serum, 2 mM L-glutamine, 50 U/mL penicillin G, and 50 µg/mL streptomycin at 37 °C in a humidified atmosphere with 5% CO<sub>2</sub>. The cells were trypsinized every three days according to the manufacturer's instructions, and they were seeded in 96-well plates.

## 2.6. Antiproliferative activity assay

To study the effect of *N. oleoabundans* extracts on the proliferation of HT-29, SW480 and HGUE-C-1 cell lines, the cells were seeded at a density of  $5 \times 10^3$  cells/well, permitted to adhere overnight at 37 °C, and exposed to algae extracts of 27, 83 or 250 µg/mL for 24 h. After incubations

in the presence of the extract, the cells were washed with PBS and incubated with MTT (3-(4,5-dimethylthiazol-2-yl)-2,5-diphenyltetrazolium bromide) for 3–4 h at 37 °C and 5% CO<sub>2</sub>. MTT is reduced to formazan by the succinate dehydrogenase system of active mitochondria, and hence, specifically used to assay for the viable cells as measurement of cell proliferation. The medium was removed, and 100 µL of DMSO per well was added to dissolve the formazan crystals. The plates were shaken for 15 min and analyzed by using a microplate reader (SPECTROstar Omega, BMG LabTech GmbH, Offenburg, Germany) at 570 nm.

## 2.7. Statistical analysis

Data sets obtained from chemical analysis, as well as those obtained from the antiproliferative activity assay were analyzed with one-way analysis of variance (ANOVA) and Tukey's post hoc analysis at the ( $p < 0.05$ ) significance level. To get additional evidences on the relationship between carotenoid content and the antiproliferative activity, a stepwise multiple regression analysis was applied. This approach was applied to find predictive equations for the antiproliferative activity with the carotenoids concentrations as the predictor variables. Regression (Beta) coefficients were analyzed to evaluate key variables for the prediction of the antiproliferative activity. The magnitude of Beta coefficients allows comparing the relative contribution of each independent variable in the prediction of the dependent variable. All the statistical analyses were performed using statistical package Statistica 7.1 (StatSoft Inc., OK, USA).

## 3. Results and discussion

### 3.1. Analysis and quantification of carotenoids

Previous works have shown that *N. oleoabundans* can be considered as a novel source of natural carotenoids when grown under certain conditions (Castro-Puyana et al., 2013). Considering that different cultivation conditions (such as nitrogen concentration, light intensity and carbon supply) have an important impact on the accumulation of carotenoids (Urreta et al., 2014), it is relevant a deeper analysis to know how these conditions affect the type and amount of carotenoids produced.

Nine extracts marked as N3, N6, N9, LL, HL, CO<sub>2</sub> (-), CO<sub>2</sub> (+), D10, and PS, were obtained from cultures of *N. oleoabundans* grown under different controlled conditions (see Section 2.2) by PLE. Table 1 shows the values of extraction yield (determined as extract dry weight/initial dry weight expressed as a percentage) obtained for each algae extract, which ranged from 23.4 to 35.5%.

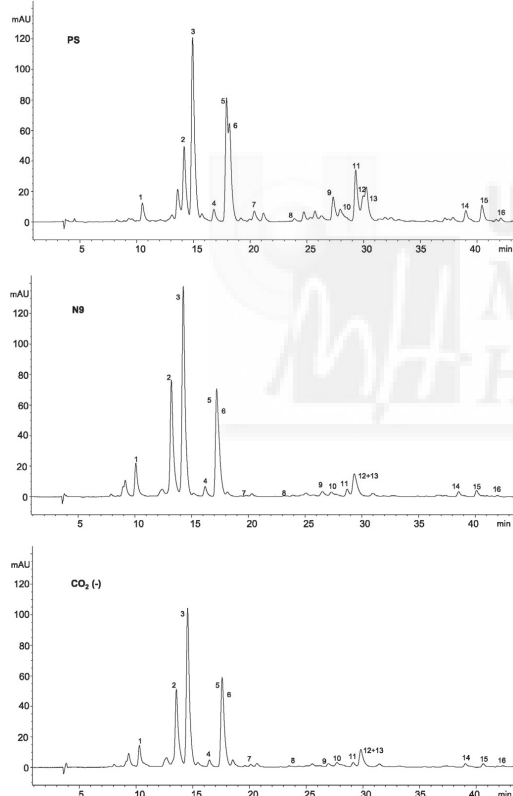
To establish differences in the carotenoid and chlorophyll composition of each *N. oleoabundans* extract and to evaluate the influence of the different nutritional and environmental factors in their production, it is essential to carry out the chemical characterization of each extract and an accurate quantification of each component.

The application of the LC-(APCI)-MS methodology previously described (Castro-Puyana et al., 2013) provided information on the main pigments (carotenoids and chlorophylls) found in the PLE extracts. Fig. 1 depicts, as example, the chromatographic profiles (at a wavelength equal to 450 nm) obtained for three different *N. oleoabundans* extracts (PS, N9, and CO<sub>2</sub> (-)). In spite all extracts have a similar chromatographic profile, important differences were obtained in terms of the amount of carotenoids and chlorophylls produced by *N. oleoabundans* at the different cultivation conditions (Table 1).

The quantitation of carotenoids whose standards were not commercially available was performed using as standards those with higher similarity in terms of spectra and structure. In addition, a molecular-weight-correction factor (determined by dividing the molecular weight of the carotenoid to be quantified by that of the standard) was applied to consider the difference in detector response (Chandra, Rana, & Li, 2001; Dhooqhe et al., 2008). Thus, violaxanthin (peak 1), lutein (peak 3), canthaxanthin (peak 5), canthaxanthin related-compound (peak

**Table 1**Extraction yield, total amount of carotenoid and chlorophylls, and content of the main carotenoids identify in *N. oleobundans* PLE extracts cultivated under different grown conditions.

Sample	Extraction yield (%)	Total carotenoids mg/g extract	Violaxanthin mg/g extract (peak 2)	Lutein mg/g extract (peak 5)	Zeaxanthin mg/g extract (peak 7)	Canthaxanthin mg/g extract (peak 8)	Monoesters mg/g extract (peaks 13–16)	$\beta$ -Carotene mg/g extract (peak 17)	Diesters mg/g extract (peaks 18–20)	Total chlorophylls mg/g extract
N9	29.7 ± 0.7	129.4 d,e,h	11.0 <sup>d</sup>	62.6 <sup>d,g</sup>	6.0 <sup>a,b,d,e</sup>	13.6 <sup>d,g,h</sup>	16.3 <sup>a,c,f</sup>	17.4 <sup>d,e,g,h</sup>	2.0 <sup>d,g,h</sup>	42.7 <sup>d</sup>
N6	24.4 ± 1.0	142.8 d,e	6.8 <sup>e,g</sup>	46.3 <sup>e</sup>	6.1 <sup>a,b,d,h</sup>	17.3 <sup>e,g</sup>	40.3 <sup>e</sup>	20.9 <sup>d,e,h</sup>	3.0 <sup>e</sup>	24.9 <sup>e</sup>
N3	35.5 ± 0.8	76.7 b,c	2.7 <sup>a,b,c,f,h</sup>	21.2 <sup>b,c,h</sup>	5.5 <sup>a,b,d,h</sup>	5.3 <sup>a,b,f,i</sup>	27.9 <sup>b</sup>	11.4 <sup>a,b,c,f,g</sup>	1.2 <sup>a,b,c,g,i</sup>	10.7 <sup>a,b,c,h</sup>
HL	33.6 ± 0.7	62.0 a,c,f	2.0 <sup>a,b,c,f,h,i</sup>	17.2 <sup>a</sup>	6.3 <sup>a,b,d,e</sup>	5.9 <sup>a,b,c,f,i</sup>	20.0 <sup>a,c,d,i</sup>	8.1 <sup>a,b,c,i</sup>	1.0 <sup>a,b,c,i</sup>	7.6 <sup>a,b,c,h</sup>
LL	30.0 ± 0.7	66.1 a,b,c,f	3.1 <sup>a,b,c,f,h</sup>	23.1 <sup>b,c,h</sup>	2.8 <sup>c,g,h,i</sup>	7.6 <sup>a,c,f</sup>	17.5 <sup>a,c,d</sup>	10.4 <sup>a,b,c,f,g</sup>	1.1 <sup>a,b,c,i</sup>	11.8 <sup>a,b,c,f,h</sup>
CO <sub>2</sub> (+)	26.6 ± 0.7	62.6 a,c,f	3.5 <sup>a,b,c,f,h</sup>	26.9 <sup>f,h</sup>	12.8 <sup>f</sup>	6.0 <sup>a,b,c,f,i</sup>	12.7 <sup>c,d,f,g</sup>	0.3 <sup>f</sup>	14.1 <sup>c,f</sup>	
CO <sub>2</sub> (-)	26.3 ± 1.0	113.8 g,h	7.0 <sup>e,g</sup>	62.2 <sup>d,g</sup>	3.0 <sup>g,h,i</sup>	16.2 <sup>d,e,g</sup>	9.0 <sup>f,g</sup>	13.5 <sup>b,c,d,f,g,h</sup>	1.7 <sup>b,d,g,h</sup>	38.9 <sup>g</sup>
PS	23.4 ± 0.7	118.6 h	2.9 <sup>a,b,c,f,h</sup>	24.7 <sup>b,c,f,h</sup>	3.3 <sup>b,c,g,h,i</sup>	13.1 <sup>d,h</sup>	53.1 <sup>h</sup>	16.9 <sup>d,e,f,g,h</sup>	2.2 <sup>d,g,h</sup>	10.9 <sup>a,b,c,h</sup>
D10	32.8 ± 0.8	45.2 i	0.8 <sup>a,i</sup>	6.7 <sup>i</sup>	2.0 <sup>c,g,h,i</sup>	4.7 <sup>a,f,i</sup>	22.6 <sup>a,i</sup>	6.1 <sup>a,i</sup>	0.9 <sup>a,b,c,i</sup>	2.3 <sup>i</sup>

<sup>a–i</sup>Means in a column without a common superscript letter differ ( $p < 0.05$ ), as analyzed by one-way ANOVA.

are set outdoor (for instance, to the temperature fluctuations in outdoor cultures). However, these differences support the importance of culture factors on the pigment content of microalgae.

The ability of microalgae to adapt their pigment content to environmental changes is well documented and it is considered as a cellular mechanism to quickly optimize the photosynthetic efficiency or even as a survival mechanism to face long-term unfavorable environmental conditions. Among these unfavorable conditions, nutrient limitation, and especially nitrogen starvation, is a well-known factor affecting microalgae pigment content (Del Campo et al., 2000; Jin, Polle, Lee, Hyund, & Chang, 2003; Li, Horsman, Wang, Wu, & Lan, 2008; Solovchenko, Khozin-Goldberg, Didi-Cohen, Cohen, & Merzlyak, 2008). Several authors indicates that when nitrogen availability become limiting for growth, cellular nitrogen-rich compounds (mainly photosynthetic proteins and chlorophylls), are degraded and used as an internal source of nitrogen to face its unavailability in the surrounding media (Li et al., 2008; Pruvost, Vooren, Cogne, & Legrand, 2009; Rismani-Yazdi, Haznedaroglu, Hsin, & Peccial, 2012). This process of degradation can explain the inverse relationship observed between the nitrogen supplied to the cultures and chlorophyll content in the analyzed samples. Furthermore, as chlorophylls, those known as primary carotenoids are closely bound to photosynthetic proteins, so degradation of photosynthetic structures inevitably would lead to a concomitant reduction of carotenoid content (Solovchenko et al., 2008). This justifies the observed similar pattern for the content of both types of pigments in relation to culture conditions.

It must be noted that, regardless of the specific culture conditions applied, all the extracts analyzed in this work come from cultures maintained for at least 6 days in stationary growth-phase and that the stationary growth-phase was triggered by the complete depletion of the nitrogen initially supplied to the medium (whatever the others culture factors applied). Therefore, there is an additive effect to nitrogen starvation exerted over the other applied culture factors. In this context, higher amounts of nitrogen could provide to the cells higher reserve of nitrogen-rich compounds to face the nitrogen unavailability, thus leading to a lesser pigment reduction under the same starvation time. Likewise, by removing the CO<sub>2</sub> supply, cells are subjected to a lesser imbalance between the availability of carbon and nitrogen, which would reduce the internal nitrogen demand and the degradation of photosynthetic pigment in the sample CO<sub>2</sub> (−) (Urreta et al., 2014). In an opposite way, long-term nitrogen-starvation would give rise to further pigment degradation, which would explain the found lowest chlorophyll content in the sample named D10.

Culture conditions not only affected the total carotenoid content, but also the carotenoid composition. This can be observed in Table 1, which shows the concentration of specific carotenoids in the extracts (as well as in Fig. 2 which displays their relative content). Regardless of the cultivation conditions, lutein and carotenoid monoesters were the most abundant carotenoids, representing more than 60% of the total content in all extracts. However, the relative content of these two compounds displayed an opposite pattern regarding the culture conditions. For instance, lutein account for the largest fraction of the total carotenoids in the extract obtained from cultures with the highest nitrogen dosage (N9) and from those lacking of carbon (CO<sub>2</sub> (−)), 48.4% and 54.7% respectively, which also show the lowest percentage of monoesters (12.6% and 7.9%, respectively). It is worth mentioning that these same samples showed the highest pigment values (chlorophylls and carotenoids). On the contrary, the highest fraction of monoesters, along with the lowest of lutein, was found in the extract D10 (that exhibited the lowest pigment content) and in the extract PS. Therefore, the latter extract stands out both for its high content of total carotenoids as for a significant fraction of monoesters. In spite of the pattern above described, the absolute value of lutein and monoesters in the extract differs from the percentage due to the differences in the total carotenoid content among samples from different culture conditions. This makes that sample D10 displays a monoester content halved compared to PS (22.6 and 53.1 mg/g extract, respectively), despite having a similar percentage (close to 45% of the total carotenoids).

Among monoesters produced by *N. oleoabundans*, we identified two specific esters of astaxanthin by applying the LC-(APCI)-MS methodology. Astaxanthin (which is one of the most valuable microalgae carotenoid due to its antioxidative properties) is synthetized and massively accumulated in the cytoplasmatic oil bodies by certain microalgae under some stressful environmental conditions (Jin et al., 2003). For instance, under stressful culture conditions, esters of astaxanthin can account for more than 95% of total carotenoids in *Haematococcus pluvialis*, where it seems to act for preventing photo-oxidative damage of cellular lipids (Solovchenko, Chivkunova, & Maslova, 2011). In this sense, astaxanthin play a very different role compared to lutein, which is a structural and functional component of the photosynthetic apparatus of most of green microalgae.

Among the other major carotenoids identified in the extracts, only violaxanthin displayed a clear pattern regarding to the culture conditions. Violaxanthin content was directly proportional to that of lutein, so the highest absolute content of this carotenoid was found in samples N9, N6 and CO<sub>2</sub> (−).

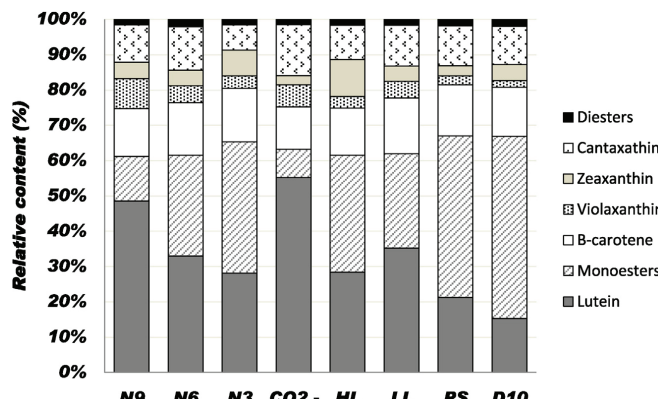


Fig. 2. Relative content of the carotenoids obtained from the different *N. oleoabundans* cultures analyzed.

### 3.2. Anti-proliferative activity

In previous studies, HT-29 cell line has shown to be more refractory to the anti-proliferative activity of natural compounds than other established colon cancer cell lines (Valdés et al., 2013). Besides, this cell line constitutes a paradigm of the colon carcinogenesis pathway proposed by Fearon and Vogelstein (1990). Thus, in the present work, we screened the algae extracts on HT-29 line as a previous step in order to select the most active extract. To attain this, HT-29 cells were incubated with 250 µg/mL of the different algae extracts for 24 h, and cell proliferation was analyzed by the MTT assay. In general, most of the extracts reduced the proliferation of HT-29 human colon cells at an initial concentration of 250 µg/mL after 24 h treatment (Fig. 3). As a general trend, those extracts with high total carotenoid content showed comparably high antiproliferative activity. An exception to this observation was N6 extract that showed the highest carotenoid concentration, but only inhibited proliferation by 16%. A possible explanation for the low inhibitory potency observed with this extract is that the presence of certain carotenoids or other constituents in the extract may have potential contrasting effects. Then, the contribution of each carotenoid to the antiproliferative activity was evaluated using a step-wise multiple regression model. This analysis showed that when six variables (violaxanthin, lutein, zeaxanthin, monoesters, β-carotene and diesters) were fitted to the cell proliferation data, the value of the adjusted coefficient of multiple determination (adjusted R<sup>2</sup>) was 0.981 ( $p < 0.05$ ). This means that 98% of the variation in the cell proliferation data was explained by the six variables. It was found that monoesters showed the highest contribution to inhibit cell proliferation ( $\text{Beta} = -1.83$ ,  $p < 0.01$ ). Likewise, lutein and violaxanthin showed negative correlation ( $\text{Beta} = -1.39$ ,  $p < 0.05$ ;  $\text{Beta} = -0.83$ ,  $p < 0.05$ ; respectively) with cell proliferation. In contrast, diesters and zeaxanthin showed positive significant contribution ( $\text{Beta} = 1.41$ ,  $p < 0.05$ ;  $\text{Beta} = 1.06$ ,  $p < 0.01$ ) to cell proliferation. The anti-proliferative effect of violaxanthin has been previously demonstrated on MCF-7 human mammary cancer cells, in which a concentration as low as 1 µg/mL of a violaxanthin-enriched fraction obtained from *Dunaliella tertiolecta* microalgae exerted significant inhibition on cell proliferation after 24 h exposure (Pasquet et al., 2011). In agreement with this, two of the most potent extracts tested in the present study contained violaxanthin at concentrations (~1.8 and ~2.8 µg/mL in N9 and CO<sub>2</sub>(-), respectively) that were close to that previously reported. In another report, violaxanthin was found as possibly involved in the antiproliferative and pro-apoptotic activity of *Chlorella ellipsoidea* extracts on

HCT-116 human colon cancer cells (Cha et al., 2008). On the other side, low-micromolar concentration (10 µM) of lutein has been shown to protect HT-29 cells against deoxynivalenol-induced oxidative stress and apoptosis (Krishnaswamy, Devaraj, & Padma, 2010). In our present study, the assayed lutein concentrations (~15 µg/mL) in two of the most potent extracts (N9 and CO<sub>2</sub>(-)) were higher than 10 µM (~5.6 µg/mL) and exerted significant inhibition (~35%) of HT-29 cell proliferation. These contrasting results compared with those reported in the literature support the idea that factors including the lutein concentration, the presence of other constituents in the extracts, or cell culture conditions such as cell density might influence the outcome of the anti-proliferative studies with these compounds. In agreement with other reports, our data suggested that the presence of zeaxanthin did not enhance the growth inhibitory activity of the extracts on cancer cells (Kotake-Nara et al., 2001). To further characterize the anti-proliferative effect of the most active algae extracts (N9, PS, and CO<sub>2</sub>(-)), the effective concentration range of the extracts was determined on different colon cancer cell lines exhibiting different drug resistance patterns. To that aim, the dose-effect of the most potent algae extracts (N9, PS, and CO<sub>2</sub>(-)) on proliferation of primary colon cancer cells (HGUE-C-1) and two cell lines (HT-29 and SW480) was evaluated after exposure of the cells to different concentrations of each extract by MTT assay. As it can be observed in Fig. 4, in general, the treatments with algae extracts resulted in a reduction of cell proliferation in dose-dependent manner. However, cells showed different sensitivity to the extracts. In particular, SW480 line (Fig. 4 B) was the most sensitive to the three extracts exhibiting significant decrease on cell proliferation after exposure to the lowest assayed concentration (i.e., 27 µg/mL) of the extracts. By contrast, HGUE-C-1 cells (Fig. 4 C) were more resistant to the effect of the extracts, showing to be especially refractory to PS extract that, in comparison with its effect on the other cell lines, exhibited negligible activity at the highest assayed concentration (250 µg/mL). In the same cell line, N9 extract at highest concentration inhibited the cell proliferation 36.4% compared to control (Fig. 4 C). The strongest resistance of HGUE-C-1 cell line could be in correlation to the higher presence of a mesenchymal phenotype which is associated to the invasion and metastasis linked to cancer stem cells in numerous carcinomas (Grasso et al., 2015).

Besides the cytoprotective attributes of carotenoids, in recent years, rising evidence suggest that these compounds may inhibit cancer cell proliferation and, in some cases, induce cell death. Although several mechanisms on their mode of action have been suggested, the exact molecular mechanisms by which carotenoids exert their anticancer effects are still unclear.

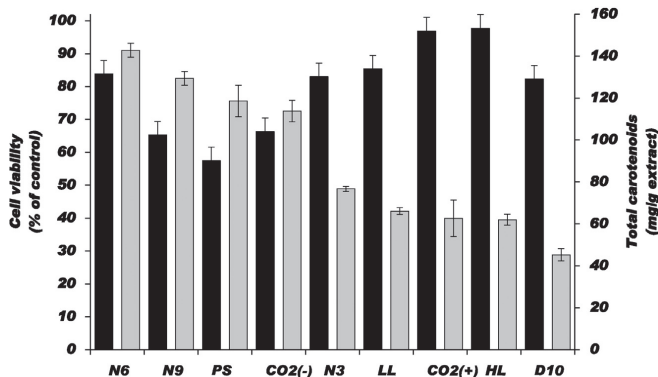


**Fig. 3.** Effect of 250 µg/mL of the different algae extracts on HT-29 cell proliferation upon treatment for 24 h (black bars). Error bars are given as the 95% confidence interval of three independent experiments each performed in triplicate. Total carotenoids (mg/g extract) (grey bars). The data are given as the mean ± SD.

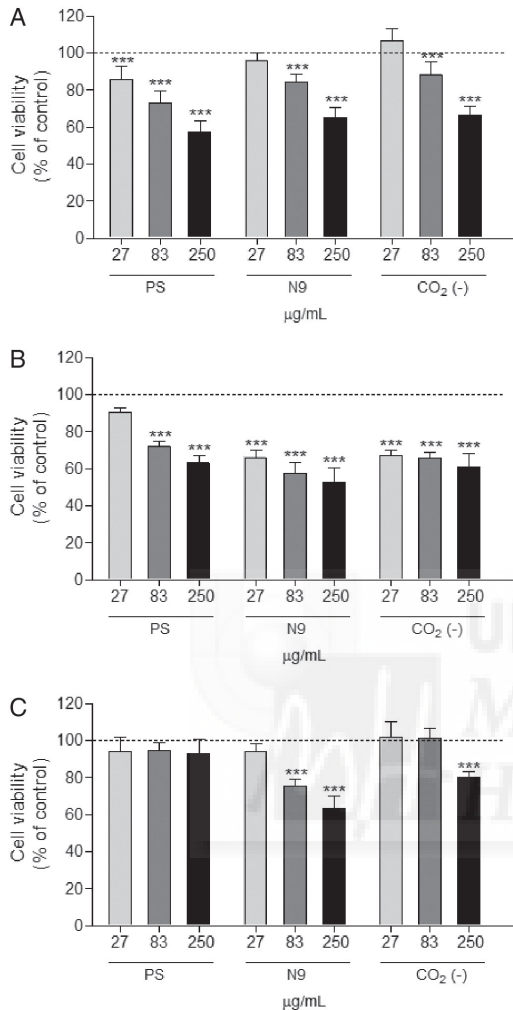


**Fig. 4.** Dose-dependent effect of the algae extracts PS, N9 and CO<sub>2</sub> (-) on HT-29 (A), SW-480 (B) and HGUE-C-1 (C) cell proliferation upon treatment for 24 h. The data are given as the mean  $\pm$  SD. One-way analysis of variance (ANOVA) and statistical comparisons of the different treatments were performed using Tukey's test. \*\*\*p < 0.001 versus control group.

#### 4. Conclusions

The study of *N. oleoabundans* extracts obtained by PLE has enabled to demonstrate that under appropriate culture conditions, these green microalgae are able to produce considerable amounts of carotenoids that provide to the biomass an added value. Lutein, carotenoids monoesters and violaxanthin were the most abundant carotenoids, regardless the cultivation conditions. In addition to evaluate the composition and total carotenoid content of each *N. oleoabundans* PLE extract, the activity of these extracts against colon cancer cell lines has been also investigated. The results obtained demonstrated that those extracts with high carotenoid content showed comparably high antiproliferative activity. In this way, it was possible to correlate the cell proliferation values and the carotenoid constituents. Thus, while carotenoids monoesters

showed the highest contribution to inhibit cell proliferation, lutein and violaxanthin showed negative correlation and diesters and zeaxanthin showed a positive significant contribution to cell proliferation. This work opens new possibilities in the use of carotenoids from *N. oleoabundans* as a functional food ingredient or nutraceutical that can help in the prevention of colon cancer development. However, more in depth studies are needed in order to scientifically demonstrate the observed effects in-vivo.

#### Acknowledgments

M.C.P. thanks the Ministry of Economy and Competitiveness (Spain) for her "Ramón y Cajal" research contract (RYC-2013-12688). This work was supported by the projects AGL2014-53609-P and AGL2015-67995-C3-1-R (Ministerio de Economía y Competitividad, Spain). A.V. thanks the Ministerio de Economía y Competitividad for his FPI pre-doctoral fellowship (BES-2012-057014).

#### References

- Andersen, R. A., Berges, J. A., Harrison, P. J., & Watanabe, M. M. (2005). In R. A. Andersen (Ed.), *Algal culturing techniques* (pp. 429–538). Elsevier: Amsterdam.
- Barba, F. J., Grimi, N., & Vorobiev, E. (2015). New approaches for the use of non-conventional cell disruption technologies to extract potential food additives and nutraceuticals from microalgae. *Food Engineering Reviews*, 7(1), 45–62 (2015).
- Castro-Puyana, M., Herrero, M., Urreta, I., Mendiola, J. A., Cifuentes, A., Ibáñez, E., & Suárez-Alvarez, S. (2013). Optimization of clean extraction methods to isolate carotenoids from the microalgae *Neochloris oleoabundans* and subsequent chemical characterization using liquid chromatography tandem mass spectrometry. *Analytical and Bioanalytical Chemistry*, 405, 4607–4616.
- Cha, K. H., Koo, S. Y., & Lee, D.-U. (2008). Antiproliferative effects of carotenoids extracted from *Chlorella ellipsoidea* and *Chlorella vulgaris* on human colon cancer cells. *Journal of Agricultural and Food Chemistry*, 56, 10521–10526.
- Cha, K. H., Lee, H. J., Koo, S. Y., Song, D.-G., Lee, D.-U., & Pan, C.-H. (2010). Optimization of pressurized liquid extraction of carotenoids and chlorophylls from *Chlorella vulgaris*. *Journal of Agricultural and Food Chemistry*, 58, 793–797.
- Chandra, A., Rana, J., & Li, Y. (2001). Separation, identification, quantification, and method validation of anthocyanins in botanical supplement raw materials by HPLC and HPLC–MS. *Journal of Agricultural and Food Chemistry*, 49, 3515–3521.
- Christakis, E., Bonos, E., Giannenas, I., & Florou-Paneri, P. (2013). Functional properties of carotenoids originated from algae. *Journal of the Science of Food and Agriculture*, 93, 5–11.
- Chue, K. T., Ten, L. N., Oh, Y. K., Woo, S.-G., Lee, M., & Yoo, S.-A. (2012). Carotenoids compositions of five microalgae species. *Chemistry of Natural Compounds*, 48, 141–142.
- Del campo, J. A., Moreno, J., Rodríguez, H., Vargas, M. A., Rivas, J., & Guerrero, M. G. (2000). *Journal of Biotechnology*, 76, 51–59.
- Denery, J. R., Dragull, K., Tang, C. S., & Li, Q. X. (2004). Pressurized fluid extraction of carotenoids from *Haematococcus pluvialis* and *Dunaliella salina* and kavalactones from *Piper methysticum*. *Analytica Chimica Acta*, 501, 175–181.
- Dhooghe, L., Mesia, K., Kohtala, E., Tona, L., Pieters, L., Vlietinck, A. J., & Apers, S. (2008). Development and validation of a HPLC-method for the determination of alkaloids in the stem bark extract of *Nauclea pobeguini*. *Talanta*, 76, 462–468.
- Fearon, E. R., & Vogelstein, B. (1990). A genetic model for colorectal tumorigenesis. *Cell*, 61, 759–767.
- Goiris, K., Muylaert, K., Fraeye, I., Foubert, I., De Brabanter, J., & De Cooman, L. (2012). Antioxidant potential of microalgae in relation to their phenolic and carotenoid content. *Journal of Applied Phycology*, 24, 1477–1486.
- Grasso, S., Martínez-Lacaci, I., Barberá, V. M., Castillo, A., Soto, J. L., Gallego-Plazas, J., ... Saceda, M. (2015). HGUE-C-1 is an atypical and novel colon carcinoma cell line. *BMC Cancer*, 15, 240.
- Guedes, A. C., Amaro, H. M., & Malcata, F. X. (2011). Microalgae as sources of carotenoids. *Marine Drugs*, 9, 625–644.
- Herrero, M., & Ibáñez, E. (2015). Green processes and sustainability: An overview on the extraction of high added-value products from seaweeds and microalgae. *Journal of Supercritical Fluids*, 95, 211–216.
- Herrero, M., Castro-Puyana, M., Mendiola, J. A., & Ibáñez, E. (2013). Compressed fluids for the extraction of bioactive compounds. *TRAC Trends in Analytical Chemistry*, 43, 67–83.
- Herrero, M., Jaime, L., Martín-Alvarez, P. J., Cifuentes, A., & Ibáñez, E. (2006). Optimization of the extraction of antioxidants from *Dunaliella salina* microalgae by pressurized liquids. *Journal of Agricultural and Food Chemistry*, 54, 5597–5603.
- Herrero, M., Mendiola, J. A., Castro-Puyana, M., & Ibáñez, E. (2012). Extraction and characterization of bioactive compounds with health benefits from marine resources: Macro and micro algae, cyanobacteria, and invertebrates. In M. M. Hayes (Ed.), *Marine bioactive compounds: Sources, characterization and applications* (pp. 55–98). USA: Springer Science + Business Media.
- Ibáñez, E., & Cifuentes, A. (2013). Benefits of using algae as natural sources of functional ingredients. *Journal of the Science of Food and Agriculture*, 93, 703–709.
- Jáime, L., Mendiola, J. A., Herrero, M., Soler-Rivas, C., Santoyo, S., Señorans, F. J., ... Ibáñez, E. (2005). Separation and characterization of antioxidants from *Spirulina platensis*.

# ARTICLE IN PRESS

- microalgae combining pressurized liquid extraction, TLC, and HPLC-DAD. *Journal of Separation Science*, 28, 2111–2119.
- Jáime, L., Rodríguez-Mézoso, I., Cíuentes, A., Santoyo, S., Suárez, S., Ibáñez, E., & Señorans, F.J. (2010). Pressurized liquids as an alternative process to antioxidant carotenoids' extraction from *Haematococcus pluvialis* microalgae. *LWT- Food Science and Technology*, 43, 105–112.
- Jin, E., Polle, J. E. W., Lee, H. K., Hyund, S. M., & Chang, M. (2003). Xanthophylls in microalgae: From biosynthesis to biotechnological mass production and application. *Microbial Biotechnology*, 13, 165–174.
- Kotake-Nara, E., Kushiro, M., Zhang, H., Sugawara, T., Miyashita, K., & Nagao, A. (2001). Carotenoids affect proliferation of human prostate cancer cells. *The Journal of Nutrition*, 131, 3303–3306.
- Krishnaswamy, R., Devaraj, S. N., & Padma, V. V. (2010). Lutein protects HT-29 cells against Dexoxynivalenol-induced oxidative stress and apoptosis: Prevention of NF- $\kappa$ B nuclear localization and down regulation of NF- $\kappa$ B and Cyclo-Oxygenase-2 expression. *Free Radical Biology & Medicine*, 49, 50–60.
- Li, Y., Horsman, M., Wang, B., Wu, N., & Lan, C. Q. (2008). Effects of nitrogen sources on cell growth and lipid accumulation of green alga *Neochloris oleoabundans*. *Applied Microbiology and Biotechnology*, 2008, 629–636.
- Moghadamtousi, S. Z., Karimian, H., Khanabdali, R., Razavi, M., Firrozinia, M., Zandi, K., & Kadir, H. A. (2014). Anticancer and antitumor potential of fucoidan and fucoxanthin, two main metabolites isolated from brown algae. *The Scientific World Journal*, 768323, 1–10 (article ID).
- Parniakov, O., Apicella, E., Koubaa, M., Barba, F. J., Grimi, N., Lebovka, N., ... Vorobiev, E. (2015a). Ultrasound-assisted green solvent extraction of high-added value compounds from microalgae *Nannochloropsis* spp. *Bioresource Technology*, 198, 262–267.
- Parniakov, O., Barba, F. J., Grimi, N., Marchal, L., Jubéau, S., Lebovka, N., & Vorobiev, E. (2015b). Pulsed electric field assisted extraction of nutritionally valuable compounds from microalgae *Nannochloropsis* spp. using the binary mixture of organic solvents and water. *Innovative Food Science & Emerging Technologies*, 27, 79–85.
- Parniakov, O., Barba, F. J., Grimi, N., Marchal, L., Jubéau, S., Lebovka, N., & Vorobiev, E. (2015c). Pulsed electric field and pH assisted selective extraction of intracellular components from microalgae *Nannochloropsis*. *Algal Research*, 8, 128–134.
- Pasquet, V., Moriset, P., Ihammoune, S., Chepied, A., Aumailley, L., Berard, J.-P., ... Picot, L. (2011). Antiproliferative activity of violaxanthin isolated from bioguided fractionation of *Dunaliella tertiolecta* extracts. *Marine Drugs*, 9, 819–931.
- Plaza, M., Santoyo, S., Jaime, L., Avalo, B., Cíuentes, A., Reglero, G., ... Ibáñez, E. (2012). Comprehensive characterization of the functional activities of pressurized liquid and ultrasound-assisted extracts from *Chlorella vulgaris*. *LWT- Food Science and Technology*, 46, 245–256.
- Pruvost, J., Vooren, G. V., Cogne, G., & Legrand, J. (2009). Investigation of biomass and lipids production with *Neochloris oleoabundans* in photobioreactor. *Bioresource Technology*, 100, 5988–5995.
- Rismani-Yazdi, H., Haznedaroglu, B. Z., Hsin, C., & Peccial, J. (2012). Transcriptomic analysis of the oleaginous microalgae *Neochloris oleoabundans* reveals metabolic insights into triacylglyceride accumulation. *Biotechnology for Biofuels*, 5, 74. <http://dx.doi.org/10.1186/1754-6834-5-74>.
- Roselló-Soto, E., Galanakis, C. M., Brnici, M., Orlien, V., Trujillo, F. J., Mawson, R., ... Barba, F. J. (2015). Clean recovery of antioxidant compounds from plant foods, by-products and algal assisted by ultrasounds processing. Modeling approaches to optimize processing conditions. *Trends in Food Science and Technology*, 42(2), 134–149.
- Solovchenko, A. E., Chivkunova, O. B., & Maslova, I. P. (2011). Pigment composition, optical properties, and resistance to photodamage of the microalgae *Haematococcus pluvialis* cultivated under high light. *Russian Journal of Plant Physiology*, 58, 9–17.
- Solovchenko, A. E., Khozin-Goldberg, I., Didi-Cohen, S., Cohen, Z., & Merzlyak, M. N. (2008). Effects of light and nitrogen starvation on the content and composition of carotenoids of the green microalgae *Parietochloris incisa*. *Russian Journal of Plant Physiology*, 20, 245–251.
- Talero, E., García-Mauriño, S., Ávila-Román, J., Rodríguez-Luna, A., Alcaide, A., & Motilva, V. (2015). Bioactive compounds isolated from microalgae in chronic inflammation and cancer. *Marine Drugs*, 13, 6152–6209.
- Urreta, I., Ikarai, Z., Janices, I., Ibáñez, E., Castro-Puyana, M., Castañón, S., & Suárez-Alvarez, S. (2014). Revalorization of *Neochloris oleoabundans* biomass as source of biodiesel by concurrent production of lipids and carotenoids. *Algal Research*, 5, 16–22.
- Valdés, A., García-Cañas, V., Rocamora-Reverte, L., Gómez-Martínez, A., Ferragut, J. A., & Cíuentes, A. (2013). Effect of rosemary polyphenols on human colon cancer cells: Transcriptomic profiling and functional enrichment analysis. *Genes Nutrition*, 8, 43–60.

ORIGINAL ARTICLE

## Skin photoprotective and antiageing effects of a combination of rosemary (*Rosmarinus officinalis*) and grapefruit (*Citrus paradisi*) polyphenols

Vincenzo Nobile<sup>1\*</sup>, Angela Michelotti<sup>1</sup>, Enza Cestone<sup>1</sup>, Nuria Caturla<sup>2</sup>, Julián Castillo<sup>3,4</sup>, Obdulio Benavente-García<sup>3,5</sup>, Almudena Pérez-Sánchez<sup>6</sup> and Vicente Micol<sup>6</sup>

<sup>1</sup>Complife Group, Pavia, Italy; <sup>2</sup>Monteloeder S.L., Alicante, Spain; <sup>3</sup>Nutrafur S.A. (Frutarom Group), Murcia, Spain;

<sup>4</sup>Universidad Católica San Antonio, Murcia, Spain; <sup>5</sup>Institute of Research Into Aging, University of Murcia, Murcia, Spain;

<sup>6</sup>Instituto de Biología Molecular y Celular, Universidad Miguel Hernández (UMH), Alicante, Spain

### Abstract

**Background:** Plant polyphenols have been found to be effective in preventing ultraviolet radiation (UVR)-induced skin alterations. A dietary approach based of these compounds could be a safe and effective method to provide a continuous adjunctive photoprotection measure. In a previous study, a combination of rosemary (*Rosmarinus officinalis*) and grapefruit (*Citrus paradisi*) extracts has exhibited potential photoprotective effects both in skin cell model and in a human pilot trial.

**Objective:** We investigated the efficacy of a combination of rosemary (*R. officinalis*) and grapefruit (*C. paradisi*) in decreasing the individual susceptibility to UVR exposure (redness and lipoperoxides) and in improving skin wrinkledness and elasticity.

**Design:** A randomised, parallel group study was carried out on 90 subjects. Furthermore, a pilot, randomised, crossover study was carried out on five subjects. Female subjects having skin phototype from I to III and showing mild to moderate chrono- or photoageing clinical signs were enrolled in both studies. Skin redness (a\* value of CIELab colour space) after UVB exposure to 1 minimal erythema dose (MED) was assessed in the pilot study, while MED, lipoperoxides (malondialdehyde) skin content, wrinkle depth (image analysis), and skin elasticity (suction and elongation method) were measured in the main study.

**Results:** Treated subjects showed a decrease of the UVB- and UVA-induced skin alterations (decreased skin redness and lipoperoxides) and an improvement of skin wrinkledness and elasticity. No differences were found between the 100 and 250 mg extracts doses, indicating a plateau effect starting from 100 mg extracts dose. Some of the positive effects were noted as short as 2 weeks of product consumption.

**Conclusions:** The long-term oral intake of Nutroxsun™ can be considered to be a complementary nutrition strategy to avoid the negative effects of sun exposure. The putative mechanism for these effects is most likely to take place through the inhibition of UVR-induced reactive oxygen species and the concomitant inflammatory markers (lipoperoxides and cytokines) together with their direct action on intracellular signalling pathways.

Keywords: plants extracts; *Rosmarinus officinalis*; *Citrus paradisi*; clinical study; photoprotection; antiageing

Received: 18 April 2016; Revised: 4 June 2016; Accepted: 4 June 2016; Published: 1 July 2016

**E**xposure to solar ultraviolet radiation (UVR) is one of the most important environmental factors affecting skin physiology. Solar UVR reaching the earth's surface can be classified according to wavelength as UVB (290–320 nm) and UVA (320–380 nm) radiation. UVA and UVB radiation ratio reaching earth's surface is 95%:5%, and it is dependent on geo-orbital factors (latitude, season, time) and on environmental factors (ozone layer, cloud thickness, pollutants, UV rays reflection from ground) (1, 2).

Historically, UVB radiation has been considered responsible for early and late consequences of solar UVR exposure. UVB radiation is, in fact, the main cause of the cardinal sign of acute solar UVR exposure: the erythema sign characterising the inflammatory reaction typical of sunburn (3–7). Erythema starts approximately 3–5 h after UVB radiation exposure, reaches its maximum at 12–24 h, and fades over 72 h (8). Skin inflammation due to acute exposure to UVR has been shown to be characterised by the release of neuropeptides, histamine, prostaglandins,

serotonin, and oxygen radicals (4–6, 9, 10), and the upregulation of pro-inflammatory cytokines such as interleukin 1 (IL-1), interleukin 6 (IL-6), and tumour necrosis factor alpha (TNF- $\alpha$ ) (11–16). Histologically, sunburn is characterised by dyskeratotic and vacuolated keratinocytes (sunburn cells), mild epidermal spongiosis, depletion of Langerhans cells, dermal oedema, endothelial cell enlargement, and later by a neutrophilic dermal infiltrate (17). Accumulated evidence on the effects of prolonged or repetitive UVB exposure during the past two decades has been reported to lead to generalised immunosuppression leading to carcinogenesis (18, 19) through the production/secretion of anti-inflammatory cytokines such as IL-4 and IL-10 (11, 20, 21).

In recent years, an increasing use of artificial sources of UVA radiation both for medical treatment (phototherapy and photochemotherapy) and for aesthetic purposes (solarium) has revealed the harmful role of UVA radiation in the pathophysiology of skin alterations due to sun exposure. UVA radiation penetrates deeper within the skin and is mostly responsible for the generation of reactive oxygen species (ROS) including singlet oxygen ( $^1\text{O}_2$ ), and other non-radical and radical ROS, such as hydrogen peroxide ( $\text{H}_2\text{O}_2$ ) and the superoxide radical ( $\text{O}_2^-$ ) (22–26) and, to a lesser extent than UVB radiation, can also induce DNA damage (27, 28). UVA-induced oxidative stress increases the potential for reactions like the oxidation of lipids and proteins (29). Both UVA and UVB contribute significantly to photoageing.

The protection of the skin from solar exposure is consigned to topical sunscreens. However, topical sunscreens have drawbacks including seasonal application (generally sunscreens are applied only during holidays) and inadequate application methods (e.g. quantity and spreading). Furthermore, the sun protection factor (SPF) provided by sunscreens seems to be overestimated, under testing conditions, when compared to the real-life condition of use (30, 31). Therefore, a dietary approach to photoprotection could be an effective method to provide a continuous adjunctive protection measure, with population-level impact (32).

Several plant extracts have been found to be effective in preventing UV-induced skin alterations. The most important group of compounds includes phenolic acid, flavonoids, and high-molecular-weight polyphenols (33–39). Several studies have shown the flavonoids to act as scavengers of superoxide anions, singlet oxygen, hydroxyl radicals, and lipid peroxy radicals (37, 40–43). There are also reports of flavonoids inhibiting the activities of many enzymes, including lipoxygenase, cyclooxygenase, monooxygenase, xanthine oxidase, mitochondrial succinate dehydrogenase, NADH oxidase, phospholipase A2, protein kinases, and nuclear transcription factor (NF- $\kappa$ B) (44, 45).

A previous study demonstrated the efficacy of a commercially available mixture of citrus and rosemary extracts (Nutroxsun™, Nutrafur S.A. & Monteloeder S.L., Spain) in skin cell models and on humans. The following was reported: 1) a protective effect on cells viability after UVB radiation, a decrease of UVB-induced intracellular ROS, and prevention of DNA damage in an immortalised human keratinocyte cell line (HaCaT), 2) a decreased chromosomal aberrations in X-irradiated human lymphocytes, and 3) an increase of the minimal erythema dose (MED) 8 and 12 weeks after the oral daily consumption (250 mg) of the extracts (46). Based on these preliminary data, in the current study we investigated the efficacy of the tested product (100 and 250 mg doses) in decreasing the individual susceptibility to UVR exposure (redness and lipoperoxides [LPO]), in decreasing wrinkle depth, and in improving skin elasticity. To our knowledge, no other studies have investigated the photoprotective and antiaging efficacy of the tested product.

## Methods

### Study design

This was a monocentric, randomised, crossover (short-term study), parallel group (long-term study) study conducted in Italy. The study protocol and the informed consent form were approved by the 'Independent Ethical Committee for Non-Pharmacological Clinical trials' during its meeting on 15 December 2014. All subjects provided written informed consent before initiation of any study-related procedures. No changes to treatment regimen or to methods were necessary after study starting.

### Subjects

Eligible subjects were all adult, female subject, having skin phototype from I to III (Fitzpatrick classification) (47) and showing mild to moderate chrono- or photoageing clinical signs. The subjects were of general good health, had no alimentary/eating disorders (i.e. bulimia, psychogenic eating disorders, etc.), and have known history of metabolic syndrome. Exclusion criteria were pregnancy or intention to become pregnant, lactation, food intolerances/allergy, pharmacological treatments known to interfere with the test product or having an effect on metabolism, participation in another similar study, unwillingness or inability to comply with the requirements of the study protocol. The study further excluded subjects using food supplements containing active ingredients that have an influence on skin response to UV rays or on skin ageing. During all the study period, subjects were asked to avoid any UV exposure (artificial UV light or sunlight). The study took place at Farcoderm Srl facilities in San Martino Siccomario (PV), Italy. Farcoderm Srl is an independent testing laboratory for *in vitro* and *in vivo*

safety and efficacy assessment of cosmetics, food supplements and medical devices.

#### Intervention

The test product was a commercially available mixture of rosemary and citrus extracts (Nutroxsun™, supplied by Monteloeder S.L., Miguel Servet 16, Elche, Alicante, Spain), obtained from dried rosemary (*Rosmarinus officinalis*) leaves and grapefruits (*Citrus paradisi*), respectively. Nutroxsun™ total phenolic standard content is higher than 35 gallic acid equivalents/100 g dry weight (dw) as determined by Folin assay (48), being the total rosemary phenolic content higher than 7% dw and total grapefruit flavones content higher than 20% dw.

Both in the long-term and in the short-term tests, subjects were randomly assigned to receive 100 mg

Nutroxsun™, 250 mg Nutroxsun™, or the placebo (100% maltodextrin) product. In the short-term study, subjects received the first dose (100 or 250 mg) of the test product or the placebo product 15–30 min before UVB exposure to 1 MED. Two supplementary doses were given 24 and 48 h after UV exposure (Fig. 1). In the long-term study, subjects received 100 mg Nutroxsun™, 250 mg Nutroxsun™, or the placebo product once a day at breakfast.

#### Primary and secondary outcomes

The primary endpoints with respect to the photoprotective efficacy were the measurement of the UVB-induced skin redness, the assessment of the erythema response of the skin after UVB exposure (290–320 nm), and the measurement of the basal and UVA-stimulated (320–400 nm)

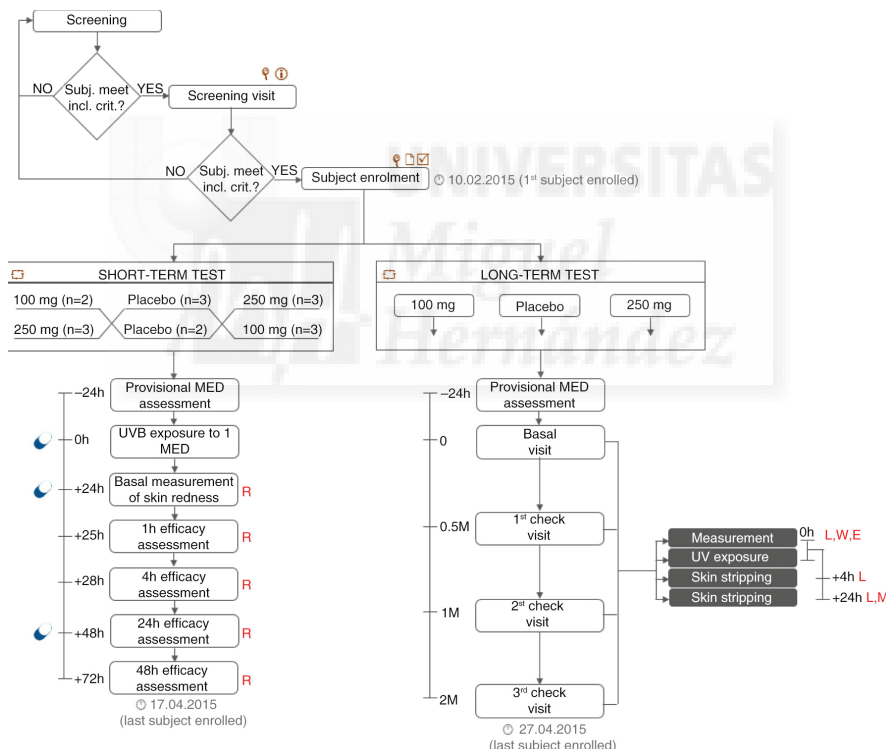


**Fig. 1.** Study flow and schedule of assessments chart. Subjects were first screened in the Farcoform volunteers database (keywords: Sex = 'female', Age = '18', Skin phototype = 'I < phototype < III', Skin type: 'ageing or photoageing', Testing preferences: 'food supplements'). Eligible participants were then screened by a board certified dermatologist. During the screening visit, a physical examination was carried out in order to assess the uniformity of the test area (back) and the clinical sign of skin ageing on the face. Subjects meeting the inclusion criteria were then enrolled and randomised to participate in the short- or in the long-term study. Legend: ♀, physical examination; ☐, informed consent signature; ☑, eligibility check; □, randomisation; PM\*, provisional MED measurement (carried out only before study start); M, MED; L, lipoperoxides; W, wrinkle depth; E, skin elasticity; R, skin redness.

skin LPO content. The primary endpoint with respect to the antiageing efficacy was the measurement of the wrinkle depth. Skin elasticity was measured as a secondary efficacy endpoint. The study flow and the schedule of assessments chart are reported in Fig. 1.

#### *Measurement of skin redness*

A spectrophotometer/colorimeter CM-700D (Konica Minolta, Milano, Italy) was used to measure skin redness in the CIELab colour space. The  $a^*$  (red-green) parameter was measured in the UVB-exposed skin site to 1 MED. Measurements were taken excluding the specular reflection. The specular component excluded mode, provides results similar to those observed visually.

#### *Assessment of minimal erythema dose*

One day before the study began, a provisional MED was determined in order to centre the UV doses ranges for the MED assessment through the study. A series of UVB doses (geometric progression of  $1.25 \times$ ), were applied on six small subsites (Fig. 2) of the skin of the back. MED was then assessed, under blind conditions,  $20 \pm 4$  h after UV exposure. MED assessment was carried out in a room with matt neutral wall colour and sufficient illumination conditions (at least 450 lux). MED assessment was considered invalid when: 1) the series of UVB exposures on a subject failed to elicit an erythema response on any sub-site, 2) all subsites in the exposure series showed an erythema response, and 3) erythema responses within an exposure series were randomly absent. The source of UVB radiation was a Multiport 601–300 W Solar simulator (Solar® Light Co. Inc., Philadelphia, USA) compliant

with ISO 24444:2010 standard requirements (49). UVB dose was adjusted with a model PMA 2100 radiometer (Solar® Light Co. Inc., Philadelphia, USA) equipped with a PMA 2103 LLG SUV detector (Solar® Light Co. Inc., Philadelphia, USA). Both the solar simulator and the radiometers were calibrated externally.

#### *Assessment of LPO*

Basal and UVA-induced ( $10 \text{ J/cm}^2$ ) skin LPO were measured in the 10th skin layer obtained using the skin stripping technique. Skin stripping was performed in the back (Fig. 2) using Corneofix® foils (Courage + Khazaka Electronic, Köln, Germany) under standard pressure conditions ( $225 \text{ g/cm}^2$ ). The first stripping was discarded while strip no. 11 was collected and stored at  $-80^\circ\text{C}$  until further analysis. Malondialdehyde (MDA) was measured according to the assay described by Erdelmeier et al. in 1998 (50) with minor modification, as follows: 1) skin strippings were layered in 12 multiwell plates containing  $500 \mu\text{l}$  of a  $0.5 \text{ mM CuSO}_4$  aqueous solution, 2) multiwell plates were incubated at  $37^\circ\text{C}$ , using a microplate incubator/shaker under continuous agitation for 1 h, 3) after incubation  $1.3 \text{ ml R1 solution}$  ( $2.13 \text{ mg N-methyl-2-phenylindole/ml acetonitrile}$ ) and  $0.3 \text{ ml } 37\% \text{ HCl}$  was added and samples were further incubated at  $45^\circ\text{C}$  for 60 min under continuous agitation, 4) the reaction was stopped in ice for 10 min followed by 10 min at room temperature, 5)  $1 \text{ ml}$  of solution was centrifuged at  $13,000 \text{ rpm per 10 min}$ , and 6) absorbance was read at  $586 \text{ nm}$  using a multiwell plates reader (programmable MPT reader model DV 990BV6; Gio DeVita & C, Rome, Italy).

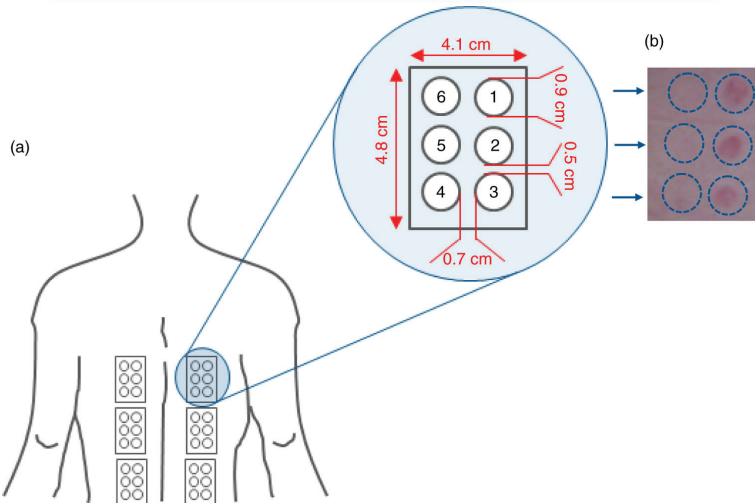


**Fig. 2.** (a) UV exposure site and subsites. (b) Minimal erythema dose (MED).

The source of UVA radiation was a Multiport 601–300 W Solar simulator (Solar<sup>®</sup> Light Co. Inc., Philadelphia, USA) compliant with the Japan Cosmetic Industry Association (JCIA) measurement standard for UVA protection (51) and ISO 24442:2011 standard requirements (52) (Table 1). UVA dose was adjusted with a model PMA 2100 radiometer (Solar<sup>®</sup> Light Co. Inc., Philadelphia, USA) equipped with a PMA 2113 LLG UVA detector (Solar<sup>®</sup> Light Co. Inc., Philadelphia, USA). Both the solar simulator and the radiometers were calibrated and compliant to ISO 24444:2010 standard.

#### Wrinkle depth

Wrinkles depth was measured using a three-dimensional (3-D) microtopography imaging system (PRIMOS 3D lite, GFMesstechnik GmbH, Teltow, Germany). The imaging system projects structured light on a specific surface of the skin with a digital micro-mirror device (DMD, Texas Instruments, Irving, TX, USA) and records the image with a CCD camera. Skin surface microtopography is then reconstructed using temporal phase shift algorithms to generate 3-D images. The imaging system has an overlap feature which enables precise matching of photos taken at different visits. In order to improve image overlap, subjects' position was regulated using a stereotactic device (Canfield Scientific, Inc., Fairfield, NJ, USA). Wrinkle depth was measured in the periocular area ('crow's feet wrinkles') using the appropriate software routine.

#### Skin elasticity

A skin viscoelasticity analyser (Cutometer<sup>®</sup> MPA 580, Courage + Khazaka Electronic, Köln, Germany) was used to measure skin elasticity. The skin surface of the face (cheek) was drawn into the aperture (3 mm) of the probe by a negative pressure (450 mbar) for 3 sec and thereafter released for 3 sec. The penetration depth of the skin inside the probe, during the suction and the release phase, was measured by a non-contact optical measuring system. Two skin elasticity indices were measured: 1) R2 ( $U_a/U_f$ ), gross elasticity or overall elasticity, Fig. 3a represents the ability of redeformation of the skin to its basal state, and 2) R5 ( $U_r/U_e$ , net elasticity, Fig. 3b represents the elastic

recovery of the skin deformation to its basal state due to its elastic component.

#### Sample size

Sample size was calculated, for the long-term study, with a two-sided 5% significance level and a power of 80% taking into account a 20% variation of the primary endpoints due to both inter-individual human variability and error in the measurement techniques. Sample size was calculated using PASS 11 statistical software (version 11.0.8 for Windows) running on Windows Server 2008 R2 Standard SP1 64 bit edition (Microsoft, USA). A sample size of 20 subjects per group was necessary given an anticipated dropout rate of 20%.

#### Randomisation

A restricted randomisation list was created using PASS 11 (version 11.0.8; PASS, LLC, Kaysville, UT, USA) statistical software running on Windows Server 2008 R2 Standard SP1 64 bit edition (Microsoft, USA) by a biostatistician and stored in a safe place. Randomisation sequence was stratified using 10% maximum allowable % deviation with a 1:1:1 allocation ratio. The allocation sequence was concealed from the study director in sequentially numbered, opaque, and sealed envelopes, reporting the unblinded treatment allocation (based on subject entry number in the study). The A4 sheet reporting the unblinded treatment was folded to render the envelope impermeable to intense light. After acceptance of the subject in the study the appropriate numbered envelope was opened. An independent technician dispensed either active or placebo products according to the card inside the envelope. The study adhered to established procedures to maintain separation between the investigator and its collaborators and the staff that delivered the intervention. Investigator and its collaborators who obtained outcome measurements were not informed on the product group assignment. Staff who delivered the intervention did not take outcome measurements. Subjects, investigator and collaborators were kept masked to products assignment. The active and the placebo products were in capsule form and identical in appearance. They were prepacked in

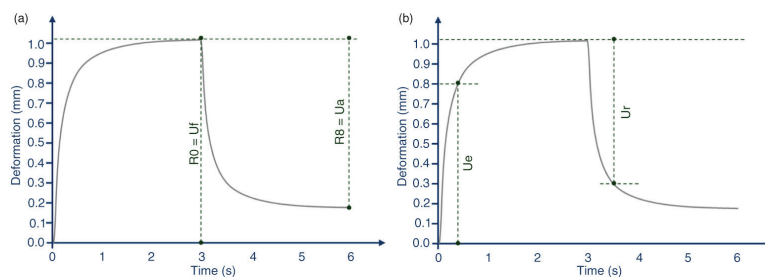


**Fig. 3.** Skin elasticity curve. (a) R2 parameter calculation. (b) R5 parameter calculation.

blisters and consecutively numbered for each subject according to the randomisation schedule. Each subject was assigned an order number and received the capsules in the corresponding prepacked blister.

#### Statistical methods

Statistical analysis was performed using NCSS 8 (version 8.0.4 for Windows; NCSS, Kaysville, UT, USA) running on Windows Server 2008 R2 Standard SP1 64 bit edition (Microsoft, USA). Data normality was checked using Shapiro-Wilk W normality test and data shape. Intragroup (vs. baseline) statistical analysis was carried out using repeated measures analysis of variance (RM-ANOVA) followed by Tukey-Kramer post-test. Inter-group (between treatments) statistical analysis was carried out using multivariate analysis of variance (M-ANOVA) followed by two-way t test of Student. A  $p < 0.05$  was considered statistically significant. Statistical analysis output was reported as follows: \*  $p < 0.05$ , \*\*  $p < 0.01$ , and \*\*\*  $p < 0.001$ .

## Results

### Subjects

The study was conducted between February and April 2015. A total of 90 female subjects were successfully randomised (Fig. 4) in the long-term study while a total of five female subjects were enrolled in the short-term study. The population was Caucasian. Demographic and baseline characteristics (Table 2) were similar across treatment arms, indicating an unbiased randomisation and the absence of covariates. Subjects participating in the short-term pilot study attended clinic visits at the time of

randomisation (baseline) and 24, 48 and 72 h after UVB exposure and the first product intake; while remained at our clinical facilities where the measure was done 1 and 4 h the day after UVB exposure. In the long-term study, subjects attended clinic visits at the time of randomisation (baseline) and after 14 days, 1, and 2 months of product use. Data analysis was intention-to-treat and involved all subjects who were randomly assigned. Subjects' compliance to treatment was assessed by means of product accountability, as follows: at each visit, the expected amount of consumed capsule was compared with the amount dispensed minus the amount the subject returned. No major deviation was observed in the treatment regimen. All subjects were included in the safety analysis data set. All the tested products were well tolerated. No adverse reactions occurred during the study period.

### Effect of the extracts on UVB-induced skin redness

Twenty-four hours after UVB exposure to 1 MED, skin redness was increased by 40.5% ( $p = 0.0099$ ) in the placebo group, by 37.0% ( $p = 0.0011$ ) in the 100 mg dose group, and 39.6% ( $p = 0.0006$ ) in the 250 mg dose group (Fig. 5). The effect of UVB on skin redness was similar for all treatments ( $p = 0.9387$ ). Skin redness time course (variation vs. 24 h) exhibited a decrease compared to placebo as the extract dose was increased from 100 to 250 mg. A statistical significant variation was observed at 48 h in the 100 mg dose group ( $p = 0.0252$ ), and at 25 h ( $p = 0.0437$ ) in the 250 mg dose group, compared to 24 h data point. At 72 h for both the 100 and 250 mg dose groups skin redness returned to its basal (pre-UVB-exposure) value. In the placebo-treated group, skin redness showed a significant decrease at 72 h ( $p = 0.0112$ ), but even it remained slightly higher when compared to its basal value ( $p = 0.0289$ ).

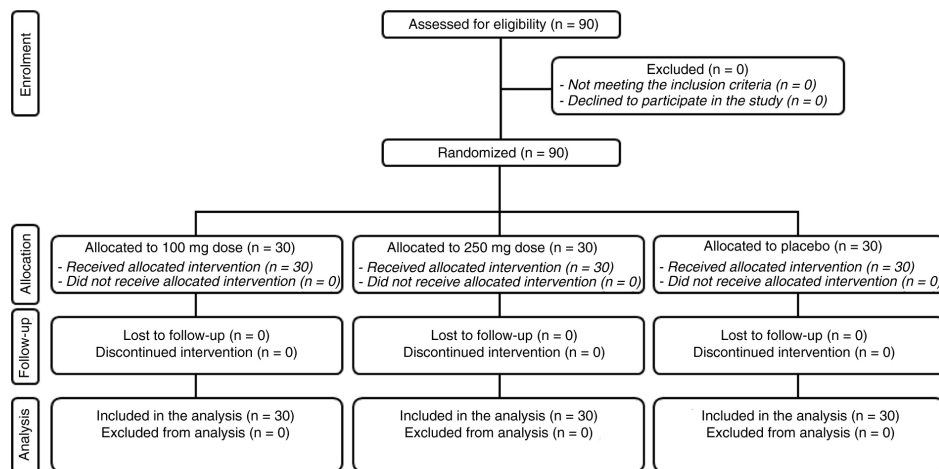


Fig. 4. Flow chart of inclusion of subjects.

**Table 1.** UVB and UVA solar simulator specifications

Spectral range (nm)	% RCEE		Spectral range (nm)	Limit (%)
	Lower limit	Upper limit		
<290	—	<0.1	UVA I (340–400 nm) irradiance	≥60
290–300	2.0	8.0	UVA II (320–340 nm) irradiance	≥20
290–310	49.0	65.0	<b>Total energy</b>	<150 mW/cm <sup>2</sup>
290–320	85.0	90.0	<b>UVA/Total</b>	92–100
290–330	91.5	95.5	<b>UVB/UVA</b>	<0.1
290–340	94.0	97.0	<b>UVA2/UVA</b>	8.0–20.0
290–350	95.5	98.5	<b>Spectrum continuity</b>	Continuous

Despite the evident differences in time course behaviour of skin redness between 100 and 250 mg dose groups, this variation was not statistically significant ( $p = 0.3720$ ) when 100 and 250 mg data were compared (Fig. 6). The variation of skin redness observed for both 100 and 250 mg extracts dose treatment regimen was statistically significant when compared to placebo treatment regimen (100 mg group,  $p = 0.020$ ; 250 mg group,  $p = 0.0182$ ).

#### Effects on MED

A significant increase of the MED was observed for both 100 and 250 mg dose groups (Fig. 7). MED increased by 4.0 (+15.2%), 5.2 (+20.5%), and 7.7 (+29.8%) mJ/cm<sup>2</sup>, after 0.5, 1, and 2 months treatment, respectively ( $p = 0.0000$ ) in the 100 mg dose group. A similar efficacy profile was seen for the 250 mg dose group, where MED was increased by 3.1 (+11.7%), 5.5 (+20.2%), and

7.5 (+26.9%) mJ/cm<sup>2</sup>, after 0.5, 1, and 2 months treatment, respectively ( $p = 0.0007$  at 0.5 months and  $p = 0.0000$  at 1 and 2 months). Variation of MED was not statistically significant ( $p = 0.1857$ ) when 100 mg and 250 mg data were compared. MED variation observed for both 100 mg and 250 mg extract dose groups was statistically significant when compared to placebo group (100 mg group,  $p = 0.0001$ ; 250 mg group,  $p = 0.0000$ ). MED was unchanged ( $p = 0.4049$ ) in the placebo-treated subjects (Fig. 8).

#### Horny layer lipoperoxides content

##### Basal lipid peroxidation

A significant decrease of the basal, not UVA stimulated, LPO content was observed for both 100 and 250 mg dose groups (Table 3). Skin horny layer MDA content was decreased by 14.4, 18.5 and 18.7% after 0.5, 1, and 2 months treatment, respectively ( $p = 0.0000$ ) in the 100 mg

**Table 2.** Demographic and baseline characteristics

	STT			LTT			Units
	100 mg	250 mg	Placebo	100 mg	250 mg	Placebo	
<b>Sex</b>							
Male	0	0	0	0	0	0	No.
Female	5	5	5	30	30	30	No.
<b>Skin phototype</b>							
I	—	—	—	6.7%	6.7%	6.7%	%
II	40%	40%	40%	33.3%	30.0%	36.7%	%
III	60%	60%	60%	60.0%	56.7%	50.0%	%
<b>Age</b>	30.8	30.8	30.8	52.9	51.0	50.9	years
Skin erythema (basal)	7.1	7.0	7.1	—	—	—	a.u.
Skin erythema (after UVB)	9.7	9.5	9.9	—	—	—	a.u.
Minimal erythema dose (MED)	—	—	—	29.0	30.3	29.3	mJ/cm <sup>2</sup>
LPO (basal)	—	—	—	2.61	2.72	2.58	µM MDA
LPO 4 h at D0	—	—	—	3.60	3.64	3.54	µM MDA
LPO 24 h at D0	—	—	—	3.23	3.30	3.21	µM MDA
Wrinkle depth	—	—	—	296.6	257.7	282.6	µm
Skin elasticity (R2 = Ur/Uf)	—	—	—	0.7233	0.7271	0.7214	Ratio
Skin elasticity (R5 = Ur/Ue)	—	—	—	0.2856	0.2940	0.2907	Ratio

Data are means ± SE.

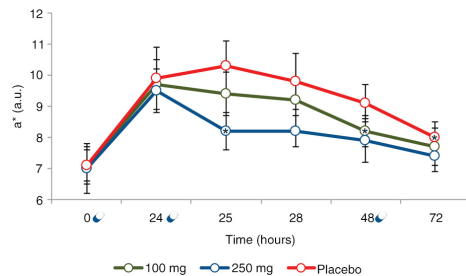


**Fig. 5.** Skin redness time course after 1 MED UVB exposure. Data are means (arbitrary units)  $\pm$  SE. \*Statistically significant ( $p < 0.05$ ) when compared to 24 h;  $\clubsuit$  Product intake.

dose group. A bigger decrease ( $p = 0.0038$  compared to 100 mg) in the horny layer MDA content was observed for the 250 mg dose group, where MDA content was decreased by 25.5, 37.7, and 32.6% respectively ( $p = 0.0000$ ). MDA variation observed for both 100 and 250 mg dose groups was statistically significant when compared to placebo treatment regimen ( $p = 0.0000$ ). MDA was unchanged ( $p = 0.1054$ ) in the placebo-treated subjects.

#### UVA-stimulated lipid peroxidation

A significant decrease of the UVA-stimulated LPO content was also observed, after 4 and 24 h from UVA exposure ( $10 \text{ J/cm}^2$ ), for both 100 and 250 mg dose groups (Table 3) compared to baseline. Skin horny layer MDA content 4 h after UVA exposure was decreased by 9.7, 16.2 and 20.1% after 0.5, 1, and 2 months treatment, respectively ( $p = 0.0000$ ) in the 100 mg dose group while 24 h after UVA exposure the MDA content was decreased by 8.7, 13.4, and 15.1% after 0.5, 1, and 2 months treatment, respectively ( $p = 0.0000$ ). A similar efficacy profile was seen for the 250 mg dose group, where MDA, 4 h after UVA exposure, was decreased by 10.2, 16.4, and 21.7% after 0.5, 1, and 2 months treatment, respectively ( $p = 0.0000$ ); while 24 h after UVA exposure the MDA content was decreased by 9.1, 13.3, and 15.8% after 0.5, 1, and 2 months treatment, respectively ( $p = 0.0000$ ). MDA variation observed for both 100 and 250 mg dose groups was also statistically significant when compared to placebo treatment (Table 3). MDA was unchanged ( $p = 0.7952$  at 4 h, and  $p = 0.7384$  at 24 h) in the placebo-treated subjects.

#### Wrinkle depth

A significant decrease of the wrinkle depth in the ‘crow’s feet’ was observed for both 100 and 250 mg dose groups (Fig. 9). Wrinkle depth decrease was by 27.4 (−8.8%), 42.4 (−13.4%), and 43.7 (−14.8%)  $\mu\text{m}$ , in the 100 mg dose group, after 0.5, 1, and 2 months treatment, respectively ( $p = 0.0000$ ). A similar efficacy profile was seen for the

250 mg extracts dose treatment regimen, where wrinkle depth was decreased by 22.7 (−9.1%), 31.5 (−12.6%), and 35.9 (−13.9%)  $\mu\text{m}$ , after 0.5, 1, and 2 months treatment, respectively ( $p = 0.0001$  at 0.5 months and  $p = 0.0000$  at 1 and 2 months). Variation of wrinkle depth was not statistically significant ( $p = 0.7731$ ) when 100 and 250 mg data were compared. Wrinkle depth variation observed for both 100 and 250 mg dose groups was statistically significant when compared to placebo treatment ( $p = 0.0000$ ). Wrinkle depth was unchanged ( $p = 0.9740$ ) in the placebo-treated subjects throughout the study.

#### Skin elasticity

##### Gross elasticity (R2 parameter)

A significant increase of the skin gross elasticity (Fig. 3a) was observed for both 100 and 250 mg extracts dose treatment regimen (Table 4). Skin elasticity increased by 1.8, 3.2, and 4.6%, in the 100 mg dose group after 0.5, 1, and 2 months treatment, respectively ( $p = 0.0026$  at 0.5 months and  $p = 0.0000$  at 1 and 2 months). A similar efficacy profile was seen for the 250 mg dose group, where skin elasticity was increased by 1.5, 2.9, and 3.7%, after 0.5, 1, and 2 months treatment, respectively ( $p = 0.0010$  at 0.5 months;  $p = 0.000$  at 1 month and  $p = 0.002$  at 2 months). Variation of skin elasticity was not statistically significant ( $p = 0.9253$ ) when 100 and 250 mg were compared. Skin elasticity variation observed for both 100 and 250 mg dose groups was statistically significant when compared to placebo group (100 mg group,  $p = 0.0455$ ; 250 mg group,  $p = 0.0281$ ). Skin elasticity was unchanged ( $p = 0.1355$ ) in the placebo-treated subjects throughout the study.

##### Net elasticity (R5 parameter)

A significant increase of the skin net elasticity (Fig. 3b) was also observed for both 100 and 250 mg dose groups (Table 4). Skin elasticity increase was by 3.3, 5.8 and 9.0%, in the 100 mg dose group after 0.5, 1, and 2 months treatment, respectively ( $p = 0.0000$ ). A similar efficacy profile was seen for the 250 mg extracts dose treatment regimen, where skin elasticity was increased by 2.9, 5.5, and 7.4%, after 0.5, 1, and 2 months treatments, respectively ( $p = 0.0000$ ). Variation of skin elasticity was not statistically significant ( $p = 0.2061$ ) when compared 100 and 250 mg data were compared each other. Skin elasticity variation observed for both 100 and 250 mg extracts dose treatment regimen was statistically significant when compared to placebo group ( $p = 0.0000$ ). Skin elasticity was unchanged ( $p = 0.2984$ ) in the placebo-treated subjects throughout the study.

#### Discussion

In recent years, different extracts derived from plants have been investigated for therapeutic application due to their pharmacological activity on inflammatory processes and other physiopathological conditions. Dietary interventions



**Fig. 6.** Skin redness variation after 1 MED UVB exposure. Digital pictures of (a) placebo, (b) 100 mg extracts dose, and (c) 250 mg extracts dose were taken using a Nikon D300 camera (Nikon corporate, Japan) equipped with a Nikon macro lens (AF-S Micro Nikkor 60 mm f/2.8 G ED) and parallel-polarised filters.

can interfere with several cell-signalling pathways and molecular targets may be involved in their efficacy in preventing or treating altered physiopathological conditions (53). Many plants, herbs and spices typically used for food flavouring and nutrition are excellent sources of phenolic compounds, which have been reported to show antioxidant activity. The anti-inflammatory activity of natural extracts has been associated to their antioxidant

activity, and to a specific role on nitric oxide (NO) production suppression (54–56).

In a previous study, it was reported (46) the synergistic effects of a mixture of rosemary and citrus extracts in decreasing the generation of UVB-induced intracellular ROS and in preventing UVR-induced DNA damage in the comet assay. The mixture also showed genoprotective and antimutagenic properties in a model for massive

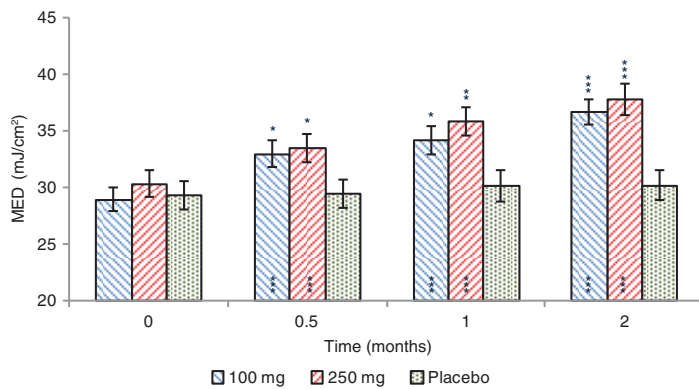


**Fig. 7.** Minimal erythema dose (MED) before and after 0.5, 1, and 2 months treatment. Intragroup (vs. 0) statistical analysis is reported inside the bars of the histogram. Intergroup (vs. placebo) statistical analysis is reported upon the bars of the histogram. Statistical analysis is reported as follows: \* $p < 0.05$ , \*\* $p < 0.01$ , and \*\*\* $p < 0.001$ . Data are means ( $\text{mJ}/\text{cm}^2$ )  $\pm$  SE.

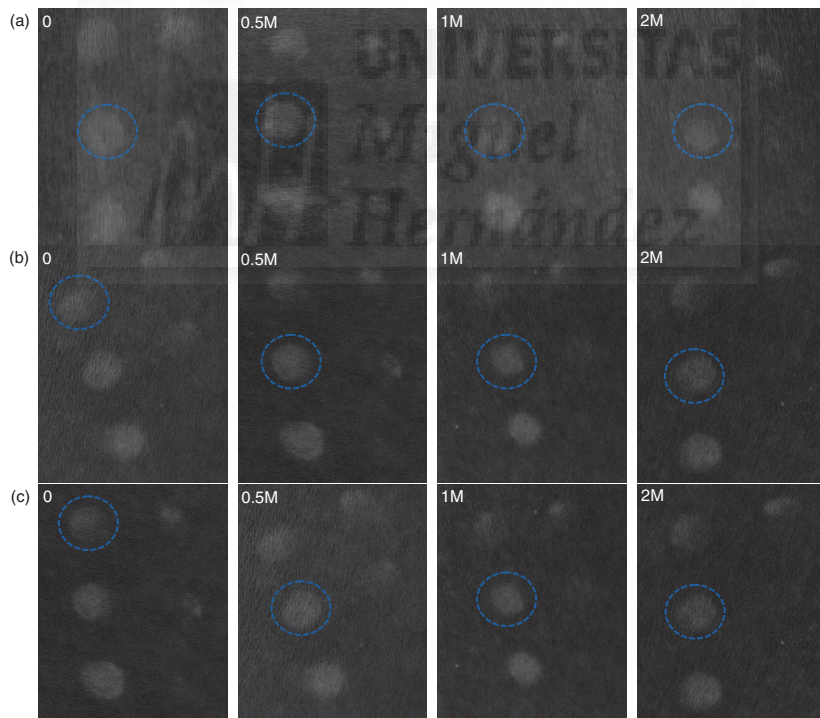


**Fig. 8.** Digital pictures of (a) placebo, (b) 100 mg extracts dose, and (c) 250 mg extracts dose were taken using a Nikon D300 camera (Nikon corporate, Japan) equipped with a Nikon macro lens (AF-S Micro Nikkor 60 mm f/2.8 G ED) and parallel-polarised filters. The a\* (CIELab chromatic space) channel image is reported in order to enhance image contrast. The blue circle indicates the MED.

**Table 3.** Basal and UVA-stimulated horny layer MDA content

Basal level	0		0.5 M		1 M		2 M	
	100 mg	2.61 ± 0.13	2.17 ± 0.09*** (- 14.4%)	2.01 ± 0.07*** (- 18.5%) <th>1.98 ± 0.05*** (- 18.7%)</th> <th>2.50 ± 0.09 (- 1.2%)</th> <td>2.47 ± 0.09 (- 2.3%)</td> <th></th>	1.98 ± 0.05*** (- 18.7%)	2.50 ± 0.09 (- 1.2%)	2.47 ± 0.09 (- 2.3%)	
250 mg	2.72 ± 0.16	1.94 ± 0.12*** (- 25.5%)	1.60 ± 0.08*** (- 37.7%)	1.69 ± 0.07*** (- 32.6%)				
Placebo	2.58 ± 0.10	2.60 ± 0.11 (+ 1.3%)	2.50 ± 0.09 (- 1.2%)	2.47 ± 0.09 (- 2.3%)				
UVA stimulated	0		0.5 M		1 M		2 M	
	4 h	24 h	4 h	24 h	4 h	24 h	4 h	24 h
100 mg	40.8%	25.6%	31.1%**	16.9%***	24.6%***	12.2%***	20.7%***	10.5%***
250 mg	37.5%	24.0%	27.3%***	14.9%***	21.1%***	10.7%***	15.8%***	8.2%***
Placebo	39.7%	26.3%	44.7%***	30.8%***	45.1%***	30.7%***	49.0%***	30.1%***

Data are means ( $\mu\text{M MDA}$ )  $\pm$  SE. Values in brackets: % variation vs. 0. \* $p < 0.05$ , \*\* $p < 0.01$ , \*\*\* $p < 0.001$ . UVA stimulated LPOs are % variation vs. baseline.

generation of radical species using ionising radiation. A pilot trial in humans also showed the preliminary effect of the combination in increasing MED. Therefore, our present study aimed to investigate the anti-inflammatory, photoprotective, and antiaging effects of this combination. Two doses of the combination (100 and 250 mg) were investigated in order to assess if a dose-effect relationship between the measured parameters and the product intake exists.

The *in vivo* anti-inflammatory effect of the extracts on UVB-induced skin inflammation was investigated in a pilot ( $n = 5$  subjects) crossover study. Both 100 and 250 mg combination doses proved to be effective in decreasing the skin redness induced by 1 MED UVB exposure. As observed in the skin redness time course curves, the group having 250 mg dose of the combination recovered basal level in a much faster manner than that of the 100 mg dose group, clearly revealing a dose-dependent anti-inflammatory effect. The results also indicate the potential

effect of the tested products in decreasing the UVB-induced skin redness with only 2 days of product consumption; however the small sample size and the associated high standard deviation was a limitation of the study and further studies would be required. Anyway, the results obtained in the pilot study provided the basis for sample size calculation.

In most studies on photoprotection based on nutritional ingredients, there is a time frame of approximately 6–10 weeks until protection against erythema becomes significant (57). A time frame much longer than we have seen in this study where the individual susceptibility to UVB radiation exposure (erythema) was decreased (+ 15.2 and + 11.7% for 100 and 250 mg dose group, respectively) after 2 weeks of product use (Fig. 7). Two months after product use, the lowest dose of UVB radiation to produce the erythematous reaction was increased by about  $7 \text{ mJ/cm}^2$ , corresponding to an increase around 33% of the time of sun exposure without experiencing sunburn. A result

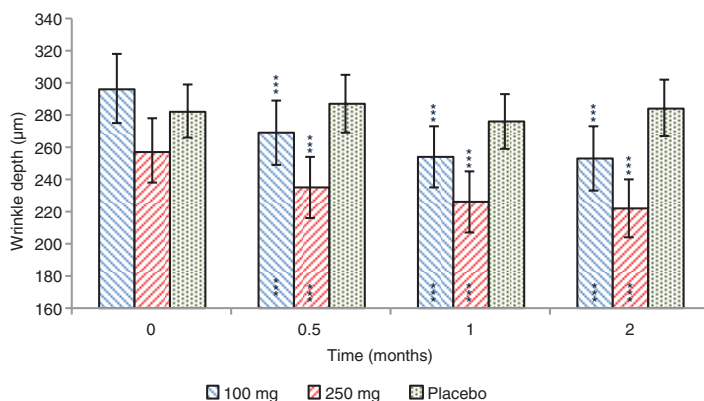


**Fig. 9.** Wrinkle depth before and after 0.5, 1, and 2 months treatment. Intragroup (vs. 0) statistical analysis is reported inside the bars of the histogram. Intergroup (vs. placebo) statistical analysis is reported upon the bars of the histogram. Statistical analysis is reported as follows: \* $p < 0.05$ , \*\* $p < 0.01$ , and \*\*\* $p < 0.001$ . Data are means ( $\mu\text{m}$ )  $\pm$  SE.

**Table 4.** Skin elasticity

R2 (skin gross elasticity)	0	0.5 M	1 M	2 M
100 mg	0.7233 ± 0.0135	0.7360 ± 0.0134*** (+ 1.8%)	0.7462 ± 0.0135*** (+ 3.2%)	0.7557 ± 0.0136*** (+ 4.6%)
250 mg	0.7271 ± 0.0127	0.7375 ± 0.0129*** (+ 1.5%)	0.7475 ± 0.0127*** (+ 2.9%)	0.7525 ± 0.0113*** (+ 3.7%)
Placebo	0.7214 ± 0.0114	0.7195 ± 0.0116 (- 0.3%)	0.7250 ± 0.0120 (+ 0.5%)	0.7233 ± 0.0121 (+ 0.2%)
R5 (skin net elasticity)	0	0.5 M	1 M	2 M
100 mg	0.2856 ± 0.0111	0.2948 ± 0.0115*** (+ 3.3%)	0.3020 ± 0.0119*** (+ 5.8%)	0.3112 ± 0.0121*** (+ 9.0%)
250 mg	0.2940 ± 0.0098	0.3024 ± 0.0101*** (+ 2.9%)	0.3093 ± 0.0096*** (+ 5.5%)	0.3147 ± 0.0098*** (+ 7.4%)
Placebo	0.2907 ± 0.0091	0.2907 ± 0.0096 (- 0.1%)	0.2926 ± 0.0089 (+ 0.8%)	0.2888 ± 0.0088 (- 0.5%)

Data are means ± SE. Values in brackets: % variation vs. 0. \*\*\* $p$  < 0.001.

similar to that was obtained in a previous study where volunteers showed a 37% increase in the MED after 8 weeks of product use (46).

In the previous cell study using the same extract combination, part of the protective effect of rosemary and citrus polyphenols was assigned to their capacity of absorption/scattering of UVB radiation. However, this factor may have a negligible contribution *in vivo* due to the low concentration of polyphenols' metabolites in skin cells.

The antioxidant properties of the skin metabolites derived from the compounds of the extracts combination may have a significant contribution to the observed UVR protective effects but further effects are expected to take place. The terpenes and caffeoic acid derivatives from rosemary and citrus flavanones and flavones of the combination showed the capacity to scavenge first stage intracellular free radicals induced by UVR and ionising radiations such as such as superoxide radical anions ( $O_2^-$ ),  $H_2O_2$ , and hydroxyl radicals ( $OH^\bullet$ ) (46, 58, 59). Furtherly, some of these radicals generate second stage lipoperoxy radicals ( $R-OO^\bullet$ ) which are responsible for the generation of inflammatory mediators and generate DNA damage and protein oxidation. ROS are also considered inflammatory mediators through the activation of the NF- $\kappa$ B signalling, which controls the expression of pro-inflammatory cytokines. Therefore, the clinically visible increase of MED and the decrease of UVB-induced skin redness of the ingredient is not only due to their antioxidant capacity but also to their ability to attenuate the subsequent inflammatory response.

Moreover, it has been proven that some of these compounds are capable to reach intracellular targets and modulate multiple metabolic processes that go beyond their antioxidant properties (60). Hence, the polyphenols in the combination may be able to exert a direct modulation of the NF- $\kappa$ B signalling regardless their antioxidant capacity. In fact, rosemary polyphenols were shown *in vivo* to reduce the expression of several inflammation-associated genes which are regulated by NF- $\kappa$ B such as IL-1 $\beta$ , TNF- $\alpha$ , COX-1 and COX-2 in a mouse inflamed skin model, (61). In a keratinocyte HaCaT cell model

stimulated with sodium lauryl sulphate, rosemary diterpenes also blocked the translocation of nuclear factor NF- $\kappa$ B by directly inhibiting its upstream signalling including (spleen tyrosine kinase) Syk/Src, phosphoinositide 3-kinase (PI3K) and protein kinase B (Akt) tyrosine kinases (62).

Skin LPO basal content (Table 3) was decreased indicating an effect of the extracts in improving the skin antioxidant status. Interestingly, the skin ability to counteract UVA-induced lipoperoxidation was also increased starting from 2 weeks of product use. Two months after product use, the UVA-induced LPO content was decreased by about 20 and 15%, 4 and 24 h after UVA exposure (Table 3). These results indicate that the metabolites derived from the ingredient are able to decrease the level of lipid peroxidation in the skin cells in only 2 weeks of consumption and therefore diminish the levels of skin LPO (lipoperoxy radicals, and MDA and hydroxynonenal as final products), which have been demonstrated to induce DNA and protein oxidation (63). Since LPO are also considered as inflammatory response mediators, their drop is also consistent with the observed decrease in skin redness after 2 weeks of product consumption.

In the present study, an improvement of the wrinkle depth (Fig. 9) and skin elasticity (Table 4) was also observed starting from 2 weeks of product use. No differences in the measured outcomes were found between 100 and 250 mg extracts dose regimen, indicating a *plateau* effect starting from the lowest dose.

This result reveals an improvement of the extracellular matrix status that is composed of proteoglycans, polysaccharides and proteins, which are responsible for skin elasticity and stiffness. UVR-induced ROS and inflammatory mediators have been shown to induce the activation of nuclear transcription complex AP-1, through intracellular kinases signalling activation (MAP kinases, p38 and JNK), leading to metalloproteinases (MMPs) activation and decreased expression of collagen and other matrix proteins with the final consequence of reduced dermal matrix formation (64). Therefore, the combined antioxidant and anti-inflammatory effects of the *in vivo* product metabolites together with their direct action on

intracellular signalling pathways may be the responsible factors for the decreased signs of photoaged skin.

As the study protocol was implemented for all ages, skin phenotype from I to III (the most susceptible to UVR), chrono- and photoaged skin, study results can be extended to the general population. The female gender selection does not represent a limitation for study results extending to the general population since the molecular, cellular, and tissue-specific events leading to inflammation, chrono- or photoageing are shared among genders.

### Conclusions

Our results confirm the previous *in vitro* and *in vivo* results (46) indicating a photoprotective and antiaging efficacy of a combination of two plants extracts obtained from dried rosemary (*R. officinalis*) leaves and grapefruits (*C. paradisi*). Long-term oral extract supplementation can contribute to skin protection by maintaining a steady-state systemic concentration of compounds capable of protecting the skin cells from UVR-induced alteration. Positive effects such as reduced UVR-induced erythema, decreased skin LPO, decreased wrinkle depth, and increased elasticity are noted as short as 2 weeks of product consumption. The putative mechanism for these effects is most probably to take place through the inhibition of UVR-induced ROS and the concomitant inflammatory markers (LPO and cytokines) together with their direct action on intracellular signalling pathways which are responsible for extracellular matrix degradation. In conclusion, the intake of Nutrox-sun™ can be considered a complementary nutrition strategy to avoid the negative effects of sun exposure and photoageing. To the best of our knowledge, this is the first study demonstrating the antioxidant, photoprotective, and antiaging efficacy of this combination of plants extracts.

### Acknowledgements

The authors thank all of the Faroderm staff who contributed to and recruited subjects for this study for their professionalism and support during the study development. This investigation was partially supported by project AGL2015-67995-C3-1-R from the Spanish Ministry of Science and Innovation.

### Conflict of interest and funding

This study was funded by Monteloeder S.L. and Nutrafur S.A. Monteloeder was involved in the design of the study protocol and provided the test products samples. Employees of the Sponsor were not involved in data analysis. The manuscript was prepared by Dr. Vincenzo Nobile. Monteloeder and Nutrafur were permitted to review the manuscript and suggest changes, but the final decision on content was exclusively retained by the corresponding author. Dr. Vincenzo Nobile is the guarantor for this article, and takes responsibility for the integrity of

the work as a whole. NC works for Monteloeder S.L. JC and OB-G work for Nutrafur S.A.

### References

1. Sabziparvar AA, Shine KP, Forster PM. A model-derived global climatology of UV irradiation at the Earth's surface. *Photochem Photobiol* 1999; 69: 193–202.
2. Tewari A, Grage MM, Harrison GI, Sarkany R, Young AR. UV-A is skin deep: molecular and clinical implications. *Photochem Photobiol Sci* 2013; 12: 95–103. doi: <http://dx.doi.org/10.1039/c3pp25323b>
3. Cotran RS, Pathak MA. The pattern of vascular leakage induced by monochromatic UV irradiation in rats, guinea pigs and hairless mice. *J Invest Dermatol* 1968; 51: 155–64.
4. Hruza LL, Pentland AP. Mechanisms of UV-induced inflammation. *J Invest Dermatol* 1993; 100: 35S–41S.
5. Benrath J, Eschenfelder C, Zimmermann M, Gillardon F. Calcitonin gene-related peptide, substance P and nitric oxide are involved in cutaneous inflammation following ultraviolet irradiation. *Eur J Pharmacol* 1995; 293: 87–96.
6. Eschenfelder CC, Benrath J, Zimmermann M, Gillardon F. Involvement of substance P in ultraviolet irradiation-induced inflammation in rat skin. *Eur J Neurosci* 1995; 7: 1520–6.
7. Gillardon F, Schröck H, Morano I, Zimmerman M. Long-term increase in CGRP levels in rat spinal dorsal horn following skin ultraviolet irradiation. A mechanism of sunburn pain. *Ann N Y Acad Sci* 1992; 657: 493–6.
8. Rother M, Rother I. Placebo controlled, crossover validation study of oral ibuprofen and topical hydrocortisone-21-acetate for a model of ultraviolet B radiation (UVR)-induced pain and inflammation. *J Pain Res* 2011; 4: 357–63.
9. Greaves MW, Sondergaard J. Pharmacologic agents released in ultraviolet inflammation studied by continuous skin perfusion. *J Invest Dermatol* 1970; 54: 365–7.
10. Hawk JLM, Black AK, Jaenicke KF, Barr RM, Soter NA, Mallett AI, et al. Increased concentrations of arachidonic acid, prostaglandins E<sub>2</sub>, D<sub>2</sub>, and 6-oxo-F<sub>1α</sub>, and histamine in human skin following UVA irradiation. *J Invest Dermatol* 1983; 80: 496–9.
11. Araneo BA, Dowell T, Moon HB, Daynes RA. Regulation of murine lymphokine production *in vivo*. Ultraviolet radiation exposure depresses IL-2 and enhances IL-4 production by T cells through an IL-1-dependent mechanism. *J Immunol* 1989; 143: 1737–44.
12. Gahrung L, Baltz M, Pepys MB, Daynes R. Effect of ultraviolet radiation on production of epidermal cell thymocyte-activating factor/interleukin 1 *in vivo* and *in vitro*. *Proc Natl Acad Sci USA* 1984; 81: 1198–202.
13. Kupper TS, Chua AO, Flood P, McGuire J, Gubler U. Interleukin 1 gene expression in cultured human keratinocytes is augmented by ultraviolet irradiation. *J Clin Invest* 1987; 80: 430–6.
14. Urbanski A, Schwarz T, Neuner P, Krutmann J, Kirnbauer R, Köck A, et al. Ultraviolet light induces increased circulating interleukin-6 in humans. *J Invest Dermatol* 1990; 94: 808–11.
15. Köck A, Schwarz T, Kirnbauer R, Urbanski A, Perry P, Ansel JC, et al. Human keratinocytes are a source for tumor necrosis factor  $\alpha$ : evidence for synthesis and release upon stimulation with endotoxin or ultraviolet light. *J Exp Med* 1990; 172: 1609–14.
16. Oxholm A, Oxholm P, Staberg B, Bendzen K. Immunohistochemical detection of interleukin 1-like molecules and tumour necrosis factor in human epidermis before and after UVB-irradiation *in vivo*. *Br J Dermatol* 1988; 118: 369–76.

17. Gilchrest BA, Soter NA, Stoff JS, Mihm MC Jr. The human sunburn reaction: histologic and biochemical studies. *J Am Acad Dermatol* 1981; 5(4): 411–22.
18. Strelein JW, Taylor JR, Vincek V, Kurimoto I, Richardson J, Tie C, et al. Relationship between ultraviolet radiation-induced immunosuppression and carcinogenesis. *J Invest Dermatol* 1994; 103: 107S–11S.
19. De Fabo EC, Noonan FP. Mechanism of immune suppression by ultraviolet radiation *in vivo*. I. Evidence for the existence of a unique photoreceptor in skin and its role in photoimmunology. *J Exp Med* 1983; 157: 84–98.
20. Rivas JM, Ullrich SE. Systemic suppression of delayed-type hypersensitivity by supernatants from UV-irradiated keratinocytes. An essential role for keratinocyte-derived IL-10. *J Immunol* 1992; 149: 3865–71.
21. Shreedhar V, Giese T, Sung VW, Ullrich SE. A cytokine cascade including prostaglandin E2, IL-4, and IL-10 is responsible for UV-induced systemic immune suppression. *J Immunol* 1998; 160: 3783–9.
22. Grether-Beck S, Olaizola-Horn S, Schmitt H, Grewel M, Jahnke A, Johnson JP, et al. Activation of transcription factor AP-2 mediates UVA radiation- and singlet oxygen-induced expression of the human intercellular adhesion molecule 1 gene. *Proc Natl Acad Sci USA* 1996; 93(25): 14586–91.
23. Berneburg M, Grether-Beck S, Kürten V, Ruzicka T, Briviba K, Sies H, et al. Singlet oxygen mediates the UVA-induced generation of the photoaging-associated mitochondrial common deletion. *J Biol Chem* 1999; 274(22): 15345–9.
24. Klotz LO, Holbrook NJ, Sies H. UVA and singlet oxygen as inducers of cutaneous signaling events. *Curr Probl Dermatol* 2001; 29: 95–113.
25. Bachelor MA, Bowden GT. UVA-mediated activation of signaling pathways involved in skin tumor promotion and progression. *Semin Cancer Biol* 2004; 14(2): 131–8.
26. Halliday GM. Inflammation, gene mutation and photoimmunosuppression in response to UVR-induced oxidative damage contributes to photocarcinogenesis. *Mutat Res* 2005; 571(1–2): 107–20.
27. Agar NS, Halliday GM, Barnett RS, Ananthaswamy HN, Wheeler M, Jones AM. The basal layer in human squamous tumors harbors more UVA than UVB fingerprint mutations: a role for UVA in human skin carcinogenesis. *Proc Natl Acad Sci USA* 2004; 101(14): 4954–9.
28. Tewari A, Sarkany RP, Young AR. UVA1 induces cyclobutane pyrimidine dimers but not 6-4 photoproducts in human skin *in vivo*. *J Invest Dermatol* 2012; 132: 394–400.
29. Vile GF, Tyrrell RM. UVA radiation-induced oxidative damage to lipids and proteins *in vitro* and in human skin fibroblasts is dependent on iron and singlet oxygen. *Free Radic Biol Med* 1995; 18(4): 721–30.
30. Ferguson J. European guidelines (COLIPA) for evaluation of sun protection factors. In: NJ Lowe, NA Shaath, MA Pathak (eds). *Sunscreens: development, evaluation and regulatory aspects*, p. 513–25. New York: Marcel Dekker; 1997.
31. Azurdia RM, Pagliaro JA, Diffey BL, Rhodes LE. Sunscreen application by photosensitive patients is inadequate for protection. *Br J Dermatol* 1999; 140: 255–8.
32. Jansen R, Wang SQ, Burnett M, Osterwalder U, Lim HW. Photoprotection: part I. Photoprotection by naturally occurring, physical, and systemic agents. *J Am Acad Dermatol* 2013; 69: 853.e1–12.
33. Robbins RJ. Phenolic acids in foods: an overview of analytical methodology. *J Agric Food Chem* 2003; 51: 2866–87.
34. Gao Z, Huang K, Xu H. Protective effects of flavonoids in the roots of *Scutellaria baicalensis Georgii* against hydrogen peroxide-induced oxidative stress in HSSY5Y cells. *Pharmacol Res* 2001; 43: 173–8.
35. Vostálová J, Zdarilová A, Svobodová A. *Prunella vulgaris* extract and rosmarinic acid prevent UVB-induced DNA damage and oxidative stress in HaCaT keratinocytes. *Arch Dermatol Res* 2010; 302: 171–81.
36. Psotova J, Svobodova A, Kolarova H, Walterova D. Photoprotective properties of *Prunella vulgaris* and rosmarinic acid on human keratinocytes. *J Photochem Photobiol B* 2006; B84: 167–74.
37. Sánchez-Campillo M, Gabaldón JA, Castillo J, Benavente-García O, Del Baño MJ, Alcaraz M, et al. Rosmarinic acid, a photoprotective agent against UV and other ionizing radiations. *Food Chem Toxicol* 2009; 47: 386–92.
38. Wei H, Zhang X, Wang Y, Lebwohl M. Inhibition of ultraviolet light-induced oxidative events in the skin and internal organs of hairless mice by isoflavone genistein. *Cancer Lett* 2002; 185: 21–9.
39. Singh RP, Agarwal R. Mechanisms and preclinical efficacy of silibinin in preventing skin cancer. *Eur J Cancer* 2005; 41(13): 1969–79.
40. Torel J, Cillard J. Antioxidant activity of flavonoids and reactivity with peroxy radical. *Phytochemistry* 1986; 25: 383–5.
41. Robak J, Gryglewski RJ. Flavonoids are scavengers of superoxide anions. *Biochem Pharmacol* 1988; 37: 837–41.
42. Del Baño MJ, Castillo J, Benavente-García O, Lorente J, Martín-Gil R, Acevedo C, Alcaraz M. Radioprotective-antimutagenic effects of rosemary phenolics against chromosomal damage induced in human lymphocytes by gamma-rays. *J Agric Food Chem* 2006; 54(6): 2064–8.
43. Alcaraz M, Acevedo C, Castillo J, Benavente-García O, Armero D, Vicente V, et al. Liposoluble antioxidants provide an effective radioprotective barrier. *Br J Radiol* 2009; 82(979): 605–9.
44. Morton LW, Caccetta RAA, Pudsey IB, Croft KD. Chemistry and biological effect of dietary phenolic compounds: relevance to cardiovascular disease. *Clin Exp Pharmacol Physiol* 2000; 27: 152–9.
45. Cao G, Sofic E, Prior RL. Antioxidant and prooxidant behavior of flavonoids: structure-activity relationships. *Free Radic Biol Med* 1996; 5: 749–60.
46. Pérez-Sánchez A, Barrajón-Catalán E, Caturla N, Castillo J, Benavente-García O, Alcaraz M, et al. Protective effects of citrus and rosemary extracts on UV-induced damage in skin cell model and human volunteers. *J Photochem Photobiol B* 2014; 136: 12–18.
47. Fitzpatrick TB. The validity and practicability of sun-reactive skin types I through VI. *Arch Dermatol* 1988; 124: 869–71.
48. Huang D, Ou B, Prior RL. The chemistry behind antioxidant capacity assays. *J Agric Food Chem* 2005; 53: 1841–56.
49. ISO 24444:2010. Cosmetics – sun protection test methods – *in vivo* determination of the sun protection factor (SPF). Available from: [http://www.iso.org/iso/catalogue\\_detail.htm?csnumber=46523](http://www.iso.org/iso/catalogue_detail.htm?csnumber=46523) [cited 12 February 2016].
50. Erdelmeier I, Gérard-Monnier D, Yadan JC, Chaudière J. Reactions of N-methyl-2-phenylindole with malondialdehyde and 4-hydroxyalkenals. Mechanistic aspects of the colorimetric assay of lipid peroxidation. *Chem Res Toxicol* 1998; 11(10): 1184–94.
51. JCIA Measurement Standard for UVA Protection Efficacy (1995). Japan Cosmetic Industry Association - JCIA, 9–14, Toranomon 2-Chome, Minato-Ku Tokyo, 105.
52. ISO 24442:2011. Cosmetics – sun protection test methods – *in vivo* determination of sunscreen UVA protection. Available from: [http://www.iso.org/iso/iso\\_catalogue/catalogue\\_tc/catalogue\\_detail.htm?csnumber=46521](http://www.iso.org/iso/iso_catalogue/catalogue_tc/catalogue_detail.htm?csnumber=46521) [cited 12 February 2016].

53. Wang Q, Kuang H, Su Y, Sun Y, Feng J, Guo R, et al. Naturally derived anti-inflammatory compounds from Chinese medicinal plants. *J Ethnopharmacol* 2013; 146(1): 9–39.
54. Nworu CS, Akah PA, Okoye FB, Esimone CO. Inhibition of pro-inflammatory cytokines and inducible nitric oxide by extract of *Emilia sonchifolia* L. aerial parts. *Immunopharmacol Immunotoxicol* 2012; 34(6): 925–31.
55. Shimoda H, Shan SJ, Tanaka J, Seki A, Seo JW, Kasajima N, et al. Anti-inflammatory properties of red ginger (*Zingiber officinale* var. *Rubra*) extract and suppression of nitric oxide production by its constituents. *J Med Food* 2010; 13(1): 156–62.
56. Tao S, Zheng Y, Lau A, Jaramillo MC, Chau BT, Lantz RC, et al. Tanshinone I activates the Nrf2-dependent antioxidant response and protects against As(III)-induced lung inflammation *in vitro* and *in vivo*. *Antioxid Redox Signal* 2013; 19(14): 1647–61.
57. Sies H, Stahl W. Nutritional protection against skin damage from sunlight. *Ann Rev Nutr* 2004; 24: 173–200.
58. Pérez-Fons L, Garzón MT, Micol V. Relationship between the antioxidant capacity and effect of rosemary (*Rosmarinus officinalis* L.) polyphenols on membrane phospholipid order. *J Agric Food Chem* 2010; 58(1): 161–71.
59. Offord EA, Gautier JC, Avanti O, Scaletta C, Runge F, Krämer K, et al. Photoprotective potential of lycopene, beta-carotene, vitamin E, vitamin C and carnosic acid in UVA-irradiated human skin fibroblasts. *Free Radic Biol Med* 2002; 32(12): 1293–303.
60. Barrajón-Catalán E, Herranz-López M, Joven J, Segura-Carretero A, Alonso-Villaverde C, Menéndez JA, et al. Molecular promiscuity of plant polyphenols in the management of age-related diseases: far beyond their antioxidant properties. *Adv Exp Med Biol* 2014; 824: 141–59.
61. Mengoni ES, Vichera G, Rigano LA, Rodriguez-Puebla ML, Galliano SR, Cafferata EE, et al. Suppression of COX-2, IL-1 $\beta$  and TNF- $\alpha$  expression and leukocyte infiltration in inflamed skin by bioactive compounds from *Rosmarinus officinalis* L. *Fioterapia* 2011; 82(3): 414–21.
62. Oh J, Yu T, Choi SJ, Yang Y, Baek HS, An SA, et al. Syk/Src pathway-targeted inhibition of skin inflammatory responses by carnosic acid. *Mediators Inflamm* 2012; 2012: 781375.
63. Braconi D, Bernardini G, Santucci A. Post-genomics and skin inflammation. *Mediators Inflamm* 2010; 2010: pii: 364823.
64. Fisher GJ, Kang S, Varani J, Bata-Csorgo Z, Wan Y, Datta S, et al. Mechanisms of photoaging and chronological skin aging. *Arch Dermatol* 2002; 138: 1462–70.

---

\*Vincenzo Nobile

Via Mons  
Angelini 21  
IT-27028 San Martino  
Siccomario, Pavia  
Italy  
Email: vincenzo.nobile@farcoderm.com





## Lemon balm extract (*Melissa officinalis*, L.) promotes melanogenesis and prevents UVB-induced oxidative stress and DNA damage in a skin cell model



Almudena Pérez-Sánchez<sup>a,1</sup>, Enrique Barrajón-Catalán<sup>a,b,1</sup>, María Herranz-López<sup>a</sup>, Julián Castillo<sup>c,d,2</sup>, Vicente Mico<sup>a,e,\*</sup>

<sup>a</sup> Institute of Molecular and Cell Biology (IBMC), Miguel Hernández University (UMH), Avenida de la Universidad s/n, E-03202 Elche, Alicante, Spain

<sup>b</sup> INVITROTECNIA S.L., Santiago Grisolía 2, 28760 Tres Cantos, Madrid, Spain

<sup>c</sup> Nutrafur S.A., Camino Viejo de Pliego km.2, 30820 Alcantarilla, Murcia, Spain

<sup>d</sup> Department of Food Technology and Nutrition, Universidad Católica San Antonio, Murcia, Spain

<sup>e</sup> CIBER (CB12/03/30038, Fisiopatología de la Obesidad y la Nutrición, CIBERobn, Instituto de Salud Carlos III), Spain

### ARTICLE INFO

#### Article history:

Received 30 March 2016

Received in revised form 27 May 2016

Accepted 3 August 2016

#### Keywords:

Lemon balm extract

Rosmarinic acid

UV radiation

Keratinocytes

Reactive oxygen species (ROS)

DNA damage

### ABSTRACT

**Background:** Solar ultraviolet (UV) radiation is one of the main causes of a variety of cutaneous disorders, including photoaging and skin cancer. Its UVB component (280–315 nm) leads to oxidative stress and causes inflammation, DNA damage, p53 induction and lipid and protein oxidation. Recently, an increase in the use of plant polyphenols with antioxidant and anti-inflammatory properties has emerged to protect human skin against the deleterious effects of sunlight.

**Objective:** This study evaluates the protective effects of lemon balm extract (LBE) (*Melissa Officinalis*, L) and its main phenolic compound rosmarinic acid (RA) against UVB-induced damage in human keratinocytes.

**Methods:** The LBE composition was determined by HPLC analysis coupled to photodiode array detector and ion trap mass spectrometry with electrospray ionization (HPLC-DAD-ESI-IT-MS/MS). Cell survival, ROS generation and DNA damage were determined upon UVB irradiation in the presence of LBE. The melanogenic capacity of LBE was also determined.

**Results:** RA and salvianolic acid derivatives were the major compounds, but caffeic acid and luteolin glucuronide were also found in LBE. LBE and RA significantly increased the survival of human keratinocytes upon UVB radiation, but LBE showed a stronger effect. LBE significantly decreased UVB-induced intracellular ROS production. Moreover, LBE reduced UV-induced DNA damage and the DNA damage response (DDR), which were measured as DNA strand breaks in the comet assay and histone H2AX activation, respectively. Finally, LBE promoted melanogenesis in the cell model.

**Conclusions:** These results suggest that LBE may be considered as a candidate for the development of oral/topical photoprotective ingredients against UVB-induced skin damage.

© 2016 Japanese Society for Investigative Dermatology. Published by Elsevier Ireland Ltd. All rights reserved.

### 1. Introduction

The skin is the largest organ of the human body, participates in sensitivity and temperature maintenance and offers protection from chemicals, microorganisms and UV radiation [1]. An excessive UV exposition can lead to several skin pathological disorders, including erythema, immunosuppression, edema, sunburn, hyperplasia, hyperpigmentation, premature aging and skin cancer [2]. UV radiation is divided into long wave UVA (315–400 nm, 90% of UV radiation), medium wave UVB (280–315 nm, 5% of UV radiation), and short wave UVC (200–280 nm). UVB is one thousand times more capable of

**Abbreviations:** 6-4PPs, pyrimidine (6-4) pyrimidone; CPDs, cyclobutane pyrimidine dimers; DDR, DNA damage response; DMSO, dimethyl sulfoxide; DSBs, double-strand breaks; H<sub>2</sub>DCF-DA, 2',7'-dichlorofluorescein diacetate; HNE, 4-hydroxy-2-nonenal; IBMX, 3-isobutyl-1-methylxanthine; LBE, lemon balm extract; MDA, malondialdehyde; ORAC, oxygen radical absorbance capacity; PBS, phosphate-buffered saline; RA, rosmarinic acid; ROS, reactive oxygen species; SSBs, single-strand breaks; TEAC, trolox equivalent antioxidant capacity; UV, ultraviolet.

\* Corresponding author at: Instituto de Biología Molecular y Celular, Universidad Miguel Hernández, Avda. de la Universidad S/N, 03202 Elche, Alicante, Spain.

E-mail address: [vmicol@umh.es](mailto:vmicol@umh.es) (V. Mico).

<sup>1</sup> These authors have equally contributed to this research and are listed in random order.

<sup>2</sup> Frutarom Group.

causing sunburn than UVA and is considered the most damaging and genotoxic [3].

Melanin is the main skin protective barrier that acts by absorbing and scattering UV radiation. Nevertheless, other intracellular molecules are targeted (DNA, RNA, lipids and proteins). The direct effect of UVB on DNA leads to the formation of cyclobutane pyrimidine dimers (CPDs) and to a lesser extent pyrimidine (6–4) pyrimidone (6-4PPs) photoproducts. When these alterations are not well repaired, the resulting substitution/transition mutations (cytosine-thymine) in the epidermal cells can lead to the development of skin cancer [4,5].

UVB, together with UVA, generates superoxide ( $O_2^{\bullet}$ ), either directly or through enzyme activation [6,7]. This is the most promptly generated oxygen radical species (ROS) and is rapidly derived into  $H_2O_2$ , which forms OH upon the Fenton reaction [4]. UVB induced  $^{\bullet}OH$  is postulated to be responsible for the formation of DNA single-strand breaks (SSBs) and also for lipid peroxidation through the generation of lipoperoxy radicals (ROO), malondialdehyde (MDA) and 4-hydroxy-2-nonenal (HNE). Additionally, UVB-induced ROS interact with numerous cellular targets and receptors that regulate crucial pathways related to inflammation, cell survival, cell growth and differentiation in human keratinocytes: the NF- $\kappa$ B, the AP-1 transcription factor, the mitogen-activated protein kinase (MAPK) and extracellular signal-regulated kinase (ERK1/2) pathways [8–10]. Most of these effects lead to extracellular matrix degeneration by proteases activation and skin photoaging [1].

Plant polyphenols possess strong free radical scavenging properties and have exhibited the capacity to modulate multiple cellular pathways [11]. Recently, their potential skin photo-protective effects have gained considerable attention [12]. The UVB protective effects of botanical extracts, such as *Punica granatum* [13], citrus and rosemary [14], green tea polyphenols [15] and pure compounds, such as resveratrol [16], genistein [17,18] and hydroxytyrosol [19] has been reported. Recently our group has demonstrated the synergistic protective effect of rosemary and citrus polyphenolic extracts both *in vitro* and *in vivo* [14].

Lemon balm (*Melissa officinalis*, L.) is representative of the *Lamiaceae* family, native to Europe but with a worldwide distribution. This herb is used not only for ornamental purposes but also for medicine and cosmetics. It is commonly used for insomnia and anxiety [20], herpes [21], and indigestion [22], as an antioxidant [23] and as an antimicrobial agent [24]. Lemon balm extraction may lead to the essential oil and the lemon balm polyphenolic extract (LBE), which is enriched in phenylpropanoid derivatives and flavonoids. The major phenolic compound found in the polyphenolic extract is rosmarinic acid (RA), which is an ester of caffeic acid, and 3,4-dihydroxyphenyllactic acid [25] (Fig. 1, see

insert). The antioxidant activity of LBE has been previously characterized in both *in vitro* and *in vivo* models [26–29].

In the present study, the UVB protective effects of LBE and its major polyphenol RA were explored and compared in human keratinocytes. The potential of LBE to protect human keratinocytes from UVB-induced oxidative stress and to alleviate DNA damage was studied. The protective effect through melanogenesis activation was also studied in a cellular model.

## 2. Materials and methods

### 2.1. Materials and LBE

Human keratinocytes (the spontaneously immortalized cell line HaCaT) were obtained from Cell lines Service GmbH, CLS (Eppelheim, Germany). Dulbecco's modified Eagle's medium (DMEM), fetal bovine serum (FBS), and penicillin-streptomycin were obtained from Gibco/Thermo Fisher Scientific (Waltham, MA, USA). RA (96%) and the rest of the reagents were purchased from Sigma-Aldrich (St. Louis, MO, USA). LBE standardized containing  $18.0 \pm 0.3\%$  RA (w/w) was kindly provided by NUTRAFUR, SA – Frutaron Group (Alcantarilla, Murcia, Spain).

### 2.2. Cell culture

HaCaT cells were grown in DMEM with 10% (v/v) FBS and 1% (v/v) penicillin-streptomycin (0.1 mg/mL penicillin and 100 U/mL) in a humidified atmosphere with  $CO_2$  (5% v/v) at 37 °C. The HaCaT cells were trypsinized every third day following the purchaser instructions and seeded in 96- or 6-well plates depending on the assay. B16-F10 mouse melanoma cells were obtained from the American Type Culture Collection (ATCC, Manassas, VA, USA) and grown using the same conditions described for the HaCaT cells.

### 2.3. HPLC-DAD-ESI-IT-MS/MS analysis of LBE

LBE was dissolved in DMSO:PBS (1:10) and filtered through a 0.45  $\mu$ m nylon membrane. The extract was analyzed using a LC-MS system consisting of an Agilent LC 1100 series (Agilent Technologies, Inc., Palo Alto, CA, USA) controlled by the Chemstation software. The HPLC instrument was coupled to an Esquire 3000 (Bruker Daltonics, GmbH, Germany) mass spectrometer equipped with an ESI source and ion trap mass analyzer. The electrospray ionization source was operated in negative mode to generate  $[M-H]^-$  ions using the following conditions: desolvation temperature was set at 300 °C, and the dry gas (nitrogen) and nebulizer were set at 10 L/min and 60 psi, respectively. The MS and MS/MS spectra were acquired over 100–1000  $m/z$  at 10 ms, and the capillary voltage was 4.0 kV. A Teknokroma C-18 Tracer Excel 120 ODSB 5  $\mu$ m  $\times$  0.4 cm column was used for analytical purposes. The mobile phase was (A) formic acid (1%) and (B) acetonitrile, and the following linear gradient was used: 20% B at 0 min, 70% at 25 min, 70% at 30 min, 20% at 31 min and 5 more minutes for re-equilibration. The flow rate was 1 mL/min. Diode-array detection was set at 280, 320 and 340 nm. The MS data were acquired as full scan mass spectra at 50–1100  $m/z$  using 200 ms for collection of the ions in the trap. Identification of the main compounds was performed by HPLC-DAD analysis. The retention times, UV spectra and MS/MS data of the peaks in the samples were compared with those of authentic standards or data reported in the literature. Quantitation of the RA content was performed using a commercial standard (Sigma-Aldrich, Europe) at 280 nm. The linearity range of the responses was determined on eight concentration levels of RA (ranging from 0.18 mg/mL to 5.4 mg/mL) with three injections for each level. Calibration graphs for the quantitative evaluation of the compounds were performed using a seven-point regression curve

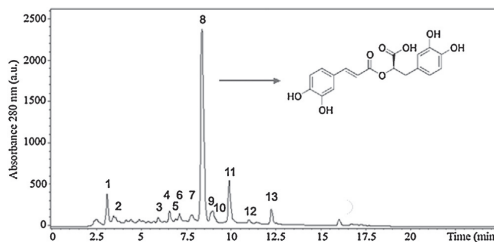


**Fig. 1.** HPLC-DAD chromatogram for LBE at 280 nm. Insert shows RA structure.

( $r^2 > 0.9973$ ). The limit of detection (LOD) and limit of quantification (LOQ) for RA were 1 µg/mL and 10 µg/mL respectively.

#### 2.4. LBE and RA absorption spectra

Absorption spectra collection was performed on an UV-1603 UV-vis spectrophotometer (SHIMADZU, Kyoto, Japan). The 5 ppm RA and LBE solutions (used at an equivalent RA concentration) were prepared by dissolving the compounds in ultra-pure water. The calculations were performed with the Origin software (OriginLab Co.) using data from at least two independent experiments in the range from 190 to 400 nm at 2 nm intervals.

#### 2.5. UVB cell treatment and survival quantitation

For UVB treatment, cells were cultured in 96-well plates and maintained in medium for 24 h. When 50–70% confluence was reached, the cells were washed with phosphate-buffered saline (PBS) and treated with a thin layer of PBS containing LBE (15–100 µg/mL) or RA (2.7–18 µg/mL), followed by UVB light treatment (800 or 1200 J/m<sup>2</sup>) emitted from the Bio-Link Crosslinker BLX-E312. Afterwards, the PBS was replaced with fresh medium and the cells were incubated for 72 h. Then, the 3-(4,5-dimethylthiazol-2-yl)-2,5-diphenyltetrazolium (MTT) assay was used as a simple, quantitative and reliable assay to determine cell viability after irradiation as previously described [30]. The protection percentage was obtained using the following formula:

$$\text{Protection\%} = 100 - 100 \cdot \left( \frac{PC - \text{sample}}{PC - NC} \right)$$

where all parameters represent the survival percentage of each sample obtained from the MTT assay as follows: PC (% survival in the non-irradiated control and the non-treated and non-irradiated sample) and NC (% survival in the irradiated control and the non-treated but irradiated sample).

#### 2.6. Melanogenesis assays

B16 mouse melanoma cells were seeded into a 96-well plate to obtain a confluent monolayer. The cells were incubated with the LBE samples or the melanin induction agent 3-isobutyl-1-methylxanthine (IBMX) at the indicated concentrations for 72 h. Both extracellular (cell supernatants) and intracellular (after dissolving the cell layer with 1 M NaOH for 1 h at 80 °C with moderate shaking) melanin were analyzed using a microplate reader at 405 nm. Cell viability was not modified by the treatments as determined by a MTT assay performed in parallel (data not shown).

#### 2.7. In vitro antioxidant assays and ROS generation measurement

The Trolox equivalent antioxidant capacity assay (TEAC) was performed as described elsewhere through decoloration of the ABTS radical cation (ABTS<sup>•+</sup>) by reducing agents [30]. The results were expressed in mmol of Trolox per 100 g of extract dry weight. The oxygen radical absorbance capacity (ORAC) assay was performed as previously described using fluorescein and AAPH as the radical generator [31]. The final ORAC values were calculated using a regression equation between the Trolox concentration and the net area of the fluorescence decay curve.

The H<sub>2</sub>DCF-DA fluorescence probe was used to monitor the intracellular ROS generation induced by UVB radiation. Cells were cultured in 96-well black plates and maintained in medium for 24 h. When 90–100% confluence was reached, the cells were treated with LBE, followed by treatment with UVB light (800 or 1200 J/m<sup>2</sup>) emitted from the Bio-Link Crosslinker BLX-E312. Afterwards, PBS was replaced with fresh medium and the cells were incubated with H<sub>2</sub>DCF-DA (10 µg/mL) for 1 h at 37 °C and 5% CO<sub>2</sub>. Fluorescence was measured using a microplate reader (POLAstar Omega, BMG LabTech GmbH, Offenburg, Germany) with 495 nm excitation and 520 nm emission filters.

#### 2.8. Comet assay

Cells were cultured in 6-well plates and maintained in medium until they reached 80–90% confluence. Then, the cells were washed with PBS and treated with a thin layer of PBS containing LBE, followed by treatment with UVB light (1200 J/m<sup>2</sup>) emitted from the Bio-Link Crosslinker BLX-E312. Subsequently, the cells were trypsinized, pelleted, resuspended in PBS and mixed with low melting point agarose (1%). The alkaline single cell electrophoresis assay was performed as previously reported [14] (Supplementary information).

#### 2.9. H2AX activation

HaCaT cells were cultured in 6-well plates and maintained in medium for 24 h. When 70–90% confluence was reached, the cells were washed with PBS and treated with LBE (15, 60 or 100 µg/mL) dissolved in a thin layer of PBS, followed by UVB irradiation (1200 J/m<sup>2</sup>). Then, the PBS was replaced with fresh medium and the cells were incubated for 24 h. The phosphorylated form of the H2AX protein (a marker for DNA damage; T-H2AX) was measured with the Activation Dual Detection Kit (Merck Millipore, Darmstadt, Germany) according to the manufacturer's instructions using the Muse Cell Analyzer (Millipore Corporation, Darmstadt, Germany).

**Table 1**

Relevant mass spectral data of the compounds identified in LBE obtained by HPLC-DAD-ESI-IT-MS/MS.

Peak no.	Retention time (min)	[M-H] <sup>-</sup>	Main fragments	Proposed compound
1	3.1	196.9	179, 135, 73	3-(3,4-Dihydroxyphenyl) lactic acid
2	3.6	178.9	135	Caffeic acid
3	6.0	597.1	579, 535, 399, 337, 293, 267, 197	Yunnaneic acid F
4	6.6	521.0	359, 161	Rosmarinic acid hexoside
5	6.9	717.0	519, 475, 359, 297	Salvianolic acid B isomer
6	7.1	719.2	607, 539, 409, 359, 297	Sagerinic acid
7	7.8	438.9	359, 259, 215, 179, 135	Sulphated rosmarinic acid
8	8.4	358.8	223, 197, 161	Rosmarinic acid
9	8.9	460.9	461, 285	Luteolin-3'-O-glucuronide
10	9.0	536.9	527, 493, 447, 359, 313, 177	Lithospermic acid A
11	9.9	829.2	697, 667, 577, 535 491, 311	Salvianolic acid C derivative
12	11.0	492.9	359, 313, 161	Salvianolic acid A
13	12.2	715.1	535, 491, 311	Salvianolic acid C derivative

### 2.10. Statistical analysis

The data were represented as the mean  $\pm$  standard deviation of the mean. All cellular measurements derived from three independent experiments with each experiment performed in 4–6 determinations unless specified. One-way ANOVA and statistical comparisons of the different treatments were performed using Tukey's test in GraphPad Prism version 5.00 (GraphPad Software, San Diego, CA, USA). The differences were considered statistically significant at  $p < 0.05$ . Statistical significance is detailed in the figures using the following symbols: \*  $p < 0.05$ , \*\*  $p < 0.01$  and \*\*\*  $p < 0.001$ .

## 3. Results

### 3.1. Characterization of LBE by HPLC-MS/MS

The major components of LBE were identified by HPLC-DAD-ESI-IT-MS/MS as described in the Methods section. The main polyphenolic compounds were identified using a library of phenolic compounds by comparing their retention times, UV spectra and MS/MS data with those of commercial standards or reports in the literature. Fig. 1 shows the chromatogram obtained at 280 nm for LBE. Thirteen major phenolic compounds were identified in LBE as detailed in Table 1 and were assigned numbers

1–13 according to their elution order. RA (insert in Fig. 1) was the major phenolic compound in the extract and corresponded to peak number 8, with a parental ion at  $m/z$  359 and fragment ions at  $m/z$  223, 197 and 161 [32]. RA represented 18% (w/w) of LBE as determined by HPLC-DAD using a RA commercial standard. The biosynthetic precursors of RA, caffeic acid and 3-(3,4-dihydroxyphenyl) lactic acid were also detected (peaks 1 and 2), and up to 10 RA derivatives were identified (peaks 3–8 and 10–13), with salvianolic acid the most abundant. An additional non-structurally related compound (the flavone luteolin-3'-O-glucuronide) was detected based on previous studies [33]. Structures of all identified compounds are displayed in Supplementary Fig. 3.

### 3.2. LBE and RA protect human keratinocytes against UVB radiation

LBE and RA were challenged in a cell survival assay to determine their capacity to protect human keratinocytes from UVB-induced damage at different UVB radiation doses (800 or 1200 J/m<sup>2</sup>). The LBE extract contained 18% w/w RA; therefore, LBE and RA were compared at equivalent RA concentrations so that the data points at the abscissa axis contained equivalent RA concentrations (Fig. 2A). After irradiation with 800 J/m<sup>2</sup> of UVB, only LBE showed a level of photoprotection based on the significant increase in the percentage of cell viability. The LBE protective effect exhibited a dose-response behavior and showed significant differences ( $p$

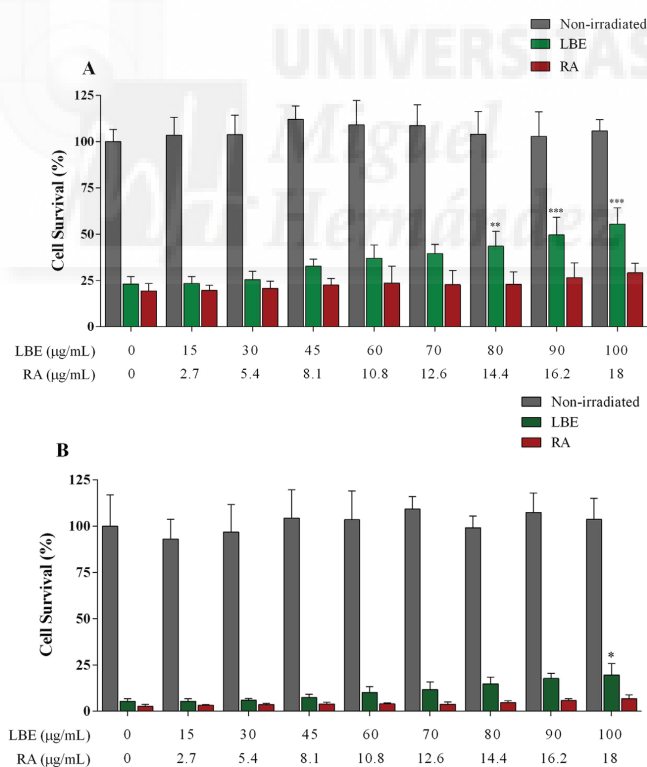


**Fig. 2.** Cell survival of human keratinocytes after irradiation with 800 J/m<sup>2</sup> (Fig. 2A) or 1200 J/m<sup>2</sup> (Fig. 2B) doses of UVB in the presence of LBE or RA and determined using MTT assay after incubation of cells for 72 h post-irradiation. Data points at the abscissa axis contain equivalent concentrations of RA in µg/mL for comparison purpose. The data are expressed as the mean of 6 replicates  $\pm$  SD. \* ( $p < 0.05$ ), \*\* ( $p < 0.01$ ) or \*\*\* ( $p < 0.001$ ) indicate statistically significant differences compared with irradiated sample in the absence of the extracts.

<0.05 or lower) starting at 80 µg/mL of LBE compared with the untreated cells or cells treated with different RA concentrations (Fig. 2A). A similar effect was observed after irradiation of keratinocytes with 1200 J/m<sup>2</sup> UVB. At this UVB dose, only the highest concentration of LBE (100 µg/mL) exhibited a protective effect with a significant difference compared with the untreated cells or cells treated with different RA concentrations ( $p < 0.05$ ) (Fig. 2B). Although a noticeable increasing trend was observed for cell viability in irradiated cells incubated with different RA concentrations, no statistically significant differences were observed compared to controls, indicating that pure RA had no effect on cell survival at the studied UV doses. LBE or RA concentrations higher than 100 µg/mL were not used because these concentrations had a cytotoxic effect on human keratinocytes (data not shown).

The protection magnitude was calculated as the difference between cell survival in the irradiated control (cells irradiated in the absence of agents) and cells treated with different LBE or RA concentrations (Supplementary Table S1). The levels of protection of 42% for LBE and 12% for pure RA were observed at 800 J/m<sup>2</sup> UVB at the highest concentration used. These percentages were reduced to 12% and 4% for LBE and RA, respectively, when the UVB irradiation dose was increased to 1200 J/m<sup>2</sup>.

### 3.3. In vitro antioxidant activity and attenuation of ROS generation in UVB-irradiated keratinocytes by LBE

To test whether the free radical scavenging capacity of LBE significantly contributed to the observed photoprotective effect,

the antioxidant capacity of LBE was evaluated both *in vitro* and in a cellular model after UVB irradiation. First, *in vitro* antioxidant activity was studied using the electron transfer-based TEAC assay and the hydrogen atom transfer-based ORAC assay as described in the Methods section. LBE exhibited a value of  $271.46 \pm 6.37$  mmol Trolox equivalent/100 g DW for TEAC assay. The ORAC measurement for LBE revealed a high oxygen radical absorbance capacity for the extract, *i.e.*,  $14,246 \pm 621$  µmol Trolox equivalent/g DW.

To study the potential protective effect of LBE on the intracellular ROS generation induced by UVB radiation, cells were exposed to 800 or 1200 J/m<sup>2</sup> UVB in the presence of several LBE concentrations. ROS generation was measured using H<sub>2</sub>DCF-DA, which is a probe that becomes fluorescent when oxidized by intracellular ROS. Fig. 3 shows the increase in fluorescence linked to ROS generation in HaCaT cells after UVB radiation in the presence and absence of various LBE concentrations. A certain level of fluorescence was detected in the non-irradiated cells due to basal cell metabolism (white bars). Upon irradiation with UVB and in the absence of LBE, the fluorescence showed a significant increase of 33% or 45% in cells irradiated with the 800 or 1200 J/m<sup>2</sup> doses, respectively, compared with their respective non-irradiated controls. In contrast, significant decreases of 19% and 23% were observed compared to the irradiated controls when the cells were irradiated with 800 J/m<sup>2</sup> and 1200 J/m<sup>2</sup> UVB ( $p < 0.001$ ), respectively, in the presence of 60 µg/mL of LBE. An enhanced capacity to decrease ROS generation was achieved when LBE was used at the 100 µg/mL concentration, with a 29% ROS decrease at 800 J/m<sup>2</sup> and a 33% decrease at 1200 J/m<sup>2</sup> compared with the irradiated and non-treated cells.

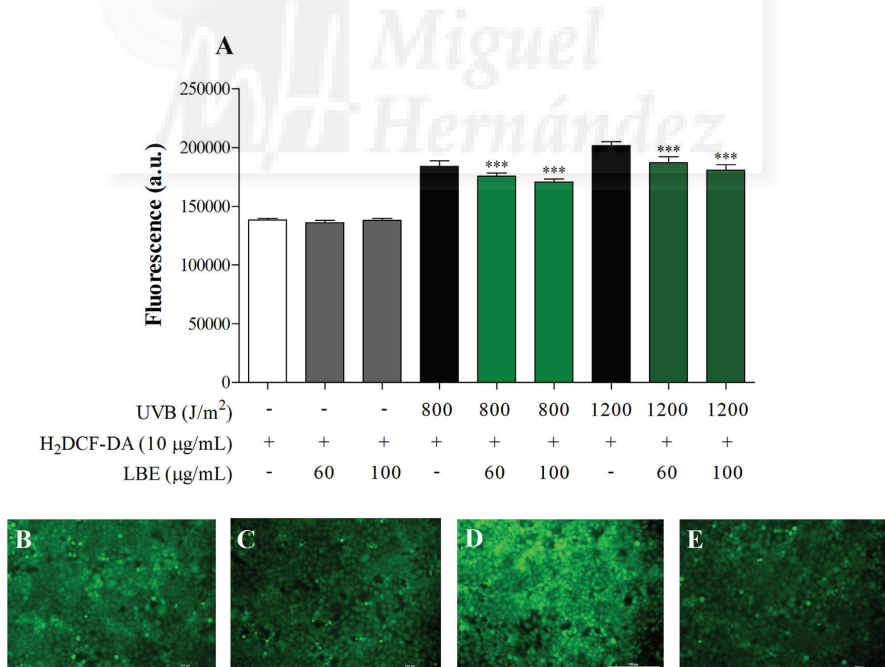


**Fig. 3.** LBE decreases UVB-induced intracellular ROS generation in HaCaT cells (A). Keratinocytes were treated with different concentrations of LBE and exposed to UVB radiation (800 or 1200 J/m<sup>2</sup>). Total fluorescence is expressed as arbitrary units. Pictures are representative of control of irradiated HaCaT cells at 800 J/m<sup>2</sup> (B), irradiated cells at 800 J/m<sup>2</sup> in the presence of LBE (100 µg/mL) (C), irradiated cells at 1200 J/m<sup>2</sup> (D) and irradiated cells at 1200 J/m<sup>2</sup> in the presence of LBE (100 µg/mL) (E). Data are expressed as the mean ± SD. \*\*\* ( $p < 0.001$ ) indicates significant differences compared to irradiated cells at the same UVB dose in the absence of LBE.

### 3.4. LBE protects against UVB-induced DNA damage and triggers the DNA damage response (DDR) in human keratinocytes

To test the hypothesis that the inhibition of ROS generation by LBE observed in UVB-irradiated human keratinocytes correlated with the protection of DNA damage, the presence of nuclear DNA damage was studied using the alkaline comet assay. The alkaline single cell comet assay primarily detects single-strand DNA breaks (SSDs), alkali-labile sites (base or phosphate alkylations that become strand breaks upon alkali treatment), incomplete excision repair sites and DNA:DNA crosslinking at the level of the individual cell; double-strand breaks (DSBs) are also partially detected [34]. The presence of smeared bands reflects smaller structures that can be correlated to the level of DNA damage. Fig. 4(B–E) shows representative pictures of the effect of LBE treatment on the comet electrophoresis gels for keratinocytes irradiated at 1200 J/m<sup>2</sup>, and Fig. 4A shows the corresponding quantitation of the comet score. The incubation of non-irradiated HaCaT cells with LBE did not significantly change the comet score (Fig. 4C) compared to the control cells (Fig. 4B), suggesting the absence of LBE genotoxicity in the cellular model. In contrast, when keratinocytes were UVB irradiated at 1200 J/m<sup>2</sup>, the comet score was considerably increased (Fig. 4A) and the nucleoid DNA adopted a strong smeared pattern (Fig. 4D). The presence of 100 µg/mL of LBE

reduced UVB-induced DNA damage by 64% ( $p < 0.001$ ) (Figs. 4A and E) compared with the irradiated but untreated cells.

The activated form of H2AX ( $\gamma$ -H2AX) was evaluated to study the potential correlation of a lesser degree of the DNA damage response (DDR) with a lower level of DNA damage in UVB irradiated keratinocytes incubated with LBE. The phosphorylated form of H2AX was assessed in keratinocytes irradiated at 1200 J/m<sup>2</sup> in the presence and absence of increasing LBE concentrations (Fig. 5). As expected, UVB irradiation of HaCaT cells in the absence of LBE led to a remarkable 16-fold increase in H2AX activation compared to non-irradiated cells. The presence of 15 µg/mL of LBE at the moment of irradiation gave rise to a significant decrease in  $\gamma$ -H2AX of almost 50% compared to irradiated cells in the absence of LBE ( $p < 0.01$  or lower). A dose response effect was observed with 60 µg/mL of LBE, whereas no further decrease was detected at the highest LBE concentration tested (100 µg/mL).

### 3.5. LBE promotes endogenous melanin production in melanogenesis cell model

Melanin is one of the main endogenous defenses in human skin against UV radiation, and an increase in melanin production correlates with improved UV radiation protection [12]. Therefore, we explored the ability of LBE to modulate melanin synthesis in a

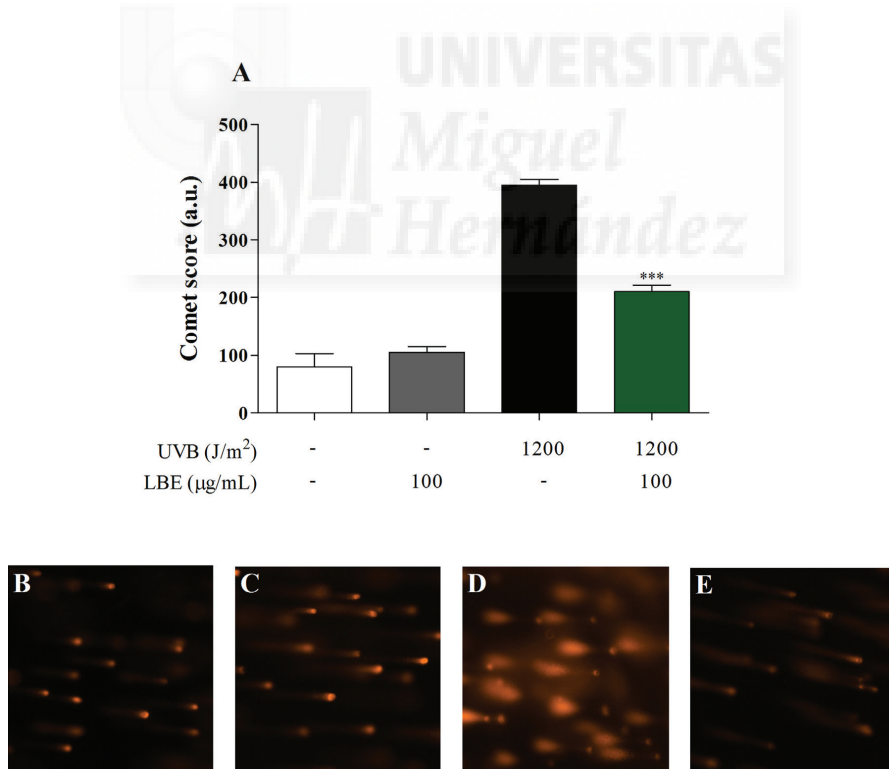


**Fig. 4.** LBE protects HaCaT cells from UVB-induced DNA damage in comet assay (A). Cells were treated with 100 µg/mL LBE and exposed to 1200 J/m<sup>2</sup> of UVB. DNA damage was expressed in arbitrary units and determined as described in Methods section. Pictures are representative of control of non-irradiated HaCaT cells (B), non-irradiated cells in the presence of LBE (C), irradiated cells at 1200 J/m<sup>2</sup> (D) and irradiated cells at 1200 J/m<sup>2</sup> in the presence of LBE (100 µg/mL) (E). The data are expressed as mean ± SD. \*\*\* ( $p < 0.001$ ) indicates significant differences compared with irradiated cells in the absence of LBE.

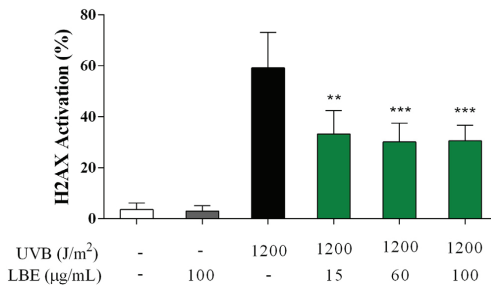


**Fig. 5.** LBE decreases DNA damage response in UVB irradiated HaCaT cells through a reduction of H2AX histone activation. Total damage was expressed as % of activation of H2AX and determined as described in Methods section. The data are expressed as the mean  $\pm$  SD. \*\* ( $p < 0.01$ ) and \*\*\* ( $p < 0.001$ ) indicate significant differences compared to irradiated but non-treated cells.

cell model as a potential contributor to skin photoprotection. Melanin production was determined using the well-established melanogenesis model with B-16 melanoma cells. The cells were incubated in the presence of IBMX, which is a well-known melanogenic compound [35], or increasing concentrations of LBE for 72 h; then, the total melanin (extracellular + intracellular) concentration was determined. As shown in Fig. 6, an increasing trend in total melanin was observed as the concentration of LBE was enhanced, showing a significant difference at 100 µg/mL LBE compared to the control ( $p < 0.01$ ), concentration at which melanin was increased by 40%. The increase was stronger in the intracellular melanin (Supplementary Fig. S2), which exhibited statistically significant differences at 90 and 100 µg/mL LBE compared to the control and achieved >50% increase at the maximum concentration of LBE tested.

#### 4. Discussion

In this study, the capacity of a lemon balm extract to prevent signs of cellular damage induced by UVB was explored. The major compound in LBE was RA (18% w/w), but other phenylpropanoid derivatives were also present (caffeoic acid, salvianolic acid, yunnaneic acid, sagerinic acid and lithospermic acid; Supplementary Fig. S3). Additionally, small amounts of the flavone luteolin-3'

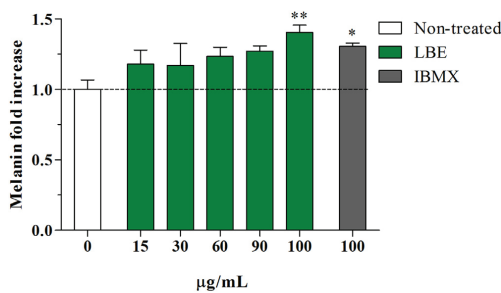


**Fig. 6.** LBE increases melanin synthesis in B16 melanoma cells. Melanin fold increase of B16 cells incubated in the presence of different concentrations of LBE (green bars) compared to control cells (white bar). Grey bar corresponds to the melanogenic inducer IBMX in µM. Data are expressed as the mean  $\pm$  SD. \* ( $p < 0.05$ ) and \*\* ( $p < 0.01$ ) indicate significant differences compared to cells in the absence of LBE (white bar).

O-glucuronide were found. Hence, most of the effects observed must be due to RA and related polyphenols. Our results show that LBE exhibits a higher protective capacity (almost 2-fold protection) than does the equivalent RA concentration in preventing UVB-induced cell death, indicating that other compounds present in the extract at low concentrations significantly contribute to the protective effect. The total polyphenolic content of the extract as measured by the Folin Ciocalteu assay was  $34.04 \pm 0.83$ %. Hence, the rest of the compounds that account for the phenolic content must contribute to the higher preventive effect of the extract. Because LBE revealed stronger photoprotective properties than the pure compound, the extract was selected for studies in the cellular model.

To examine the possible causes that may account for the additional photoprotective properties of LBE compared to RA, the LBE and RA absorption spectra were analyzed and compared (Supplementary Fig. S1). The spectra of both agents (the extract and pure compound) showed two absorption maxima at approximately 285 nm and 325 nm within the ultraviolet B spectra, which was typical for a hydroxycinnamic acid moiety. Thus, the absorption capacity of LBE and RA at this wavelength might contribute to their photoprotective properties. Theoretically, this finding limits the effectiveness of LBE when given orally because low concentrations of polyphenol metabolites must be presumed to reach skin cells. However, plant polyphenols bearing a UV protective capacity in the skin cell model and similar absorption spectra also exhibited efficacy in a human trial [14]. Moreover, higher concentrations could be achieved after topical application of LBE.

UVB radiation has been reported to induce first stage intracellular ROS, such as superoxide radical anions ( $O_2^-$ ),  $H_2O_2$ , and hydroxyl radicals ( $^{\bullet}OH$ ), either directly or through enzyme activation [4,6,7]. Our results using the fluorescent probe H<sub>2</sub>DCF-DA, which is sensitive to the above mentioned ROS and most likely to OH [36], indicated that LBE decreased the intracellular UVB-induced ROS level in a dose-dependent manner with a higher efficacy at high UVB doses (i.e., 1200 J/m<sup>2</sup>), revealing almost 33% protection against ROS-induced damage. ROS are considered inflammatory mediators that function through the activation of NF-κB signaling, which controls the expression of pro-inflammatory cytokines and enzymes such as IL-1β, IL-6, IL-9 and COX-2. Therefore, we postulate that LBE polyphenols may be capable of reducing the inflammatory response concomitant with intracellular ROS generation as reported for RA in several *in vitro* and *in vivo* models [25]. Recently, other polyphenols, such as the flavone naringin, have shown the capacity to protect against UVB-induced p38-mediated keratinocyte apoptosis in a manner correlated with a decrease in intracellular ROS and inflammation [9,37].

Oxidative stress-driven lipid peroxidation is responsible for continuous chromosomal and DNA damage and protein oxidation and is involved in the pathogenesis of several human diseases. Lipid peroxidation has been shown to be generated by UVB-induced ROS, such as OH. Hydroxyl radicals trigger lipoperoxyl radicals (R-OO<sup>•</sup>), which are a class of radical species derived from the oxidation of membrane unsaturated fatty acids, leading to MDA and HNE as the final products. The electrophilic addition of MDA or HNE to DNA guanine bases exerts their mutagenic action not only by forming DNA adducts but also at least partially by compromising the base excision repair pathway [38]. Our results confirmed the capability of LBE to decrease the generation of UVB-induced OH. Therefore, we propose that the extract should contribute to decreased lipid peroxidation and consequently the formation of mutagenic peroxide DNA adducts. We found similar protective behavior using lipophilic antioxidants such as rosemary diterpenes, which avoid the generation of OH induced by ionizing radiation [39]. Using the ORAC assay, which primarily detects the

lipoperoxy radical scavenging capacity [40], we found a high ORAC value for the LBE extract, than those reported for strong antioxidant extracts such as African potato or lemon verbena extract [30,41], which strengthened our hypothesis.

UV light and ionizing radiation induce transient SSBs (initial damage) and DSBs, which are the most dangerous type of DNA damage and lead to cell death, mutations or genome aberrations when incorrectly repaired [42,43]. Cells have evolved repair pathways to detect DNA lesions, signal their presence and promote their repair through the DNA damage response (DDR). The protein kinases ATM (ataxia telangiectasia mutated) and ATR (ataxia telangiectasia and Rad3-related protein) are key DDR-signaling components in mammalian cells. When activated by damaged DNA, these kinases phosphorylate serine 139 of the histone H2A variant H2AX, which acts as a sensor and promotes the recruitment of DDR factors plus other chromatin-modifying components that together promote DNA repair and regulate cell-cycle checkpoints or apoptosis through p53 and checkpoint kinase 1 (CHK1) [44]. UVB irradiation induces H2AX phosphorylation and recruits DDR proteins to CDP and 6-4PP damaged DNA sites, which persist for several hours after irradiation. Resolution of DDR proteins occurs when the nucleotide excision repair system acts. If DNA damage is not repaired and DDR persists, apoptosis usually occurs [43]. The UVB-induced accumulation of γ-H2AX foci results from the collapse of replication forks at unrepaired CPDs, leading to the generation of SSBs and DSBs [4]. In our cellular system, we found a correlation between the level of UVB-induced DNA damage in the alkaline comet assay (probably SSBs, DSBs and alkali-labile sites) and the phosphorylation of histone H2AX as a sign of DDR. The incubation of keratinocytes with LBE at the time of UVB irradiation significantly decreased both DNA damage and γ-H2AX, suggesting that the extract prevented the generation of CDP and 6-4PP photoproducts in the DNA of HaCaT cells and concomitantly less of a DDR arose. Therefore, the ability of LBE to decrease DNA damage and the subsequent activation of the DDR and repair systems suggested that the extract might enable fewer chances for incorrectly repaired DNA or mutations.

The analysis of the composition of the LBE extract used in this study by HPLC-MS highlighted the abundance of RA and its biosynthetically related compounds 3-(3,4-dihydroxyphenyl) lactic acid and salvianolic acid, which was in agreement with previous reports [45,46]. The presence of other cinnamate derivatives, such as the salvianolic, sagerinic, lithospermic and yunnaneic acids, indicates that the predominant secondary metabolic pathway in LBE polyphenols is the phenylpropanoid derivative pathway, which proceeds from phenylalanine via *trans*-*p*-coumaric acid directly to *trans*-caffeic acid. Previous studies have reported the presence of phenolic acids, gallic acid, ellagic acid, flavones and flavonols as major compounds in dichloromethane, ethyl acetate and butanolic fractions derived from lemon balm leaves analyzed by regular HPLC-DAD [46]. However, we have found that phenylpropanoid compounds related to RA, as identified by HPLC-DAD-ESI-IT-MS/MS, were maximized in our extract probably due to the use of acetone extraction in the manufacturing process of the extract.

The exceptional antioxidant, antiinflammatory and cytoprotective capacities of RA in parallel with its effects on cell signaling pathways and gene expression have been thoroughly studied [25]. The capacity of RA to protect human keratinocytes from UVB-induced ROS generation, apoptosis, IL-6 release and DNA breakage have also been reported [29]. Moreover, RA was especially efficient in inhibiting MDA formation *in vitro* [47] and showed a unique capability to penetrate lipid bilayers and protect them from oxidation without disturbing their structure [23]. Therefore, we hypothesize that part of the DNA protective effects of LBE in our cellular system may be due to the capacity of RA to interact with cell membranes and therefore inhibit lipid peroxidation.

In contrast to previous studies, we found a higher protective effect for LBE than for pure RA when both were used at equivalent RA concentrations. The presence of other caffeic acid derivatives structurally related to RA (Supplementary Fig. S3) in the extract may be responsible for this effect. The flavone luteolin also exhibited UV protection activity in cellular models [10,48], but the LBE extract contained only small quantities of this compound. The whole extract is definitely more convenient, less expensive and easier to produce for nutraceutical or nutricosmetic applications. However, the stronger photoprotective activity of LBE compared to RA deserves further attention to identify the compounds responsible for the additional performance of the extract.

Finally, the melanogenic capacity of LBE was studied in a cellular system. The extract showed the capacity to promote melanogenesis as determined by the increase in both intracellular and extracellular melanin in melanoma cells. Flavonoids, such as the flavonols quercetin or kaempferol, and flavones, such as apigenin or luteolin, were reported to promote melanogenesis in a melanoma cell model [49]. Whether the melanogenic capacity of the LBE extract is due to the small quantities of luteolin or other compounds present in the extract requires further research. Regardless, the melanogenic capacity of LBE may be an interesting feature of the extract that should be explored for its application (topically or by oral consumption) as a UV protector.

Theoretically, the relevance of these results is limited by the bioavailability of the bioactive polyphenols in LBE. The physiological concentration of RA and its metabolites in the plasma of rats after oral ingestion was reported to vary within the low micromolar range (1.5–5 μM) [50], which represented an RA concentration of approximately 0.5–1.8 μg/mL; this concentration is below those used in our cell model. However, topical application of RA to rat skin resulted in the percutaneous absorption of RA, which was subsequently distributed in the skin, blood, bone and muscle [51]. Thus, higher concentrations may be achieved in skin tissue.

In summary, the present study demonstrates the higher capacity of LBE compared to pure RA to increase the survival of human keratinocytes upon UVB irradiation, which is reflected in the inhibition of the generation of intracellular ROS and the concomitant decrease in DNA damage. We postulated that the DNA protective capacity of LBE was partially due to a decrease in direct DNA damage and CPD and 6-4PP photoproduct production, leading to a lower level of DNA strand breaks in the comet assay. Additionally, LBE may exert an indirect DNA protective effect through the inhibition of lipid peroxidation triggered by OH. These effects were correlated with a decrease in the DNA damage response that diminished the chances for incorrectly repaired DNA or mutations. Nevertheless, the complete understanding of the molecular mechanism requires further research.

Although the efficacy of the ingredients must be tested topically and by oral ingestion in a human trial, the photoprotective properties of LBE together with its melanogenic capacity suggest its potential as a candidate for the protection of human skin against the deleterious effects of sunlight and will allow the future development of new topical and nutraceutical products.

#### Conflict of interest

The authors declare no conflicts of interest.

#### Acknowledgements

This investigation was supported by project AGL2015-67995-C3-1-R and the Torres-Quevedo (PTQ-14-07243) fellowship to E. Barrajón-Catalán from the Spanish Ministry of Science and Innovation, grants PROMETEO/2012/007 and 2016/006 and VALiD fellowships (ACIF/2010/162 and ACIF/2013/064) from

Generalitat Valenciana (GV) and CIBER (CB12/03/30038, Fisiopatología de la Obesidad y la Nutrición, CIBERobn, Instituto de Salud Carlos III). We thank NUTRAFUR, SL for providing us with the raw materials. We also thank Cristina Ibáñez for her invaluable help with the state of the art bibliographic revision.

## Appendix A. Supplementary data

Supplementary data associated with this article can be found, in the online version, at <http://dx.doi.org/10.1016/j.jdermisci.2016.08.004>.

## References

- [1] J. Krutmann, P. Humbert, Skin aging, in: J.K.A.P. Humbert (Ed.), *Nutrition for Healthy Skin: Strategies for Clinical and Cosmetic Practice*, Springer, Berlin Heidelberg, 2011.
- [2] F. Afq, H. Mukhtar, Botanical antioxidants in the prevention of photocarcinogenesis and photoaging, *Exp. Dermatol.* 15 (2006) 678–684.
- [3] A. Svobodová, J. Psotova, D. Walterová, Natural phenolics in the prevention of UV-induced skin damage. A review, *Biomed. Pap. Med. Fac. Univ. Palacky Olomouc Czech. Repub.* 147 (2003) 137–145.
- [4] J. Cadet, T. Douki, J.L. Ravanat, Oxidatively generated damage to cellular DNA by UVB and UVA radiation, *Photochem. Photobiol.* 91 (2015) 140–155.
- [5] H. Ichihara, T. Ono, The mechanisms of UV mutagenesis, *J. Radiat. Res.* 52 (2011) 115–125.
- [6] D.E. Heck, A.M. Vetrano, T.M. Mariano, J.D. Laskin, UV light stimulates production of reactive oxygen species: unexpected role for catalase, *J. Biol. Chem.* 278 (2003) 22432–22436.
- [7] S.M. Beak, Y.S. Lee, J.A. Kim, NADPH oxidase and cyclooxygenase mediate the ultraviolet B-induced generation of reactive oxygen species and activation of nuclear factor-kappaB in HaCaT human keratinocytes, *Biochimie* 86 (2004) 425–429.
- [8] M.M. Bashir, M.R. Sharma, V.P. Werth, TNF-alpha production in the skin, *Arch. Dermatol. Res.* 301 (2009) 87–91.
- [9] X. Ren, Y. Shi, D. Zhao, M. Xu, X. Li, Y. Tang, et al., Naringin protects ultraviolet B-induced skin damage by regulating p38 MAPK signal pathway, *J. Dermatol. Sci.* 70 (2015).
- [10] Y.P. Hwang, K.N. Oh, H.J. Yun, H.G. Jeong, The flavonoids apigenin and luteolin suppress ultraviolet A-induced matrix metalloproteinase-1 expression via MAPKs and AP-1-dependent signaling in HaCaT cells, *J. Dermatol. Sci.* 61 (2011) 23–31.
- [11] E. Barragón-Catalán, M. Herranz-López, J. Joven, A. Segura-Carretero, C. Alonso-Villaverde, J.A. Menéndez, et al., Molecular promiscuity of plant polyphenols in the management of age-related diseases: far beyond their antioxidant properties, *Adv. Exp. Med. Biol.* 824 (2014) 141–159.
- [12] A. Godic, B. Poljsak, M. Adamic, R. Dahmane, The role of antioxidants in skin cancer prevention and treatment, *Oxid. Med. Cell Longev.* 860479 (2014) 2014.
- [13] M.A. Zaid, F. Afq, D.N. Syed, M. Dreher, H. Mukhtar, Inhibition of UVB-mediated oxidative stress and markers of photoaging in immortalized HaCaT keratinocytes by pomegranate polyphenol extract POMx, *Photochem. Photobiol.* 83 (2007) 882–888.
- [14] A. Pérez-Sánchez, E. Barragón-Catalán, N. Caturla, J. Castillo, O. Benavente-García, M. Alcaraz, et al., Protective effects of citrus and rosemary extracts on UV-induced damage in skin cell model and human volunteers, *J. Photochem. Photobiol. B* 136 (2014) 12–18.
- [15] L.Y. Wu, X.Q. Zheng, J.L. Lu, Y.R. Liang, Protective effect of green tea polyphenols against ultraviolet B-induced damage to HaCaT cells, *Hum. Cell* 22 (2009) 18–24.
- [16] K. Park, J.H. Lee, Protective effects of resveratrol on UVB-irradiated HaCaT cells through attenuation of the caspase pathway, *Oncol. Rep.* 19 (2008) 413–417.
- [17] H. Wei, X. Zhang, Y. Wang, M. Lebwohl, Inhibition of ultraviolet light-induced oxidative events in the skin and internal organs of hairless mice by isoflavone genistein, *Cancer Lett.* 185 (2002) 21–29.
- [18] Y. Wang, X. Zhang, M. Lebwohl, V. Deleo, H. Wei, Inhibition of ultraviolet B (UVB)-induced c-fos and c-jun expression in vivo by a tyrosine kinase inhibitor genistein, *Carcinogenesis* 19 (1998) 649–654.
- [19] W. Guo, A. An, L. Jiang, C. Geng, L. Zhong, The protective effects of hydroxytyrosol against UVB-induced DNA damage in HaCaT cells, *Phytother. Res.* 24 (2010) 352–359.
- [20] B.S. Weeks, Formulations of dietary supplements and herbal extracts for relaxation and anxiolytic action: relarian, *Med. Sci. Monit.* 15 (2009) RA256–RA262.
- [21] P. Schnitzler, A. Schuhmacher, A. Astani, J. Reichling, *Melissa officinalis* oil affects infectivity of enveloped herpesviruses, *Phytomedicine* 15 (2008) 734–740.
- [22] A. Madisch, G. Holtmann, G. Mayr, B. Vinson, J. Hotz, Treatment of functional dyspepsia with a herbal preparation. A double-blind, randomized, placebo-controlled, multicenter trial, *Digestion* 69 (2004) 45–52.
- [23] O. Fadel, K. El Kirat, S. Morandat, The natural antioxidant rosmarinic acid spontaneously penetrates membranes to inhibit lipid peroxidation in situ, *BBA Biophys.* 1808 (2011) 2973–2980.
- [24] M. Hancianu, A.C. Aprotosoaie, E. Gilie, A. Poiata, C. Tuchilus, A. Spac, et al., Chemical composition and in vitro antimicrobial activity of essential oil of *Melissa officinalis* L. from Romania, *Rev. Med. Chir. Soc. Med. Nat. Iasi* 112 (2008) 843–847.
- [25] S.K. Amoah, L.P. Sandjo, J.M. Kratz, M.W. Biavatti, Rosmarinic acid – pharmaceutical and clinical aspects, *Planta Med.* (2016), doi:<http://dx.doi.org/10.1055/s-0035-1568274>.
- [26] J.P. Kamdem, A. Adeniran, A.A. Boligon, C.V. Klimaczewski, O.O. Elekofehinti, W. Hassan, et al., Antioxidant activity, genotoxicity and cytotoxicity evaluation of lemon balm (*Melissa officinalis* L.) ethanolic extract: its potential role in neuroprotection, *Ind. Crop Prod.* 51 (2013) 26–34.
- [27] E. Skotti, E. Anastassi, K. Kanellou, M. Polissiou, P.A. Tarantilis, Total phenolic content: antioxidant activity and toxicity of aqueous extracts from selected Greek medicinal and aromatic plants, *Ind. Crop Prod.* 53 (2014) 46–54.
- [28] A. Zeraatpishe, S. Oryan, M.H. Bagheri, A.A. Pilevarian, A.A. Malekiрад, M. Baeri, et al., Effects of *Melissa officinalis* L. on oxidative status and DNA damage in subjects exposed to long-term low-dose ionizing radiation, *Toxicol. Ind. Health* 27 (2011) 205–212.
- [29] J. Vostalová, A. Zdrálová, A. Svobodová, *Prunella vulgaris* extract and rosmarinic acid prevent UVB-induced DNA damage and oxidative stress in HaCaT keratinocytes, *Arch. Dermatol. Res.* 302 (2010) 171–181.
- [30] O. Laporta, L. Pérez-Fons, R. Mallavia, N. Caturla, V. Micó, Isolation, characterization and antioxidant capacity assessment of the bioactive compounds derived from *Hypoxis rooperi* corm extract (African potato), *Food Chem.* 101 (2007) 1425–1437.
- [31] E. Barragón-Catalán, S. Fernández-Arroyo, D. Saura, E. Guillén, A. Fernandez-Gutiérrez, A. Segura-Carretero, et al., *Cistaceae* aqueous extracts containing ellagitannins show antioxidant and antimicrobial capacity, and cytotoxic activity against human cancer cells, *Food Chem. Toxicol.* 48 (2010) 2273–2282.
- [32] L. Pérez-Fons, M.T. Garzon, V. Micó, Relationship between the antioxidant capacity and effect of rosemary (*Rosmarinus officinalis* L.) polyphenols on membrane phospholipid order, *J. Agric. Food Chem.* 58 (2016) 161–171.
- [33] A. Heitz, A. Carnat, D. Fraisse, A.P. Carnat, J.L. Lamaison, Luteolin 3'-glucuronide, the major flavonoid from *Melissa officinalis* subsp. *officinalis*, *Fitoterapia* 71 (2000) 201–202.
- [34] R.R. Tice, G.H. Strauss, The single cell gel electrophoresis/comet assay: a potential tool for detecting radiation-induced DNA damage in humans, *Stem Cells* 13 (Suppl. 1) (1995) 207–214.
- [35] J. Lee, Y.S. Kim, D. Park, Rosmarinic acid induces melanogenesis through protein kinase A activation signaling, *Biochem. Pharmacol.* 74 (2007) 960–968.
- [36] C.P. Lebel, H. Ischiropoulos, S.C. Bondy, Evaluation of the probe 2',7'-dichlorofluorescein as an indicator of reactive oxygen species formation and oxidative stress, *Chem. Res. Toxicol.* 5 (1992) 227–231.
- [37] D. Peus, R.A. Vasa, A. Beyerle, A. Meves, C. Krautmacher, M.R. Pittelkow, UVB activates ERK1 and p38 signaling pathways via reactive oxygen species in cultured keratinocytes, *J. Invest. Dermatol.* 112 (1999) 751–756.
- [38] A. Winczura, A. Czubaty, K. Winczura, K. Maslowska, M. Nalecz, D.A. Dudzinska, et al., Lipid peroxidation product 4-hydroxy-2-nonenal modulates base excision repair in human cells, *DNA Repair (Amst.)* 22 (2014) 1–11.
- [39] M. Alcaraz, C. Acevedo, J. Castillo, O. Benavente-García, D. Armero, V. Vicente, et al., Liposomal antioxidants provide an effective radioprotective barrier, *Br. J. Radiol.* 82 (2009) 605–609.
- [40] D. Huang, O.U. Boxin, R.L. Prior, The chemistry behind antioxidant capacity assays, *J. Agric. Food Chem.* 53 (2005) 1841–1856.
- [41] L. Funés, S. Fernández-Arroyo, O. Laporta, A. Pons, E. Roche, A. Segura-Carretero, et al., Correlation between plasma antioxidant capacity and verbascoside levels in rats after oral administration of lemon verbena extract, *Food Chem.* 117 (2009) 589–598.
- [42] S.P. Jackson, J. Bartek, The DNA-damage response in human biology and disease, *Nature* 461 (2009) 1071–1078.
- [43] K.S. Oh, M. Bustin, S.J. Mazur, E. Appella, K.H. Kraemer, UV-induced histone H2AX phosphorylation and DNA damage related proteins accumulate and persist in nucleotide excision repair-deficient XP-B cells, *DNA Repair (Amst.)* 10 (2011) 5–15.
- [44] O. Fernandez-Capetillo, A. Lee, M. Nussenzweig, A. Nussenzweig, H2AX: the histone guardian of the genome, *DNA Repair* 3 (2004) 959–967.
- [45] T.L. Miron, M. Herrero, E. Ibáñez, Enrichment of antioxidant compounds from lemon balm (*Melissa officinalis*) by pressurized liquid extraction and enzyme-assisted extraction, *J. Chromatogr. A* 1288 (2013) 1–9.
- [46] R.P. Pereira, A.A. Boligon, A.S. Appel, R. Fachinetto, C.S. Ceron, J.E. Tanus-Santos, et al., Chemical composition: antioxidant and anticholinesterase activity of *Melissa officinalis*, *Ind. Crop Prod.* 53 (2014) 34–45.
- [47] M. Sanchez-Campillo, J.A. Gabaldón, J. Castillo, O. Benavente-García, M.J. Del Bano, M. Alcaraz, et al., Rosmarinic acid: a photo-protective agent against UV and other ionizing radiations, *Food Chem. Toxicol.* 47 (2009) 386–392.
- [48] S.H. Lim, S.K. Jung, S. Byun, E.J. Lee, J.A. Hwang, S.G. Seo, et al., Luteolin suppresses UVB-induced photoaging by targeting JNK1 and p90 RSK2, *J. Cell. Mol. Med.* 17 (2013) 672–680.
- [49] S. Takekoshi, H. Nagata, K. Kitatani, Flavonoids enhance melanogenesis in human melanoma cells, *Tokai J. Exp. Clin. Med.* 39 (2014) 116–121.
- [50] S. Baba, N. Osakabe, M. Natsume, J. Terao, Orally administered rosmarinic acid is present as the conjugated and/or methylated forms in plasma, and is degraded and metabolized to conjugated forms of caffeic acid, ferulic acid and m-cumaric acid, *Life Sci.* 75 (2004) 165–178.
- [51] W.A. Ritschel, A. Starzacher, A. Sabouni, A.S. Hussain, H.P. Koch, Percutaneous absorption of rosmarinic acid in the rat, *Methods Find. Exp. Clin. Pharmacol.* 11 (1989) 345–352.



# Cell Cycle

ISSN: 1538-4101 (Print) 1551-4005 (Online) Journal homepage: <http://www.tandfonline.com/loi/kccy20>

## STAT3-targeted treatment with silibinin overcomes the acquired resistance to crizotinib in ALK-rearranged lung cancer

Elisabet Cuyàs, Almudena Pérez-Sánchez, Vicente Micol, Javier A. Menendez & Joaquim Bosch-Barrera

To cite this article: Elisabet Cuyàs, Almudena Pérez-Sánchez, Vicente Micol, Javier A. Menendez & Joaquim Bosch-Barrera (2016) STAT3-targeted treatment with silibinin overcomes the acquired resistance to crizotinib in ALK-rearranged lung cancer, *Cell Cycle*, 15:24, 3413-3418, DOI: [10.1080/15384101.2016.1245249](https://doi.org/10.1080/15384101.2016.1245249)

To link to this article: <http://dx.doi.org/10.1080/15384101.2016.1245249>



Accepted author version posted online: 18 Oct 2016.  
Published online: 18 Oct 2016.



Submit your article to this journal 



Article views: 190



View related articles 



View Crossmark data 



Citing articles: 1 View citing articles 

Full Terms & Conditions of access and use can be found at  
<http://www.tandfonline.com/action/journalInformation?journalCode=kccy20>

REPORT

## STAT3-targeted treatment with silibinin overcomes the acquired resistance to crizotinib in ALK-rearranged lung cancer

Elisabet Cuyàs<sup>a,b</sup>, Almudena Pérez-Sánchez<sup>c</sup>, Vicente Micol<sup>c</sup>, Javier A. Menendez<sup>a,b</sup>, and Joaquim Bosch-Barrera <sup>b,d,e</sup>

<sup>a</sup>Program Against Cancer Therapeutic Resistance (ProCURE), Metabolism and Cancer Group, Catalan Institute of Oncology, Girona, Catalonia, Spain;

<sup>b</sup>Molecular Oncology Group, Girona Biomedical Research Institute (IDIBGI), Girona, Spain; <sup>c</sup>Molecular and Cell Biology Institute, Miguel Hernández University, Elche, Spain; <sup>d</sup>Department of Medical Oncology, Catalan Institute of Oncology, Girona, Catalonia, Spain; <sup>e</sup>Department of Medical Sciences, Medical School, University of Girona, Girona, Spain

### ABSTRACT

The signal transducer and activator of transcription 3 (STAT3) has been suggested to play a prominent role in mediating non-small-cell lung cancer (NSCLC) resistance to some tyrosine kinase inhibitor (TKI)-mediated therapies. Using a model of anaplastic lymphoma kinase gene (ALK)-translocated NSCLC with acquired resistance to the ALK TKI crizotinib, but lacking amplifications or mutations in the kinase domain of ALK, we herein present evidence that STAT3 activation is a novel mechanism of crizotinib resistance that involves the upregulation of immune escape and epithelial to mesenchymal transition (EMT) signaling pathways. Taking advantage of the flavonolignan silibinin as a naturally occurring STAT3-targeted pharmacological inhibitor, we confirmed that STAT3 activation protects ALK-translocated NSCLC from crizotinib. Accordingly, silibinin-induced inhibition of STAT3 worked synergistically with crizotinib to reverse acquired resistance and restore sensitivity in crizotinib-resistant cells. Moreover, silibinin treatment significantly inhibited the upregulation of the immune checkpoint regulator PD-L1 and also EMT regulators (e.g., SLUG, VIM, CD44) in crizotinib-refractory cells. These findings provide a valuable strategy to potentially improve the efficacy of ALK inhibition by cotreatment with silibinin-based therapeutics, which merit clinical investigation for ALK TKI-resistant NSCLC patients.

### ARTICLE HISTORY

Received 19 September 2016

Revised 28 September 2016

Accepted 30 September 2016

### KEYWORDS

ALK; crizotinib; EMT; lung cancer; silibinin; STAT3

### Introduction

Genetic abnormalities with “driver” characteristics have been extensively reported in several distinct subsets of non-small-cell lung cancer (NSCLC). Among these rare genetic changes, transforming rearrangements in the anaplastic lymphoma kinase gene (ALK) are present in about 2–5% of NSCLC tumors. The most often encountered rearrangement is an inversion of chromosome 2 leading to the fusion of ALK with echinoderm microtubule-associated protein like 4 (EML4), which results in the abnormal expression and activation of ALK in the cytoplasm of NSCLC cells.<sup>1</sup>

Patients with ALK-EML4 translocation obtain clinical benefit from molecularly targeted therapy with precision ALK tyrosine kinase inhibitors (TKIs). Crizotinib, a first-in-class multitargeting TKI with activity against ALK, c-MET, and ROS1, is particularly effective in ALK-rearranged NSCLC, resulting in a median progression-free survival of 6–10 months and an overall survival of nearly 75% at one year.<sup>2</sup> Unfortunately, despite the dramatic and prolonged responses with low toxicity, systemic acquired resistance invariably develops over time and the median progression-free survival does not exceed 11 months in crizotinib-treated ALK-positive NSCLC patients.<sup>3</sup> Intriguingly, while ALK TK mutations appear to be major determinants of acquired resistance to crizotinib, over 2

thirds of cases of ALK-rearranged NSCLC with acquired resistance to crizotinib lack kinase mutations. Accordingly, several studies have revealed that ALK-rearranged tumors activate other oncogene kinases (e.g., HERs) to circumvent the inhibition of ALK phosphorylation conferred by crizotinib and more potent TKIs, thereby maintaining the downstream PI3K/AKT and ERK/MAPK signals in the presence of TKIs.<sup>4–8</sup> Using a model of ALK-translocated NSCLC with acquired resistance to crizotinib, but lacking amplifications or mutations in the kinase domain of ALK, we here evaluated the molecular and therapeutic relevance of signal transducer and activator of transcription 3 (STAT3) as a nongenetic mechanism mediating crizotinib resistance in ALK-rearranged tumors.

### Results

#### ALK-rearranged NSCLC cells with acquired resistance to crizotinib exhibit crizotinib-unresponsive hyperactivation of STAT3

Because constitutive ALK activation results in tumorigenic activity through activation not only of PI3K/AKT and ERK1/2/MAPK but also of STAT3 signaling, we envisioned that if acquisition of crizotinib resistance was accompanied by

changes in STAT3 activity, then therapies targeted to STAT3 might be effective to overcome crizotinib resistance in *ALK*-rearranged NSCLC. To test this hypothesis, we utilized the crizotinib-responsive NSCLC cell line H3122, which harbors the fusion variant *EML4-ALK* E13; A20, and a derived resistant variant capable of growth in the presence of 1  $\mu\text{mol/L}$  crizotinib (H3122/CR) but lacking amplification or mutations in the kinase domain of *ALK*.<sup>9</sup>

To characterize the relationship between crizotinib resistance and STAT3 signaling, we measured the phosphorylation status of STAT3 at Tyr705, which is known to induce its activation via dimerization, nuclear translocation, and DNA binding. Using a commercially available solid phase enzyme-linked immunosorbent assay (ELISA) that specifically detects endogenous phospho-STAT3<sup>Tyr705</sup> protein, we observed a marked induction ( $\sim$ 3-fold) of phospho-STAT3<sup>Tyr705</sup> expression in crizotinib-refractory H3122/CR cells relative to crizotinib-responsive H3122 parental cells (Fig. 1A). To establish a causal relationship between the activation of STAT3 and the acquisition of resistance to crizotinib, we examined the effect of crizotinib on STAT3 signaling in crizotinib-sensitive and resistant H3122 cells. We found that STAT3 activity was significantly lower in crizotinib-sensitive H3122 cells than in resistant cells (80% reduction in the presence of 0.2  $\mu\text{mol/L}$  crizotinib). Although an equimolar concentration of crizotinib reduced the expression of phospho-STAT3<sup>Tyr705</sup> by 40–45% in H3122/CR cells, it failed to return STAT3 activation to the baseline levels found in crizotinib-sensitive H3122 cells. Consequently, the residual activation of STAT3 in crizotinib-treated H3122/CR cells remained significantly higher (1.5-fold) than that observed in crizotinib-responsive cells (Fig. 1A). These results expand earlier findings by Tanizaki et al.,<sup>8</sup> who showed that inhibition of STAT3 phosphorylation by the ALK inhibitor NVP-TAE684 in crizotinib-responsive H3122 cells was largely prevented in H3122 cells with acquired resistance to TAE684. These findings suggested that inhibition of STAT3 signaling is a potential therapeutic strategy to overcome the acquired resistance to ALK inhibitors in *ALK*-rearranged NSCLC cells.

#### **Silibinin deactivates STAT3 in ALK TKI-sensitive and -resistant NSCLC cells**

We have recently reviewed the effects of silibinin, a natural polyphenolic flavonoid isolated from seed extracts of milk thistle (*Silybum marianum*), and concluded that its robust preclinical activity against diverse human cancer types including NSCLC can be explained, at least in part, by its capacity to operate as a *bona fide* STAT3-targeted inhibitor.<sup>10</sup> To examine whether STAT3-targeting by the flavonolignan silibinin could overcome NSCLC acquired resistance to crizotinib, we tested its effect on crizotinib sensitivity of *ALK*-rearranged NSCLC cells. Silibinin dose-dependently blocked STAT3 activation in both parental and crizotinib-resistant H3122 cells at 24 and 48 h (Fig. 1B). Although crizotinib-refractory H3122/CR cells experienced a delay of 24 h in achieving the same degree of STAT3 inhibition as that observed in H3122 cells treated with silibinin, it appeared that the mechanism underlying crizotinib-unresponsive STAT3 hyperactivation did not preclude the

ability of silibinin to fully inhibit STAT3 activity in crizotinib-resistant H3122/CR cells.

We next assessed the effect of silibinin-induced inhibition of STAT3 for apoptosis of parental and resistant cells. Using a cell death ELISA to measure DNA fragmentation and histone release by apoptotic cells, we found that the extent of apoptosis in H3122/CR cells by high concentrations of silibinin was significantly greater (up to  $\sim$ 3 fold) than that induced by silibinin in crizotinib-sensitive H3122 cells (Fig. 1C). These findings strongly suggest that H3122/CR cells use STAT3 signaling to engage anti-apoptotic survival mechanisms. Consistent with this notion, the silibinin IC<sub>50</sub> in H3122/CR cells (63  $\pm$  10  $\mu\text{mol/L}$ ) was moderately less than the silibinin IC<sub>50</sub> of crizotinib-sensitive H3122 cells (76  $\pm$  13  $\mu\text{mol/L}$ ).

#### **Silibinin synergistically reverses acquired resistance to crizotinib**

We evaluated the tumocidal potential of combining crizotinib and silibinin in H3122/CR cells. The IC<sub>50</sub> of crizotinib for the inhibition of cell viability of H3122 cells was 0.27  $\mu\text{mol/L}$ , whereas it was almost 3-fold higher for crizotinib-resistant H3122/CR cells (Fig. 1D, left). Remarkably, cell viability was significantly more inhibited by combined silibinin and crizotinib treatment when compared with either agent on its own in crizotinib-resistant H3122/CR but not in crizotinib-sensitive H3122 cells. Accordingly, whereas combined treatment with crizotinib and 50  $\mu\text{mol/L}$  silibinin modestly decreased the crizotinib IC<sub>50</sub> value by 1.5-fold in crizotinib-sensitive H3122 cells, co-treatment reduced the crizotinib IC<sub>50</sub> value by more than 5-fold in H3122/CR cells (Fig. 1D, left). These results indicate that silibinin-induced suppression of STAT3 hyperactivation generates a crizotinib-hypersensitive phenotype in crizotinib-resistant H3122/CR cells. To confirm the ability of STAT3-targeted silibinin treatment to overcome the acquired resistance to crizotinib in *ALK*-rearranged lung cancer, we explored the effect of silibinin on the long-term proliferative ability of H3122 and H3122/CR cells grown in the presence of crizotinib. The immediate and highly significant arrest in growth observed in crizotinib treated H3122 cells was followed by a conspicuous late burst of cell proliferation, illustrating the rapid adaption of *ALK*-rearranged NSCLC cells to crizotinib exposure. Importantly, silibinin fully abolished the late proliferative burst of H3122 parental cells exposed to crizotinib (Fig. 1D, right). Moreover, long-term co-exposure to silibinin promoted cytostatic and cytotoxic effects in H3122/CR cells, which likewise demonstrated their ability to proliferate in the presence of crizotinib (Fig. 1D, right).

#### **Silibinin suppresses the activation of PD-L1/EMT in crizotinib-resistant NSCLC cells**

It has been recently reported that upregulation of the immuno-regulatory protein, programmed cell death ligand 1 (PD-L1), might mediate immune escape in *ALK*-positive NSCLC tumor cells.<sup>11</sup> We therefore assessed how silibinin might affect PD-L1 expression in crizotinib-sensitive and -resistant NSCLC cells. Quantitative real-time PCR analysis revealed that PD-L1 expression was markedly ( $\sim$ 4-fold) higher in H3122/CR cells

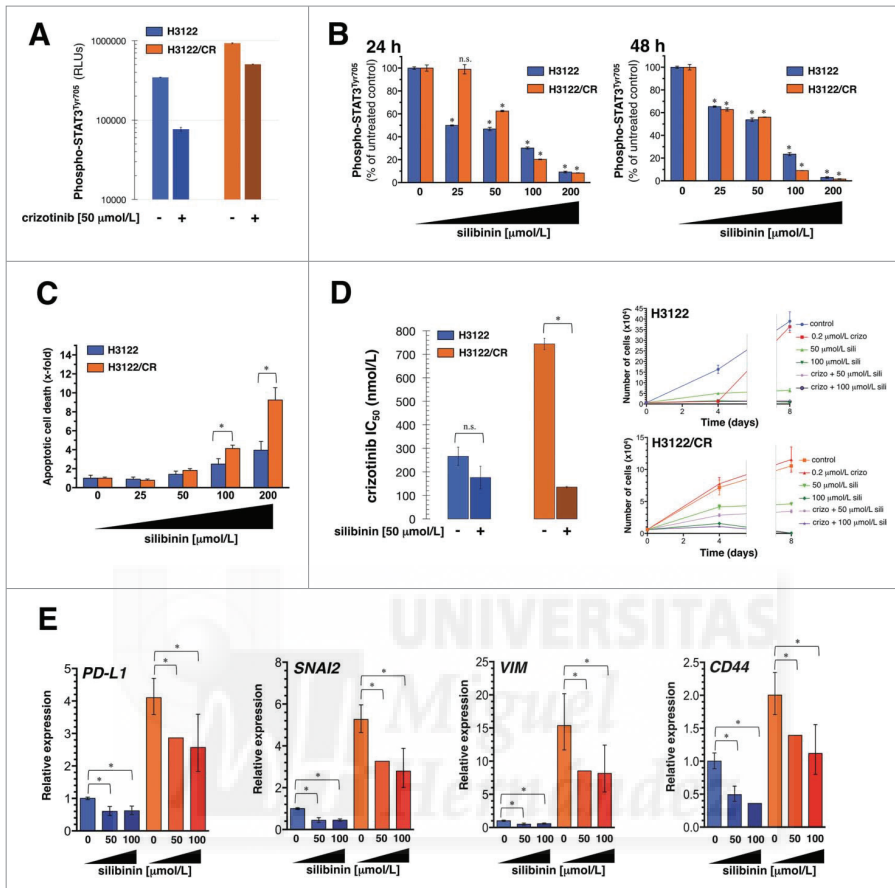


**Figure 1.** Silibinin reverts STAT3-driven acquired resistance to crizotinib in ALK-rearranged NSCLC cells. (A) H3122 and H3122/CR cells were treated with 0.2 μmol/L crizotinib for 48 h. Whole cell lysates were subjected to phospho-STAT3<sup>Tyr705</sup> ELISA. Results are expressed in relative light units (RLU) and represent the mean (columns) ± SD (bars) of 2 independent experiments performed in duplicate. (B) H3122 and H3122/CR cells were treated with graded concentrations of silibinin for 24 and 48 h. Whole cell lysates were subjected to phospho-STAT3<sup>Tyr705</sup> ELISA. Results are expressed as the % of phospho-STAT3<sup>Tyr705</sup> expression relative to untreated controls and represent the mean (columns) ± SD (bars) of 2 independent experiments performed in duplicate (n.s., non-significant differences were identified by ANOVA followed by Scheffé's multiple contrasts; \*P < 0.01 relative to control cells by ANOVA followed by Scheffé's multiple contrasts) (C) Quantification of apoptosis-related cell death in H3122 and H3122/CR cells in response to 48 h treatment with graded concentrations of silibinin was determined as described in "Materials and methods." Results are shown as mean (columns) ± SD (error bars) from at least 2 experiments in which duplicate wells were analyzed (\*P < 0.01 relative to control cells by Student's t test for paired values) (D) Left: Cell viability of H3122 and H3122/CR cells cultured with graded concentrations of crizotinib was assessed using an MTT assay. Concentrations causing 50% reduction in cell viability (IC<sub>50</sub> values) were calculated in the absence or presence of 50 μmol/L silibinin (n.s., non-significant differences were identified by Student's t test for paired values; \*P < 0.01 relative to control cells by Student's t test for paired values). Right: H3122 and H3122/CR cells were plated in 24-well plates at 5,000 cells/well and treated with crizotinib, silibinin or crizotinib plus silibinin as specified. The data presented are mean of number of cells × 10<sup>3</sup>/well (columns) ± SD (bars). All assays were performed at least 2 times in triplicate. (E) Total RNA from H3122 and H3122/CR cells cultured in the absence or presence of graded concentrations of silibinin was characterized in technical triplicates for the relative abundance of PD-L1, SNAI2 (SLUG), VIM, and CD44. The transcript abundance was calculated using the delta Ct method and presented as fold-change vs. basal expression in H3122 parental cells. \*P < 0.01 relative to untreated control cells by ANOVA followed by Scheffé's multiple contrasts.

than in H3122 cells (Fig. 1E, left). Treatment with silibinin significantly downregulated the high baseline levels of PD-L1 expression in crizotinib-sensitive H3122 cells<sup>11</sup> and significantly inhibited the up-regulation of PD-L1 in H3122/CR cells.

Given the molecular and clinical correlation between high expression of immune checkpoint regulators such as PD-L1 and the activation of mesenchymal markers following epithelial to mesenchymal transition (EMT) phenomena,<sup>12–18</sup> we finally

questioned whether silibinin, which has been shown to regulate the EMT program,<sup>19–21</sup> might affect the close relationship between EMT and immune escape signaling pathways for acquired resistance to crizotinib. Interestingly, silibinin's ability to downregulate PD-L1 expression was accompanied by the parallel downregulation of the EMT markers SNAI2 (SLUG), VIM, and CD44, all of which were significantly upregulated in crizotinib-resistant H3122/CR cells (Fig. 1E, right).

## Discussion

Crizotinib received Food and Drug Administration approval in 2011 for the treatment of metastatic NSCLC that is positive for *ALK* rearrangements. However, systemic acquired resistance remains the main limitation to prolonged clinical efficacy of crizotinib in patients with *ALK*-positive NSCLC. It is therefore important to understand crizotinib resistance mechanisms and to identify potential therapeutic strategies against this resistance. Our present results show that STAT3 activation plays an important role in the acquisition of resistance to pathway-targeted drug therapies such as crizotinib,<sup>8,22</sup> a STAT3-centered mechanism that appears to involve the concomitant upregulation of immune escape and EMT signaling pathways in *ALK*-positive NSCLC cells.

First, in our present study, we confirm that crizotinib treatment represses STAT3 activation in crizotinib-sensitive NSCLC cells,<sup>8,23,24</sup> but not in crizotinib-resistant cells. Second, we show that inhibition of STAT3 with the flavonolignan silibinin markedly inhibits cellular growth of *ALK*-positive NSCLC cells with acquired resistance to crizotinib, which is associated with significant apoptotic cell death. Third, we provide evidence that STAT3 activation forms part of the intrinsic mechanisms that control the expression of the immunoregulatory ligand PD-L1. Because PD-L1 upregulation represents an innate immune resistance mechanism in *ALK*-positive NSCLC and blockade of PD-L1 may be a promising optional treatment for NSCLC patients with resistance to crizotinib,<sup>11</sup> our present findings showing for the first time that silibinin significantly downregulates PD-L1 opens new horizons for the therapeutic use of silibinin to increase the immunogenicity of *ALK*-positive NSCLC. Fourth, given the close correlation between EMT and immune escape in driving cancer aggressiveness and therapeutic resistance,<sup>12-18,25</sup> the capacity for silibinin to "switch-off" signals expressed by tumor cells to escape the immune system (e.g., PD-L1) while also reducing the expression of EMT-associated core genes (e.g., vimentin, Slug) strongly suggests that the combination of silibinin with new immunotherapeutic agents, such as checkpoint blockers, may be particularly useful for the treatment of *ALK*-positive NSCLC with the most mesenchymal (EMT) features.

Because crizotinib-resistant H3122/CR cells have been found to significantly hyperactivate the epidermal growth factor receptor (EGFR),<sup>9</sup> it appears reasonable to suggest that STAT3 might operate as a signaling molecule activated specifically and persistently by overactivated EGFR in crizotinib-resistant cells, but not by normal levels of EGFR activity in crizotinib-sensitive cells. If activation of the EGFR-STAT3 signaling axis is confirmed as a predominant mechanism of acquired cross-resistance to first- and second generation *ALK* TKIs (e.g., crizotinib, ceritinib, alectinib),<sup>26,27</sup> the use of silibinin as a STAT3-targeted treatment *plus* *ALK*/EGFR TKIs could be explored to clinically manage the *ALK*-rearranged cohort of NSCLC patients. However, we are aware that the use of one cell system (i.e., H3122 vs. H3122/CR cells) represents a great limitation of our study; further work using series of *ALK* TKI-resistant patient-derived cell lines is needed before proposing activation of STAT3 as a major nongenetic mechanism that drives *ALK* TKIs resistance.<sup>28</sup> Moreover, it remains to be

established whether in the absence of STAT3 hyperactivation, the occurrence of acquired resistance to crizotinib might remain sensitive to silibinin. We are currently exploring the STAT3-independent capability of silibinin to circumvent EMT-related crizotinib resistance in *ALK*-rearranged NSCLC cells.<sup>29</sup>

Our present findings highlight the potential of STAT3-targeted treatment with silibinin as a therapeutic strategy with an alternative mechanism of action to overcome crizotinib resistance in *ALK*-rearranged lung cancer. We have recently reported the first evidence that an oral nutraceutical product containing silibinin has significant clinical efficacy against brain metastasis in NSCLC patients.<sup>30</sup> Although further studies are needed, we believe that these encouraging results should drive the translation of the experimental crizotinib-silibinin combination to the clinical setting to assess and profile the safety and efficacy of crizotinib plus silibinin in overcoming the acquired resistance to crizotinib in *ALK*-rearranged lung carcinomas.

## Materials and methods

### Reagents

Crizotinib was kindly provided by Pfizer. Silibinin was purchased from Sigma-Aldrich (St. Louis, MO). All reagents were dissolved in dimethylsulfoxide (DMSO) to prepare 10 mmol/L stock solutions, which were stored at -80°C until use.

### Cell culture

NCI-H3122 (H3122) cells, which harbor *EML4-ALK* E13; A20 and are dependent on *ALK* signaling, were made resistant to crizotinib by incremental and continuous exposure to crizotinib. H3122/crizotinib-resistant (CR) cell derivation, sequencing of *ALK*, and evaluation of DNA copy numbers has been described elsewhere.<sup>9</sup>

### Cell viability

Cell viability effects of crizotinib and silibinin were determined using the standard colorimetric MTT reduction assay. Dose-response curves were plotted as a percentage of the control cell absorbance, which was obtained from control wells containing the vehicle (DMSO) processed simultaneously. For each treatment, cell viability was evaluated as a percentage using the following equation: (OD<sub>570</sub> of the treated sample/OD<sub>570</sub> of the untreated sample) × 100. Sensitivity to agents was expressed in terms of the concentrations required for 50% (IC<sub>50</sub>) reduction of cell viability. Since the percentage of control absorbance was considered to be the surviving fraction of cells, the IC<sub>50</sub> values were defined as the concentration of drug that produced 50% reduction in control absorbance (by interpolation).

### STAT3 elisa

Cells were treated with crizotinib or silibinin for 48 h. Cells were harvested and equivalent aliquots of protein were subjected to a PathScan® phospho-Stat3 (Tyr705) sandwich ELISA (Cell Signaling Technology, Danvers, MA) following the manufacturer's instructions.

### Apoptosis assay

Apoptosis was assessed using the Cell Death Detection ELISA<sup>PLUS</sup> Kit from Roche Diagnostics (Barcelona, Spain). Briefly, cells ( $5-10 \times 10^3$  cells per well) were grown in 96-well plates and treated in triplicate with the indicated doses of silibinin for 48 h. Pelleted cells were treated with lysis buffer for 30 min at room temperature. Anti-histone biotin and anti-DNA peroxidase antibodies were then added to each well followed by incubation at room temperature for 2 h. After three washes, the peroxidase substrate was added to each well, and the plates were read at 405 nm at multiple time intervals. The enrichment of histone-DNA fragments in treated cells was expressed as the fold increase in absorbance relative to control (vehicle-treated) cells using the following formula:  $[A_{405} - A_{490}]_{\text{TREATED}} / [A_{405} - A_{490}]_{\text{UNTREATED}}$

### Cell proliferation assays

Semi-confluent H3122 and H3122/CR cultures were trypsinized and cells were seeded into 24-well plates at a density of 5,000 cells/well. Cells were allowed to attach for 18 h, after which time a 0-time point measurement was determined. Cells were then cultured in standard medium containing 5% serum in the absence or presence of crizotinib, silibinin, and crizotinib plus silibinin and counted at day 2, 4, and 8 using a Coulter Counter (Coulter Electronics, Inc., Hialeah, FL). All assays were performed at least 3 times in duplicate.

### Quantitative real-time polymerase chain reaction (qRT-PCR)

Total RNA was extracted from cell cultures using the Qiagen RNeasy Kit and QIAshredder columns according to the manufacturer's instructions. One microgram of total RNA was reverse-transcribed to cDNA using the Reaction Ready<sup>TM</sup> First Strand cDNA Synthesis Kit (SABiosciences, Frederick, MD) and applied to a customized PCR array (96-well format) containing the following panel of genes: *PD-L1*, *SLUG*, *VIM*, and *CD44*. The arrays were processed according to the SABiosciences RT-PCR manual and analyzed using an Applied Biosystems 7500 Fast Real-Time PCR System with an automated baseline and threshold cycle detection. The data were interpreted using the web-based PCR array analysis tool from SABiosciences.

### Disclosure of potential conflicts of interest

No potential conflicts of interest were disclosed.

### Acknowledgments

We are greatly indebted to Prof. Daniel B. Costa (Beth Israel Deaconess Medical Center, Harvard Medical School, Boston, MA, USA) for providing the H3122 and H3122/CR cells used in this work. Joaquim Bosch-Barrera and Javier A. Menendez thank a charity collection organized by Fundació Roses Contra el Càncer (Roses, Girona, Catalonia) that allowed this line of research to be initiated in 2011. The authors would like to thank Dr. Kenneth McCreathe for editorial support.

### Funding

This work was supported by grants from the Ministerio de Ciencia e Innovación (Grant SAF2012-38914), Plan Nacional de I+D+I, Spain and the Agència de Gestió d'Ajuts Universitaris i de Recerca (AGAUR) (Grant 2014 SGR229), Departament d'Economia i Coneixement, Catalonia, Spain to Javier A. Menendez. Elisabet Cuyàs received the Sara Borrell post-doctoral contract (CD15/00033) from the Ministerio de Sanidad y Consumo, Fondo de Investigación Sanitaria (FIS), Spain. Joaquim Bosch-Barrera was supported by an Emerging Research Grant (2013) from the Spanish Society of Medical Oncology (SEOM, Madrid, Spain), and a Research Grant from Pfizer (W1190764). Vicente Micó was supported by grants PROMETEO/2016/006, AGL2015-67995-C3-1-R, and CIBEROnco CB12/03/30038. Almudena Pérez-Sánchez was supported by the VALi+d fellowship ACIF/2013/064.

### ORCID

Joaquim Bosch-Barrera  <http://orcid.org/0000-0002-0893-7821>

### References

- [1] Gridelli C, Peters S, Sgambato A, Casaluce F, Adjei AA, Ciardiello F. ALK inhibitors in the treatment of advanced NSCLC. *Cancer Treat Rev* 2014; 40:300-6; PMID:23931927; <http://dx.doi.org/10.1016/j.ctrv.2013.07.002>
- [2] Shaw AT, Kim DW, Nakagawa K, Seto T, Crino L, Ahn MJ, De Pas T, Besse B, Solomon BJ, Blackhall F, et al. Crizotinib versus chemotherapy in advanced ALK-positive lung cancer. *N Engl J Med* 2013; 368:2385-94; PMID:23724913; <http://dx.doi.org/10.1056/NEJMoa1214886>
- [3] Solomon BJ, Mok T, Kim DW, Wu YL, Nakagawa K, Mekhail T, Felip E, Cappuzzo F, Paolini J, Usari T, et al. PROFILE 1014 Investigators. First-line crizotinib versus chemotherapy in ALK-positive lung cancer. *N Engl J Med* 2014; 371:2167-77; PMID:25470694; <http://dx.doi.org/10.1056/NEJMoa1408440>
- [4] Lovly CM, Pao W. Escaping ALK inhibition: mechanisms of and strategies to overcome resistance. *Sci Transl Med* 2012; 4:120ps2; PMID:22323827; <http://dx.doi.org/10.1126/scitranslmed.3003728>
- [5] Katayama R, Shaw AT, Khan TM, Mino-Kenudson M, Solomon BJ, Halmos B, Jessop NA, Wain JC, Yeo AT, Benes C, et al. Mechanisms of acquired crizotinib resistance in ALK-rearranged lung cancers. *Sci Transl Med* 2012; 4:120ra17; PMID:22277784; <http://dx.doi.org/10.1126/scitranslmed.3003316>
- [6] Doebele RC, Pilling AB, Aisner DL, Kuteladze TG, Le AT, Weickhardt AJ, Kondo KL, Linderman DJ, Heasley LE, Franklin WA, et al. Mechanisms of resistance to crizotinib in patients with ALK gene rearranged non-small cell lung cancer. *Clin Cancer Res* 2012; 18:1472-82; PMID:22235099; <http://dx.doi.org/10.1158/1078-0432.CCR-11-2906>
- [7] Costa DB, Kobayashi S. Acquired resistance to the ALK inhibitor crizotinib in the absence of an ALK mutation. *J Thorac Oncol* 2012; 7:623-5; PMID:22334013; <http://dx.doi.org/10.1097/JTO.0b013e318241daab>
- [8] Tanizaki J, Okamoto I, Okabe T, Sakai K, Tanaka K, Hayashi H, Kaneda H, Takezawa K, Kuwata K, Yamaguchi H, et al. Activation of HER family signaling as a mechanism of acquired resistance to ALK inhibitors in EML4-ALK-positive non-small cell lung cancer. *Clin Cancer Res* 2012; 18:6219-26; PMID:22843788; <http://dx.doi.org/10.1158/1078-0432.CCR-12-0392>
- [9] Yamaguchi N, Lucena-Araujo AR, Nakayama S, de Figueiredo-Pontes LL, Gonzalez DA, Yasuda H, Kobayashi S, Costa DB. Dual ALK and EGFR inhibition targets a mechanism of acquired resistance to the tyrosine kinase inhibitor crizotinib in ALK rearranged lung cancer. *Lung Cancer* 2014; 83:37-43; PMID:24199682; <http://dx.doi.org/10.1016/j.jlungcan.2013.09.019>
- [10] Bosch-Barrera J, Menendez JA. Silibinin and STAT3: A natural way of targeting transcription factors for cancer therapy. *Cancer Treat Rev* 2015; 41:540-6; PMID:25944486; <http://dx.doi.org/10.1016/j.ctrv.2015.04.008>
- [11] Hong S, Chen N, Fang W, Zhan J, Liu Q, Kang S, He X, Liu L, Zhou T, Huang J, et al. Uregulation of PD-L1 by EML4-ALK fusion

- protein mediates the immune escape in ALK positive NSCLC: Implication for optional anti-PD-1/PD-L1 immune therapy for ALK-TKIs sensitive and resistant NSCLC patients. *Oncoimmunology* 2015; 5: e1094598; PMID:27141355; <http://dx.doi.org/10.1080/2162402X.2015.1094598>
- [12] Wang Y, Wang H, Zhao Q, Xia Y, Hu X, Guo J. PD-L1 induces epithelial-to-mesenchymal transition via activating SREBP-1c in renal cell carcinoma. *Med Oncol* 2015; 32:212; PMID:26141060; <http://dx.doi.org/10.1007/s12032-015-0655-2>
- [13] Alsuliman A, Colad D, Al-Harazi O, Fitwi H, Tulbah A, Al-Tweigeri T, Al-Alwan M, Ghebeh H. Bidirectional crosstalk between PD-L1 expression and epithelial to mesenchymal transition: significance in claudin-low breast cancer cells. *Mol Cancer* 2015; 14:149; PMID:26245467; <http://dx.doi.org/10.1186/s12943-015-0421-2>
- [14] Ritprajak P, Azuma M. Intrinsic and extrinsic control of expression of the immunoregulatory molecule PD-L1 in epithelial cells and squamous cell carcinoma. *Oral Oncol* 2015; 51:221-8; PMID:25500094; <http://dx.doi.org/10.1016/j.oraloncology.2014.11.014>
- [15] Ock CY, Kim S, Keam B, Kim M, Kim TM, Kim JH, Jeon YK, Lee JS, Kwon SK, Hah JH, et al. PD-L1 expression is associated with epithelial-mesenchymal transition in head and neck squamous cell carcinoma. *Oncotarget* 2016; 7:15901-14; PMID:26893364
- [16] Mak MP, Tong P, Diao L, Cardnell RJ, Gibbons DL, William WN, Skoulidis F, Parra ER, Rodriguez-Canales J, Wistuba II, et al. A Patient-Derived, Pan-Cancer EMT Signature Identifies Global Molecular Alterations and Immune Target Enrichment Following Epithelial-to-Mesenchymal Transition. *Clin Cancer Res* 2016; 22:609-20; PMID:26420858; <http://dx.doi.org/10.1158/1078-0432.CCR-15-0876>
- [17] Satelli A, Bath IS, Brownlee Z, Rojas C, Meng QH, Kopetz S, Li S. Potential role of nuclear PD-L1 expression in cell-surface vimentin positive circulating tumor cells as a prognostic marker in cancer patients. *Sci Rep* 2016 Jul 1; 6:28910; <http://dx.doi.org/10.1038/srep28910>
- [18] Lee Y, Shin JH, Longmire M, Wang H, Kohrt HE, Chang HY, Sunwoo JB. CD44+ Cells in Head and Neck Squamous Cell Carcinoma Suppress T-Cell-Mediated Immunity by Selective Constitutive and Inducible Expression of PD-L1. *Clin Cancer Res* 2016; 22:3571-81; PMID:26864211; <http://dx.doi.org/10.1158/1078-0432.CCR-15-2665>
- [19] Corominas-Faja B, Oliveras-Ferraro C, Cuyàs E, Segura-Carretero A, Joven J, Martin-Castillo B, Barrajón-Catalán E, Micol V, Bosch-Barrera J, Menéndez JA. Stem cell-like ALDH(bright) cellular states in EGFR-mutant non-small cell lung cancer: a novel mechanism of acquired resistance to erlotinib targetable with the natural polyphenol silibinin. *Cell Cycle* 2013; 12:3390-404; PMID:24047698; <http://dx.doi.org/10.4161/cc.26417>
- [20] Cufí S, Bonavia R, Vazquez-Martín A, Oliveras-Ferraro C, Corominas-Faja B, Cuyàs E, Martin-Castillo B, Barrajón-Catalán E, Visa J, Segura-Carretero A, et al. Silibinin suppresses EMT-driven erlotinib resistance by reversing the high miR-21/low miR-200c signature in vivo. *Sci Rep* 2013; 3:2459
- [21] Cufí S, Bonavia R, Vazquez-Martín A, Corominas-Faja B, Oliveras-Ferraro C, Cuyàs E, Martin-Castillo B, Barrajón-Catalán E, Visa J, Segura-Carretero A, et al. Silibinin meglumine, a water-soluble form of milk thistle silymarin, is an orally active anti-cancer agent that impedes the epithelial-to-mesenchymal transition (EMT) in EGFR-mutant non-small-cell lung carcinoma cells. *Food Chem Toxicol* 2013; 60:360-8; <http://dx.doi.org/10.1016/j.fct.2013.07.063>
- [22] Lee HJ, Zhuang G, Cao Y, Du P, Kim HJ, Settleman J. Drug resistance via feedback activation of Stat3 in oncogene-addicted cancer cells. *Cancer Cell* 2014; 26:207-21; PMID:25065853; <http://dx.doi.org/10.1016/j.ccr.2014.05.019>
- [23] Hamedani FS, Cinar M, Mo Z, Cervania MA, Amin HM, Alkan S. Crizotinib (PF-2341066) induces apoptosis due to downregulation of pSTAT3 and BCL-2 family proteins in NPM-ALK(+) anaplastic large cell lymphoma. *Leuk Res* 2014; 38:503-8; PMID:24486291; <http://dx.doi.org/10.1016/j.leukres.2013.12.027>
- [24] You L, Shou J, Deng D, Jiang L, Jing Z, Yao J, Li H, Xie J, Wang Z, Pan Q, et al. Crizotinib induces autophagy through inhibition of the STAT3 pathway in multiple lung cancer cell lines. *Oncotarget* 2015; 6:40268-82; PMID:26384345
- [25] Shimoji M, Shimizu S, Sato K, Suda K, Kobayashi Y, Tomizawa K, Takemoto T, Mitsudomi T. Clinical and pathologic features of lung cancer expressing programmed cell death ligand 1 (PD-L1). *Lung Cancer* 2016; 98:69-75; PMID:27393509; <http://dx.doi.org/10.1016/j.lungcan.2016.04.021>
- [26] Lucena-Araujo AR, Moran JP, VanderLaan PA, Dias-Santagata D, Folch E, Majid A, Kent MS, Gangadharan SP, Rangachari D, Huberman MS, et al. De novo ALK kinase domain mutations are uncommon in kinase inhibitor-naïve ALK rearranged lung cancers. *Lung Cancer* 2016; 99:17-22; PMID:27565908; <http://dx.doi.org/10.1016/j.lungcan.2016.06.006>
- [27] Gainor JF, Dardaei L, Yoda S, Friboulet L, Leshchiner I, Katayama R, Dagogo-Jack I, Gadgil S, Schultz K, Singh M, et al. Molecular Mechanisms of resistance to first- and second-generation ALK inhibitors in ALK-Rearranged Lung Cancer. *Cancer Discov* 2016; 6:1118-1133
- [28] Zhao C, Li H, Lin H, Yang S, Lin J, Liang G. Feedback Activation of STAT3 as a Cancer Drug-Resistance Mechanism. *Trends Pharmacol Sci* 2016; 37:47-61; PMID:26576830; <http://dx.doi.org/10.1016/j.tips.2015.10.001>
- [29] Kim HR, Kim WS, Choi YJ, Choi CM, Rho JK, Lee JC. Epithelial-mesenchymal transition leads to crizotinib resistance in H2228 lung cancer cells with EML4-ALK translocation. *Mol Oncol* 2013; 7:1093-102; PMID:23993685; <http://dx.doi.org/10.1016/j.molonc.2013.08.001>
- [30] Bosch-Barrera J, Sais E, Cañete N, Marruecos J, Cuyàs E, Izquierdo A, Porta R, Haro M, Brunel J, Pedraza S, et al. Response of brain metastasis from lung cancer patients to an oral nutraceutical product containing silibinin. *Oncotarget* 2016; 7:32006-14; PMID:26959886

